



**HAL**  
open science

# The impact of the acidic tumor microenvironment on ion channel expression and regulation, in the progression of pancreatic ductal adenocarcinoma

Julie Schnipper

► **To cite this version:**

Julie Schnipper. The impact of the acidic tumor microenvironment on ion channel expression and regulation, in the progression of pancreatic ductal adenocarcinoma. *Tissues and Organs [q-bio.TO]*. Université de Picardie Jules Verne, 2022. English. NNT : 2022AMIE0071 . tel-04327741

**HAL Id: tel-04327741**

**<https://theses.hal.science/tel-04327741>**

Submitted on 6 Dec 2023

**HAL** is a multi-disciplinary open access archive for the deposit and dissemination of scientific research documents, whether they are published or not. The documents may come from teaching and research institutions in France or abroad, or from public or private research centers.

L'archive ouverte pluridisciplinaire **HAL**, est destinée au dépôt et à la diffusion de documents scientifiques de niveau recherche, publiés ou non, émanant des établissements d'enseignement et de recherche français ou étrangers, des laboratoires publics ou privés.



# Thèse de Doctorat

*Mention Biologie – Santé  
Spécialité Physiopathologie Humaine*

présentée à l'Ecole Doctorale en Sciences Technologie et Santé (ED 585)

de l'Université de Picardie Jules Verne

par

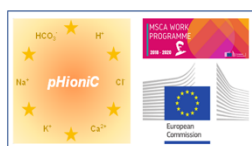
**Julie Schnipper**

pour obtenir le grade de Docteur de l'Université de Picardie Jules Verne

*The impact of the acidic tumor microenvironment on ion channel expression and regulation, in the progression of pancreatic ductal adenocarcinoma*

Soutenue le 10 Novembre 2022, après avis des rapporteurs, devant le jury d'examen :

<b>M. L. COUNILLON, Professeur, Professeur des Universités</b> Université Côte d'Azur	<b>Rapporteur</b>
<b>M. F. VAN COPPENOLLE, Professeur des Universités</b> Université Claude Bernard Lyon 1	<b>Rapporteur</b>
<b>M. L. PARDO, Professeur des Universités</b> Max Planck Institute for Multidisciplinary Sciences	<b>Examineur</b>
<b>M. S. ROGER, Maître de Conférences HDR,</b> Université de Tours	<b>Examineur</b>
<b>M. H. SEVESTRE, Professeur des Universités</b> Université de Picardie Jules Verne	<b>Examineur</b>
<b>M. L. GARÇON, Professeur des Universités</b> Université de Picardie Jules Verne	<b>Examineur</b>
<b>M<sup>me</sup> H. OUADID-AHIDOUCH, Professeur des Universités,</b> Université de Picardie Jules Verne	<b>Directrice de thèse</b>





## Acknowledgments

During my Ph.D. studies, I have had the opportunity to work with a number of excellent people to whom I am profoundly grateful and who should be acknowledged for their invaluable contributions to this thesis work.

First, I would like to thank Prof. Laurent Counillon, Prof. Fabien Van Coppenolle, Prof. Luis Pardo, Dr. Sébastien Roger, Prof. Loic Garçon, and Prof. Henri Sevestre for agreeing to take part in my jury. Thank you in advance for showing interest in my research and for taking the time to evaluate and discuss my thesis and my following thesis defense.

I would like to thank my supervisor Prof. Halima Ouadid-Ahidouch for giving me the opportunity to carry out this thesis project in her laboratory. Thank you for challenging me and guiding me and for our many inspiring scientific discussions throughout the last three years. Your door has always been open to me, and even during my bad times, you have encouraged and supported me to work on. I am exceptionally thankful that you have welcomed and included me in your group as an international student, even though the French have challenged me. Again, thank you for taking good care of me during the lockdown and for our many travels we, after all, have had the opportunity to accomplish.

I owe a special thank you to Prof. Stine Falsig Pedersen for welcoming me into her laboratory for my secondments during my Ph.D. I started my very early scientific career in your laboratory, and you inspired me to take this opportunity to go abroad, and you keep inspiring me. Thank you for always helping and caring for me, both scientifically and personally. Thanks to everyone in your group who always included me, no matter how long I had to stay.

I wish to thank everyone in the AnaPath Department at CHU Amiens-Picardie. Especially thanks to Prof. Henri Sevestre for welcoming me with open arms and including me in the department and your family. It has been such a pleasure to work with you. Thank you for teaching me and encouraging me to work in pathology. Thank you for all our good times, even during the lockdown.

Thanks to Dr. Pierre Rybarczyk for taking the time to analyze many IHC slides with me during the years and for some great moments meanwhile. Thanks to Dr. Riad Tebbakha for taking care of all administration related to ethical procedures during this project, and thank you for warmly welcoming me to the AnaPath. Here, I would also like to thank Marie-Pierre Mabilie for carrying out the experimental procedures during this Ph.D., and for being brave to try to work with me in English.

I would like to thank everyone in LPCM for welcoming me and making an effort to work with me in English. Especially thanks to Marie-Sophie Telliez, who helped me with all experimental procedures during my Ph.D.

Thank you for some good moments. It has been a pleasure and challenging (I think for both of us), but at least we have tried to collaborate in English and French. Thanks to Lucille Dubuisson for taking very good care of me and installing me in Amiens, when I arrived back in 2019, I could not have integrated so well without your help all along. Also, thanks to Nathalie Guingand for the administrative help the last year. Thanks to Dr. Alban Girault for helping me out experimentally with biotinylation assays and scientific discussions and personally for cheering on me during the ups and downs. Thanks to Dr. Frédéric Hague for helping me with calcium imaging and scientific debates, where you have always made great perspectives of my work, encouraging me to think of further experiments to do, and personally, thanks for joking and cheering in the early mornings. Thanks to Dr. Sana Kouba for helping me with many experimental procedures, such as co-IP and PLA. No matter what, you have always been a great friend, smiling, laughing, and encouraging. Thanks to Prof. Mathieu Gautier, Dr. Isabelle Dhennin-Duthille, and Dr. Lise Rodat-Despoix for welcoming me and for scientific and personal encouragement during the years. I would also like to thank all the current and previous students, Mohamed, Julie, Melanie, Sarah, Riadh, Hiba, and Sylvie, for their support, help, and great time during the last three years.

Thanks to everyone at the CRRBM for help and collaboration the last three years. I owe a special thanks to Dr. Stéphanie Guénin for helping me with everything I needed during my daily laboratory work and for your friendship.

Moreover, I wish to thank all members, fellows, and PIs of the Marie Curie international training network pHioniC for their great friendship, collaborations, and all the memorable moments.

Thereby I would like to thank my family and friends who have been a part of my life for the last three years. Especially thanks to my little sister, who cheered on me and helped me with whatever I needed help with, even with this distance between us. You have always been patient with me, made me brave, and stood by me all along. Thanks to my dear friend Ida, who has always supported me, taking her time to talk, discuss and listen to whatever I say. Thank you for still being as close, and even closer to me, as we have ever been.

I would like to dedicate this thesis and the last three years of work to my angel-Mom who raised me and gave me the strength and courage to take this path in my life. You have made me who I am.

Finally, my deepest thankfulness and appreciation to my better half, Mohamed. I am beyond grateful for everything you have done and still do for me, which words cannot describe. I am forever indebted to you.

## Abbreviations

2-ABP	2-aminoethoxydiphenyl borate	MAPK	Mitogen-activated protein kinase
5PTase	Polyphosphate-5-phosphatase A	MEK	Mitogen-activated protein kinase kinase
5hmC	5-hydroxymethylcytosine	MCN	Mucinous cystic neoplasm
ACh	Acetylcholine	MCT	Monocarboxylate transporters
ADEX	Aberrantly differentiated endocrine exocrine	MCU	Mitochondrial calcium uniporter
AKT	Protein kinase B	MMP	Matrix metalloprotease
ATCC	American Type Culture Collection	MPP <sup>+</sup>	1-methyl-4-phenylpyridinium ion
ATP	Adenosine triphosphate	MRI	Magnetic resonance imaging
BS-MSP	Bisulfite conversion-specific methylation-specific PCR	mTOR	Mammalian target of rapamycin
CA	Carbonic anhydrase	Na <sup>+</sup>	Sodium
Ca <sup>2+</sup>	Calcium	NaCl	Sodium chloride
CAF	Cancer-associated fibroblast	NBCs	Na <sup>+</sup> /HCO <sub>3</sub> <sup>-</sup> co-transporters
CaM	Calmodulin	NBCn1	Na <sup>+</sup> /HCO <sub>3</sub> <sup>-</sup> co-transporter 1
CaMK	Ca <sup>2+</sup> /CaM-kinases	NCLX	Na <sup>+</sup> /Ca <sup>2+</sup> exchangers
cAMP	Cyclic adenosine monophosphate	NFAT	Nuclear factor of activated T-cells
CaR	Ca <sup>2+</sup> -sensing receptor	NFκB	Nuclear factor kappa-light-chain-enhancer of activated B cells
CDK	Cyclin dependent kinase	NHEs	Na <sup>+</sup> /H <sup>+</sup> exchangers
CDKI	Cyclin dependent kinase inhibitor	NHE1	Na <sup>+</sup> /H <sup>+</sup> exchanger 1
CDK2NA	Cyclin-dependent kinase inhibitor 2A	NSCLC	Non-small cell lung cancer
CFTR	Cystic fibrosis transmembrane conductance regulator	O <sub>2</sub>	Dioxygen
Cl <sup>-</sup>	Chloride	PanIN	Pancreatic intraepithelial neoplasia
CKK	Cholecystokinin	PDAC	Pancreatic ductal adenocarcinoma
CO <sub>2</sub>	Carbon dioxide	PET	Positron emission tomography
CpG	Cytosine-phosphate-guanine	pH <sub>i</sub>	Intracellular pH
CRC	Colorectal cancer	pH <sub>o</sub>	Extracellular pH
CT	Computed tomography	PI	Propidium iodide
DNMT	DNA methyltransferases	PI3K	Phosphoinositide 3-kinase
DPC4	Deleted in Pancreatic Cancer-4	PKC	Protein kinase C
ECM	Extracellular matrix	PSCs	Pancreatic stellate cells
ECOG	Eastern Cooperative Oncology Group	qPCR	Quantitative real-time PCR
EGF	Epidermal growth factor	Rb	Retinoblastoma
EGFR	Epidermal growth factor receptor	RKIP	Raf kinase inhibitory protein
ERK1/2	Extracellular signal-regulated kinase	RT-PCR	Reverse transcription polymerase chain reaction
EMT	Epithelial-to-mesenchymal transition	SERCA	ER/SR Ca <sup>2+</sup> -ATPases
ER	Endoplasmic reticulum	shRNA	Short-hairpin RNA
FdG	<sup>18</sup> fluorodeoxyglucose	siRNA	Small-interfering RNA
FGFR1	Fibroblast growth factor receptor 1	SP-1	Sphingosine-1
G6PDH	Glucose-6-phosphate dehydrogenase	SPCA	Ca <sup>2+</sup> ATPases
GAPDH	Glyceraldehyde hosphate dehydrogenase	SR	Sarcoplasmic reticulum
GBM	Glioblastoma multiforme	STIM	Stromal interaction molecule
GLUT1	Glucose transporter 1	TET	Ten-eleven translocation methylcytosine dioxygenases
GPCR	G-protein coupled receptor	TCGA	The Cancer Genome Atlas
GTP	Guanosine triphosphate	TGFβ	Transforming growth factor β
H <sup>+</sup>	Proton	TNM	Tumor, node, metastasis
HAT	Histone acetyltransferases	TP53	Tumor protein 53
HCO <sub>3</sub> <sup>-</sup>	Bicarbonate	TRP	Transient receptor potential
HCX	Ca <sup>2+</sup> /H <sup>+</sup> exchangers	TSCC	Tongue squamous cell carcinoma
HDAC	Histone deacetylases	V-ATPase	Vacuolar-type (V)-ATPase
HIF	Hypoxia-inducible factors	VEGF	Vascular endothelial growth factor
IHC	Immunohistochemistry	VGFR	Vascular endothelial growth factor receptor
IL-6	Interleukin-6	VGCC	Voltage-gated calcium channels
K <sup>+</sup>	Potassium	VGSC	Voltage-gated sodium channels
KCa	Ca <sup>2+</sup> -activated K <sup>+</sup> channels		
KD	Knockdown		
KRAS	Kirsten rat sarcoma virus		
LAMP2	Lysosomal-associated membrane protein 2		
m5C	5-methylcytosine		

# Table of Contents

<b>ACKNOWLEDGMENTS .....</b>	<b>1</b>
<b>ABBREVIATIONS.....</b>	<b>3</b>
<b>INTRODUCTION .....</b>	<b>7</b>
<b>CHAPTER 1: PANCREATIC ANATOMY, PHYSIOLOGY AND PDAC CARCINOGENESIS.....</b>	<b>8</b>
THE PANCREAS .....	8
1. <i>Pancreatic anatomy</i> .....	8
2. <i>The endocrine pancreas</i> .....	8
3. <i>The exocrine pancreas</i> .....	8
4. <i>Pancreatic fluid secretion and pH regulation</i> .....	10
HALLMARKS OF CANCER .....	13
1. <i>Pancreatic carcinogenesis</i> .....	13
2. <i>The three steps of PDAC development and progression</i> .....	16
3. <i>Cell cycle regulation in PDAC</i> .....	18
4. <i>Consequences of aberrant cell cycle progression in PDAC</i> .....	20
5. <i>Metastatic properties of PDAC</i> .....	22
6. <i>Genetic alterations and signaling causing PDAC metastasis</i> .....	24
EPIDEMIOLOGY OF PANCREATIC CANCER.....	25
1. <i>Risk factors and causes of PDAC</i> .....	26
2. <i>TNM Classification</i> .....	27
3. <i>Grade classification of PDAC</i> .....	28
4. <i>Molecular classification of PDAC</i> .....	28
5. <i>Diagnosis and treatment</i> .....	28
<b>CHAPTER 2: THE PANCREATIC TUMOR MICROENVIRONMENT AND THE INVOLVEMENT OF PH IN CANCER PROGRESSION.....</b>	<b>32</b>
THE PANCREATIC TUMOR MICROENVIRONMENT.....	32
1. <i>pH regulation in cancer progression</i> .....	33
2. <i>Metabolic reprogramming</i> .....	33
3. <i>pH regulatory transport proteins</i> .....	35
4. <i>Changes in pH shape PDAC development</i> .....	38
5. <i>Cellular adaptation to extracellular acidosis in carcinogenesis</i> .....	39
<b>CHAPTER 3: ION CHANNELS AND CALCIUM HOMEOSTASIS IN THE PANCREATIC TUMOR MICROENVIRONMENT.....</b>	<b>44</b>
ION CHANNELS IN THE PANCREAS AND PDAC .....	44
1. <i>Calcium homeostasis</i> .....	45
2. <i>Calcium signaling in the pancreas</i> .....	45
3. <i>Transmembrane calcium channels</i> .....	46
4. <i>Intracellular calcium channels</i> .....	48
5. <i>Calcium pumps and transporters</i> .....	48
6. <i>Other calcium-binding proteins and processes</i> .....	49
7. <i>Calcium in cellular processes</i> .....	50
8. <i>Calcium in cancer</i> .....	53
CALCIUM CHANNELS IN THE TUMOR MICROENVIRONMENT.....	55
1. <i>Calcium and pH</i> .....	55

2. <i>pH-sensitive calcium channels</i> .....	57
<b>CHAPTER 4: THE TRPC1 CHANNEL</b> .....	<b>60</b>
CLASSIFICATION OF TRP CHANNELS .....	60
1. <i>TRPC1; Expression and structure</i> .....	60
2. <i>TRPC1; Activation and regulation</i> .....	62
3. <i>The contribution of TRPC1 in the SOCE scenario</i> .....	63
4. <i>Pharmacological inhibition of TRPC1</i> .....	64
5. <i>TRPC1 in pathologies</i> .....	65
6. <i>TRPC1 in the pancreatic tumor microenvironment</i> .....	70
7. <i>The TRPC1 interactome</i> .....	71
<b>OBJECTIVES</b> .....	<b>73</b>
<b>MATERIALS AND METHODS</b> .....	<b>75</b>
CELL CULTURING .....	76
1. <i>Cell lines</i> .....	76
2. <i>Cell maintenance</i> .....	77
3. <i>Freezing and thawing of cells</i> .....	79
TRANSFECTION .....	79
GENERATION OF SPHEROIDS .....	80
CELL PROLIFERATION ASSAYS .....	80
CALCIUM IMAGING .....	81
TRANSCRIPTIONAL EXPRESSION .....	83
PROTEIN EXPRESSION .....	85
CO-IMMUNOPRECIPITATION .....	86
PROXIMITY LIGATION ASSAY .....	87
BIOTINYLATION .....	87
INTRACELLULAR pH.....	87
IMMUNOFLUORESCENCE ANALYSIS .....	89
MIGRATION ASSAY.....	89
CALCIUM DEPLETION AND CALMODULIN INHIBITION.....	90
IMMUNOHISTOCHEMISTRY.....	90
STATISTICAL ANALYSIS .....	91
BISULFITE SEQUENCING.....	92
<b>RESULTS</b> .....	<b>97</b>
PART 1: THE TRPC1 CHANNEL FORMS A PI3K/CAM COMPLEX AND REGULATES PANCREATIC DUCTAL ADENOCARCINOMA CELL PROLIFERATION IN A $Ca^{2+}$ -INDEPENDENT MANNER .....	98
<i>Ca<sup>2+</sup> channels are overexpressed in human PDAC tissue and cell lines</i> .....	98
<i>Summary</i> .....	102
<i>Complementary results</i> .....	105
PART 2: ACID ADAPTATION PROMOTES TRPC1 PLASMA MEMBRANE LOCALIZATION LEADING TO PANCREATIC DUCTAL ADENOCARCINOMA CELL PROLIFERATION AND MIGRATION THROUGH $Ca^{2+}$ ENTRY AND INTERACTION WITH PI3K/CAM .....	106
<i>Summary</i> .....	106
<i>Complementary results</i> .....	109
<i>TRPC1 silencing does not change the expression of other store-operated channels</i> .....	109
<i>Acid adaptation does not affect the transcriptional expression of other <math>Ca^{2+}</math> channels</i> .....	109
<i>Acute acidification increases <math>Ca^{2+}</math> entry through TRPC1</i> .....	110
<i>The TRPC1 localization correlates with the acidic tumor microenvironment</i> .....	110
<b>DISCUSSION</b> .....	<b>113</b>
DISCUSSION, PART 1 & 2 .....	114
<i>TRPC1 is a potential biomarker of PDAC</i> .....	115

<i>TRPC1 localizes to the plasma membrane and is functionally active solely in acid-adapted and -recovered PANC-1 cells</i> .....	115
<i>TRPC1 regulates proliferation and migration through Ca<sup>2+</sup>-dependent mechanisms in acid-adapted and -recovered conditions</i> .....	116
<i>TRPC1 regulates proliferation and migration through the PI3K/AKT and MAPK/ERK1/2 axis in acid-recovered conditions</i> .....	117
<b>EPIGENETIC PROJECT</b> .....	<b>119</b>
<b>THE ACIDIC MICROENVIRONMENT AFFECTS THE DNA METHYLATION OF ION CHANNELS</b> .....	<b>120</b>
INTRODUCTION .....	120
<i>DNA methylation patterns in PDAC</i> .....	120
RESULTS.....	124
<i>ASIC1 and Nav1.6 expression is dysregulated in human PDAC tissue and affected by acid adaptation in PDAC cell lines</i> .....	124
<i>ASIC1 seems to be hypomethylated in acid-adapted MiaPaCa-2 cells, but hypermethylated in acid-adapted PANC-1 cells</i> .....	124
<i>The quantitative analysis method reveals that the ASIC1 region is not hypomethylated upon acid-adaptation</i> ...	126
<i>The SCN8A gene promoter is hypermethylated in acid-adapted PANC-1 cells</i> .....	127
<i>The TRPC1 gene promoter is hypomethylated upon acid-adaptation</i> .....	129
DISCUSSION .....	130
<b>CONCLUSION AND FUTURE PERSPECTIVES</b> .....	<b>132</b>
<b>RÉSUMÉ</b> .....	<b>137</b>
<b>REFERENCES</b> .....	<b>148</b>
<b>APPENDICES</b> .....	<b>171</b>
APPENDIX 1 .....	171

# INTRODUCTION

# CHAPTER 1: Pancreatic anatomy, physiology and PDAC carcinogenesis

## The pancreas

### 1. Pancreatic anatomy

The pancreas is a transversally retroperitoneal organ in the abdomen, located posterior to the stomach. It weighs about 100 grams and is 14-23 cm long. It is divided into the head, neck, body, and tail. The head of the pancreas is located in the loop of the duodenum where it exits the stomach (Figure 1A). The neck and body lie posterior to the distal portion of the stomach, and the tail lies near the hilum of the spleen. The blood supply of the pancreatic head departs from the superior pancreatic duodenal artery (branches from the hepatic artery) and the inferior pancreatic duodenal artery (branches from the superior mesenteric artery). The tail of the pancreas is supplied through branches from the splenic artery. The venous blood from the head is drained into the superior mesenteric vein, and the blood from the body and tail is drained into the splenic veins, which both end up in the portal vein. The pancreatic ducts extend through the whole organ, from the tail to the head, where the principal duct (duct of Wirsung) and the accessory duct (duct of Santorini) merge with the distal common bile duct. These end up in the central pancreatic draining duct (papilla of Vater), which terminates in the second part of the duodenum. On the cellular level, the pancreas originates from the endodermal germ layer and is made up of two major types of tissue; the endocrine and the exocrine part (Figure 1D) (Longnecker 2021, Talathi *et al.* 2022).

### 2. The endocrine pancreas

The endocrine tissue of the pancreas is composed of the islets of Langerhans and looks like small islets under the microscope. More than a million islets of Langerhans are distributed all over the adult human pancreas, but these islets comprise only 1-2% of the pancreatic mass (Longnecker 2021). The islets of Langerhans consist of four cell types; the alpha, beta, and delta cells and pancreatic polypeptide cells (PP cells), which all secrete metabolic regulatory hormones into the bloodstream (Figure 1D). The alpha cells produce and secrete glucagon, the beta cells insulin, the delta cells somatostatin, and the PP cells pancreatic polypeptide (Figure 1D). The main deficiencies of the endocrine pancreas are type I or II diabetes mellitus, and the endocrine cells are also the source of pancreatic neuroendocrine tumors (Bardeesy and DePinho 2002, Longnecker 2021, Talathi *et al.* 2022).

### 3. The exocrine pancreas

The exocrine pancreas comprises more than 95% of the pancreatic volume and is responsible for producing and secreting pancreatic juices containing essential digestive enzymes and fluids to the intestine. The exocrine tissue contains mainly two cell types necessary for its function; acinar cells (make up >80% of the pancreatic mass) that produce the digestive enzymes and the duct cells, which add mucus and bicarbonate to the enzyme mixture (Figure 1B, C). The acini are arranged in an anastomosing tubular network, consisting of acinar and



centroacinar cells forming a central lumen, which is the beginning of the branching duct system. The acinar cells are polarized in a basolateral and apical axis, and the secretory zymogen granules are stored in the apical domain. The zymogen granules contain precursors of pancreatic digestive enzymes, including lipases, alpha-amylases, carboxypolypeptidase, trypsin, and chymotrypsin. In addition, the granules contain trypsin inhibitors preventing enzyme activation. The zymogen granules are continuously secreted, with the highest rate after a meal (Bardeesy and DePinho 2002, Longnecker 2021, Talathi et al. 2022).

The lobules formed by the acinar cells are connected to the ductules, which are constructed of duct cells, transporting the secreted pancreatic enzymes to the major pancreatic duct ending in the duodenum. The acinar lobule ends, and the duct system begins with the centroacinar cells marking the transition between acinar and duct cells. The duct cells have several segments based on size and location, and the ducts have several cell types, including secretory, mucosal, and ciliated cells. The secretory duct cells start the branch of the ductal tree with small intercalated duct cells that join together and are sequentially followed by the intralobular, interlobular and interlobar duct segments. In humans, the interlobar ducts unite and form the principal duct (duct of Wirsung). The intercalated and intralobular ducts are the major sites of  $\text{HCO}_3^-$  secretion. These cells contain a high number of mitochondria to meet the high energy demand of the transcellular  $\text{HCO}_3^-$  and fluid secretion. In contrast, they have a relatively small amount of organelles required for protein secretion (Bardeesy and DePinho 2002, Longnecker 2021, Talathi et al. 2022).

Additionally, the pancreas contains a third and minor cell type; the pancreatic stellate cells (PSCs). They are located both at the periacinar and periductal space or surrounding the islets of Langerhans, thus participating in the maintenance of the pancreatic tissue architecture (Bachem *et al.* 1998, Apte *et al.* 2012, Zhou *et al.* 2019).

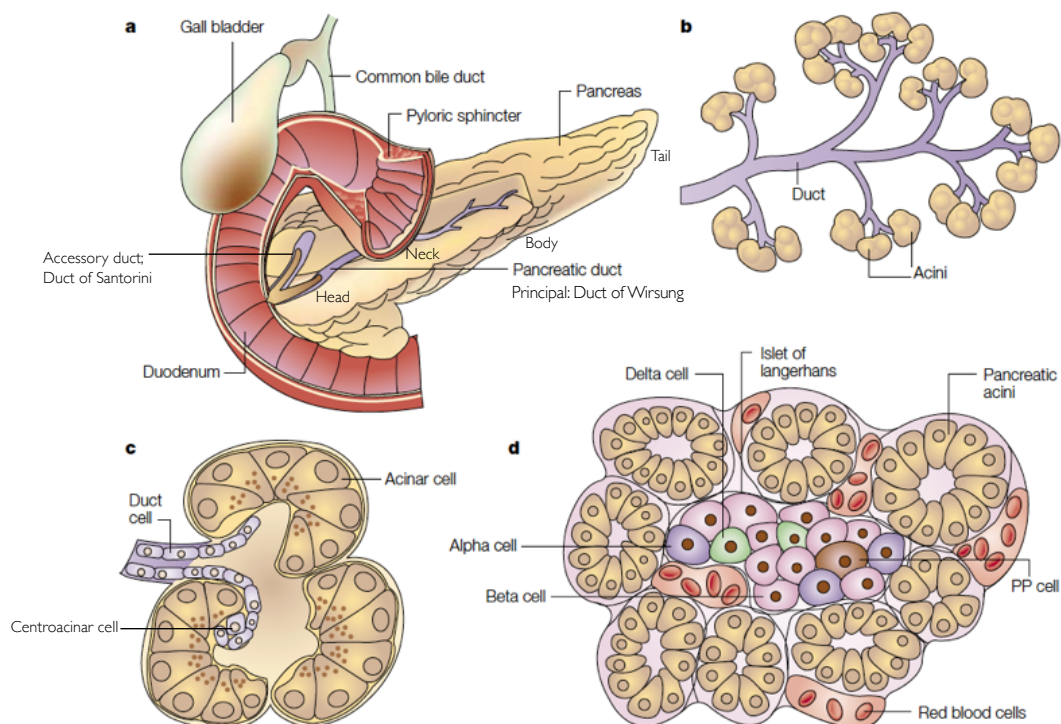


Figure 1. Graphical overview of the anatomy of the pancreas. A) Overview of the anatomy of the pancreas and the main ducts. B) Anatomy of the exocrine pancreas consisting of acini and ductal branches. C) A single acinus containing several acinar cells and centroacinar cells assembles into a duct. D) Overview of endocrine cells and how they are organized between acini (Modified from (Bardeesy and DePinho 2002).

#### 4. Pancreatic fluid secretion and pH regulation

The functional unit formed by acinar and ductal cells secretes 1-2 L/day of pancreatic juice, an alkaline isotonic fluid containing several digestive enzymes, as described above (Lee *et al.* 2012). The high bicarbonate ( $\text{HCO}_3^-$ ) concentration provides an optimal pH for the digestive enzymes and neutralizes the acidic chyme entering the duodenum from the stomach (Hegyi *et al.* 2011). The pancreatic exocrine secretion is controlled by multiple neurohormonal inputs (Lee *et al.* 2012). The activation of acinar cells is regulated by  $\text{Ca}^{2+}$ -mobilizing agents, whereas duct cells are primarily regulated by cyclic adenosine monophosphate (cAMP) generating receptors. The main stimulation of acinar cells is through receptors responding to the hormone cholecystinin (CKK) and the neurotransmitter acetylcholine (ACh). In comparison, duct cells respond to a cholinergic vagal output and the hormone secretin. Both secretin and CCK are secreted by the duodenum and enter the pancreas from the bloodstream. The secretion of these hormones is due to the digestive phase the human body enters, during the intake of a meal, enhancing the pancreatic fluid secretion (Lee *et al.* 2012).

During the secretion of the pancreatic fluids, the acini and ductal cells performing net acid-base transport are exposed to very different extracellular pH values on the apical and basolateral membranes, respectively (Novak *et al.* 2013). At the luminal site of the pancreatic duct system, the acinar cells secrete an isotonic sodium chloride (NaCl) and proton ( $\text{H}^+$ ) -rich fluid containing different digestive enzymes, which can

decrease the luminal pH to 6.8 (Hegyí et al. 2011, Hegyí and Petersen 2013, Pallagi *et al.* 2015). In the duct cells, chloride  $\text{Cl}^-$  stimulate the excretion of  $\text{HCO}_3^-$  to produce an alkaline fluid that can contain up to 140 mM  $\text{HCO}_3^-$  and increase the luminal pH to 8 (Ishiguro *et al.* 2012, Hegyí and Petersen 2013, Pallagi et al. 2015). This  $\text{HCO}_3^-$  secretion is regulated by ion channels and transporters along the pancreatic ducts.

Acini and ductal cells absorb ions in a periodic pattern, alternating between the resting and digestive phases. When the digestive phase is initiated, CCK or ACh can stimulate receptors (e.g., G-protein coupled receptors GPCRs) at the apical pole of acinar cells, which evokes a rise in the intracellular  $\text{Ca}^{2+}$  concentration (Lee et al. 2012). The calcium ( $\text{Ca}^{2+}$ ) signal activates a  $\text{Cl}^-$  uptake across the basolateral membrane through sodium ( $\text{Na}^+$ )-potassium ( $\text{K}^+$ )- $2\text{Cl}^-$  cotransporters, which cooperate with the  $\text{Ca}^{2+}$ -activated  $\text{K}^+$  channels and the  $\text{Na}^+/\text{K}^+$  pump. The increased  $\text{Ca}^{2+}$  concentration stimulates  $\text{Ca}^{2+}$ -activated  $\text{Cl}^-$  channels at the apical pole, producing  $\text{Cl}^-$  and zymogen granules into the acinar lumen (Hegyí and Petersen 2013). Along with the  $\text{Cl}^-$  transport is the  $\text{Na}^+$  and water movement from the interstitial fluid to the acinar lumen through the leaky tight junctions. On the luminal side of the proximal duct cells, secretin stimulated rises of intracellular cAMP and high  $\text{Cl}^-$  concentrations will activate the SLC26A6  $\text{Cl}^-/\text{HCO}_3^-$  exchanger, secreting  $\text{HCO}_3^-$  to the ductal lumen and absorb  $\text{Cl}^-$ . As the  $\text{Cl}^-$  concentrations fall and the  $\text{HCO}_3^-$  concentration rises in the distal part of the ducts, the SLC26A6 approaches equilibrium, and the  $\text{HCO}_3^-$  secretion will mainly be mediated by the cystic fibrosis transmembrane conductance regulator (CFTR) (Ishiguro et al. 2012). Indeed, a high load of  $\text{HCO}_3^-$  from the basolateral side is required to satisfy the high demand for  $\text{HCO}_3^-$  excretion. The  $\text{HCO}_3^-$  are transported directly across the basolateral membrane into the duct cells through  $\text{Na}^+/\text{HCO}_3^-$  cotransporters (NBCs) or indirectly by passive diffusion of carbon dioxide ( $\text{CO}_2$ ) through the cell membrane.  $\text{CO}_2$  is converted to  $\text{HCO}_3^-$  and  $\text{H}^+$  by carbonic anhydrases (CAs) and  $\text{HCO}_3^-$ . Thus,  $\text{HCO}_3^-$  can be transported into the lumen, and a backward transport of  $\text{H}^+$  to the basolateral membrane is maintained by  $\text{Na}^+/\text{H}^+$  exchangers (NHEs) and  $\text{H}^+$ -ATPases (Figure 2) (Pallagi et al. 2015) (transporters are described in detail in the section ‘pH regulatory transport proteins’).

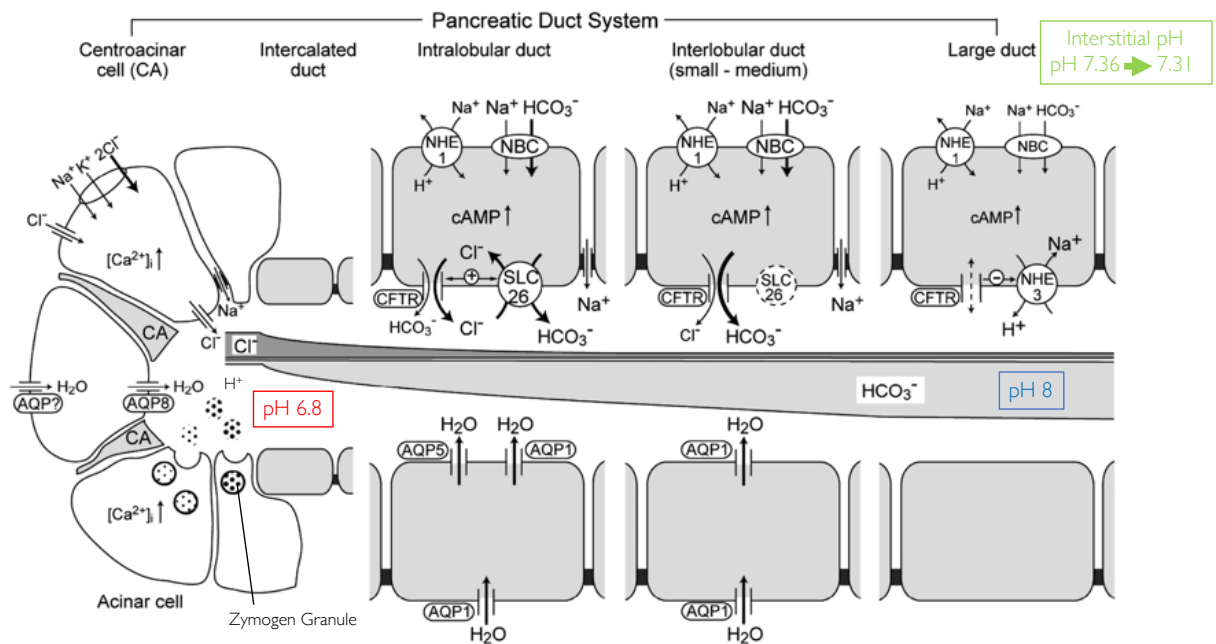


Figure 2. Overview of the pancreatic ducts and the transporters involved in the secretion of the alkaline  $\text{HCO}_3^-$  rich pancreatic fluids and ductal cell pH regulation (Modified from (Ishiguro *et al.* 2012)).

Thus, under normal conditions, the production of  $\text{H}^+$  and  $\text{HCO}_3^-$  along the pancreatic duct system results in changing pH values of the pancreatic juices. The varying extracellular pH ( $\text{pH}_o$ ) challenges the buffer capacity of the cells in the pancreatic ducts and can result in a variable intracellular pH ( $\text{pH}_i$ ) landscape (Pedersen *et al.* 2017). The regulation of the  $\text{pH}_i$  in pancreatic duct cells is maintained by ion transporters that contribute to cellular pH homeostasis. The major pH regulator is the NHEs. It is reported that NHEs contribute to  $\text{pH}_i$  regulation of pancreatic ducts of different species, including rats, mice, guinea pigs, pigs, and human duct cell lines (Novak and Praetorius 2020). One of the nine members of the NHE family, NHE1, is ubiquitously expressed and is often regarded as the central cellular acid extruder. Several studies indicate that NHE1 is localized on the basolateral membrane of pancreatic duct cells, contributing to normal duct function by regulating  $\text{pH}_i$  (Novak and Praetorius 2020). As described above, NBCs translocate  $\text{HCO}_3^-$  into the cell, which alkalizes the cytosol (Bardeesy and DePinho 2002). One family of NBCs was cloned from the pancreas; pNBC (NBCe1B). This isoform was found in the basolateral membrane of human pancreatic duct cells. The isoform NBCn1 is also expressed in the pancreatic ductal cells of mice, but rather in the luminal membrane, where it probably regulates  $\text{HCO}_3^-$  salvage (Novak and Praetorius 2020). Additional pH regulators of pancreatic duct cells are the anion exchangers, which are expressed on the basolateral membrane. Not surprisingly have, other  $\text{H}^+$  pumps (the V-ATPases and  $\text{H}^+/\text{K}^+$ -ATPases) shown to be involved in the regulation of  $\text{pH}_i$ , however, with a relatively small contribution, compared to NHE1 (Novak and Praetorius 2020). As described above, the  $\text{HCO}_3^-$  secretion creates alkaline apical conditions, where the

extrusion of  $H^+$  and  $CO_2$  across the basolateral membrane will create acidity. This phenomenon is proposed as the acid tide, reflecting pancreatic interstitial acidosis (Rune and Lassen 1968, Ashley *et al.* 1994, Novak *et al.* 2013).

## Hallmarks of cancer

In a multicellular organism, cancer is defined as the abnormal growth of a (multi)clonal cell population, which can invade and degrade surrounding and distant tissue within the host to form secondary tumors (Greaves and Maley 2012). For this to occur, a cell displays six characteristics called the Hallmarks of cancer during its transformation from normal to malignant. These characteristics were described and classified by Hanahan and Weinberg in 2000 as (1) an unlimited potential to replicate; (2) resisting apoptosis; (3) sustaining proliferative signaling; (4) evasion of growth suppressors (5) inducing angiogenesis; and (6) activation of invading and metastatic processes. These six characteristics are now divided in two 14 subcategories (Figure 3) (Hanahan and Weinberg 2011, Hanahan 2022).

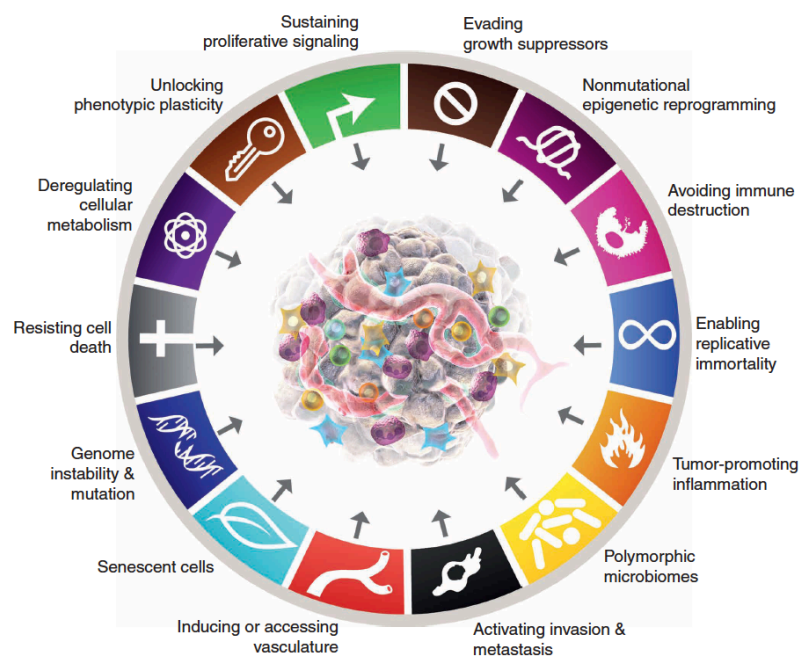


Figure 3. The updated 14 hallmarks of cancer (Hanahan 2022).

### 1. Pancreatic carcinogenesis

On gross inspection, pancreatic ductal adenocarcinomas (PDAC) are a firm white-yellow mass with poorly detectable demarcates. The tumor is surrounded by a non-malignant pancreas showing fibrosis, atrophy, and dilated ducts due to obstructive effects during carcinoma expansion (Ying *et al.* 2016). On the microscopic level, PDAC presents a heterogeneous growth pattern with atypical tubular glands resembling small or medium-sized pancreatic ducts. The irregular tubular glands are embedded in a desmoplastic stroma consisting of stromal and inflammatory cells and extracellular matrix proteins, which all contribute to the aggressive



behavior of these neoplasms (Figure 4) (Haeberle and Esposito 2019). They are classified by well-, moderately-, or poorly differentiated PDAC.

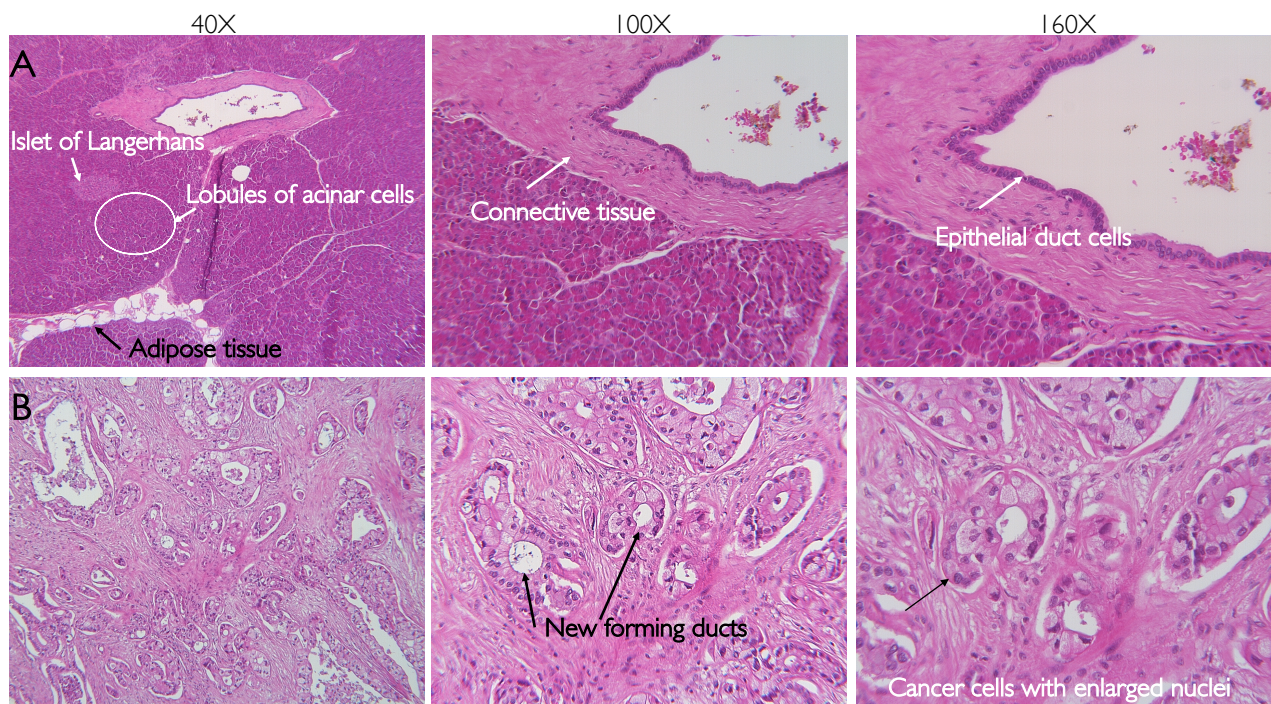


Figure 4. Histology of normal pancreas and PDAC. Panel A) shows normal well-organized pancreatic tissue, and different elements of the normal pancreas are indicated. Acinar cells form lobules and ducts formed by connective tissue aligned with epithelial duct cells. Indicated are the endocrine part of the pancreas, the islets of Langerhans, and adipose tissue. Panel B) shows well-differentiated cancer cells that are enlarged, with enlarged nuclei, forming new ducts (a feature of PDAC). In PDAC tissue, the acini are disrupted by the pressure created by the cancer cells, and only cancer cells and stroma are left. (Magnification indicated above the images. All images represent slides stained with hematoxylin (nuclei, purple) and eosin (extracellular matrix, pink). Images are taken in collaboration with Prof. Sevestre at Amiens Hospital).

PDAC evolves from well-characterized precursor lesions, where the most widely described are the microscopic pancreatic intraepithelial neoplasia (PanIN), followed by the macroscopic cysts called the intraductal papillary mucinous neoplasm (IPMN) and the mucinous cystic neoplasm (MCN) (Ying et al. 2016). Precursor lesions are usually described as bearing the characteristics of ductal epithelial cells. However, several studies support the notion that various cell types of the pancreas exhibiting the malignant potential of duct cells. For instance, acinar cells can, through a reprogramming process called acinar-to-ductal metaplasia, give rise to pancreatic cancer, which is often associated with the cell damage and inflammation that occurs during acute or chronic pancreatitis (Ying et al. 2016).

The most common and widely studied putative precursor lesions of PDAC are the PanINs. The PanINs are classified into three different stages: PanIN1a to PanIN3. As illustrated in Figure 5 normal duct cells have a low columnar epithelium. The epithelium becomes taller at the PanIN1a stage, and at the PanIN1B stage, the epithelium displays papillary structures. During the PanIN2 stage, the ductal cells lose their polarity, showing

nuclear crowding, cell enlargement, and hyperchromasia. In the PanIN3 stage, the cells display advanced lesions with severe nuclear atypia, luminal necrosis, and epithelial cell budding into the ductal lumen (Makohon-Moore and Iacobuzio-Donahue 2016, Ying et al. 2016). The PanIN1 and PanIN2 stages can be classified as low-grade with a low risk of PDAC development. PanIN3 is classified as high-grade and is almost exclusively found in patients with invasive PDAC and recognizes this precursor lesion as the one with the most significant biological potential for progression (Makohon-Moore and Iacobuzio-Donahue 2016, Ying et al. 2016).

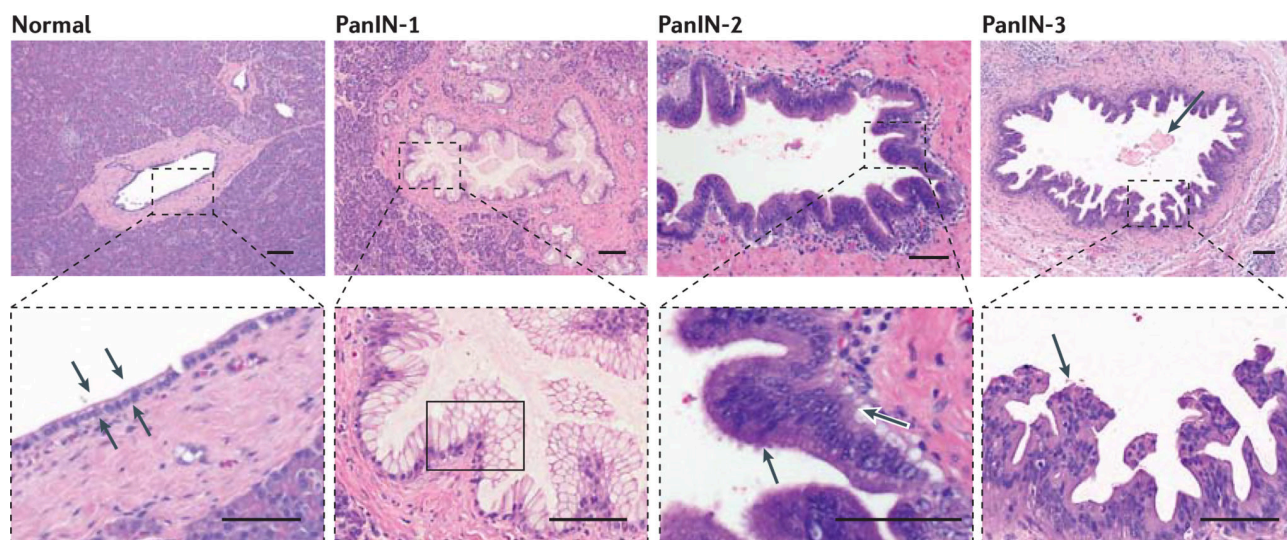


Figure 5. Morphology of pancreatic intraepithelial neoplasia (PanIN-1-3) Scale bar: 100  $\mu$ m (Makohon-Moore and Iacobuzio-Donahue 2016).

Besides the morphological changes in PanINs, genetic alterations are taken into account during the classification of the PanINs. It has been shown that the genetic modifications of PanINs do not occur randomly but rather in a specific order during the PanIN development, which is thought to be required for malignant transformation (Morris *et al.* 2010). There are four common mutations associated with the progression of PDAC. Sequencing of PanINs demonstrates that activating mutations in the Kirsten rat sarcoma virus gene (*KRAS*) are present in PanIN1 lesions (99% of cases), and the proportion of cells containing *KRAS* mutations increases with the PanIN grade. The most common cancer-associated mutations are found in residues G12, G13, or Q61 (Waters and Der 2018). Inactivating mutations in the cyclin-dependent kinase inhibitor 2A (*CDKN2A/p16INK4A*) are present as early as PanIN2 lesions (90% of cases), and loss of protein expression increases in PanIN3. Similarly, the inactivation of Tumor protein 53, coding for the P53 protein (*TP53*) (85% of cases) and the Deleted in Pancreatic Cancer-4 gene (*DPC4/SMAD4*) (55% of cases) are found in the PanIN3 stage and with a higher frequency in invasive cancers (Figure 6) (Morris *et al.* 2010, Makohon-Moore and Iacobuzio-Donahue 2016, Gao *et al.* 2020).

In the view of PanINs, pancreatic carcinogenesis occurs through a three-step process: initiation of the tumor by acquiring a gene mutation, clonal expansion of the already mutation-carrying cell, and the



introduction of the transformed and neoplastic cell population into local and/or distal environments (Makohon-Moore and Iacobuzio-Donahue 2016).

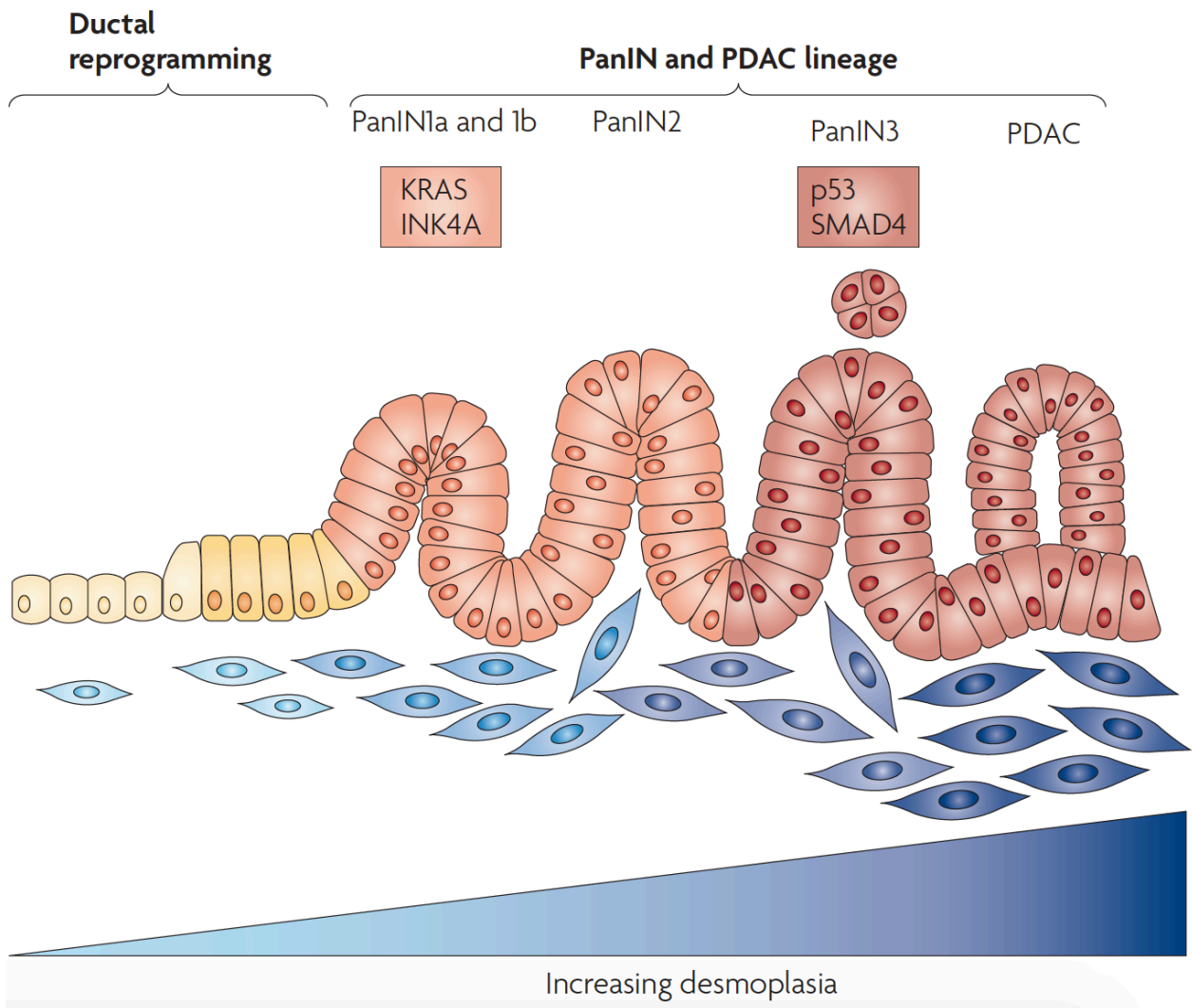


Figure 6. Genetic alterations during PanIN stages. KRAS mutation functions as an initiating mutation, sequentially followed by mutations in the tumor suppressor genes CDKN2A/INK4A, p53, and SMAD4. (Modified from (Morris et al. 2010).

## 2. The three steps of PDAC development and progression

- Initiation

A single cell can undergo genetic alterations of either intrinsic (DNA repair defects, inherited genetic mutations, reactive oxygen species) or extrinsic (environmental factors, such as radiation or chemical exposure) origin that the cell cannot repair. In most instances, this initiating mutation will lead to cell apoptosis or senescence or be lost owing to immune surveillance. If these mechanisms fail and the initiating mutation causes the cell to escape from senescence and immunosuppression or rather apoptosis, the cell will transform and continuously promotes its growth and survival advantages (Makohon-Moore and Iacobuzio-Donahue



2016). During cell transformation, two types of genes can be altered: (1) proto-oncogenes: gain-of-function mutation. Several oncogenes are known to code for growth factor receptors, transcription factors, and genes that initiate cell proliferation. (2) tumor-suppressor genes: loss of function mutation, meaning that the gene cannot exert its inhibitory effect (Lee and Muller 2010). A well-known tumor suppressor gene is the TP53 gene, which is found in more than 50% of cancers, making it impossible for cells to repair DNA, undergo cell cycle arrest, and activate apoptosis (Muller and Vousden 2013).

The oncogenic *KRAS* mutations are the best known to initiate PDAC development, as described for PanINs. However, studies have shown that the mutation needs to be subsequently combined with the inactivation of the other tumor suppressor genes (*TP53*, *CDK2NA*, and *SMAD4*) to promote and maintain PDAC progression (Figure 7A) (Grant *et al.* 2016).

- Clonal expansion

The cell possessing the initiating mutation that selected it to survive and grow creates a clonal population defined by the presence of the driver gene mutation, which in PDAC will be an oncogenic *KRAS* mutation. As the cell population progressively grows in number and geographical space, the descendants gradually acquire additional driver and passenger mutations (as seen for PanINs) to increase the clonal heterogeneity of the neoplasm. This phase is known as the phase between the precancerous lesions (PanIN3) and the development of full-blown PDAC (Figure 7B) (Makohon-Moore and Iacobuzio-Donahue 2016).

- Progression

The ongoing clonal expansion can promote a population of neoplastic cells to escape through the basement membrane into the surrounding stroma. Degradation of the dense extracellular matrix (ECM) and immune infiltrates provide selective and adaptive forces that shape these cells into subclonal populations with high fitness advantages. The dissemination process from where a cell population breaks free from the primary neoplasm might be an ongoing process during tumor development. However, these cells possessing a high fitness may have the most excellent chance of migrating to and surviving in a new microenvironment, such as in the liver, lung, or peritoneum, all common metastatic sites of PDAC (Figure 7C) (Makohon-Moore and Iacobuzio-Donahue 2016).

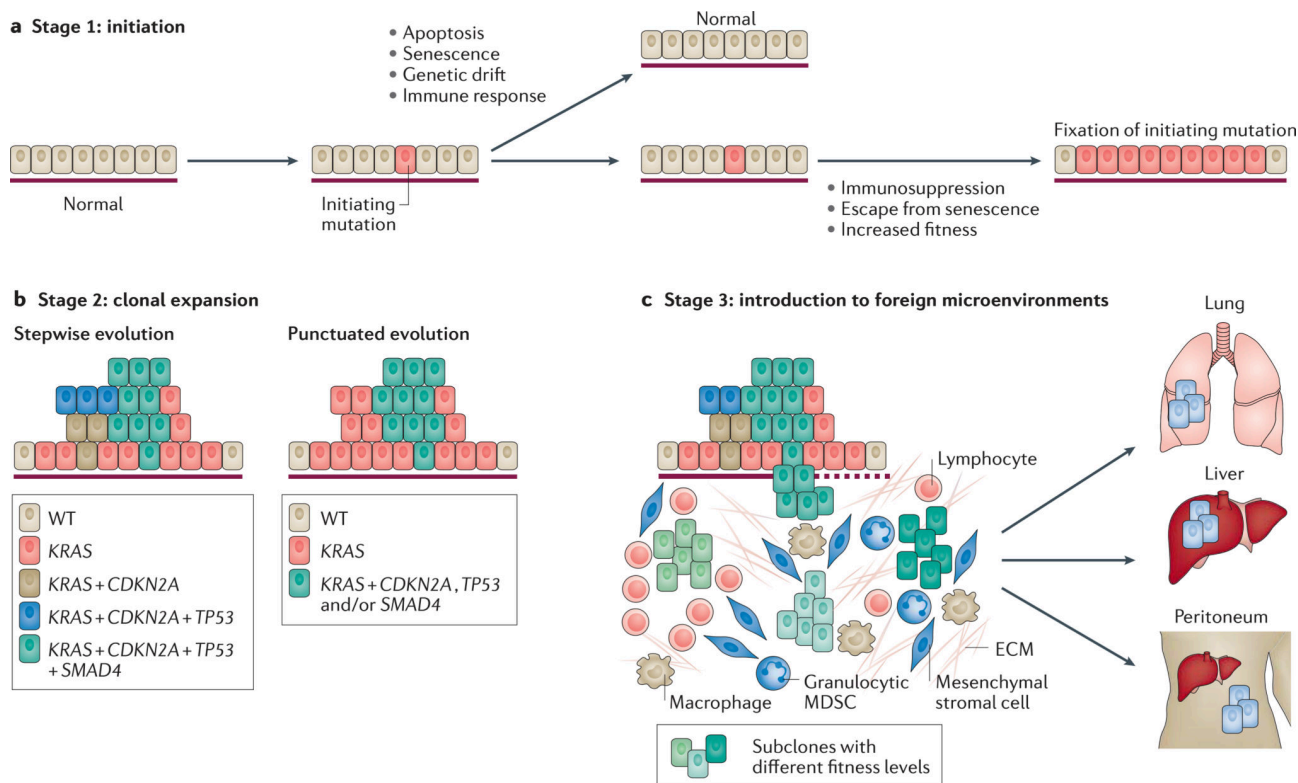


Figure 7. The three steps in PDAC progression. A) Stage 1/Initiation: Cells with initiating driver mutations that escape apoptosis and senescence are fixed in the epithelium. B) Stage 2/Clonal expansion: Cells acquire further mutations as they evolve. C) Stage 3/Progression: Cells can break free from their population, and by degrading the extracellular matrix with the help of immune infiltration, they can migrate and colonize in a new organ (Makohon-Moore and Iacobuzio-Donahue 2016).

### 3. Cell cycle regulation in PDAC

Eukaryotic cells reproduce themselves through a highly regulated series of events, collectively known as the eukaryotic cell cycle. These events include cell growth, replication of genetic material and organelles, and segregation of the genetic material and organelles to separate them into two different daughter cells. Every event in the cell cycle comprises a corresponding phase: the G1, S, G2, and M phases. The G1 phase prepares the cell for DNA synthesis; the chromosomes are replicated during the S phase. The G2 phase prepares for mitosis, which occurs during the M phase, where chromosomes are separated into two individual cells. The G phases have been referred to as Gap-phases, where visually, nothing is happening. However, the G phases are now known as Growth-phases as it was recognized that the cell uses this time to grow. Under favorable conditions, a somatic cell can remain in the G1 phase for half of the cell cycle time. Under stress conditions, this time is even longer, and some cells will remain outside the active division events, entering the so-called G0 phase. The length of the cell cycle is highly variable between cell types. Yet, in rapidly growing cells, such as cancer cells in culture, the cycle length is approximately 24 h (Lewis 2010).

Positive or negative regulating proteins control the cell cycle. Positive regulating proteins are the four cyclins and their belonging cyclin-dependent kinases (CDKs), which must undergo phosphorylation to be

activated. The proteins form complexes responsible for the progress through the cell cycle, and the levels of the CDKs remain relatively stable while it is the concentration of the cyclins that fluctuates (Figure 8B). The levels of the cyclins are induced through transcriptional activation upon a receipt of the appropriate signal to move through the cell cycle, allowing the formation of the suitable cyclin/CDK complex. The different complexes are formed at specific points in the cell cycle, thus regulating individual checkpoints (Lewis 2010).

The progression through the G1 phase of the cell cycle is regulated by the cyclin D/CDK4 and D/CDK6 complexes. Three types of cyclin D exist (D1, 2, and 3). Initially, cyclin D expression levels respond to external stimuli such as mitogens, inducing the transport of CDK4 and CDK6 into the nucleus. Cyclin D forms an active complex with CDK4 or CDK6, which can phosphorylate members of the retinoblastoma (Rb) protein family (Malumbres and Barbacid 2005). Rb proteins exert a negative regulation to repress transcription of cyclins by binding and modulating the activity of transcription factors of the E2F family. Once phosphorylated, Rb loses its affinity for E2F, and E2F-mediated transcription of cyclin E (E1 and 2), cyclin A (A1 and 2), and E2F itself is initiated. When cyclin E binds to CDK2, it provides a positive feedback loop by phosphorylating Rb (Bertoli *et al.* 2013). The activity of the cyclin E/CDK2 complex is required for S phase progression. During the S phase, cyclin A levels rise, and cyclin E dissociates from CDK2, allowing cyclin A to bind, which is required for proper completion and exit from the S phase (Malumbres and Barbacid 2005). During the G2 phase, cyclin A is degraded by ubiquitin-mediated proteolysis, whereas cyclin B (B1 and 2) are actively synthesized. When cyclin A is degraded, CDK1 forms a complex with cyclin B. This complex is thought to regulate several events during both the G2-M transition and through mitosis (Figure 8A) (Malumbres and Barbacid 2005).

- **CDK inhibitors**

The cyclin/CDKs complexes are regulated by inhibitory proteins, the so-called repressor proteins or CDK inhibitors (CKIs). CKIs act as allosteric inhibitors of the CDKs and block their kinase activity (Kahl and Means 2003). The two groups of CKIs are; the (1) INK4 protein family (p15, p16, p18, and p19), which arrest cells in the G1 phase by binding to cyclin D/CDK complexes, and (2) the Cip/Kip (p21 and p27) protein family, which inhibit cyclin/CDK2 complexes, inducing both G1 and G2 cell cycle arrest. Another inhibitor of the G1/S transitions checkpoint is the TP53, which suppresses the transcriptional activation of the CDKI proteins Cip/Kip (p21 and p27). Cip/Kip proteins bind and inhibit the activity of cyclin E/CDK2 and cyclin A/CDK2 complexes, preventing the progression through the G1/S transition. In the M phase, the function of the cyclin B/CDK1 is activated upon the removal of inhibitory phosphates by the Cdc25 phosphatase, allowing cells to enter the M phase (Figure 8A) (Lewis 2010).

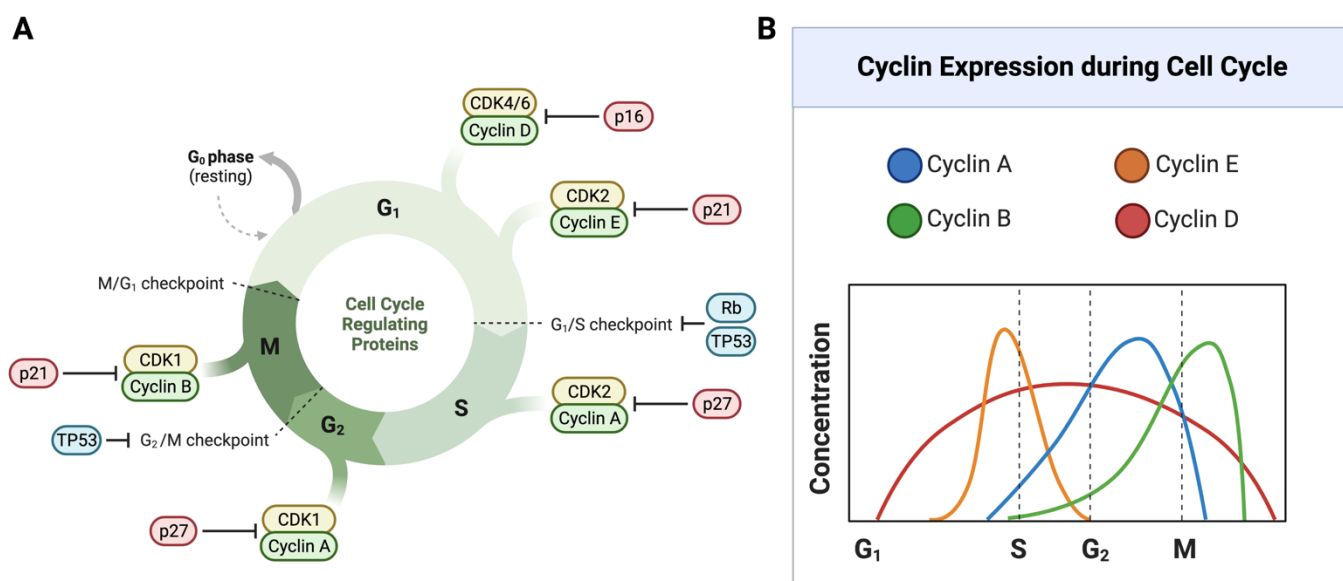


Figure 8. Graphic overview of the cell cycle regulatory proteins. A) Indicate the cyclins, their respective cyclin-dependent kinases, and inhibitors of the cell cycle checkpoints, controlling the progression through the cell cycle. B) Schematic illustration of how the cyclins fluctuate during the cell cycle (Generated with Biorender).

This simplified description represents that many key regulators are involved in cell proliferation and differentiation. Perturbation of these features can result in the formation of a tumor. Five out of the six hallmarks of cancers influence the proliferative capacity, thus the cell cycle. Concerning sustained proliferative signaling, cancer cells display upregulation of growth factor receptors or mutations that activates them, so they no longer require ligand binding for activation, resulting in increased downstream signaling and hence cell proliferation. These involve oncogenes, such as transcription factors, resulting in an upregulation of several cell cycle regulatory proteins that promote cancer progression (Lewis 2010).

Cancer cells often inactivate molecules that constrain the progression through the cell cycle, for instance, tumor suppressors such as Rb, TP53, and INK4 inhibitors, where the latter two are frequently mutated in PDAC. The genes encoding the Cip/Kip family proteins are not commonly mutated in cancers. Still, the expression of the genes is often reduced, leading to induced expression and activity of cyclin E- and cyclin A/CDK2 complexes. Thus, when negative regulators of cell cycle progression become inactive, cells exhibit aberrant cell cycle progression.

#### 4. Consequences of aberrant cell cycle progression in PDAC

PDAC displays a wide range of genetic modifications. The before-mentioned alteration of the oncogenic *KRAS* that results in a constitutive active Kras protein is involved in the cell cycle regulation of PDAC. Ras proteins activate downstream effector pathways, where two of the best studied are the Ras-MAP kinase (MAPK) and Phosphoinositide 3-kinase (PI3K)/ protein kinase B (AKT) pathways, which are both associated with enhanced proliferation, survival, and cell growth. Stimulation of Ras proteins leads to subsequent phosphorylation of

downstream Raf, mitogen-activated protein kinase-activated protein kinases (MEK), and extracellular signal-regulated kinase 1/2 (ERK1/2) (Figure 9). The activated kinases phosphorylate their targets to regulate cellular functions. Among them are transcription factors and other regulators implicated in the expression of cyclin/CDK and CDKIs (Lewis 2010).

The second pathway activated by the Kras protein is the PI3K/AKT signaling pathway. The PI3K protein is overexpressed in 70% of PDAC cases (Edling *et al.* 2010), where the kinase AKT is consistently activated in 40% of all PDAC cell lines (Bondar *et al.* 2002). The constitutively active Ras can phosphorylate PI3K, which binds and phosphorylates phosphatidylinositol (4,5)-biphosphate (PIP<sub>2</sub>) to phosphatidylinositol (3,4,5)-trisphosphate (PIP<sub>3</sub>), activating AKT. One of the downstream targets of AKT is the mammalian target of rapamycin (mTOR) kinase, an essential regulator of several translation proteins involved in proliferation and survival (Figure 9). In addition, Kras can activate an anti-apoptotic signal, thus reducing the cell's ability to undergo cell death.

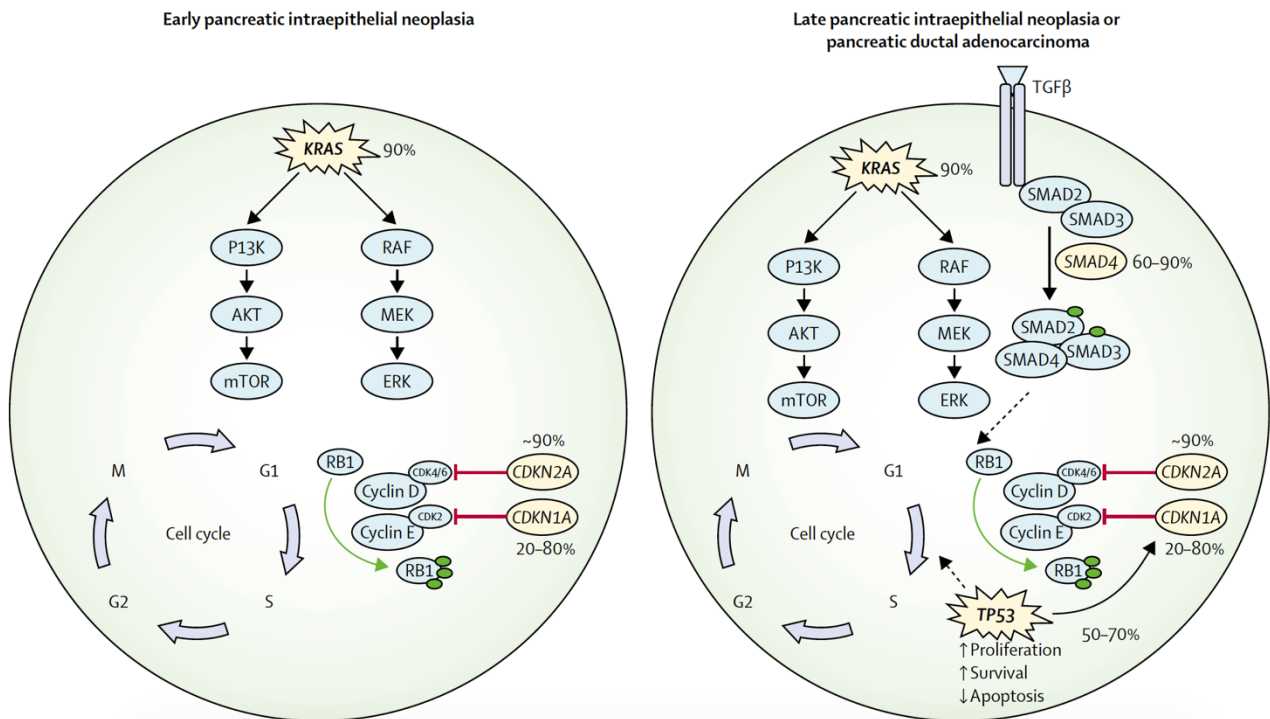


Figure 9. Schematic overview of the common genetic alterations that affect cell cycle progression and proliferation in PDAC (Mizrahi *et al.* 2020).

The *INK4A* (also mentioned as *CDK2A*) protein p16 inhibits CDK complexes and is frequently mutated in PDAC as early as in PanIN2 lesions, resulting in loss of function. p16 binds to cyclin D/CDK complexes and inhibits the Rb proteins at the G1/S checkpoint. Loss of p16 will eliminate its inhibitory function and allow the cells to continuously pass through this checkpoint, underscoring the relevance of the *INK4A* mutation in PDAC development (Lewis 2010).

The tumor suppressor *TP53*, also frequently mutated in PDAC, is a target of p21. TP53 is a key pro-apoptotic regulator of apoptosis. When a cell becomes insensitive to apoptotic signals, it fails to undergo cell death. Thus, the evasion of apoptosis results in cell survival and the continued proliferation of cells. TP53 deficiency impairs cell death in response to apoptotic stimuli, blocks the senescence induced by oncogenes, and enhances the transformation of cells activated by oncogenes as *KRAS*. Emphasizing the relevance of TP53 in cell cycle progression, it has been found that *TP53*-deficient mice are more likely to develop spontaneous carcinogen-induced tumors and accelerate the development and metastatic potential of PDAC (Hingorani *et al.* 2005).

The canonical transforming growth factor  $\beta$  (TGF $\beta$ )/SMAD4 pathway plays a tumor suppressive role in the early stages of cancer by inducing cell cycle arrest and apoptosis. The activation of SMAD4 through TGF $\beta$  serves its functions in the G1/S phase transition, as it promotes the transcription of the inhibitors p15 and p21. An early study reported that TGF $\beta$  failed to induce the expression of p21 in pancreatic cancer cell lines in the absence of SMAD4, resulting in enhanced cell growth (Grau *et al.* 1997).

Taken together, all the mutations appearing during PDAC development lead to uncontrolled cell cycle progression, hence PDAC growth and progression.

## 5. Metastatic properties of PDAC

During cancer progression, cells acquire aggressive properties to invade and spread to surrounding and distant tissues, where they can form secondary tumors, namely metastases (Pantel and Brakenhoff 2004, Quail and Joyce 2013). The steps of tumor metastasis concerning epithelial-derived carcinomas include loss of epithelial polarity, migration, and invasion of the ECM and surrounding tissue, intravasation into the blood and/or lymphatic vessels, survival here, and the extravasation and colonization at different organ sites (Yilmaz and Christofori 2010, Fares *et al.* 2020). The migratory and invasive abilities of cancer cells present essential parameters in the metastatic cascade. Several molecular pathways define distinct types of migration and invasion in a cancer cell-autonomous fashion, including single-cell amoeboid and mesenchymal migration and collective cell migration. For these processes to succeed, cancer cells lose their polarity and function to adhere to the ECM, allowing them to move (Figure 10) (Bravo-Cordero *et al.* 2012). In general, cancer cells acquire a migratory phenotype by undergoing epithelial-mesenchymal transition (EMT), which is a process associated with a profound reorganization of the cytoskeleton and focal adhesions in order to diminish cell-cell attachment and strengthen cell-matrix adhesions (Bravo-Cordero *et al.* 2012, Leggett *et al.* 2021). Here, the EMT process is described with respect to cancer cell migration. However, all epithelial cells can undergo EMT, which occurs during embryonic development, wound healing, and other diseases. The EMT process is initiated by inflammatory stimuli in the tumor microenvironment, such as growth factors, hypoxia, or acidosis, which act through developmental transcription factors (e.g., SNAIL, TWIST, and ZEB) to repress the expression of epithelial markers (e.g., E-cadherin and claudin) and induce the expression of mesenchymal markers (e.g., N-cadherin and vimentin) (Yilmaz and Christofori 2010). A complete EMT occurs when the cancer cells undergo



cytoskeletal reorganization, with a loss of apicobasal polarity and a gain of front-back polarity. In particular, the cells weaken their cell-cell junctions and form actin-rich protrusions at the leading edge (Leggett et al. 2021). The formation of these protrusions is driven by localized actin polymerization and often occurs in response to chemotactic signals. Carcinoma cells in primary tumors will form protrusions called pseudopods and lamellipodia at the migrating front, allowing them to attach and crawl on the ECM fibers (Yamaguchi *et al.* 2005). To migrate through the physical barrier of the dense ECM, cancer cells protrude invadopodia and podosomes. Invadopodia and podosomes are remarkably similar structures (Yamaguchi et al. 2005). However, invadopodia formation is only observed in highly invasive cancer cells, thus implicated in tumor cell metastasis (Chen *et al.* 1994, Yamaguchi et al. 2005, Bravo-Cordero et al. 2012), while podosomes are formed by monocyte-derived cells. Both can produce or exhibit matrix metalloproteases (MMPs) and plasminogen, which are responsible for ECM degradation, the intravasation to the vessels, and the extravasation, from where they locate to other organs (Yamaguchi et al. 2005, Bravo-Cordero et al. 2012). The Rho-family guanosine triphosphate (GTP)-ases are among many regulating proteins linked to motility and protrusion formation as they can activate signaling targets that direct upstream actin cytoskeleton-altering proteins. The most studied Rho-GTPases include RhoA, Rac1, and Cdc42 (Bravo-Cordero et al. 2012).

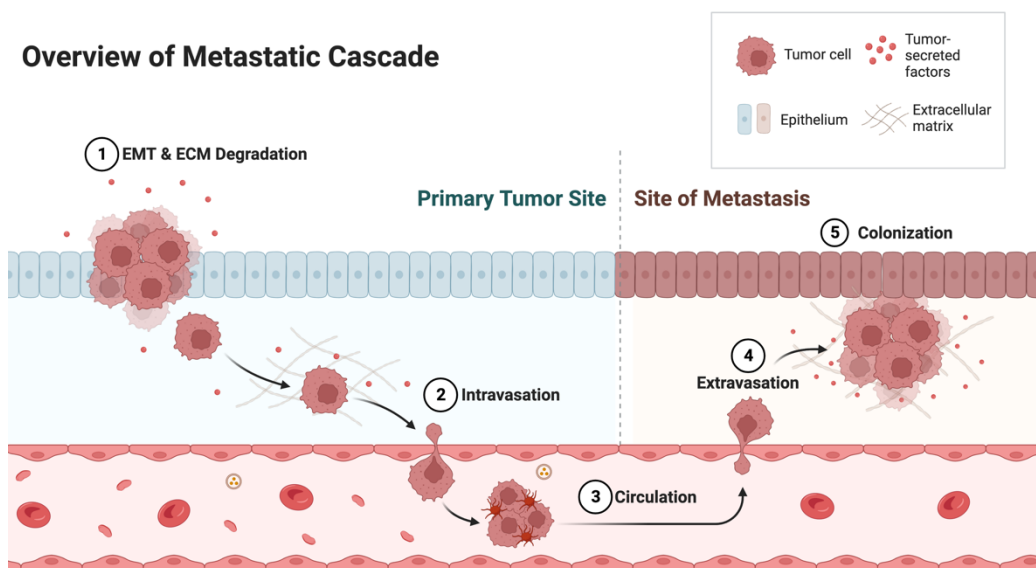


Figure 10. Overview of the metastatic cascade. (1) Cancer cells undergo epithelial-to-mesenchymal transition and degrade the extracellular matrix through tumor cell-secreted factors such as metalloproteases. (2) Next, they intravade the bloodstream, where they (3) are in circulation. Finally, (4) they extravade to a local or distant organ where they can (5) colonize and form metastasis (Generated with Biorender).

## 6. Genetic alterations and signaling causing PDAC metastasis

The metastatic potential of PDAC is one of the main reasons for the poor outcome of patients. Indeed, driver and passenger gene mutations are involved in these metastatic processes. Comparative analysis of primary PDAC tumors with matched metastatic tissue revealed that 90% of tissues had concordant driver gene mutations between the primary and metastatic material (Yachida *et al.* 2010, Yachida *et al.* 2012). The number of mutational driver genes in a tumor correlated to the metastatic burden of the patients and disease-free survival (Yachida *et al.* 2012). Notably, *TP53* and *SMAD4* (Iacobuzio-Donahue *et al.* 2009, Whatcott *et al.* 2015, Grant *et al.* 2016) mutations were associated with a higher metastatic burden and poor prognosis of PDAC patients, compared to *KRAS* and *CDKN2A*, which were related to oligometastases (Yachida *et al.* 2012).

The *KRAS* mutations affect numerous downstream signaling pathways. One of them, as described before, is the PI3K/AKT/mTOR pathway, most often involved in cell proliferation and survival and less in migration and invasion. However, several studies have found that the PI3K pathway is involved in forming PDAC metastasis. In an orthotopic mouse model, the treatment with the PI3K inhibitor LY294002 decreased metastasis and tumor growth and increased tumor cell death (Bondar *et al.* 2002). Tumor intrinsic activation of PI3K signaling, in particular PI3K $\alpha$ , has been associated with an inflammatory metastatic phenotype, which led to enhanced accumulation of protumorigenic-like macrophages in PDAC (Thibault *et al.* 2021). In addition, inhibition of the PI3K $\gamma$  isoform in a mouse model with PDAC resulted in the reprogramming of immunosuppressive tumor-associated macrophages to promote T-cell-mediated anti-tumor immune response, which reduced PDAC metastasis and desmoplasia (Kaneda *et al.* 2016). Targeting PI3K/AKT and mTOR has proven more effective than targeting one alone (Mehra *et al.* 2021). Treatment of PDAC cell lines with Urolithin A, a natural compound inhibiting PI3K/AKT and mTOR simultaneously, resulted in reduced migration, tumor growth, and proliferation *in vitro*, along with improving overall survival in a mouse model with highly aggressive PDAC (Totiger *et al.* 2019). These results suggest that PI3K signaling is also involved in migration, besides being involved in proliferation and survival.

ERK signaling is primarily associated with tumor growth. However, evidence has revealed that ERK signaling is a critical regulator of cell motility (Tanimura and Takeda 2017), also in PDAC. Indeed, one study has shown that the MAPK signaling pathway was involved in PDAC migration upstream from several receptors, including the TGF $\beta$ -activated kinase 1 (Huang *et al.* 2017) and several isoforms of the  $\beta$ -Adrenergic receptor (Huang *et al.* 2012). Yang *et al.* demonstrated that overexpression of *KRAS* decreased the expression of the tumor suppressor Raf kinase inhibitory protein (RKIP) and, through ERK activation, regulated EMT and migration of PANC-1 and SW1990 PDAC cell lines (Yang *et al.* 2018). Furthermore, ERK has been shown to regulate EMT and hence migration through the non-canonical SMAD4 pathway, indicating that the function of ERK can be controlled through other pathways than *KRAS* (Derynck and Zhang 2003, Javadrashid *et al.* 2021).



## Epidemiology of pancreatic cancer

PDAC accounts for more than 90% of pancreatic cancer cases. Other subtypes of pancreatic cancer include neuroendocrine tumors, acinar carcinoma, and pancreatic blastoma (Park *et al.* 2021). According to cancer statistics, it was estimated that in the 27 countries of the European Union (EU), approximately 111500 people (55000 males and 56500 females) will die from PDAC by 2025 (Ferlay *et al.* 2016). In 2020, there were 14461 new cases and 13793 PDAC-related deaths in France (source; GLOBOCAN 2020). In 2020, the global number of incidences was 495773, and the number of deaths was 466003, indicating almost as many deaths as new cases. A systematic analysis showed that the incidences and deaths increased 2.3-fold from 1990 to 2017, reflecting that the number of incidences increased and the overall survival rate remains low. The 5-year survival rate of PDAC varies globally in different countries and regions but does not exceed 10%. PDAC is thought to be the second cause of cancer-related deaths in 2030, only surpassed by lung cancer (Figure 11) (Rahib *et al.* 2014).

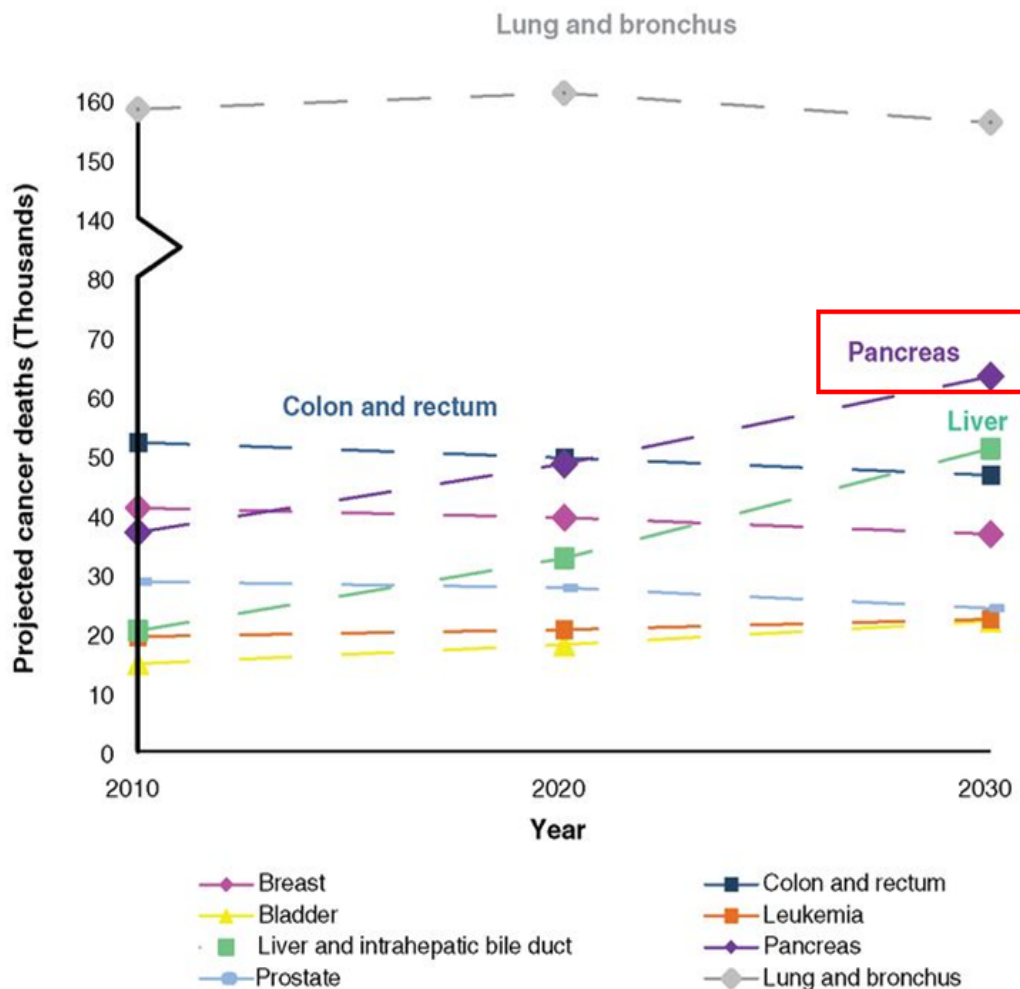


Figure 11. Projected cancer-related deaths in 2030, presenting that PDAC is thought to be the second leading cause of cancer in 2030. (Modified from (Rahib *et al.* 2014)),

## 1. Risk factors and causes of PDAC

The progress from normal epithelium, PanIN1-2 (low/intermediate-grade) to PanIN3/invasive PDAC (high grade) requires a considerable period of development. The process before high-grade PanIN3 and invasive PDAC is the golden phase of prevention of PDAC progression through effective interventions. Thus, a comprehensive understanding of PDAC risk factors is fundamental in preventing PDAC.

The cause of PDAC is relatively unknown. Yet, many non-modifiable and modifiable risk factors are associated with the development of PDAC.

### Non-modifiable risk factors

- Age: the risk of developing PDAC increases with age, and new cases are most frequently diagnosed in patients between 65-74 years of age
- Gender: the worldwide incidence and mortality of PDAC are higher among males than females
- ABO blood group: different studies have found a significantly higher risk of developing PDAC in patients with A or AB blood types than those with type O.
- Genetic susceptibility and family history: hereditary PDACs include inherited cancer syndromes with a known germline mutation associated with an increased risk of PDAC and familial PDAC, with two or more cases within a family (Chang *et al.* 2014). PDAC related to hereditary syndromes or familial PDAC occurrence accounts for about 10% of cases. The most known genetic mutations associated with an increased risk of PDAC development include *CDKN2A* (associated with familial atypical multiple mole melanoma), *BRCA1/2* (associated with hereditary breast cancer ovarian cancer syndrome), and *MLH1/MSH6/MSH2/PMS2* (associated with hereditary non-polyposis colorectal carcinoma syndrome) and *CFTR* (associated with hereditary cystic fibrosis) (McWilliams *et al.* 2010, Ghiorzo 2014, Cazacu *et al.* 2018, Rawla *et al.* 2019)
- Diabetes mellitus and obesity: compared to patients without any form of diabetes (based on hyperglycemia), those who were recently diagnosed with diabetes had an almost 7-fold increased risk of developing PDAC (Huang *et al.* 2020). Furthermore, relevant studies have shown that obese patients have an increased risk of developing PDAC with a potentially worse outcome

### Modifiable risk-factors

- Smoking: Cigarette smoking has the strongest positive association with the risk of developing cancer. A recent European case-control study showed that current smokers have a 72% higher risk of developing PDAC than never-smokers. Furthermore, 16% of all PDAC diagnoses could be avoided through tobacco preventive measures (Molina-Montes *et al.* 2020). Tobacco smoking also increases the risk of developing PDAC in individuals with a family history of cancer (Molina-Montes *et al.* 2018)

- Alcohol: In general, there is no doubt that high alcohol consumption (more than three drinks per day) is associated with the risk of developing PDAC (Rawla et al. 2019)
- Dietary factors: As a whole, consuming diets high in vegetables, fruits, and other plant-based foods can reduce the risk of developing PDAC, while a diet rich in meat and animal products can increase the risk of PDAC development (Tsai and Chang 2019)
- Pancreatitis: It has been reported that acute pancreatitis, an inflammatory disease of the exocrine pancreas, is associated with damage and necrosis of tissue (Habtezion *et al.* 2019). Furthermore, when acute pancreatitis progress to chronic pancreatitis, the risk of developing PDAC increases 9-fold, compared to patients with the first incidence of acute pancreatitis (Rijkers *et al.* 2017)

## 2. TNM Classification

PDAC classification is based on the international cancer classification system developed by the American Joint Committee of Cancer (AJCC) (Gress *et al.* 2017). It is defined as the tumor (T), node (N), metastasis (M) (TNM) staging system (Table 1):

- T; primary tumor is classified by existence, size, or extent of the tumor by a coefficient ranging from 0-4, where 0 assigns no evidence of a primary tumor
- N; regional lymph nodes are classified by their existence and extent, ranging from 0-3 (0-2 in PDAC diagnosis), where 0 assigns no regional lymph node involvement with cancer
- M; distant metastases specifies whether distant metastases are present and is classified by either 0 or 1, where the M1 category may be specified further, according to the location of metastases

Category	Definition
T1	Tumor $\leq 2$ cm in greatest dimension
T1a	Tumor $\leq 0.5$ cm in greatest dimension
T1b	Tumor $\geq 0.5$ cm and $< 1$ in greatest dimension
T1c	Tumor 1-2 cm in greatest dimension
T2	Tumor $> 2$ and $\leq 4$ cm in greatest dimension
T3	Tumor $> 4$ cm in greatest dimension
T4	Tumor involves CA, SMA, and/or CHA regardless of size
N1	Metastasis in 1-3 regional lymph nodes
N2	Metastasis in $\geq 4$ regional lymph nodes
M0	No metastasis in distant organ
M1	Metastasis in distant organ

Table 1 TNM Classification of PDAC. CA: celiac axis, SMA: superior mesenteric artery, CHA: common hepatic artery (Gress *et al.* 2017).

### 3. Grade classification of PDAC

The grade of PDAC is classified by a qualitative assessment of histological material and describes the degree of tumor differentiation. It can reflect to which extent the tumor resembles the normal tissue and may provide important information on the risk of metastasis and prognosis. The grades range from 0-3 (Makohon-Moore and Iacobuzio-Donahue 2016).

- Grade 1: Well differentiated
- Grade 2: Moderately differentiated
- Grade 3: Poorly differentiated

### 4. Molecular classification of PDAC

As described in the 'Pancreatic carcinogenesis' section, the pathophysiology and progression of PDAC are characterized by complex multistep genetic alterations, including *KRAS*, *CDKN2A*, *TP53*, and *SMAD4* (Mizrahi *et al.* 2020). Recent advances in molecular classification pathology have impacted clinical practice. In 2011, Collisson *et al.* described three subtypes based on micro-dissected tumor samples: the classical, exocrine-like, and quasi-mesenchymal (Collisson *et al.* 2011). In 2015, Moffitt *et al.* subtyped PDAC into 'basal-like' or 'classical' type by RNA transcriptional analysis. The classical subtype is characterized by a higher level of differentiation, fibrosis, and inflammation. In contrast, the basal-like subtype is associated with loss of differentiation and a poorer clinical outcome (Moffitt *et al.* 2015). In 2016, another categorization of PDAC subtypes, based on genomic analysis, classified tumors into four distinct subtypes: the squamous, pancreatic progenitor, immunogenic, and aberrantly differentiated endocrine exocrine (ADEX) (Bailey *et al.* 2016). Cross-study analysis suggested that the squamous, basal-like, and quasi-mesenchymal subtypes displayed similar molecular profiles and likely represented the same subset of PDAC tumors. Tumors categorized within these three subtypes were also similar in their clinical outcomes, possessing a poor prognosis and response to chemotherapy compared to the pancreatic progenitor or classical subtypes (Mizrahi *et al.* 2020). The latest study, which has been categorizing PDAC subtypes, was made in 2018 (Puleo *et al.* 2018). Here, they confirmed the presence of the pancreatic progenitor, basal-like, squamous, and quasi-mesenchymal subtypes. Further, they characterized the pancreatic tumor microenvironment and classified three additional subtypes: desmoplastic, immune classical, and stroma-activated (Puleo *et al.* 2018). However, the latter three are not yet evaluated for clinical implications.

### 5. Diagnosis and treatment

PDAC is often diagnosed at a late onset, and about 50% of patients present with distant metastasis at the time of diagnosis (Mizrahi *et al.* 2020). There are no cardinal symptoms for PDAC, and to date, no recommendation exists for screening in asymptomatic adults. Many patients develop few if any, symptoms before the disease are advanced. Unfortunately, the symptoms of PDAC overlap with other benign or malignant conditions (Loveday *et al.* 2019). The patients often have non-specific complaints such as epigastric or back pain, nausea,

bloating, abdominal fullness, or change in stool consistency. All symptoms are more frequently related to alternative benign causes than PDAC, which may delay the time of diagnosis. At the time of diagnosis, more specific symptoms occur, including abdominal and back pain, abnormal liver function herein, jaundice, new-onset diabetes, dyspepsia, vomiting, nausea, and weight loss (Loveday *et al.* 2019, Mizrahi *et al.* 2020). The presentation of symptoms is often correlated with the location of the tumor within the pancreas. As 60-70% of PDACs arise from the pancreatic head or the body, these patients are more likely to develop painless jaundice caused by biliary obstruction (Schmidt-Hansen *et al.* 2016). However, the positive predictive value of jaundice for diagnosing PDAC is only 4-13% (Schmidt-Hansen *et al.* 2016). Patients with tumors in the body of the pancreas tend to invade vascular structures such as the celiac, hepatic, and superior mesenteric vessels and the portal vein, which can all cause back pain. Tumors in the pancreatic tail often grow unrestricted due to fewer anatomical neighbors, thus presenting in an advanced stage at the time of diagnosis (Figure 12) (Walter *et al.* 2016).

The diagnosis of PDAC requires cross-sectional imaging, preferably computed tomography (CT), using a pancreas protocol, which carries a sensitivity of at least 90% (Valls *et al.* 2002, Al-Hawary *et al.* 2014). Magnetic resonance imaging (MRI) can provide a detailed assessment of the biliary tract and has a high sensitivity in detecting liver sections (Vachiranubhap *et al.* 2009). Endoscopic ultrasound is a supplemental tool for identifying local lymph nodes and tumors in nearby vascular structures (DeWitt *et al.* 2004). Positron emission tomography (PET)-CT scans are not routinely used in the diagnosis of PDAC but are considered when patients display a high risk for metastasis, which is detected by the serum marker carbohydrate antigen 19-19. The concentration of this antigen in the blood is proportional to the suspected high disease stage (Mizrahi *et al.* 2020).

At present, surgical resection remains the only treatment that offers curative potential. Local tumors can be defined as resectable, whereas borderline resectable and locally advanced PDAC are usually categorized as inoperable. Tumors arising in the pancreatic head are typically resected with a pancreaticoduodenectomy (Whipple procedure). This includes the resection of the pancreatic head, duodenum, proximal jejunum, a segment of the stomach, the common bile duct, and gall bladder. Tumors in the tail and body are usually resected with distal pancreatectomy combined with splenectomy (Park *et al.* 2021).

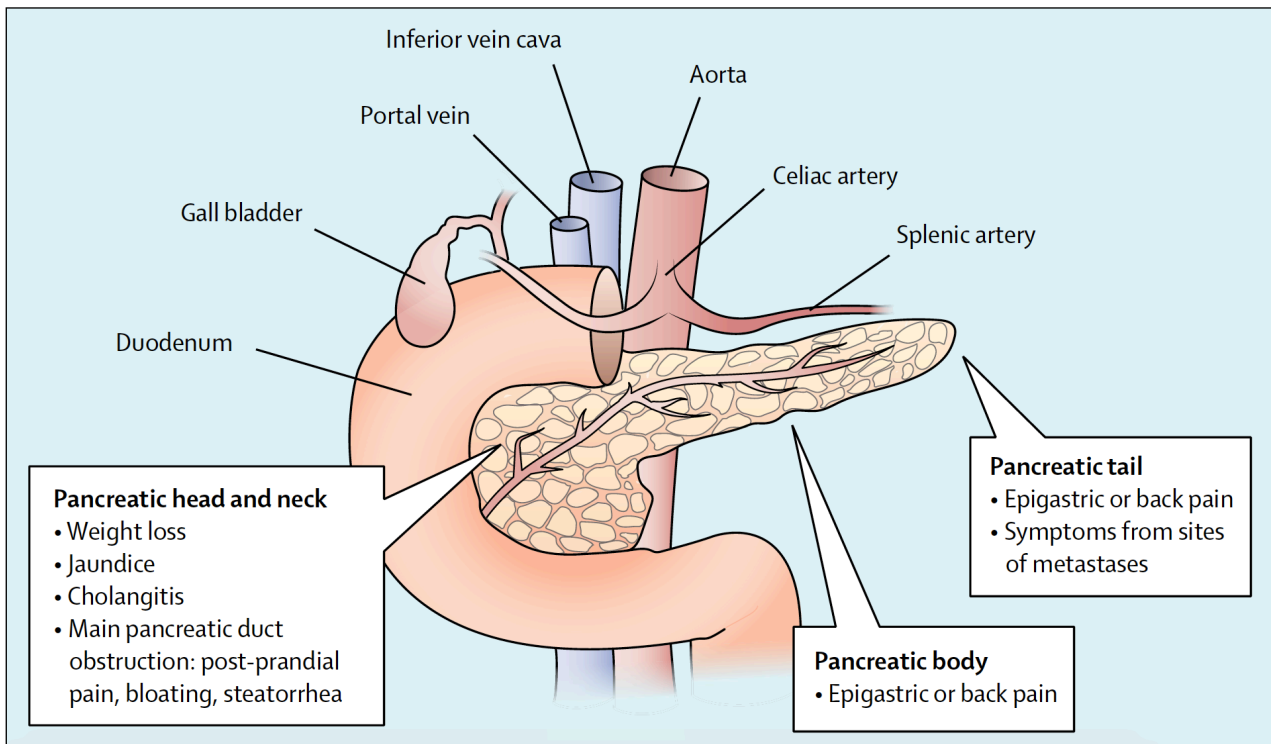


Figure 12. Graphic illustration of the symptoms that patients present developing PDAC; usually, these symptoms are not occurring until the time of diagnosis. (Mizrahi et al. 2020)

After the resection of PDAC, the recommended adjuvant chemotherapy used is either modified FOLFIRINOX (fluorouracil, oxaliplatin, irinotecan, leucovorin) or gemcitabine and capecitabine or gemcitabine alone. FOLFIRINOX is given for individuals with a high functional status according to the Eastern Cooperative Oncology Group (ECOG) classifications, where performance status is ranged from 0-5, where 0 is fully active, and 5 is dead. Gemcitabine and capecitabine or gemcitabine alone are given to individuals with poor functional status, according to the ECOG. The main components of these chemotherapies are DNA-damaging agents directly affecting DNA synthesis and repair (oxaliplatin, irinotecan) and antimetabolites (gemcitabine and fluorouracil) (Park et al. 2021). Most clinical trials represent a modest prolongation of survival for PDAC patients treated with these chemotherapeutic agents. However, a recent clinical trial presenting 493 patients with resected PDAC, a low carbohydrate antigen 19-9 concentration, and a 0 or 1 in ECOG functional status, were randomized to receive six months of adjuvant FOLFIRINOX or gemcitabine (Conroy et al. 2018). Here, patients receiving FOLFIRINOX had an overall survival of 54.4 months compared to 35 months in patients only treated with gemcitabine (Conroy et al. 2018).

Recently, novel therapies for PDAC patients started to evolve, and several clinical trials are ongoing to test immunotherapeutic combinations (Park et al. 2021). For instance, single-agent PD1-blockade (monoclonal antibody) has been approved for mismatch repair deficiency in any tumor by US Food and Drug Administration. Mismatch repair deficiencies occur in around 1% of patients with PDAC and are defined by either germline or somatic alterations or loss in mismatch repair deficiency genes such as *MLH1* and *MSH2*.

Additionally, targeting immunosuppressive metabolite adenosine of the tumor microenvironment, using small molecule targeting agents (e.g., AB680) or antibody therapy (e.g., oleclumab) displays a novel metabolism-directed approach for targeting PDAC, and a Phase I study is ongoing (Bendell *et al.* 2020).

## CHAPTER 2: The pancreatic tumor microenvironment and the involvement of pH in cancer progression

### The pancreatic tumor microenvironment

PDACs are solid tumors and constitute two major components: the pancreatic cancer cells and the tumor stroma. The desmoplastic stroma is heterogeneous and comprises both cellular and acellular components. Among cellular components are the pancreatic PSCs, cancer-associated fibroblasts (CAFs), immune cells, endothelial cells, and cancer stem cells. The acellular characteristics include poor vascularization, low nutrient concentrations, increased inflammatory stress, high interstitial fluid pressure, stiffness of the ECM, hypoxia, and extracellular acidosis that in general are known to occur together (Feig *et al.* 2012, Pedersen *et al.* 2017, Li *et al.* 2021, Truong and Pauklin 2021, Elingaard-Larsen *et al.* 2022). However, several studies demonstrate that  $H^+$  accumulation occurs outside of regions with dioxygen ( $O_2$ ) depletion, for instance, in highly proliferative areas of the tumor-stroma border (Figure 13) (Helmlinger *et al.* 1997, Fukumura *et al.* 2001, Rohani *et al.* 2019). Thus, the PDAC tumor microenvironment forms hostile conditions, and only adapted cells can survive, proliferate and exert other malignant effects (Boedtkjer and Pedersen 2020). The following section will focus on the importance of microenvironmental pH in cancer cell development and progression.

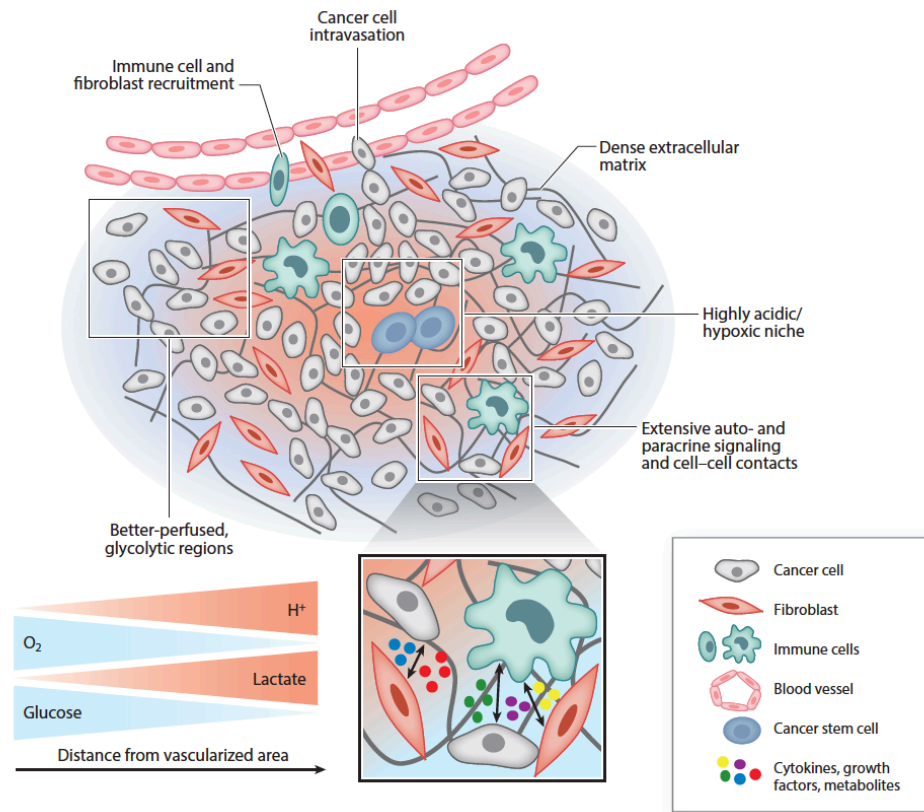


Figure 13. Illustration of the solid tumor microenvironment and the cellular and acellular components. Low  $O_2$  levels (hypoxia) and glucose levels correspond to high production of  $H^+$  and lactate, which occur with the increasing distance from the well-vascularized



areas. (Fibroblast represents cancer-associated fibroblasts and pancreatic stellate cells). Adapted from (Boedtkjer and Pedersen 2020).

## 1. pH regulation in cancer progression

The cytosol of normal cells is usually slightly acidic (~7.0-7.2) due to the production of acid as a byproduct of metabolism and to the inward negative membrane potential that drives the influx of  $H^+$  and efflux of negatively charged ions (Casey *et al.* 2010). The  $pH_i$  is determined by the combined effects of pH buffering capacity and ion carriers (Casey *et al.* 2010) (see pH regulatory transport proteins). Precise and tight regulation of  $pH_i$  is necessary as numerous essential processes are regulated by pH, including cell cycle progression, cell signaling, cell motility, cell volume, and cancer development and progression (Casey *et al.* 2010, Webb *et al.* 2011, Corbet and Feron 2017, Flinck *et al.* 2018, Boedtkjer and Pedersen 2020). Indeed, pH directly influences the activity of all proteins that undergo protonation (Srivastava *et al.* 2007, Schonichen *et al.* 2013, White *et al.* 2017, Swietach 2019), and these proteins appear to operate optimally near pH 7.3. Thus, it should be of interest to maintain a stable cytosolic pH near this level (Swietach 2019).

In general, normal cells exhibit a  $pH_i$  lower than the extracellular pH of ~7.4. However, in cancer cells, the pH gradient is reversed with a  $pH_i$  of 7.1-7.6 (when measured at physiological pH) and a  $pH_o$  in the range of 6.2-6.9 (Vaupel *et al.* 1989, Helmlinger *et al.* 1997, Swietach *et al.* 2014, Rohani *et al.* 2019, Boedtkjer and Pedersen 2020). The decline of  $pH_o$  can promote a decrease of  $pH_i$  to a similar extent as for normal cells. Thus, tumor cells in acidic areas will experience a very low  $pH_o$  and are expected to exhibit a relatively low  $pH_i$  (although higher than non-transformed cells in the same conditions). Whilst other cancer cells in areas with a neutral pH are expected to have a relatively high  $pH_i$  (Boedtkjer and Pedersen 2020). The increase of  $pH_i$  is a hallmark of transformed cells and is permissive for growth factor-induced proliferation, cell cycle progression, and differentiation (Cardone *et al.* 2005, Webb *et al.* 2011, Corbet and Feron 2017). The decreased  $pH_o$  is known to promote ECM degradation leading to invasion and migration (Riemann *et al.* 2014, Riemann *et al.* 2016, Riemann *et al.* 2019, Thews and Riemann 2019). The alkaline  $pH_i$  of cancer cells can seem paradoxical, as high proliferative and glycolytic rates, caused by metabolic reprogramming, generate acid production as described below (Webb *et al.* 2011).

## 2. Metabolic reprogramming

Most normal cells generate the energy necessary for cellular processes primarily through oxidative phosphorylation. On the contrary, many cancer cells reprogram their energy production by limiting their energy metabolism mainly to glycolysis, even in the presence of oxygen, a state termed 'aerobic glycolysis' or 'the Warburg Effect' (Warburg 1956) (Figure 14). Poor vascularization in desmoplastic solid tumors, such as PDAC, leads to inadequate  $O_2$  delivery and, subsequently, hypoxia, which limits oxidative phosphorylation (Hanahan and Weinberg 2011). The hypoxic response in cancer cells works pleiotropically by upregulating glucose transporters and enzymes of the glycolytic pathways, leading to increased glycolysis (Semenza 2010,

Wicks and Semenza 2022). In addition, hypoxia increases levels of the transcription factors hypoxia-inducible factors (HIF1 $\alpha$  and HIF2 $\alpha$ ), which, in turn, upregulates glycolysis (Kroemer and Pouyssegur 2008, Semenza 2010). The increased glucose uptake and utilization in tumors are used in the diagnostic imaging technique PET, which uses the glucose analog tracer <sup>18</sup>fluorodeoxyglucose (FdG) to visualize primary and metastatic lesions by their glucose uptake, which depends on the rate of glycolysis (Gatenby and Gillies 2004).

Even though aerobic glycolysis is far less efficient than oxidative phosphorylation given the relatively poor adenosine triphosphate (ATP) generation by glycolysis, glycolysis supplies highly proliferative cancer cells with biosynthetic precursors of nucleotides, proteins, and lipids which are needed to sustain tumor growth. In fact, cancer cells can consume at least ten times more glucose than normal cells (Icard and Lincet 2012, Andersen *et al.* 2014). As mentioned above, several oncogenes and their related pathways favor the switch to aerobic glycolysis, including *PI3K*, *mTOR*, *Myc*, *TP53*, and the regulation of *HIF*. In addition, oncogenes can promote glycolysis. This is, for instance, true for *KRAS*, which upregulates glucose transporters and glycolytic enzymes (Chen *et al.* 2016, Andersen *et al.* 2021). Concerning PDAC, a metabolic and transcriptional profiling study of 38 pancreatic cancer cell lines revealed that they belonged to a glycolytic subtype, defined by displaying high levels of gene expression and metabolites from the glycolytic, serine and pentose phosphate pathways (Daemen *et al.* 2015). Another study showed an upregulation of glycolytic pathway genes in clinical resectable and metastatic PDAC samples. The samples classified as a glycolytic subtype showed amplification of the *KRAS* and *Myc* oncogenes, which further correlated with the basal, squamous, and quasi-mesenchymal molecular subtypes, associated with poor clinical outcomes (Karasinska *et al.* 2020, Andersen *et al.* 2021).

The increased proliferation combined with the glycolytic shift leads to large metabolic acid production. The glucose metabolism through aerobic glycolysis will result in only 2 ATP per glucose molecule and a high amount of lactate and H<sup>+</sup>. In contrast, the metabolism of glucose to ATP from oxidative phosphorylation generates up to 36 ATPs per molecule of glucose and acid in the form of CO<sub>2</sub> (Andersen *et al.* 2014) (Figure 14).

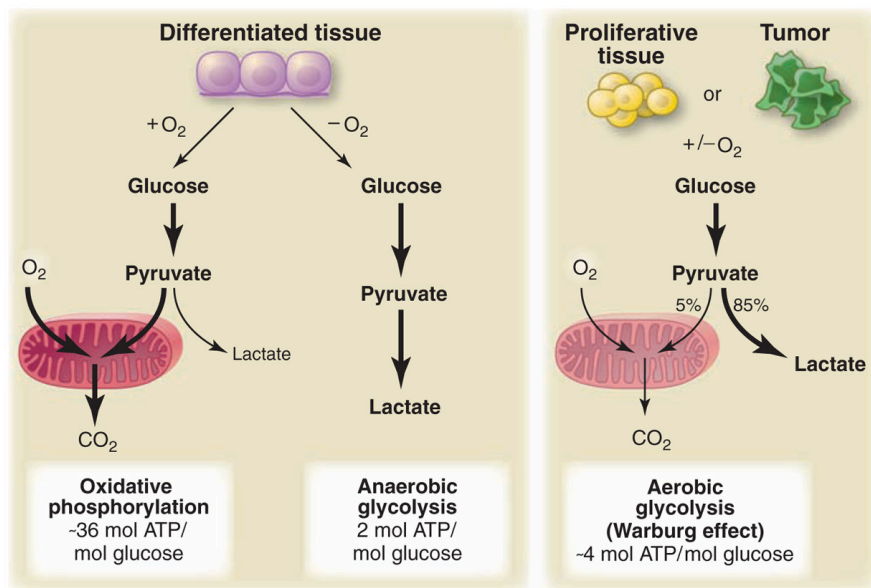


Figure 14. A simplified overview of the differences between the use and effects of oxidative phosphorylation, anaerobic and aerobic glycolysis (Warburg effect). In the presence of oxygen (oxidative phosphorylation) in normal differentiated/non-proliferating tissues, glucose is first metabolized to pyruvate via glycolysis, then completely oxidized in the mitochondria to  $\text{CO}_2$ , producing 36 ATP/glucose. When oxygen is absent (anaerobic glycolysis), cells can redirect the pyruvate generated by glycolysis by generating lactate, producing only 2 ATP/glucose. During the Warburg effect (aerobic glycolysis), proliferating/tumor cells convert glucose to lactate in the presence or absence of oxygen, even though mitochondrial function and oxidative phosphorylation continue to function. To overcome the low amount of ATP generated by cancer cells, utilize  $\sim 10\%$  of glucose in biosynthetic pathways such as glutamine or fatty acid metabolism. Adapted from (Vander Heiden *et al.* 2009)

Thus, the metabolic acid production can be substantial in both hypoxic and oxidative parts of the tumor (Helmlinger *et al.* 1997, Rohani *et al.* 2019). The lack of blood supply in many tumor areas limits acid venting. It causes an acid accumulation inside the cells, decreasing cell proliferation and cell death (L'Allemain *et al.* 1984, Yamagata *et al.* 1998, Gatenby and Gillies 2004). Hence, cancer cells need a robust pH regulatory system to overcome intracellular acidosis and to maintain an alkaline  $\text{pH}_i$  permissive growth. To overcome this acidic burden, the pH-regulatory system facilitates  $\text{CO}_2$ ,  $\text{HCO}_3^-$  and  $\text{H}^+$  diffusion and transport across the plasma membrane (Damaghi *et al.* 2013, Swietach 2019).

### 3. pH regulatory transport proteins

The regulatory pH system of cancer cells is highly regulated by plasma membrane-localized acid-base transporters and the pH regulatory enzymes CAs (Figure 15).

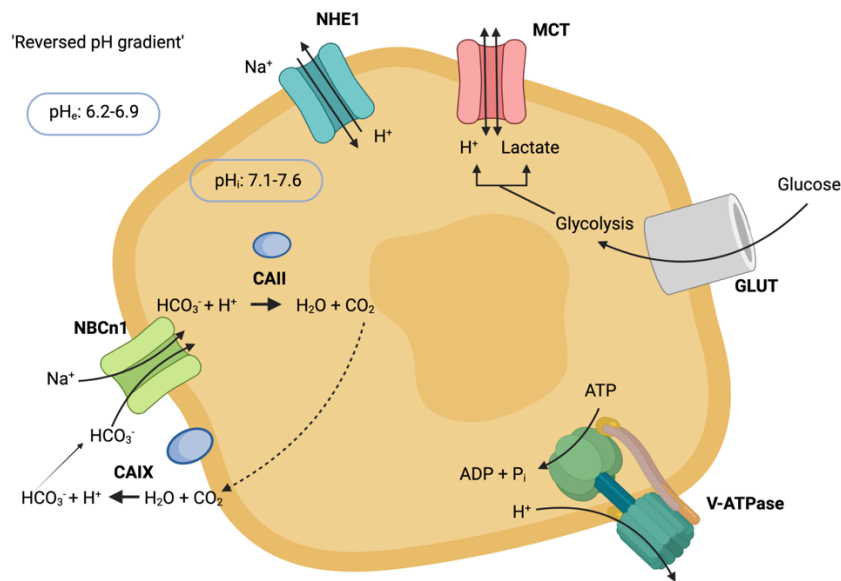


Figure 15. Simplified schematic representation of the main transporters involved in pH regulation in cancer cells contributes to maintaining the 'reversed pH gradient'. Due to the glycolytic shift in cancer cells, a large amount of acids in the form of  $H^+$ , lactate, and  $CO_2$  are produced, and tumor cells rely on increased acid extrusion to avoid intracellular acidosis. Glucose transporters (GLUT) import glucose to fuel glycolysis. The  $Na^+/H^+$  exchanger 1 (NHE1) extrude  $H^+$  directly, by the uptake of  $Na^+$ , while the  $Na^+$ ,  $HCO_3^-$ -cotransporter 1 (NBCn1) imports  $HCO_3^-$  to neutralize  $H^+$ . This reaction is facilitated by intracellular carbonic anhydrase II (CAII) forms  $H_2O$  and  $CO_2$ , which can passively exit across the plasma membrane. Extracellular membrane-bound CAIX rehydrate  $H_2O$  and  $CO_2$  to  $HCO_3^-$ , which can be taken up by NBCn1. Monocarboxylate transporters (MCTs) as MCT1 and -4 co-export lactate and  $H^+$  where the Vacuolar  $H^+$ -ATPase V-ATPase pumps out  $H^+$  at the expense of ATP. Overall, these transporters establish a slightly alkaline pH while creating an acidic extracellular tumor microenvironment (Figure generated with Biorender).

- NHEs

The mammalian  $Na^+/H^+$  exchangers (NHEs) mediate the electroneutral exchange of extracellular  $Na^+$  with intracellular  $H^+$  in a 1:1 stoichiometry (Aronson 1985, Montrose and Murer 1988). It is a secondary active transporter driven by the inward-directed chemical  $Na^+$  gradient maintained by the  $Na^+/K^+$  ATPase (Skou and Esmann 1992, Keener and Sneyd 2009, Counillon *et al.* 2016, Pedersen and Counillon 2019). The NHE1 is a member of the Solute Carrier 9A (SLC9A) gene family and is expressed in essential all types of tissue and localizes to the basolateral membrane of epithelial cells. Other NHE isoforms are more tissue-specific, and their subcellular location differs (Coupaye-Gerard *et al.* 1996, Peti-Peterdi *et al.* 2000, Park *et al.* 2001, Orłowski and Grinstein 2011, Pedersen and Counillon 2019).

NHE1 remains the most widely studied among NHEs, both in the context of pH regulation and disease. NHE1 is active when  $pH_i$  acidifies and is nearly quiescent at physiological pH (unless activated by other stimuli such as mitogens and growth factors), keeping the pH in a narrow range (Stock and Pedersen 2017, Pedersen and Counillon 2019). This homeostatic pH regulation connects NHE1 to several physiological and pathophysiological functions. NHE1 has been linked to cancer progression, and upregulation of its expression

and activity is often correlated with tumor malignancy (Stock and Pedersen 2017) through the roles of NHE1 in cell cycle progression (Flinck *et al.* 2018), proliferation (Amith *et al.* 2015, Andersen *et al.* 2016), invasion (Cardone *et al.* 2015), migration (Stuwe *et al.* 2007, Martin *et al.* 2011), and apoptosis (Rich *et al.* 2000).

- NBCs

The electroneutral  $\text{Na}^+/\text{HCO}_3^-$ -cotransporter NBCn1, moving 1  $\text{Na}^+$  and 1  $\text{HCO}_3^-$  from the extracellular space to the cytosol, is often co-expressed with NHE1 (Boedtkjer *et al.* 2012). NBCn1 has a broad expression profile and belongs to the Solute Carrier 4A gene family, which consists of nine other members. However, NBCn1 is the isoform most widely studied concerning  $\text{pH}_i$  regulation. NBCn1 extrudes acid secondarily by the uptake of  $\text{HCO}_3^-$  which neutralizes cytosolic  $\text{H}^+$  and converts it into  $\text{H}_2\text{O}$  and  $\text{CO}_2$  with help from intracellular carbonic anhydrases (CA) (Boedtkjer *et al.* 2012). When  $\text{CO}_2$  diffuses across the plasma membrane, it is then converted back to  $\text{HCO}_3^-$  by membrane-bound extracellular facing CA and can be reutilized by NBCn1. NBCn1 is less studied than NHE1 in relation to cancer. However, NBCn1 protein is two- to threefold upregulated during breast cancer carcinogenesis and is the dominant mechanism of net acid extrusion in both murine and human breast cancer tissue (Boedtkjer *et al.* 2013, Gorbatenko *et al.* 2014, Lee *et al.* 2015, Andersen *et al.* 2018). In addition, extracellular acidification ( $\text{pH} \leq 6.8$ ) upregulates the expression of NBCn1 in cultured rat hippocampal neurons, suggesting that NBCn1 not only regulates but also is a sensor of the tumor microenvironment (Cooper *et al.* 2009).

- MCTs

The consequence of high glycolytic activity is an increased production of lactate and  $\text{H}^+$ . The monocarboxylate transporters (MCT) of the SLC16 family, where two isoforms (MCT1 and MCT4) contribute to acid extrusion by mediating electroneutral transport of 1 monocarboxylate and 1  $\text{H}^+$  (Halestrap and Wilson 2012). Both MCT1 and MCT4 mediate the co-transport of  $\text{H}^+$  and monocarboxylates, such as lactate, pyruvate, and ketone bodies, across the plasma membrane, thus eliminating the acid load associated with increased glycolysis (Halestrap and Wilson 2012). The lactate concentration in the cytosol of tumor cells can reach levels as high as 40 mM (Walenta and Mueller-Klieser 2004). It has been proposed that both transporters are essential for tumor growth by mediating a continuous lactic efflux, thereby securing a sustained high glycolytic flow (Halestrap and Wilson 2012). MCT1 and MCT4 are upregulated in several cancers and have been linked to poor prognosis (Felmlee *et al.* 2020). Interestingly, the elevated lactate levels in the extracellular space can be a nutrient source for stroma cells or other cancer cells as long as they have access to oxygen. MCT1 in neighboring cells can take up and utilize lactate for energy production through oxidative metabolism (Perez-Escuredo *et al.* 2016).

- Vacuolar-type ATPase

The vacuolar-type (V)-ATPase, a member of the VATP6 family, is mainly located in lysosomes or late endosomes, where it ensures the  $H^+$  flux into the lumen of these organelles to maintain an acidic pH, which is essential for their function (Nishi and Forgac 2002). However, the V-ATPase pump has been found in the plasma membrane of different cell types, including tumor cells (Martinez-Zaguilan *et al.* 1993). Here, it acidifies the extracellular space by extruding protons. It has been shown that the plasma membrane localization of this pump contributes to cell migration and invasion by facilitating a local acidic extracellular microenvironment (Sennoune *et al.* 2004, Sennoune *et al.* 2004, Rojas *et al.* 2006, McGuire *et al.* 2016).

#### 4. Changes in pH shape PDAC development

As described above, metabolic reprogramming and poor vascularization lead to the acidic microenvironment, a hallmark of cancer carcinogenesis. Pedersen *et al.* hypothesized that the acid-base challenges that the epithelial cells in the normal pancreas are exposed to can facilitate cancer development (Pedersen *et al.* 2017) (Figure 16). The so-called acidic tide occurring in the interstitium when  $HCO_3^-$  is secreted to neutralize the acidic pancreatic juice extruded by the acini (see section Pancreatic fluid secretion and pH regulation) could cause an acid preconditioning, which could increase the survival potential of cancer cells in the acidic tumor microenvironment (Pedersen, 2017). The alternating digestion phases that stimulate pancreatic  $HCO_3^-$  secretion affect the interstitial  $pH_o$  in a cyclic manner. At the onset of PDAC, either (1) decreased extracellular acidosis develops due to reduced transepithelial  $HCO_3^-$  secretion along with reduced epithelial integrity; or (2) an inflammatory state is induced, such as chronic pancreatitis, where the epithelial environment is exposed to moderately increased and sustained acidity. Thus, the epithelial cells are constantly exposed to unstable pH conditions, which can contribute to the dormancy of premalignant stages of PDAC and favor proliferation, invasion, migration, metastasis, and resistance to chemotherapy (Pedersen *et al.* 2017).



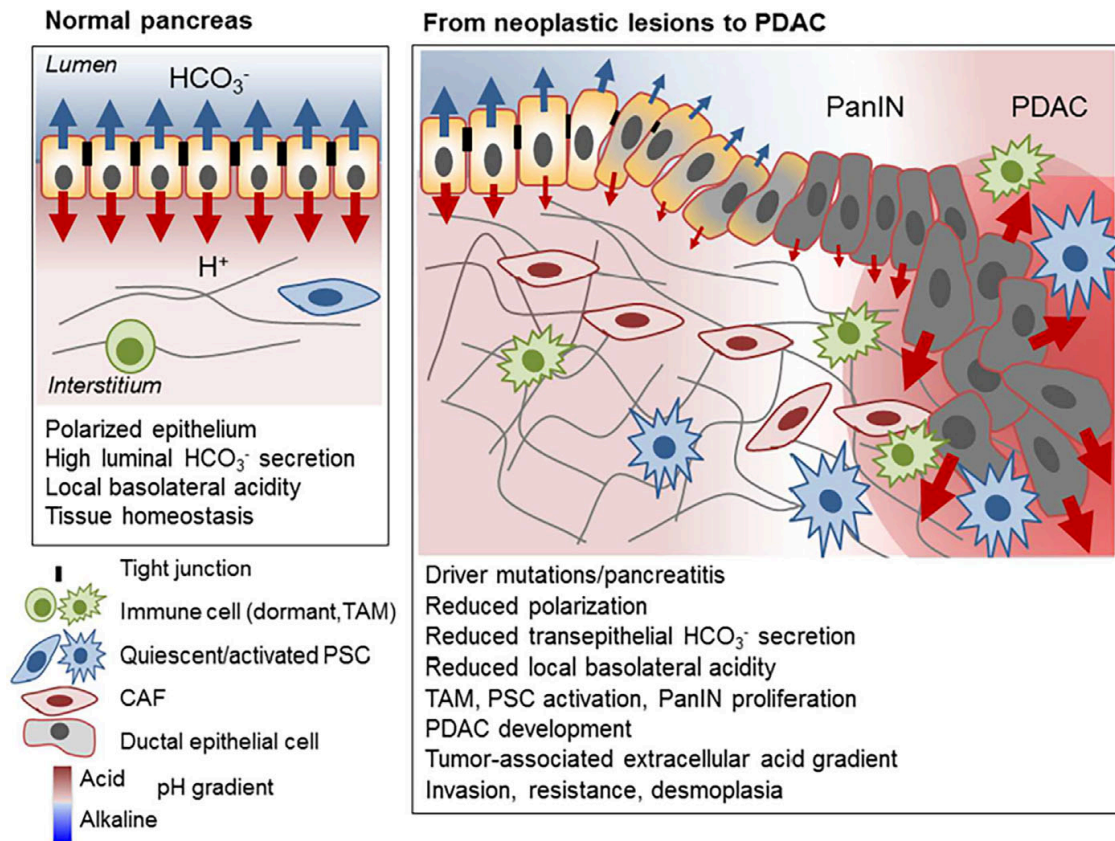


Figure 16. Schematic representation of the hypothesis proposed by Pedersen et al., 2017. The left panel represents normal pancreatic duct cells and the unique acid (red) – base (blue) transport occurring across membranes in the exocrine pancreas. The right panel represents the acidic microenvironment contributing to PDAC development and progression by adapting and preconditioning epithelial cells to become intraepithelial neoplasias (PanIN) and PDAC (Pedersen et al. 2017).

## 5. Cellular adaptation to extracellular acidosis in carcinogenesis

It is now well established that the  $\text{pH}_o$  of cancer cells is acidic and that this property is associated with aggressive behaviors of solid tumors. Early studies by Thomlinson and Gray reported that human tumors surrounded blood vessels as cords. As the tumor grew, the blood supply decreased, and the central region of the tumor became hypoxic, even though the diffusion distance of glucose remained (Thomlinson and Gray 1955). As already described above, hypoxia upregulates glycolysis, thus acid extrusion is required to maintain the  $\text{pH}_i$ , leading to the acidic  $\text{pH}_o$ , which in turn can provide an evolutionary selection pressure and initiate adaptive responses in cancer cells, enhancing malignant and invasive phenotypes (Damaghi et al. 2015, Pillai et al. 2019, Elingaard-Larsen et al. 2022). There is evidence that the acid-adapted phenotype may be particularly aggressive when the cancer cells encounter a less acidic environment (Robey et al. 2009, Riemann et al. 2014, Riemann et al. 2016, Boedtkjer and Pedersen 2020, de Bem Prunes et al. 2022). As described below, the mechanisms of adaptation to the acidic microenvironment are pleiotropic.

The adaptation and selection to the acidic environment will initially slow the growth of cancer cells. Early studies have shown that strongly acidic  $\text{pH}_o$  can cause double-stranded DNA breaks (Morita et al. 1992),

and recovery from DNA damage from other stressors is inhibited at acidic  $\text{pH}_o$ , leading to the accumulation of chromosomal aberrations (Jayanth *et al.* 1994). Furthermore, acidosis favors epigenetic changes and oncogenic mutations (Rohani *et al.* 2019, Boedtkjer and Pedersen 2020). Thus, acidic stress may cause genetic instability and a risk of malignant transition. Acidic stress occurs in several precancerous inflammatory states, such as chronic pancreatitis, a known risk factor for PDAC development (Kirkegard *et al.* 2017). The dual roles of the acidic environment, inhibiting growth and increasing oncogenic mutations could explain why the PanINs can be dormant for years and subsequently turn into full-blown PDAC, suggesting that the preneoplastic cells adapt to the microenvironment and hence turn into a malignant state (Pedersen *et al.* 2017, Boedtkjer and Pedersen 2020).

The genetic instability and accumulation of oncogenes caused by acid adaptation can lead to metabolic changes. Acidosis reduces the glycolytic rate, for instance, by inhibiting the rate-limiting enzyme phosphofructokinase (Trivedi and Danforth 1966, Blaszcak and Swietach 2021), which can force cancer cells to rely more on oxidative phosphorylation and a shift towards glutamine and fatty acid metabolism. This shift can supply the cancer cells with the energy necessary for the high proliferative rate (Lamonte *et al.* 2013, Corbet *et al.* 2016, Wu *et al.* 2016, Boedtkjer and Pedersen 2020, Dierge *et al.* 2021, Michl *et al.* 2022).

The acidic microenvironment also facilitates cancer cells' invasion and migration properties. To initiate the invasive process and spread through blood and lymphatic vessels and subsequently infiltrate the surrounding tissue, cancer cells have to penetrate the ECM (Riemann *et al.* 2019). This process is initiated by the aid of the acidic  $\text{pH}_o$ , which activates (MMPs and cathepsins secreted from the cancer cells to the extracellular space to catalyze the degradation of the ECM (Martin *et al.* 2011, Kato *et al.* 2013, Stock and Pedersen 2017, Sutoo *et al.* 2020). Additionally, the translocation of lysosomes to the plasma membrane where they fuse and release their acidic content is proposed to contribute to ECM remodeling and local invasion. Here, it has been found that the lysosomal-associated membrane protein 2 (LAMP2) protects the plasma membrane from acid hydrolysis (Damaghi *et al.* 2015). Interestingly, local acidification is of more importance than total acidification, as it is the leading edge of the migrating cells that contribute to the ECM degradation process. Indeed, it has been shown that NHE1 alone or in a complex with NBCn1 and CAIX are located in invadopodia (Busco *et al.* 2010, Boedtkjer *et al.* 2016). This acid-exporting machinery can establish an acidic  $\text{pH}_o$  at the leading edge of the cell, which facilitates directional migration and, thereby, degradation of the ECM (Busco *et al.* 2010, Boedtkjer *et al.* 2016).

Cells can undergo EMT that initiate invading and migratory processes. Acidosis stimulates epithelial cells to lose their apicobasal polarity and cell-cell adhesion, whereas they become mesenchymal-like and gain invasive and migratory properties (Riemann *et al.* 2019). However, the underlying mechanisms are not fully understood. Indeed, it has been found that acidic  $\text{pH}_o$  reduces the expression of E-cadherin and upregulates vimentin, N-cadherin, twist, and other EMT markers in breast cancer, lung cancer, prostate cancer, PDAC, and melanoma cells (Suzuki *et al.* 2014, Peppicelli *et al.* 2015, Riemann *et al.* 2019, Sadeghi *et al.* 2020, Shin *et*



*al.* 2020, Wu *et al.* 2022). Recently, several markers of EMT and invasion have been found dysregulated in PDAC cell lines, and their expression depended on the time of acidosis duration. The expression of E-cadherin was decreased after three weeks and completely abolished after 4-5 and 10-12 months of acid adaptation. The opposite effect was found on the expression of N-cadherin, SNAIL, fibronectin1, vimentin, and laminin (Wu *et al.* 2022).

Not surprisingly, the low  $pH_o$  favors invasion in various cell types (Martinez-Zaguilan *et al.* 1996, Moellering *et al.* 2008, Estrella *et al.* 2013, Riemann *et al.* 2014). The effect can be ascribed to long-term acidosis as exposure to low  $pH_o$  for as short as 24 h selects for invasive phenotypes in colorectal cancer and melanoma cells (Martinez-Zaguilan *et al.* 1996, Zhou *et al.* 2017). The hypothesis that acidic pH promotes invasion by  $H^+$  diffusing from the proximal tumor and remodeling the adjacent tissue has been tested *in vivo* (Rofstad *et al.* 2006, Estrella *et al.* 2013). Intravital microscopy of HCT116 tumors found that areas with low acidic  $pH_o$  of peritumoral tissues corresponded to regions with the highest tumor invasion. In addition, tumors did not invade regions with normal  $pH_o$ . Immunohistochemical (IHC) analysis revealed that the tumor edge showed an increased expression of NHE1 and the glucose transporter (GLUT1), both of which were associated with peritumoral acidosis (Estrella *et al.* 2013).

The invading process is accompanied by migration and may result in near or distant metastases. Numerous studies have shown that acidic pH increases cell migration. *In vitro*, this was demonstrated by scratch and transwell assays or by time-lapse microscopy (Chen *et al.* 2008, Parks and Pouyssegur 2015, Peppicelli *et al.* 2015, Peppicelli *et al.* 2017, Wu *et al.* 2017). Enhanced migration was found in cells treated upon acute acidification, and long-term acidosis, including in PDAC cell lines (Riemann *et al.* 2016, Wu *et al.* 2022), suggesting enhanced migration is a long-lasting feature of tumor cells. Early and recent studies have shown that oxygen deficiency and hypoxia lead to a higher rate of distant metastases (Ishikawa *et al.* 2004, Chang *et al.* 2011, Schito and Rey 2017). As described in the ‘Metabolic reprogramming’ section, hypoxia intensifies glycolytic metabolism, enhancing lactic acid and  $H^+$  production. Lactate concentration can be measured using bioluminescence assays of cervical cancer. In this way, it was shown that primary tumors with a high level of intratumoral lactate exhibit a significantly higher rate of metastases (Walenta *et al.* 2000, Ellingsen *et al.* 2013, Walenta *et al.* 2016). Regarding acidification, different outcomes have been found. In two studies on melanoma and prostate cancer cells, respectively, it was found that acid-primed tumor cells injected into a xenograft mouse model immediately after incubation increased the metastatic rate (Rofstad *et al.* 2006, Riemann *et al.* 2014). In contrast, another study of sarcoma and melanoma cell mouse models found that cells incubated at pH 6.5 did not increase the number of lung metastases, except if they were re-cultured in physiological pH conditions for at least 24 h (Schlappack *et al.* 1991). Furthermore, it has been found that primary tumors with low metastatic potential exhibit a homogeneous pH distribution, whereas primary tumors with a high metastatic potential exhibit low pH values in the tumor periphery (Wang *et al.* 2015).

Even though the features of the increased glycolytic activity and upregulation of  $H^+$  pumps lead to enhanced proliferation of cancer cells, it is well known that extracellular acidosis decreases  $pH_i$ , which inhibits cell cycle progression and hence proliferation (Flinck et al. 2018, Boedtkjer and Pedersen 2020). Thus, tight regulation and a transient increase in  $pH_i$  are essential for progression through cell cycle-specific checkpoints (Putney and Barber 2003, Flinck M *et al.* 2018). However, long-term acidosis will eventually select and adapt cancer cells to grow in an acidic environment (Pillai et al. 2019). For instance, PDAC cells lines grown in acidic pH (6.7) for 2-3 weeks accumulate in the G1 phase, whereas the number of cells in the S-phase is reduced, along with a reduced expression of CDK4, CDK6, Cyclin D1, Cyclin E, and an increase in  $p21^{Kip1}$ . When the same cells are cultured for a period of 4-5 months or 10-12 months, the expression of cell cycle regulating proteins and the number of cells in different cell cycle phases return to similar as for cells grown in pH 7.4 (Wu et al. 2022), indicating that cells can adapt their growth to the hostile acidic microenvironment. Interestingly, dual roles can be attributed to the acidic  $pH_o$  (Boedtkjer and Pedersen 2020). An acidic  $pH_o$  can acidify  $pH_i$ , thus limiting proliferation, but acidic  $pH_o$  can also act directly on extracellular  $H^+$  sensors such as GPCRs or acid-sensing ion channels (ASIC), which facilitate increased intracellular  $Ca^{2+}$  levels that may conversely promote proliferation and growth (Zhu *et al.* 2017).

Taken together, these reports indicate that the reciprocal interactions between the tumor microenvironment and tumor cells affect cancer development and their ability to grow and metastasize to other organs (Figure 17).

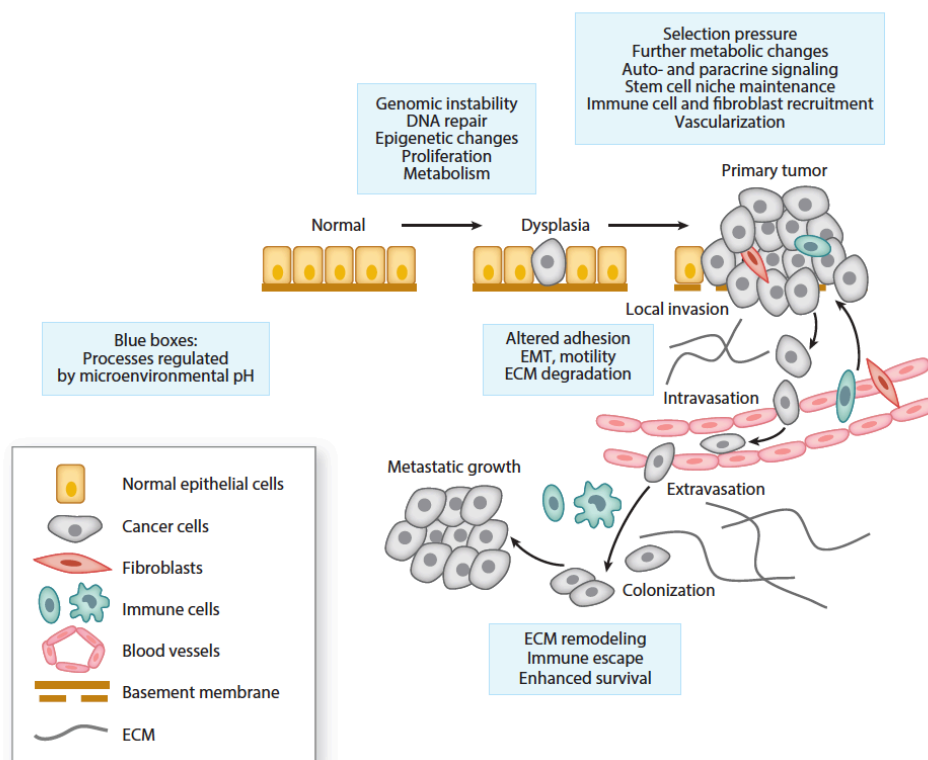


Figure 17. Overview of processes occurring carcinogenesis caused by the acidic microenvironment. Acidosis affects normal cells to acquire genomic instability, which leads to dysplasia. Long-time acidosis creates a selection pressure resulting in metabolic changes

*and other characteristics contributing to a malignant phenotype. Cancer cells can perform local invasion epithelial to mesenchymal transition (EMT), extracellular matrix (ECM) degradation, migration, and metastasis to distant organs, where they escape the immune system and exhibit enhanced survival potentials. Adapted from (Boedtkjer and Pedersen 2020).*

To target cancer cells and kill them without side effects on normal cells, it is favorable to target characteristics of cancer cells that differ from normal cells (Jin and Jin 2020). Increased glycolytic metabolism and the subsequent upregulation of acid extrusion, leading to acidic pH<sub>o</sub>, are shared features of most solid tumors (Andersen et al. 2014). Thus, inhibition of cancer cell metabolism or direct targeting of the acidity has been proposed as promising strategies to selectively kill tumor cells (Neri and Supuran 2011, Porporato *et al.* 2011, Parks *et al.* 2013, Margetis 2022). Hence, tumor acidosis is a relevant therapeutic target and can be approached by; 1) targeting acidity directly or indirectly by inhibiting acid-extruding transporters; 2) inhibiting the metabolic processes responsible for producing acids in the first place (Pillai et al. 2019). Several challenges exist for drug delivery to cancer cells due to the acidic, hypoxic, and poorly vascularized tumor microenvironment. Most of the commonly used chemotherapeutics are weak bases, and they become protonated in the acidic pH<sub>o</sub> of the tumor, which prevents the drugs from passively diffusing across the plasma membrane of the tumor and reaching the intracellular target (Raghunand *et al.* 1999, Gerweck *et al.* 2006, Webb et al. 2011). This challenge could be circumvented by raising the pH<sub>o</sub> of solid tumors (Webb et al. 2011). Oral buffers, such as NaHCO<sub>3</sub>, have been shown to increase the pH<sub>o</sub> of xenograft tumors without affecting the systemic pH balance. The increased tumor pH<sub>o</sub> reduced the formation of spontaneous metastases but did not decrease primary tumor growth (Robey et al. 2009). However, the issue with this so-called systemic buffer therapy where oral supplementation of NaHCO<sub>3</sub> is given in humans is the required dose, which is too high for agreeable administration (Yang *et al.* 2020). The systemic treatment could potentially be replaced by local delivery of bicarbonate (Chao *et al.* 2016) as NaHCO<sub>3</sub> treatment can increase the uptake of other conventional chemotherapies, such as doxorubicin and oxaliplatin (Yang et al. 2020).

The tumor acidity can also be targeted by inhibiting acid extruders, such as NHE1, NBCn1, MCTs, and the V-ATPase. This inhibition would lead to dual effects, as it would raise the pH<sub>o</sub> of tumors, allowing for more optimal conditions to distribute chemotherapeutic drugs, and the intracellular acid accumulation could enforce cancer cell death (Reshkin *et al.* 2003, Lauritzen *et al.* 2010, Le Floch *et al.* 2011, Amith et al. 2015). Targeting the glycolytic pathway can be done by inhibiting enzymes involved in glycolysis, such as glyceraldehyde phosphate dehydrogenase (GAPDH) or glucose-6-phosphate dehydrogenase (G6PDH), or by inhibiting the glucose uptake (Pillai et al. 2019).

Collectively, tumor acidosis offers the prospect that treatments interfering with pH as a target have great potential, both directly and to optimize the conditions for conventional chemotherapy.

## CHAPTER 3: Ion channels and calcium homeostasis in the pancreatic tumor microenvironment

### Ion channels in the pancreas and PDAC

Ion channels are transmembrane proteins that form aqueous pores across the plasma membrane. Open pores provide a low resistance pathway for ion movement down a concentration gradient. Ion channels are, in general, classified by their ion permeability (e.g.,  $\text{Ca}^{2+}$ ,  $\text{K}^+$ ,  $\text{Na}^+$ ,  $\text{Cl}^-$ , or non-selective) (Niemeyer *et al.* 2001). Accordingly, ion channels provide signaling and modulation of transmembrane solutes and water, and each cell expresses hundreds to thousands of channels that differ according to the cell and tissue requirements (Niemeyer *et al.* 2001, Gouaux and Mackinnon 2005). On a cellular level, the redistribution of ions changes electrical and chemical properties, which regulates numerous cellular processes, including; cell volume, transcription, and intracellular signaling and trafficking. These processes are tightly regulated to ensure normal tissue homeostasis through cell cycle progression, proliferation, invasion, migration, and apoptosis (Chen *et al.* 1994, Stock and Schwab 2015).

In the exocrine pancreas, ion channels, in cooperation with transporters, mainly contribute to the secretion of enzymes and bicarbonate (as described in ‘Pancreatic fluid secretion and pH regulation’). Thus, a correct ion channel and transporter distribution are needed to maintain accurate fluid secretion. An aberrant expression, distribution, and/or activity of ion channels are associated with several diseases, and the term ‘channelopathies’ has been widely used to describe these disorders (Niemeyer *et al.* 2001, Kim 2014). While many channelopathies are associated with neuromuscular and cardiac diseases, many also affect epithelial cell and organ function. Classical channelopathies result from mutations in a gene coding for ion channel proteins (Kim 2014). These mutations result in under- or overexpression, non-function, or dysfunctional regulation of the corresponding ion channel protein. In the pancreas, an often occurring channelopathy is cystic fibrosis. Mutations in the *CFTR* gene leads to altered  $\text{Cl}^-$  and  $\text{HCO}_3^-$  secretion, clotting of the ducts, pancreatic dysfunction, and eventually pancreatic insufficiency (McWilliams *et al.* 2010).

The abnormal regulation of ion channel expression and/or activity is also classified as a ‘hallmark of cancer’ (Hanahan and Weinberg 2011, Kim 2014, Prevarskaya *et al.* 2018, Hanahan 2022). Thus, changes in the pancreas ion channel distribution, expression, and function can result in the malignant transformation from normal epithelial cells to full-blown PDAC (Pedersen *et al.* 2017, Schnipper *et al.* 2020). Several studies have found that ion channel dysregulation is involved in cellular processes driving PDAC progression. However, the comparison between the role of ion channels in the healthy pancreas and PDAC has never been synthesized. Hence, we made a comprehensive review describing the localization and function of  $\text{K}^+$ ,  $\text{Ca}^{2+}$ ,  $\text{Cl}^-$ , Aquaporin, and  $\text{Na}^+$  channels in the healthy exocrine pancreas. Furthermore, we summarized the role of these ion channels

in PDAC development and progression and how they can function as novel biomarkers of PDAC (Schnipper et al. 2020). In this thesis manuscript, we will be focusing on the role of  $\text{Ca}^{2+}$  channels.

## 1. Calcium homeostasis

$\text{Ca}^{2+}$  is an essential element in the human body, and maintaining a constant free ionized  $\text{Ca}^{2+}$  concentration is biologically necessary for the function of excitable and non-excitable tissues. Normal  $\text{Ca}^{2+}$  concentrations in the body are tightly regulated by ion transport in the intestinal tract, kidneys, and bone. 99% of  $\text{Ca}^{2+}$  in the human body is stored in the bones.  $\text{Ca}^{2+}$  in the blood constitutes 50% in its free ionized form, and it is available for all tissues. The remaining 10% is combined with various anions, and 40% is bound to serum proteins, mainly albumin (Maalouf 2011).

In its ionized form,  $\text{Ca}^{2+}$  has a vital role in intracellular signaling processes, where it can regulate fertilization, differentiation, transcription, proliferation, cell death, protein phosphorylation, and migration (Berridge *et al.* 2000). In the exocrine pancreas, intracellular  $\text{Ca}^{2+}$  plays a central role in regulating enzyme,  $\text{HCO}_3^-$ , and fluid secretion (Petersen 2014). Fine-tuning of  $\text{Ca}^{2+}$  levels is essential to avoid uncontrolled  $\text{Ca}^{2+}$  release,  $\text{Ca}^{2+}$  overload, and toxicity, which can lead to the development of several pathologies. A high concentration of  $\text{Ca}^{2+}$  leads to subsequent harmful events, such as lipid and membrane damage or nucleic acid and protein aggregation (Case *et al.* 2007). Thus, the precise intracellular  $\text{Ca}^{2+}$  concentration is tightly regulated by various  $\text{Ca}^{2+}$  transport proteins (ion channels, exchangers, and ATPases) and buffer proteins. Due to membrane impermeability, extracellular  $\text{Ca}^{2+}$  concentrations are higher (1-2 mM) than intracellular  $\text{Ca}^{2+}$  concentrations, which are maintained close to 100 nM but can reach 1 or 2  $\mu\text{M}$  after stimulation (Berridge *et al.* 2003). This increased intracellular  $\text{Ca}^{2+}$  concentration is responsible for multiple  $\text{Ca}^{2+}$ -dependent cellular processes. Two main pathways permit the increase of intracellular  $\text{Ca}^{2+}$ ; (1) entry of extracellular  $\text{Ca}^{2+}$  through channels permeable to  $\text{Ca}^{2+}$  or exchangers, and (2) the release of  $\text{Ca}^{2+}$  through the endoplasmic reticulum (ER) or sarcoplasmic reticulum (SR), which are the central intracellular  $\text{Ca}^{2+}$  reserves. The release from ER or SR occurs via stimulation of channel receptors, such as inositol triphosphate ( $\text{IP}_3$ ) receptors ( $\text{IP}_3\text{R}$ ) or ryanodine receptors (RyR). These two pathways are responsible for activating downstream  $\text{Ca}^{2+}$ -dependent signaling and permit a spatiotemporal regulation of cellular processes (Berridge et al. 2000, Berridge et al. 2003).

## 2. Calcium signaling in the pancreas

In pancreatic acinar and ductal cells, the intracellular increase of  $\text{Ca}^{2+}$  is mainly evoked by ACh and CCK, respectively (Petersen 2014). This increase of intracellular  $\text{Ca}^{2+}$  activates epithelial  $\text{Ca}^{2+}$ -dependent  $\text{K}^+$  and  $\text{Cl}^-$  ion channels, which are required for the enzyme,  $\text{HCO}_3^-$  and fluid secretion (described in section Pancreatic fluid secretion and pH regulation). The binding of ACh or CCK to specific receptors activates phospholipase C  $\beta$  ( $\text{PLC}\beta$ ), which binds and hydrolyzes  $\text{PIP}_2$  in the plasma membrane, and releases  $\text{IP}_3$  and diacylglycerol.  $\text{IP}_3$  binds to the  $\text{IP}_3\text{R}$  in the membrane of ER, located in the apical pole of acinar cells, mediating a  $\text{Ca}^{2+}$  wave to the basal pole. The  $\text{IP}_3\text{R}$  stimulation promotes a  $\text{Ca}^{2+}$  ER store depletion leading to clustering of the ER  $\text{Ca}^{2+}$

sensor, the stromal interaction molecule 1 (STIM1), which activates store-operated channels (SOCs) and transient receptor potential (TRP) channels, leading to the  $\text{Ca}^{2+}$  influx known as SOC entry (SOCE) Figure 18.

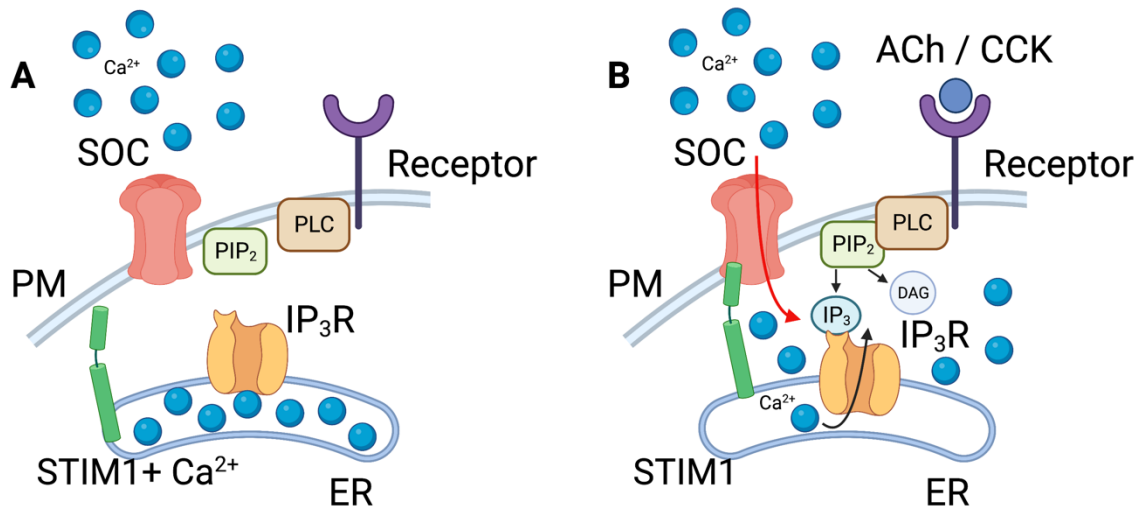


Figure 18. Simplified graphic of Store-operated channel entry of  $\text{Ca}^{2+}$  (SOCE). A) At rest,  $\text{Ca}^{2+}$  is stored in the ER. B) The binding of ligands (such as acetylcholine (ACh) or cholecystinin (CCK) leads to the activation of PLC, which hydrolyzes  $\text{PIP}_2$  into  $\text{IP}_3$  and diacylglycerol (DAG). This activates  $\text{IP}_3\text{R}$ , which promotes ER  $\text{Ca}^{2+}$  release, leading to activation of STIM1 and hence SOCE (Generated with Biorender).

Since the sustained elevation of intracellular  $\text{Ca}^{2+}$  concentrations can be toxic, it is necessary to extrude  $\text{Ca}^{2+}$  from the cytoplasm. In addition, also intracellular buffer proteins and organelles, such as the mitochondria, are involved in maintaining intracellular  $\text{Ca}^{2+}$  homeostasis (Berridge et al. 2000).

This  $\text{Ca}^{2+}$  homeostasis is general for most epithelial cells and is maintained by transmembrane ion channels, intracellular ion channels, pumps, and transporters, briefly described below and summarized in Figure 19.

### 3. Transmembrane calcium channels

The primary source of intracellular  $\text{Ca}^{2+}$  is extracellular  $\text{Ca}^{2+}$ , which is transported across the plasma membrane through activated ion channels. The electrochemical gradient allows the  $\text{Ca}^{2+}$  influx from the extracellular space through different types of ion channels, classified according to the genes that encode their components and their functional properties:

Voltage-gated calcium channels (VGCCs) are present in the membrane of all excitable cells. VGCC are key signal transducers of electrical excitability, as they convert the electrical signal of the action potential in the cell membrane to intracellular  $\text{Ca}^{2+}$  signals. Hence, regulated changes in the membrane potential and membrane depolarization will activate them, leading to the  $\text{Ca}^{2+}$  entry regulating essential functions for excitable cells, such as contraction, transmitter release, hormone secretion, and gene transcription (Zamponi et al. 2015). These channels are classified into six subtypes: the L-, N-, P-, Q, R, and T-type. They are

assembled by complexes of  $\alpha 1$ ,  $\beta$ ,  $\gamma$ , and  $\alpha 2$ - $\delta$  subunits, where the  $\alpha 1$  is the pore-forming subunit, but confer more gating properties when co-expressed with  $\alpha 2\delta$  subunit and especially the  $\beta$ -subunit (Catterall 2011). VGCCs are mainly expressed in excitable cells, such as neurons and muscle cells, and endocrine cells. However, they are found to be expressed in epithelial cells. Specifically, VGCCs are overexpressed in different epithelial-derived cancers (Tajada and Villalobos 2020).

Receptor-operated channels (ROCs) are directly gated by extracellular stimuli such as ligands. They are found in excitable cells responding to neurotransmitters and non-excitable cells responding to agonists such as ATP. They are provided with a cation-permeable pore that allows the influx of  $\text{Ca}^{2+}$  (Penner *et al.* 1993). One type of ubiquitously expressed ROCs is the purinergic receptors which are ATP-gated; their activation is associated with increased intracellular  $\text{Ca}^{2+}$  and cyclic AMP levels (North 2002). Indeed, TRP channels can be activated as ROCs (Pedersen and Nilius 2007).

Second-messenger-operated channels (SMOCs) share many properties with ROC. The main difference is that SMOCs are gated by intracellular second messengers binding to G-proteins or messengers secondary to receptor stimulation (Penner *et al.* 1993), leading to the entry of extracellular  $\text{Ca}^{2+}$ . For instance, some TRP channels are activated by second messengers, such as diacylglycerol, which is the case for TRPC3, TRPC6, and TRPC7. In addition is the Arachidonate-Regulated  $\text{Ca}^{2+}$  channel, in association with ORAI1, ORAI3, and STIM1, which are activated by arachidonic acid allowing  $\text{Ca}^{2+}$  entry (Penner *et al.* 1993).

SOCs are the main pathway for  $\text{Ca}^{2+}$  entry in non-excitable cells, such as epithelial cells. As described above, these channels generate SOCE. Upon ER  $\text{Ca}^{2+}$  store depletion from 700  $\mu\text{M}$  to 200  $\mu\text{M}$  (Alvarez and Montero 2002, Tajada and Villalobos 2020), cytoplasmic  $\text{Ca}^{2+}$  concentration increases. This partial depletion of ER stores activates STIM1, which oligomerizes and interacts with plasma membrane-localized SOC channels such as ORAI or TRP channels, allowing  $\text{Ca}^{2+}$  influx. ORAI channels appear in three isoforms (ORAI1, ORAI2, and ORAI3) and are mainly involved in the inwardly  $\text{Ca}^{2+}$  release-activated  $\text{Ca}^{2+}$  ( $I_{\text{CRAC}}$ ) current (Prakriya and Lewis 2015). STIM1 (and STIM2) are distributed in the ER- and plasma membrane and contain an EF-hand  $\text{Ca}^{2+}$  binding domain, which binds free  $\text{Ca}^{2+}$  ions, thus sensing the changes in  $\text{Ca}^{2+}$  concentrations of the ER upon store depletion (Grabmayr *et al.* 2020).

TRP channels represent a large family of non-selective ion channels mainly expressed in the plasma membrane. They can form homo- and hetero-tetramers and are activated upon different stimuli. The mammalian TRP channels are grouped into seven subfamilies: The ankyrin (TRPA), canonical (TRPC), melastatin (TRPM), mucolipin (TRPML), polycystin (TRPP), vanilloid (TRPV), and NO-mechano-potential C (TRPN) (Samanta *et al.* 2018). The latter is only found in invertebrates and fish (Nilius and Owsianik 2011). The role of TRP channels in mediating SOCE is a controversial issue. Certain members of the TRP family display properties similar to the operation of other SOC channels. At least, TRPC1, TRPC3, TRPC6, and TRPV6 act as SOC channels by interacting with STIM1 (Trebak *et al.* 2003, Vanden Abeele *et al.* 2003). However, the relationship



of TRP channels to SOC is likely cell-specific and influenced by factors such as endogenous expression and their capability to form heteromultimeric structures (Ong *et al.* 2016).

#### 4. Intracellular calcium channels

Intracellular organelles can function as  $\text{Ca}^{2+}$  stores as they rapidly respond to the need for intracellular  $\text{Ca}^{2+}$ . The main store of intracellular  $\text{Ca}^{2+}$  is the ER. The release of  $\text{Ca}^{2+}$  from the ER occurs mainly through the activation of the  $\text{IP}_3\text{R}$  and  $\text{RyR}$  (Mikoshiha 2007, Van Petegem 2012). Even though the two receptors share sequence homology, their activation of them is distinct. The three  $\text{IP}_3\text{R}$  isoforms ( $\text{IP}_3\text{R1}$ ,  $\text{IP}_3\text{R2}$ ,  $\text{IP}_3\text{R3}$ ) are mainly activated by  $\text{IP}_3$  as a product of the hydrolysis of  $\text{PIP}_2$  into  $\text{IP}_3$  and diacylglycerol, as described above. In contrast,  $\text{RyR}$ , which also appears in three isoforms ( $\text{RyR1}$ ,  $\text{RyR2}$ , and  $\text{RyR3}$ ), is activated by low concentrations of  $\text{Ca}^{2+}$  (in the  $\mu\text{M}$  range) or ryanodine (an alkaloid inhibitor only found in plants) (Van Petegem 2012). The mitochondrial calcium uniporter (MCU) is responsible for the passage of  $\text{Ca}^{2+}$  from the cytosol into mitochondria. MCUs are activated upon increased cytosolic  $\text{Ca}^{2+}$  concentrations and a depolarization of the mitochondrial membrane (Marchi and Pinton 2014).

#### 5. Calcium pumps and transporters

Besides,  $\text{Ca}^{2+}$  channels, pumps, and transporters are essential to maintain the intracellular  $\text{Ca}^{2+}$  concentration. Indeed,  $\text{Ca}^{2+}$  channels allow the influx of  $\text{Ca}^{2+}$ , where transporters and pumps remove  $\text{Ca}^{2+}$  from the cytosol by the extrusion across the plasma membrane or into organellar  $\text{Ca}^{2+}$  stores. Together, these mechanisms restore basal  $\text{Ca}^{2+}$  levels and prevent intracellular  $\text{Ca}^{2+}$  overload. The removal of  $\text{Ca}^{2+}$  requires energy in the form of ATP hydrolysis for  $\text{Ca}^{2+}$  pumps or in the electrochemical gradient of other cations for transporters. Both types of  $\text{Ca}^{2+}$  removers have been characterized:

In the plasma membrane are two critical players in  $\text{Ca}^{2+}$  removal described. The  $\text{Na}^+/\text{Ca}^{2+}$  exchange transporter (NCX) is a bi-directional transporter and removes  $\text{Ca}^{2+}$  from the cytosol in exchange for three  $\text{Na}^+$  into the cell. However, the transporter can, in specific modes, provide  $\text{Ca}^{2+}$  entry (Jeffs *et al.* 2007). In addition, the plasma membrane  $\text{Ca}^{2+}$ -ATPase (PMCA) pumps  $\text{Ca}^{2+}/\text{ATP}$  in a 1:1 stoichiometry, which provides a high affinity but low capacity for  $\text{Ca}^{2+}$  extrusion, compared to NCX (Khananshvili 2014, Krebs 2017). The two transporters cooperate in such a way as the PMCA ensures a cytosolic  $\text{Ca}^{2+}$  concentration around the basal level, where the NCX eliminates significant rises of intracellular  $\text{Ca}^{2+}$  (Brini and Carafoli 2011).

The ER and mitochondria, recognized as  $\text{Ca}^{2+}$  stores, hold their own  $\text{Ca}^{2+}$  transporters.  $\text{Ca}^{2+}$  is constantly leaking from channels in the ER membrane. Still, the  $\text{Ca}^{2+}$  concentration remains high due to the continuous activity of the ER/SR  $\text{Ca}^{2+}$ -ATPases (SERCA) that recharge  $\text{Ca}^{2+}$  stores by pumping two  $\text{Ca}^{2+}$  for every hydrolyzed ATP molecule (Periasamy and Kalyanasundaram 2007). In the mitochondria, the  $\text{Ca}^{2+}$  uptake is provided by MCU and the  $\text{Na}^+/\text{Ca}^{2+}$  (NCLX) and  $\text{Ca}^{2+}/\text{H}^+$  (HCX) exchangers, respectively. The Golgi-associated secretory  $\text{Ca}^{2+}$ -ATPases (SPCAs) are responsible for loading the Golgi apparatus with  $\text{Ca}^{2+}$  (Vandecaetsbeek *et al.* 2011).



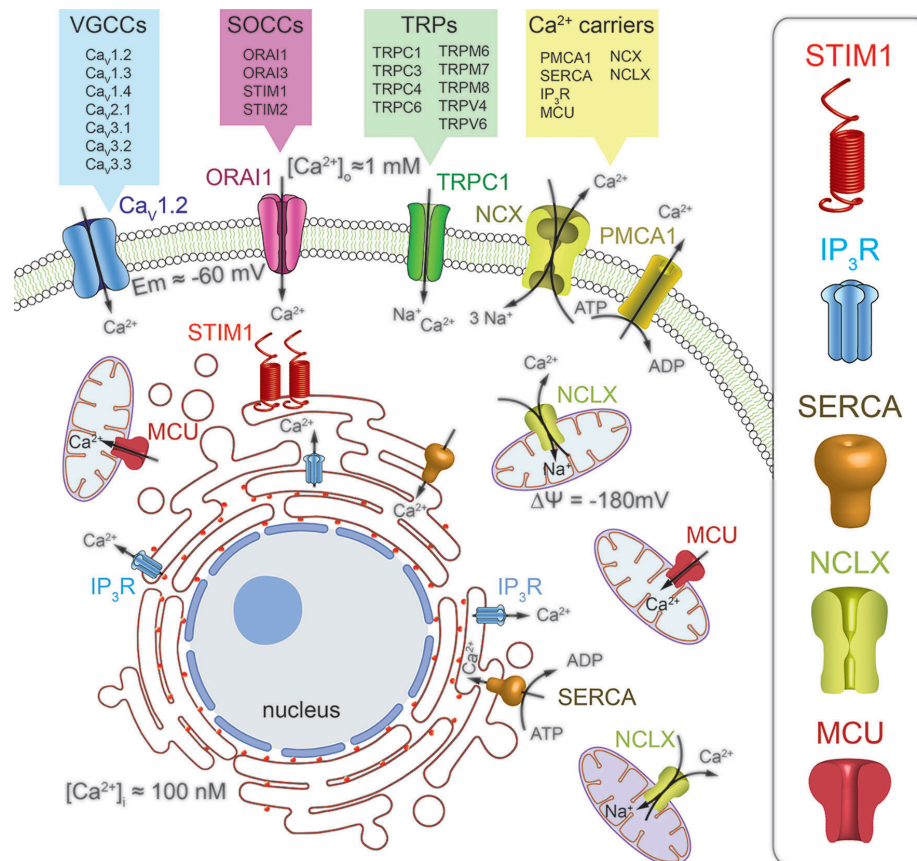


Figure 19. Schematic overview of ion channels, transporters, pumps, and receptors involved in  $\text{Ca}^{2+}$  homeostasis in mammalian cells (Tajada and Villalobos 2020).

## 6. Other calcium-binding proteins and processes

Besides ion channels, transporters, and pumps, other proteins maintain  $\text{Ca}^{2+}$  homeostasis. Intracellular changes in  $\text{Ca}^{2+}$  concentrations promote the binding of  $\text{Ca}^{2+}$  to specific  $\text{Ca}^{2+}$  binding proteins, modulating  $\text{Ca}^{2+}$  signaling and the transduction of cellular signaling pathways (Lewit-Bentley and Rety 2000). A common characteristic between all  $\text{Ca}^{2+}$  binding proteins is the expression of the EF-hand  $\text{Ca}^{2+}$ -binding domain, which forms a high-affinity binding site for  $\text{Ca}^{2+}$ . Most EF-hand-containing proteins belong to a group of ‘ $\text{Ca}^{2+}$  sensors’; that is, binding  $\text{Ca}^{2+}$  induces a conformational change, allowing them to interact with specific targets, such as downstream signaling pathways, in a  $\text{Ca}^{2+}$ -dependent manner (Kretsinger and Nockolds 1973, Ikura 1996). The  $\text{Ca}^{2+}$  binding proteins can be divided into two families; buffer proteins and effector proteins. Buffer proteins do not work as  $\text{Ca}^{2+}$  sensors. Depending on their affinity and kinetics, they function as ‘ $\text{Ca}^{2+}$  chelators’ as they reduce the quantity of free  $\text{Ca}^{2+}$  available in the cytosol, thus contributing to regulating the spatiotemporal aspects of  $\text{Ca}^{2+}$  signaling (Schwaller 2010). Some intracellular buffer proteins are expressed in the cytosol (e.g., calretinin and calbindin), and others at the reticular level (e.g., calnexin and calreticulin). Unlike buffer proteins, effector proteins work as  $\text{Ca}^{2+}$  sensors and lead to conformational changes. Indeed, the binding of  $\text{Ca}^{2+}$  to effector proteins as calmodulin (CaM) modifies the conformational architecture of the latter

and transduces changes in  $\text{Ca}^{2+}$  concentrations into cellular signals by binding to a range of target proteins (Ikura 1996, Halling *et al.* 2016). S100 proteins are also essential  $\text{Ca}^{2+}$  sensors. The activity of S100 proteins depends on  $\text{Ca}^{2+}$  binding followed by conformational shifts. Interestingly, the expression of the subfamily S100P protein has been found to increase during the progression from PanIN to invasive adenocarcinoma, and it is used as a specific diagnostic marker of PDAC (Deng *et al.* 2008, Ezzat *et al.* 2016).

## 7. Calcium in cellular processes

### *Focus on calcium and calcium channels in proliferation and migration*

$\text{Ca}^{2+}$  is a universal second messenger that regulates numerous cellular processes, including cell proliferation and motility. The mechanism by which  $\text{Ca}^{2+}$  regulates cell division and proliferation is by (1) acting directly on target proteins involved in cell cycle progression or (2) its effect can be mediated by  $\text{Ca}^{2+}$  binding proteins, such as CaM (Kahl and Means 2003).

Early studies have demonstrated that the cell's ability to proliferate depends on its sensitivity to external  $\text{Ca}^{2+}$  concentrations. Non-transformed cells are highly dependent, and neoplastic cells are less dependent on external  $\text{Ca}^{2+}$ . Proliferating human or mouse non-transformed cells, incubated in a medium containing low extracellular  $\text{Ca}^{2+}$  levels (10-60  $\mu\text{M}$ ) ceased cellular division and accumulated in the G1 phase (Boynton *et al.* 1976, Hazelton *et al.* 1979, Whitfield *et al.* 1979). This G1 arrest was reversible in mouse fibroblasts, and returning to a medium with normal extracellular  $\text{Ca}^{2+}$  levels (1.25 and 1.80 mM  $\text{Ca}^{2+}$ ) enabled cells to undergo DNA synthesis within hours (Boynton *et al.* 1976). Indeed, the cells were susceptible to  $\text{Ca}^{2+}$  depletion at two points during the cell cycle: (1) in the early G1 phase and (2) near the G1/S boundary (Boynton *et al.* 1977). When human endothelial cells were stimulated with growth factors, the chelation of  $\text{Ca}^{2+}$  (0.03 mM extracellular  $\text{Ca}^{2+}$ ) would, at any time during the first eight hours after stimulation, result in inhibited DNA synthesis (Takuwa *et al.* 1992). At any other time, after these eight hours, the depletion of  $\text{Ca}^{2+}$  did not affect the ability of the cells to pass into the S-phase. Beyond these two critical time points, no further influx of extracellular  $\text{Ca}^{2+}$  signal is required (Reddy 1994, Capiod 2013). It was demonstrated 30 years ago that the  $\text{Ca}^{2+}$  influx decreased during cell division, probably through uncoupling store depletion from SOCE (Volpi and Berlin 1988, Preston *et al.* 1991), ORAI1 internalization during cell division (Yu *et al.* 2009), or STIM1 phosphorylation (Smyth *et al.* 2009). Since has it been confirmed, in several cell lines, that SOCE decreases during mitosis (Tani *et al.* 2007, Russa *et al.* 2008, El Boustany *et al.* 2010). However,  $\text{Ca}^{2+}$  transients released from intracellular stores are required for a cell to progress through the M-phase. Studies performed in sea urchin eggs and mammalian cells revealed that single  $\text{Ca}^{2+}$  transients and sustained increases occur during pronuclear migration, envelope break-down, and the meta- and anaphase transition of mitosis and cytokinesis (Kao *et al.* 1990). The cyclic increases in  $\text{IP}_3$  and  $\text{IP}_3\text{R}$  generate this  $\text{Ca}^{2+}$  release from internal stores (Poenie *et al.* 1985, Kahl and Means 2003, Hodeify *et al.* 2018). In general, cells need extracellular  $\text{Ca}^{2+}$  levels, thus the influx of  $\text{Ca}^{2+}$ , to control G1 and S-phase transitions, but it is not necessary during late S-phase and G2/M transitions. Here, cell division depends on the release of intracellular  $\text{Ca}^{2+}$  (Hodeify *et al.* 2018).

Once intracellular  $\text{Ca}^{2+}$  levels increase,  $\text{Ca}^{2+}$  binding proteins such as CaM can propagate the signal (Chin and Means 2000). When CaM is activated, it binds to other proteins bearing CaM domains, including the family of  $\text{Ca}^{2+}$ /CaM-kinases (CaMK). CaMK turns on different cellular downstream pathways mediated by transcription factors, such as nuclear factor of activated T-cells (NFAT) and nuclear factor kappa-light-chain-enhancer of activated B cells (NF $\kappa$ B), among others, which regulate gene expression of Cyclin/CDK complexes and other cell cycle relevant inhibitors (Figure 20A) (Berridge et al. 2000, Humeau *et al.* 2018).

$\text{Ca}^{2+}$  channels are needed for the influx of  $\text{Ca}^{2+}$  to regulate the cell cycle. The link between  $\text{Ca}^{2+}$  channel expression and proliferation was demonstrated in knockdown (KD) experiments, where many cases showed that the KD of several TRP channels and ORAI/STIM reduced  $\text{Ca}^{2+}$  entry and hence cell cycle progression and proliferation (Borowiec *et al.* 2014) (Figure 20B). However, several exceptions are now found where reducing the expression of the channel has no effect on  $\text{Ca}^{2+}$  entry, which provides evidence for additional channel functions, except for mediating  $\text{Ca}^{2+}$  influx. The  $\text{Ca}^{2+}$ -independent role of ion channels can, to some extent, explain the fact that untransformed cells exceed proliferative capacity in the presence of as little as 50-100  $\mu\text{M}$  free  $\text{Ca}^{2+}$ . Yet, transformed cells can proliferate even in the presence of only 20  $\mu\text{M}$   $\text{Ca}^{2+}$  (Borowiec *et al.* 2014, Humeau *et al.* 2018).

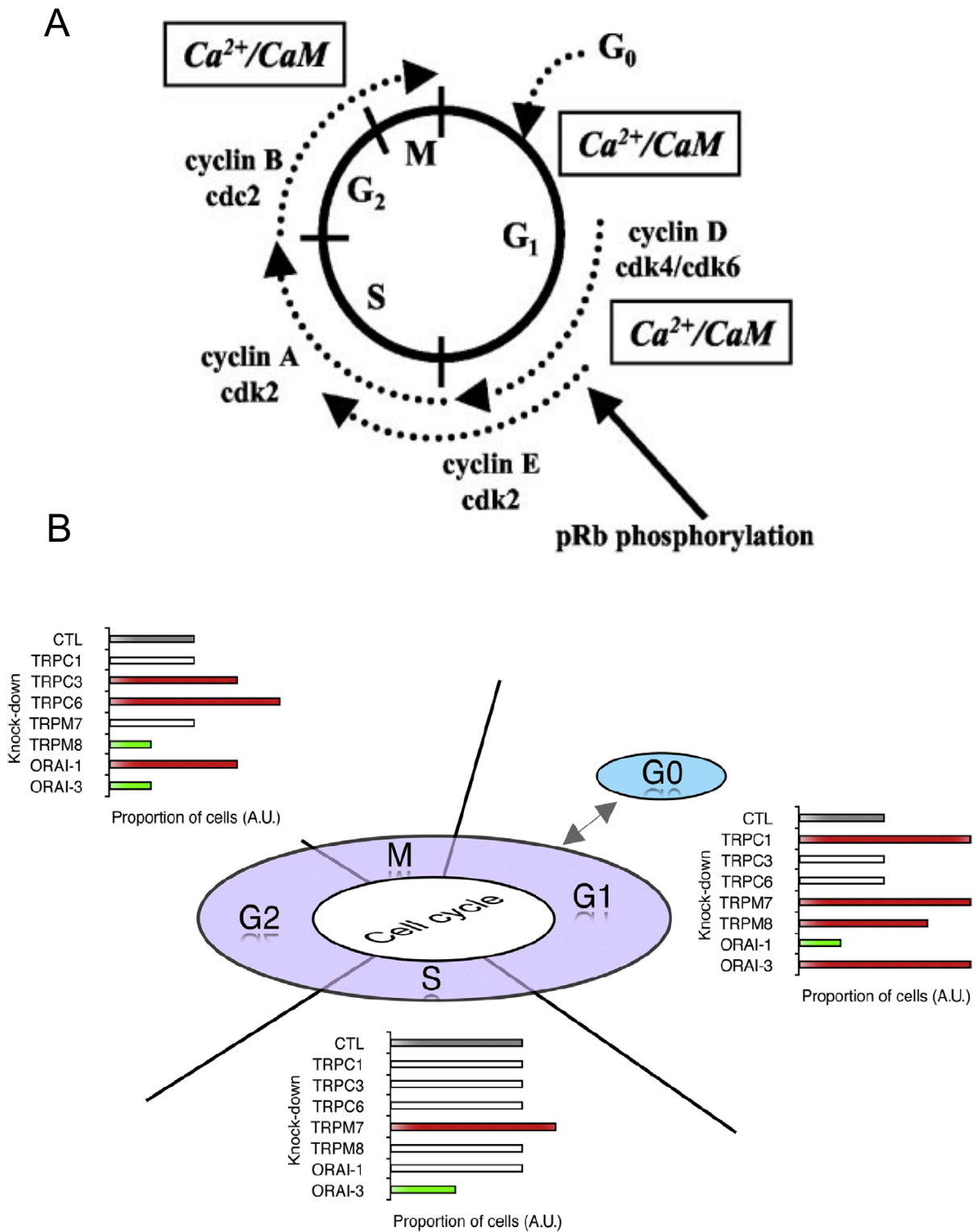


Figure 20.  $Ca^{2+}$  signaling and  $Ca^{2+}$  channels in cell cycle progression. A) Schematic overview of  $Ca^{2+}$  and CaM regulating cell cycle progression,  $Ca^{2+}$ /CaM is required at two points during the reentry from G0 and later near the G1/S boundary. Additionally,  $Ca^{2+}$ /CaM is implicated in the G2/M transition, M phase progression, and exit from mitosis. B) Representation of the proportion of decreased or increased calcium channel expression (arbitrary units A.U.) and its consequence on cell cycle distribution (Modified from (Kahl and Means 2003) and (Borowiec et al. 2014)).

As for proliferation,  $\text{Ca}^{2+}$  signaling is essential for regulating cell migration. Early and recent studies have shown that migrating eosinophils and embryonic lung fibroblasts display a front-to-rear end-increasing gradient of  $\text{Ca}^{2+}$  concentrations (Brundage *et al.* 1991, Brundage *et al.* 1993, Wei *et al.* 2009). When chemoattractants are present or during cell turning, the  $\text{Ca}^{2+}$  signals are enhanced, and the resting  $\text{Ca}^{2+}$  concentration is elevated (Brundage *et al.* 1991, Brundage *et al.* 1993, Wei *et al.* 2009). The spatially and temporally patterned activation of local  $\text{Ca}^{2+}$  concentrations affects cell migration in the form of  $\text{Ca}^{2+}$ -dependent processes in the leading lamella (Figure 21) (Wei *et al.* 2012). Among many signaling pathways,  $\text{Ca}^{2+}$  regulates actin-myosin-based cytoskeletal networks and integrin-based focal adhesion complexes.  $\text{Ca}^{2+}$  can activate protein kinase C (PKC) and CaMK, which interact with actin, thus affecting its dynamics (Ohta *et al.* 1986, Larsson 2006, Hoffman *et al.* 2013). In addition,  $\text{Ca}^{2+}$  can regulate Rho GTPases and PI3K, which are essential for actin polymerization, and involved in cytoskeletal remodeling and adhesion formation (Holinstat *et al.* 2003, Evans and Falke 2007). Indeed, several TRP channels have been reported as contributors to cell migration and cancer metastasis (Canales Coutino and Mayor 2021).

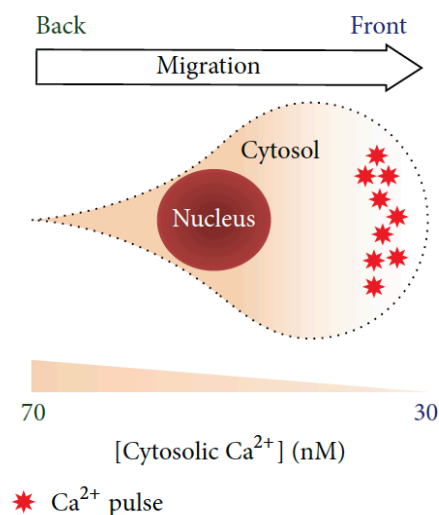


Figure 21. A simple model of  $\text{Ca}^{2+}$  concentrations in the migration process. The cytosolic  $\text{Ca}^{2+}$  concentration is lower overall in the front of the cell, but during migration, the local  $\text{Ca}^{2+}$  concentration increases and creates  $\text{Ca}^{2+}$  pulses (Modified from (Tsai *et al.* 2015)).

## 8. Calcium in cancer

### *A focus on pancreatic cancer*

It is well-established that  $\text{Ca}^{2+}$  is one of the essential intracellular regulators of physiological and pathophysiological conditions, including cancer (Tajada and Villalobos 2020).  $\text{Ca}^{2+}$  is involved in all tumor processes, from malignant transformation to the formation of metastases. The  $\text{Ca}^{2+}$  signaling mechanism in terms of speed, amplitude, and spatio-temporal patterning results in interactions and crosstalk with other

signaling pathways in cancer progression (Berridge et al. 2000). There is often a significant remodeling in the expression and function of the proteins directly involved in  $\text{Ca}^{2+}$  signaling, for instance, ion channels (Monteith *et al.* 2017). Several ion channels, including  $\text{Ca}^{2+}$  permeable, are associated with cell cycle progression, proliferation, apoptosis, invasion, and migration (Prevorskaya et al. 2018, Schnipper et al. 2020). However, the dysregulation of  $\text{Ca}^{2+}$  channels in PDAC is less explored compared to other types of cancer, such as breast-cervical-, and colorectal cancer (Chen *et al.* 2019). Below is summarized the known role of  $\text{Ca}^{2+}$  regulating ion channels in PDAC;

ORAI1 and STIM1 are expressed in several PDAC cell lines. ORAI1 plays a role in proliferation, survival, and apoptosis through SOCE in PANC-1, AsPC-1, MiaPaCa-2, and Capan-1 cells (Kondratska *et al.* 2014, Khan *et al.* 2020). Furthermore, ORAI1 promotes an  $I_{\text{CRAC}}$  current leading to proliferation in colony formation in MiaPaCa-2 and L3.6pl cells. This proliferation is regulated by the  $\text{Ca}^{2+}$ -activated AKT/mTOR/NFAT signaling pathway. In contrast, one study has found a decrease in ORAI1 gene expression in human PDAC tissues (Khan et al. 2020). STIM1 is involved in proliferation and invasion, and EMT is co-expressed with HIF-1 $\alpha$  in human PDAC samples. In cooperation, they regulate PANC-1 cell proliferation, invasion, and EMT in a hypoxic environment. Furthermore, STIM1 and IP<sub>3</sub>R, redistributing to the leading edge of focal adhesion, lead to SOCE-dependent PANC-1 cell migration (Okeke *et al.* 2016).

TRPV1 regulates the Epidermal growth factor receptor (EGFR) in PANC-1 cells, where a high expression of TRPV1 is associated with a decrease in EGFR expression and vice versa. The overexpression of TRPV1 leads to decrease proliferation through the MAPK signaling pathway. In contrast, another study has demonstrated that low expressions of TRPV1 reduce cell proliferation and induce cell proliferation (Hartel *et al.* 2006).

TRPV6 is overexpressed in human pancreatic cancer tissues and two PDAC cell lines, Capan2 and SW1990. Here, TRPV6 promotes cell cycle progression, proliferation, migration, invasion, and reduced apoptosis (Song *et al.* 2018). On the contrary, two other studies have found downregulation of TRPV6 in human PDAC samples and a PDAC cell line A818-6 grown in a highly malignant undifferentiated monolayer (Zaccagnino *et al.* 2016, Tawfik *et al.* 2020).

TRPM2, TRPM7, and TRPM8 are overexpressed in human PDAC samples and several cell lines, which drives cell cycle progression, proliferation, migration, and invasion (Yee *et al.* 2010, Rybarczyk *et al.* 2012, Cucu *et al.* 2014, Yee *et al.* 2014, Rybarczyk *et al.* 2017, Ulareanu *et al.* 2017). For TRPM7, are these processes usually regulated through  $\text{Mg}^{2+}$  entry (Rybarczyk et al. 2012, Rybarczyk et al. 2017).

The VGCCs Cav2.1 and Cav3.1 are upregulated and downregulated, respectively, in human PDAC tissue; however, there is no evidence of how these channels are involved in PDAC progression (Zaccagnino et al. 2016).

$\text{Ca}^{2+}$  pumps and transporters are also known to be dysregulated in PDAC. MCU, SERCA, and several isoforms of PMCA and NCX are involved in PDAC progression (Bettaieb *et al.* 2021).  $\text{Ca}^{2+}$  signaling affects

the activity of other ion channels in the pancreas (described in Calcium signaling in the pancreas), Thus,  $\text{Ca}^{2+}$ -activated channels or different types of ion channel families such as  $\text{K}^+$ ,  $\text{Cl}^-$ , and  $\text{Na}^+$  channels are dysregulated in PDAC, summarized in (Schnipper et al. 2020). In addition, it has been proposed that ion channels are a good target in cancer therapy, found in ovarian-, breast-, prostate-, and esophageal cancers (Prevarskaya et al. 2018).

## Calcium channels in the tumor microenvironment

Several studies have reasonably focused their search for  $\text{Ca}^{2+}$  signaling in cancer cells themselves. However, the tumor microenvironment has become of great interest, also in terms of  $\text{Ca}^{2+}$  signaling. In different types of cancer, the tumor microenvironment in terms of  $\text{Ca}^{2+}$  signaling is studied in immune-cancer interactions, tumor vasculature, angiogenesis, hypoxia, and CAFs and adipocytes (Liot et al. 2021). The role of  $\text{Ca}^{2+}$  signaling in the tumor microenvironment of PDAC has so far only been investigated by a handful of studies.

PSCs express several  $\text{Ca}^{2+}$  channels, particularly TRP and ORAI channels.  $\text{Ca}^{2+}$  entry through ORAI1 promotes cell proliferation in activated PSCs by controlling cell cycle progression and  $\text{TGF}\beta$  secretion, through the activation of AKT signaling (Radoslavova et al. 2021).

TRPC6 is proposed to regulate autocrine stimulation of PSCs in hypoxic conditions (Nielsen et al. 2017).  $\text{Ca}^{2+}$  entry through TRPC3 activates neighboring  $\text{KCa}3.1$  channels, which results in increased PDGF-stimulated PSC migration (Storck et al. 2017). Furthermore, TRPV4 expression decreases in PSC when cultured under elevated ambient pressure, mimicking the conditions found in PDAC (Sharma et al. 2019). Several  $\text{Ca}^{2+}$  channels have been found expressed in different cell types of the immune system, such as neutrophils, macrophages, T-cells, and B-lymphocytes. In these cell types,  $\text{Ca}^{2+}$  channels also contribute to controlling cellular responses, which have been associated with PDAC progression and development (Hofschroer et al. 2020).

Taken together,  $\text{Ca}^{2+}$  signaling through ion channels is essential for neighboring cells in the tumor microenvironment.  $\text{Ca}^{2+}$  transients in the crosstalk between cells in the tumor microenvironment and PDAC cells could be vital for PDAC development and progression. As described before, the challenged pH gradient is a prominent factor in the tumor microenvironment.

### 1. Calcium and pH

Separately, pH and  $\text{Ca}^{2+}$  regulate the same physiological processes equally, and disrupted homeostasis of both is involved in tumor progression. In addition,  $\text{Ca}^{2+}$  and pH are linked together, and crosstalk between  $\text{pH}_i$  and intracellular  $\text{Ca}^{2+}$  exists (Molinari and Nervo 2021). In aqueous solutions, the solubility of calcium salts in water is pH-dependent since the  $\text{H}^+$  competes with calcium for the same binding sites and can easily replace it (McCudden 2013). The replacement of calcium to  $\text{H}^+$  increases ionized  $\text{Ca}^{2+}$  in the solution. Thus, in solution,  $\text{H}^+$  reduces the binding affinity of ligands and promotes  $\text{Ca}^{2+}$  release. This indicates a direct chemical interdependence between  $\text{H}^+$  and  $\text{Ca}^{2+}$  ions and that an increase in pH (alkalization) promotes the storage of bound calcium, decreasing the concentration of free  $\text{Ca}^{2+}$ . In contrast, a decrease in pH (acidification) fosters



the breaking/solubilization of bound calcium, hence increasing  $\text{Ca}^{2+}$  concentrations (McCudden 2013). An example of the relationship between ionized and bound calcium and changes in pH is illustrated in the blood (Figure 22).

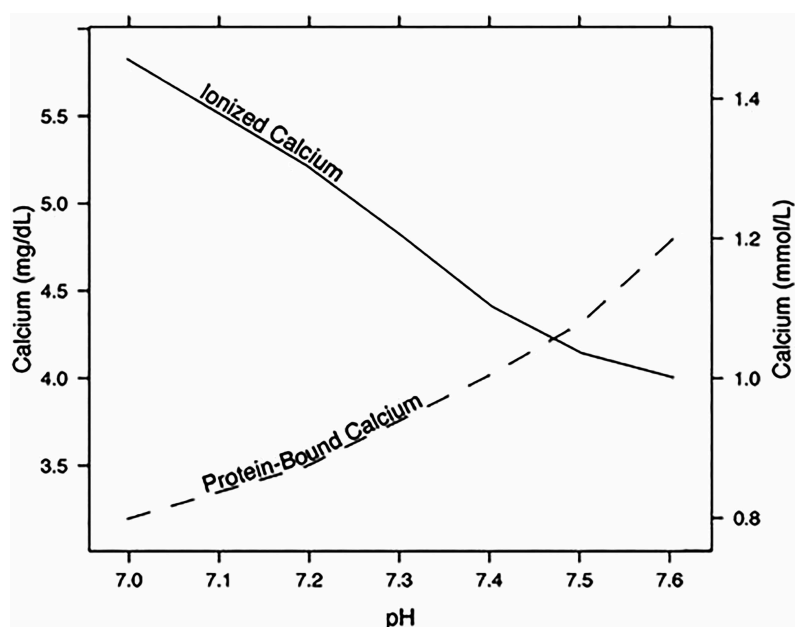


Figure 22. The effect of pH on protein-bound  $\text{Ca}^{2+}$  and the ionized  $\text{Ca}^{2+}$  in blood. When pH decreases,  $\text{H}^+$  competes for the binding site of  $\text{Ca}^{2+}$ , and the amount of ionized  $\text{Ca}^{2+}$  increases. On the contrary, when the blood pH increases, albumin and globulin become more negatively charged, which leads to more binding of  $\text{Ca}^{2+}$ , causing the total amount of circulating ionized  $\text{Ca}^{2+}$  to decrease (McCudden 2013).

However, the interdependence of  $\text{H}^+$  and  $\text{Ca}^{2+}$  inside a cell should be considered part of the cell's overall metabolic system in the cytoplasm (Molinari and Nervo 2021). One could expect that acidification of the cytosol would increase intracellular  $\text{Ca}^{2+}$  concentrations and that, on the other hand, alkalization would promote decreased intracellular  $\text{Ca}^{2+}$  concentrations. However, the structure of the cell is highly complex, and due to various biological systems and processes, which control  $\text{H}^+$  and  $\text{Ca}^{2+}$  concentrations, they are modified according to the physiological needs of the cell. Hence, experimental studies do not demonstrate consistent results, and some studies show that increased  $\text{Ca}^{2+}$  concentrations are produced by acidification in different cell systems (Orchard *et al.* 1987, Kim and Smith 1988, Cairns *et al.* 1993, Daugirdas *et al.* 1995, Donoso *et al.* 1996, Nishiguchi *et al.* 1997, Gonzalez *et al.* 1998, Chen *et al.* 2001, Thomas 2002, Marin *et al.* 2010, Krizaj *et al.* 2011, Swietach *et al.* 2013, Paillamanque *et al.* 2016, Hu *et al.* 2017, Berra-Romani *et al.* 2019, Sun *et al.* 2021). Whilst other have shown that alkalization produces increased  $\text{Ca}^{2+}$  concentrations (Kiang 1991, Guse *et al.* 1994, Alfonso *et al.* 2000, Minelli *et al.* 2000, Li *et al.* 2012, Chowdhury *et al.* 2013). Ionized  $\text{Ca}^{2+}$  indirectly has a role in the cytosolic pH (Molinari and Nervo 2021). When  $\text{Ca}^{2+}$  influx is activated, PLC is hydrolyzed. PLCs are acidifying enzymes because when PLC hydrolyzes  $\text{PIP}_2$ , it produces diacylglycerol, an alcohol, and  $\text{IP}_3$ , an acid.  $\text{IP}_3$  is protonated and must completely dissociate to bring itself into balance with



the pH of the cytosol (pH 7.2) and, therefore quickly release an  $H^+$ . The same occurs when  $IP_3$  is further degraded to inositol 1,4 biphosphate by polyphosphate-5-phosphatase A (5PTase). The two hydrolysis events are likely interrelated and are a part of the mechanisms that control the influx of  $Ca^{2+}$  through SOCs (Molinari and Nervo 2021). Thus, it can be hypothesized that  $Ca^{2+}$  oscillations, in combination with other processes, originate from the diffusion of  $H^+$  in the cytoplasm and the activation of  $Ca^{2+}$ -dependent enzymes.

Early studies have been carried out regarding pancreatic cells, showing how pH affects  $Ca^{2+}$  fluctuations. These studies on isolated rat pancreatic acinar cells (Speake and Elliott 1998) showed that changing pH affected  $Ca^{2+}$  signals. Indeed, cytosolic alkalization of non-stimulated acinar cells increased  $Ca^{2+}$  release from intracellular stores, where acidification had no effect. On the contrary, when the acinar cells were agonist stimulated with either ACh or CCK, acidification enhanced  $Ca^{2+}$  signals, whereas alkalization had an inhibitory effect (Speake and Elliott 1998). In other studies, performed on rat pancreatic acinar cells, the authors found the opposite result, where extracellular acidification and intracellular alkalization had an inhibitory effect on  $Ca^{2+}$  entry upon CCK stimulation. In contrast, extracellular alkalization and intracellular acidification enhanced the  $Ca^{2+}$  entry (Muallem *et al.* 1989, Tsunoda 1990), leading to amylase secretion (Tsunoda *et al.* 1990). In mouse pancreatic acinar cells, acidification of the cytosol decreased  $Ca^{2+}$  wave propagations upon ACh stimulation (Gonzalez *et al.* 1998).

The interdependency between pH and  $Ca^{2+}$  signaling in cancer models is less studied. In a colon carcinoma cell line, alkaline  $pH_i$  release  $Ca^{2+}$  from intracellular  $Ca^{2+}$  stores via an  $IP_3$ -independent mechanism, leading to activation of  $Ca^{2+}$  influx. Acidic  $pH_i$  could induce small and slow intracellular  $Ca^{2+}$  changes. Furthermore, thapsigargin or carbachol stimulated  $Ca^{2+}$  influxes were decreased upon acidification but enhanced by alkaline  $pH_i$  changes (Nitschke *et al.* 1996). In androgen-independent prostate cancer cells, ATP induced growth arrest by increasing  $Ca^{2+}$  entry, leading to a rapid and sustained decrease of  $pH_i$ . On the other hand, intracellular acidification reduces  $Ca^{2+}$  release from ER and thus cell proliferation (Humez *et al.* 2004). In two pancreatic cancer cell lines (PANC-1 and BxPC-3), acidification increased intracellular  $Ca^{2+}$  influxes. This acid-induced  $Ca^{2+}$  influx was evoked by the expression of two acid-sensing ion channels (ASIC) ASIC1 and ASIC3, resulting in  $Ca^{2+}$ -activated RhoA activity and hence EMT (Zhu *et al.* 2017)

## 2. pH-sensitive calcium channels

Changes in both  $pH_i$  and  $pH_o$  can modulate ion channel function through multiple mechanisms. Often acidosis is the best-described pH state, as it is associated with inflammation, ischemia, and inadequate acid venting, as found in the tumor microenvironment due to poor vascularization (Elingaard-Larsen *et al.* 2022). In addition, ion channels are described as acid sensors, as they appear to contribute to sensing pain and acid-induced feedback regulation in homeostatic reactions (Holzer 2009, Petho *et al.* 2020, Audero *et al.* 2022). Even though it is well known that the tumor microenvironment is acidic and ion channels can function as acid sensors, it is not understood how acidosis affects ion channel expression and function in cancer. Petho *et al.* have recently reviewed which ion channels are affected by acidification. Each ion channel activity was linked to channel

expression and function in different types of cancer (Petho et al. 2020). The same considerations have been made for  $\text{Ca}^{2+}$  channels, which have been shown to be pH sensitive (Audero et al. 2022). As this thesis is mainly focused on TRP isoforms, these channels and their cooperative partners (ORAI/STIM) (Figure 23), as acid sensors will be briefly described here:

- TRPM

Among different stimuli, some TRPM are sensitive to low pH. TRPM2 channel currents are completely inhibited by a  $\text{pH}_i$  of 6 due to ion competition (Starkus *et al.* 2007) or conformational changes induced by  $\text{H}^+$  binding (Du *et al.* 2009, Yang *et al.* 2010). TRPM6 and TRPM7 channel currents are also sensitive to acidosis. However, the effect seems controversial as some studies have shown that both TRPM6 and TRPM7 are inhibited by acidic  $\text{pH}_o$ , and others have shown that they are activated (Jiang *et al.* 2005, Li *et al.* 2007).

- TRPC

In contrast to TRPM channels, some TRPC channels can be activated by acidic pH. Both TRPC4 and TRPC5 are activated by acidic  $\text{pH}_o$  (6.5) but inhibited when  $\text{pH}_o$  decreases below 6 and 5.5, respectively (Semtner *et al.* 2007, Holzer 2009). Activation of TRPC4 currents by acidosis is mediated by GPCRs and requires an increase in intracellular  $\text{Ca}^{2+}$  concentrations (Thakur *et al.* 2020). On the contrary, TRPC5 can be activated directly by protonation and through GPCR activation (Semtner *et al.* 2007). Conversely to TRPC5 and TRPC4, TRPC6 currents are slightly inhibited by acidic pH. This modest inhibition could be explained by the lack of glutamate residues which are present in both TRPC4 and TRPC5 (Semtner *et al.* 2007).

- TRPV

TRPV1 was the first TRP channel demonstrated to be activated by protonation. A direct effect of protons on channel opening occurs at  $\text{pH} \leq 5.9$ . This proton-induced activation depends on glutamic acid and phenylalanine, and the negatively charged form of Glu is crucial for proton sensing (Jordt *et al.* 2000, Aneiros *et al.* 2011), as seen for TRPC4 and TRPC5. Similar to TRPV1, TRPV4 is activated by an extracellular pH below 6 (Suzuki *et al.* 2003).

- TRPA

Less studied is the TRPA subfamily, which is activated by acidic pH in a concentration-dependent manner. TRPA1 currents were induced until pH 5.4, and  $\text{Ca}^{2+}$  influx was around 50% enhanced at pH 6.0 and 5.0 compared to pH 6.4, indicating that TRPA1 induces  $\text{Ca}^{2+}$  entry upon acidification (de la Roche *et al.* 2013).

- ORAI/STIM complexes

In contrast to TRP channels, which show paradoxical results whether they are activated or inactivated by acidification, then it is well accepted that all three ORAI isoforms and at least STIM1 are inhibited by acidic pH's around 6 (Yu *et al.* 2018, Audero *et al.* 2022). In addition, they are activated upon alkalization at a pH of

about 8. Both effects have been studied in a wide range of cell lines and show that SOCE is decreased upon acidosis while enhanced by alkalization (Scrimgeour *et al.* 2012, Beck *et al.* 2014). Conserved intracellular and extracellular glutamate and histidine residues have been described as the pH sensitivity among all three ORAI isoforms (Tsujikawa *et al.* 2015). In addition, negatively charged amino acid residues of STIM1 also seem responsible for the  $\text{pH}_i$ -dependent inactivity of STIM1 (Tsujikawa *et al.* 2015). Interestingly, a recent study has shown that ORAI1 and ORAI2  $I_{\text{CRAC}}$  amplitudes depend on  $\text{pH}_i$  in the same manner, where ORAI3  $I_{\text{CRAC}}$  amplitude does not depend on  $\text{pH}_i$ , suggesting that the pH sensitivity is different among the three ORAI isoforms (Rychkov *et al.* 2022).

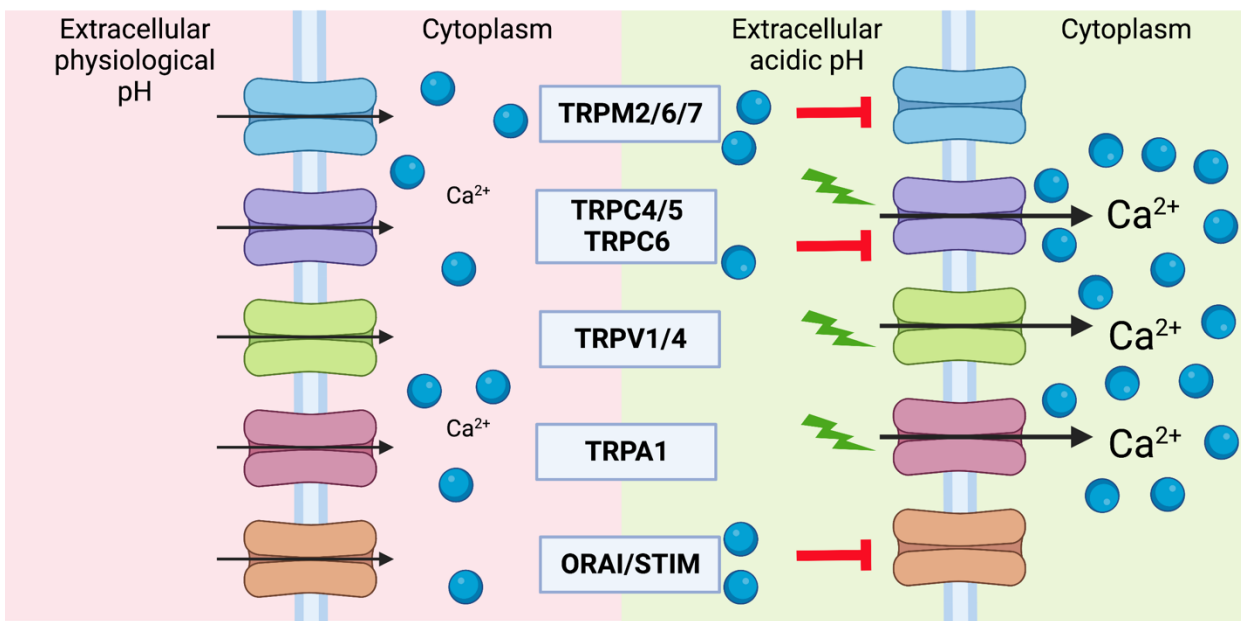


Figure 23. Graphical overview of  $\text{Ca}^{2+}$  channels known to be either inhibited or activated by acidic pH (Generated with Biorender).

## CHAPTER 4: The TRPC1 channel

### Classification of TRP channels

TRP genes were first described in *Drosophila melanogaster* in 1969. Studies of this fruit fly's visual system identified a visually impaired mutant fly with a transient response to steady light instead of a sustained electroretinogram, which was recorded in the wild-type fly. Thus, the mutant was named transient receptor potential (Cosens and Manning 1969). However, it was not until 1989 that the *trp* gene was identified by Montell and Rubin (Montell and Rubin 1989). To date, more than 100 *trp* genes have been identified across species, including 28 mammalian *TRP* genes. This superfamily is divided into seven subfamilies (mentioned in Transmembrane calcium channels), where the number of channels within one subfamily varies. They are distinguished from one another based on differences in their primary amino acid sequence rather than ligand affinity or selectivity (Nilius and Owsianik 2011). All TRP channels comprise six putative transmembrane spanning domains and a cation-permeable pore formed by a short hydrophobic region between transmembrane domains 5 and 6. TRP channels are widely expressed across tissues, including epithelial cells. They are activated by environmental stresses, such as; changes in temperature, pressure, pH, and osmolarity, as well as chemicals, hormones, and cytokines. In general, their activation is potentiated by PLC activation mediated by GPCRs. This activation leads to an inward current of  $\text{Ca}^{2+}$  and  $\text{Na}^{+}$  ions, defining that TRP channels are non-selective cation channels (Nilius and Owsianik 2011). However, some channels are more selective for  $\text{Ca}^{2+}$  than others (Vangeel and Voets 2019).

The first subfamily of mammalian TRP channels studied is the TRPC subfamily canonical TRP channels. TRPC channels can form homo or hetero-tetramers with other families of the TRP channel family. Like most other TRP channels, they function as  $\text{Ca}^{2+}$  permeable plasma membrane channels and display varying  $\text{Ca}^{2+}$  selectivity (Vangeel and Voets 2019, Wang *et al.* 2020). The following section will focus on the first identified TRPC member, TRPC1.

#### 1. TRPC1; Expression and structure

The TRPC family comprises seven members, and this TRP subfamily shares 30%–47% amino acid homology (Wang *et al.* 2020). The first identified member out of the seven in the TRPC subfamily is TRPC1. The DNA, an amino acid sequence, and the expression pattern of TRPC1 were published in 1995 (Wes *et al.* 1995, Zhu *et al.* 1995), followed by the first functional data in 1996 (Zitt *et al.* 1996). The human gene coding for TRPC1 is localized on chromosome 3, while the murine homolog is on chromosome 9. TRPC1 protein expression pattern is ubiquitously expressed across tissue types, with a low expression in the pancreas, compared to high expression in the retina and ovaries (Figure 24). The TRPC1 mRNA is expressed in five splice variants, but only three ( $\alpha$ ,  $\beta$ , and  $\epsilon$ ) seem to be translated and form functional proteins (Sakura and Ashcroft 1997, Ong *et al.* 2013). The predicted size of TRPC1 is around 90 KDa. However, in native tissues, the actual size was more

remarkable than first anticipated and can be explained by its glycosylation between the transmembrane domain 5 and the pore region (Rychkov and Barritt 2007).

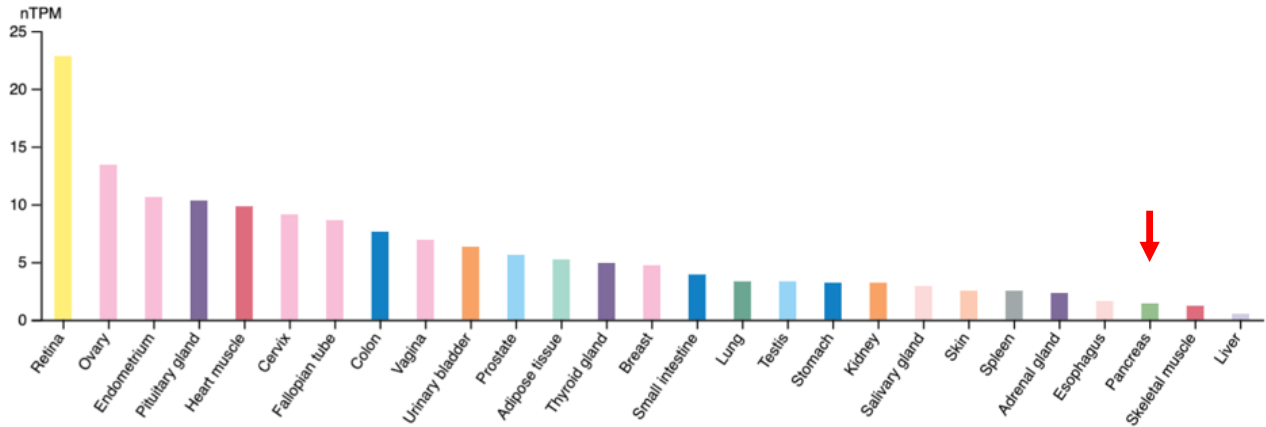


Figure 24. Protein expression of TRPC1 in different tissues. Generated with GTEx data and the human protein atlas. (nTPM: normalized protein-coding transcripts per million).

TRPC1 shows structural similarities with the other members of the TRPC subfamily (Nesin and Tsiokas 2014). The putative transmembrane structure of TRPC1 consists of the following (Figure 25):

- Coiled-coil domains in intracellular N- and C- termini, where the C-terminus is a proline-rich region
- Six membrane-spanning helices (S1-S6)
- A hydrophobic pore-forming loop (P), with negatively charged aspartic acid (D) and glutamic acid (E) residues, and a putative selectivity filter (SYGEE) between S5 and S6
- A TRP box/motif (EWKKFAR)
- A CaM-binding domain that partially overlaps with an IP<sub>3</sub>R-binding domain
- Four ankyrin repeats that may be important for binding and interactions with other proteins

The localization of TRPC1 in native tissues has been questioned. Indeed, in HEK and CHO cell models, TRPC1 localized in ER and intracellular vesicles (Alfonso *et al.* 2008, Cheng *et al.* 2011), whereas in tsA 201 cells, TRPC1 was localized in the plasma membrane (Barrera *et al.* 2007). TRPC1 has also been shown to localize in lipid raft domains (Lockwich *et al.* 2000). Besides, TRPC1 can form functional channels with other TRP family members. TRPC1 has been shown to form heterotetrameric channel complexes in the plasma membrane with TRPC3, -4, -5, 6- and -7 (Dietrich *et al.* 2014). Additionally, TRPC1 physically interacts with TRPP1 channels, which are mutated in patients with polycystic kidney disease (Bai *et al.* 2008). TRPC1 also interacts with the highly Ca<sup>2+</sup> selective channels TRPV6 and TRPV4. Apart from TRP channels, TRPC1 can also form a complex with ORAI1 and STIM1, which are implicated in SOCE (Ong *et al.* 2016). These findings clearly demonstrate that TRPC1 is functional, at least in heteromeric channel complexes.

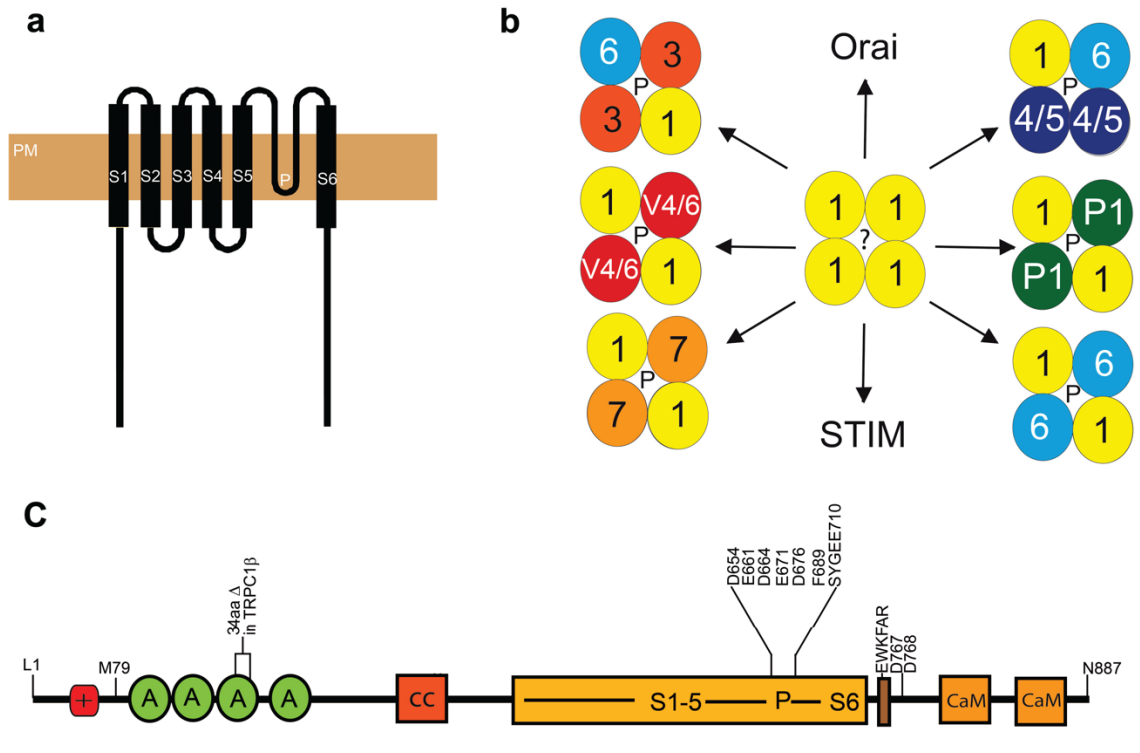


Figure 25. Overview of TRPC1 structure and interacting partners. A) TRPC1 topology in the plasma membrane indicating transmembrane regions (S1-S6) and pore domain. B) Heteromultimerisation potential of TRPC. Possible interacting partners from the TRP family, as well as ORAI and STIM proteins. C) Domain structure of TRPC1, as described in the text (Dietrich *et al.* 2014).

## 2. TRPC1; Activation and regulation

Various TRP channels are mechanosensitive, gated directly by physical forces like membrane stretch or temperature, biochemically by ligands, or downstream signaling cascades. TRP channels are involved in several cellular processes, including  $\text{Ca}^{2+}$  homeostasis, nociception, inflammation, and cell motility (Wang *et al.* 2020). In general terms, TRPC1 is a member of ion channels called ‘cellular sensors’ (Pedersen and Nilius 2007, Eijkelkamp *et al.* 2013). TRPC1 has shown to be activated via:

- Stretch; leading to TRPC1-dependent  $\text{Ca}^{2+}$  entry in several cell types, such as frog oocytes, cells from cerebral arteries, and skeletal and smooth muscle cells (Maroto *et al.* 2005, Dietrich *et al.* 2007, Formigli *et al.* 2009)
- Light; TRPC1-deficient mice exhibited nearly a 50% decrease in behavioral responses to both the light-stroke and light punctate mechanical assays (Garrison *et al.* 2012)
- Ambient pressure; TRPC1-mediated  $\text{Ca}^{2+}$  influx rises when PSCs are kept under elevated pressure (Staaf *et al.* 2009, Fels *et al.* 2016, Radoslavova *et al.* 2022)
- Hypoxia; TRPC1 expression is induced and mediates  $\text{Ca}^{2+}$  entry in non-cancerous and cancerous cell lines (Sukumaran *et al.* 2015, Azimi *et al.* 2017)
- Growth factors; EGF,  $\text{TGF}\beta$ , Platelet-derived growth factor (PDGF), and vascular endothelial growth factor (VEGF), lead to the regulation of different cellular processes involved in cancer progression

through TRPC1 and  $\text{Ca}^{2+}$  entry (Tajeddine and Gailly 2012, Asghar *et al.* 2015, Schaar *et al.* 2016, Azimi *et al.* 2017)

- Interaction with other proteins, such as GPCRs, other channels, and classical channel activations, such as store-depletion (Nesin and Tsiokas 2014, Ong *et al.* 2016). For instance, by forming a complex with the GTPase RhoA in intestinal epithelial cells (Chung *et al.* 2015)

### 3. The contribution of TRPC1 in the SOCE scenario

With the discovery of TRPC channels, none of these  $\text{Ca}^{2+}$  permeable channels seemed to generate currents that resembled  $I_{\text{CRAC}}$ . Thus, identifying the role of these channels and other regulatory components of SOCE led to the identification of the CRAC channel component ORAI1. This four-transmembrane domain protein assembles into a hexamer to form the pore of a CRAC channel (Ong *et al.* 2016). ORAI1 and two other isoforms (ORAI 2 and ORAI3) display store-dependent activation (Feske *et al.* 2006, Vig *et al.* 2006). Furthermore, were the STIM1 and STIM2 proteins identified as  $\text{Ca}^{2+}$  sensing proteins localized in the ER membrane, from where they sense intracellular  $\text{Ca}^{2+}$  levels and regulate SOCE (Cahalan 2009). It is now known that at least STIM1 can activate both ORAI1 and TRPC1 (Ambudkar *et al.* 2017). TRPC1 is reported to have a role in SOCE in various cell types. However, the contribution of TRPC1 in SOCE has not been consistent since several reports found that exogenous TRPC1 expression did not increase SOCE, while the KD of endogenous TRPC1 expression significantly decreased SOCE (DeHaven *et al.* 2009, Ong *et al.* 2016). The latter was found in different cell types, such as smooth muscle and endothelial cells, but interestingly also in human salivary glands and pancreatic acinar cells (Liu *et al.* 2007, Hong *et al.* 2011, Sun *et al.* 2015). Several studies in TRPC1 deficient mice (TRPC1<sup>-/-</sup>) displayed low SOCE, which decreased the  $\text{Ca}^{2+}$  dependent activation of  $\text{Ca}^{2+}$ -activated  $\text{K}^+$  channels ( $\text{K}_{\text{Ca}}$ ) and  $\text{Cl}^-$  channel activity, inhibiting fluid and protein secretion (Liu *et al.* 2007, Hong *et al.* 2011, Sun *et al.* 2015). Notably, the expression of ORAI1 did not change in the salivary gland or pancreatic acinar cells from the TRPC1<sup>-/-</sup> mice, meaning that this channel does not compensate for the lack of TRPC1 or support the  $\text{Ca}^{2+}$  signaling on its own. In these secretory glands, the decreased secretion is primarily a result of the loss of TRPC1-mediated SOCE (Hong *et al.* 2011).

Albeit from these results, other reports show that ORAI1 is required for TRPC1 function, as silencing of ORAI1 abolished TRPC1 channel activation, despite the presence of STIM1. Here, it was shown that the  $\text{Ca}^{2+}$  influx through ORAI1 triggered the insertion of TRPC1 in the plasma membrane. Furthermore, is STIM1 required for TRPC1 channel activation, as a KD of STIM1 reduced endogenous TRPC1-mediated SOCE and  $\text{Ca}^{2+}$  current, whereas co-expression of both TRPC1 and STIM1 enhanced SOCE (Ong *et al.* 2007). ORAI1 and STIM1 form a complex with TRPC1 in response to ER  $\text{Ca}^{2+}$  store depletion in several cell types, including salivary gland and pancreatic acinar cells (Ong *et al.* 2007, Lu *et al.* 2010, Zhang *et al.* 2010, Almirza *et al.* 2012, Ng *et al.* 2012, Pani *et al.* 2013). Co-localization experiments revealed that TRPC1 localized in the same ER-plasma membrane junctions where the ORAI1/STIM1 complex was localized. This localization allows for



Ca<sup>2+</sup> entry through TRPC1 by assembling with STIM1 (Ong *et al.* 2007, Cheng *et al.* 2008, Kim *et al.* 2009, Cheng *et al.* 2011).

Additionally, the lipid raft domain caveolae-residing protein, caveolin-1 (Cav-1), is an essential modifier of TRPC1 activity and plasma membrane localization depends on this protein. When Cav-1 is lacking, TRPC1 displays abnormal localization and is not able to interact with STIM1, which is essential for the TRPC1 activation and SOCE (Pani *et al.* 2009, Pani *et al.* 2013, Lee *et al.* 2014). TRPC1 localization and trafficking can also be modulated by several cytoskeletal and microtubule proteins. It has been shown that the monomeric GTPase, RhoA, promotes TRPC1 translocation to the plasma membrane in pulmonary artery endothelial cells and intestinal epithelial cells (Mehta *et al.* 2003, Chung *et al.* 2015). Whilst in retinal epithelial cells,  $\beta$ -tubulin determines the plasma membrane expression of TRPC1 (Bollimuntha *et al.* 2005). The inhibition of TRPC1 of either RhoA or  $\beta$ -tubulin abolished SOCE (Mehta *et al.* 2003, Bollimuntha *et al.* 2005, Chung *et al.* 2015).

Taken together, TRPC1 can interact with STIM1 and form a SOC that generates an I<sub>SOC</sub> current. When TRPC1 interacts with ORAI1 and STIM1, it can participate in the generation of the I<sub>CRAC</sub> or I<sub>SOC</sub> current (Figure 26). Furthermore, its interaction with other proteins is required for TRPC1 plasma membrane localization where SOCE is regulated.

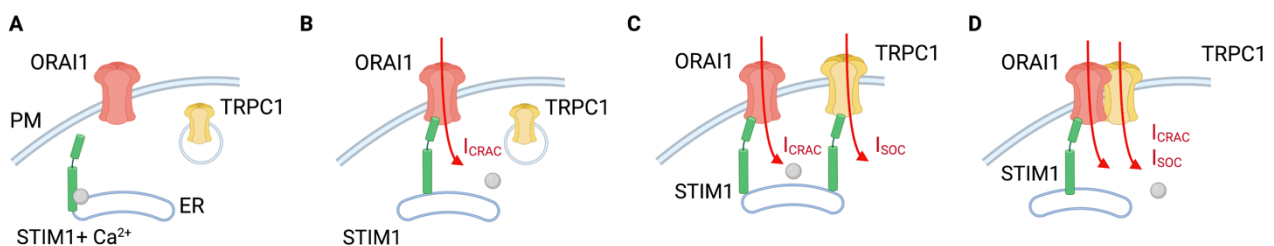


Figure 26. Hypothetical models of TRPC1 to store-operated Ca<sup>2+</sup> entry. A) When in resting conditions, TRPC1 resides in the intracellular compartments or vesicles. Upon activation, B) ORAI1 interacts with STIM1 (in the ER) and creates an I<sub>CRAC</sub> current, and TRPC1 will move to the plasma membrane (PM) as shown in C) where TRPC1 interacts with STIM1 and create an I<sub>SOC</sub> current. The last scenario in D) is where TRPC1 will form a complex with ORAI1 and contribute to an I<sub>CRAC</sub> and/or I<sub>SOC</sub> current (Generated with Biorender).

#### 4. Pharmacological inhibition of TRPC1

To date, no pharmacological inhibitors have proven to be specific and selective for TRPC1. It is typically genetically encoded approaches used to decrease the expression and function of TRPC1, such as small-interfering RNA (siRNA) or short-hairpin RNA (shRNA) strategies (Zhong *et al.* 2022). TRP channels can be inhibited by the lanthanides La<sup>3+</sup> and Gd<sup>3+</sup>, which are widely used in electrophysiological experiments (Bouron *et al.* 2015).

Some pharmacological inhibitors often utilized are SOC inhibitors 2-APB, SKF96365, and MRS1845. 2-aminoethoxydiphenyl borate (2-ABP) is frequently used as a reasonably non-selected SOC inhibitor but was

initially discovered as an IP<sub>3</sub>R inhibitor. Similarly, SKF96365 was developed to inhibit receptor-mediated Ca<sup>2+</sup> entry, but the compounds showed pleiotropic effects, as it inhibits SOCE via STIM1 and several TRPC channels, as well as voltage-gated Ca<sup>2+</sup> and K<sup>+</sup> channels. Furthermore, the dihydropyridine MRS1845 has been reported to inhibit the SOCE pathway (Gautier *et al.* 2014). However, its potential effect on TRPC1 has now been proven in electrophysiological studies. Interestingly, compounds including AM12, AC1903, Clemizole, Galangin, M084, and PICO 145 have been described as more specific antagonists of TRPC1 in combination with TRPC4 and TRPC5 (Elzamzamy *et al.* 2020).

## 5. TRPC1 in pathologies

### *A focus on cancer*

The biological role of TRPC1 has been studied in genetically engineered TRPC1<sup>-/-</sup> mouse models. Although the mice survived TRPC1 depletion, they showed defects in several organs and tissues, and this loss of TRPC1 leads to the decreased fluid secretion of exocrine glands such as salivary glands and pancreatic acinar cells (Nesin and Tsiokas 2014). Furthermore, the TRPC1 deficiency showed; reduced response to hemodynamic stress in terms of developing cardiac hypertrophy; slow regeneration of skeletal muscle cells; dysfunctional development and growth of bones; reduced production of cytokines and chemokines; increased development of lung edemas; reduced vascular remodeling after chronic hypoxia; epilepsy-induced neurodegeneration, and increased unfolded protein response and a reduced number of dopaminergic neurons concerning Parkinson's disease (Dietrich *et al.* 2014, Nesin and Tsiokas 2014).

Widely studied is the implication of TRPC1 in cancer progression. Numerous studies have shown that dysregulation of TRPC1, both beside and through Ca<sup>2+</sup> entry, and as a biomarker of several types of cancer (Elzamzamy *et al.* 2020). The following section will summarize the role of TRPC1 in different kinds of cancer.

- **Breast cancer**

TRPC1 has been widely studied in breast cancer (Elzamzamy *et al.* 2020). Azimi *et al.* found that TRPC1 was overexpressed in MDA-MB-468, MDA-MB-231, and HCC1569 breast cancer cell lines under hypoxic conditions, which increased expression of Snail, Vimentin, and Twist, leading to EMT. This effect was regulated through an AKT/HIF1 $\alpha$  pathway. Furthermore, it was found that reducing TRPC1 expression under hypoxic conditions decreased basal Ca<sup>2+</sup> entry (Azimi *et al.* 2017). However, silencing of TRPC1 slightly increased SOCE activity, indicating that the TRPC1/AKT/HIF1 $\alpha$  pathway regulating EMT is SOCE-independent. AKT/TRPC1 dependency was shown in another study where downregulation of TRPC1 reduced the activation of AKT (Kaemmerer *et al.* 2018). Schaar *et al.* found that TRPC1-mediated SOCE in TGF $\beta$  stimulated breast cell lines and breast cancer cell lines, which resulted in increased calpain activity and, thus, EMT and cell migration (Schaar *et al.* 2016). Davis *et al.* showed that silencing of TRPC1 inhibited constitutively active ERK1/2 and led to S-phase reduction and, thus, attenuation of cell proliferation. However, this seemed to be in a SOCE-independent manner as the downregulation of TRPC1 also slightly increased

SOCE (Davis *et al.* 2012). In a phenotypic distant breast cancer cell line, MCF-7, the silencing of TRPC1 attenuated ERK1/2 phosphorylation mediated by the activation of the Ca<sup>2+</sup>-sensing receptor (CaR), thus arresting cells in the G1 phase and decreasing cell proliferation (El Hiani *et al.* 2006, El Hiani *et al.* 2009). Furthermore, a feed-forward loop was described where TRPC1 expression required activation of EGFR and ERK activity (El Hiani *et al.* 2009, El Hiani *et al.* 2009). In the same cell line was, cell cycle progression dependent on TRPC1 expression mediating the activity of KCa3.1 (Faouzi *et al.* 2016). The role of TRPC1 was MCF7 cells is dependent on Ca<sup>2+</sup> entry (El Hiani *et al.* 2009, El Hiani *et al.* 2009, Faouzi *et al.* 2016). Several studies have found that TRPC1 is upregulated in human breast cancer tissue, which correlates with TNM stage, clinical stage, and lymph node metastasis (Dhennin-Duthille *et al.* 2011, Mandavilli *et al.* 2012, Zhang *et al.* 2020). However, a recent study has shown a high TRPC1 expression in different breast cancer compared to a corresponding normal-like cell line. Here, they found that the increased expression of TRPC1 inhibited the expression of AKT and EMT markers leading to subsequent inhibition of cell proliferation, migration, and invasion. Furthermore, they found that upregulation of TRPC1 in breast tumor tissue correlated with a better prognosis in estrogen receptor<sup>+</sup> patients (Zhang *et al.* 2020). These contradictory results indicate that TRPC1, in some breast cancer patient populations, seems to have a protective effect while showing a more aggressive role in others.

- Lung cancer

In the lung cancer cell line A549, exposure to high nicotine levels resulted in increased HIF1 $\alpha$  levels, leading to an upregulation of the SOC components, ORAI1, TRPC6, and TRPC1, as found in breast cancer (Azimi *et al.* 2017, Wang *et al.* 2018). On the other hand, the downregulation of HIF1 $\alpha$  was associated with low levels of ORAI1, TRPC6, and TRPC1, decreasing cell proliferation. Interestingly, high nicotine levels were related to enhanced basal intracellular Ca<sup>2+</sup> concentrations. Downregulation of TRPC1 decreased hypoxia-induced autophagy, which is known to promote survival in hypoxic environments (Wang *et al.* 2018). Another report demonstrated in the same cell line that silencing of TRPC1 decreased the expression of cyclins D1 and D3 along with induced G0/G1 cell cycle arrest, resulting in reduced cell growth. This TRPC1 silencing was associated with a decreased phosphorylation and activation of EGFR and subsequent disruption of AKT and ERK pathways. The stimulation of EGFR led to induced TRPC1-mediated SOCE (Tajeddine and Gailly 2012). Moreover, another study showed that inhibition with 2-ABP or a specific TRPC1 inhibiting antibody (T1E3) repressed cell proliferation (Jiang *et al.* 2013). Several studies have demonstrated that a high expression of TRPC1 in non-small cell lung cancer (NSCLC) human specimens correlated with well-differentiated tumors, advanced TNM stage, and low disease-free survival (Jiang *et al.* 2013, Ke and Long 2022).

- Colorectal cancer

TRPC1 has been shown to be overexpressed in several colorectal cancer (CRC) cell lines (HT29, HCT116, SW620, SW480, and CaCo2, compared to a corresponding normal-like cell line (Sobradillo *et al.* 2014, Sun

*et al.* 2021). Even though SOCE is highly upregulated in several of these cell lines, TRPC1 silencing has until now only been shown to significantly decrease SOCE levels in SW620 and HCT116 cells (Gueguinou *et al.* 2016, Sun *et al.* 2021). However, TRPC1 seems to have a role in CRC progression. It was demonstrated that reducing TRPC1 expression levels and disrupting a complex consisting of TRPC1, ORAI1, and the Ca<sup>2+</sup>-activated K<sup>+</sup> channel (SK3) in the lipid rafts led to decreased cell migration. It was shown that this mechanism was regulating migration via AKT and EGFR activation in a Ca<sup>2+</sup>-dependent manner (Gueguinou *et al.* 2016). In a recent study, it was demonstrated that TRPC1 regulated CRC cell and tumor growth and metastasis by forming a complex with CaM and PI3K (Sun *et al.* 2021). *In vitro*, silencing of TRPC1 inhibited cell migration, EMT, and invasion, decreased expression levels of Cyclin B1 and CDK1, and accumulated cells in G2/M phases, leading to reduced cell proliferation. *In vivo*, TRPC1 silencing decreased tumor growth and metastasis, and tumorigenesis was attenuated in TRPC1<sup>-/-</sup> mice. In contrast, the upregulation of TRPC1 promoted cell growth and migration, both *in vitro* and *in vivo*. TRPC1 interacted and co-localized with both PI3K and CaM. In addition, AKT activation induced by an overexpression of TRPC1 was decreased upon inhibition of the PI3K with LY294002 (Sun *et al.* 2021). Furthermore, TRPC1 was upregulated in human CRC tissue samples, which correlated with a poor prognosis in the form of low survival (Ibrahim *et al.* 2019, Sun *et al.* 2021).

- Prostate

It has been shown that TRPC1 is a SOC component in LNCaP and ATP-stimulated primary human prostate cancer epithelial cells, and the silencing of TRPC1 decreases SOCE levels (Vanden Abeele *et al.* 2003, Pigozzi *et al.* 2006, Thebault *et al.* 2006). However, the expression levels of TRPC1 are known to decrease with the progression of prostate cancer from androgen-dependent to androgen-independent (Shapovalov *et al.* 2016). In addition, one study has demonstrated that TRPC1 expression was increased in the early stages of prostate cancer compared to late stages and that the high expression was associated with lower proliferation and more prolonged recurrence-free survival (Perrouin Verbe *et al.* 2016, Perrouin-Verbe *et al.* 2019). These results suggest that TRPC1 could have a protective role in prostate cancer.

- Glioblastoma and neuroblastoma

In a glioma/glioblastoma multiforme (GBM) cell model, D54MG cells, the inhibition of SOCE inhibitors 2-APB, SKF96365, and MRS1845, significantly decreased both Ca<sup>2+</sup> influx and proliferation, as well as the formation of multinucleated cells, a known characteristic of GBM (Bomben and Sontheimer 2010). Specific inhibition of TRPC1 with either a polyclonal-TRPC1 antibody or shRNA targeting decreased Ca<sup>2+</sup> entry significantly (Bomben and Sontheimer 2010). This inhibition led to reduced proliferation and enlargement of multinucleated cells (Bomben and Sontheimer 2010). The role of TRPC1 in GBM was assessed *in vivo* by injecting mice with glioma cells that ectopically expressed a doxycycline-inducible shRNA targeting TRPC1. Mice with this inducible TRPC1 KD exhibited a smaller tumor size than mice with a wild-type TRPC1 expression (Bomben and Sontheimer 2010). Another study demonstrated that TRPC1 co-localized with Cav-

1 in the lipid rafts of the leading edge of D54MG cells (Bomben *et al.* 2011). This localization involved chemotaxis and directional migration of cells towards EGF, as the mechanism was attenuated upon TRPC1 silencing (Bomben *et al.* 2011). The use of SOCE inhibitors MRS1845 and SKF96365 inhibited glioma cell migration, suggesting that  $\text{Ca}^{2+}$  signaling is involved in this migration process (Bomben *et al.* 2011).

The role of TRPC1 has been studied in SH-SY5Y neuroblastoma cells. It was shown that SH-SY5Y cells treated with an exogenous neurotoxin, 1-methyl-4-phenylpyridinium ion ( $\text{MPP}^+$ ), exhibited low TRPC1 protein and mRNA expression (Bollimuntha *et al.* 2005). The inhibition with  $\text{MPP}^+$  induced translocation of TRPC1 from the plasma membrane to the cytosol. They found that overexpression of TRPC1 maintained the plasma membrane localization, even upon  $\text{MPP}^+$  treatment. In addition, they demonstrated that TRPC1 overexpression protected SH-SY5Y cells from cell death upon  $\text{MPP}^+$  treatment. On the contrary, TRPC1 silencing could not protect cells from cell death. This protection partially depended on a  $\text{Ca}^{2+}$  influx (Bollimuntha *et al.* 2005).

- **Hepatocellular carcinoma**

In the hepatocellular carcinoma cell line Huh7, the KD of TRPC1 increased SOCE levels and suppressed cell proliferation (Selli *et al.* 2015). The same authors found that silencing of TRPC1 in Huh7 cells changed the SOC and proliferation gene expression pattern (Selli *et al.* 2016). Different genes of the MAPK signaling pathway were upregulated upon TRPC1 silencing. The same was found for the cell cycle progression regulating genes CDK11A/B and URGCP (Up-regulator of Cell Proliferation). Interestingly, STIM1 was reciprocally upregulated, suggesting a compensatory role of STIM1 in TRPC1-deficient Huh7 cells (Selli *et al.* 2016).

- **Nasopharyngeal carcinoma and thyroid cancer**

In a study in a nasopharyngeal carcinoma cell line, CNE2, it was demonstrated that both shRNA silencing of TRPC1 and 2-ABP treatment decreased the expression levels of TRPC1. Both types of TRPC1 abolishment decreased expression of MMP2 and 9, resulting in reduced CNE2 cell migration and invasion. It was not further investigated if the inhibition of TRPC1 affected  $\text{Ca}^{2+}$  entry (He *et al.* 2012).

In the endocrine follicular thyroid cancer cell line ML-1, the silencing of TRPC1 resulted in the attenuation of sphingosine-1 (SP-1) induced proliferation, invasion, and migration (Asghar *et al.* 2015). TRPC1 KD decreased SOCE upon SP-1 stimulation but failed to inhibit both basal  $\text{Ca}^{2+}$  entry and SOCE. Furthermore, the SP1 receptor, VGFR, HIF1 $\alpha$ , MMP2, and 9 decreased upon TRPC1 silencing and CaM inhibition. Along was a decrease in the expression of PKC isoforms, ERK1/2, cyclin D2, and D3 CDK6, and an upregulation of p21 and p27, which resulted in a significant increase in cell population in the G0/G1 phase, and a substantial decrease in S and G2 phases (Asghar *et al.* 2015). These results suggest that TRPC1 regulates thyroid cell proliferation, invasion, and downstream migration mechanisms.

- Ovarian and endometrial cancer

The role of TRPC1 in ovarian cancer was investigated in a cell line called SKOV-3. First, the two SOCE inhibitors, 2-ABP and SKF96365, decreased cell proliferation in a concentration-dependent manner. Next, cell proliferation was enhanced by stimulation with trypsin. Both antibody inhibition of TRPC1 and siRNA transfection reduced the proliferation rate of SKOV-3 cells, whereas overexpression of TRPC1 promoted cell proliferation and colony formation (Zeng *et al.* 2013). The inhibition of SKOV-3 cell proliferation could result from the decreased number in the G2/M cell cycle phases upon the inhibition of SK96365 or TRPC1 silencing. Furthermore, the expression of TRPC1 was investigated in human tissue samples where the mRNA TRPC1 expression was significantly lower in undifferentiated ovarian cancer than in normal ovarian tissue (Zeng *et al.* 2013). Similar results were found upon IHC analysis where the expression of TRPC1 was significantly lower in undifferentiated tissue (Grade 3) compared to well-differentiated tissue (Grade 1-2) (Zeng *et al.* 2013). Microarray analysis showed that TRPC1 was downregulated in human ovarian cancer samples, compared to adjacent tissue samples, and in drug-resistant ovarian cancer cell lines, compared to sensitive cell lines (Liu *et al.* 2016). mRNA-microRNA analysis showed that TRPC1 was interacting with several genes involved in the drug resistance of ovarian cancer. Additionally, the authors made a TCGA investigation which revealed that TRPC1 expressions were lower the higher the histological grade (Liu *et al.* 2016).

The role of TRPC1 in endometrial carcinoma is poorly understood among many other cancers. However, one study made a TCGA and micro-array-based investigation. Here, they found that a high expression of TRPC1 in samples from endometrial cancer patients was correlated with low overall survival, even though the expression of TRPC1 was downregulated between endometrial cancer and adjacent tissue samples (Wang *et al.* 2021).

- Tongue-, esophageal-, and gastric cancer

TRPC1 is overexpressed in tongue squamous cell carcinoma (TSCC) cell lines and tissue, compared to a normal control cell line and adjacent tissue (Xu *et al.* 2017). The high protein expression of TRPC1 in TSCC specimens was significantly correlated with EphA2, ephrinA1, e-NOS, VEGF-A expression, and microvessel density, indicative markers of angiogenesis upregulation. In terms of prognosis, high TRPC1 expression was positively correlated with clinical stage, lymph node metastasis, and tumor differentiation of TSCC (Xu *et al.* 2017). In a recent study, it was demonstrated by IHC analysis and mRNA expression that TRPC1 was a good value for differentiating TSCC tissue from adjacent tissue. The high expression of TRPC1 positively correlated with pathological grade and lymph node metastasis. However, a high TRPC1 expression negatively correlated with overall survival, especially in patients who received adjuvant radiotherapy (Shi *et al.* 2022).

The role of TRPC1 in esophageal cancer cell lines is, to some extent, a little complicated. EC9706 cells, which natively have a high expression of TRPC1, were transfected with siRNA targeting TRPC1,



resulting in increased cell proliferation, migration, and invasion rates (Zeng *et al.* 2021). Intriguingly, the KD of TRPC1 induced the activation of AKT and the levels of p27. In the KYSE150 cells, natively expressing low levels of TRPC1, overexpression resulted in decreased proliferation, migration, and invasion rates, along with reduced activation of AKT and p27 (Zeng *et al.* 2021). The authors performed IHC analysis on human esophageal cancer samples, where they found a low expression compared to adjacent tissue. The low expression correlated with high proliferation, lymph node metastasis, and low survival (Zeng *et al.* 2021).

TRPC1 was involved in TGF $\beta$  induced EMT in a gastric cancer cell line, SGC-7901 cells. Specific TRPC1 silencing and inhibition with SKF96365 and 2-APB increased mRNA and protein levels of E-cadherin and decreased the levels of vimentin and  $\alpha$ -SMA. The inhibition with SKF96365 and 2-APB significantly reduced protein levels of TRPC1 along with Ras and Raf1 and the phosphorylation of ERK1/2, suggesting that the MAPK signaling pathway is involved in EMT of gastric cancer cells (Ge *et al.* 2018)

Zhiyong *et al.* developed two stable gastric cancer cell lines; BGC-823 cells with a low expression of TRPC1 and MKN-45 cells with a high expression of TRPC1 (Zhang *et al.* 2020). While BGC-823, with low TRPC1, exhibited decreased cell migration, MKN-45, with a high TRPC1 expression, displayed enhanced cell migration. The authors speculated if miRNA involved in the pathogenesis of gastric cancer could regulate TRPC1 expression. By a database prediction, they found that miR-135a-5p could be a possible TRPC1 target. This mechanism was further analyzed and confirmed by luciferase, qRT-PCR, and protein expression assays demonstrating that co-transfection with miR-135a-5p decreased and increased TRPC1 levels in BGC-823 and MKN-45 cells, respectively (Zhang *et al.* 2020). Furthermore, they found that a circulating RNA (ciRS-7) acted as a sponge of miR-135a-5p and reversed miR-135a-5p-mediated downregulation of TRPC1. In addition, they demonstrated that both TRPC1 and ciRS-7 were upregulated in human gastric cancer tissue, which correlated with low survival (Zhang *et al.* 2020).

- **Renal Cell Carcinoma**

It has recently been shown that TRPC1 is overexpressed in renal cell carcinoma (Chen *et al.* 2022). IHC analysis and qRT-PCR demonstrated that TRPC1 levels were elevated in human tissue samples from renal cell carcinoma patients. Here, the high TRPC1 expression did not correlate with tumor properties. However, an increased expression of TRPC1 protein, but not mRNA, was associated with a low overall survival (Chen *et al.* 2022).

## 6. TRPC1 in the pancreatic tumor microenvironment

A high expression of TRPC1 and TRPC4 and TRPC6 has been found in the PDAC cell line BxPC-3. Here, TRPC1 increased intracellular Ca<sup>2+</sup> levels upon TGF $\beta$  stimulation, followed by PKC- $\alpha$  activation, initiating cell motility and migration (Chow *et al.* 2008, Dong *et al.* 2010). The authors proved this with three approaches; (1) Pharmacological inhibition of SOCE with 2-ABP and La<sup>3+</sup>, which abolished the TGF $\beta$ -



mediated  $\text{Ca}^{2+}$  entry. (2) Blocking of PKC- $\alpha$  with selective inhibitors inhibited the TGF $\beta$ -induced  $\text{Ca}^{2+}$  entry, and (3) KD of TRPC1, but not the KD of TRPC4 or TRPC6, reversed the TGF $\beta$ -induced motility and migration (Dong et al. 2010).

TRPC1 has been associated with pressure-induced activation of PSC (Fels et al. 2016, Radoslavova et al. 2022). In both murine and human PSCs, TRPC1 partially mediate PSC activation under high pressure by promoting  $\alpha$ SMA expression. Elevated pressure increased the stiffness and the emitted traction forces of PSCs in a TRPC1-dependent manner. Furthermore, TRPC1 cooperated with the phosphorylated form of SMAD2 and regulated cell cycle progression and interleukin-6 (IL-6) secretion through an ERK1/2 and SMAD2-dependent pathway (Radoslavova et al. 2022). In addition, pressure-induced activation of PSCs leads to TRPC1-dependent stimulation of migration and  $\text{Ca}^{2+}$  influx (Fels et al. 2016).

Taken together, there is sparse evidence about the role of TRPC1 in the pancreatic tumor microenvironment.

## 7. The TRPC1 interactome

Besides interacting with other ion channels (especially TRPCs), TRPC1 interacts with other regulatory and scaffolding proteins to regulate downstream processes. Indeed, TRPC1 forms a complex with ORAI1 and STIM1 in the lipid rafts to allow the activation of SOCE. Additionally, the plasma membrane localization of TRPC1 is promoted by the monomeric GTPase, RhoA, as described in ‘The contribution of TRPC1 in the SOCE scenario’. Upon thrombin activation, RhoA interacts with IP<sub>3</sub>R and TRPC1 in the plasma membrane of pulmonary artery endothelial cells, which is required for  $\text{Ca}^{2+}$  entry. This Rho-activated  $\text{Ca}^{2+}$  entry through TRPC1 enhances endothelial permeability (Mehta et al. 2003). In intestinal epithelial cells, the physical interaction between RhoA and TRPC1 mediates SOCE and stimulates cell migration after wounding (Chung et al. 2015). Besides RhoA, the Rho GTPase Rac1 and TRPC1 are associated with colon cancer cell migration by being involved in a complex positive feedback loop. SOCE induced by EGF activates Rac1 and STIM1 through the AKT pathway, which in turn promotes the translocalization of a TRPC1/SK3/ORAI1 complex into the lipid rafts, which triggers SOCE. Simultaneously, AKT-mediated Rac1 activation promotes SOCE-dependent cell migration through the AKT pathway, leading to lamellipodia formation and calpain activation (Gueguinou et al. 2016).

TRPC1 interacts with other membrane-bound proteins, such as metabotropic glutamate receptors, tumor necrosis factor receptors, and growth factor receptors (Nesin and Tsiokas 2014). For instance, in isolated rat embryonic neural stem cells, TRPC1 physically interacts with the fibroblast growth factor receptor (FGFR-1). The silencing of TRPC1 suppresses  $\text{Ca}^{2+}$  entry, cation conductance, and cell proliferation of these cells (Fiorio Pla *et al.* 2005).

Furthermore, TRPC1 interacts with cytosolic proteins, such as Homer protein, caveolins, and CaM (Ong and Ambudkar 2011, Nesin and Tsiokas 2014). Deleting the second CaM binding domain in the C-terminal tail of TRPC1 resulted in a  $\text{Ca}^{2+}$ -dependent inactivation of SOC currents in human salivary gland

cells, suggesting that TRPC1 displays  $\text{Ca}^{2+}$ -dependent inactivation (Singh *et al.* 2002). Additionally, as described above (in TRPC1 in the pancreatic tumor microenvironment), our group has recently shown that TRPC1 forms a complex  $\alpha$ SMA and phosphorylated SMAD2 in PSCs (Radoslavova *et al.* 2022). Interestingly, TRPC1 interacts with PI3K and CaM in colorectal cancer cells, regulating tumor growth and metastasis (as described in TRPC1 in pathologies; colon cancer).

Taken together, several reports suggest that TRPC1 channel activity can rely on the interaction with different partner proteins, such as other ion channels, GTPases, other cytosolic proteins, and membrane-bound proteins. The interaction of TRPC1 with various proteins involved in up- and downstream mechanisms of several signaling cascades emphasizes the importance of a TRPC1 interactome (Figure 27).

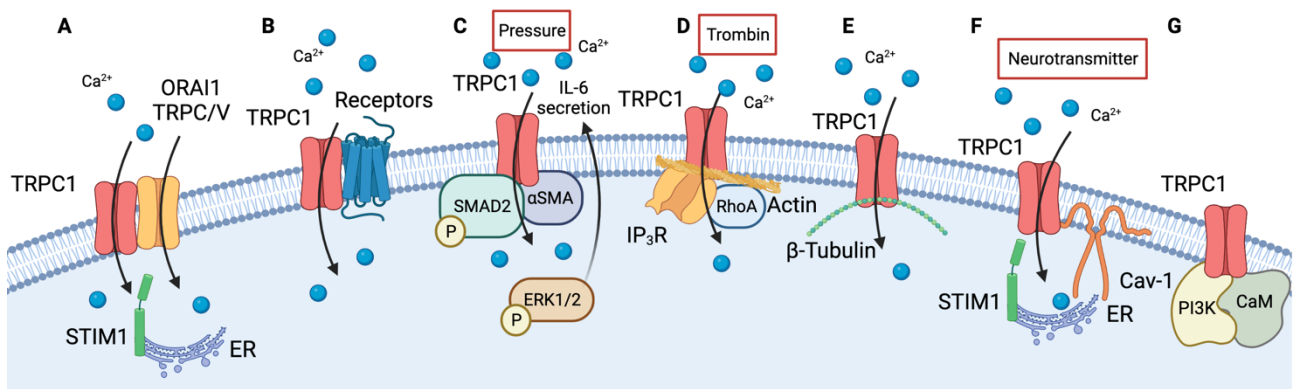


Figure 27. Illustration of TRPC1 as an interactome. A) TRPC1 can interact with other ion channels, such as ORAI1, STIM1, TRPCs, or TRPVs leading to  $\text{Ca}^{2+}$  entry. B) TRPC1 can interact with receptors, such as growth factor receptors. C) Pressure activates TRPC1, which forms a complex with SMAD2 and  $\alpha$ SMA that activates ERK1/2, leading to IL-6 secretion. D) Thrombin enhances the formation of a TRPC1/RhoA/IP3R complex in an actin filament polymerization-dependent manner, leading to SOCE. E) TRPC1 interacts with  $\beta$ -tubulin, which promotes plasma membrane localization and  $\text{Ca}^{2+}$  entry. D) Agonist-stimulation promotes TRPC1 to form a complex with Cav-1 in the plasma membrane. This complex is needed for TRPC1 to interact with STIM1 and allow  $\text{Ca}^{2+}$  entry. G) TRPC1 forms a complex with PI3K and CaM (Generated with Biorender).



# Ion Channel Signature in Healthy Pancreas and Pancreatic Ductal Adenocarcinoma

Julie Schnipper<sup>1</sup>, Isabelle Dhennin-Duthille<sup>1</sup>, Ahmed Ahidouch<sup>1,2</sup> and Halima Ouadid-Ahidouch<sup>1\*</sup>

<sup>1</sup> Laboratory of Cellular and Molecular Physiology, UR-4667, University of Picardie Jules Verne, Amiens, France,

<sup>2</sup> Department of Biology, Faculty of Sciences, Ibn Zohr University, Agadir, Morocco

## OPEN ACCESS

### Edited by:

Sébastien Roger,  
Université de Tours, France

### Reviewed by:

David Cottès,  
University of California, San Francisco,  
United States

Nelson Shu-Sang Yee,  
Penn State Milton S. Hershey Medical  
Center, United States

### \*Correspondence:

Halima Ouadid-Ahidouch  
halima.ahidouch-ouadid@u-picardie.fr

### Specialty section:

This article was submitted to  
Pharmacology of Ion Channels  
and Channelopathies,  
a section of the journal  
Frontiers in Pharmacology

**Received:** 02 June 2020

**Accepted:** 16 September 2020

**Published:** 16 October 2020

### Citation:

Schnipper J, Dhennin-Duthille I,  
Ahidouch A and Ouadid-Ahidouch H  
(2020) Ion Channel Signature in  
Healthy Pancreas and Pancreatic  
Ductal Adenocarcinoma.  
*Front. Pharmacol.* 11:568993.  
doi: 10.3389/fphar.2020.568993

Pancreatic ductal adenocarcinoma (PDAC) is the fourth most common cause of cancer-related deaths in United States and Europe. It is predicted that PDAC will become the second leading cause of cancer-related deaths during the next decades. The development of PDAC is not well understood, however, studies have shown that dysregulated exocrine pancreatic fluid secretion can contribute to pathologies of exocrine pancreas, including PDAC. The major roles of healthy exocrine pancreatic tissue are secretion of enzymes and bicarbonate rich fluid, where ion channels participate to fine-tune these biological processes. It is well known that ion channels located in the plasma membrane regulate multiple cellular functions and are involved in the communication between extracellular events and intracellular signaling pathways and can function as signal transducers themselves. Hereby, they contribute to maintain resting membrane potential, electrical signaling in excitable cells, and ion homeostasis. Despite their contribution to basic cellular processes, ion channels are also involved in the malignant transformation from a normal to a malignant phenotype. Aberrant expression and activity of ion channels have an impact on essentially all hallmarks of cancer defined as; uncontrolled proliferation, evasion of apoptosis, sustained angiogenesis and promotion of invasion and migration. Research indicates that certain ion channels are involved in the aberrant tumor growth and metastatic processes of PDAC. The purpose of this review is to summarize the important expression, localization, and function of ion channels in normal exocrine pancreatic tissue and how they are involved in PDAC progression and development. As ion channels are suggested to be potential targets of treatment they are furthermore suggested to be biomarkers of different cancers. Therefore, we describe the importance of ion channels in PDAC as markers of diagnosis and clinical factors.

**Keywords:** ion channels, exocrine pancreas, pancreatic ductal adenocarcinoma, signaling pathways, biomarkers

## INTRODUCTION

Ion channels are plasma membrane spanning proteins found in all human tissues, allowing rapid transport of ions and fluids between the extracellular and intracellular milieu (Niemeyer et al., 2001; Gouaux and Mackinnon, 2005). Opening of ion channels can result in redistribution of different ions, which changes the electrical and chemical properties of the cell leading to several cellular processes (Roux, 2017). These include multiple signal transduction and downstream signaling events, including regulation of gene expression, secretion of enzymes and hormones, and intracellular communication between compartments (Chen et al., 1994; Tolon et al., 1996; Stock and Schwab, 2015). A stable regulation of these processes maintains normal tissue homeostasis, such as cell cycle progression, migration, and apoptosis (Kunzelmann, 2005; Kunzelmann, 2016; Prevarskaya et al., 2018; Anderson et al., 2019). Accordingly, dysregulated expression as well as altered function of ion channels are related to a great number of diseases (Kim, 2014), and can drive the transformation from normal to malignant cell behavior (Litan and Langhans, 2015). Over the past decades, aberrant and even cancer-specific expression of numerous ion channels have been demonstrated in various types of cancers (Pedersen and Stock, 2013; Djamgoz et al., 2014). Together, the abnormal expression and activity of ion channels can be categorized as “hallmarks of cancer” (Hanahan and Weinberg, 2011).

The pancreas is a complex organ, which has two main functions exerted by an exocrine and endocrine compartment (Pandiri, 2014). Dysregulation of exocrine pancreatic fluid secretion can contribute to pathologies such as pancreatitis and neoplasms such as pancreatic ductal adenocarcinoma (PDAC), whereas a well-known disorder related to dysfunction of the endocrine pancreas is diabetes mellitus (Pallagi et al., 2015; Kirkegard et al., 2017). The exocrine pancreas ensures enzymatic secretion for digesting fats and proteins in the intestines and, in parallel, the secretion of abundant fluid rich in bicarbonate ions, which serves to neutralize the acidic chime in the duodenum (Ishiguro et al., 2012; Lee et al., 2012; Pallagi et al., 2015). The bicarbonate secretion involves a tightly coordinated network of ion channels and transporters (Novak et al., 2013). The ductal epithelial cells comprising the exocrine pancreas are, as other types of epithelia, well-organized and exhibit epithelial features such as a polarized morphology and specialized cell-to-cell contact with tight junctions (Rodriguez-Boulan and Nelson, 1989). The ductal cells are equipped with a highly polarized set of ion channels and transporters, enabling the net bicarbonate excretion at the apical membrane, balanced by the net efflux of acid *via* the basolateral membrane to maintain their intracellular pH (Steward et al., 2005). Therefore, a correct distribution of ion channels and transporters is important to maintain the secreting function of exocrine pancreas (Lee et al., 2012). Moreover, expression, function, and localization of ion channels in the plasma membrane are involved in the development and progression of PDAC (Pedersen et al., 2017). PDAC can arise from ductal cells (Schneider et al., 2005) or from acinar cells transforming to

ductal cells by acinar-to-ductal-metaplasia, resulting in these cells possessing a ductal phenotype (Aichler et al., 2012). The transformation-associated loss of cell polarity and cell-cell adhesions of the epithelial cell layer will result in an altered localization of ion channels (Coradini et al., 2011; Pedersen and Stock, 2013).

Several reports and reviews about the role of transporters in bicarbonate, pancreatic fluid secretion and PDAC have been published (Novak, 2000; Lee et al., 2001; Novak et al., 2011; Ishiguro et al., 2012; Lee et al., 2012; Kong et al., 2014; Lemstrova et al., 2014; Pedersen et al., 2017; Yamaguchi et al., 2017). However, the role of ion channels in exocrine pancreas and in PDAC is not well understood. In this review, we aim to make a synthesis of the important role of ion channels and their localization and function in fluid secretion in healthy exocrine pancreatic tissue (see **Table 1** and **Figure 1**). Next, we summarize the sparse knowledge of the involvement of ion channels in PDAC progression and development *via* effects on proliferation, apoptosis, invasion and migration (see **Table 2** and **Figure 2**). Finally, we describe how ion channels are important novel biomarkers in PDAC (see **Table 2** and **Figure 3**).

## EXPRESSION, LOCALIZATION, AND ROLE OF ION CHANNELS IN HEALTHY PANCREATIC EPITHELIAL CELLS

### Potassium Channels

The relevance of K<sup>+</sup> channels in the exocrine pancreas received great attention in the 1970s–1980s, notably by Petersen’s team, thanks to electrophysiological studies of ion channels on acinar pancreatic epithelial cells dissociated from the pancreas of different animal species. While several studies have shown the expression of different families of K<sup>+</sup> channels on both acinar and duct pancreatic cells (Petersen and Findlay, 1987; Bleich and Warth, 2000; Thevenod, 2002; Hayashi and Novak, 2013; Venglovecz et al., 2015), few studies have shown their physiological role in exocrine secretion.

Two excellent reviews have summarized the role of these channels in physiological process of ductal fluid secretion, likely by contributing to maintain the membrane potential and thereby providing driving forces for anion transport (Hayashi and Novak, 2013; Venglovecz et al., 2015). Among these channels the voltage- and Ca<sup>2+</sup>-activated K<sup>+</sup>, big conductance (BK, maxi-K), and the intermediate (IK, KCa3.1) Ca<sup>2+</sup>-activated K<sup>+</sup> channels have been intensely studied in pancreatic ductal cells. The BK which is activated by cAMP and PKA is found on the basolateral membrane of rat pancreatic duct cells (Gray et al., 1990a). The authors suggest its role in pancreatic bicarbonate secretion. BK is also found mainly expressed in the apical membrane of guinea-pig non-transformed pancreatic duct epithelial cells (PDEC) (Venglovecz et al., 2011) where it regulates the bicarbonate secretion stimulated by the bile acid chenodeoxycholate likely through changes of the membrane potential. KCa3.1 was first characterized in cultured PDEC where it is expressed on the basolateral membrane of duct

**TABLE 1 |** Expression, localization, and the potential role of ion channels in exocrine pancreas.

Channel type	Species	Pancreatic Acini	Pancreatic Duct	Localization	Function	Ref.
<b>K<sup>+</sup> Channels</b>						
Kir2, Kir2.3, Kir7.1, Kir1.3	Rat	+		Basolateral	Unknown	(Kim et al., 2000) (Shuck et al., 1997)
Kir5.1 & Kir4.2	Rat Human	+	+	Unknown	Kir5.1 forms heteromeric channels with Kir4.2. Might have a role in the pH-dependent regulation of K <sup>+</sup> fluxes?	(Pessia et al., 2001) (Liu et al., 2000)
TALK-1 & TALK-2	Human	+		Unknown	Highly modulated (activation) by NOS and ROS	(Duprat et al., 2005) (Girard et al., 2001)
TASK-2	Human	+	+	Luminal in duct	Might drive the force for electrogenic HCO <sub>3</sub> <sup>-</sup> secretion?	(Duprat et al., 1997) (Duprat et al., 2005) (Hayashi and Novak, 2013)
minK	Rat	+		Unknown in acinar		(Kim and Greger, 1999)
KCNQ1(KvLQT1/Kv7.) & KCNE1 (minK)	Mouse Rat	+	+	Luminal in duct Lateral and basolateral in acini	Cell volume regulation in ducts Membrane potential in acini Electrolyte/enzyme secretion with minK	(Kottgen et al., 1999) (Warth et al., 2002) (Demolombe et al., 2001) (Hayashi et al., 2012)
KCa1.1 (BK, maxi-K)		+	+	Basolateral in acini/Luminal in duct	Activate luminal secretion	(Gray et al., 1990a) (Hede et al., 1999) (Hede et al., 2005)
BK (maxi-K)	Pig		+	Basolateral	Cl <sup>-</sup> secretion	(Iwatsuki and Petersen, 1985a) (Iwatsuki and Petersen, 1985b) (Suzuki et al., 1985) (Petersen and Findlay, 1987) (Gallacher et al., 1984) (Petersen et al., 1985) (Venglovecz et al., 2011)
BK (maxi-K) BK (maxi-K)	Human Guinea-pig	+	+	Unknown Luminal	Regulation of HCO <sub>3</sub> <sup>-</sup> secretion-induced by the bile acid Chenodeoxycholate	
BK (maxi-K)	Rat	+		Basolateral	Might regulate membrane potential hyperpolarization?	(Gray et al., 1990a) (Hede et al., 2005)
IK1 (KCa3.1)	Dog (cell lines, PDEC)	+	+	Basolateral/Luminal in duct	Driving force for Cl <sup>-</sup> efflux Regulate HCO <sub>3</sub> <sup>-</sup> secretion Hyperpolarization	(Nguyen and Moody, 1998) (Thompson-Vest et al., 2006) (Jung et al., 2006)
IK1 (KCa3.1)	Mouse & Human		+	Luminal/basolateral	Setting the RMP. Involvement in anion and K <sup>+</sup> transport in stimulated ducts	(Hayashi et al., 2012)
IK1 (KCa3.1)	Human & Rat					(Ishii et al., 1997) (Joiner et al., 1997) (Hede et al., 2005)
Kv3.4 Kv1.5	Mouse Human	+		Unknown Unknown	Unknown Might regulate membrane potential?	(Kalman et al., 1998) (Bielanska et al., 2009) (Venglovecz et al., 2015)
Kv11.1 (ERG1) Kv10.2	Human Human		+	Luminal Luminal	Might regulate membrane potential? Might regulate membrane potential?	(Hayashi et al., 2012) (Hayashi et al., 2012)
<b>Calcium</b>						
Orai1	Mouse	+		Both in acinar Mostly basolateral	Might drive exocytosis of secretory granules or stimulate fluid and electrolyte secretion?	(Lur et al., 2009) (Hong et al., 2011)
Orai2 Orai3	Dog Dog		+	Unknown Basolateral	Unknown Unknown	(Kim et al., 2013) (Kim et al., 2013)
STIM1	Mouse	+		Both in acinar Mostly basolateral	Might drive exocytosis of secretory granules or stimulate fluid and electrolyte secretion?	(Lur et al., 2009) (Hong et al., 2011)
TRPC1	Mouse	+	+	Lateral side of the basolateral membrane	Might drive exocytosis of secretory granules or stimulate fluid and electrolyte secretion?	(Hong et al., 2011)
TRPC3	Mouse	+	+	Basolateral in acini	Might drive exocytosis of secretory granules or stimulate fluid and electrolyte secretion?	(Kim et al., 2006) (Kim et al., 2009)

(Continued)

TABLE 1 | Continued

Channel type	Species	Pancreatic Acini	Pancreatic Duct	Localization	Function	Ref.
TRPC6	Mouse	+		Unknown	Might drive exocytosis of secretory granules or stimulate fluid and electrolyte secretion?	(Kim et al., 2006)
TRPV6	Dog		+	Unknown	Unknown	(Kim et al., 2013)
TRPM7	Zebra fish		+	Luminal	Regulating epithelial cell-cycle progression, growth, and, consequently, acinar and ductal morphogenesis, also during embryogenesis	(Yee et al., 2011)
TRPM8	Human	+	(To some extend)	Unknown	Unknown	(Yee et al., 2010)
<b>Chloride</b>						
CFTR	Rat Guinea-pig Dog Human	+	+	Luminal in ducts	Drive fluid and HCO <sub>3</sub> <sup>-</sup> secretion	(Gray et al., 1988) (Gray et al., 1989) (Gray et al., 1990b) (Marino et al., 1991; Gray et al., 1993) (Zeng et al., 1997)
CaCC (TMEM16A)	Mouse Rat Guinea-pig Dog Bovine	+	+	Luminal on both	Drive fluid and HCO <sub>3</sub> <sup>-</sup> secretion	(Park et al., 2001) (al-Nakkash and Cotton, 1997) (Winpenney et al., 1995) (Nguyen et al., 1997) (Yokoyama et al., 2019) (Zdebik et al., 1997) (Wang and Novak, 2013) (Park et al., 2001) (Yang et al., 2008) (Bergmann et al., 2011) (Ousingsawat et al., 2009) (Huang et al., 2009) (Randriamampita et al., 1988) (Kasai and Augustine, 1990) (Marty et al., 1984) (Gray et al., 1989) (Gray et al., 1990b)
<b>Sodium</b>						
ENaC (δ -subunit)	Mouse Human	+	+	Luminal	Unknown	(McDonald et al., 1994; Waldmann et al., 1995; Zeiher et al., 1995; Novak and Hansen, 2002; Pascua et al., 2009) (Waldmann et al., 1995)
<b>Other</b>						
AQP1	Mouse Rat Human	+	+	Both on ducts	Facilitates water flow	(Gabbi et al., 2008) (Ko et al., 2002) (Furuya et al., 2002) (Burghardt et al., 2003)
AQP5	Mouse Rat Human		+	Luminal	Facilitates water flow	(Hurley et al., 2001) (Ko et al., 2002) (Burghardt et al., 2003)
AQP8	Rat Human	+		Luminal	Facilitates water flow	(Hurley et al., 2001) (Burghardt et al., 2003)
AQP12	Mouse Chicken Human	+		Intracellular	Synthesis of digestive enzymes	(Itoh et al., 2005) (Isokpehi et al., 2009)

epithelial cells (Nguyen and Moody, 1998). Activation of P2Y2R induced an increase of free intracellular calcium ([Ca<sup>2+</sup>]<sub>i</sub>) that activates KCa3.1, which in turn hyperpolarized the membrane potential, leading to a Cl<sup>-</sup> dependent bicarbonate secretion (Jung et al., 2006). KCa3.1 was also found located on the basolateral and luminal membrane of pancreatic mouse and human duct

cells (Hayashi et al., 2012). The same authors demonstrated that both luminal and basolateral KCa3.1 channels were involved in the regulation of membrane potential.

In acinar cells, the membrane potential created by K<sup>+</sup> channels, and waves of [Ca<sup>2+</sup>]<sub>i</sub> provide the necessary driving force for Cl<sup>-</sup> efflux through the luminal membrane, which is a key



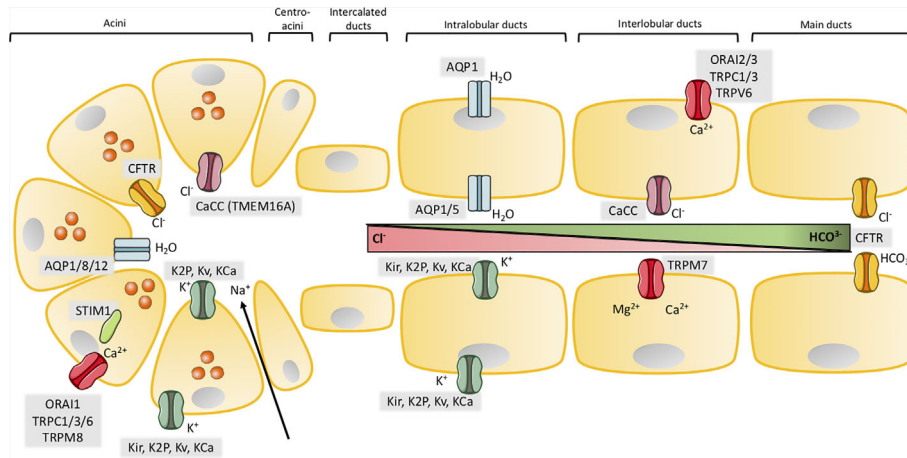


**FIGURE 1 |** Ion channels in exocrine pancreas. Illustration of the structure of acinar and major ductal segments of secretory glands in pancreas. Acinar cells secrete digestive enzymes (orange circles in acini) and an isotonic NaCl rich fluid which transports the enzymes to the ducts. Fluid secretion in acini cells is regulated by a Cl<sup>-</sup> secretion process. Cl<sup>-</sup> secretion is activated by [Ca<sup>2+</sup>]<sub>i</sub>, from a Ca<sup>2+</sup> influx through SOCs in the basolateral membrane, where Cl<sup>-</sup> channels, Ca<sup>2+</sup> activated Cl<sup>-</sup> channels (CaCC) and different types of K<sup>+</sup> channels are activated to provide the efflux of their respected ions. K<sup>+</sup> channels also create a driving force by maintaining a negative membrane potential. The negative charge mediated by a high concentration of Cl<sup>-</sup> ions results in transport of Na<sup>+</sup> through tight junctions to the luminal space. NaCl makes the driving force for water to efflux through aquaporins and a cell shrinkage. This cell shrinkage reduces [Ca<sup>2+</sup>]<sub>i</sub>, which inhibits Cl<sup>-</sup> and K<sup>+</sup> efflux through their channels and in parallel activates basolateral transporters and pumps to restore both Cl<sup>-</sup> and K<sup>+</sup>. The digestive enzymes are transported in the NaCl isotonic fluid to the ducts, which is low in HCO<sub>3</sub><sup>-</sup> concentration in the proximal ducts, but this concentration increases through the transport to the distal duct cells. The ductal fluid becomes rich in HCO<sub>3</sub><sup>-</sup>, by a two-step process. The first step takes place in the proximal ducts, where Cl<sup>-</sup>/HCO<sub>3</sub><sup>-</sup> exchangers secretes HCO<sub>3</sub><sup>-</sup> and absorb Cl<sup>-</sup> and Cl<sup>-</sup> channels recycle Cl<sup>-</sup>. As in the acinar cells an osmotic reaction happens, where efflux of negative HCO<sub>3</sub><sup>-</sup> and Na<sup>+</sup> drives water flow through aquaporins. This results in high concentration of HCO<sub>3</sub><sup>-</sup> (~100 mM), a low concentration of Cl<sup>-</sup> (~25 mM) and a high fraction of water in the pancreatic juice. The second step takes place in the distal part of the ducts, where the specific Cl<sup>-</sup> channel CFTR changes selectivity to HCO<sub>3</sub><sup>-</sup> and function as a HCO<sub>3</sub><sup>-</sup> efflux channel to determine the final concentration of the HCO<sub>3</sub><sup>-</sup> rich fluid (~140 mM). K<sup>+</sup> channels may, as in acini, take part in the secretion of K<sup>+</sup> and regulation of anion transport by maintaining the membrane potential in both the basolateral and luminal membrane. SOCs ensure the influx of Ca<sup>2+</sup> which takes part in regulation of ion channels through [Ca<sup>2+</sup>]<sub>i</sub>, as in acini. Activation or inhibition of P2 receptors by Ca<sup>2+</sup> signaling also regulate anion secretion through K<sup>+</sup> and Cl<sup>-</sup> channels.

**TABLE 2 |** Profile expression of ion channels in pancreatic ductal adenocarcinoma (PDAC) cell lines and tissue and how they are involved in driving PDAC formation and how channel expression correlate with clinical factors.

Channel	Profile expression Up/Downregulated (method used for expression profiling)	Cell line/Solid tumor	Driving PDAC formation in form of	Downstream regulation and signaling	Channel expression correlates with clinical factors	Ref.
<b>Potassium</b>						
KCa3.1	Upregulated (mRNA, IHC, Microarray, electrophysiological, transcriptome data, TCGA analysis)	BxPC-3 Capan-1 MiaPaCa-2 PANC-1 Solid tumors	Proliferation Cell cycle progression Migration Invasion	Ras Oxidative Phosphorylation	High expression: Low overall survival Advanced tumor stage	(Bonito et al., 2016) (Jager et al., 2004) (Hayashi et al., 2012) (Jiang et al., 2017) (Shen et al., 2017) (Kovalenko et al., 2016) (Zaccagnino et al., 2016)
KCa4.1	mRNA	Capan-1 PANC-1				(Hayashi et al., 2012)
KCa4.2	mRNA	CFPAC PANC-1				(Hayashi et al., 2012)
K <sub>v</sub> 1.3	Downregulated in tumors (mRNA, IHC) Upregulated in cell lines (mRNA, protein)	AsPC-1 BxPC-3 Capan-1 Colo357 MiaPaCa-2 Panc-89	Apoptosis Hypermethylation		Low expression: Hypermethylation correlates with survival (not significant)	(Brevet et al., 2009) (Zaccagnino et al., 2017) (Bielanska et al., 2009)

(Continued)



TABLE 2 | Continued

Channel	Profile expression Up/Downregulated (method used for expression profiling)	Cell line/Solid tumor	Driving PDAC formation in form of	Downstream regulation and signaling	Channel expression correlates with clinical factors	Ref.
K <sub>v</sub> 1.5	Upregulated (IHC)	Panc-TUI Solid tumors Solid tumors				(Bielanska et al., 2009)
K <sub>v</sub> 7.1	Downregulated (Microarray, Nanostring electrophysiological)	A818-6 HPAF Solid tumors				(Tawfik et al., 2020) (Fong et al., 2003) (Zaccagnino et al., 2016)
minK	Downregulated (Microarray)	Solid tumors				(Zaccagnino et al., 2016)
K <sub>v</sub> 10.1	Unknown	Solid tumors	Tumor growth	Blocking shows antitumor activity		(Gomez-Varela et al., 2007) (Pardo and Stuhmer, 2014)
K <sub>v</sub> 11.1	Upregulated (mRNA, protein, IHC, Sequencing analysis)	BxPC-3 CFPAC-1 MiaPaCa-2 PANC-1 SW1990 T3M4 Solid tumors	Proliferation Cell cycle progression Migration Invasion Metastasis	miR96 EGFR-pathway ERK1/2 F-actin assembly	High expression: Low overall survival High Ki67 expression Advanced tumor grade	(Manoli et al., 2019) (Lastraioli et al., 2015b) (Zhou et al., 2012) (Feng et al., 2014) (Sette et al., 2013)
TREK-1	Upregulated (protein, electrophysiological)	AsPC-1 BxPC-3 Capan-1 Solid tumors	Proliferation Migration	pH/Vm activated		(Sauter et al., 2016)
TASK-1	Downregulated (Microarray database analysis)	Solid tumors				(Williams et al., 2013)
TASK-2	(mRNA, protein electrophysiological)	HPAF				(Fong et al., 2003)
TWIK-1	Upregulated (Microarray database analysis)	Solid tumors				(Williams et al., 2013)
TWIK-3	Downregulated (Microarray)	Solid tumors	Cell differentiation			(Zaccagnino et al., 2016)
Kir3.1	Upregulated (mRNA, IHC)	Solid tumors				(Brevet et al., 2009)
Kir4.2	Downregulated (Microarray)	Solid tumors	Cell differentiation			(Zaccagnino et al., 2016)
Kir5.1	Downregulated (Microarray)	Solid tumors				(Zaccagnino et al., 2016)
<b>Sodium</b>						
VGSC SCN9A SCNA3	Downregulated (Microarray)	MiaPaCa-2 CAV Solid tumors	Proliferation	Inhibition of growth with phenytoin		(Sato et al., 1994; Koltai, 2015) (Zaccagnino et al., 2016)
ASIC1	Upregulated (mRNA, protein, IHC)	AsPC-1 BxPC-3 PANC-1 SW1990 Solid tumors	EMT Metastasis	RhoA		(Zhu et al., 2017)
ASIC3	Upregulated (mRNA, protein, IHC)	AsPC-1 BxPC-3 PANC-1 SW1990 Solid tumors	EMT Metastasis	RhoA		(Zhu et al., 2017)
<b>Calcium</b>						
ORAI1	Different expression in different cell lines (mRNA, protein) Downregulated (Microarray)	AsPC-1 BxPC-3 Capan-1 MiaPaCa-2 PANC-1 Solid tumors	Apoptosis Proliferation	Calcium-regulated Akt/ mTOR/NFAT signaling		(Kondratska et al., 2014) (Khan et al., 2020) (Zaccagnino et al., 2016)

(Continued)

TABLE 2 | Continued

Channel	Profile expression Up/Downregulated (method used for expression profiling)	Cell line/Solid tumor	Driving PDAC formation in form of	Downstream regulation and signaling	Channel expression correlates with clinical factors	Ref.
STIM1	Different expression in different cell lines Upregulated in chemo-resistant cells (mRNA, protein, TCGA analysis, IHC)	AsPC-1 BxPC-3 Capan-1 CFAPC-1 MiaPaCa2 Panc-1 Solid tumors	Apoptosis Proliferation Invasion EMT Gemcitabine resistance	Regulated by HIF1-alpha	High expression: Low disease-free survival Advanced tumor grade	(Kondratska et al., 2014) (Zhou et al., 2020) (Wang et al., 2019)
TRPM2	Upregulated (mRNA, TCGA analysis)	PANC-1 Solid tumors	Proliferation Migration Invasion		High expression: Low overall survival	(Lin et al., 2018) Reviewed in: (Stoklosa et al., 2020)
TRPM7	Upregulated (mRNA, protein, IHC, electrophysiological)	BxPC-3 Capan-1 HPAF-II MiaPaCa2 PL45 Panc-1 Panc 02.03 Solid tumors	Proliferation Cell cycle progression Migration Invasion	Mg <sup>2+</sup> -sensitive Socs3a-pathway Hsp90α/uPA/ MMP-2 proteolytic axis	High expression: Low overall survival Advanced tumor grade Advanced tumor stage Large tumor size Metastasis Molecular phenotype Treatment response	(Yee et al., 2011; Yee et al., 2012a; Yee et al., 2015) (Rybarczyk et al., 2012; Rybarczyk et al., 2017)
TRPM8	Upregulated (mRNA, protein, IHC, electrophysiological)	BxPC-3 Capan-1 HPAF-II MiaPaCa2 Panc-1 Panc 02.03 PL45 Solid tumors	Proliferation Cell cycle progression Apoptosis Invasion Migration	Glycosylation states	High expression: Low overall survival Low disease-free survival Poor prognosis Metastasis Molecular phenotype Treatment response	(Yee et al., 2010) (Yee et al., 2012a) (Liu et al., 2018) (Yee et al., 2014) (Du et al., 2018) (Cucu et al., 2014) (Ulareanu et al., 2017)
TRPC1	(mRNA, protein)	BxPC-1 CAPAN-1 CFPAC PANC-1	Motility	TGF-β-induced Ca/PKCα signaling		(Kim et al., 2013) (Dong et al., 2010)
TRPC4	(mRNA, protein)	BxPC-1				(Dong et al., 2010)
TRPC6	(mRNA, protein)	BxPC-1				(Dong et al., 2010)
TRPV1	Upregulated (mRNA, protein, IHC)	Capan-1 MiaPaCa-2 PANC-1 Solid tumors	Proliferation Apoptosis	EGFR/MAPK		(Huang et al., 2020) (Hartel et al., 2006) Reviewed in: (Liddle, 2007)
TRPV6	Upregulated (mRNA, protein, IHC) Downregulated (Microarray, Nanostring)	A818-6 AsPC-1 BxPC-3 CAPAN-1 CFPAC PANC-1 SW1990 Solid tumors	Cell cycle Apoptosis Metastasis	Numb protein	High expression: Low overall survival Advanced tumor stage Large tumor size Vascular infiltration	(Kim et al., 2013; Song et al., 2018) (Tawfik et al., 2020) (Zaccagnino et al., 2016)
IP3R	Immunoblotting (IF)	PANC-1	Migration	Colocalization with STIM1/ER-PM junctions		(Okeke et al., 2016)
CACNA1	Upregulated (Microarray)	Solid tumors				(Zaccagnino et al., 2016)
CACNA1G	Downregulated	Solid tumors				(Zaccagnino et al., 2016)
<b>Chloride</b>						
CLCA1	Upregulated (IHC, Proteomics)	Solid tumors	Unclear		Low expression correlates with poor prognosis Low overall survival	(Hu et al., 2018a) (Hu et al., 2018b; Hu et al., 2019)
CLCNKB	Downregulated (Microarray)	Solid tumors				(Zaccagnino et al., 2016)
CLCN1	Downregulated (Microarray)	Solid tumors				(Zaccagnino et al., 2016)

(Continued)

TABLE 2 | Continued

Channel	Profile expression Up/Downregulated (method used for expression profiling)	Cell line/Solid tumor	Driving PDAC formation in form of	Downstream regulation and signaling	Channel expression correlates with clinical factors	Ref.
CLIC1	Upregulated (IHC)	MiaPaCa-2 PANC-1 Solid tumors	Proliferation Invasion		High expression: Low overall survival Advanced tumor grade Advanced tumor stage Large tumor size	(Jia et al., 2016) (Lu et al., 2015)
CLIC2	mRNA, protein, electrophysiological	HPAF				(Fong et al., 2003)
CLIC3	Upregulated (mRNA, protein, electrophysiological, immunohistochemistry)	HPAF Solid tumors	Promote integrin recycling		High expression: Low overall survival	(Dozynkiewicz et al., 2012) (Fong et al., 2003)
CLIC4	Upregulated (IHC)	Solid tumors	Invasion			(Zou et al., 2016)
CLIC5	(mRNA, protein electrophysiological) Downregulated (Microarray)	HPAF Solid tumors	Cell differentiation			(Fong et al., 2003) (Zaccagnino et al., 2016)
TMEM16A	Upregulated (mRNA, electrophysiological, TCGA analysis)	AsPC-1 BxPC-3 Capan-1 MiaPaCa-2 PANC-1 Solid tumors	Migration	TMEM16A-dependent store-operated calcium entry (SOCE). EGFR-signaling pathways	High expression: Low overall survival	(Sauter et al., 2015) (Wang and Novak, 2013) (Crottes et al., 2019)
TMEM16E	Upregulated (mRNA, protein, IHC)	BxPC-3 HPAC PANC-1 Solid tumors	Proliferation Migration			(Song et al., 2019)
TMEM16J	Upregulated (mRNA, protein, IHC)	AsPC-1 BxPC-3 Capan-2 PANC-1 Solid tumors	Proliferation	ERK1/2 EGFR	High expression: Low overall survival	(Jun et al., 2017)
CFTR	Downregulated (mRNA, Microarray, Sequencing analysis) Immunoblotting (IF)	AsPC-1 BxPC-3 Capan-1 Capan-2 Colo357 CFPAC1 HPAC HPAF HS766T MiaPaCa-2 PANC-1 QGP1 S2CP9 Suit2 SW1990 T3M4 Solid tumors Organoids	EMT	Regulate expression of MUC4	CFTR mutation leads to a higher risk of getting pancreatic cancer	(Chambers and Harris, 1993) (Singh et al., 2007) (McWilliams et al., 2010; Cazacu et al., 2018) (Hennig et al., 2019) (Zaccagnino et al., 2016)
<b>Aquaporins</b>						
AQP1	Upregulated (mRNA, protein, IHC)	Solid tumors			High expression: Low overall survival Advanced tumor stage Large tumor size Lymph node metastasis Tumor differentiation Invasion	(Burghardt et al., 2003) (Zou et al., 2019)
AQP3	Upregulated (mRNA, Microarray, protein, IHC)	BxPC-3 Capan-2 HPAC	Proliferation Apoptosis EMT	mTOR/S6 signaling Simultaneous overexpression of	High expression: Low overall survival Advanced tumor stage	(Burghardt et al., 2003) (Huang et al., 2017)

(Continued)

TABLE 2 | Continued

Channel	Profile expression Up/Downregulated (method used for expression profiling)	Cell line/Solid tumor	Driving PDAC formation in form of	Downstream regulation and signaling	Channel expression correlates with clinical factors	Ref.
		HPAFII Solid tumors		EGFR, Ki-67, and CK7, down-regulation of E-cadherin and vimentin	Large tumor size Lymph node metastasis Tumor differentiation Invasion	(Zou et al., 2019) (Direito et al., 2017) (Zaccagnino et al., 2016) (Burghardt et al., 2003)
AQP4	(mRNA)	Capan-1 Capan-2 Solid tumors				
AQP5	Upregulated (mRNA, IHC)	Capan-1 Capan-2 HPAF Solid tumors	Proliferation Differentiation EMT	Simultaneous overexpression of EGFR, Ki-67, and CK7. Downregulation of E-cadherin and vimentin.	High expression: Low overall survival Tumor differentiation	(Burghardt et al., 2003) (Direito et al., 2017)
AQP8	mRNA Downregulated (Microarray)	Solid tumors				(Burghardt et al., 2003) (Zaccagnino et al., 2016)
<b>Ionotropic receptors</b>						
P2X4	mRNA	AsPC-1 BxPC-3 Capan-1 CFPAC-1 MiaPaCa-2 PANC-1				(Kunzli et al., 2007) (Hansen et al., 2008) (Giannuzzo et al., 2015)
P2X6	mRNA	AsPC-1 BxPC-3 Capan-1 CFPAC-1 MiaPaCa-2 PANC-1				(Kunzli et al., 2007) (Hansen et al., 2008) (Giannuzzo et al., 2015)
P2X7	Upregulated (mRNA, protein, IHC)	AsPC-1 BxPC-3 Capan-1 CFPAC-1 MiaPaCa-2 PANC-1 Solid tumors	Proliferation Apoptosis Invasion Migration	PKC, PLD ERK1/2, and JNK Decreased nitric oxide synthase		(Giannuzzo et al., 2015) (Kunzli et al., 2007) (Hansen et al., 2008) (Choi et al., 2018)
NMDAR	(IHC, Microarray)	BxPC-3 HPAFII SUIT2 Solid tumors	Proliferation Survival			(Li and Hanahan, 2013) (North et al., 2017)

step in initiating fluid and electrolyte secretion (Lee et al., 2012). The activation of K<sup>+</sup> channels located on the basolateral membrane hyperpolarizes the resting membrane potential, promoting the driving force for luminal Cl<sup>-</sup> efflux through Cl<sup>-</sup> channels (Petersen, 2005). A Ca<sup>2+</sup>-dependent maxi- K<sup>+</sup> channel (200 pS) has been characterized upon stimulation with acetylcholine (ACh), cholecystokinin (CCK), and bombesin in pancreatic acinar cells (Maruyama et al., 1983; Iwatsuki and Petersen, 1985a; Iwatsuki and Petersen, 1985b; Petersen et al., 1985; Suzuki et al., 1985; Petersen and Findlay, 1987). Moreover, Pearson et al. (1984) showed, on isolated pancreas acinar pig cells, that neural and hormonal (ACh, bombesin and pentagastrin) stimulation evokes a Ca<sup>2+</sup>-dependent cell hyperpolarization by causing an increase in membrane K<sup>+</sup> conductance (Pearson et al., 1984). An intermediate Ca<sup>2+</sup>-activated K<sup>+</sup> channel is also expressed in both the basolateral and the apical membranes of acinar cells (Thompson-Vest et al., 2006), but its role has not been studied.

KCNQ1 (KVLQT1, Kv7.1) and KCNE1 (IsK, minK) have been found in abundance in pancreatic acinar cells (Kottgen et al., 1999; Bleich and Warth, 2000; Demolombe et al., 2001; Warth and Barhanin, 2002; Warth et al., 2002; Hayashi et al., 2012). By using mouse models associated with electrophysiological studies, Warth et al. (2002) showed that KCNQ1 was predominantly located at the basolateral membrane and its co-assemblage with KCNE1 leads to a voltage-dependent K<sup>+</sup> current that was increased by cholinergic stimulation and inhibited by the KCNQ1 blocker (Kim and Greger, 1999; Kottgen et al., 1999; Warth et al., 2002). The fact that inhibition of KCNQ1 channels diminishes intestinal Cl<sup>-</sup> secretion, made the authors suggest its involvement in pancreatic electrolyte secretion process.

K<sup>+</sup> inwardly rectifying channels (Kir) channels are expressed in exocrine pancreas. Kir 2.1, Kir2.3, Kir7.1, Kir5.1, and Kir4.2 were detected in rat pancreatic acini (Kim et al., 2000; Pessia et al., 2001). *In-situ* hybridization analysis confirmed the expression of Kir5.1 in human pancreatic acinar and ductal

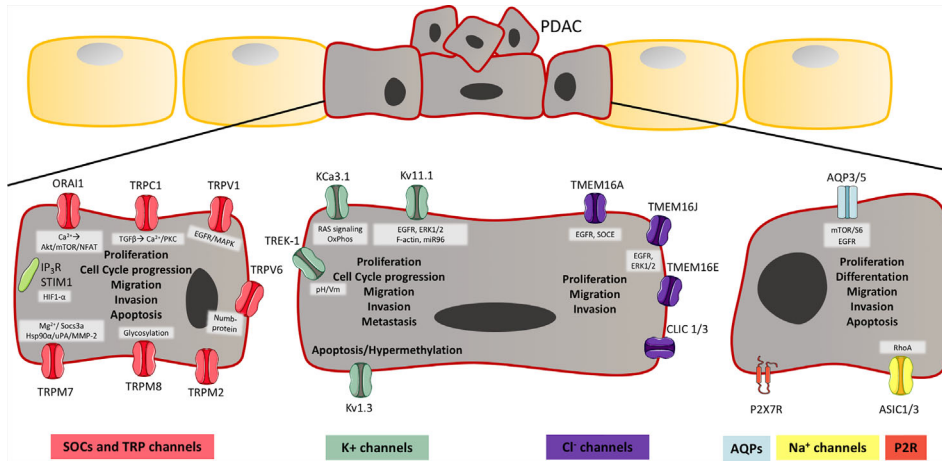


**FIGURE 2 |** Ion channels in pancreatic ductal adenocarcinoma (PDAC). Illustration of ion channels, which have been shown to have a role in hallmarks of cancer, thereby PDAC development and progression. As cancer cells lose their polarity, the localization of the channels is unknown, and on the illustration, it should be considered that the channels have no particular localization. The aberrant expression in PDAC cells, are shown for; Store-operated channels (SOCs) and transient receptor potential (TRP) channels, K<sup>+</sup> channels, Cl<sup>-</sup> channels, aquaporins (AQP), Na<sup>+</sup> channels and P2X7R. These channels are known to be involved in PDAC development and progression through proliferation, cell cycle progression, differentiation, migration, invasion, metastasis, and apoptosis. The known pathways and mechanism, which have been shown to be involved in these processes are shown in a grey box next to the channel and are mentioned in **Table 2**. The channels shown to be expressed in PDAC, but where the role is unknown are also shown in **Table 2**.

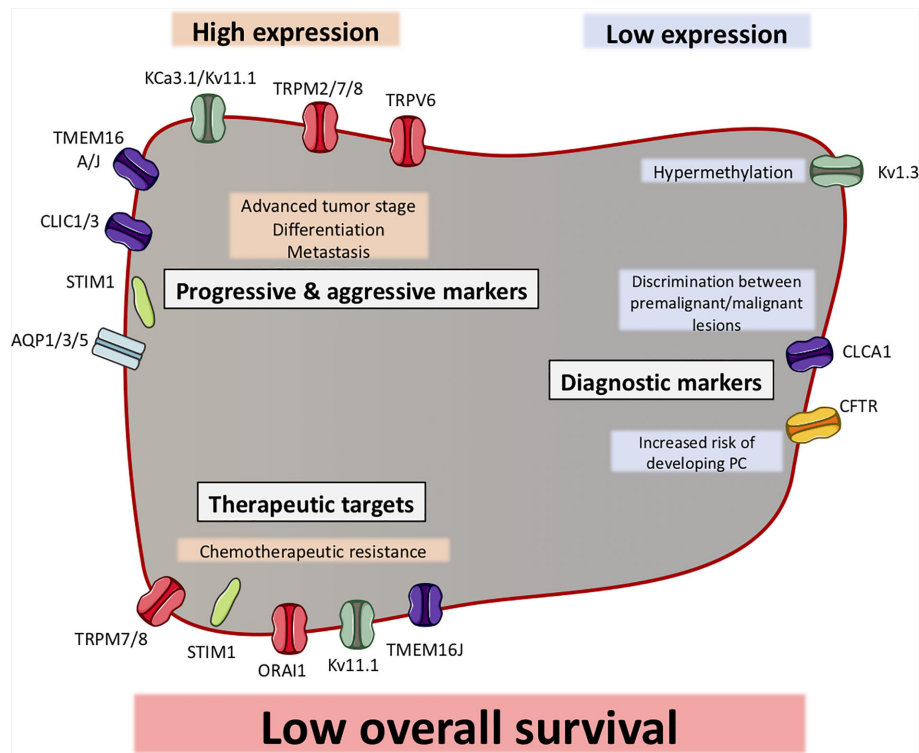


**FIGURE 3 |** Ion channels can function as biomarkers in pancreatic ductal adenocarcinoma (PDAC). Illustration of ion channels, where the expression has been shown to be correlated with clinical factors. Most of the ion channels show a high expression in PDAC, which correlates with clinical factors (indicated in grey boxes). Some ion channels have shown to be to have a low expression in PDAC, which correlates with other clinical factors. The ion channels are grouped as progression and aggressiveness markers, diagnostic markers or therapeutic targets. Among all ion channels, their expression (except CFTR) have been shown to be correlated with a low overall survival.

cells (Liu et al., 2000). Moreover, it has been suggested that Kir5.1 forms heteromeric channels with Kir4.2 in rat pancreas and is involved in the pH-dependent regulation of  $K^+$  flux (Pessia et al., 2001). Kir1.3 was also detected by northern blot analysis, in human pancreas (Shuck et al., 1997). The 2-Pore  $K^+$  channel ( $K_2P$ ) family has also been found in human exocrine pancreas; however, their localization and function are still unknown. For example, TALK-1 and TALK-2 are very specifically expressed in exocrine pancreas where they are activated by NOS and ROS (Girard et al., 2001; Duprat et al., 2005), while TASK-2 is expressed in both exocrine and endocrine pancreas (Duprat et al., 1997; Duprat et al., 2005).

## Calcium Channels

As Petersen and co-workers showed the relevance of  $K^+$  channels in exocrine pancreas, they have also described the role of  $Ca^{2+}$  signaling, in pancreatic acinar cells (Petersen, 2014). In the early 70's they showed that movements of  $Ca^{2+}$  was evoked upon ACh stimulation released  $Ca^{2+}$  from intracellular stores and that only a small part of  $Ca^{2+}$  was taken up from the extracellular solution (Case and Clausen, 1973; Matthews et al., 1973). This  $Ca^{2+}$  signaling is involved in exocrine pancreatic fluid secretion as both acinar and duct cells in pancreas are regulated by receptors that change  $[Ca^{2+}]_i$ , which activates epithelial  $Ca^{2+}$ -dependent  $K^+$  and  $Cl^-$  ion channels, thereby enzyme and fluid secretion (Petersen, 2014). The  $Ca^{2+}$  signal is initiated by ACh or CCK, binding to specific receptors (Case and Clausen, 1973; Matthews et al., 1973; Petersen and Ueda, 1976), which generates specific  $Ca^{2+}$  signals. These signals start by  $Ca^{2+}$  activating phospholipase C, which hydrolyzes  $PIP_2$ , hence generating  $IP_3$  and diacylglycerol.  $IP_3$  binds to  $IP_3$  receptors located in the ER at the apical pole of the acinar cells mediating a  $Ca^{2+}$  wave to the basal pole (Mogami et al., 1997; Hong et al., 2011). This evokes a  $Ca^{2+}$  ER store depletion that results in clustering of the ER  $Ca^{2+}$  sensor STIM1, which activates store-operated channels (SOCs) and transient receptor potential (TRP) channels, leading to  $Ca^{2+}$  influx (Petersen and Tepikin, 2008). Members and regulators of SOCs are the SOC channel pore-forming ORAI proteins (ORAI1-3) and their regulators STIM (STIM1-2) (Hoth and Niemeyer, 2013). ORAI1 is the best described among these and are found to be expressed at the apical membrane of pancreatic acinar cells where it colocalizes with  $IP_3R$  (Hong et al., 2011; Lur et al., 2011) and at the basolateral membrane where it colocalizes with STIM1 (Lur et al., 2011). Recently, it has been shown that inhibition of ORAI1 in pancreatic acinar cells abolished SOC entry upon stimulation with thapsigargin, CCK, and the bile acid taurothiocholic acid 3-sulfate, indicating that ORAI1 mediates SOC entry in pancreatic acinar cells (Gerasimenko et al., 2013; Wen et al., 2015).

TRPC channels have also been found to participate or influence store-dependent  $Ca^{2+}$  influx in pancreatic acinar cells. TRPC1 was found to localize both at the apical and lateral regions of the basolateral membrane, and pancreatic acinar cells isolated from TRPC1 $^{-/-}$  mice showed reduced  $Ca^{2+}$  influx and  $Ca^{2+}$  oscillation frequency (Hong et al., 2011). The role of TRPC1 in pancreatic acinar cells is not yet known, but it is

suggested to have a similar role as in salivary glands, where they regulate fluid secretion and  $Ca^{2+}$  activated  $K^+$  channels (Liu et al., 2007). TRPC3 was found in the junctional site of the apical pole and the basolateral membrane of pancreatic acini cells and in TRPC3 $^{-/-}$  mice a reduction of  $Ca^{2+}$  influx was seen (Kim et al., 2006). Furthermore, TRPC6 seemed to be expressed in the pancreatic acini cells, but its localization and role are unknown (Kim et al., 2006). These data suggest that TRPC channels are involved in the SOC entry of pancreatic acini cells and could contribute to fluid secretion. Other TRP channels have been found to be expressed in exocrine pancreas; TRPV6 (Kim et al., 2013), TRPM7 (Yee et al., 2011) and TRPM8 (Yee et al., 2010). However, only the role of TRPM7 is described. In a zebra fish model, it has been found that TRPM7 is involved in the developmental processes of exocrine pancreas, which was linked to  $Mg^{2+}$  signaling (Yee et al., 2011). Diminish of cell cycle progression and cell growth in TRPM7-mutated zebra fish models attenuated proliferation of exocrine pancreatic epithelia. This was partially rescued by adding extra  $Mg^{2+}$  to the embryo medium (Yee et al., 2011). Furthermore, the proliferation was also regulated by suppressor of cytokine signaling 3a (socs3a), indicating that TRPM7 plays a role in the development of exocrine pancreas (Yee et al., 2011), but the physiological role in fluid secretion is yet to be determined.

In duct cells,  $HCO_3^-$  secretion is mediated by cAMP/ $Ca^{2+}$  signaling systems. Through specific  $Ca^{2+}$  channels and  $Ca^{2+}$  activated ion channels ( $Ca^{2+}$ -activated  $K^+$  and  $Cl^-$  channels),  $Ca^{2+}$  can act as key player in regulation and secretion of pancreatic juices (Lee M. G. et al., 2012). The localization of SOCs in duct cells, due to  $HCO_3^-$  fluid secretion, is not well studied. However, it has been found that SOC-mediated  $Ca^{2+}$  influx can be a driving force for exocytosis, evoked by trypsin (Kim et al., 2008) in dog PDEC. The same authors have shown the function of SOCs in dog PDEC where the typical inward rectifying current was found, as for other types of epithelial cells (Kim et al., 2013). Furthermore, it was found that STIM1, STIM2, ORAI1, ORAI2, and ORAI3 as well as TRPC1 and TRPV6 are all expressed in dog PDEC, where ORAI3 was shown to be the dominant expressing type (Kim et al., 2013). Moreover, STIM1 and ORAI3 are colocalized in both single cell PDEC and polarized monolayers upon thapsigargin treatment (Kim et al., 2013). Using thapsigargin, the same authors showed an increased  $[Ca^{2+}]_i$  only at the basolateral membrane, indicating that SOCs are mainly located at this site of the plasma membrane (Kim et al., 2013). It might be hypothesized that the localization of SOCs and  $Ca^{2+}$ -activated ion channels are the same in pancreatic duct cells as in acinar cells, and that they play a role in  $HCO_3^-$  secretion, as they play a role in enzyme and fluid secretion in acinar cells (Maleth and Hegyi, 2014).

## Aquaporin Channels

Aquaporins (AQPs) are activated by  $Ca^{2+}$  and mediate a water flow through the luminal membrane. The role of some AQP types in physiological and pathophysiological processes of exocrine pancreas has already been reviewed (Burghardt et al., 2006; Delporte, 2014; Arsenijevic et al., 2019). AQP1 is expressed



at the apical and basolateral membrane of centro-acinar cells and intercalated ductal cells (Burghardt et al., 2003; Burghardt et al., 2006) and is also expressed in capillary endothelial cells and at the pancreatic zymogen granule membrane (Cho et al., 2002; Burghardt et al., 2003). AQP5 has been found to be co-localized with AQP1 in the apical membrane of centro-acinar cells and intercalated ductal cells (Burghardt et al., 2003). Otherwise, AQP8 is expressed only in acinar cells in the apical membrane (Isokpehi et al., 2009). In the two-step process of pancreatic fluid secretion, AQP8 in the pancreatic acinar cells ensures the water flow across the plasma membrane, where NaCl makes the driving force. In the pancreatic ductal cells the driving force is maintained by HCO<sub>3</sub><sup>-</sup> and Na<sup>+</sup> through AQP1 and AQP5 (Burghardt et al., 2006). However, this theory is not well explained, since pancreatic fluid secretion was not found to be altered in AQP1, AQP5, AQP8, or AQP12 knockout mice (Ma et al., 2001; Yang et al., 2005; Ohta et al., 2009). Recently, the role of AQP1 has been confirmed to be involved in pancreatic fluid and bicarbonate secretion in an AQP1-knockout mouse model (Venglovecz et al., 2018).

## Chloride Channels

In the early 80's the evidence for Ca<sup>2+</sup> activated Cl<sup>-</sup> channels (CaCC) were presented by whole-cell patch clamp and single-channel currents in rat lacrimal acinar. Marty and co-workers showed that Cl<sup>-</sup> currents were evoked by muscarinic receptor activation and Ca<sup>2+</sup>, as previously demonstrated for the K<sup>+</sup> current (Marty et al., 1984; Petersen, 1992). Shortly after, following investigations confirmed this Ca<sup>2+</sup> activated Cl<sup>-</sup> current in rat pancreatic acinar cells (Randriamampita et al., 1988). The localization of these Ca<sup>2+</sup>-dependent channels was proposed to be both on the basolateral and the luminal site, but speculations and further studies revealed that the localization of CaCC was found in the luminal membrane of pancreatic acinar cells, where an early activation of Cl<sup>-</sup> currents was seen upon ACh stimulation (Kasai and Augustine, 1990; Zdebik et al., 1997). A small delayed current was found after Ca<sup>2+</sup> has spread to the basal pole of the cell, suggesting that CaCC are highly located at the luminal membrane and to some extent in the basolateral of pancreatic acinar cells (Kasai and Augustine, 1990). New evidence shows clearly that CaCC are exclusively localized to the apical membrane and regulate pancreatic fluid secretion (Marty et al., 1984; Kasai and Augustine, 1990; Park et al., 2001).

Gray and his team have investigated the properties and roles of Cl<sup>-</sup> channels in pancreatic duct epithelial cells. They and others, found two types of Cl<sup>-</sup> channels in pancreatic ducts cells; cystic fibrosis transmembrane conductance regulator (CFTR), regulated by rises in [cAMP]<sub>i</sub> and CaCC, regulated by an increase in [Ca<sup>2+</sup>]<sub>i</sub> (Gray et al., 1989; Riordan et al., 1989; Gray et al., 1990b; Gray et al., 1993; al-Nakkash and Cotton, 1997; Nguyen et al., 1997). Both types of channels have been found in several species and to be localized in the apical membrane of duct cells (Gray et al., 1990b; Marino et al., 1991; Ashton et al., 1993; Evans et al., 1996; al-Nakkash and Cotton, 1997; Zeng et al., 1997; Ishiguro et al., 2002; Wang and Novak, 2013; Yokoyama

et al., 2019). CaCC have been found in rodent pancreatic ducts. Here, it was shown that increases in [Ca<sup>2+</sup>]<sub>i</sub>, evoked by either ionomycin or ACh activated the Cl<sup>-</sup> channels (Gray et al., 1990b; Gray et al., 1995). Furthermore, Cl<sup>-</sup> currents were detected in mouse pancreatic ducts with no detectable function of CFTR, which indicates that these currents are carried by an ion channel that is distinct from CFTR (Gray et al., 1994; Winpenny et al., 1995).

Until now, it has been shown that mammalian TMEM16 proteins have different physiological functions. TMEM16A and B are suggested to be CaCC, where both of TMEM16E and F are suggested to have scramblase and channel activities. TMEM16D, G, and J are suggested to only have a scramblase activity. Therefore, the channel nature of all TMEM16 proteins is still not clearly identified [Reviewed in (Falzone et al., 2018)]. Recently, it has been suggested that TMEM16A, of the TMEM16/Anoctamin family, is the CaCC gene candidate for Cl<sup>-</sup> secretion (Caputo et al., 2008; Schroeder et al., 2008; Yang et al., 2008). In rodent pancreatic acinar cells and intercalated ducts, expression of TMEM16A was found by immunostaining and RT-PCR (Huang et al., 2009; Yokoyama et al., 2019). The biophysical properties of the channel agreed with Ca<sup>2+</sup>-dependent Cl<sup>-</sup> currents, described elsewhere (Yang et al., 2008). Another study demonstrated that Ca<sup>2+</sup>-dependent Cl<sup>-</sup> secretion was defective in acinar cells from TMEM16A-null mice, indicating that TMEM16A has a physiological role in pancreatic fluid secretion (Ousingsawat et al., 2009).

The model of how Cl<sup>-</sup> is secreted through channels in exocrine pancreas is described as a two-step process, starting by the activation by ACh or CCK, which trigger an IP<sub>3</sub>-mediated rise of cytosolic Ca<sup>2+</sup> (Iwatsuki and Petersen, 1977; Reubi et al., 2003; Gautam et al., 2005; Wang and Cui, 2007). In response to this stimulation, the NaCl rich fluid starts to be produced (Hegyí and Petersen, 2013). At the basolateral membrane the Na<sup>+</sup>-K<sup>+</sup>-2Cl<sup>-</sup> cotransporters (NKCC), Cl<sup>-</sup>/HCO<sub>3</sub><sup>-</sup> exchangers and Na<sup>+</sup>/K<sup>+</sup> pumps are activated, to function together to establish the Cl<sup>-</sup> uptake mechanism. The increased [Ca<sup>2+</sup>]<sub>i</sub> enhances the Cl<sup>-</sup> conductance of the luminal membrane and a K<sup>+</sup> channel-mediated hyperpolarization of the basolateral membrane creates the driving force for Cl<sup>-</sup> efflux to the luminal space. At the apical membrane, Cl<sup>-</sup> ions pass through the Cl<sup>-</sup> channels. This hormonal stimulation by ACh and CCK, leading to increased [Ca<sup>2+</sup>]<sub>i</sub>, plays the central role in activating enzyme release and electrogenic Cl<sup>-</sup> secretion (Petersen and Gallacher, 1988; Mogami et al., 1997; Giovannucci et al., 2002; Petersen, 2005). While Cl<sup>-</sup> passes through the acinar cells a negative charge in the luminal space arises, which moves Na<sup>+</sup> from the interstitial space to the acinar lumen *via* the paracellular pathway through leaky tight junctions, resulting in NaCl secretion. In physiological circumstances the acinar luminal Cl<sup>-</sup> concentration contains 135 mM Cl and 25 mM HCO<sub>3</sub><sup>-</sup> (Park et al., 2010). The second step in pancreatic fluid secretion occurs in the duct cells and depends on the high concentration of luminal Cl<sup>-</sup> as it activates HCO<sub>3</sub><sup>-</sup> efflux through Cl<sup>-</sup>/HCO<sub>3</sub><sup>-</sup> exchangers, which elevates the luminal HCO<sub>3</sub><sup>-</sup> concentration and thereby activates CFTR functioning to secrete



Cl<sup>-</sup> and to some extent HCO<sub>3</sub><sup>-</sup> (Ishiguro et al., 2009; Wilschanski and Novak, 2013). The HCO<sub>3</sub><sup>-</sup> concentration in the fluid increases along the ducts, while the Cl<sup>-</sup> concentration reciprocally decreases. By the time the pancreatic fluid leaves the ducts the ratio is inverse, with the HCO<sub>3</sub><sup>-</sup> concentration around 140 mM and the Cl<sup>-</sup> concentration around 20 mM (Park et al., 2010). These specific concentrations will inhibit CFTR and Cl<sup>-</sup>/HCO<sub>3</sub><sup>-</sup> exchangers to prevent HCO<sub>3</sub><sup>-</sup> reabsorption (Wright et al., 2004).

## Sodium Channels

The efflux of Na<sup>+</sup> through tight junctions in both the acinar and ductal cells is a part of regulating the HCO<sub>3</sub><sup>-</sup> rich fluid to be isotonic and to keep the cell osmolarity (Lee M. G. et al., 2012). The expression and function of Na<sup>+</sup> channels in normal pancreatic tissue are controversial. Some studies have shown functional expression of amiloride sensitive epithelial sodium channels (ENaC) in interlobular ducts from mice (Zeihner et al., 1995; Pascua et al., 2009). Moreover, transcripts of different subunits of ENaC have been also detected in human pancreas (McDonald et al., 1994; Waldmann et al., 1995; Novak and Hansen, 2002). Other studies have shown no functional activity of ENaC in isolated small ducts from rats or in PDAC cell lines Capan-1 and HPAF (Novak and Hansen, 2002; Fong et al., 2003; Wang and Novak, 2013), which is in accordance with the secretory nature of pancreatic ducts.

## EXPRESSION OF ION CHANNELS IN PDAC CELLS AND HUMAN TISSUES, FUNCTION, AND ASSOCIATED SIGNALING PATHWAYS IN CELL LINES

### Potassium Channels in PDAC

#### Kv Channels

It is widely accepted that Kv channels participate in cancer development and progression and their expression has shown to be aberrant in several types of tumor tissue, also in PDAC (Serrano-Novillo et al., 2019; Teisseyre et al., 2019). It has been shown that Kv1.3 is expressed in different human PDAC cell lines, harboring mutation in p53 (Zaccagnino et al., 2017). The authors demonstrate that the inhibition of Kv1.3 by clofazimine, induces apoptosis *in-vitro* and reduces tumor weight *in-vivo* (Zaccagnino et al., 2017). Another study has reported a remodeling of Kv1.3 and Kv1.5 on a large cohort of human tissue samples (Bielanska et al., 2009). In fact, they showed that protein expression of Kv1.3 was lower in PDAC tissue, while Kv1.5 had a higher protein expression in PDAC tissue compared to healthy tissue (Bielanska et al., 2009; Comes et al., 2013). The low expression of Kv1.3 in PDAC can be explained by a hypermethylation of the *KCNA3* gene promoter (Brevet et al., 2009). Similar to Kv1.3 the expression of Kv7.1 has recently been shown to be down-regulated in PDAC (Zaccagnino et al., 2016; Tawfik et al., 2020). *KCNQ1* (gene coding for Kv7.1) was downregulated in PDAC tissue, compared to normal tissue. In addition, downregulation of *KCNQ1* was found in a system comparing PDAC A818-6 cells grown as a

highly malignant undifferentiated monolayer (ML) or as three-dimensional (3D) single layer hollow spheres (HS). Database analysis showed that *KCNQ1* was involved in the enrichment of pancreatic secretion in normal pancreatic epithelium and HS, suggesting that a downregulation of *KCNQ1* might impair fluid secretion in PDAC and ML cells, while being maintained in normal pancreas and HS cells (Tawfik et al., 2020). Another comprehensive study has been investigating the gene-expression levels of the transportome in PDAC and normal specimens (Zaccagnino et al., 2016). The authors showed the downregulation of five different K<sup>+</sup> channels, including the K<sup>+</sup> voltage-gated channels; *KCNQ1* and *KCNE1*. Moreover, their results showed a downregulation of genes coding for the Kir4.2 (*KCNJ15*), Kir5.1 (*KCNJ16*), and the K<sub>2</sub>P channel TWIK-3 (*KCNK7*). In addition, the expression of *KCNJ15* and *KCNK7* was associated with the expression of EMT transcription factors (Zaccagnino et al., 2016). The authors also suggested that the higher expression of K<sup>+</sup> channels in normal pancreatic epithelium takes part in setting the resting membrane potential, which generates the driving force of fluid and ion secretion in the pancreatic ducts (Zaccagnino et al., 2016).

Kv10.1 is another Kv channel that has been reported in pancreatic cancer. The expression of Kv10.1 in peripheral tissues is very restricted (Hemmerlein et al., 2006), including pancreatic tissue (Pardo et al., 1999). A xenograft mouse model of pancreatic cancer showed that monoclonal antibodies blocking the Kv10.1 current exerts antitumor activity (Gomez-Varela et al., 2007). Because Kv10.1 is nearly absent in normal tissue, there is a certain tumor selectivity for Kv10.1 expression, which gives rise to the possibility that Kv10.1 can be used as a targeting channel for the delivery of cytotoxic compounds (Pardo and Stuhmer, 2014). However, the expression and function of Kv10.1 in PDAC must be further investigated.

Interestingly, another Kv channel, Kv11.1 has been implicated as an oncogene in various cancers, including PDAC (Arcangeli et al., 2014; Lastraioli et al., 2015a). In contrast, to the Kv10.1 expression, Kv11.1 is ubiquitously expressed in normal human tissues including heart where it is mainly expressed (Sanguinetti et al., 1995; McDonald et al., 1997; Pond et al., 2000; Camacho, 2006; Comes et al., 2015). *KCNH2* (gene coding for Kv11.1) was identified as a gene with somatic mutations that could drive the metastatic process of PDAC (Zhou et al., 2012). Here, exome sequencing analysis showed that *KCNH2* clustered into a single network related to cancer development. To investigate the involvement of *KCNH2* in PDAC progression, the authors showed that knockdown of Kv11.1 reduced proliferation, colony formation and migration in PDAC cell lines. Immunohistochemical analysis of Kv11.1 expression showed expression in 8 out of 38 (21%) PDAC tissues, versus one out of 37 (2.7%) in normal tissues (Zhou et al., 2012). Another study further investigated the expression and role of Kv11.1 in PDAC (Feng et al., 2014). Here, immunohistochemical analysis confirmed a strong expression in PDAC tissues, with highest expression in the cytoplasm and membrane. In contrary, normal tissue showed only weak expression. The expression was confirmed in PDAC cell lines (Feng et al., 2014). Knockdown

of Kv11.1 showed a significant decreased proliferation rate, higher number of cells undergoing apoptosis, cell cycle arrest in G1 phase and a reduction of migration and invasion, suggesting that Kv11.1 has a role in different aspects of PDAC progression (Feng et al., 2014). This was confirmed in a xenograft mouse model, where a knockdown of Kv11.1 in CFPAC-1 cells showed reduced tumor growth and fewer metastatic nodules, compared to tumors in mice injected with control cells (Feng et al., 2014). Furthermore, it was found that miR-96 was downregulated in tumor tissue and PDAC cells. The overexpression of miR-96 reduced cell proliferation, migration, and invasion *in-vitro* and reduced the Kv11.1 expression, tumor growth, and formation of metastasis *in-vivo* (Feng et al., 2014). This indicates that Kv11.1 could function as an oncogene in PDAC and be a potential target of miR-96 (Feng et al., 2014). Further investigations showed that Kv11.1 promotes pancreatic cancer cell migration, by modulation of F-actin organization and dynamics (Lastraioli et al., 2015b) suggesting its involvement in cancer metastasis (Arcangeli et al., 2014; Manoli et al., 2019).

### KCa Channels/KCa3.1/IK

IK (KCa3.1) channels are the K<sup>+</sup> channels most frequently studied among this family in PDAC. Even though, transcripts of KCa4.1 and KCa4.2 also have been shown in some cell lines (Hayashi et al., 2012). Investigation of the KCa3.1 mRNA expression in primary pancreatic cancer tumors show that 8 of 9 tumors (89%) contain a 6- to 66-fold higher expression, compared to normal pancreatic tissue (Jager et al., 2004). KCa3.1 is also found overexpressed in several PDAC cell lines (Jager et al., 2004). The over-expression of KCa3.1 was associated with an increased Ca<sup>2+</sup>-activated K<sup>+</sup>-current. Pharmacological inhibition (by TRAM-34, Clotrimazole) of KCa3.1 completely suppressed cell proliferation of MiaPaCa-2 and BxPC-3 cells but not PANC-1 cells (Jager et al., 2004). Moreover, application of [Ca<sup>2+</sup>]<sub>o</sub> while inhibiting with TRAM-34 or Clotrimazole rescued the MiaPaCa-2 and BxPC-3 cell proliferation but did not affect this of PANC-1 suggesting that PANC-1 cell line grows independently of functional KCa3.1 channels (Jager et al., 2004). Bonito and co-workers have also reported the role of KCa3.1 in PDAC cell proliferation and migration (Bonito et al., 2016). They showed a significant mRNA upregulation of KCa3.1 in MiaPaCa-2 and BxPC-3, but not in Capan-1 and PANC-1 cells. In addition, Patch clamp measurements revealed a Ca<sup>2+</sup>-activated K<sup>+</sup> current, which was reduced by TRAM-34 and clotrimazole. Interestingly, a transient gene silencing of KCa3.1 in MiaPaCa-2 cells completely abolished the Ca<sup>2+</sup> current (Bonito et al., 2016). MiaPaca-2 cell proliferation was inhibited with TRAM-34 and 1% FBS, whereas no effect was found by application of TRAM-34 and 10% FBS in the culture media, as shown before (Jager et al., 2004). Silencing of KCa3.1 removed the ability of MiaPaCa-2 cells to proliferate, and attenuated their cell invasion and migration. Surprisingly treatment upon TRAM-34 or clotrimazole increased cell migration. It was hypothesized that this could be due to Ca<sup>2+</sup> homeostasis, which was investigated by Ca<sup>2+</sup> imaging that confirmed that TRAM-34 evoked an increase of [Ca<sup>2+</sup>]<sub>i</sub> (Bonito et al., 2016)

possibly leading to promotion of cell migration (Lotz et al., 2004). This indicates that KCa3.1 expression and function are important for cell proliferation, migration and invasion (Bonito et al., 2016). Another study has identified KCa3.1 as a regulator of oxidative phosphorylation in MiaPaCa-2 cells as silencing and inhibition of KCa3.1 determined the effect of channel dependent-oxidative phosphorylation in proliferation and ATP generation (Kovalenko et al., 2016). In addition, MiaPaCa-2 cells showed mRNA and protein levels in mitochondria, suggesting that KCa3.1 is involved in proliferation through metabolic processes (Kovalenko et al., 2016). Three other studies have identified *KCNN4* (gene coding for KCa3.1) as a gene related to PDAC as its transcripts and gene-level were upregulated compared to normal pancreatic tissue (Zaccagnino et al., 2016; Jiang et al., 2017; Shen et al., 2017). The upregulation of *KCNN4* was associated with the gene expression of different EMT transcription factors (Zaccagnino et al., 2016).

### Two-Pore K<sup>+</sup> Channels (K<sub>2</sub>P)

The outward conducting, pH and membrane potential activated K<sub>2</sub>P channels have an impact on physiological processes. They can regulate the cell volume, the membrane potential in form of being pH sensitive, modulate ion transport and Ca<sup>2+</sup> homeostasis. They are involved in cancer progression due to their impact on cell growth survival and migration, as it has been shown in different types of cancer (Mu et al., 2003; Kim et al., 2004; Voloshyna et al., 2008; Alvarez-Baron et al., 2011; Lee G. W. et al., 2012; Nagy et al., 2014; Sauter et al., 2016). A broad data base analysis of K<sub>2</sub>P expression in different cancers revealed an aberrant expression of different K<sub>2</sub>P in PDAC (Williams et al., 2013). mRNA expression of *KCNK1* (gene coding for TWIK-1) was upregulated in PDAC compared to normal tissue, and *KCNK3* (gene coding for TASK-1) were downregulated (Williams et al., 2013). One study has found the functional mRNA and protein expression of *KCNK5* (gene coding for TASK-2) in PDAC cell lines HPAF, but the role in cancer progression was not further studied (Fong et al., 2003). In another study a pH sensitive K<sup>+</sup> current was identified in BxPC-3 cells and was probably mediated by TREK-1 (Sauter et al., 2016). TREK-1 protein expression was shown in PDAC cell lines where it was shown that TREK-1 was involved in proliferation (Sauter et al., 2016). A similar pattern was shown in a scratch wound healing assay where activation of TREK-1 lead to decreased migration. These results indicate that TREK-1 has a potential inhibiting role in PDAC proliferation and migration (Sauter et al., 2016). Very few studies have been done on the role of K<sub>2</sub>P channels in PDAC. However, it can be suggested from other types of cancer that these channels can be related to cancer progression (Comes et al., 2015).

### Calcium Channels in PDAC

#### ORAI and STIM

It is well known that physiological Ca<sup>2+</sup> signaling has many effects in the exocrine pancreas, and takes part in stimulating secretion of HCO<sub>3</sub><sup>-</sup> and other ions (Hegyi and Petersen, 2013; Maleth and Hegyi, 2014). In non-excitabile cells, such as cancer cells, Ca<sup>2+</sup> entry

occurs mainly through SOCs (Mo and Yang, 2018) but also through transient receptor potential channels (TRP), which are selective for both  $\text{Ca}^{2+}$  and  $\text{Na}^+$  (Worley et al., 2007).

There is increasing evidence of dysregulated  $\text{Ca}^{2+}$  signaling in cancer. This evidence is based on the implication of SOCs and TRP in key hallmarks of cancer progression and as prognostic markers in several types of cancers (Prevarskaya et al., 2007; Shapovalov et al., 2016; Chen et al., 2019). Some members of SOCs and TRP have been studied in PDAC, even though knowledge is less pronounced compared to other types of cancer, such as breast-, cervical-, and colorectal cancer (Chen et al., 2019).

The complex of ORAI1 and STIM1 has been shown to play a role in carcinogenesis and to be involved in regulation of proliferation, migration, invasion and apoptosis in different types of cancer (Chen et al., 2019). Only two studies have been performed on PDAC showing that ORAI1 and STIM1 mediate SOC entry and that they are involved in proliferation, survival and apoptosis (Kondratska et al., 2014; Khan et al., 2020). It has been shown that both ORAI1 and STIM1 were expressed in several PDAC cell lines at mRNA and protein levels, with PANC-1 showing the highest levels of both. Knockdown of ORAI1 and STIM1 with siRNA showed a significant reduction of  $\text{Ca}^{2+}$  entry. This was confirmed in PANC-1, AsPC-1, MiaPaCa-2, and Capan-1 cells, indicating that SOC entry is mediated by ORAI1 and STIM1 in different PDAC cell lines. A recent study has revealed the involvement of Calcium Release-Activated calcium (CRAC) channel (ORAI1) in proliferation of PDAC (Khan et al., 2020). An inhibition with CRAC channel inhibitor, RP4010, showed a significant reduction of cell proliferation and colony formation in MiaPaCa-2 cells and in L3.6pl (a pancreatic adenocarcinoma derived cell line). The influx of calcium was also inhibited upon treatment with RP4010, suggesting that cell proliferation is mediated by regulation of  $\text{Ca}^{2+}$  entry through CRAC channel (Khan et al., 2020). It was proposed that cell proliferation was calcium-regulated through the AKT/mTOR signaling pathway as RP4010 inhibition decreased the mRNA levels and protein expression of phosphorylated AKT, modulated the expression of proteins important for downstream AKT/mTOR signaling. Furthermore, RP4010 or ORAI1 knockdown showed a decrease in mRNA levels and in nuclear translocation of NFAT1, suggesting that CRAC channel takes part in modulating calcium signaling associated with NFAT translocation and that PDAC proliferation is regulated through the calcium-activated AKT/mTOR/NFAT signaling (Khan et al., 2020). To test if RP4010 could enhance anticancer activity of standard used treatments gemcitabine and Nab-Paclitaxel, a combination of the three drugs were used to treat PDAC cell lines. The results showed a decrease in proliferation. A synergistic effect of certain dose combinations of RP4010 with gemcitabine/Nab-Paclitaxel was found to inhibit cell growth. In addition, this synergistic treatment downregulated the expression of NFATC1 and mTOR mRNA and NFAT1, NF- $\kappa$ B, and phosphorylated S6K proteins, suggesting that inhibition of cell proliferation through CRAC channel are mediated by a downregulation of mTOR,

NFAT and NF- $\kappa$ B signaling (Khan et al., 2020). The anticancer activity and the synergistic effect of RP4010/Gemcitabine/Nab-Paclitaxel were tested *in-vivo*. In a patient-derived xenograft mouse model, it was shown that Ki-67 expression decreased with the treatment of RP4010 or by the triple combination treatment (Khan et al., 2020). The overexpression found by Kondratska and co-workers can explain increased  $[\text{Ca}^{2+}]_i$  levels in PDAC cell lines, and that this is a mechanism for survival (Kondratska et al., 2014). In contrast, another study has found decreased gene expression levels of ORAI1 (Zaccagnino et al., 2016).

A recent study has been investigating the role of STIM1 in PDAC progression (Wang et al., 2019). shRNA knockdown of STIM1 showed decreased proliferation, invasion, and upregulation of E-cadherin protein levels and downregulation of vimentin levels, suggesting that STIM1 is involved in carcinogenesis of PDAC and in some way involved in Epithelial-Mesenchymal transition (EMT). Even though, E-cadherin levels have shown to be upregulated, in contrary to what is usually seen in cells undergoing EMT where E-cadherin decrease in favor of N-cadherin (Gheldof and Berx, 2013). Furthermore, tissue microarray analysis showed that the STIM1 expression positively correlated with HIF-1 $\alpha$  (Wang et al., 2019). It was further shown that similar protein expression levels of STIM1 and HIF-1 $\alpha$  were expressed in different PDAC cell lines. STIM1 and HIF-1 $\alpha$  protein levels were also upregulated in some PDAC tumor samples compared to non-tumor samples. Knockdown of HIF-1 $\alpha$  in PANC-1 cells revealed a significantly lower mRNA and protein expression of STIM1. The co-upregulation of both proteins and the downregulation of STIM1 upon knockdown of HIF-1 $\alpha$  indicate that STIM1 is regulated by HIF-1 $\alpha$  on the transcriptional level. STIM1 promoter activity was tested in PANC-1 cells upon normoxia or hypoxia, where HIF-1 $\alpha$  binding sites, under hypoxic conditions reduced STIM1 promoter activity (Wang et al., 2019). These results indicate that HIF-1 $\alpha$  probably regulates STIM1 transcription and that STIM1 overexpression, in a hypoxic environment, can promote PDAC progression and invasion (Wang et al., 2019).

The EMT process is stimulated upon loss of cell-cell contact and occurs in migrating cancer cells (Gheldof and Berx, 2013). It has been shown in disconnected individual PANC-1 cells that ER/Plasma membrane junctions containing STIM1, together with the IP<sub>3</sub>Rs, redistribute to the leading edge of focal adhesions (Okeke et al., 2016). An inhibition of IP<sub>3</sub>Rs and SOC entry reduced the migrating capacity of PANC-1 cells. This mechanism indicates the importance of  $\text{Ca}^{2+}$  signaling in migration through SOC entry and intracellular calcium channels (Okeke et al., 2016).

### TRP Channels

TRP form an adaptable family of ion channel proteins where the majority are calcium permeable and show regulatory patterns that are sensitive to different environmental factors (Shapovalov et al., 2016). The role of TRP has been reported in different types of cancer (Prevarskaya et al., 2007). It has been proposed that



TRPC1 can regulate PDAC cell proliferation through TGF- $\beta$  signaling, as TGF- $\beta$  has been shown to be one of the key modulators of EMT in mammary epithelial cells (Radisky and LaBarge, 2008). In PDAC cell line BxPC-3, TGF- $\beta$  has shown to induce  $[Ca^{2+}]_i$  increase leading to activation of the  $Ca^{2+}$ -dependent protein kinase C $\alpha$  (PKC- $\alpha$ ) and its translocation to the plasma membrane. PKC- $\alpha$  activation by TGF- $\beta$  initiates the motility and migration by inhibiting tumor suppressor PTEN (Chow et al., 2008). Further on, it has been shown that there is a high expression of TRPC1, TRPC4 and TRPC6 in BxPC-3 cells (Dong et al., 2010). Here, it was confirmed that TGF- $\beta$  induces cytosolic  $Ca^{2+}$  concentrations through TRPC1, followed by a PKC- $\alpha$  activation, thus initiating motility and migration. This was shown by a pharmacological inhibition of SOC entry pathways with 2-APB and  $La^{3+}$ , which abolishes the TGF- $\beta$  induced cytosolic  $Ca^{2+}$  increase. Furthermore, blocking of PKC- $\alpha$  with selective PKC- $\alpha$  inhibitors inhibited the TGF- $\beta$  mediated  $Ca^{2+}$  entry. In addition, knockdown of TRPC1 with siRNA reversed the effect of TGF- $\beta$  on cell motility, although, knockdown of TRPC4 and TRPC6 did not have an effect on motility of TGF- $\beta$  mediated BxPC-3 cell motility (Dong et al., 2010). These observations suggest that dysregulated  $Ca^{2+}$  entry through TRPC1 could be involved in EMT, and thereby invasion and metastasis of PDAC.

TRPV channels function as sensors in the central and peripheral nervous system where the majority is sensitive to voltage and temperature (Premkumar and Abooj, 2013). TRPV1 has shown to be related to oncogenesis and is expressed in different types of cancer (Domotor et al., 2005; Lazzeri et al., 2005; Sanchez et al., 2005; Miao et al., 2008; Morelli et al., 2014; Vercelli et al., 2014). TRPV1 can be activated by multiple pathways, which can promote pancreatic inflammation and pain, but also pancreatic cancer (Hartel et al., 2006; Huang et al., 2020). TRPV1 was shown to be upregulated at the mRNA and protein level in PDAC tissue compared to normal pancreatic tissue (Hartel et al., 2006). TRPV1 staining has been shown in both normal acini and ducts but with highest intensity in nerves of inflamed tissue surrounding the cancer. The elevated TRPV1 expression in infiltrating nerves was associated with pain in patients with PDAC. The same authors showed that inhibition of TRPV1 with resiniferatoxin induces apoptosis by targeting mitochondrial respiration and decreases cell growth in some PDAC cell lines (Hartel et al., 2006).

Recently, it has been shown that TRPV1 regulates the Epidermal Growth Factor Receptor (EGFR) in PANC-1 cell line (Huang et al., 2020). In this study, an overexpression of TRPV1 has been associated with a decrease in protein expression of EGFR in PANC-1. Vice versa, the downregulation and inhibition of TRPV1 increases the protein expression of EGFR. In addition, an overexpression of TRPV1 showed increased levels of ubiquitinated EGFR. The membranous fractions of EGFR were reduced, while the cytoplasmic were increased compared to the control (Huang et al., 2020). This indicates that TRPV1 promotes EGFR ubiquitination and thereby a downregulation of EGFR activity, resulting in EGFR cytoplasmic translocation and degradation, which was found to be mainly through

the lysosomal pathway (Huang et al., 2020). Furthermore, it was shown that TRPV1 overexpression inhibited proliferation, probably through the MAPK signaling pathway. Overexpression of TRPV1 resulted in decreased mRNA levels of KRAS and AKT2 and a treatment with EGF reduced the protein expression of ERK, JNK, and CREB, suggesting that a TRPV1 overexpression decreases EGFR/MAPK dependent proliferation in PANC-1 cells (Huang et al., 2020). The two above mentioned studies show contrary results in form of how the expression of TRPV1 is related to proliferation. Hartel et al., demonstrated that inhibition of TRPV1 terminate cell growth and induced apoptosis, where Huang et al., found that an overexpression of TRPV1 leads to a reduced proliferation rate (Hartel et al., 2006; Huang et al., 2020).

Another member of the TRPV family, TRPV6, was also found to be overexpressed in the primary pancreatic cancer tissues at both protein and mRNA levels. Moreover, by immunohistochemical analysis, it was found that TRPV6 is mainly localized in the cytoplasm in both tumor and normal tissue (Song et al., 2018). *In-vitro*, the highest level of TRPV6 was found in two pancreatic cell lines, Capan-2 and SW1990. The knockdown of TRPV6, by siRNA, resulted in reduced proliferation, cell cycle arrest in G0/G1 phase, promotion of apoptosis, and suppression of cell migration and invasion (Song et al., 2018). Furthermore, the silencing of TRPV6 resulted in a significant increase of sensitivity to the chemotherapeutic reagent oxaliplatin (Song et al., 2018). In contrast to this finding, Zaccagnino et al., 2016 showed a downregulation of TRPV6 in PDAC tissue, compared to normal pancreatic epithelium. Moreover, Tawfik et al., 2020 found also a downregulation of TRPV6 expression in a PDAC cell line A818-6 grown in a highly malignant undifferentiated monolayer. The authors suggest that a lower expression of TRPV6 could contribute to an inhibited epithelial fluid secretion in PDAC (Tawfik et al., 2020).

The TRPM family is also constituted with several members, which have been found to be implicated in carcinogenesis. One of the most studied in PDAC is TRPM7, which is a particular channel having an intrinsic kinase, together with its closest homolog TRPM6 (Yee et al., 2012a). TRPM7 is ubiquitously expressed and controls cellular homeostasis of ions, especially  $Mg^{2+}$  and  $Ca^{2+}$ . Interpreting that the developmental role of TRPM7 in zebrafish could be the same in humans, the role of TRPM7 has been studied in the development and progression of PDAC. Here, it has been shown that there was an overexpression of TRPM7 protein in PDAC tissue compared to normal tissue, and that TRPM7 is required for  $Mg^{2+}$ -regulated proliferation. Knockdown of TRPM7 with siRNA showed that this channel is necessary to prevent cell cycle arrest in G0/G1 phases. Furthermore, the proliferation of TRPM7-deficient PDAC cells was rescued by adding  $Mg^{2+}$  to the cell culture medium (Yee et al., 2011). Another study confirmed the overexpression of TRPM7 both at mRNA and protein levels in PDAC tissue (Rybarczyk et al., 2012). Furthermore, it was shown that TRPM7 silenced BxPC-3 cells decreased  $[Mg^{2+}]_i$ , suggesting that TRPM7 takes part in regulating  $Mg^{2+}$  uptake in PDAC cells. In contrary to previous findings, these authors demonstrated that the

silencing of TRPM7 had no effect on cell viability or proliferation, but a significant decrease of BxPC-3 cell migration (Rybarczyk et al., 2012). TRPM7 has also been found to be involved in cell invasion in both MiaPaCa2- and PANC-1 cells. In the two last cell lines, TRPM7 regulates constitutive cation currents, the influx and homeostasis of  $Mg^{2+}$ , and cell invasion through the Hsp90 $\alpha$ /uPA/MMP-2 proteolytic pathway (Rybarczyk et al., 2017).

Besides TRPM7, also other TRPM channels are found to be expressed in pancreatic cancer (Yee et al., 2010; Yee et al., 2014). TRPM8 is expressed in different types of adult human tissue and has also been found to be expressed in PDAC. In a panel of PDAC cell lines, mRNA TRPM8 was consistently overexpressed compared to the control cell line (H6c7) (Yee et al., 2010). This pattern has further been confirmed by immunohistochemistry in human PDAC tumors, compared to normal pancreatic tissue (Yee et al., 2010; Yee et al., 2014). Here, it was found that TRPM8 has a role in carcinogenesis in form of proliferation, migration and senescence. TRPM8 is required for proliferation by promoting cell cycle progression in PANC-1 and BxPC-3 cells, as a knockdown of TRPM8 showed a significant decrease in proliferation rate and a cell cycle arrest in G0/G1 phase (Yee et al., 2010). In another study, the knockdown of TRPM8 showed the opposite effect on proliferation. Here, the proliferation increased by 30% in PANC-1 cells and in contrary the proliferation was suppressed in HEK/M8 cells. It was found that TRPM8 is expressed in a non-glycosylated form in different PDAC cell lines, and that the channel in this form might have a protective role in PDAC (Ulaeanu et al., 2017). Concerning the involvement of TRPM8 in migration and invasion, two studies show opposite results. One study demonstrated that TRPM8 also is required for cell migration, as a knockdown of the channel impaired migration of BxPC-3 and MiaPaCa-2 by 60% and 45%, respectively (Yee et al., 2014). Where another study found that it enhanced the motility of PANC-1 cells (Cucu et al., 2014).

Recently, it has been shown that a third member of the TRPM family, also plays a role in PDAC progression (Lin et al., 2018). An overexpression of TRPM2 enhanced the proliferative, migrative and invasive abilities of PANC-1 cells, compared to the control cells and the results were inverted when TRPM2 was silenced in PANC-1 cells. It should be noted, that the study does not mention the application of a proliferation inhibitor during the Scratch wound-healing assay, which investigates the migratory role of TRPM2. Therefore, one can speculate if the wound-healing could be caused by proliferation, and not migration. Nevertheless, these results suggest that TRPM2 is involved at least in cell growth and invasion (Lin et al., 2018).

### Voltage-Dependent Calcium Channels

The expression of two voltage dependent  $Ca^{2+}$  channels have been found to be dysregulated in PDAC, namely, CaV2.1 (*CACNA1A*) and CaV3.1 (*CACNA1G*) are upregulated and downregulated, respectively (Zaccagnino et al., 2016). These sparse data indicate that voltage-dependent  $Ca^{2+}$  channels might have a role in PDAC progression.

## Chloride Channels in PDAC

### $Ca^{2+}$ -Activated Chloride Channel (CaCC) and TMEM Proteins

Aberrant expression and dysregulated function of  $Cl^-$  channels have shown to be involved in carcinogenesis, especially their role in cell volume regulation has shown to be important for cancer cell migration and infiltration (Duran et al., 2010; Prevarskaya et al., 2010; Anderson et al., 2019). In Capan-1 cells, CaCC are expressed at the apical membrane, as shown for normal pancreatic acinar and ductal cells (Park et al., 2001; Wang et al., 2013; Wang and Novak, 2013).

The functional role of TMEM16A has been found to vary between different types of cancer (Ayoub et al., 2010; Liu et al., 2012; Ruiz et al., 2012; Britschgi et al., 2013). While a pro-proliferative role was found in breast and prostate cancer, the role in pancreatic cancer has been found to be contradictory. An anti-proliferative effect was found by a knockdown and overexpression strategy in CFPAC-1 cells (Ruiz et al., 2012), where another study found that inhibition with the TMEM16A specific inhibitor T16A<sub>inh</sub>-A01 decreased the proliferation rate in CFPAC-1 cells (Mazzone et al., 2012). Both studies lack the comparison of PDAC cell lines with a normal pancreatic epithelial control cell line. This was considered in a recent study, where the role of TMEM16A was investigated in PDAC cell lines and compared to a normal pancreatic epithelial control cell line (Sauter et al., 2015). The mRNA expression of TMEM16A was upregulated, with a 1,450-fold, in AsPC-1, BxPC-3, and especially in Capan-1 cells (Sauter et al., 2015). The upregulation was confirmed by an increase in TMEM16A protein expression for all three cell lines. Furthermore, it was shown that TMEM16A carries the major component of CaCC current in these cell lines (Sauter et al., 2015). Moreover, the authors found that knockdown of TMEM16A had no effect on proliferation. Inhibition, by T16A<sub>inh</sub>-A01 or other CaCC inhibitors, failed to affect PDAC cell lines proliferation, while T16A<sub>inh</sub>-A01 had a significant effect on the control cell line cell proliferation, which almost completely lack the expression of TMEM16A. These results suggest that the inhibition by T16A<sub>inh</sub>-A01 is unspecific for TMEM16A, and that this channel has no implication in proliferation, at least in these three PDAC cell lines (Sauter et al., 2015). According to the role of TMEM16A in migration, gene silencing reduced the migratory capability of AsPC-1 and BxPC-3 cells, where the inhibition with T16A<sub>inh</sub>-A01 was ineffective (Sauter et al., 2015). Other CaCC inhibitors caused a decrease in migration of BxPC-3 cells. Nevertheless, Capan-1 cells showed the highest expression of TMEM16A, the migration was very slow, suggesting that TMEM16A is not implicated in the role of migration in Capan-1 cells and supporting that TMEM16A has different roles in carcinogenesis of PDAC cells (Sauter et al., 2015).

Another recent study has performed a database investigation on the expression of TMEM16A and found that mRNA TMEM16A expression is upregulated in pancreatic cancer (Crottes et al., 2019). The authors found that extracellular application of EGF increased  $[Ca^{2+}]_i$  and the outward-rectifying  $Cl^-$  current, which were both inhibited by different

TMEM16A inhibitors. The regulation of  $\text{Cl}^-$  currents and the  $\text{Ca}^{2+}$  response were probably due to SOC entry. Furthermore, silencing of TMEM16A in AsPC-1 cells reduced migration even under EGF treatments, while EGF induced migration in the control cell line. This indicates that TMEM16A is involved in EGF-induced PDAC migration and progression, probably through  $\text{Ca}^{2+}$  signaling. In addition, this study investigated the possible role of TMEM16A to classify PDAC patients (Crottes et al., 2019). They found 10 genes involved in EGF-induced TMEM16A-dependent  $\text{Ca}^{2+}$  signaling, which could distinguish neuro-endocrine tumors from other pancreatic cancers. In PDAC, these genes formed three clusters with different genetic profiles that could reflect different molecular characterizations (Crottes et al., 2019).

Another TMEM16 protein expressed in pancreatic cancer is the TMEM16J protein, which also has been found to be overexpressed (Jun et al., 2017). TMEM16J is not a well characterized protein, but it is proposed that it might function as a cation channel activated by the cAMP/PKA signaling pathway (Falzone et al., 2018; Kim et al., 2018). An upregulation of TMEM16J gene-, mRNA-, and protein overexpression were found in AsPC-1, BxPC-3, and Capan-2 cell lines and a small overexpression in PANC-1 cells. An overexpression of TMEM16J in PANC-1 cells resulted in phosphorylated ERK1/2 levels, but not total ERK1/2 levels. Furthermore, both EGFR and phosphorylated EGFR levels were upregulated in PANC-1 cells overexpressing TMEM16J and an immunoprecipitation assay revealed that both TMEM16A and TMEM16J formed protein complexes with EGFR, but the binding affinity for TMEM16J was 132% higher, than for the one of TMEM16A (Jun et al., 2017), suggesting that TMEM16J are involved in upregulation and activation of EGFR. In contrary, a knockdown of TMEM16J in AsPC-1 cells resulted in inhibition of phosphorylated ERK1/2, EGFR and phosphorylated EGFR and a decreased proliferation rate. These results were confirmed *in-vivo*, were a xenograft mouse model was made by implanting PANC-1 cells stably overexpressing TMEM16J. It was shown that tumor growth was significantly increased and immunohistochemistry of these tumors confirmed the TMEM16J overexpression (Jun et al., 2017). These results indicate that TMEM16J is implicated in cell proliferation and tumor growth. Another member of the TMEM16 family, TMEM16E, has been shown to be implicated in PDAC. It is not yet clear whether the TMEM16E protein function as an ion channel or scramblase (Falzone et al., 2018). It has been shown, by immunohistochemical analysis, that TMEM16E is entirely expressed in PDAC but not in normal pancreatic tissue (Song et al., 2019). The highest expression of both mRNA and protein of TMEM16E was found in PANC-1 cells. The impact of TMEM16E on migration was investigated by a wound-scratch assay and a siRNA knockdown of TMEM16E showed a significant decrease in PANC-1 cell migration (Song et al., 2019). Even though, it should be mentioned that the authors do not account for the possible effect of proliferation in this assay. The migration was in some ways confirmed by the downregulation of vimentin protein expression, compared to the control, which showed a higher

expression of vimentin, suggesting that TMEM16E is implicated in migration of PANC-1 cells. In addition, the proliferation of PANC-1 cells was significantly decreased upon knockdown of TMEM16E suggesting its role in proliferation (Song et al., 2019). This assay supports the speculation on the TMEM16E role in migration.

Besides being activated by  $\text{Ca}^{2+}$ , CaCC can also be activated and regulated by specific proteins, namely Calcium-activated Chloride channel regulators (CLCAs) also called Calcium Chloride channel accessory proteins. CLCAs are expressed in different types of cancer and have been implicated in regulation of proliferation, migration and metastasis (Yurtsever et al., 2012; Lang and Stourmaras, 2014; Stock and Schwab, 2015). CLCA1 has been shown to be overexpressed in pancreatic cancer (Hu et al., 2018a; Hu et al., 2018b). However, the expression pattern and underlying molecular mechanism of its role in PDAC is less known. Finally, low gene expression of Chloride Channel Kb (*CLCNKB*) and Chloride Voltage-Gated Channel 1 (*CLCN1*) have been reported in human PDAC tissue compared to normal pancreatic epithelium (Zaccagnino et al., 2016).

## CFTR

It has been shown that CFTR is expressed in some PDAC cell lines. An early study showed that CFTR only was expressed in Capan-1 cells among nine different pancreatic cell lines and that the expression varied as a function of confluence (Chambers and Harris, 1993). Singh et al., confirmed the almost non-existent expression of CFTR in PDAC cell lines. Indeed, mRNA levels were detectable in normal pancreatic tissue and three (Capan-1, Suit2 and SW1990) out of 16 pancreatic cell lines (Singh et al., 2007). Furthermore, Zaccagnino et al., reported the downregulation of CFTR, at gene-level, in human PDAC tissue compared to normal pancreatic epithelium. This downregulation was associated with gene expression of EMT transcription factors (Zaccagnino et al., 2016). Furthermore, Singh et al., showed that wild type CFTR negatively regulated MUC4 expression while silencing of CFTR upregulated MUC4 expression. As MUC4 is a protein involved in tumor migration and metastasis, the negative regulation by CFTR indicates a protective role and a tumor suppressing function by inhibiting MUC4 and hence pancreatic cancer progression (Singh et al., 2007).

A recent study has investigated CFTR expression in patient derived PDAC organoids, in order to enable routine organoid subtyping for personalized treatment (Hennig et al., 2019). It has been suggested that subtyping could be based on the expression of cytokeratin 81 (KRT81) and hepatocyte nuclear factor 1A (HNF1A). As the antibody for HNF1A was no longer available, the authors permitted CFTR to replace it as a potential marker instead of HNF1A (Hennig et al., 2019). Organoids can be categorized into the established quasi-mesenchymal, exocrine-like, and classical subtypes. Immunofluorescence staining showed a mutual expression pattern where exocrine-like organoids were  $\text{CFTR}^+/\text{KRT81}^-$  and quasi-mesenchymal  $\text{CFTR}^+/\text{KRT81}^+$ . The protein expression revealed by IF was compared to mRNA levels of CFTR, which matched in 8 out of 10 cases (Hennig et al., 2019). In addition, it was confirmed, by immunohistochemical analysis, that both CFTR and KRT81



were preserved in 6 out of 7 tumors, indicating that the organoids had the same subtype as their primary tumor (Hennig et al., 2019). These results suggest that CFTR could be a supplement marker for HFN1A and that CFTR/KRT81 together might be a suitable way to evaluate subtype organoids for personal treatments (Hennig et al., 2019).

### Cl<sup>-</sup> Intracellular Channel Proteins (CLICs)

CLICs are ubiquitously expressed and have been identified in several types of cancer, where they are either overexpressed or downregulated compared to the normal tissue (Peretti et al., 2015). In PDAC, CLICs are mostly found upregulated, even though their specific role in PDAC progression and development is not yet understood. CLIC2, CLIC3, and CLIC5 have been shown to be expressed at mRNA and protein levels in a HPAF cell line. By an electrophysiological study, the authors revealed that there was no single channel/conductance for apical Cl<sup>-</sup> secretion, but that these CLICs rather contributed to provide a constant net conductance across the plasma membrane (Fong et al., 2003). Another study has shown the importance of CLIC3 in PDAC, as immunohistochemical analysis and mRNA levels showed an overexpression of CLIC3 in PDAC tissue compared to normal pancreatic tissue (Dozynkiewicz et al., 2012). It was also found that CLIC3 in collaboration with Rab25 promoted cancer cell invasion and migration by integrin recycling from late endosomes/lysosomes (Dozynkiewicz et al., 2012). CLIC1 was overexpressed in primary tumors compared to normal pancreatic tissue, and strongly expressed in MiaPaCa-2 and PANC-1 cells (Lu et al., 2015). Silencing of CLIC1 showed a significant decrease in the proliferation rate, colony formation and the invasive abilities of both MiaPaCa-2 and PANC-1 cells, suggesting that CLIC1 contributes to the aggressive role of these PDAC cells (Lu et al., 2015). In addition, gene expression levels of CLIC5 has been found to be downregulated in PDAC tissue, compared to normal pancreatic epithelium and to be associated with gene expression of transcription factors related to cell differentiation (Zaccagnino et al., 2016).

### Aquaporins (AQPs) in PDAC

AQPs are expressed in various types of cancers and are predicted to be key regulators in tumor development and progression (Papadopoulos and Saadoun, 2015). The expression and role of AQPs in PDAC is poorly studied, yet few studies have described their involvement in PDAC progression (Burghardt et al., 2003; Direito et al., 2017; Huang et al., 2017; Zou et al., 2019). Burghardt and co-workers have found mRNA expression of AQP1, AQP3, AQP4, AQP5, and AQP8 in PDAC. All subtypes were expressed in solid tumors, where only AQP3, AQP4, and AQP5 were expressed in PDAC cell lines (Burghardt et al., 2003). Further studies have found an upregulation of AQP1 and AQP3 in PDAC tissue compared to normal pancreatic tissue (Zou et al., 2019). The expression of AQP1 correlated with the expression of AQP3, suggesting that these two channels cooperate during PDAC development. Another study has shown the overexpression of AQP3 and AQP5 in PDAC tissue (Direito et al., 2017). AQP5 localization in PDAC was found to be in the entire plasma

membrane and in the cytoplasm of ducts cells, where in normal pancreas the localization is in the apical membrane. Furthermore, AQP5 and AQP3 were suggested to be involved in proliferation and tumor transformation as a simultaneous overexpression was found to be correlated with an increased expression of EGFR, Ki-67, CK7, and a decrease of E-cadherin and increase of Vimentin (Direito et al., 2017). Another study investigating AQP has, through TCGA analysis, revealed that AQP3 shows the highest expression among AQPs in PDAC (Huang et al., 2017). The authors investigated the role of AQP3 further, with a focus on how microRNA (miR-874) regulates gene expression and post-translational events in PDAC. In a panel of eight pancreatic cell lines, they detected that cell lines with high AQP3 mRNA levels had lower miR-874 levels, where cell lines with high miR-874 had lower AQP3 levels suggesting that AQP3 expression is regulated by miR-874 (Huang et al., 2017). It was found that both modulation of AQP3 and miR-874 altered the expression and activity of mTOR and its downstream target S6, suggesting that an overexpression of AQP3 is associated with proliferation and cell survival by mTOR signaling in PDAC. In contrast to other studies, Zaccagnino et al. (2016) showed a downregulation of AQP3 and AQP8 expression in PDAC tissue compared to normal pancreatic one. Furthermore, they showed that AQP3 expression was associated with several cell differentiation related transcription factors.

### Sodium Channels in PDAC ASIC

It has recently been shown that acid-sensing ion channels (ASICs), an H<sup>+</sup>-gated subgroup of ENaC, are expressed in PDAC cell lines and tissue (Zhu et al., 2017). ASIC1 and ASIC3 were found functionally expressed and mRNA and protein expression were also found in PDAC cell lines. In all cases, the expression was upregulated compared to the normal control cell line. These results were confirmed in PDAC tissue where immunohistochemical analysis and qPCR revealed the overexpression compared to non-cancerous pancreatic tissue, suggesting that ASIC1 and ASIC3 have a pathophysiological role in PDAC (Zhu et al., 2017). Separate inhibition or knockdown of ASIC1 and ASIC3 decreased the acidity-promoted invasion and migration capacity of PDAC cell lines, but did not decrease the proliferation rate, suggesting that ASIC1 and ASIC3 are involved in the metastatic process of PDAC, but not tumor cell growth (Zhu et al., 2017). Furthermore, it was shown that ASIC1 and ASIC3 are involved in acidity-promoted EMT, as silencing or inhibition of ASIC1 or ASIC3 in PDAC cells showed decreased protein expression of mesenchymal markers Vimentin, N-cadherin, Snail, and ZEB1, while the epithelial marker E-cadherin showed increased protein expression. In contrary, PDAC cells overexpressing ASIC1 and ASIC3 showed an increase in mesenchymal markers and a decrease in epithelial markers, under acidic conditions. This was confirmed in human PDAC tissue samples by IF analysis. It was further investigated whether this mechanism was regulated by [Ca<sup>2+</sup>]<sub>i</sub>, where it was found that inhibition of ASIC1 or ASIC3 resulted in a decrease of [Ca<sup>2+</sup>]<sub>i</sub> upon acidification. In addition, the removal of [Ca<sup>2+</sup>]<sub>i</sub> upon acidic conditions decreased mesenchymal markers and



increased the epithelial ones. It was determined that the RhoA pathway, which is involved in cytoskeleton re-arrangement and cell migration, was a major effector of EMT induced by ASIC1/3- $[Ca^{2+}]_i$  activation in acidic conditions (Zhu et al., 2017). The role of ASIC1 and ASIC3 was further confirmed *in-vivo*, where a xenograft mouse model injected with BxPC-3 cells with a stable knockdown of ASIC1 and ASIC3 showed a significant decrease in lung and liver metastasis, but no obvious effect on tumor growth (Zhu et al., 2017).

### VGSCs

Another subfamily of  $Na^+$  channels, namely voltage gated sodium channels (VGSCs), has shown to be implicated in cancer progression (Angus and Ruben, 2019). An early study has shown that  $Ca^{2+}$  blockers Phenytoin and Verapamil inhibited the growth of pancreatic cancer cell lines MiaPaCa-2 and CAV, both *in-vitro* and *in-vivo* (Sato et al., 1994). Phenytoin and Verapamil were chosen because they appeared to be blocking different  $Ca^{2+}$  channels; T-type and L-type voltage dependent  $Ca^{2+}$  channels, respectively (Sato et al., 1994). It has been suggested that this growth-inhibition of pancreatic cancer cell was rather due to the block of VGSC than the block of  $Ca^{2+}$  channels, as both Phenytoin and Verapamil show high affinity for VGSC in the inactivated state of the channel (Ragsdale et al., 1991; Koltai, 2015). In addition, the expression of VGSC (*SCN9A* and *SCN3A*) was downregulated in PDAC (Zaccagnino et al., 2016).

## IONOTROPIC RECEPTORS IN PDAC

### Purinergic Receptors (P2XR) and N-Methyl-D-Aspartate Receptors (NMDAR)

Different types of ionotropic receptors including P2XR and NMDAR have been reported to be expressed in PDAC (Kunzli et al., 2007; Hansen et al., 2008; Burnstock and Novak, 2012; Li and Hanahan, 2013; North et al., 2017). Among P2XR, P2X7R is the most well described (Kunzli et al., 2007; Hansen et al., 2008; Burnstock and Novak, 2012). This ionotropic receptor has shown to be overexpressed in PDAC cell lines and tissue (Kunzli et al., 2007; Giannuzzo et al., 2015), and to be implicated in the proliferating, apoptotic, migrating, and invading processes of PDAC (Kunzli et al., 2007; Hansen et al., 2008; Giannuzzo et al., 2015; Giannuzzo et al., 2016; Choi et al., 2018). In addition, the expression of NMDAR was found in both PDAC cell lines and PDAC tumors, and their inhibition and blocking resulted in reduced different PDAC cell lines viability and survival (Li and Hanahan, 2013; North et al., 2017). Furthermore, an inhibition of NMDAR prevented growth of tumor xenografts (Li and Hanahan, 2013; North et al., 2017).

## ION CHANNELS AS PDAC BIOMARKERS

A growing number of studies have investigated ion channel expression in pancreatic cell lines and human tissues, showing

modulation of mRNA and/or protein expression between normal and cancer cells. Among all the studied channels, only CFTR has lower expression in cancer cell lines compared to normal cells (Singh et al., 2007), while Kv1.3, Kv7.1, and TASK-1 were downregulated in PDAC tissue compared to healthy tissue (Brevet et al., 2009; Williams et al., 2013; Tawfik et al., 2020), suggesting a protective role and tumor suppressive function for these channels. Although most of the ion channels are overexpressed in PDAC, studies on ion channel expression patterns in correlation with clinical parameters are more limited.

### Diagnostic Markers

Some attention has been given to the connection between pancreatic cancer risk and CFTR deficiency. Mutations in the *CFTR* gene cause the hereditary life shortening disease cystic fibrosis (CF). Severe clinical manifestations occur upon CF in secretory epithelial tissues and in pancreas, mutations causing loss of function lead to pancreatic insufficiency (Wilschanski and Novak, 2013; Castellani and Assael, 2017). Different cohort studies have investigated how different variants of *CFTR* affect the risk of pancreatic cancer (Sheldon et al., 1993; Neglia et al., 1995). It has been shown that CF patients present an elevated risk to develop pancreatic cancer, even though the overall risk of developing cancer is the same as for the general population (Sheldon et al., 1993; Neglia et al., 1995). Furthermore, studies also indicate that patients who are *CFTR* mutant carriers develop pancreatic cancer in a younger age, compared to patients carrying a wildtype form of *CFTR* (McWilliams et al., 2010; Hamoir et al., 2013), and patients carrying a germline mutation to some degree have an increased risk of developing PDAC (Cazacu et al., 2018). One mechanism of which a *CFTR* mutation could cause pancreatic cancer is by the defect of CFTR and ion transport leading to dysregulated mucus secretion and obstruction of the pancreatic ducts, which all are events that could result in pancreatitis (McWilliams et al., 2010). Patients with chronic pancreatitis have a 26-fold higher risk for developing pancreatic cancer compared to the general population (Lowenfels et al., 1993; Kirkegard et al., 2017), suggesting that *CFTR* mutation could be considered as a new risk factor for developing PDAC.

In order to discriminate pancreatic premalignant/malignant lesions from benign lesions, an explorative proteomic approach was performed on a cohort of 24 patients using targeting mass spectrometry analysis of different biomarkers (Jabbar et al., 2018). This study proposed CLCA1 to be a supportive marker, which together with mucin-5AC (*MUC5AC*) and prostate stem-cell antigen (*PSCA*) could distinguish cystic precursor lesions from PDAC, suggesting that CLCA1 is a potential biomarker in PDAC diagnosis.

### Prognostic Markers of Cancer Progression and Aggressiveness

Different studies have investigated ion channels as potential biomarkers of PDAC development and progression. Using immunohistochemical analysis, high KCa3.1 expression in PDAC tissue was correlated with TNM stages III and IV

(Jiang et al., 2017), and high expression of STIM1 was correlated with tumor grade (Wang et al., 2019). Upregulation of Kv11.1 expression was associated with advanced tumor grade and high expression of Ki67 proliferative marker (Lastraioli et al., 2015b), whereas TRPV6, TRPM8 and AQP1/AQP3 channels were positively correlated with tumor stages III and IV and large tumor size (Yee et al., 2014; Du et al., 2018; Liu et al., 2018; Song et al., 2018; Zou et al., 2019). Finally, TRPM7 and Cl<sup>-</sup> intracellular channel proteins (CLIC1-3). CLIC1 overexpression was shown to be correlated with the three clinical parameters: advanced tumor grade, advanced tumor stage and large tumor size (Rybarczyk et al., 2012; Lu et al., 2015; Yee et al., 2015; Jia et al., 2016). These results suggest that all the ion channels cited above are associated with pancreatic tumor growth.

Regarding the metastatic status, immunohistochemistry experiments showed that TRPV6 expression was higher in cases where PDAC was infiltrating (Song et al., 2018). The same results were observed at mRNA and protein levels for CLIC3, with a highly detectable expression in regions where the tumor was invading normal pancreatic tissue (Dozynkiewicz et al., 2012). Other studies revealed higher TRPM7 and TRPM8 staining in metastatic tumors than in non-metastatic tumors (Yee et al., 2015; Liu et al., 2018), which was confirmed by qPCR for TRPM8 (Du et al., 2018). AQP1 and AQP3 were also more expressed in PDAC patients with lymph node metastasis and invasion, than in non-invasive cancers (Zou et al., 2019), whereas overexpression of Kir3.1 potassium channel (GIRK1) was not found to be correlated with metastatic status (Brevet et al., 2009).

Gene expression correlation analysis demonstrated that TRPM2 is strongly correlated with different genes including toll-like receptor 7 (TLR7) (Lin et al., 2018), which has already been associated with PDAC progression (Ochi et al., 2012; Grimmig et al., 2015; Wang et al., 2016). Moreover, AQP1 and AQP3 protein expression was highest in poorly differentiated tumors (Direito et al., 2017; Zou et al., 2019), whereas AQP5 is more expressed in moderately differentiated tumors (Direito et al., 2017), suggesting that AQPs are associated with tumor aggressiveness.

Finally, most of the studied ion channels in PDAC tissue were associated with overall survival of the patients. The authors usually used immunohistochemical staining on large cohorts and Kaplan-Meier survival analysis, to observe a correlation between high channel expression and short patient survival. This is the case for KCa3.1 (Jiang et al., 2017), STIM1 (Wang et al., 2019), TRPM8 (Liu et al., 2018), TRPV6 (Song et al., 2018), TMEM16J (Jun et al., 2017), CLIC1 (Lu et al., 2015; Jia et al., 2016), and AQP1/AQP3 (Zou et al., 2019). The same correlation was obtained on gene expression using qPCR for TRPM8 (Du et al., 2018) or TCGA for TRPM2 (Lin et al., 2018) and TMEM16A (Crottes et al., 2019). Furthermore, the mutation status of TRPM2 was also analyzed using Kaplan-Meier in 10 patients out of 159, and the mutated *TRPM2* gene revealed a negative correlation with patient survival, compared to patients expressing wildtype *TRPM2* (Lin et al., 2018). Studies on shorter cohorts also revealed that high protein expression of Kv11.1 and

TRPM7 channels are inversely correlated with overall survival using Pearson correlation on 18 patients, and multivariate overall survival analysis on 44 samples, respectively (Rybarczyk et al., 2012; Lastraioli et al., 2015a). Comparison of ion channels expression level in 9 patients with short survival (<12 months) and 10 patients with long survival (>45 months) showed that short survival was correlated with high expression of CLIC3 and low expression of CLCA1 (Hu et al., 2018b). This low CLCA1 expression correlated with shorter disease-free survival was confirmed using tissue microarrays, immunohistochemistry and Kaplan-Meier analysis in 140 patients (Hu et al., 2018a). Except for CLCA1 which could be proposed as a good prognostic marker, all the other studied ion channels could be proposed as poor prognostic markers.

These studies on human tissues highlighted the major clinical relevance of ion channels expression in pancreatic cancer development (Table 2 and Figure 3). Indeed, the expression of potassium, calcium, chloride channels, and aquaporins is mainly associated with aggressiveness and invasiveness and inversely correlated to patient survival, suggesting that they may be potential markers of poor prognosis.

## Therapeutic Targets

In general, PDAC cells are resistant to pro-apoptotic reagents, and overexpression of ion channels was shown to be involved in this resistance. Knockdown of TRPM7 in combination with gemcitabine treatment enhanced cytotoxicity in PANC-1 cells even though the precise mechanisms are not yet determined (Yee et al., 2012b), whereas the silencing of TRPV6 in Capan-2 PDAC cells resulted in a significant increase of sensitivity to the chemotherapeutic reagent oxaliplatin, but had little effect on gemcitabine and cisplatin treatments (Song et al., 2018). Another study has shown that silencing of TRPM8 in combination with gemcitabine suppressed the proliferation and invasion properties of PANC-1 and BxPC-3 cells. In addition, gemcitabine-sensitivity depended on TRPM8 silencing in these cell lines, where mRNA level of multi-drug related proteins was decreased, and expression of apoptosis-related proteins was also affected, suggesting that TRPM8 is involved in multi-drug resistance and apoptosis of PDAC cells (Liu et al., 2018). PANC-1 cells apoptosis was also increased after treatment with chemotherapeutic reagents 5-fluorouracil or gemcitabine in combination with a knockdown of ORAI1, STIM1, or both (Kondratska et al., 2014). Furthermore, it was shown that cells treated with either 5-fluorouracil or gemcitabine increased ORAI1 and STIM1 expression as well as SOC entry suggesting that ORAI1 and STIM1 confer resistance to chemotherapy, probably through the increase of SOC entry (Kondratska et al., 2014). More recently, STIM1 was found to be involved in gemcitabine resistance in PDAC (Zhou et al., 2020). The transcriptome sequencing analysis in established gemcitabine resistant PDAC cell lines, showed that STIM1 was significantly upregulated in the gemcitabine resistant cell lines, compared to the parental cell line (Zhou et al., 2020). Among the chloride channels, knockdown of TMEM16J provided an additive effect on inhibiting proliferation upon treatment with gemcitabine and

erlotinib, suggesting that a TMEM16J inhibitor can help to prevent gemcitabine resistance associated with the prolonged use of gemcitabine (Jun et al., 2017). The team of Arcangeli has been investigating another therapeutic perspective with the development of a novel anti-Kv11.1 antibody-conjugated PEG-TiO<sub>2</sub> nanoparticles for targeting PDAC cells (Sette et al., 2013).

## CONCLUSION

Increasing evidence indicates that ion channels are involved in the regulation of cancer proliferation, apoptosis, chemoresistance, migration, and invasion. The field of ion channels in PDAC still constitutes a novel area of research and even studies conclude their involvement in the malignancy and aggressiveness of PDAC, only relatively few studies provide the complete signaling pathways. Moreover, the majority of the studies cited in this review were carried out on 2D cultured cell lines. It appears thus necessary to develop and/or increase better approaches (organoids, 3D culture, and/or animal models) to investigate the candidate channel(s) as well as its (their) function and associated signaling pathways in PDAC. However, recently, an increasing number of publications on signaling in

pancreatic cancer take the tumor microenvironment into account. This reflects the interest in ionic channels and their potential promising use as therapeutic targets in the fight against pancreatic cancer.

## AUTHOR CONTRIBUTIONS

JS, ID-D, AA, and HO-A: design and manuscript preparation. All authors contributed to the article and approved the submitted version.

## FUNDING

JS is grateful for the funding by the Marie Skłodowska-Curie Innovative Training Network (ITN) Grant Agreement number: 813834 - pHioniC - H2020-MSCA-ITN-2018. HO-A is grateful for the funding by the Ministère de l'Enseignement Supérieur et de la Recherche, the Région Hauts-de-France (Picardie), the FEDER (Fonds Européen de Développement Économique Régional), the Université Picardie Jules Verne, and the Ligue Contre le Cancer (Septentrion).

## REFERENCES

- Aichler, M., Seiler, C., Tost, M., Siveke, J., Mazur, P. K., Da Silva-Buttkus, P., et al. (2012). Origin of pancreatic ductal adenocarcinoma from atypical flat lesions: a comparative study in transgenic mice and human tissues. *J. Pathol.* 226 (5), 723–734. doi: 10.1002/path.3017
- al-Nakkash, L., and Cotton, C. U. (1997). Bovine pancreatic duct cells express cAMP- and Ca(2+)-activated apical membrane Cl<sup>-</sup> conductances. *Am. J. Physiol.* 273 (1 Pt 1), G204–G216. doi: 10.1152/ajpgi.1997.273.1.G204
- Alvarez-Baron, C. P., Jonsson, P., Thomas, C., Dryer, S. E., and Williams, C. (2011). The two-pore domain potassium channel KCNK5: induction by estrogen receptor alpha and role in proliferation of breast cancer cells. *Mol. Endocrinol.* 25 (8), 1326–1336. doi: 10.1210/me.2011-0045
- Anderson, K. J., Cormier, R. T., and Scott, P. M. (2019). Role of ion channels in gastrointestinal cancer. *World J. Gastroenterol.* 25 (38), 5732–5772. doi: 10.3748/wjg.v25.i38.5732
- Angus, M., and Ruben, P. (2019). Voltage gated sodium channels in cancer and their potential mechanisms of action. *Channels (Austin)* 13 (1), 400–409. doi: 10.1080/19336950.2019.1666455
- Arcangeli, A., Crociani, O., and Bencini, L. (2014). Interaction of tumour cells with their microenvironment: ion channels and cell adhesion molecules. A focus on pancreatic cancer. *Philos. Trans. R. Soc. Lond. B. Biol. Sci.* 369 (1638), 20130101. doi: 10.1098/rstb.2013.0101
- Arsenijevic, T., Perret, J., Van Laethem, J. L., and Delporte, C. (2019). Aquaporins Involvement in Pancreas Physiology and in Pancreatic Diseases. *Int. J. Mol. Sci.* 20 (20). doi: 10.3390/ijms20205052
- Ashton, N., Evans, R. L., Elliott, A. C., Green, R., and Argent, B. E. (1993). Regulation of fluid secretion and intracellular messengers in isolated rat pancreatic ducts by acetylcholine. *J. Physiol.* 471, 549–562. doi: 10.1113/jphysiol.1993.sp019915
- Ayoub, C., Wasylyk, C., Li, Y., Thomas, E., Marisa, L., Robe, A., et al. (2010). ANO1 amplification and expression in HNSCC with a high propensity for future distant metastasis and its functions in HNSCC cell lines. *Br. J. Cancer* 103 (5), 715–726. doi: 10.1038/sj.bjc.6605823
- Bergmann, F., Andrusis, M., Hartwig, W., Penzel, R., Gaida, M. M., Herpel, E., et al. (2011). Discovered on gastrointestinal stromal tumor 1 (DOG1) is expressed in pancreatic centroacinar cells and in solid-pseudopapillary neoplasms—novel evidence for a histogenetic relationship. *Hum. Pathol.* 42 (6), 817–823. doi: 10.1016/j.humpath.2010.10.005
- Bielanska, J., Hernandez-Losa, J., Perez-Verdaguer, M., Moline, T., Somoza, R., Ramon, Y. C. S., et al. (2009). Voltage-dependent potassium channels Kv1.3 and Kv1.5 in human cancer. *Curr. Cancer Drug Targets* 9 (8), 904–914. doi: 10.2174/156800909790192400
- Bleich, M., and Warth, R. (2000). The very small-conductance K<sup>+</sup> channel KvLQT1 and epithelial function. *Pflugers Arch.* 440 (2), 202–206. doi: 10.1007/s004240000257
- Bonito, B., Sauter, D. R., Schwab, A., Djamgoz, M. B., and Novak, I. (2016). KCa3.1 (IK) modulates pancreatic cancer cell migration, invasion and proliferation: anomalous effects on TRAM-34. *Pflugers Arch.* 468 (11-12), 1865–1875. doi: 10.1007/s00424-016-1891-9
- Brevet, M., Fucks, D., Chatelain, D., Regimbeau, J. M., Delcenserie, R., Sevestre, H., et al. (2009). Deregulation of 2 potassium channels in pancreas adenocarcinomas: implication of KV1.3 gene promoter methylation. *Pancreas* 38 (6), 649–654. doi: 10.1097/MPA.0b013e3181a56ebf
- Britschgi, A., Bill, A., Brinkhaus, H., Rothwell, C., Clay, I., Duss, S., et al. (2013). Calcium-activated chloride channel ANO1 promotes breast cancer progression by activating EGFR and CAMK signaling. *Proc. Natl. Acad. Sci. U. S. A.* 110 (11), E1026–E1034. doi: 10.1073/pnas.1217072110
- Burghardt, B., Elkaer, M. L., Kwon, T. H., Racz, G. Z., Varga, G., Steward, M. C., et al. (2003). Distribution of aquaporin water channels AQP1 and AQP5 in the ductal system of the human pancreas. *Gut* 52 (7), 1008–1016. doi: 10.1136/gut.52.7.1008
- Burghardt, B., Nielsen, S., and Steward, M. C. (2006). The role of aquaporin water channels in fluid secretion by the exocrine pancreas. *J. Membr. Biol.* 210 (2), 143–153. doi: 10.1007/s00232-005-0852-6
- Burnstock, G., and Novak, I. (2012). Purinergic signalling in the pancreas in health and disease. *J. Endocrinol.* 213 (2), 123–141. doi: 10.1530/JOE-11-0434
- Camacho, J. (2006). Ether a go-go potassium channels and cancer. *Cancer Lett.* 233 (1), 1–9. doi: 10.1016/j.canlet.2005.02.016
- Caputo, A., Caci, E., Ferrera, L., Pedemonte, N., Barsanti, C., Sondo, E., et al. (2008). TMEM16A, a membrane protein associated with calcium-dependent chloride channel activity. *Science* 322 (5901), 590–594. doi: 10.1126/science.1163518



- Case, R. M., and Clausen, T. (1973). The relationship between calcium exchange and enzyme secretion in the isolated rat pancreas. *J. Physiol.* 235 (1), 75–102. doi: 10.1113/jphysiol.1973.sp010379
- Castellani, C., and Assael, B. M. (2017). Cystic fibrosis: a clinical view. *Cell Mol. Life Sci.* 74 (1), 129–140. doi: 10.1007/s00018-016-2393-9
- Cazacu, I. M., Farkas, N., Garami, A., Balasko, M., Mosdosi, B., Alizadeh, H., et al. (2018). Pancreatitis-Associated Genes and Pancreatic Cancer Risk: A Systematic Review and Meta-analysis. *Pancreas* 47 (9), 1078–1086. doi: 10.1097/MPA.0000000000001145
- Chambers, J. A., and Harris, A. (1993). Expression of the cystic fibrosis gene and the major pancreatic mucin gene, MUC1, in human ductal epithelial cells. *J. Cell Sci.* 105 (Pt 2), 417–422.
- Chen, C., Vincent, J. D., and Clarke, I. J. (1994). Ion channels and the signal transduction pathways in the regulation of growth hormone secretion. *Trends Endocrinol. Metab.* 5 (6), 227–233. doi: 10.1016/1043-2760(94)p3080-q
- Chen, Y. F., Lin, P. C., Yeh, Y. M., Chen, L. H., and Shen, M. R. (2019). Store-Operated Ca(2+) Entry in Tumor Progression: From Molecular Mechanisms to Clinical Implications. *Cancers (Basel)* 11 (7), 899. doi: 10.3390/cancers11070899
- Cho, S. J., Sattar, A. K., Jeong, E. H., Satchi, M., Cho, J. A., Dash, S., et al. (2002). Aquaporin 1 regulates GTP-induced rapid gating of water in secretory vesicles. *Proc. Natl. Acad. Sci. U. S. A.* 99 (7), 4720–4724. doi: 10.1073/pnas.072083499
- Choi, J. H., Ji, Y. G., Ko, J. J., Cho, H. J., and Lee, D. H. (2018). Activating P2X7 Receptors Increases Proliferation of Human Pancreatic Cancer Cells via ERK1/2 and JNK. *Pancreas* 47 (5), 643–651. doi: 10.1097/MPA.0000000000001055
- Chow, J. Y., Dong, H., Quach, K. T., Van Nguyen, P. N., Chen, K., and Carethers, J. M. (2008). TGF-beta mediates PTEN suppression and cell motility through calcium-dependent PKC-alpha activation in pancreatic cancer cells. *Am. J. Physiol. Gastrointest. Liver Physiol.* 294 (4), G899–G905. doi: 10.1152/ajpgi.00411.2007
- Comes, N., Bielanska, J., Vallejo-Gracia, A., Serrano-Albarras, A., Marruecos, L., Gomez, D., et al. (2013). The voltage-dependent K(+) channels Kv1.3 and Kv1.5 in human cancer. *Front. Physiol.* 4, 283. doi: 10.3389/fphys.2013.00283
- Comes, N., Serrano-Albarras, A., Capera, J., Serrano-Novillo, C., Condom, E., Ramon, Y. C. S., et al. (2015). Involvement of potassium channels in the progression of cancer to a more malignant phenotype. *Biochim. Biophys. Acta* 1848 (10 Pt B), 2477–2492. doi: 10.1016/j.bbame.2014.12.008
- Coradini, D., Casarsa, C., and Oriana, S. (2011). Epithelial cell polarity and tumorigenesis: new perspectives for cancer detection and treatment. *Acta Pharmacol. Sin.* 32 (5), 552–564. doi: 10.1038/aps.2011.20
- Crottes, D., Lin, Y. T., Peters, C. J., Gilchrist, J. M., Wiita, A. P., Jan, Y. N., et al. (2019). TMEM16A controls EGF-induced calcium signaling implicated in pancreatic cancer prognosis. *Proc. Natl. Acad. Sci. U. S. A.* 116 (26), 13026–13035. doi: 10.1073/pnas.1900703116
- Cucu, D., Chiritoiu, G., Petrescu, S., Babes, A., Stanica, L., Duda, D. G., et al. (2014). Characterization of functional transient receptor potential melastatin 8 channels in human pancreatic ductal adenocarcinoma cells. *Pancreas* 43 (5), 795–800. doi: 10.1097/MPA.000000000000106
- Delporte, C. (2014). Aquaporins in salivary glands and pancreas. *Biochim. Biophys. Acta* 1840 (5), 1524–1532. doi: 10.1016/j.bbagen.2013.08.007
- Demolombe, S., Franco, D., de Boer, P., Kupersmidt, S., Roden, D., Pereon, Y., et al. (2001). Differential expression of KvLQT1 and its regulator IsK in mouse epithelia. *Am. J. Physiol. Cell Physiol.* 280 (2), C359–C372. doi: 10.1152/ajpcell.2001.280.2.C359
- Direito, I., Paulino, J., Vigia, E., Brito, M. A., and Soveral, G. (2017). Differential expression of aquaporin-3 and aquaporin-5 in pancreatic ductal adenocarcinoma. *J. Surg. Oncol.* 115 (8), 980–996. doi: 10.1002/jso.24605
- Djamgoz, M. B., Coombes, R. C., and Schwab, A. (2014). Ion transport and cancer: from initiation to metastasis. *Philos. Trans. R. Soc. Lond. B. Biol. Sci.* 369 (1638), 20130092. doi: 10.1098/rstb.2013.0092
- Domotor, A., Peidl, Z., Vincze, A., Hunyady, B., Szolcsanyi, J., Kereskay, L., et al. (2005). Immunohistochemical distribution of vanilloid receptor, calcitonin-gene related peptide and substance P in gastrointestinal mucosa of patients with different gastrointestinal disorders. *Inflammopharmacology* 13 (1-3), 161–177. doi: 10.1163/156856005774423737
- Dong, H., Shim, K. N., Li, J. M., Estrema, C., Ornelas, T. A., Nguyen, F., et al. (2010). Molecular mechanisms underlying Ca2+-mediated motility of human pancreatic duct cells. *Am. J. Physiol. Cell Physiol.* 299 (6), C1493–C1503. doi: 10.1152/ajpcell.00242.2010
- Dozynkiewicz, M. A., Jamieson, N. B., Macpherson, I., Grindlay, J., van den Berghe, P. V., von Thun, A., et al. (2012). Rab25 and CLIC3 collaborate to promote integrin recycling from late endosomes/lysosomes and drive cancer progression. *Dev. Cell* 22 (1), 131–145. doi: 10.1016/j.devcel.2011.11.008
- Du, J. D., Zheng, X., Chen, Y. L., Huang, Z. Q., Cai, S. W., Jiao, H. B., et al. (2018). Elevated Transient Receptor Potential Melastatin 8 (TRPM8) Expression Is Correlated with Poor Prognosis in Pancreatic Cancer. *Med. Sci. Monit.* 24, 3720–3725. doi: 10.12659/MSM.909968
- Duprat, F., Lesage, F., Fink, M., Reyes, R., Heurteaux, C., and Lazdunski, M. (1997). TASK, a human background K+ channel to sense external pH variations near physiological pH. *EMBO J.* 16 (17), 5464–5471. doi: 10.1093/emboj/16.17.5464
- Duprat, F., Girard, C., Jarretou, G., and Lazdunski, M. (2005). Pancreatic two P domain K+ channels TALK-1 and TALK-2 are activated by nitric oxide and reactive oxygen species. *J. Physiol.* 562 (Pt 1), 235–244. doi: 10.1113/jphysiol.2004.071266
- Duran, C., Thompson, C. H., Xiao, Q., and Hartzell, H. C. (2010). Chloride channels: often enigmatic, rarely predictable. *Annu. Rev. Physiol.* 72, 95–121. doi: 10.1146/annurev-physiol-021909-135811
- Evans, R. L., Ashton, N., Elliott, A. C., Green, R., and Argent, B. E. (1996). Interactions between secretin and acetylcholine in the regulation of fluid secretion by isolated rat pancreatic ducts. *J. Physiol.* 496 (Pt 1), 265–273. doi: 10.1113/jphysiol.1996.sp021683
- Falzone, M. E., Malvezzi, M., Lee, B. C., and Accardi, A. (2018). Known structures and unknown mechanisms of TMEM16 scramblases and channels. *J. Gen. Physiol.* 150 (7), 933–947. doi: 10.1085/jgp.201711957
- Feng, J., Yu, J., Pan, X., Li, Z., Chen, Z., Zhang, W., et al. (2014). HERG1 functions as an oncogene in pancreatic cancer and is downregulated by miR-96. *Oncotarget* 5 (14), 5832–5844. doi: 10.18632/oncotarget.2200
- Fong, P., Argent, B. E., Guggino, W. B., and Gray, M. A. (2003). Characterization of vectorial chloride transport pathways in the human pancreatic duct adenocarcinoma cell line HPAF. *Am. J. Physiol. Cell Physiol.* 285 (2), C433–C445. doi: 10.1152/ajpcell.00509.2002
- Furuya, S., Naruse, S., Ko, S. B., Ishiguro, H., Yoshikawa, T., and Hayakawa, T. (2002). Distribution of aquaporin 1 in the rat pancreatic duct system examined with light- and electron-microscopic immunohistochemistry. *Cell Tissue Res.* 308 (1), 75–86. doi: 10.1007/s00441-002-0527-x
- Gabbi, C., Kim, H. J., Hultenby, K., Bouton, D., Toresson, G., Warner, M., et al. (2008). Pancreatic exocrine insufficiency in LXRbeta-/- mice is associated with a reduction in aquaporin-1 expression. *Proc. Natl. Acad. Sci. U. S. A.* 105 (39), 15052–15057. doi: 10.1073/pnas.0808097105
- Gallacher, D. V., Maruyama, Y., and Petersen, O. H. (1984). Patch-clamp study of rubidium and potassium conductances in single cation channels from mammalian exocrine acini. *Pflugers Arch.* 401 (4), 361–367. doi: 10.1007/BF00584336
- Gautam, D., Han, S. J., Heard, T. S., Cui, Y., Miller, G., Bloodworth, L., et al. (2005). Cholinergic stimulation of amylase secretion from pancreatic acinar cells studied with muscarinic acetylcholine receptor mutant mice. *J. Pharmacol. Exp. Ther.* 313 (3), 995–1002. doi: 10.1124/jpet.105.084855
- Gerasimenko, J. V., Gryshchenko, O., Ferdek, P. E., Stapleton, E., Hebert, T. O., Bychkova, S., et al. (2013). Ca2+ release-activated Ca2+ channel blockade as a potential tool in antipancreatitis therapy. *Proc. Natl. Acad. Sci. U. S. A.* 110 (32), 13186–13191. doi: 10.1073/pnas.1300910110
- Gheldof, A., and Bex, G. (2013). Cadherins and epithelial-to-mesenchymal transition. *Prog. Mol. Biol. Transl. Sci.* 116, 317–336. doi: 10.1016/B978-0-12-394311-8.00014-5
- Giannuzzo, A., Pedersen, S. F., and Novak, I. (2015). The P2X7 receptor regulates cell survival, migration and invasion of pancreatic ductal adenocarcinoma cells. *Mol. Cancer* 14, 203. doi: 10.1186/s12943-015-0472-4
- Giannuzzo, A., Saccomano, M., Napp, J., Ellegaard, M., Alves, F., and Novak, I. (2016). Targeting of the P2X7 receptor in pancreatic cancer and stellate cells. *Int. J. Cancer* 139 (11), 2540–2552. doi: 10.1002/ijc.30380
- Giovannucci, D. R., Bruce, J. I., Straub, S. V., Arreola, J., Sneyd, J., Shuttleworth, T. J., et al. (2002). Cytosolic Ca(2+) and Ca(2+)-activated Cl(-) current dynamics: insights from two functionally distinct mouse exocrine cells. *J. Physiol.* 540 (Pt 2), 469–484. doi: 10.1113/jphysiol.2001.013453

- Girard, C., Duprat, F., Terrenoire, C., Tinel, N., Fosset, M., Romey, G., et al. (2001). Genomic and functional characteristics of novel human pancreatic 2P domain K(+) channels. *Biochem. Biophys. Res. Commun.* 282 (1), 249–256. doi: 10.1006/bbrc.2001.4562
- Gomez-Varela, D., Zwick-Wallasch, E., Knotgen, H., Sanchez, A., Hettmann, T., Ossipov, D., et al. (2007). Monoclonal antibody blockade of the human Eag1 potassium channel function exerts antitumor activity. *Cancer Res.* 67 (15), 7343–7349. doi: 10.1158/0008-5472.CAN-07-0107
- Gouaux, E., and Mackinnon, R. (2005). Principles of selective ion transport in channels and pumps. *Science* 310 (5753), 1461–1465. doi: 10.1126/science.1113666
- Gray, M. A., Greenwell, J. R., and Argent, B. E. (1988). Secretin-regulated chloride channel on the apical plasma membrane of pancreatic duct cells. *J. Membr. Biol.* 105 (2), 131–142. doi: 10.1007/BF02009166
- Gray, M. A., Harris, A., Coleman, L., Greenwell, J. R., and Argent, B. E. (1989). Two types of chloride channel on duct cells cultured from human fetal pancreas. *Am. J. Physiol.* 257 (2 Pt 1), C240–C251. doi: 10.1152/ajpcell.1989.257.2.C240
- Gray, M. A., Greenwell, J. R., Garton, A. J., and Argent, B. E. (1990a). Regulation of maxi-K+ channels on pancreatic duct cells by cyclic AMP-dependent phosphorylation. *J. Membr. Biol.* 115 (3), 203–215. doi: 10.1007/bf01868636
- Gray, M. A., Pollard, C. E., Harris, A., Coleman, L., Greenwell, J. R., and Argent, B. E. (1990b). Anion selectivity and block of the small-conductance chloride channel on pancreatic duct cells. *Am. J. Physiol.* 259 (5 Pt 1), C752–C761. doi: 10.1152/ajpcell.1990.259.5.C752
- Gray, M. A., Plant, S., and Argent, B. E. (1993). cAMP-regulated whole cell chloride currents in pancreatic duct cells. *Am. J. Physiol.* 264 (3 Pt 1), C591–C602. doi: 10.1152/ajpcell.1993.264.3.C591
- Gray, M. A., Winpenny, J. P., Porteous, D. J., Dorin, J. R., and Argent, B. E. (1994). CFTR and calcium-activated chloride currents in pancreatic duct cells of a transgenic CF mouse. *Am. J. Physiol.* 266 (1 Pt 1), C213–C221. doi: 10.1152/ajpcell.1994.266.1.C213
- Gray, M. A., Winpenny, J. P., Verdon, B., McAlroy, H., and Argent, B. E. (1995). Chloride channels and cystic fibrosis of the pancreas. *Biosci. Rep.* 15 (6), 531–541. doi: 10.1007/BF01204355
- Grimmig, T., Matthes, N., Hoeland, K., Tripathi, S., Chandraker, A., Grimm, M., et al. (2015). TLR7 and TLR8 expression increases tumor cell proliferation and promotes chemoresistance in human pancreatic cancer. *Int. J. Oncol.* 47 (3), 857–866. doi: 10.3892/ijo.2015.3069
- Hamoir, C., Pepermans, X., Piessevaux, H., Jouret-Mourin, A., Weynand, B., Habyalimana, J. B., et al. (2013). Clinical and morphological characteristics of sporadic genetically determined pancreatitis as compared to idiopathic pancreatitis: higher risk of pancreatic cancer in CFTR variants. *Digestion* 87 (4), 229–239. doi: 10.1159/000348439
- Hanahan, D., and Weinberg, R. A. (2011). Hallmarks of cancer: the next generation. *Cell* 144 (5), 646–674. doi: 10.1016/j.cell.2011.02.013
- Hansen, M. R., Krabbe, S., and Novak, I. (2008). Purinergic receptors and calcium signalling in human pancreatic duct cell lines. *Cell Physiol. Biochem.* 22 (1–4), 157–168. doi: 10.1159/000149793
- Hartel, M., di Mola, F. F., Selvaggi, F., Mascetta, G., Wente, M. N., Felix, K., et al. (2006). Vanilloids in pancreatic cancer: potential for chemotherapy and pain management. *Gut* 55 (4), 519–528. doi: 10.1136/gut.2005.073205
- Hayashi, M., and Novak, I. (2013). Molecular basis of potassium channels in pancreatic duct epithelial cells. *Channels (Austin)* 7 (6), 432–441. doi: 10.4161/chan.26100
- Hayashi, M., Wang, J., Hede, S. E., and Novak, I. (2012). An intermediate-conductance Ca<sup>2+</sup>-activated K<sup>+</sup> channel is important for secretion in pancreatic duct cells. *Am. J. Physiol. Cell Physiol.* 303 (2), C151–C159. doi: 10.1152/ajpcell.00089.2012
- Hede, S. E., Amstrup, J., Christoffersen, B. C., and Novak, I. (1999). Purinoceptors evoke different electrophysiological responses in pancreatic ducts. P2Y inhibits K(+) conductance, and P2X stimulates cation conductance. *J. Biol. Chem.* 274 (45), 31784–31791. doi: 10.1074/jbc.274.45.31784
- Hede, S. E., Amstrup, J., Klaerke, D. A., and Novak, I. (2005). P2Y2 and P2Y4 receptors regulate pancreatic Ca(2+)-activated K+ channels differently. *PLoS Arch.* 450 (6), 429–436. doi: 10.1007/s00424-005-1433-3
- Hegy, P., and Petersen, O. H. (2013). The exocrine pancreas: the acinar-ductal tango in physiology and pathophysiology. *Rev. Physiol. Biochem. Pharmacol.* 165, 1–30. doi: 10.1007/112\_2013\_14
- Hemmerlein, B., Weseloh, R. M., Mello de Queiroz, F., Knotgen, H., Sanchez, A., Rubio, M. E., et al. (2006). Overexpression of Eag1 potassium channels in clinical tumours. *Mol. Cancer* 5:41. doi: 10.1186/1476-4598-5-41
- Hennig, A., Wolf, L., Jahnke, B., Polster, H., Seidlitz, T., Werner, K., et al. (2019). CFTR Expression Analysis for Subtyping of Human Pancreatic Cancer Organoids. *Stem Cells Int.* 2019:1024614. doi: 10.1155/2019/1024614
- Hong, J. H., Li, Q., Kim, M. S., Shin, D. M., Feske, S., Birnbaumer, L., et al. (2011). Polarized but differential localization and recruitment of STIM1, Orai1 and TRPC channels in secretory cells. *Traffic* 12 (2), 232–245. doi: 10.1111/j.1600-0854.2010.01138.x
- Hoth, M., and Niemeyer, B. A. (2013). The neglected CRAC proteins: Orai2, Orai3, and STIM2. *Curr. Top. Membr.* 71, 237–271. doi: 10.1016/B978-0-12-407870-3.00010-X
- Hu, D., Ansari, D., Pawlowski, K., Zhou, Q., Sasor, A., Welinder, C., et al. (2018a). Proteomic analyses identify prognostic biomarkers for pancreatic ductal adenocarcinoma. *Oncotarget* 9 (11), 9789–9807. doi: 10.18632/oncotarget.23929
- Hu, D., Ansari, D., Zhou, Q., Sasor, A., Hilmersson, K. S., Bauden, M., et al. (2018b). Calcium-activated chloride channel regulator 1 as a prognostic biomarker in pancreatic ductal adenocarcinoma. *BMC Cancer* 18 (1), 1096. doi: 10.1186/s12885-018-5013-2
- Hu, D., Ansari, D., Bauden, M., Zhou, Q., and Andersson, R. (2019). The Emerging Role of Calcium-activated Chloride Channel Regulator 1 in Cancer. *Anticancer Res.* 39 (4), 1661–1666. doi: 10.21873/anticancer.13271
- Huang, F., Rock, J. R., Harfe, B. D., Cheng, T., Huang, X., Jan, Y. N., et al. (2009). Studies on expression and function of the TMEM16A calcium-activated chloride channel. *Proc. Natl. Acad. Sci. U. S. A.* 106 (50), 21413–21418. doi: 10.1073/pnas.0911935106
- Huang, X., Huang, L., and Shao, M. (2017). Aquaporin 3 facilitates tumor growth in pancreatic cancer by modulating mTOR signaling. *Biochem. Biophys. Res. Commun.* 486 (4), 1097–1102. doi: 10.1016/j.bbrc.2017.03.168
- Huang, J., Liu, J., and Qiu, L. (2020). Transient receptor potential vanilloid 1 promotes EGFR ubiquitination and modulates EGFR/MAPK signalling in pancreatic cancer cells. *Cell Biochem. Funct.* 38 (4), 401–408. doi: 10.1002/cbf.3483
- Hurley, P. T., Ferguson, C. J., Kwon, T. H., Andersen, M. L., Norman, A. G., Steward, M. C., et al. (2001). Expression and immunolocalization of aquaporin water channels in rat exocrine pancreas. *Am. J. Physiol. Gastrointest. Liver Physiol.* 280 (4), G701–G709. doi: 10.1152/ajpgi.2001.280.4.G701
- Ishiguro, H., Naruse, S., Kitagawa, M., Mabuchi, T., Kondo, T., Hayakawa, T., et al. (2002). Chloride transport in microperfused interlobular ducts isolated from guinea-pig pancreas. *J. Physiol.* 539 (Pt 1), 175–189. doi: 10.1113/jphysiol.2001.012490
- Ishiguro, H., Steward, M. C., Naruse, S., Ko, S. B., Goto, H., Case, R. M., et al. (2009). CFTR functions as a bicarbonate channel in pancreatic duct cells. *J. Gen. Physiol.* 133 (3), 315–326. doi: 10.1085/jgp.200810122
- Ishiguro, H., Yamamoto, A., Nakakuki, M., Yi, L., Ishiguro, M., Yamaguchi, M., et al. (2012). Physiology and pathophysiology of bicarbonate secretion by pancreatic duct epithelium. *Nagoya J. Med. Sci.* 74 (1–2), 1–18.
- Ishii, T. M., Silvia, C., Hirschberg, B., Bond, C. T., Adelman, J. P., and Maylie, J. (1997). A human intermediate conductance calcium-activated potassium channel. *Proc. Natl. Acad. Sci. U. S. A.* 94 (21), 11651–11656. doi: 10.1073/pnas.94.21.11651
- Isokpehi, R. D., Rajnarayanan, R. V., Jeffries, C. D., Oyeleye, T. O., and Cohly, H. H. (2009). Integrative sequence and tissue expression profiling of chicken and mammalian aquaporins. *BMC Genomics* 10 Suppl 2, S7. doi: 10.1186/1471-2164-10-S2-S7
- Itoh, T., Rai, T., Kuwahara, M., Ko, S. B., Uchida, S., Sasaki, S., et al. (2005). Identification of a novel aquaporin, AQP12, expressed in pancreatic acinar cells. *Biochem. Biophys. Res. Commun.* 330 (3), 832–838. doi: 10.1016/j.bbrc.2005.03.046
- Iwatsuki, N., and Petersen, O. H. (1977). Pancreatic acinar cells: localization of acetylcholine receptors and the importance of chloride and calcium for acetylcholine-evoked depolarization. *J. Physiol.* 269 (3), 723–733. doi: 10.1113/jphysiol.1977.sp011925

- Iwatsuki, N., and Petersen, O. H. (1985a). Action of tetraethylammonium on calcium-activated potassium channels in pig pancreatic acinar cells studied by patch-clamp single-channel and whole-cell current recording. *J. Membr. Biol.* 86 (2), 139–144. doi: 10.1007/BF01870780
- Iwatsuki, N., and Petersen, O. H. (1985b). Inhibition of Ca<sup>2+</sup>-activated K<sup>+</sup> channels in pig pancreatic acinar cells by Ba<sup>2+</sup>, Ca<sup>2+</sup>, quinine and quinidine. *Biochim. Biophys. Acta* 819 (2), 249–257. doi: 10.1016/0005-2736(85)90180-4
- Jabbar, K. S., Arike, L., Verbeke, C. S., Sadik, R., and Hansson, G. C. (2018). Highly Accurate Identification of Cystic Precursor Lesions of Pancreatic Cancer Through Targeted Mass Spectrometry: A Phase IIc Diagnostic Study. *J. Clin. Oncol.* 36 (4), 367–375. doi: 10.1200/JCO.2017.73.7288
- Jager, H., Dreker, T., Buck, A., Giehl, K., Gress, T., and Grissmer, S. (2004). Blockage of intermediate-conductance Ca<sup>2+</sup>-activated K<sup>+</sup> channels inhibit human pancreatic cancer cell growth in vitro. *Mol. Pharmacol.* 65 (3), 630–638. doi: 10.1124/mol.65.3.630
- Jia, N., Dong, S., Zhao, G., Gao, H., Li, X., and Zhang, H. (2016). CLIC1 overexpression is associated with poor prognosis in pancreatic ductal adenocarcinomas. *J. Cancer Res. Ther.* 12 (2), 892–896. doi: 10.4103/0973-1482.154057
- Jiang, S., Zhu, L., Yang, J., Hu, L., Gu, J., Xing, X., et al. (2017). Integrated expression profiling of potassium channels identifies KCNN4 as a prognostic biomarker of pancreatic cancer. *Biochem. Biophys. Res. Commun.* 494 (1–2), 113–119. doi: 10.1016/j.bbrc.2017.10.072
- Joiner, W. J., Wang, L. Y., Tang, M. D., and Kaczmarek, L. K. (1997). hSK4, a member of a novel subfamily of calcium-activated potassium channels. *Proc. Natl. Acad. Sci. U. S. A.* 94 (20), 11013–11018. doi: 10.1073/pnas.94.20.11013
- Jun, I., Park, H. S., Piao, H., Han, J. W., An, M. J., Yun, B. G., et al. (2017). ANO9/TMEM16J promotes tumorigenesis via EGFR and is a novel therapeutic target for pancreatic cancer. *Br. J. Cancer* 117 (12), 1798–1809. doi: 10.1038/bjc.2017.355
- Jung, S. R., Kim, K., Hille, B., Nguyen, T. D., and Koh, D. S. (2006). Pattern of Ca<sup>2+</sup> increase determines the type of secretory mechanism activated in dog pancreatic duct epithelial cells. *J. Physiol.* 576 (Pt 1), 163–178. doi: 10.1113/jphysiol.2006.114876
- Kalman, K., Nguyen, A., Tseng-Crank, J., Dukes, I. D., Chandry, G., Hustad, C. M., et al. (1998). Genomic organization, chromosomal localization, tissue distribution, and biophysical characterization of a novel mammalian Shaker-related voltage-gated potassium channel, Kv1.7. *J. Biol. Chem.* 273 (10), 5851–5857. doi: 10.1074/jbc.273.10.5851
- Kasai, H., and Augustine, G. J. (1990). Cytosolic Ca<sup>2+</sup> gradients triggering unidirectional fluid secretion from exocrine pancreas. *Nature* 348 (6303), 735–738. doi: 10.1038/348735a0
- Khan, H. Y., Mpilla, G. B., Sexton, R., Viswanadha, S., Penmetsa, K. V., Aboukameel, A., et al. (2020). Calcium Release-Activated Calcium (CRAC) Channel Inhibition Suppresses Pancreatic Ductal Adenocarcinoma Cell Proliferation and Patient-Derived Tumor Growth. *Cancers (Basel)* 12 (3), 750. doi: 10.3390/cancers12030750
- Kim, S. J., and Greger, R. (1999). Voltage-dependent, slowly activating K<sup>+</sup> current (I(K<sub>s</sub>)) and its augmentation by carbachol in rat pancreatic acini. *Pflugers Arch.* 438 (5), 604–611. doi: 10.1007/s004249900071
- Kim, S. J., Kerst, G., Schreiber, R., Pavenstadt, H., Greger, R., Hug, M. J., et al. (2000). Inwardly rectifying K<sup>+</sup> channels in the basolateral membrane of rat pancreatic acini. *Pflugers Arch.* 441 (2–3), 331–340. doi: 10.1007/s004240000427
- Kim, C. J., Cho, Y. G., Jeong, S. W., Kim, Y. S., Kim, S. Y., Nam, S. W., et al. (2004). Altered expression of KCNK9 in colorectal cancers. *APMIS* 112 (9), 588–594. doi: 10.1111/j.1600-0463.2004.apm1120905.x
- Kim, J. Y., Zeng, W., Kiselyov, K., Yuan, J. P., Dehoff, M. H., Mikoshiba, K., et al. (2006). Homer 1 mediates store- and inositol 1,4,5-trisphosphate receptor-dependent translocation and retrieval of TRPC3 to the plasma membrane. *J. Biol. Chem.* 281 (43), 32540–32549. doi: 10.1074/jbc.M602496200
- Kim, M. H., Choi, B. H., Jung, S. R., Sernka, T. J., Kim, S., Kim, K. T., et al. (2008). Protease-activated receptor-2 increases exocytosis via multiple signal transduction pathways in pancreatic duct epithelial cells. *J. Biol. Chem.* 283 (27), 18711–18720. doi: 10.1074/jbc.M801655200
- Kim, M. S., Hong, J. H., Li, Q., Shin, D. M., Abramowitz, J., Birnbaumer, L., et al. (2009). Deletion of TRPC3 in mice reduces store-operated Ca<sup>2+</sup> influx and the severity of acute pancreatitis. *Gastroenterology* 137 (4), 1509–1517. doi: 10.1053/j.gastro.2009.07.042
- Kim, M. H., Seo, J. B., Burnett, L. A., Hille, B., and Koh, D. S. (2013). Characterization of store-operated Ca<sup>2+</sup> channels in pancreatic duct epithelia. *Cell Calcium* 54 (4), 266–275. doi: 10.1016/j.ceca.2013.07.002
- Kim, H., Kim, H., Lee, J., Lee, B., Kim, H. R., Jung, J., et al. (2018). Anoctamin 9/TMEM16J is a cation channel activated by cAMP/PKA signal. *Cell Calcium* 71, 75–85. doi: 10.1016/j.ceca.2017.12.003
- Kim, J. B. (2014). Channelopathies. *Korean J. Pediatr.* 57 (1), 1–18. doi: 10.3345/kjp.2014.57.1.1
- Kirkegard, J., Mortensen, F. V., and Cronin-Fenton, D. (2017). Chronic Pancreatitis and Pancreatic Cancer Risk: A Systematic Review and Meta-analysis. *Am. J. Gastroenterol.* 112 (9), 1366–1372. doi: 10.1038/ajg.2017.218
- Ko, S. B., Naruse, S., Kitagawa, M., Ishiguro, H., Furuya, S., Mizuno, N., et al. (2002). Aquaporins in rat pancreatic interlobular ducts. *Am. J. Physiol. Gastrointest. Liver Physiol.* 282 (2), G324–G331. doi: 10.1152/ajpgi.00198.2001
- Koltai, T. (2015). Voltage-gated sodium channel as a target for metastatic risk reduction with re-purposed drugs. *F1000Res* 4, 297. doi: 10.12688/f1000research.6789.1
- Kondratska, K., Kondratskyi, A., Yassine, M., Lemonnier, L., Lepage, G., Morabito, A., et al. (2014). Orai1 and STIM1 mediate SOCE and contribute to apoptotic resistance of pancreatic adenocarcinoma. *Biochim. Biophys. Acta* 1843 (10), 2263–2269. doi: 10.1016/j.bbamcr.2014.02.012
- Kong, S. C., Giannuzzo, A., Novak, I., and Pedersen, S. F. (2014). Acid-base transport in pancreatic cancer: molecular mechanisms and clinical potential. *Biochem. Cell Biol.* 92 (6), 449–459. doi: 10.1139/bcb-2014-0078
- Kottgen, M., Hofer, A., Kim, S. J., Beschoner, U., Schreiber, R., Hug, M. J., et al. (1999). Carbachol activates a K<sup>+</sup> channel of very small conductance in the basolateral membrane of rat pancreatic acinar cells. *Pflugers Arch.* 438 (5), 597–603. doi: 10.1007/s004249900070
- Kovalenko, I., Glasauer, A., Schockel, L., Sauter, D. R., Ehrmann, A., Sohler, F., et al. (2016). Identification of KCa3.1 Channel as a Novel Regulator of Oxidative Phosphorylation in a Subset of Pancreatic Carcinoma Cell Lines. *PLoS One* 11 (8), e0160658. doi: 10.1371/journal.pone.0160658
- Koyama, Y., Yamamoto, T., Kondo, D., Funaki, H., Yaoita, E., Kawasaki, K., et al. (1997). Molecular cloning of a new aquaporin from rat pancreas and liver. *J. Biol. Chem.* 272 (48), 30329–30333. doi: 10.1074/jbc.272.48.30329
- Kunzelmann, K. (2005). Ion channels and cancer. *J. Membr. Biol.* 205 (3), 159–173. doi: 10.1007/s00232-005-0781-4
- Kunzelmann, K. (2016). Ion channels in regulated cell death. *Cell Mol. Life Sci.* 73 (11–12), 2387–2403. doi: 10.1007/s00018-016-2208-z
- Kunzli, B. M., Berberat, P. O., Giese, T., Csizmadia, E., Kaczmarek, E., Baker, C., et al. (2007). Upregulation of CD39/NTPDases and P2 receptors in human pancreatic disease. *Am. J. Physiol. Gastrointest. Liver Physiol.* 292 (1), G223–G230. doi: 10.1152/ajpgi.00259.2006
- Lang, F., and Stourmaras, C. (2014). Ion channels in cancer: future perspectives and clinical potential. *Philos. Trans. R. Soc. Lond. B. Biol. Sci.* 369 (1638), 20130108. doi: 10.1098/rstb.2013.0108
- Lastraioli, E., Lottini, T., Bencini, L., Bernini, M., and Arcangeli, A. (2015a). hERG1 Potassium Channels: Novel Biomarkers in Human Solid Cancers. *BioMed. Res. Int.* 2015:896432. doi: 10.1155/2015/896432
- Lastraioli, E., Perrone, G., Sette, A., Fiore, A., Crociani, O., Manoli, S., et al. (2015b). hERG1 channels drive tumour malignancy and may serve as prognostic factor in pancreatic ductal adenocarcinoma. *Br. J. Cancer* 112 (6), 1076–1087. doi: 10.1038/bjc.2015.28
- Lazzeri, M., Vannucchi, M. G., Spinelli, M., Bizzoco, E., Beneforti, P., Turini, D., et al. (2005). Transient receptor potential vanilloid type 1 (TRPV1) expression changes from normal urothelium to transitional cell carcinoma of human bladder. *Eur. Urol.* 48 (4), 691–698. doi: 10.1016/j.eururo.2005.05.018
- Lee, M. G., Ahn, W., Lee, J. A., Kim, J. Y., Choi, J. Y., Moe, O. W., et al. (2001). Coordination of pancreatic HCO<sub>3</sub><sup>-</sup> secretion by protein-protein interaction between membrane transporters. *JOP* 2 (4 Suppl), 203–206.
- Lee, G. W., Park, H. S., Kim, E. J., Cho, Y. W., Kim, G. T., Mun, Y. J., et al. (2012). Reduction of breast cancer cell migration via up-regulation of TASK-3 two-pore domain K<sup>+</sup> channel. *Acta Physiol. (Oxf)* 204 (4), 513–524. doi: 10.1111/j.1748-1716.2011.02359.x



- Lee, M. G., Ohana, E., Park, H. W., Yang, D., and Muallem, S. (2012). Molecular mechanism of pancreatic and salivary gland fluid and HCO<sub>3</sub> secretion. *Physiol. Rev.* 92 (1), 39–74. doi: 10.1152/physrev.00011.2011
- Lemstova, R., Soucek, P., Melichar, B., and Mohelnikova-Duchonova, B. (2014). Role of solute carrier transporters in pancreatic cancer: a review. *Pharmacogenomics* 15 (8), 1133–1145. doi: 10.2217/pgs.14.80
- Li, L., and Hanahan, D. (2013). Hijacking the neuronal NMDAR signaling circuit to promote tumor growth and invasion. *Cell* 153 (1), 86–100. doi: 10.1016/j.cell.2013.02.051
- Liddle, R. A. (2007). The role of Transient Receptor Potential Vanilloid 1 (TRPV1) channels in pancreatitis. *Biochim. Biophys. Acta* 1772 (8), 869–878. doi: 10.1016/j.bbdis.2007.02.012
- Lin, R., Wang, Y., Chen, Q., Liu, Z., Xiao, S., Wang, B., et al. (2018). TRPM2 promotes the proliferation and invasion of pancreatic ductal adenocarcinoma. *Mol. Med. Rep.* 17 (6), 7537–7544. doi: 10.3892/mmr.2018.8816
- Litan, A., and Langhans, S. A. (2015). Cancer as a channelopathy: ion channels and pumps in tumor development and progression. *Front. Cell Neurosci.* 9, 86. doi: 10.3389/fncel.2015.00086
- Liu, Y., McKenna, E., Figueroa, D. J., Blevins, R., Austin, C. P., Bennett, P. B., et al. (2000). The human inward rectifier K(+) channel subunit kir5.1 (KCNJ16) maps to chromosome 17q25 and is expressed in kidney and pancreas. *Cytogenet. Cell Genet.* 90 (1-2), 60–63. doi: 10.1159/000015662
- Liu, X., Cheng, K. T., Bandyopadhyay, B. C., Pani, B., Dietrich, A., Paria, B. C., et al. (2007). Attenuation of store-operated Ca<sup>2+</sup> current impairs salivary gland fluid secretion in TRPC1(-/-) mice. *Proc. Natl. Acad. Sci. U. S. A.* 104 (44), 17542–17547. doi: 10.1073/pnas.0701254104
- Liu, W., Lu, M., Liu, B., Huang, Y., and Wang, K. (2012). Inhibition of Ca(2+)-activated Cl(-) channel ANO1/TMEM16A expression suppresses tumor growth and invasiveness in human prostate carcinoma. *Cancer Lett.* 326 (1), 41–51. doi: 10.1016/j.canlet.2012.07.015
- Liu, J., Hu, G., Gong, Y., Yu, Q., He, B., Li, W., et al. (2018). Silencing of TRPM8 inhibits aggressive tumor phenotypes and enhances gemcitabine sensitivity in pancreatic cancer. *Pancreatology* 18 (8), 935–944. doi: 10.1016/j.pan.2018.08.011
- Lotz, M. M., Wang, H., Song, J. C., Pories, S. E., and Matthews, J. B. (2004). K<sup>+</sup> channel inhibition accelerates intestinal epithelial cell wound healing. *Wound Repair Regen.* 12 (5), 565–574. doi: 10.1111/j.1067-1927.2004.012509.x
- Lowenfels, A. B., Maisonneuve, P., Cavallini, G., Ammann, R. W., Lankisch, P. G., Andersen, J. R., et al. (1993). Pancreatitis and the risk of pancreatic cancer. International Pancreatitis Study Group. *N. Engl. J. Med.* 328 (20), 1433–1437. doi: 10.1056/NEJM199305203282001
- Lu, J., Dong, Q., Zhang, B., Wang, X., Ye, B., Zhang, F., et al. (2015). Chloride intracellular channel 1 (CLIC1) is activated and functions as an oncogene in pancreatic cancer. *Med. Oncol.* 32 (6), 616. doi: 10.1007/s12032-015-0616-9
- Lur, G., Haynes, L. P., Prior, I. A., Gerasimenko, O. V., Feske, S., Petersen, O. H., et al. (2009). Ribosome-free terminals of rough ER allow formation of STIM1 puncta and segregation of STIM1 from IP(3) receptors. *Curr. Biol.* 19 (19), 1648–1653. doi: 10.1016/j.cub.2009.07.072
- Lur, G., Sherwood, M. W., Ebisui, E., Haynes, L., Feske, S., Sutton, R., et al. (2011). InsP(3) receptors and Orai channels in pancreatic acinar cells: co-localization and its consequences. *Biochem. J.* 436 (2), 231–239. doi: 10.1042/BJ20110083
- Ma, T., Jayaraman, S., Wang, K. S., Song, Y., Yang, B., Li, J., et al. (2001). Defective dietary fat processing in transgenic mice lacking aquaporin-1 water channels. *Am. J. Physiol. Cell Physiol.* 280 (1), C126–C134. doi: 10.1152/ajpcell.2001.280.1.C126
- Maleth, J., and Hegyi, P. (2014). Calcium signaling in pancreatic ductal epithelial cells: an old friend and a nasty enemy. *Cell Calcium* 55 (6), 337–345. doi: 10.1016/j.ceca.2014.02.004
- Manoli, S., Coppola, S., Duranti, C., Lulli, M., Magni, L., Kuppalu, N., et al. (2019). The Activity of Kv 11.1 Potassium Channel Modulates F-Actin Organization During Cell Migration of Pancreatic Ductal Adenocarcinoma Cells. *Cancers (Basel)* 11 (2), 135. doi: 10.3390/cancers11020135
- Marino, C. R., Matovcik, L. M., Gorelick, F. S., and Cohn, J. A. (1991). Localization of the cystic fibrosis transmembrane conductance regulator in pancreas. *J. Clin. Invest.* 88 (2), 712–716. doi: 10.1172/JCI115358
- Marty, A., Tan, Y. P., and Trautmann, A. (1984). Three types of calcium-dependent channel in rat lacrimal glands. *J. Physiol.* 357, 293–325. doi: 10.1113/jphysiol.1984.sp015501
- Maruyama, Y., Petersen, O. H., Flanagan, P., and Pearson, G. T. (1983). Quantification of Ca<sup>2+</sup>-activated K<sup>+</sup> channels under hormonal control in pig pancreas acinar cells. *Nature* 305 (5931), 228–232. doi: 10.1038/305228a0
- Matthews, E. K., Petersen, O. H., and Williams, J. A. (1973). Pancreatic acinar cells: acetylcholine-induced membrane depolarization, calcium efflux and amylase release. *J. Physiol.* 234 (3), 689–701. doi: 10.1113/jphysiol.1973.sp010367
- Mazzone, A., Eisenman, S. T., Strege, P. R., Yao, Z., Ordog, T., Gibbons, S. J., et al. (2012). Inhibition of cell proliferation by a selective inhibitor of the Ca(2+)-activated Cl(-) channel, Ano1. *Biochem. Biophys. Res. Commun.* 427 (2), 248–253. doi: 10.1016/j.bbrc.2012.09.022
- McDonald, F. J., Snyder, P. M., McCray, P. B. Jr., and Welsh, M. J. (1994). Cloning, expression, and tissue distribution of a human amiloride-sensitive Na<sup>+</sup> channel. *Am. J. Physiol.* 266 (6 Pt 1), L728–L734. doi: 10.1152/ajplung.1994.266.6.L728
- McDonald, T. V., Yu, Z., Ming, Z., Palma, E., Meyers, M. B., Wang, K. W., et al. (1997). A minK-HERG complex regulates the cardiac potassium current I(Kr). *Nature* 388 (6639), 289–292. doi: 10.1038/40882
- McWilliams, R. R., Petersen, G. M., Rabe, K. G., Holtegaard, L. M., Lynch, P. J., Bishop, M. D., et al. (2010). Cystic fibrosis transmembrane conductance regulator (CFTR) gene mutations and risk for pancreatic adenocarcinoma. *Cancer* 116 (1), 203–209. doi: 10.1002/ncr.24697
- Miao, X., Liu, G., Xu, X., Xie, C., Sun, F., Yang, Y., et al. (2008). High expression of vanilloid receptor-1 is associated with better prognosis of patients with hepatocellular carcinoma. *Cancer Genet. Cytogenet.* 186 (1), 25–32. doi: 10.1016/j.cancergencyto.2008.05.011
- Mo, P., and Yang, S. (2018). The store-operated calcium channels in cancer metastasis: from cell migration, invasion to metastatic colonization. *Front. Biosci. (Landmark Ed.)* 23, 1241–1256. doi: 10.2741/4641
- Mogami, H., Nakano, K., Tepikin, A. V., and Petersen, O. H. (1997). Ca<sup>2+</sup> flow via tunnels in polarized cells: recharging of apical Ca<sup>2+</sup> stores by focal Ca<sup>2+</sup> entry through basal membrane patch. *Cell* 88 (1), 49–55. doi: 10.1016/s0092-8674(00)81857-7
- Morelli, M. B., Amantini, C., Nabissi, M., Liberati, S., Cardinali, C., Farfariello, V., et al. (2014). Cross-talk between alpha1D-adrenoceptors and transient receptor potential vanilloid type 1 triggers prostate cancer cell proliferation. *BMC Cancer* 14, 921. doi: 10.1186/1471-2407-14-921
- Mu, D., Chen, L., Zhang, X., See, L. H., Koch, C. M., Yen, C., et al. (2003). Genomic amplification and oncogenic properties of the KCNK9 potassium channel gene. *Cancer Cell* 3 (3), 297–302. doi: 10.1016/s1535-6108(03)00054-0
- Nagy, D., Goncz, M., Dienes, B., Szoor, A., Fodor, J., Nagy, Z., et al. (2014). Silencing the KCNK9 potassium channel (TASK-3) gene disturbs mitochondrial function, causes mitochondrial depolarization, and induces apoptosis of human melanoma cells. *Arch. Dermatol. Res.* 306 (10), 885–902. doi: 10.1007/s00403-014-1511-5
- Neglia, J. P., FitzSimmons, S. C., Maisonneuve, P., Schoni, M. H., Schoni-Affolter, F., Corey, M., et al. (1995). The risk of cancer among patients with cystic fibrosis. Cystic Fibrosis and Cancer Study Group. *N. Engl. J. Med.* 332 (8), 494–499. doi: 10.1056/NEJM199502233280803
- Nguyen, T. D., and Moody, M. W. (1998). Calcium-activated potassium conductances on cultured nontransformed dog pancreatic duct epithelial cells. *Pancreas* 17 (4), 348–358. doi: 10.1097/00006676-199811000-00005
- Nguyen, T. D., Koh, D. S., Moody, M. W., Fox, N. R., Savard, C. E., Kuver, R., et al. (1997). Characterization of two distinct chloride channels in cultured dog pancreatic duct epithelial cells. *Am. J. Physiol.* 272 (1 Pt 1), G172–G180. doi: 10.1152/ajpki.1997.272.1.G172
- Niemeyer, B. A., Mery, L., Zawar, C., Suckow, A., Monje, F., Pardo, L. A., et al. (2001). Ion channels in health and disease. 83rd Boehringer Ingelheim Fonds International Titisee Conference. *EMBO Rep.* 2 (7), 568–573. doi: 10.1093/embo-reports/kve145
- North, W. G., Liu, F., Lin, L. Z., Tian, R., and Akerman, B. (2017). NMDA receptors are important regulators of pancreatic cancer and are potential targets for treatment. *Clin. Pharmacol.* 9, 79–86. doi: 10.2147/CPAA.S140057
- Novak, I., and Hansen, M. R. (2002). Where have all the Na<sup>+</sup> channels gone? In search of functional ENaC in exocrine pancreas. *Biochim. Biophys. Acta* 1566 (1-2), 162–168. doi: 10.1016/s0005-2736(02)00598-9



- Novak, I., Wang, J., Henriksen, K. L., Haanes, K. A., Krabbe, S., Nitschke, R., et al. (2011). Pancreatic bicarbonate secretion involves two proton pumps. *J. Biol. Chem.* 286 (1), 280–289. doi: 10.1074/jbc.M110.136382
- Novak, I., Haanes, K. A., and Wang, J. (2013). Acid-base transport in pancreas—new challenges. *Front. Physiol.* 4, 380. doi: 10.3389/fphys.2013.00380
- Novak, I. (2000). Keeping up with bicarbonate. *J. Physiol.* 528 Pt 2, 235. doi: 10.1111/j.1469-7793.2000.00235.x
- Ochi, A., Graffeo, C. S., Zambirinis, C. P., Rehman, A., Hackman, M., Fallon, N., et al. (2012). Toll-like receptor 7 regulates pancreatic carcinogenesis in mice and humans. *J. Clin. Invest.* 122 (11), 4118–4129. doi: 10.1172/JCI63606
- Ohta, E., Itoh, T., Nemoto, T., Kumagai, J., Ko, S. B., Ishibashi, K., et al. (2009). Pancreas-specific aquaporin 12 null mice showed increased susceptibility to caerulein-induced acute pancreatitis. *Am. J. Physiol. Cell Physiol.* 297 (6), C1368–C1378. doi: 10.1152/ajpcell.00117.2009
- Okeke, E., Parker, T., Dingsdale, H., Concannon, M., Awais, M., Voronina, S., et al. (2016). Epithelial-mesenchymal transition, IP3 receptors and ER-PM junctions: translocation of Ca<sup>2+</sup> signalling complexes and regulation of migration. *Biochem. J.* 473 (6), 757–767. doi: 10.1042/BJ20150364
- Ousingsawat, J., Martins, J. R., Schreiber, R., Rock, J. R., Harfe, B. D., and Kunzelmann, K. (2009). Loss of TMEM16A causes a defect in epithelial Ca<sup>2+</sup>-dependent chloride transport. *J. Biol. Chem.* 284 (42), 28698–28703. doi: 10.1074/jbc.M109.012120
- Pallagi, P., Hegyi, P., and Rakonczay, Z. Jr. (2015). The Physiology and Pathophysiology of Pancreatic Ductal Secretion: The Background for Clinicians. *Pancreas* 44 (8), 1211–1233. doi: 10.1097/MPA.00000000000000421
- Pandiri, A. R. (2014). Overview of exocrine pancreatic pathobiology. *Toxicol. Pathol.* 42 (1), 207–216. doi: 10.1177/0192623313509907
- Papadopoulos, M. C., and Saadoun, S. (2015). Key roles of aquaporins in tumor biology. *Biochim. Biophys. Acta* 1848 (10 Pt B), 2576–2583. doi: 10.1016/j.bbame.2014.09.001
- Pardo, L. A., and Stuhmer, W. (2014). The roles of K<sup>+</sup> channels in cancer. *Nat. Rev. Cancer* 14 (1), 39–48. doi: 10.1038/nrc3635
- Pardo, L. A., del Camino, D., Sanchez, A., Alves, F., Bruggemann, A., Beckh, S., et al. (1999). Oncogenic potential of EAG K<sup>+</sup> channels. *EMBO J.* 18 (20), 5540–5547. doi: 10.1093/emboj/18.20.5540
- Park, M. K., Lomax, R. B., Tepikin, A. V., and Petersen, O. H. (2001). Local uncaging of caged Ca<sup>2+</sup> reveals distribution of Ca<sup>2+</sup>-activated Cl<sup>-</sup> channels in pancreatic acinar cells. *Proc. Natl. Acad. Sci. U. S. A.* 98 (19), 10948–10953. doi: 10.1073/pnas.181353798
- Park, H. W., Nam, J. H., Kim, J. Y., Namkung, W., Yoon, J. S., Lee, J. S., et al. (2010). Dynamic regulation of CFTR bicarbonate permeability by [Cl<sup>-</sup>]<sub>i</sub> and its role in pancreatic bicarbonate secretion. *Gastroenterology* 139 (2), 620–631. doi: 10.1053/j.gastro.2010.04.004
- Pascua, P., Garcia, M., Fernandez-Salazar, M. P., Hernandez-Lorenzo, M. P., Calvo, J. J., Colledge, W. H., et al. (2009). Ducts isolated from the pancreas of CFTR-null mice secrete fluid. *Pflugers Arch.* 459 (1), 203–214. doi: 10.1007/s00424-009-0704-9
- Pearson, G. T., Flanagan, P. M., and Petersen, O. H. (1984). Neural and hormonal control of membrane conductance in the pig pancreatic acinar cell. *Am. J. Physiol.* 247 (5 Pt 1), G520–G526. doi: 10.1152/ajpgi.1984.247.5.G520
- Pedersen, S. F., and Stock, C. (2013). Ion channels and transporters in cancer: pathophysiology, regulation, and clinical potential. *Cancer Res.* 73 (6), 1658–1661. doi: 10.1158/0008-5472.CAN-12-4188
- Pedersen, S. F., Novak, I., Alves, F., Schwab, A., and Pardo, L. A. (2017). Alternating pH landscapes shape epithelial cancer initiation and progression: Focus on pancreatic cancer. *Bioessays* 39 (6). doi: 10.1002/bies.201600253
- Peretti, M., Angelini, M., Savalli, N., Florio, T., Yuspa, S. H., and Mazzanti, M. (2015). Chloride channels in cancer: Focus on chloride intracellular channel 1 and 4 (CLIC1 AND CLIC4) proteins in tumor development and as novel therapeutic targets. *Biochim. Biophys. Acta* 1848 (10 Pt B), 2523–2531. doi: 10.1016/j.bbame.2014.12.012
- Pessia, M., Imbrici, P., D'Adamo, M. C., Salvatore, L., and Tucker, S. J. (2001). Differential pH sensitivity of Kir4.1 and Kir4.2 potassium channels and their modulation by heteropolymerisation with Kir5.1. *J. Physiol.* 532 (Pt 2), 359–367. doi: 10.1111/j.1469-7793.2001.0359f.x
- Petersen, O. H., and Findlay, I. (1987). Electrophysiology of the pancreas. *Physiol. Rev.* 67 (3), 1054–1116. doi: 10.1152/physrev.1987.67.3.1054
- Petersen, O. H., and Gallacher, D. V. (1988). Electrophysiology of pancreatic and salivary acinar cells. *Annu. Rev. Physiol.* 50, 65–80. doi: 10.1146/annurev.ph.50.030188.000433
- Petersen, O. H., and Tepikin, A. V. (2008). Polarized calcium signaling in exocrine gland cells. *Annu. Rev. Physiol.* 70, 273–299. doi: 10.1146/annurev.physiol.70.113006.100618
- Petersen, O. H., and Ueda, N. (1976). Pancreatic acinar cells: the role of calcium in stimulus-secretion coupling. *J. Physiol.* 254 (3), 583–606. doi: 10.1113/jphysiol.1976.sp011248
- Petersen, O. H., Findlay, I., Iwatsuki, N., Singh, J., Gallacher, D. V., Fuller, C. M., et al. (1985). Human pancreatic acinar cells: studies of stimulus-secretion coupling. *Gastroenterology* 89 (1), 109–117. doi: 10.1016/0016-5085(85)90751-6
- Petersen, O. H. (1992). Stimulus-secretion coupling: cytoplasmic calcium signals and the control of ion channels in exocrine acinar cells. *J. Physiol.* 448, 1–51. doi: 10.1113/jphysiol.1992.sp019028
- Petersen, O. H. (2005). Ca<sup>2+</sup> signalling and Ca<sup>2+</sup>-activated ion channels in exocrine acinar cells. *Cell Calcium* 38 (3–4), 171–200. doi: 10.1016/j.ceca.2005.06.024
- Petersen, O. H. (2014). Calcium signalling and secretory epithelia. *Cell Calcium* 55 (6), 282–289. doi: 10.1016/j.ceca.2014.01.003
- Pond, A. L., Scheve, B. K., Benedict, A. T., Petrecca, K., Van Wagoner, D. R., Shrier, A., et al. (2000). Expression of distinct ERG proteins in rat, mouse, and human heart. Relation to functional I(Kr) channels. *J. Biol. Chem.* 275 (8), 5997–6006. doi: 10.1074/jbc.275.8.5997
- Premkumar, L. S., and Abooj, M. (2013). TRP channels and analgesia. *Life Sci.* 92 (8–9), 415–424. doi: 10.1016/j.lfs.2012.08.010
- Prevarkaya, N., Zhang, L., and Barritt, G. (2007). TRP channels in cancer. *Biochim. Biophys. Acta* 1772 (8), 937–946. doi: 10.1016/j.bbadis.2007.05.006
- Prevarkaya, N., Skryma, R., and Shuba, Y. (2010). Ion channels and the hallmarks of cancer. *Trends Mol. Med.* 16 (3), 107–121. doi: 10.1016/j.molmed.2010.01.005
- Prevarkaya, N., Skryma, R., and Shuba, Y. (2018). Ion Channels in Cancer: Are Cancer Hallmarks Oncochannelopathies? *Physiol. Rev.* 98 (2), 559–621. doi: 10.1152/physrev.00044.2016
- Radisky, D. C., and LaBarge, M. A. (2008). Epithelial-mesenchymal transition and the stem cell phenotype. *Cell Stem Cell* 2 (6), 511–512. doi: 10.1016/j.stem.2008.05.007
- Ragsdale, D. S., Scheuer, T., and Catterall, W. A. (1991). Frequency and voltage-dependent inhibition of type IIA Na<sup>+</sup> channels, expressed in a mammalian cell line, by local anesthetic, antiarrhythmic, and anticonvulsant drugs. *Mol. Pharmacol.* 40 (5), 756–765.
- Randriamampita, C., Chanson, M., and Trautmann, A. (1988). Calcium and secretagogues-induced conductances in rat exocrine pancreas. *Pflugers Arch.* 411 (1), 53–57. doi: 10.1007/BF00581646
- Reubi, J. C., Waser, B., Gugger, M., Friess, H., Kleeff, J., Kaye, H., et al. (2003). Distribution of CCK1 and CCK2 receptors in normal and diseased human pancreatic tissue. *Gastroenterology* 125 (1), 98–106. doi: 10.1016/s0016-5085(03)00697-8
- Riordan, J. R., Rommens, J. M., Kerem, B., Alon, N., Rozmahel, R., Grzelczak, Z., et al. (1989). Identification of the cystic fibrosis gene: cloning and characterization of complementary DNA. *Science* 245 (4922), 1066–1073. doi: 10.1126/science.2475911
- Rodriguez-Boulan, E., and Nelson, W. J. (1989). Morphogenesis of the polarized epithelial cell phenotype. *Science* 245 (4919), 718–725. doi: 10.1126/science.2672330
- Roux, B. (2017). Ion channels and ion selectivity. *Essays Biochem.* 61 (2), 201–209. doi: 10.1042/EBC20160074
- Ruiz, C., Martins, J. R., Rudin, F., Schneider, S., Dietsche, T., Fischer, C. A., et al. (2012). Enhanced expression of ANO1 in head and neck squamous cell carcinoma causes cell migration and correlates with poor prognosis. *PLoS One* 7 (8), e43265. doi: 10.1371/journal.pone.0043265
- Rybarczyk, P., Gautier, M., Hague, F., Dhennin-Duthille, I., Chatelain, D., Kerr-Conte, J., et al. (2012). Transient receptor potential melastatin-related 7 channel is overexpressed in human pancreatic ductal adenocarcinomas and regulates human pancreatic cancer cell migration. *Int. J. Cancer* 131 (6), E851–E861. doi: 10.1002/ijc.27487
- Rybarczyk, P., Vanlaeys, A., Brassart, B., Dhennin-Duthille, I., Chatelain, D., Sevestre, H., et al. (2017). The Transient Receptor Potential Melastatin 7

- Channel Regulates Pancreatic Cancer Cell Invasion through the Hsp90alpha/uPA/MMP2 pathway. *Neoplasia* 19 (4), 288–300. doi: 10.1016/j.neo.2017.01.004
- Sanchez, M. G., Sanchez, A. M., Collado, B., Malagarie-Cazenave, S., Olea, N., Carmena, M. J., et al. (2005). Expression of the transient receptor potential vanilloid 1 (TRPV1) in LNCaP and PC-3 prostate cancer cells and in human prostate tissue. *Eur. J. Pharmacol.* 515 (1–3), 20–27. doi: 10.1016/j.ejphar.2005.04.010
- Sanguinetti, M. C., Jiang, C., Curran, M. E., and Keating, M. T. (1995). A mechanistic link between an inherited and an acquired cardiac arrhythmia: HERG encodes the IKr potassium channel. *Cell* 81 (2), 299–307. doi: 10.1016/0092-8674(95)90340-2
- Sato, K., Ishizuka, J., Cooper, C. W., Chung, D. H., Tsuchiya, T., Uchida, T., et al. (1994). Inhibitory effect of calcium channel blockers on growth of pancreatic cancer cells. *Pancreas* 9 (2), 193–202. doi: 10.1097/00006676-199403000-00009
- Sauter, D. R. P., Novak, I., Pedersen, S. F., Larsen, E. H., and Hoffmann, E. K. (2015). ANO1 (TMEM16A) in pancreatic ductal adenocarcinoma (PDAC). *Pflugers Arch.* 467 (7), 1495–1508. doi: 10.1007/s00424-014-1598-8
- Sauter, D. R., Sorensen, C. E., Rapedius, M., Bruggemann, A., and Novak, I. (2016). pH-sensitive K(+) channel TREK-1 is a novel target in pancreatic cancer. *Biochim. Biophys. Acta* 1862 (10), 1994–2003. doi: 10.1016/j.bbadis.2016.07.009
- Schneider, G., Siveke, J. T., Eckel, F., and Schmid, R. M. (2005). Pancreatic cancer: basic and clinical aspects. *Gastroenterology* 128 (6), 1606–1625. doi: 10.1053/j.gastro.2005.04.001
- Schroeder, B. C., Cheng, T., Jan, Y. N., and Jan, L. Y. (2008). Expression cloning of TMEM16A as a calcium-activated chloride channel subunit. *Cell* 134 (6), 1019–1029. doi: 10.1016/j.cell.2008.09.003
- Serrano-Novillo, C., Capera, J., Colomer-Molera, M., Condom, E., Ferreres, J. C., and Felipe, A. (2019). Implication of Voltage-Gated Potassium Channels in Neoplastic Cell Proliferation. *Cancers (Basel)* 11 (3), 287. doi: 10.3390/cancers11030287
- Sette, A., Spadavecchia, J., Landoulsi, J., Casale, S., Haye, B., Crociani, O., et al. (2013). Development of novel anti-Kv 11.1 antibody-conjugated PEG-TiO2 nanoparticles for targeting pancreatic ductal adenocarcinoma cells. *J. Nanopart Res.* 15, 2111. doi: 10.1007/s11051-013-2111-6
- Shapovalov, G., Ritaine, A., Skryma, R., and Prevarskaya, N. (2016). Role of TRP ion channels in cancer and tumorigenesis. *Semin. Immunopathol.* 38 (3), 357–369. doi: 10.1007/s00281-015-0525-1
- Sheldon, C. D., Hodson, M. E., Carpenter, L. M., and Swerdlow, A. J. (1993). A cohort study of cystic fibrosis and malignancy. *Br. J. Cancer* 68 (5), 1025–1028. doi: 10.1038/bjc.1993.474
- Shen, S., Gui, T., and Ma, C. (2017). Identification of molecular biomarkers for pancreatic cancer with mRMR shortest path method. *Oncotarget* 8 (25), 41432–41439. doi: 10.18632/oncotarget.18186
- Shuck, M. E., Piser, T. M., Bock, J. H., Slightom, J. L., Lee, K. S., and Bienkowski, M. J. (1997). Cloning and characterization of two K+ inward rectifier (Kir) 1.1 potassium channel homologs from human kidney (Kir1.2 and Kir1.3). *J. Biol. Chem.* 272 (1), 586–593. doi: 10.1074/jbc.272.1.586
- Singh, A. P., Chauhan, S. C., Andrianifahanana, M., Moniaux, N., Meza, J. L., Copin, M. C., et al. (2007). MUC4 expression is regulated by cystic fibrosis transmembrane conductance regulator in pancreatic adenocarcinoma cells via transcriptional and post-translational mechanisms. *Oncogene* 26 (1), 30–41. doi: 10.1038/sj.onc.1209764
- Song, H., Dong, M., Zhou, J., Sheng, W., Li, X., and Gao, W. (2018). Expression and prognostic significance of TRPV6 in the development and progression of pancreatic cancer. *Oncol. Rep.* 39 (3), 1432–1440. doi: 10.3892/or.2018.6216
- Song, H. Y., Zhou, L., Hou, X. F., and Lian, H. (2019). Anoctamin 5 regulates cell proliferation and migration in pancreatic cancer. *Int. J. Clin. Exp. Pathol.* 12 (12), 4263–4270.
- Steward, M. C., Ishiguro, H., and Case, R. M. (2005). Mechanisms of bicarbonate secretion in the pancreatic duct. *Annu. Rev. Physiol.* 67, 377–409. doi: 10.1146/annurev.physiol.67.031103.153247
- Stock, C., and Schwab, A. (2015). Ion channels and transporters in metastasis. *Biochim. Biophys. Acta* 1848 (10 Pt B), 2638–2646. doi: 10.1016/j.bbame.2014.11.012
- Stoklosa, P., Borgstrom, A., Kappel, S., and Peinelt, C. (2020). TRP Channels in Digestive Tract Cancers. *Int. J. Mol. Sci.* 21 (5), 1877. doi: 10.3390/ijms21051877
- Suzuki, K., Petersen, C. C., and Petersen, O. H. (1985). Hormonal activation of single K+ channels via internal messenger in isolated pancreatic acinar cells. *FEBS Lett.* 192 (2), 307–312. doi: 10.1016/0014-5793(85)80131-9
- Tawfik, D., Zaccagnino, A., Bernt, A., Szczepanowski, M., Klapper, W., Schwab, A., et al. (2020). The A818-6 system as an in-vitro model for studying the role of the transportome in pancreatic cancer. *BMC Cancer* 20 (1), 264. doi: 10.1186/s12885-020-06773-w
- Teisseyre, A., Palko-Labuz, A., Sroda-Pomianek, K., and Michalak, K. (2019). Voltage-Gated Potassium Channel Kv1.3 as a Target in Therapy of Cancer. *Front. Oncol.* 9, 933. doi: 10.3389/fonc.2019.00933
- Thevenod, F. (2002). Ion channels in secretory granules of the pancreas and their role in exocytosis and release of secretory proteins. *Am. J. Physiol. Cell Physiol.* 283 (3), C651–C672. doi: 10.1152/ajpcell.00600.2001
- Thompson-Vest, N., Shimizu, Y., Hunne, B., and Furness, J. B. (2006). The distribution of intermediate-conductance, calcium-activated, potassium (IK) channels in epithelial cells. *J. Anat.* 208 (2), 219–229. doi: 10.1111/j.1469-7580.2006.00515.x
- Tolon, R. M., Sanchez-Franco, F., Lopez Fernandez, J., Lorenzo, M. J., Vazquez, G. F., and Cacicado, L. (1996). Regulation of somatostatin gene expression by veratridine-induced depolarization in cultured fetal cerebrocortical cells. *Brain Res. Mol. Brain Res.* 35 (1–2), 103–110. doi: 10.1016/0169-328x(95)00188-x
- Ulaoreanu, R., Chiritoiu, G., Cojocaru, F., Deftu, A., Ristoiu, V., Stanica, L., et al. (2017). N-glycosylation of the transient receptor potential melastatin 8 channel is altered in pancreatic cancer cells. *Tumour Biol.* 39 (8):1010428317720940. doi: 10.1177/1010428317720940
- Venglovecz, V., Hegyi, P., Rakonczay, Z.Jr., Tiszlavicz, L., Nardi, A., Grunnet, M., et al. (2011). Pathophysiological relevance of apical large-conductance Ca(2+)-activated potassium channels in pancreatic duct epithelial cells. *Gut* 60 (3), 361–369. doi: 10.1136/gut.2010.214213
- Venglovecz, V., Rakonczay, Z.Jr., Gray, M. A., and Hegyi, P. (2015). Potassium channels in pancreatic duct epithelial cells: their role, function and pathophysiological relevance. *Pflugers Arch.* 467 (4), 625–640. doi: 10.1007/s00424-014-1585-0
- Venglovecz, V., Pallagi, P., Kemeny, L. V., Balazs, A., Balla, Z., Becskehazi, E., et al. (2018). The Importance of Aquaporin 1 in Pancreatitis and Its Relation to the CFTR Cl(-) Channel. *Front. Physiol.* 9, 854. doi: 10.3389/fphys.2018.00854
- Vercelli, C., Barbero, R., Cuniberti, B., Racca, S., Abbadesse, G., Piccione, F., et al. (2014). Transient receptor potential vanilloid 1 expression and functionality in mcf-7 cells: a preliminary investigation. *J. Breast Cancer* 17 (4), 332–338. doi: 10.4048/jbc.2014.17.4.332
- Voloshyna, I., Besana, A., Castillo, M., Matos, T., Weinstein, I. B., Mansukhani, M., et al. (2008). TREK-1 is a novel molecular target in prostate cancer. *Cancer Res.* 68 (4), 1197–1203. doi: 10.1158/0008-5472.CAN-07-5163
- Waldmann, R., Champigny, G., Bassilana, F., Voilley, N., and Lazdunski, M. (1995). Molecular cloning and functional expression of a novel amiloride-sensitive Na+ channel. *J. Biol. Chem.* 270 (46), 27411–27414. doi: 10.1074/jbc.270.46.27411
- Wang, B. J., and Cui, Z. J. (2007). How does cholecystokinin stimulate exocrine pancreatic secretion? From birds, rodents, to humans. *Am. J. Physiol. Regul. Integr. Comp. Physiol.* 292 (2), R666–R678. doi: 10.1152/ajpregu.00131.2006
- Wang, J., and Novak, I. (2013). Ion transport in human pancreatic duct epithelium, Capan-1 cells, is regulated by secretin, VIP, acetylcholine, and purinergic receptors. *Pancreas* 42 (3), 452–460. doi: 10.1097/MPA.0b013e318264c302
- Wang, J., Haanes, K. A., and Novak, I. (2013). Purinergic regulation of CFTR and Ca(2+)-activated Cl(-) channels and K(+) channels in human pancreatic duct epithelium. *Am. J. Physiol. Cell Physiol.* 304 (7), C673–C684. doi: 10.1152/ajpcell.00196.2012
- Wang, F., Jin, R., Zou, B. B., Li, L., Cheng, F. W., Luo, X., et al. (2016). Activation of Toll-like receptor 7 regulates the expression of IFN-lambda1, p53, PTEN, VEGF, TIMP-1 and MMP-9 in pancreatic cancer cells. *Mol. Med. Rep.* 13 (2), 1807–1812. doi: 10.3892/mmr.2015.4730
- Wang, J., Shen, J., Zhao, K., Hu, J., Dong, J., and Sun, J. (2019). STIM1 overexpression in hypoxia microenvironment contributes to pancreatic

- carcinoma progression. *Cancer Biol. Med.* 16 (1), 100–108. doi: 10.20892/j.jissn.2095-3941.2018.0304
- Warth, R., and Barhanin, J. (2002). The multifaceted phenotype of the knockout mouse for the KCNE1 potassium channel gene. *Am. J. Physiol. Regul. Integr. Comp. Physiol.* 282 (3), R639–R648. doi: 10.1152/ajpregu.00649.2001
- Warth, R., Garcia Alzamora, M., Kim, J. K., Zdebik, A., Nitschke, R., Bleich, M., et al. (2002). The role of KCNQ1/KCNE1 K(+) channels in intestine and pancreas: lessons from the KCNE1 knockout mouse. *Pflugers Arch.* 443 (5–6), 822–828. doi: 10.1007/s00424-001-0751-3
- Wen, L., Voronina, S., Javed, M. A., Awais, M., Sztamary, P., Latawiec, D., et al. (2015). Inhibitors of ORAI1 Prevent Cytosolic Calcium-Associated Injury of Human Pancreatic Acinar Cells and Acute Pancreatitis in 3 Mouse Models. *Gastroenterology* 149481–492 (2), e487. doi: 10.1053/j.gastro.2015.04.015
- Williams, S., Bateman, A., and O’Kelly, I. (2013). Altered expression of two-pore domain potassium (K2P) channels in cancer. *PLoS One* 8 (10), e74589. doi: 10.1371/journal.pone.0074589
- Wilschki, M., and Novak, I. (2013). The cystic fibrosis of exocrine pancreas. *Chang Spring Harb. Perspect. Med.* 3 (5):a009746. doi: 10.1101/cshperspect.a009746
- Winpenny, J. P., Verdon, B., McAlroy, H. L., Colledge, W. H., Ratcliff, R., Evans, M. J., et al. (1995). Calcium-activated chloride conductance is not increased in pancreatic duct cells of CF mice. *Pflugers Arch.* 430 (1), 26–33. doi: 10.1007/BF00373836
- Worley, P. F., Zeng, W., Huang, G. N., Yuan, J. P., Kim, J. Y., Lee, M. G., et al. (2007). TRPC channels as STIM1-regulated store-operated channels. *Cell Calcium* 42 (2), 205–211. doi: 10.1016/j.ceca.2007.03.004
- Wright, A. M., Gong, X., Verdon, B., Linsdell, P., Mehta, A., Riordan, J. R., et al. (2004). Novel regulation of cystic fibrosis transmembrane conductance regulator (CFTR) channel gating by external chloride. *J. Biol. Chem.* 279 (40), 41658–41663. doi: 10.1074/jbc.M405517200
- Yamaguchi, M., Steward, M. C., Smallbone, K., Sohma, Y., Yamamoto, A., Ko, S. B., et al. (2017). Bicarbonate-rich fluid secretion predicted by a computational model of guinea-pig pancreatic duct epithelium. *J. Physiol.* 595 (6), 1947–1972. doi: 10.1113/JP273306
- Yang, B., Song, Y., Zhao, D., and Verkman, A. S. (2005). Phenotype analysis of aquaporin-8 null mice. *Am. J. Physiol. Cell Physiol.* 288 (5), C1161–C1170. doi: 10.1152/ajpcell.00564.2004
- Yang, Y. D., Cho, H., Koo, J. Y., Tak, M. H., Cho, Y., Shim, W. S., et al. (2008). TMEM16A confers receptor-activated calcium-dependent chloride conductance. *Nature* 455 (7217), 1210–1215. doi: 10.1038/nature07313
- Yee, N. S., Zhou, W., and Lee, M. (2010). Transient receptor potential channel TRPM8 is over-expressed and required for cellular proliferation in pancreatic adenocarcinoma. *Cancer Lett.* 297 (1), 49–55. doi: 10.1016/j.canlet.2010.04.023
- Yee, N. S., Zhou, W., and Liang, I. C. (2011). Transient receptor potential ion channel Trpm7 regulates exocrine pancreatic epithelial proliferation by Mg<sup>2+</sup>-sensitive Socs3a signaling in development and cancer. *Dis. Model Mech.* 4 (2), 240–254. doi: 10.1242/dmm.004564
- Yee, N. S., Chan, A. S., Yee, J. D., and Yee, R. K. (2012a). TRPM7 and TRPM8 Ion Channels in Pancreatic Adenocarcinoma: Potential Roles as Cancer Biomarkers and Targets. *Sci. (Cairo)* 2012, 415158. doi: 10.6064/2012/415158
- Yee, N. S., Zhou, W., Lee, M., and Yee, R. K. (2012b). Targeted silencing of TRPM7 ion channel induces replicative senescence and produces enhanced cytotoxicity with gemcitabine in pancreatic adenocarcinoma. *Cancer Lett.* 318 (1), 99–105. doi: 10.1016/j.canlet.2011.12.007
- Yee, N. S., Li, Q., Kazi, A. A., Yang, Z., Berg, A., and Yee, R. K. (2014). Aberrantly Over-Expressed TRPM8 Channels in Pancreatic Adenocarcinoma: Correlation with Tumor Size/Stage and Requirement for Cancer Cells Invasion. *Cells* 3 (2), 500–516. doi: 10.3390/cells3020500
- Yee, N. S., Kazi, A. A., Li, Q., Yang, Z., Berg, A., and Yee, R. K. (2015). Aberrant over-expression of TRPM7 ion channels in pancreatic cancer: required for cancer cell invasion and implicated in tumor growth and metastasis. *Biol. Open* 4 (4), 507–514. doi: 10.1242/bio.20137088
- Yokoyama, T., Takemoto, M., Hirakawa, M., and Saino, T. (2019). Different immunohistochemical localization for TMEM16A and CFTR in acinar and ductal cells of rat major salivary glands and exocrine pancreas. *Acta Histochem.* 121 (1), 50–55. doi: 10.1016/j.acthis.2018.10.013
- Yurtsever, Z., Sala-Rabanal, M., Randolph, D. T., Scheaffer, S. M., Roswit, W. T., Alevy, Y. G., et al. (2012). Self-cleavage of human CLCA1 protein by a novel internal metalloprotease domain controls calcium-activated chloride channel activation. *J. Biol. Chem.* 287 (50), 42138–42149. doi: 10.1074/jbc.M112.410282
- Zaccagnino, A., Pilarsky, C., Tawfik, D., Sebens, S., Trauzold, A., Novak, I., et al. (2016). In silico analysis of the transportome in human pancreatic ductal adenocarcinoma. *Eur. Biophys. J.* 45 (7), 749–763. doi: 10.1007/s00249-016-1171-9
- Zaccagnino, A., Manago, A., Leanza, L., Gontarewitz, A., Linder, B., Azzolini, M., et al. (2017). Tumor-reducing effect of the clinically used drug clobazamine in a SCID mouse model of pancreatic ductal adenocarcinoma. *Oncotarget* 8 (24), 38276–38293. doi: 10.18632/oncotarget.11299
- Zdebik, A., Hug, M. J., and Greger, R. (1997). Chloride channels in the luminal membrane of rat pancreatic acini. *Pflugers Arch.* 434 (2), 188–194. doi: 10.1007/s004240050382
- Zeiber, B. G., Eichwald, E., Zabner, J., Smith, J. J., Puga, A. P., McCray, P. B. Jr., et al. (1995). A mouse model for the delta F508 allele of cystic fibrosis. *J. Clin. Invest.* 96 (4), 2051–2064. doi: 10.1172/JCI118253
- Zeng, W., Lee, M. G., Yan, M., Diaz, J., Benjamin, I., Marino, C. R., et al. (1997). Immuno and functional characterization of CFTR in submandibular and pancreatic acinar and duct cells. *Am. J. Physiol.* 273 (2 Pt 1), C442–C455. doi: 10.1152/ajpcell.1997.273.2.C442
- Zhou, B., Irwanto, A., Guo, Y. M., Bei, J. X., Wu, Q., Chen, G., et al. (2012). Exome sequencing and digital PCR analyses reveal novel mutated genes related to the metastasis of pancreatic ductal adenocarcinoma. *Cancer Biol. Ther.* 13 (10), 871–879. doi: 10.4161/cbt.20839
- Zhou, J., Zhang, L., Zheng, H., Ge, W., Huang, Y., Yan, Y., et al. (2020). Identification of chemoresistance-related mRNAs based on gemcitabine-resistant pancreatic cancer cell lines. *Cancer Med.* 9 (3), 1115–1130. doi: 10.1002/cam4.2764
- Zhu, S., Zhou, H. Y., Deng, S. C., He, C., Li, X., et al. (2017). ASIC1 and ASIC3 contribute to acidity-induced EMT of pancreatic cancer through activating Ca(2+)/RhoA pathway. *Cell Death Dis.* 8 (5), e2806. doi: 10.1038/cddis.2017.189
- Zou, Q., Yang, Z., Li, D., Liu, Z., and Yuan, Y. (2016). Association of chloride intracellular channel 4 and Indian hedgehog proteins with survival of patients with pancreatic ductal adenocarcinoma. *Int. J. Exp. Pathol.* 97 (6), 422–429. doi: 10.1111/iep.12213
- Zou, W., Yang, Z., Li, D., Liu, Z., Zou, Q., and Yuan, Y. (2019). AQP1 and AQP3 Expression are Associated With Severe Symptoms and Poor-prognosis of the Pancreatic Ductal Adenocarcinoma. *Appl. Immunohistochem. Mol. Morphol.* 27 (1), 40–47. doi: 10.1097/PAI.0000000000000523

**Conflict of Interest:** The authors declare that the research was conducted in the absence of any commercial or financial relationships that could be construed as a potential conflict of interest.

Copyright © 2020 Schnipper, Dhennin-Duthille, Ahidouch and Ouadid-Ahidouch. This is an open-access article distributed under the terms of the Creative Commons Attribution License (CC BY). The use, distribution or reproduction in other forums is permitted, provided the original author(s) and the copyright owner(s) are credited and that the original publication in this journal is cited, in accordance with accepted academic practice. No use, distribution or reproduction is permitted which does not comply with these terms.

# OBJECTIVES

PDAC remains one of the deadliest cancers (Park et al. 2021). The dismal prognostic of PDAC is mainly due to the late manifestation of symptoms, its high metastatic potential, and strong chemoresistance (Mizrahi et al. 2020). A prominent hallmark of PDAC tumors is their unique tumor microenvironment characterized by excessive fibrosis, acidity, and depletion of oxygen and nutrients due to poor vascularity (Pedersen et al. 2017). Strong evidence shows the impact of the acidic tumor microenvironment on PDAC aggressiveness in proliferation, migration, invasion, and apoptosis (Orth *et al.* 2019). However, the underlying mechanisms are poorly understood.

The dysregulation of ion channels modulates cancerous processes to such an extent that this phenomenon is characterized as ‘onco-channelopathies’ (Prevarskaya et al. 2018). More specifically is, the role of  $Ca^{2+}$  channels and signaling known to be implicated in carcinogenesis (Prevarskaya *et al.* 2007, Shapovalov et al. 2016, Chen et al. 2019). However, the interplay between ion channel dysregulation and the acidic tumor microenvironment is not well studied.

Among ion channel families implicated in  $Ca^{2+}$  entry is the TRP channel family. The canonical TRPC subfamily of the TRP channel family is characterized as ‘pH sensing ion channels’ (Wang et al. 2020). The first member of the TRPC family is TRPC1, which is particularly known to be involved in cancer carcinogenesis both through  $Ca^{2+}$  entry and independently of  $Ca^{2+}$  entry (Elzamzamy et al. 2020).

TRPC1 is involved in the carcinogenesis of several types of cancer, including PDAC, but how it is affected by the tumor microenvironment is not well understood. Our group and others have recently shown that TRPC1 is activated by ambient pressure, a feature of the tumor microenvironment in PSCs. This activation of TRPC1 promotes the proliferation and migration of PSCs in a  $Ca^{2+}$ -dependent manner (Fels et al. 2016, Radoslavova et al. 2022). Furthermore, TRPC1 promotes  $Ca^{2+}$  entry in breast cancer carcinogenesis in a hypoxic tumor microenvironment (Azimi et al. 2017).

Several studies have shown the role of the acidic environment and TRPC1 in cancer progression, but until now, the link between them remains unknown. Thus, our objectives of this study were to determine the interplay between TRPC1 and the tumor microenvironment.

The specific aims of the present research were as follows.:

1. To make a comprehensive screen of  $Ca^{2+}$  ion channels in human PDAC tissue and cell lines
2. To elucidate the role of TRPC1 in PDAC progression in the form of proliferation
3. To characterize the effect of the acidic tumor microenvironment on  $Ca^{2+}$  channel expression
4. To evaluate the implication of the acidic tumor microenvironment and TRPC1 in PDAC proliferation and migration

Finally, we aimed to investigate if the acidic microenvironment could affect the DNA methylation of specific ion channels and their expression.

# MATERIALS AND METHODS

## Cell culturing

### 1. Cell lines

The cell lines employed in this study are one control cell line and several PDAC cell lines, where our primary focus has been PANC-1 cells. All cell lines, including their characteristics, are summarized in Table 2.

- **HPNE**

The control used in this study is the normal-like duct cell line, Human Pancreatic Nestin-Expressing cells (HPNE), which was obtained from the pancreas of a 52-year-old man after his accidental death. The cells were immortalized by transduction with a retroviral expression vector containing human telomerase (hTERT) cDNA. The cells do not exhibit mutations in three common genes of pancreatic ductal adenocarcinoma; *KRAS*, *TP53*, and *p16*.

- **Colo357**

Colo357 cells are collected from a lymph node metastasis of a 77-year-old female. After a period of 2 months, she demonstrated weight loss, anemia, anorexia, and progressive jaundice, and it was found that she had a tumor in the head of the pancreas. The tumor cells were well-differentiated, and later genotyping of Colo357 cells revealed that they exhibit a *KRAS* mutation but wildtype (WT) in the three other genes. However, a homozygous deletion in *SMAD4* has been observed.

- **BxPC-3**

BxPC-3 cells were cultured from a 61-year-old female with a tumor in the body of the pancreas. There was no evidence of metastasis found. These cells are moderate to poorly differentiated and are the only cells in this study with no mutation in the *KRAS* gene. They exhibit mutations in p53 and *CDKN2A*.

- **AsPC-1**

AsPC-1 cells are derived from a 62-year-old female with adenocarcinoma in the head of the pancreas. The cell line was obtained and established from ascitic cell components. The cells are poorly differentiated and displays mutations in all driver genes.

- **MiaPaCa-2**

The undifferentiated MiaPaCa-2 cells were derived from a 65-year-old man with 6 months of recurrent abdominal pain. The tumor was removed from the body and tail of the pancreas, where it infiltrated the periaortic area. No metastasis was detected upon tumor removal. MiaPaCa-2 cells display mutations in all four genes except *SMAD4*.

- **PANC-1**

PANC-1 cells were obtained from a specimen removed from the head of the pancreas of a 56-year-old man who demonstrated a history of jaundice. The tumor had a size of 1.5 cm and was invading the duodenal wall.



Tumor cells were malignant undifferentiated cells, showing perineural invasion and metastases to one peripancreatic lymph node. Later investigations have shown that PANC-1 cells exhibit genetic alterations in *KRAS*, *TP53* and *CDKN2A*.

All cell lines can be obtained at the American Type Culture Collection (ATCC). We kindly received our PDAC cell lines from Prof. Anna Trauzold from the Institute of Experimental Cancer Research, Kiel University, except for the MiaPaCa-2 cell line, which we kindly received from Prof. Natalia Prevarskaya from The Laboratory of Cell Physiology, INSERM U1003, University of Lille.

Cell line	Origin	Differentiation & tumor grade	KRAS	p53	CDKN2A/p16	SMAD4/DPC4
HPNE	Pancreas		None	None	None	Unknown
Colo357	Lymph node metastasis	Well, G1-G2	12 Asp mutation	Wildtype	HD, Wildtype	HD or Wildtype
BxPC-3	Primary tumor	Moderate to poor, G2	Wild type	220 Cys mutation	HD, Wildtype	HD or Wildtype
AsPC-1	Ascites	Poor, G2	12 Asp mutation	Frameshift mutation, 135 $\Delta$ 1 bp,	$\Delta$ 2 bp frameshift mutation, HD, wildtype	HD or Wildtype
MiaPaCa-2	Primary tumor	Poor, G3	12 Cys mutation	248 Trp mutation	HD	Wild type
PANC-1	Primary tumor	Poor, G3	12 Val mutation	176 Ser mutation	HD	Wild type

Table 2. Genetic alterations in human pancreatic cell lines. HD homozygous deletion,  $\Delta$ -deletion, bp- base pair (Modified from: (Moore et al. 2001, Grutzmann et al. 2003, Deer et al. 2010))

## 2. Cell maintenance

Cell culture experiments were performed under a type II microbiological safety cabinet (PSM) (Faster BH-EN-2003-S). The cells were seeded and cultured in culture flasks of 25 or 75cm<sup>2</sup> (Nunc) treated to promote cell adhesion and placed in an incubator with an atmosphere saturated with humidity at 37 °C and 5% CO<sub>2</sub>. HPNE cells were grown in a culture medium recommended by ATCC supplemented with 10% FBS (Table 3). PDAC cell lines were cultured in RPMI-1640 medium. Medium pH was adapted by adjusting the HCO<sub>3</sub><sup>-</sup> concentration by adding the appropriate amount of NaHCO<sub>3</sub>, ensuring equal osmolarity by adjusting [NaCl] (Table 4). Cells were adapted to pH 7.4 and 6.5 by adding the appropriately pH-adjusted medium to freshly split cells and maintaining cells in this medium for 30 days. Cells were, after acidic adaptation, recovered in pH 7.4 for 14 days. Normal pH (7.4) conditions simulate the physiological pH in blood and organs. Acidic pH (6.5) simulates the conditions in the tumor microenvironment. Recovery conditions (7.4) simulate the recovery phase, of where cells potentially leave the tumor microenvironment by invasion and migration (Figure 28). In

order to avoid geno- and phenotypic changes of the cells, the cells were passaged maximum 20 times, before a new vial was thawed. All cells were mycoplasma tested before freezing.

Components	HPNE media
<b>DMEM without glucose</b>	75%
<b>Medium M3 Base</b>	25%
<b>FBS</b>	10%
<b>Glucose</b>	5.5 mM
<b>Puromycin</b>	750 ng/ml

Table 3. Components of complete hTERT-HPNE medium DMEM without glucose (Sigma Cat#D-503). Medium M3 Base (Incell Corp. Cat#M300F-500) Fetal Bovine Serum was purchased from PAN Biotech (Cat#P30-3031, PAN Biotech), and 10% was added as a final concentration.

Components	pH 7.4	pH 6.5
<b>RPMI-1640</b>	500 ml	4.2 g
<b>NaHCO<sub>3</sub><sup>-</sup></b>	24 mM	3 mM
<b>NaCl</b>	5 mM	26 mM
<b>FBS</b>	10%	10%
<b>Sodium Pyruvate</b>	1 mM	1 mM
<b>GlutaMax</b>	1%	1%

Table 4. Components of pH corrected RPMI-1640 medium. For RPMI-1640 pH 7.4, 500 ml of prepared media was used (Sigma-Aldrich, Cat#R8758), for pH 6.5 RPMI-1640 powder was used for 500 ml of sterile water (Sigma-Aldrich, Cat#R6504- 10X1L). Fetal Bovine Serum was purchased from PAN Biotech (Cat#P30-3031, PAN Biotech).

To adjust the HCO<sub>3</sub><sup>-</sup> concentration, the Henderson Hasselback equation was used:

$$\text{Henderson – Hasselbalch: } pH = pKa + \log \frac{[\text{weak base}]}{[\text{weak acid}]}$$

Adapting this equation to a cell culture system will look like this:

$$pH = pK + \log \frac{[HCO_3^-]}{s * PCO_2}$$

$pK = 6.1$ .  $s$  is the inverse of the Henrys law constant for solubility of CO<sub>2</sub> in aqueous solution

$s = 0.24 \text{ mmol}/(l * kPa)$  and 5% CO<sub>2</sub> gives 1.2 mmol/l CO<sub>2</sub>

Thus, the equation to have a pH of 6.5 will be:

$$6.5 = 6.1 + \log \frac{[HCO_3^-]}{1.2 * 5}$$

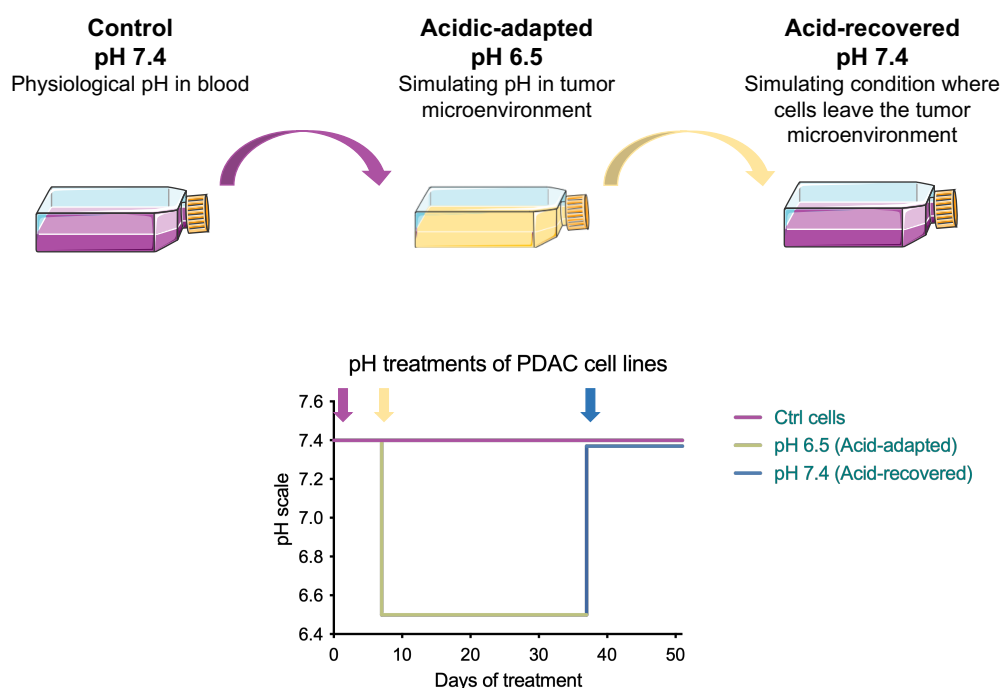


Figure 28. All cell lines were grown in pH 7.4 PANC-1 cells were adapted to acidic pH (6.5) for 30 days. After acid adaptation, cells were grown under recovery conditions (pH 7.4) for 14 days.

### 3. Freezing and thawing of cells

At 80% confluence, the cells were detached by adding trypsin. A quantity of one million cells was centrifuged at 1500 rpm for 7 min, the cell pellet was then resuspended in 1 ml of a freezing medium composed of 90% medium and 10% dimethylsulfoxide (DMSO). The cell suspension was transferred to cryopreservation ampoules, and placed in CoolCell™ freezer boxes (Biocision, Dutscher, Thermofisher, France) at -80 °C, allowing slow and progressive freezing of the cells. The cells were rapidly thawed in a water bath at 37 °C. The cells were transferred to an Eppendorf tube and then centrifuged at 1500 rpm for 5 minutes. The supernatant containing the DMSO (toxic to the cells) was then eliminated. The pellet composed of the cells was resuspended in their corresponding cell culture medium in a culture flask of 25 cm<sup>2</sup> and then placed in the incubator at 37° C and 5% CO<sub>2</sub>. Cells were kept for ~14 days before being used for experimental procedures.

### Transfection

The principle of transfection is the process of introducing e.g., genetic material such as a plasmid or mRNA into eukaryotic cells, either to suppress or overexpress a gene. In this study, we have introduced a knock-down (KD) of a gene with the siRNA transfection approach. Here, we used the technique of electroporation, which is a physical transfection method that permeabilizes the cell membrane by applying an electrical pulse to move molecules (e.g., siRNA), with the help of a cell type-specific nucleofection buffer (Nucleofector Kit V, Amaxa) via the electrical field into the cell.

For transfection, cells were detached by trypsinization and counted ( $1 \times 10^6$ ). The cells were then centrifuged for 7 min at 1500 rpm, and the pellet was resuspended in 100  $\mu$ L of transfection buffer to which we added 4  $\mu$ g of Control (siCTRL) or target siRNA, in this case, the KD of TRPC1 (siTRPC1) (Table 5). Transfection efficiency was validated by mRNA and protein expression.

siRNA	Sequence
siCTRL	5'-UAGCGACUAAACACAUCA-3' (Eurogentec)
siTRPC1	ON-TARGET plus SMART pool siRNA, (Dharmacon Research, IL #L-004191-00050 )

*Table 5. siRNA used for transfections*

## Generation of spheroids

It is well-accepted that 3D models imitate in vivo cell-cell and cell-extracellular matrix interactions better than traditional two-dimensional (2D) cell cultures. Therefore, spheroid models were included in this study to investigate ion channel expression and proliferation. In this study, both non-transfected and transfected cells were used. Monolayer PANC-1 cells were detached with trypsin and counted  $2 \times 10^3$  cells per spheroid in 200  $\mu$ L media. Cells were resuspended in ice-cold media containing 2% Geltrex (Gibco, #A1413202). Media containing cells and Geltrex<sup>TM</sup> (Gibco, A1413202) were transferred to a reservoir and then distributed to an ultra-low attachment round bottom 96-well plate (Corning, #7007). Firstly, the plate was centrifuged for 20 min at 750 RCF. It was checked whether cells formed proper spheroids in a bright field microscope. Spheroids were kept at 37° C and 5% CO<sub>2</sub>. Every second day the media was changed on spheroids by removing 100  $\mu$ L of media and adding 100  $\mu$ L of new media from each well. Pictures were taken every 2<sup>nd</sup>, 4<sup>th</sup>, 7<sup>th</sup>, and 9<sup>th</sup> day to control the spheroids' size.

## Cell proliferation assays

- Trypan blue assay

The viability of cells was analyzed by the trypan blue assay. Trypan blue is an impermeable dye, which can pass the plasma membrane of dead cells but not alive cells. Here, we used trypan blue to assess the viability of PANC-1 cells, grown under the three different pH conditions. Media was removed from cells grown in 35mm Petri dishes and washed once with 200  $\mu$ L PBS, then 200  $\mu$ L trypsin to detach the cells. The effect of trypsin was inhibited with the removed media that the cells were grown in. Cells in suspension were mixed with 0.4% Trypan Blue reagent (Sigma-Aldrich) in a ratio 1:5. Cells were counted 6 times using the standard Malassez cell method. The viability was calculated as the total number of viable cells (cells alive/white cells) normalized to the control, and the mortality was calculated as the percentage of dead cells (blue cells) compared to the control.

- **CellTiter-Glo® Assay**

The viability of 3D cultured spheroids was evaluated with the CellTiter-Glo® 3D Assay (Promega). This reagent measures ATP as an indicator of viability and generates a luminescent readout. Spheroids grown for nine days were transferred to a black 96-well plate with 100 µL of media. For each well, 100 µL of CellTiter-Glo® were added. The plate was placed on a shaker for 5 minutes and for incubating without shaking for 25 minutes. Results were obtained with a FLUOSTAR microplate reader.

- **Flow Cytometry**

Flow cytometry was carried out on ethanol-fixed cells by a propidium iodide (PI) assay. The intercalating agent PI binds DNA, which can be emitted (excitation at 535nm/ emission at 617nm) by a fluorescent signal. The premise with fluorescent dyes, such as PI, is that they are stoichiometric. That is they bind in proportion to the amount of DNA present in the cell. Cells that are in S phase will have more DNA than cells in G0/G1 phase, and cells in G2/M phase will have approximately the double amount of DNA than cells in G1. The more DNA, the more fluorescent the cells will be. Thus, the fluorescent signal can be used to distinguish between cells in G0/G1, S and cells in G2/M-phase, by a flow cytometer. Duplicates of  $2 \times 10^5$  PANC-1 cells were seeded in 60 mm Petri dishes. The cells were either non-transfected or transfected for 72 h. For each condition, cells were washed in PBS and harvested in 400 µL trypsin, and resuspended in 3 ml media. The Petri dishes were washed with 4 ml PBS, which was pooled with the rest of the media. The cells were centrifuged for 7 min at 1000 RPM, washed in PBS, and centrifuged again.  $3 \times 10^5$  cells were counted and transferred to an Eppendorf tube and centrifuged again. The pellet was resuspended in 150 µL PBS + EDTA 5 mM and fixed in 350 µL ice-cold Absolut ethanol during vortexing. Before staining with PI, the samples were kept at 4° C for at least one week. On the day of flow cytometry, cells were centrifuged for 7 min at 1000 RPM, and the supernatant was removed. Cells were resuspended in 100 µL of PBS + EDTA 5 mM. RNase A was added to a final concentration of 20 µg/mL for 30 minutes at room temperature. Nuclei staining was performed with PI (50 µg/mL) immediately before the acquisition, which was performed using BD Accuri C6 flow cytometry. Flow cytometry data was analyzed in Cyflogic, and figures were made in FCS Express 7.

## Calcium Imaging

Calcium Imaging makes it possible to detect  $\text{Ca}^{2+}$  concentrations in real-time. Variations in intracellular  $\text{Ca}^{2+}$  concentrations can be measured by using a fluorescent probe, in this case, Fura-2. The Fura-2 is loaded with an AM (acetoxymethyl ester) group, which allows the probe to cross the plasma membrane of cells. When entered, the AM group is hydrolyzed by esterases resulting in the fluorescent signal of the cell cytoplasm. Fura-2 has the characteristic of being ratiometric. Fura-2 is excited simultaneously at two wavelengths, 340 nm and 380 nm, and emitted at 510 nm. The binding of  $\text{Ca}^{2+}$  to the probe causes a variation in fluorescence. Thus, the fluorescence measured at 340 nm increases, and that at 380 nm decreases. Conversely, during a loss of affinity for  $\text{Ca}^{2+}$ , the fluorescence at 340 nm decreases and increases at 380 nm. The ratio of the intensities

emitted at 510 nm, after the excitation at the two wavelengths mentioned above, makes it possible to estimate the fluctuations of the  $\text{Ca}^{2+}$  intracellular concentration.

$20 \times 10^3$  transfected cells were seeded in the middle of an autoclaved coverslip in a 35 mm petri dish. 72 h after transfection, Fura-2 AM was loaded in a final concentration of  $3.3 \mu\text{M}$  for 45 minutes. Coverslips were rinsed two times with  $\text{Ca}^{2+}$  imaging solutions (Table 6) to remove excessive Fura-2. The coverslip was then attached to a plastic dish with a perforated bottom using silicone grease. The cells are then exposed to different excitation wavelengths using a monochromator (Polychrome V, Till Photonics). A CCD camera captures the fluorescence variations of the Fura-2 probe, and Metafluor acquisition software transforms the light signal into a digital signal. The software then quantifies the variations in Fura-2 emission fluorescence for each of the excitation wavelengths. Throughout the experiment, a perfusion/aspiration system allows the control of the extracellular environment. During the different  $\text{Ca}^{2+}$  imaging protocols, the extracellular environment is composed as described in Table 6. The data is finally analyzed using Origin8 and GraphPad Prism Software.

<b>Chemical Compounds</b>	<b>Concentration</b>
<b>NaCl</b>	140 mM
<b>KCl</b>	5 mM
<b>MgCl<sub>2</sub></b>	2 mM
<b>Hepes</b>	10 mM
<b>Glucose</b>	5 mM

*Table 6. Composition of basic extracellular  $\text{Ca}^{2+}$  imaging medium.*

- **Manganese quenching assay**

The principle of the Manganese ( $\text{Mn}^{2+}$ ) quenching assay is based on fluorescent quenching.  $\text{Mn}^{2+}$  is able to bind to Fura-2, which causes an irreversible quenching of the fluorescent signal and a conformational change of the probe. Since  $\text{Mn}^{2+}$  permeate the cell membrane by the same pathways as  $\text{Ca}^{2+}$ , the entry of extracellular  $\text{Mn}^{2+}$  into the cells represents an indirect measurement of intracellular  $\text{Ca}^{2+}$  movements. When  $\text{Mn}^{2+}$  is present in the cells, it competes with  $\text{Ca}^{2+}$  to bind Fura-2. At equal concentrations of  $\text{Ca}^{2+}$  and  $\text{Mn}^{2+}$ , the latter binds more than 99% of Fura-2, compared to  $\text{Ca}^{2+}$ , which leads to elimination of the fluorescent signal. Thus, the greater the fluorescent quenching kinetics, the greater the influx of  $\text{Mn}^{2+}$ , which can suggest a greater  $\text{Ca}^{2+}$  entry. During the  $\text{Mn}^{2+}$  quenching assay, the fluorescent probe is excited at 360 nm, corresponding to the isosbestic point of Fura-2. Excitation at this wavelength is important since the fluorescence of the probe is independent of the intracellular calcium concentration. For the experimental setup of the  $\text{Mn}^{2+}$  quenching assay, cells are perfused with basic extracellular medium containing 2 mM  $\text{Ca}^{2+}$ . After 90 sec, the extracellular medium is replaced by a medium containing 2 mM of  $\text{Mn}^{2+}$  for 3 min. Replacing extracellular  $\text{Ca}^{2+}$  with  $\text{Mn}^{2+}$  leads to quenching of the fluorescent signal of Fura-2. By measuring the slope of the  $\text{Mn}^{2+}$  quench, we can interpret the basal  $\text{Ca}^{2+}$  entry.



- Store-operated channel entry assay

To test the capacity of SOCs to allow extracellular  $\text{Ca}^{2+}$  across the plasma membrane, the cells used in this protocol were perfused with an extracellular  $\text{Ca}^{2+}$  medium containing 2 mM  $\text{Ca}^{2+}$  for 2 min. Then, this medium is replaced by an extracellular medium without  $\text{Ca}^{2+}$ , supplemented with 1  $\mu\text{M}$  thapsigargin, which allows the irreversible depletion of  $\text{Ca}^{2+}$  stocks for 11 min. Next, the cells were again perfused with an extracellular medium containing 2 mM  $\text{Ca}^{2+}$ , for 5 minutes. Finally, the cells were perfused with the 0 mM  $\text{Ca}^{2+}$  solution for 5 minutes.

## Transcriptional expression

### Transcriptional expression

- RNA extraction

Total RNA extraction was performed using the Trizol extraction method (TRI Reagent®, Sigma) on cell cultures, either transfected or non-transfected. After extraction, the RNA concentration was measured using a NanoDrop 2000 spectrophotometer (ThermoFischer). During the assay, we eliminated all samples with A260/A280 and A260/A230 ratios below 1.8, as they were considered impure. During RNA extraction, all surfaces and technical equipment are cleaned with an RNase Away solution (Molecular Bioproducts) to avoid any contamination by RNases. In addition, all the extraction steps are carried out under a chemical extraction hood.

- Reverse transcription

To transform RNA to cDNA, the extracted RNA had to undergo reverse transcription (RT). This was done using a High-Capacity cDNA Reverse Transcriptase kit (Applied Biosystems). A volume corresponding to 2  $\mu\text{g}$  RNA was completed with ultra-pure water to a final volume of 13.2  $\mu\text{L}$ . To this, 6.8  $\mu\text{L}$  of reaction mixture necessary to perform RT was added (Table 7). The heat-resistant tubes containing the RNA-reaction mixture was placed in a thermocycler to perform the RT, consisting of steps: (1) A primer fixing step for 10 min at 25°C. (2) The RT step for 2 hours at 37°C. (3) A step of stopping the reaction for 5 min at 85°C (deactivation of the enzyme). Following this step, the cDNA was stored at -20°C.

Reagents	Volume
<b>RT buffer</b>	2 $\mu\text{L}$
<b>Random primers</b>	2 $\mu\text{L}$
<b>Deoxyribonucleotides (dNTPs)</b>	0.8 $\mu\text{L}$
<b>RNase inhibitor</b>	1 $\mu\text{L}$
<b>Polymerase (MultiScribe™)</b>	1 $\mu\text{L}$

Table 7. Composition of RT reaction mixture (1 reaction)

- **Quantitative PCR**

Quantitative PCR (qPCR) allows for the amplification and detection of a specific DNA sequence in real-time. Our qPCR experiments were carried out at the Regional Resource Center for Molecular Biology in Amiens (CRRBM) with the help of Dr. Stéphanie Guénin. The qPCR was performed in a 384-well plate using a thermocycler and Light Cycler® 480 software (Roche Molecular System, Inc.). The cDNA sample obtained during the RT was diluted 1/20 in ultra-pure water, then 2 µL of this diluted cDNA was diluted in the reaction mixture containing the primers, water, and SYBR Green mixture (Roche, France) (Table 8). SYBR Green is a DNA intercalating agent which emits fluorescence is proportional to the number of amplicons formed during PCR. Fluorescence is measured at the end of the elongation phase of each cycle.

<b>Reagents</b>	<b>Volume</b>
<b>Ultra-pure water</b>	1.6 µL
<b>Forward primer (10 µM)</b>	0.5 µL
<b>Reverse primer (10 µM)</b>	0.5 µL
<b>SYBR Green</b>	4.6 µL

*Table 8. Composition of the qPCR reaction mixture (1 reaction)*

The plate containing cDNA, primer, and SYBR Green mixtures was centrifuged for 30 sec and then placed in the thermocycler for 45 cycles, where each cycle is made up of three steps: (1) a denaturation step at 95°C for 30 s (2) a hybridization step at 60°C for 10 s, and (3) an elongation step at 72°C for 15 s. To quantify the transcriptional expression of our genes of interest, we determined the number of cycles from which the fluorescence linked to the amplification is detectable (cycles above 40 were considered not expressed). This threshold signal, called cycle threshold or Cycle Threshold (Ct) is inversely proportional to the quantity of cDNA initially present in the amplified sample. The quantification of the transcriptional expression of our actors of interest was normalized against the transcriptional expression of beta-2-microglobulin (B2M) using the following formula:

$$\text{Ratio} = \frac{(\text{Efficiency}_{\text{target}})^{\Delta C_{\text{target}}(\text{control} - \text{sample})}}{(\text{Efficiency}_{\text{reference}})^{\Delta C_{\text{reference}}(\text{control} - \text{sample})}}$$

- **Public database analysis**

The mRNA expression of ion channels was investigated by using online available datasets. Whisker boxplots of ORAI, STIM and TRPC1 mRNA expression were generated using GEPIA2 (<http://gepia2.cancerpku.cn/>) that compiles Genotype-Tissue Expression (GTEx) (<http://www.GTEXportal.org/>), and The Cancer Genome Atlas (TCGA) (<http://www.cancergenome.nih.gov/>) datasets of normal and tumor samples from different organs of interest, in our case pancreas and PDAC (PAAD). Survival analysis was performed using the SurvExpress online tool (available at <http://bioinformatica.mty.itesm.mx/SurvExpress>).

## Protein expression

Either transfected or non-transfected cells were washed two times with ice-cold PBS on ice. The total protein was extracted using radioimmunoprecipitation assay (RIPA) protein extraction buffer, supplemented with protease inhibitors (Sigma), sodium orthovanadate (0.5 mM), and EDTA (5 mM). 50  $\mu$ L or 100  $\mu$ L of the complete RIPA buffer was used for 60 mm and 10 cm Petri dishes, respectively. The cells were incubated with RIPA for 30 min, scrapped, and transferred into an Eppendorf tube. The sample was centrifuged for 15 min, at 14000 RPM at 4°C. After centrifugation, the supernatant containing the proteins was transferred into a new Eppendorf tube. The protein concentration was determined using the Bradford colorimetric method (DC protein assay, Biorad) and using a BSA-based standard range. The assay is performed by measuring the optical density at 620 nm using a plate reader spectrophotometer (Tecan®) and Tecan I-Control software. The proteins were finally stored at -80°C.

- **Western blot**

Protein samples were diluted in 5X Laemmli and 1X Laemmli buffer to have the same concentration and amount of protein for each sample. The proteins were denatured at 95 °C for 10 min. After the denaturation step, the samples were loaded into an acrylamide gel, and proteins were separated by gel electrophoresis carried out in a Bio-Rad system using the Sodium dodecyl sulfate-polyacrylamide gel electrophoresis (SDS-PAGE) technique. Electrophoresis was permitted by the use of an electrophoresis buffer and carried out for 15 minutes at 100 volts (V) and 1 hour at 180 V. Following electrophoretic separation, the proteins were transferred to a nitrocellulose membrane by electroblotting. The transfer step was performed using a transfer buffer for 90 min at 60 V. The nitrocellulose membrane was then incubated for 1 h with gentle shaking at room temperature, in a Tris Buffered Saline (TBS) solution containing 0.1% Tween-20 (TBS-T) and 5% milk or 5% BSA, in order to prevent non-specific antibodies binding the membrane. The membrane was incubated in a primary antibody solution (diluted in TBS-T 5% BSA) overnight at 4°C with gentle shaking (Table 9 shows primary antibodies included in this study). After 3 washes with TBS-T of 5 minutes each, the membrane was incubated for 1 hour with gentle shaking in a secondary antibody solution (diluted in TBS-T 5% BSA), corresponding to the specie of the primary antibody, at room temperature. After the secondary antibody incubation, the membrane was finally washed with TBS-T (5 min each). The proteins recognized by the antibodies were revealed by chemiluminescence using the ECL reagent (Enhanced ChemiLuminescence, Biorad). The light signal emitted was captured by the ChemiDoc XRS device (Biorad) and integrated using the Quantity One® software (Biorad). The intensity of the signals was measured by densimetry. Photo analysis and quantification of protein bands were performed using ImageJ software. The expression of all the proteins of interest was normalized to the protein expression of GAPDH.

<b>Antibody for WB</b>	<b>Host</b>	<b>Dilution</b>	<b>Distributor</b>	<b>Reference</b>
<b>TRPC1</b>	Rabbit	1/500	Abcam	Ab110837
<b>ORAI1</b>	Mouse	1/500	ProSci Inc	PM-5205
<b>ORAI3</b>	Rabbit	1/500	Abcam	Ab254260
<b>STIM1</b>	Rabbit	1/500	Cell Signaling	5668S
<b>STIM2</b>	Rabbit	1/500	Abcam	Ab59342
<b>PI3K-p85<math>\alpha</math></b>	Rabbit	1/500	Bioworld Technology	MB9419
<b>CaM</b>	Mouse	1/500	Santa Cruz	sc-137079
<b>CDK1</b>	Rabbit	1/500	Cell Signaling	77055
<b>CDK2</b>	Rabbit	1/500	Cell Signaling	2546
<b>CDK4</b>	Rabbit	1/500	Cell Signaling	Ab82335
<b>CDK6</b>	Rabbit	1/500	Cell Signaling	Ab18528
<b>Cyclin A</b>	Mouse	1/500	Santa Cruz	sc-271682
<b>Cyclin B1</b>	Rabbit	1/500	Cell Signaling	4138
<b>Cyclin D1</b>	Rabbit	1/500	Cell Signaling	2978
<b>Cyclin D3</b>	Mouse	1/500	Cell Signaling	2936
<b>Cyclin E</b>	Rabbit	1/500	Cell Signaling	20808
<b>p21</b>	Rabbit	1/250	Cell Signaling	2947
<b>ERK1/2</b>	Rabbit	1/500	Cell Signaling	9102
<b>pERK1/2</b>	Rabbit	1/500	Cell Signaling	9101
<b>AKT</b>	Rabbit	1/500	Cell Signaling	9272
<b>pAKT</b>	Rabbit	1/500	Cell Signaling	4060
<b>GAPDH</b>	Mouse	1/4000	Cell Signaling	97166

*Table 9. Primary antibodies used in this study.*

## Co-immunoprecipitation

Co-immunoprecipitation (co-IP) is a standard technique to identify a physically relevant protein-protein interaction by using target protein-specific antibodies to capture proteins bound to a specific target protein indirectly. In this study, we aimed to investigate the protein-protein interaction between TRPC1 and the PI3K-p85 $\alpha$  subunit. In this study, we used SureBeads™ Protein A Magnetic Beads (Biorad # 161-4013) as they have a high affinity for rabbit antibodies. First,  $6 \times 10^5$  non-transfected or  $1 \times 10^6$  transfected PANC-1 cells were seeded in a 10 cm Petri dish and collected after 72 h. Co-IP was carried out according to the manufacturer's protocol. The beads were washed and preincubated with 1  $\mu$ g of the TRPC1 (Rabbit, Abcam) or PI3K-p85 $\alpha$  subunit antibody or a control Anti-rabbit IgG antibody for 30 min. After a sequential washing step, 500  $\mu$ g of protein lysates from RIPA scrapped samples were added to the beads, which were slowly rotated for 2 h at

room temperature. After another sequential washing step, the proteins were eluted according to the manufacturer's protocol. The proteins were denatured and subjected to Western blotting, as described above. To detect the input, 50 µg of proteins from the corresponding co-immunoprecipitation samples were used.

### Proximity ligation assay

Proximity ligation assay (PLA) allows in situ detection of protein interactions with high sensitivity and specificity. In this study,  $8 \times 10^4$  non-transfected or transfected PANC-1 cells were grown on coverslips 72 h before the PLA experiment. First, the cells were washed twice in PBS and fixed with 4% PFA at room temperature for 20 min. Following two washes with PBS, cells were permeabilized with 0.1% Triton™ X-100 for 10 min. The Duolink in situ PLA detection kit (Sigma-Aldrich, Saint-Quentin-Fallavier, France) was used to detect interactions/proximity between TRPC1 and the PI3K-p85 $\alpha$  subunit. Experiments were performed according to the manufacturer's protocol. The red fluorescent oligonucleotides produced as the end product of the procedure were visualized using the Zeiss Observer Z1 microscope 60X oil objective (Carl Zeiss, Oberkochen, Germany). Images were analyzed using ImageJ, where puncta per cell were counted and normalized to the respective control; normal pH conditions (pH 7.4) for non-transfected cells, and siCTRL in their respective medium (pH 6.5 or 7.4R). Approximately 20 pictures per condition were captured and analyzed and presented as relative number puncta/cell.

### Biotinylation

Biotinylation allows for specific isolation and quantification of proteins in the cell surface membrane. The biotinylation technique consists of labeling cell surface proteins with a biotin reagent before lysing the cells and isolating these biotin-tagged proteins with a streptavidin pull-down. In this study,  $1 \times 10^6$  HPNE cells or  $8 \times 10^5$  PANC-1 cells were seeded and collected after 48 h. Cells were washed three times with cold PBS, then incubated with 3 mg of Sulfo-NHS-SS-biotin (Thermo Scientific) and slightly shaken for 1 h at 4° C. The reaction was interrupted by adding cold PBS containing 10 mM glycine. Next, cells were scrapped with RIPA, and approximately 10% of the total lysate was saved as the total lysate fraction. The remaining sample was incubated with 100 µL high-capacity streptavidin-agarose beads (ThermoFisher Scientific, Waltham, MA, USA) with gentle rotation overnight at 4° C. After incubation, beads were washed 4 times with RIPA buffer. Proteins were eluted from the beads with 50 µl of Laemli buffer 2X and heated at 60° C for 30 min. Both total lysate samples and membrane fraction samples were subjected to Western Blot analysis.

### Intracellular pH

Measurements of pHi can be performed by the use of fluorescent dyes, such as the H<sup>+</sup>-dependent probe 2',7'-bis-(2-carboxyethyl)-5-(and-6)-carboxyfluorescein (BCECF) acetoxymethyl ester (AM). Initially, BCECF is esterified with acetoxymethyl esters, which allow cell entrance but leave BCECF essentially non-

fluorescent. Once inside the cells, the esterases remove the ester groups from the probe, keeping it in the cells and enabling its protonation and fluorescent activity.  $H^+$  quenches the fluorescence of BCECF, meaning that the fluorescence intensity of excited BCECF declines when lowering pH. BCECF is simultaneously excited at two wavelengths, 440 nm, and 485 nm. Excitation at 440 nm is not sensitive to pH changes, whereas excitation at a wavelength of 485 nm results in pH-dependent fluorescence, which is reduced when elevating the  $H^+$  concentration (lowering pH). The background-corrected fluorescence intensity ratio between the two excitation channels is directly related to  $pH_i$  and can be converted to pH values by calibration (described in Intracellular pH calibration).  $8 \times 10^4$  cells were seeded in WillCo glass-bottom dishes WillCo Wells. After 48 h of seeding, cells were incubated in a growth medium containing  $4 \mu M$  BCECF for 30 min in the dark at  $37^\circ C$ , 95% humidity, 5%  $CO_2$ . Cells were washed twice in  $HCO_3^-$  containing Ringer solution (Table 10). Then, the cells in the glass-bottom dish containing Ringer solution adjusted to the respective pH were placed in a temperature-controlled compartment ( $37^\circ C$ ) equipped with gas. A group of cells was focused and monitored using the software EasyRatioPro, in which a measuring area inside certain cells was marked. In this area, the 440- and 485 nm intensities were simultaneously measured, and the emission was measured at 520 nm. The steady-state  $pH_i$  measurements were carried out for 10 min.

<b><math>HCO_3^-</math> Ringer</b>	<b>pH 7.4</b>	<b>pH 6.5</b>
<b>NaHCO<sub>3</sub></b>	24 mM	3 mM
<b>NaCl</b>	115 mM	135 mM
<b>KCl</b>	5 mM	5 mM
<b>Na<sub>2</sub>HPO<sub>4</sub></b>	1 mM	1 mM
<b>CaCl<sub>2</sub></b>	1 mM	1 mM
<b>MgCl<sub>2</sub></b>	0.5 mM	0.5 mM
<b>MOPS/TES/HEPES (MTH)</b>	3.3/3.3/5 mM	3.3/3.3/5 mM

Table 10. Composition of Ringer solutions for  $pH_i$  measurements at pH 7.4 and pH 6.5.

- **Intracellular pH calibration**

Because BCECF is a quencher, its quantum yields diverge in different buffers, which is why calibration *in situ*, is required. In the present work calibration using the high  $K^+$ /Nigericin method was obtained for each cell line (Boyarsky et al. 1996). Nigericin is an ionophore antiporting  $K^+/H^+$ . Supplying the cells with  $K^+$ -based Ringer in a concentration equal to the intracellular, i.e.  $[K^+]_i=[K^+]_e$ , the transport will be driven by the electrochemical gradient of  $H^+$  only. Therefore,  $pH_i$  is clamped at the equilibrium at which  $[K^+]_i/[K^+]_e=[H^+]_i/[H^+]_e$ . By adding KCl Ringers with different pHs, BCECF at different  $pH_i$  values can be measured, and a calibration curve can be made (Appendix 1). In this study, we used KCl Ringers (Table 11) with pH 6.6, 7.0, 7.2, and 7.4 at  $37^\circ C$  infused, and  $10 \mu M$  Nigericin was added.



<b>KCl Ringer</b>	<b>Concentration</b>
<b>KCl</b>	140 mM
<b>K<sub>2</sub>HPO<sub>4</sub></b>	1 mM
<b>CaCl<sub>2</sub></b>	1 mM
<b>MgCl<sub>2</sub></b>	0.5 mM
<b>MOPS/TES/HEPES (MTH)</b>	3.3/3.3/5 mM

Table 11. Composition of KCl solutions for pH<sub>i</sub> calibrations.

## Immunofluorescence analysis

To investigate the localization of TRPC1 and the PI3K-p85 $\alpha$  subunit, we performed an immunofluorescence analysis assay with subsequent confocal imaging.  $8 \times 10^4$  non-transfected HPNE or PANC-1 cells were seeded on coverslips for 48 h. Then, cells were washed twice in cold PBS and fixed for 20 min at room temperature in 4% paraformaldehyde. The cells were washed twice in PBS and permeabilized in 0.1% TritonTMX-100 for 10 min. Next, cells were blocked in 5% Bovine Serum Albumin (BSA) for 30 min, followed by the addition of primary antibodies (Table 12) overnight at 4 °C. Cells were washed three times in PBS, and secondary antibodies (AlexaFluor® 488/550 conjugated antibody 1:600) were applied for 1 h at room temperature, followed by treatment with 1% DAPI for 5 min to stain nuclei. Coverslips were washed three times in PBS and mounted on slides using Prolong® Gold antifade reagent. Images were collected on an Olympus Cell Vivo IX83 with a Yokogawa CSU-W1 confocal scanning unit. Z-stacks were deconvoluted in Olympus Cell Sens software using a constrained iterative algorithm. Controls without primary and secondary antibodies were made to rule out unspecific binding. No or negligible labeling was seen in the absence of primary and secondary antibodies. Overlays and brightness/contrast/background adjustments were carried out using ImageJ software. Mander's overlapping R coefficient was calculated using the ImageJ software plugin JACoP, which calculates the proportion of the green signal coincident with the magenta signal over the total intensity (Bolte, 2006). The threshold setting was the same for both images.

<b>Antibody</b>	<b>Host</b>	<b>Distributor</b>	<b>Reference</b>
TRPC1	Mouse	Santa Cruz	sc-133076
PI3K-p85 $\alpha$	Rabbit	Bioworld Technology	MB9419
NBCn1	Rabbit	Abcam	Ab82335

Table 12. Antibodies used for IF analysis

## Migration assay

The Boyden Chamber assay is used to study the migration of cells across a microporous membrane. Cells are placed in the upper compartment of the chamber and allows the cells to migrate through the pores of the membrane into the lower compartment. After an appropriate incubation time, the membrane between the upper

and lower compartment is fixed and stained, and the number of cells that migrated to the lower side of the membrane can be determined. In this study we used Boyden chambers with 8  $\mu\text{m}$  pore size.  $4 \times 10^4$  non-transfected or transfected PANC-1 cells were seeded in the upper compartment of the chamber. Both the upper and lower compartment were filled with the respective culture medium containing 10% FBS (meaning that no chemo-attractant was present). After 24 h of incubation at 37 °C, 95% humidity, and 5% CO<sub>2</sub>, inserts were washed in PBS and fixed in methanol for 15 min at room temperature, followed by staining with hematoxylin for 5 min. Inserts were washed in Milli-Q water and cleaned with a cotton swab. 20 adjacent fields were counted per insert in a brightfield microscope at  $\times 400$  magnification. The number of migrating cells was normalized to their respective control. To ensure that there was no difference in viability between the conditions after 24 h, the trypan blue assay (as described above) was performed. For Ca<sup>2+</sup> chelation assays, (see below) medium in both the upper and lower chamber was changed after 8 h of seeding, and Ca<sup>2+</sup> depleted medium or new normal medium containing Ca<sup>2+</sup> were added. Then cells migrated for 24 h.

### Calcium depletion and calmodulin inhibition

To investigate the effect of extracellular Ca<sup>2+</sup> concentrations on either migration or proliferation, we chelated extracellular Ca<sup>2+</sup> concentrations by adding 0.4 mM Ethylene Glycol Tetraacetic Acid (EGTA). For proliferation assays Ca<sup>2+</sup> were chelated for 48 h, and for migration assays Ca<sup>2+</sup> were chelated for 24 h.

CaM is activated by Ca<sup>2+</sup> and is a connecting protein between TRPC1 and CaM. Therefore, we aimed to investigate the phosphorylation of AKT and ERK upon CaM inhibition. CaM was inhibited with the treatment of the antagonist W7 (25  $\mu\text{M}$ ) for 72 h.

### Immunohistochemistry

Patient samples from this study were collected at the Amiens University Hospital. 21 samples from patients diagnosed with PDAC between 2018 and 2021 were used. A physician made the diagnosis of a paraffin block. The samples were used anonymously and retrospectively in the Department of Pathological Anatomy and Cytology-Tumorotheque of Picardy in the context of research not involving the human person.

All experimental protocols were approved by the ethical committee of the University Hospital Center of Amiens (reference: PI2021\_843\_0027).

Classical immunohistochemistry was performed from formalin-fixed paraffin-embedded PDAC tumor material. First, 4  $\mu\text{M}$  thick sections were deparaffinized in xylene and then rehydrated in ethanol. Next, the endogenous peroxidase activity was blocked with a 3% hydrogen peroxide solution before the antigen retrieval. The cell conditioning solution CC1 was used for antigen retrieval. Adding of antibodies was carried out using an automatic immunohistochemical staining was carried out on a BenchMark ULTRA system. First, primary antibodies were added and next biotin-labeled secondary antibody was applied, followed by the addition of avidin–biotin–peroxidase complex treatment. Reactions were developed using a chromogenic

reaction with 3,3'-diaminobenzidine tetrahydrochloride. All tissue sections were counterstained with hematoxylin. To evaluate nerve invasion, slides were stained with S100, which marks the nerves. For vascular invasion, slides were stained with Factor VIII or ERG, which are expressed in vascular endothelial cells. Negative controls were performed with the same technique and conditions, without adding the primary antibody. The marking intensity score ranged from 0 to 3 (0 = no immunostaining, 1 = weak immunostaining, 2 = moderate immunostaining, 3 = strong immunostaining). The localization of ion channels was evaluated as a percentage of being present in the cytoplasm or membrane. Primary and secondary antibodies against ion channels were used, as described in Table 13. The dilution and incubation time of primary antibodies were chosen by orchestrated time points and a dilution curve.

<b>Antibody for IHC</b>	<b>Host</b>	<b>Dilution</b>	<b>Pretreatment/incubation time/ incubation time with secondary antibody (min)</b>	<b>Distributor</b>	<b>Reference</b>
<b>TRPC1</b>	Goat	1/50	CC1/64/32	Abcam	Ab110837
<b>ORAI1</b>	Rabbit	1/400	CC1/64/32	Sigma Aldrich	O8264- 200UL
<b>ORAI2</b>	Rabbit	1/500	CC1/64/32	Abcam	Ab155216
<b>ORAI3</b>	Rabbit	1/50	CC1/64/32	Sigma Aldrich	HPA015022
<b>STIM1</b>	Mouse	1/100	CC1/64/32	Santa Cruz	Sc-166840
<b>STIM2</b>	Rabbit	1/400	CC1/64/32	Alomone	ACC-064
<b>TRPM7</b>	Goat	1/500	CC1/64/32	Abcam	ab729
<b>ASIC1</b>	Rabbit	1/400	CC1/64/32	Alomone	ASC-014
<b>NaV1.6</b>	Rabbit	1/250	CC1/36/32	Abcam	Ab65166
<b>NBCn1</b>	Rabbit	1/400	CC1/64/32	Abcam	Ab82335
<b>LAMP2</b>	Rabbit	1/800	CC1/64/32	Abcam	Ab18528

*Table 13. Antibodies used for IHC. (The cell conditioning solution; CC1)*

## Statistical analysis

In this study, all our data are shown as representative images or mean measurements with standard error of means (SEM) error bars and represent at least three independent experiments. n refers to the number of independent experiments performed or to the number of cells analyzed (as described in either text or figure legends). Welch's correction t-test or Tukey's multiple comparison test was applied to test for statistically significant differences between the two groups. \*, \*\*, and \*\*\* and \*\*\*\* denotes  $p < 0.05$ ,  $p < 0.01$ , and  $p < 0.001$ ,  $p < 0.0001$ , respectively. All graphs and statistical analysis were generated in GraphPad Prism 9.0 software.

## Bisulfite sequencing

- Concept of bisulfite sequencing

Bisulfite sequencing is considered the ‘golden standard’ method for studying DNA methylation. Standard DNA sequencing technologies do not possess the ability to distinguish cytosine and methylcytosine. The bisulfite treatment of DNA mediates the deamination of cytosine into uracil. Uracil is converted into thymine and is determined by PCR amplification and subsequent Sanger sequencing analysis. However, 5mC residues are resistant to the conversion provided by the bisulfite treatment and, so, will remain read as cytosine. Therefore, comparing the Sanger sequencing read from an untreated DNA sample to the same sample following bisulfite treatment allows the detection of the methylated cytosines. With the advances in next-generation sequencing (NGS), the bisulfite treatment approach can be extended to DNA methylation analysis across an entire genome. However, the bisulfite treatment and conversion reduce genome complexity to three nucleotides (except the methylated cytosines, 5mC), and sequence alignment can become a more difficult task. Thus, a less complex method was taken into use in this study, namely the bisulfite conversion-specific methylation-specific PCR (BS-MSP) (Kurdyukov and Bullock 2016). Here, the DNA sequence of interest is amplified by PCR with primers specific for methylated and unmethylated DNA. The workflow of performing bisulfite sequencing is described in Figure 29.

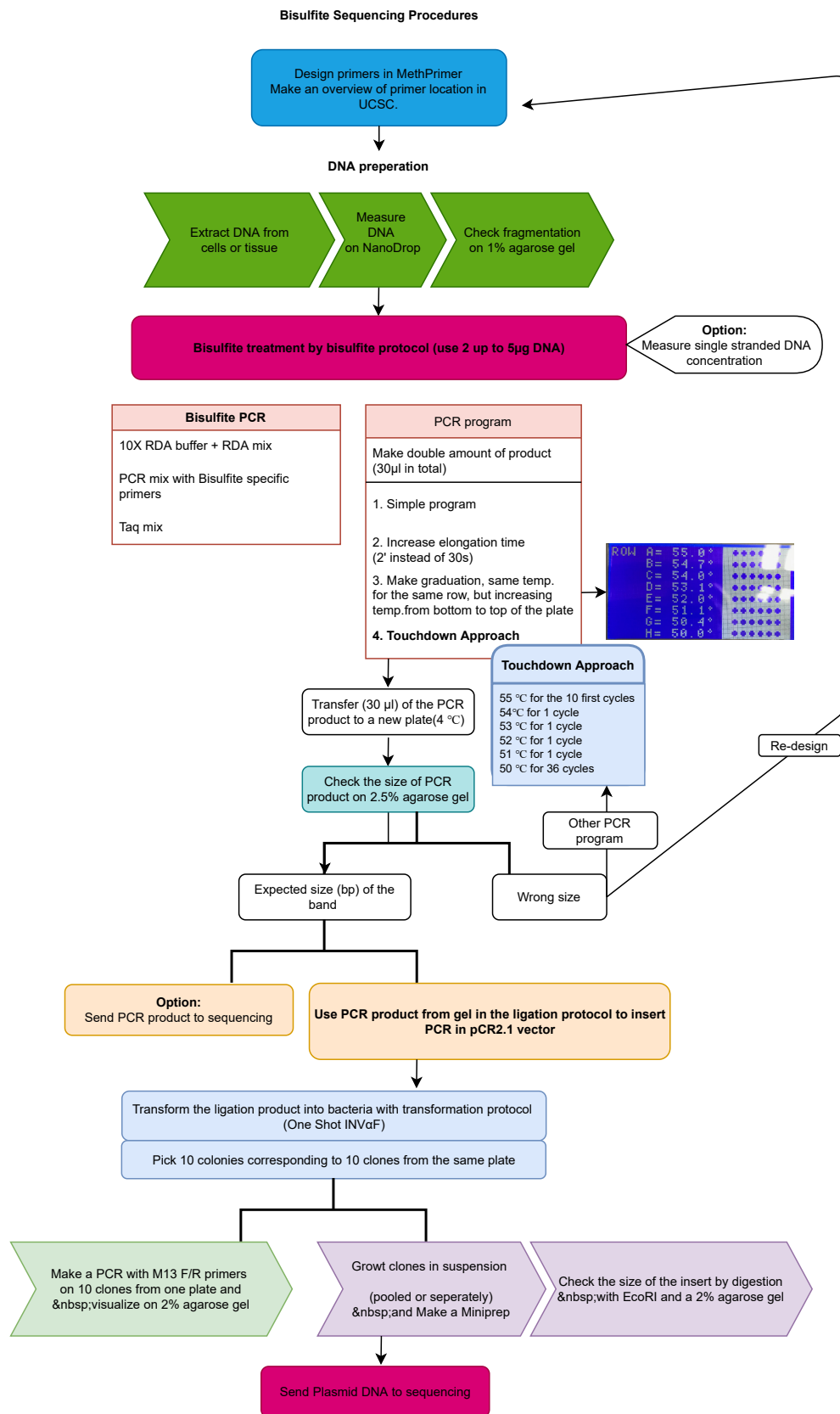


Figure 29. Workflow of bisulfite sequencing approach.

- DNA extraction

DNA was extracted from PANC-1 or MiaPaca2 cell lines, grown in either pH 7.4 or pH 6.5, with Blood & Cell Culture DNA Mini Kit (QIAGEN #13323), following the manufacturer's protocol. After the DNA extraction, the DNA concentration and purity were determined on a Nanodrop, and 100 ng of DNA samples were loaded on a 1% agarose gel to exclude DNA fragmentation.

- Bisulfite treatment

The first step is to denature the genomic DNA (5 µg) for 20 min at 50 °C in a water bath in the presence of NaOH at a final concentration of 0.3 M in a final volume of 20 µL. Next, deamination is carried out by mixing the 20 µL of denatured genomic DNA with 500 µL of a freshly prepared solution containing 2.5 M sodium bisulfite, 0.5 mM hydroquinone, and 0.35 M NaOH, which were then incubated for 3 h at 70 °C. The bisulfite-treated DNA was then desalted using Wizard DNA Cleanup Kit (Promega, #A7280) and eluted in 45 µL of low TE buffer. The genomic DNA is now converted into single-stranded DNA.

- Bisulfite conversion-specific methylation-specific PCR

CpG sites or upstream/downstream promoter regions of different ion channels were designed using the MethPrimer software (<http://www.urogene.org/methprimer/>) (Table 14). 4 µL of bisulfite-treated DNA was amplified by PCR with RDA buffer. A touchdown PCR cycling approach was used for all amplicons, and the specificity of the PCR was checked on a 2% agarose gel. The PCR product was extracted from the agarose gel with a NucleoSpin Gel and PCR Clean-up kit (Machinery Nagel #740609.250).

Gene promoter		Primer sequence	Product size (bp)	CpG sites	Tm °C
TRPC1	F	TTATTAATTTGGGGTTGTTAGTGGA	200	15	59
	R	GACCCATAAAAAAAAAACAAACCAAAA			59
ASIC1	F	GTTGTTTTTTGGGTTGGTGTG	225	26	58
	R	AAACAAACACCCTCCCTCCTA			59
SCN8A (1)	F	GGGTTTTTTAAGAGAATTGAGGAT	291	11	58
	R	CCTTAACTTCTACAATTTTAAACAAC			56
SCN8A (2)	F	GGTAGGAGAAAGGTAAGATTT	348	52	58
	R	ACCCACCTACCCCTACAAAAC			56

Table 14. Overview of bisulfite sequencing primers.

- Cloning and sequencing

After purification, the PCR product was cloned into the vector pCR<sup>®</sup>2.1 (TA Cloning kit, Invitrogen). The reaction mixture is described in Table 15.



<b>PCR Product</b>	2 $\mu$ L
<b>10X Buffer</b>	1 $\mu$ L
<b>pCR<sup>®</sup>2.1 Vector (25 ng/<math>\mu</math>l)</b>	2 $\mu$ L
<b>5X T4 DNA Ligase Reaction Buffer</b>	2 $\mu$ L
<b>Water up to 10 <math>\mu</math>L</b>	3 $\mu$ L

*Table 15. The reaction mixture of cloning product.*

This mixture is incubated overnight at 14°C then stored at -20°C. The INV $\alpha$ F<sup>+</sup> bacteria (One Shot<sup>®</sup> competent cells, Invitrogen) were transformed with the ligation product into pCR<sup>®</sup>2.1 according to the manufacturer's protocol. Competent bacteria (50  $\mu$ l) were incubated for 30 min on ice in the presence of 2  $\mu$ L of ligation product, then heat shocked for 30 s at 42° C. and finally placed again on ice for 2 min. The transformed bacteria were then incubated for 1 hour at 37°C upon shaking in SOC medium (250  $\mu$ l), and then spread (80  $\mu$ l) on LB-Agar plates containing ampicillin (50  $\mu$ g/ml) and X-Gal (40  $\mu$ l of a 50 mg/ml) on Petri dishes and incubated overnight at 37°C. The X-Gal allows for the selection of clones due to the blue color of the X-Gal substrate. The pCR<sup>®</sup>2.1 vector encodes the first 146 amino acids of  $\beta$ -galactosidase. If  $\beta$ -galactosidase is produced, X-Gal is hydrolyzed and produces an insoluble blue pigment. The colonies formed by non-recombinant cells do not contain the expected insert and will appear blue, while the recombinant ones, having the inserts, appear white. The desired recombinant colonies were picked for either the semiquantitative analysis or the quantitative analysis method. For the semiquantitative analysis method 10 clones were picked and pooled in the same falcon tube with 5 ml LB medium containing ampicillin (50  $\mu$ g/ml). For the quantitative method, single clones were picked and grown separately in falcon tubes with 5 ml LB medium containing ampicillin (50  $\mu$ g/ml). From here, two approaches can be used: (1) Clones were grown overnight, and the plasmids were extracted using the NucleoSpin Plasmid, Mini kit for plasmid DNA (Machinery Nagel, #740588.250), according to the manufacturer's protocol. 1  $\mu$ L of plasmid DNA was then mixed with the restriction enzyme EcoRI, 1  $\mu$ L of its belonging 10X digestion buffer, cutting at both sites of the insertion site of pCR<sup>®</sup>2.1 vector, and 8  $\mu$ L of water, and incubated at 1 h at 37° C. The 10  $\mu$ L of digestion product was then loaded on a 2% agarose gel to verify that the plasmid contained the bisulfite insert. (2) When clones were picked, they were first scratched on a new LB-agarose plate, and the rest of the clones were used for colony PCR. With this approach, the two primers encoded in the pCR<sup>®</sup>2.1 vector M13 forward and reverse were used to do a colony PCR. After the PCR, the products were loaded on a 2% agarose gel. This approach can be used to be sure that the different clones contain the insert before performing mini-prep. Following the ensuring steps that the plasmid contains the expected insert, the plasmid was sent to sequencing. Plasmid DNA was sequenced on both strands on an infrared-based ABI 3730 XL sequencer (GATC, Eurofins, Konstanz, Germany) using T7 and M13-RP universal primers.

- **Semiquantitative analysis method**

The semiquantitative analysis method is based on the fact that several inserts from different clones are sequenced at the same time, and it gives a notion of whether the specific CpG sites are methylated. The semiquantitative analysis distinguishes between C's or T's at the CpG site at a specific ratio. The percentage of conversion of non-CpG cytosines was used as an index of overall bisulfite reaction efficiency (Figure 30). The sequence was aligned to an '*in silico* bisulfite-converted sequence' corresponding to the same gene promoter by using Clustal Omega alignment tool. The conversion efficiency of >97% was included in the study.

- **Quantitative analysis method**

The quantitative analysis method is used for more accurate analysis. Here, only one plasmid is sequenced alone, and it can be directly interpreted if the C's remain or is converted into T's (Figure 30). Thus, the quantitative method distinguishes between methylated (100) or not methylated (0). The sequence was aligned to an '*in silico* bisulfite-converted sequence' corresponding to the same gene promoter by using Clustal Omega alignment tool. The conversion efficiency of >97% was included in the study.

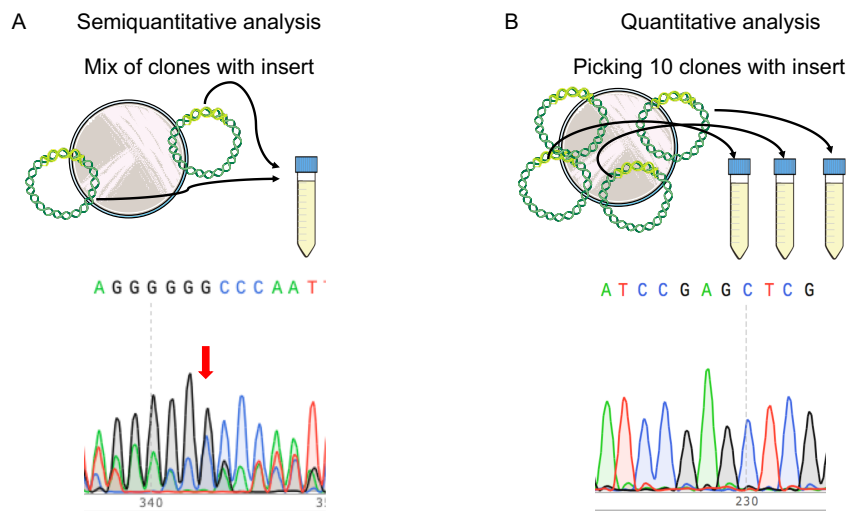


Figure 30. Overview of A) Semiquantitative and B) Quantitative sequencing analysis.

# RESULTS

## Part 1: The TRPC1 channel forms a PI3K/CaM complex and regulates pancreatic ductal adenocarcinoma cell proliferation in a $\text{Ca}^{2+}$ -independent manner

$\text{Ca}^{2+}$  channels are overexpressed in human PDAC tissue and cell lines

Several ion channels, including  $\text{Ca}^{2+}$  channels, are dysregulated in different types of cancer (Tajada and Villalobos 2020). Even though several studies have implicated these  $\text{Ca}^{2+}$  channels in PDAC progression, a comprehensive overview of their expression in human PDAC tissue has not yet been accomplished. Thus, we compared the mRNA expression of  $\text{Ca}^{2+}$  channels between normal pancreatic tissue and human PDAC samples using the PAAD TCGA dataset of normal and tumor samples. Specifically, we found that ORAI1, ORAI2, ORAI3, TRPC1, and STIM1 were overexpressed in PDAC tissue (Figure 31).

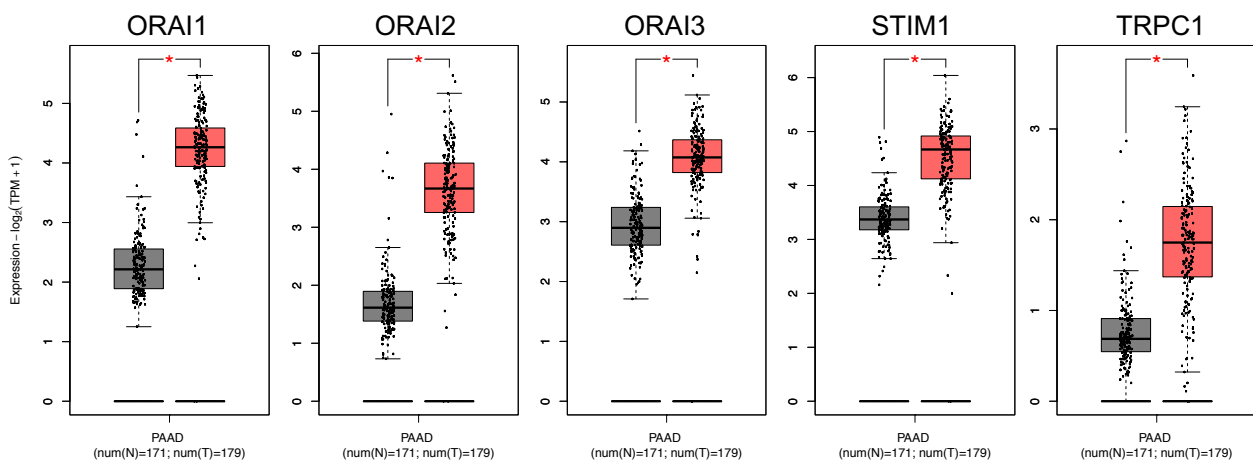


Figure 31. *ORAI*, *STIM1* and *TRPC1* are overexpressed in human PDAC samples. Whisker boxplots of *ORAI1*, *ORAI2*, *ORAI3*, *STIM1*, and *TRPC1* mRNA expression in normal samples (N) and PDAC tumor tissues (T) were generated by GEPIA2 by using data from The Cancer Genome Atlas (TCGA) cohort PAAD and Genotype-Tissue Expression (GTEx) samples. \* Indicate  $p < 0.01$ .

Hence, we aimed to investigate the protein expression of these  $\text{Ca}^{2+}$  channels in our local cohort of human PDAC samples. Our IHC results confirmed that ORAI3 (Figure 32A,  $n = 12$ ,  $p < 0.05$ ) and TRPC1 (Figure 32B  $n = 21$ ,  $p < 0.05$ ) were significantly overexpressed by  $60.2 \pm 24.3\%$  and  $33 \pm 12.5\%$ , respectively, in human PDAC tissue compared to adjacent non-tumor tissue. The other  $\text{Ca}^{2+}$  channels did not show any significant difference in expression (Figure 33). Interestingly, both ORAI3 and TRPC1 were more localized to the plasma membrane in tumor cells when compared to non-tumor cells, where both were found mainly expressed in the cytoplasm.

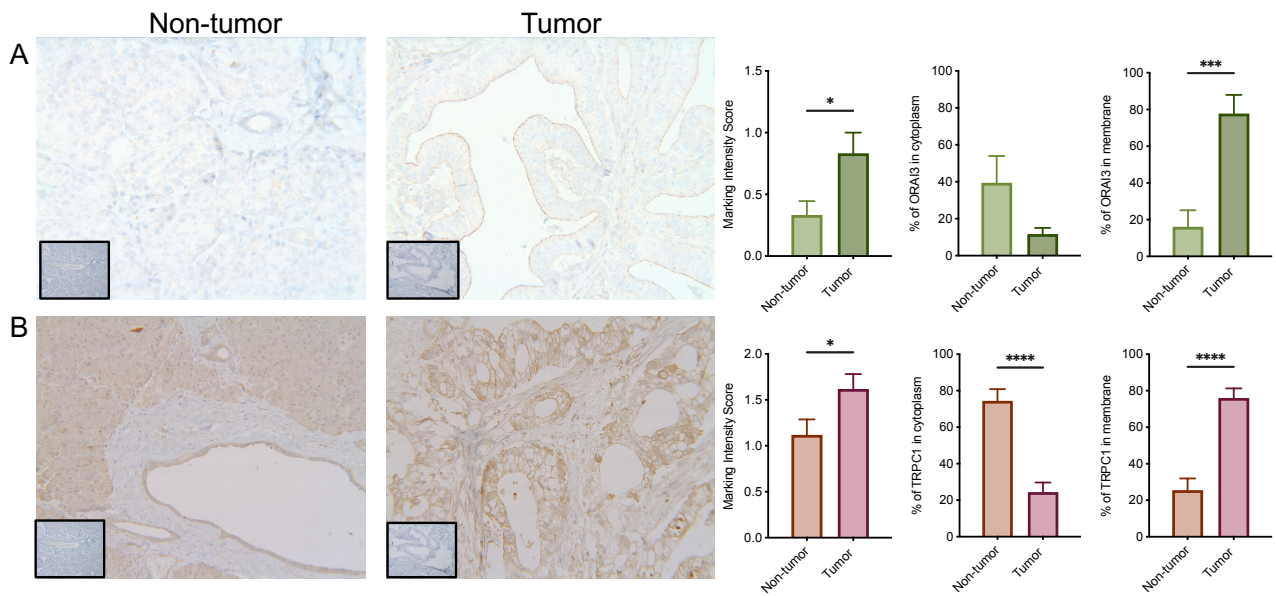


Figure 32. *ORAI3* and *TRPC1* are overexpressed in human PDAC tissue from the local cohort. A) *ORAI3* expression in PDAC tissue compared to non-tumor tissue. The marking intensity score designates the expression between 0 (low or no expression) and 3 (high expression). *ORAI3* in the cytoplasm or the membrane is designated by percentage ( $n = 12$ ). B) *TRPC1* expression in PDAC tissue compared to non-tumor tissue. The marking intensity score designates the expression between 0 (low or no expression) and 3 (high expression). *TRPC1* in the cytoplasm or the membrane is designated by percentage ( $n = 21$ ). Inserts represent negative controls. All images are shown in 160X magnification. \* and \*\*\*\* indicate  $p < 0.05$  and 0.0001, respectively.

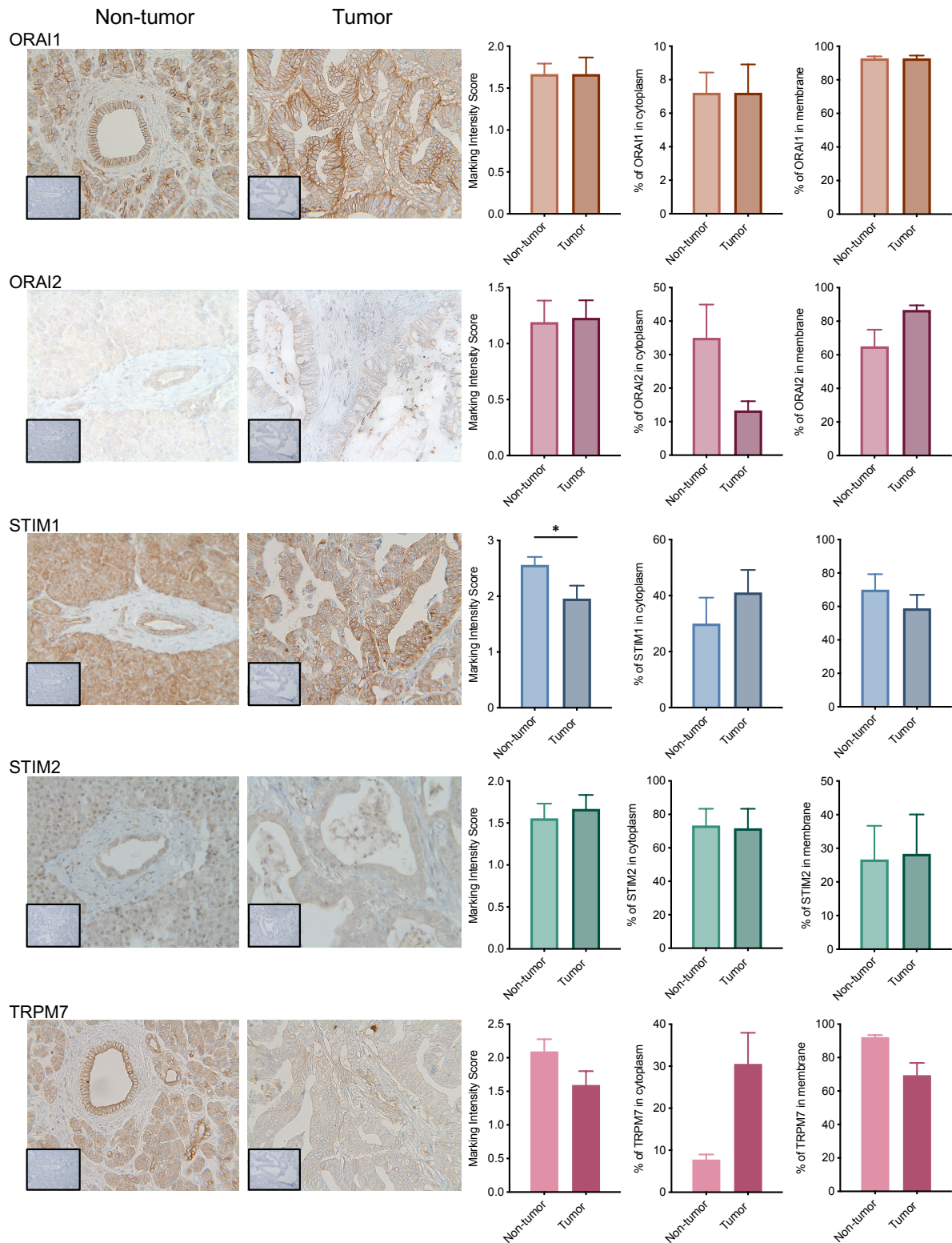


Figure 33. Protein expression of ORAI, STIM and TRPM7 in human PDAC tissue from the local cohort. The marking intensity score designates the expression between 0 (low or no expression) and 3 (high expression). The protein expression in the cytoplasm or the membrane is designated by percentage ( $n = 12-21$ ). Inserts represent negative controls. All images are shown in 160X magnification. \* indicates  $p < 0.05$ .



Further, we investigated the mRNA expression of these Ca<sup>2+</sup> channels in different PDAC cell lines. Here, we demonstrated that these Ca<sup>2+</sup> channel expression profiles differed among cell lines. Notably, TRPC1 was overexpressed in the highly aggressive PDAC cell line PANC-1 compared to the normal-like duct cell line HPNE, where ORAI3 and STIM2 seemed to be overexpressed in the less aggressive cell lines BxPC-3 and AsPC-1. STIM1 was significantly upregulated in AsPC-1 and PANC-1 cells.

These results indicate that STIM, ORAI and TRPC1 are overexpressed in human PDAC tissue, at least at the transcriptomic level. Additionally, they are differentially expressed among cell lines. The role of ORAI3 has recently been demonstrated in human PDAC cell lines and tissue (Arora *et al.* 2021, Dubois *et al.* 2021). In our study, TRPC1 was consistently overexpressed in human PDAC tissue at a transcriptomic and protein level and additionally highly expressed in the aggressive PDAC cell line, PANC-1. Combined with the sparse knowledge of TRPC1 in PDAC carcinogenesis, our further work was based on these findings and aimed to investigate the role of TRPC1 in PDAC progression.

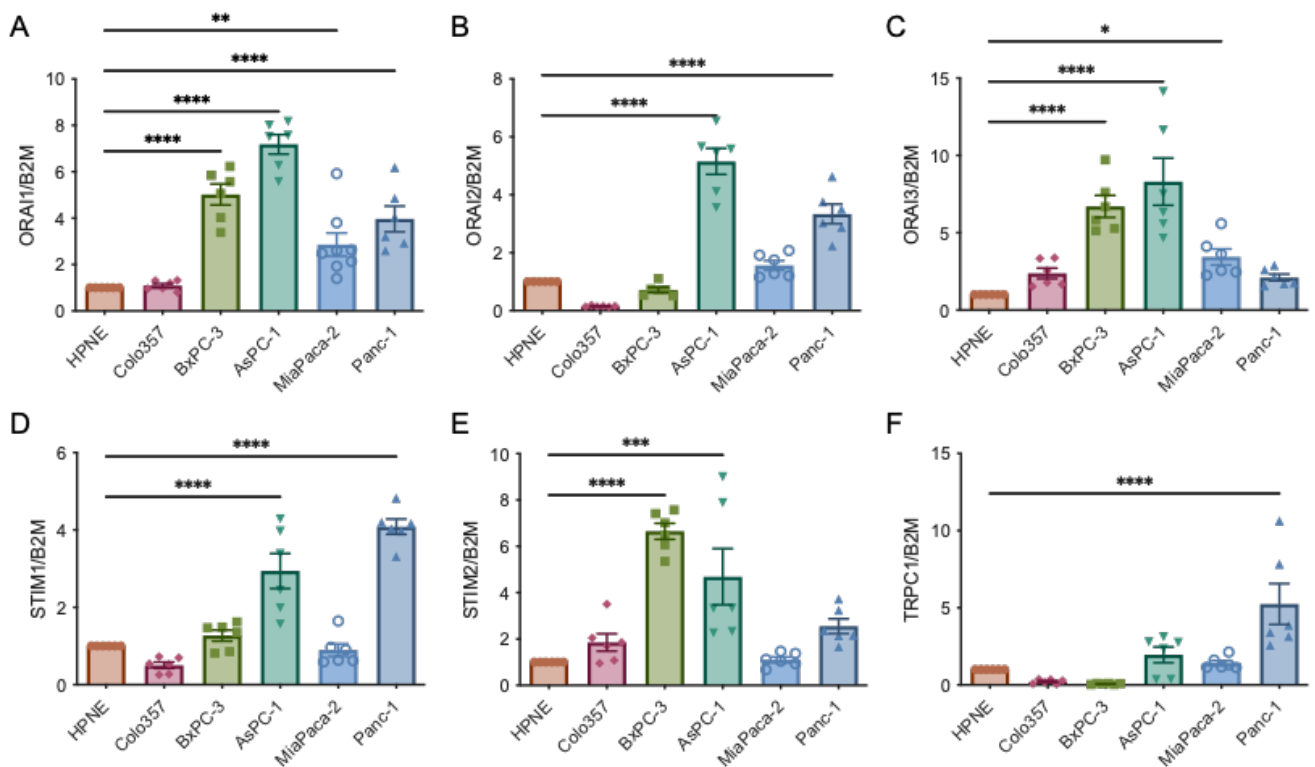


Figure 34. Ca<sup>2+</sup> channels are overexpressed differentially among PDAC cell lines. mRNA expression of A) ORAI1, B) ORAI2, C) ORAI3, D) STIM1, E) STIM2, and F) TRPC1. n = 3-4. \*, \*\*, \*\*\*, and \*\*\*\* indicate p < 0.05, 0.01, 0.001 and 0.0001, respectively.

## Summary

PDAC is a highly aggressive neoplasm and is predicted to become the second leading cause of cancer by 2030, surpassing colorectal- and breast cancer (Rahib et al. 2014). Due to the lack of diagnostic biomarkers and early-stage symptoms, diagnosis often occurs at advanced, invasive stages. Despite extensive efforts, both cytotoxic and targeted therapies have provided limited efficacy and marginally prolonged survival for patients with PDAC (Mizrahi et al. 2020). Thus, new strategies for screening and detecting PDAC tumors at earlier stages are desperately needed to make a clinically significant impact.

$\text{Ca}^{2+}$  is an intracellular messenger involved in both physio- and pathophysiological conditions, as cellular functions depend on  $\text{Ca}^{2+}$  homeostasis. The regulation of  $\text{Ca}^{2+}$  levels through  $\text{Ca}^{2+}$  channels is essential for maintaining cellular processes, such as proliferation. Transient receptor potential channels and store-operated channels (SOC) are important players in maintaining these  $\text{Ca}^{2+}$  levels in epithelial cells (Borowiec et al. 2014, Hodeify et al. 2018). The first identified member of the TRP canonical subfamily (TRPC1) is involved in tumor progression in different types of cancer and is recognized as a potential biomarker (Elzamzamy et al. 2020). The impact of TRPC1 in carcinogenesis is demonstrated through both  $\text{Ca}^{2+}$ -dependent and -independent mechanisms. One study has shown that  $\text{Ca}^{2+}$  entry through TRPC1 promotes migration of the PDAC cell line BxPC-3 (Dong et al. 2010). However, other studies have shown that TRPC1 regulates carcinogenesis in a  $\text{Ca}^{2+}$ -independent manner (El Boustany *et al.* 2008, Davis et al. 2012, Madsen *et al.* 2012, Asghar et al. 2015, Selli *et al.* 2015, Selli et al. 2016, Sun et al. 2021). Until present, the expression and role of TRPC1 in highly aggressive PDAC cell lines have not yet been demonstrated. Based on our data described above, we first aimed to investigate if TRPC1 could be a potential biomarker of PDAC and if its overexpression correlated with clinical factors. Next, we aimed to investigate the functional role of TRPC1 in PDAC progression.

In our study, we demonstrated that the mRNA overexpression of TRPC1, analyzed by PAAD TCGA datasets, was significantly higher in the aggressive basal-like PDAC subtype compared to TRPC1 expression in the classical subtype. Additionally, a Kaplan-Meier survival analysis using Survexpress revealed that patients with high levels of TRPC1 displayed a significantly low overall survival compared to patients with low levels of TRPC1.

Here, the data demonstrating the high TRPC1 expression and plasma membrane localization in human PDAC samples from our local cohort were presented. We showed that cell lines, preliminary investigated for TRPC1 mRNA expression, displayed high TRPC1 protein expression. Interestingly, the expression was significantly higher in MiaPaCa-2 and PANC-1 cells compared to the normal-like duct cell line HPNE. As TRPC1 was overexpressed in the remarkably aggressive PDAC cell line PANC-1, we chose to investigate the downstream mechanisms of TRPC1 in this cell line. In PANC-1 cells, we found a robust plasma membrane localization of TRPC1, which we did not find in HPNE cells where TRPC1 seemed to be localized in cytoplasmic compartments.

To investigate the downstream effects of TRPC1, we developed a loss-of-function model by silencing TRPC1 with a siRNA approach. The efficiency of the KD was validated by qPCR and immunoblot analysis. Subsequently, we investigated the role of TRPC1 in PANC-1 cell and spheroid proliferation. We demonstrated that TRPC1 silencing decreased cell proliferation and spheroid viability. Additionally, flow cytometric analysis revealed that TRPC1 KD resulted in an accumulation of cells in the G1 phase along with a reduced number of cells in the S phase. These observations correlated with the decreased expression of the cell cycle regulating proteins CDK6, CDK2, and Cyclin A and the increased expression of p21.

As the role of TRPC1 in  $\text{Ca}^{2+}$  entry has been contradictory among different cell lines, we sought to determine the  $\text{Ca}^{2+}$  signature specific to TRPC1 in PANC-1 cells. Indeed, we found that TRPC1 silencing did not affect either basal or SOCE. Furthermore, the proliferative role of PANC-1 cells did not depend on  $\text{Ca}^{2+}$  entry, as there was no significant difference between the proliferation of PANC-1 cells grown in a medium with normal extracellular  $\text{Ca}^{2+}$  levels or in a medium with low extracellular  $\text{Ca}^{2+}$  levels.

The PANC-1 cell line has mutations in three out of four driver genes (*KRAS*, *TP53*, *CDKN2A*), and TRPC1 has been shown to regulate cancer cell proliferation through downstream pathways of these oncogenes. Thus, we aimed to investigate if TRPC1 regulated PANC-1 cell proliferation through the PI3K/AKT and MAPK/ERK pathways. We found that TRPC1 KD mainly decreased the activation of AKT and, to less extent, ERK, indicating that TRPC1 regulates PANC-1 cell proliferation through a PI3K/AKT axis rather than the MAPK.

Hence, we investigated the physical interaction between the PI3K-p85 subunit and TRPC1. Our PLA showed proximity between TRPC1 and the PI3K-p85 subunit. Our co-IP, followed by immunoblot analysis, revealed a strong interaction between TRPC1, the PI3K, and their connecting protein calmodulin (CaM). This interaction was abolished upon TRPC1 silencing.

Taken together, our data revealed that TRPC1 is a potential biomarker of PDAC by being upregulated in human PDAC tissue and cell lines. We demonstrated that TRPC1 regulates PANC-1 cell proliferation and spheroid growth through direct interaction with the PI3K and CaM. Thus, activating downstream signaling pathways regulating G1 and S phase progression, likely through  $\text{Ca}^{2+}$ -independent mechanisms.

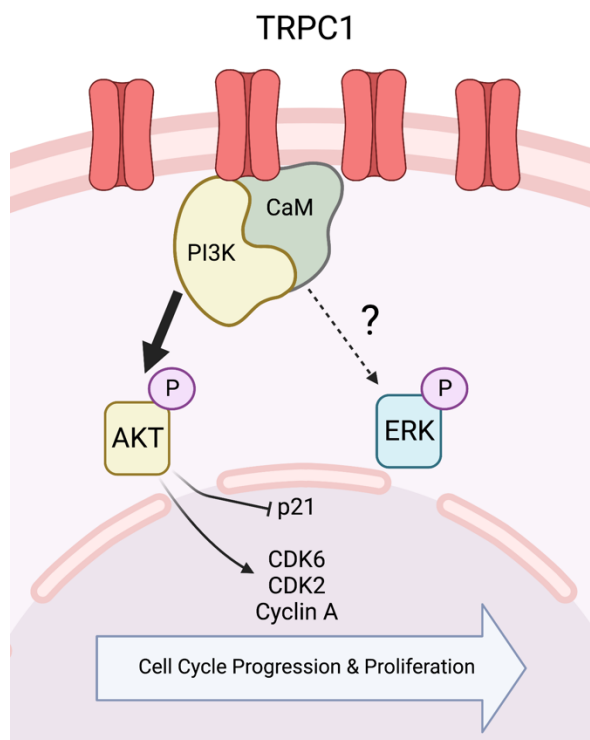


Figure 35. The role of TRPC1 in PDAC proliferation. TRPC1 is upregulated in human PDAC tissue and cell lines and localizes to the plasma membrane. Here, it forms a complex with PI3K and CaM and activates downstream signaling pathways. This activation phosphorylates, to a small extent, ERK1/2 and, notably, AKT, which regulates cell cycle progression and, thereby, PDAC cell proliferation. (The figure is generated with [www.Biorender.com](http://www.Biorender.com))



Article

# The TRPC1 Channel Forms a PI3K/CaM Complex and Regulates Pancreatic Ductal Adenocarcinoma Cell Proliferation in a Ca<sup>2+</sup>-Independent Manner

Julie Schnipper <sup>1</sup>, Sana Kouba <sup>1</sup>, Frédéric Hague <sup>1</sup>, Alban Girault <sup>1</sup>, Pierre Rybarczyk <sup>1,2</sup>, Marie-Sophie Telliez <sup>1</sup>, Stéphanie Guénin <sup>3</sup>, Riad Tebbakha <sup>1,2</sup>, Henri Sevestre <sup>1,2</sup>, Ahmed Ahidouch <sup>1,4</sup>, Stine Falsig Pedersen <sup>5</sup> and Halima Oquadid-Ahidouch <sup>1,\*</sup>

<sup>1</sup> Laboratory of Cellular and Molecular Physiology, UR UPJV 4667, University of Picardie Jules Verne, 80000 Amiens, France; julie\_schnipper@hotmail.com (J.S.); sana.kouba@hotmail.com (S.K.); fh-lnc@u-picardie.fr (F.H.); alban.girault@u-picardie.fr (A.G.); rybarczyk.pierre@chu-amiens.fr (P.R.); marie-sophie.telliez@u-picardie.fr (M.-S.T.); tebbakha.riad@chu-amiens.fr (R.T.); henrisevestre@gmail.com (H.S.); ahidouch@gmail.com (A.A.)

<sup>2</sup> Anatomy and Pathology Department, Amiens Hospital, University of Picardie Jules Verne, Tumorothèque of Picardie, 80000 Amiens, France

<sup>3</sup> Centre de Ressources Régional en Biologie Moléculaire, Université de Picardie Jules Verne, 80000 Amiens, France; stephanie.vandecasteele@u-picardie.fr

<sup>4</sup> Biology Department, University Ibn Zohr, Agadir 80000, Morocco

<sup>5</sup> Section for Cell Biology and Physiology, Department of Biology, University of Copenhagen, 1165 Copenhagen Ø, Denmark; sfpedersen@bio.ku.dk

\* Correspondence: halima.ahidouch-ouadid@u-picardie.fr; Tel.: +33-322-827-646



**Citation:** Schnipper, J.; Kouba, S.; Hague, F.; Girault, A.; Rybarczyk, P.; Telliez, M.-S.; Guénin, S.; Tebbakha, R.; Sevestre, H.; Ahidouch, A.; et al. The TRPC1 Channel Forms a PI3K/CaM Complex and Regulates Pancreatic Ductal Adenocarcinoma Cell Proliferation in a Ca<sup>2+</sup>-Independent Manner. *Int. J. Mol. Sci.* **2022**, *23*, 7923. <https://doi.org/10.3390/ijms23147923>

Academic Editors: Elena Lastraioli and Alessandra Fiorio Pla

Received: 28 June 2022

Accepted: 17 July 2022

Published: 18 July 2022

**Publisher's Note:** MDPI stays neutral with regard to jurisdictional claims in published maps and institutional affiliations.



**Copyright:** © 2022 by the authors. Licensee MDPI, Basel, Switzerland. This article is an open access article distributed under the terms and conditions of the Creative Commons Attribution (CC BY) license (<https://creativecommons.org/licenses/by/4.0/>).

**Abstract:** Dysregulation of the transient receptor canonical ion channel (TRPC1) has been found in several cancer types, yet the underlying molecular mechanisms through which TRPC1 impacts pancreatic ductal adenocarcinoma (PDAC) cell proliferation are incompletely understood. Here, we found that TRPC1 is upregulated in human PDAC tissue compared to adjacent pancreatic tissue and this higher expression correlates with low overall survival. TRPC1 is, as well, upregulated in the aggressive PDAC cell line PANC-1, compared to a duct-like cell line, and its knockdown (KD) reduced cell proliferation along with PANC-1 3D spheroid growth by arresting cells in the G1/S phase whilst decreasing cyclin A, CDK2, CDK6, and increasing p21<sup>CIP1</sup> expression. In addition, the KD of TRPC1 neither affected Ca<sup>2+</sup> influx nor store-operated Ca<sup>2+</sup> entry (SOCE) and reduced cell proliferation independently of extracellular calcium. Interestingly, TRPC1 interacted with the PI3K-p85 $\alpha$  subunit and calmodulin (CaM); both the CaM protein level and AKT phosphorylation were reduced upon TRPC1 KD. In conclusion, our results show that TRPC1 regulates PDAC cell proliferation and cell cycle progression by interacting with PI3K-p85 $\alpha$  and CaM through a Ca<sup>2+</sup>-independent pathway.

**Keywords:** pancreatic ductal adenocarcinoma; TRPC1; cell proliferation; spheroid growth; cell cycle progression; PI3K; calmodulin

## 1. Introduction

Pancreatic ductal adenocarcinoma (PDAC) is the most prevalent type of pancreatic cancer, accounting for more than 90% of all pancreatic malignancies [1]. With a mortality rate similar to its incidence, the 5-year survival rate remains one of the lowest (less than 10%) of all cancers [2]. When detected, PDAC is often at a late disease stage. Overall, the response rate for late-diagnosed patients is limited. The poor prognosis of PDAC patients is associated with rapid tumor progression and limited available treatments [3].

Calcium (Ca<sup>2+</sup>) is a ubiquitous intracellular messenger that transduces signals in cellular processes, including cell fertilization, differentiation, cell growth, and death [4]. The influx of Ca<sup>2+</sup> through Ca<sup>2+</sup> channels plays an important role in cell cycle progression

in several cell types [5,6]. However, the direct relationship between  $\text{Ca}^{2+}$  and cellular proliferation is complex, as many cell types can proliferate even in the near absence of extracellular  $\text{Ca}^{2+}$  [7]. The transient receptor potential (TRP) and store-operated channels (SOC) are recognized as major regulators of the  $\text{Ca}^{2+}$  influx in epithelial cancer cells [8]. Growing evidence demonstrates that the TRP canonical (TRPC) channel subfamily is involved in tumor development [9,10]. The first identified member of this non-selective cation channel subfamily is TRPC1. TRPC1 is a potential regulator of store-operated  $\text{Ca}^{2+}$  entry (SOCE) pathways [11] and has shown to be a potential biomarker of different cancer types, as its dysregulation correlates with several clinical parameters, including overall survival [12–21]. At the cellular level, TRPC1 contributes to a plethora of physiological and pathophysiological processes, including tumor cell proliferation and growth. However, it seems that it depends on the cancer cell type, and whether the presence or absence of TRPC1 contributes to cell growth. In a majority of studies, TRPC1 downregulation inhibits the proliferative rate in neuroblastoma [22], glioblastoma [23], thyroid [24], breast [12,25–27], lung, [28], liver [29,30], ovarian [31], and colon cancer [13]. Whereas in other studies, TRPC1 downregulation drives proliferation and growth in esophageal [32] and breast cancer [33]. Additionally, it is controversial whether the influx of  $\text{Ca}^{2+}$  causes this proliferation through TRPC1. In different cancer cell models, the depletion of TRPC1 diminishes SOCE [12,23,27–29], whereas, in others, this increased or did not affect SOCE [13,24,30,34–37]. TRPC1 principally regulates proliferation through the phosphoinositol-3-kinase (PI3K) and mitogen-activated protein kinase (MAPK) pathways in several cancers [13,26,28,38]. TRPC1 regulates PI3K and its downstream signaling kinases, such as AKT, differently, depending on whether it is an activator or an inhibitor of proliferation. Thus, in the lung (A549) and hepatocellular (Huh7) cancer cell lines, the depletion of TRPC1 inhibits cell proliferation by decreasing the activation of AKT [28,29]. Meanwhile, TRPC1 downregulation enhances cell proliferation by activating AKT in the esophageal (EC9706 cells) and breast (MCF-7 cells) carcinoma cell lines [32]. Recently, it has been shown that TRPC1 interacts with PI3K through calmodulin (CaM). Here, CaM, a multifunctional intracellular  $\text{Ca}^{2+}$ -binding protein, works as a connecting protein between TRPC1 and PI3K, thereby regulating colorectal cancer progression [13].

Nonetheless, to the best of our knowledge, nothing is known about TRPC1 expression in PDAC tumors and the possible downstream mechanisms that contribute to PDAC cell proliferation. In the present study, we demonstrated that TRPC1 upregulation correlates with low overall survival in PDAC patients. Furthermore, we revealed that TRPC1 regulates cell proliferation and cell cycle progression, particularly in aggressive PDAC cells, independently from  $\text{Ca}^{2+}$ -entry, by forming a complex with the PI3K p85 $\alpha$  subunit and CaM, leading to activation of AKT.

## 2. Results

### 2.1. TRPC1 Upregulation Correlates with the Aggressive Basal-like Subtype of PDAC and with Low Overall Survival

The expression of TRPC1 has been shown to be dysregulated in several types of cancer [1–4] and was recently shown to be correlated with poor prognosis in colorectal cancer [5]. However, little is known about its expression in PDAC. Therefore, we analyzed the expression of TRPC1 in normal pancreatic tissue and human PDAC samples using the PAAD TCGA dataset of normal and tumor samples. The results showed that TRPC1 mRNA expression was significantly upregulated in PDAC tissue samples compared to non-tumor tissue samples (N = 171 vs. 179,  $p < 0.01$ , Figure 1A). Furthermore, the results showed that the upregulation of TRPC1 was significantly higher in samples of a more aggressive basal-like PDAC subtype (N = 171 vs. 65  $p < 0.01$ , Figure 1B) compared to TRPC1 expression in the classical PDAC subtype (N = 171 vs. 86, Figure 1B). To investigate the prognostic significance of TRPC1, we analyzed whether TRPC1 overexpression was associated with survival in PDAC patients. The Kaplan–Meier survival analysis using SurvExpress, an online resource to correlate gene expression with overall survival, showed that patients



with high levels of TRPC1 ( $N = 110$ ) expression were associated with a significantly low overall survival compared to patients with low expression ( $N = 66$ ,  $p < 0.01$ , Figure 1C). Altogether, these online available expression data reveal that TRPC1 is overexpressed in human PDAC tissue, which correlates with low overall survival.

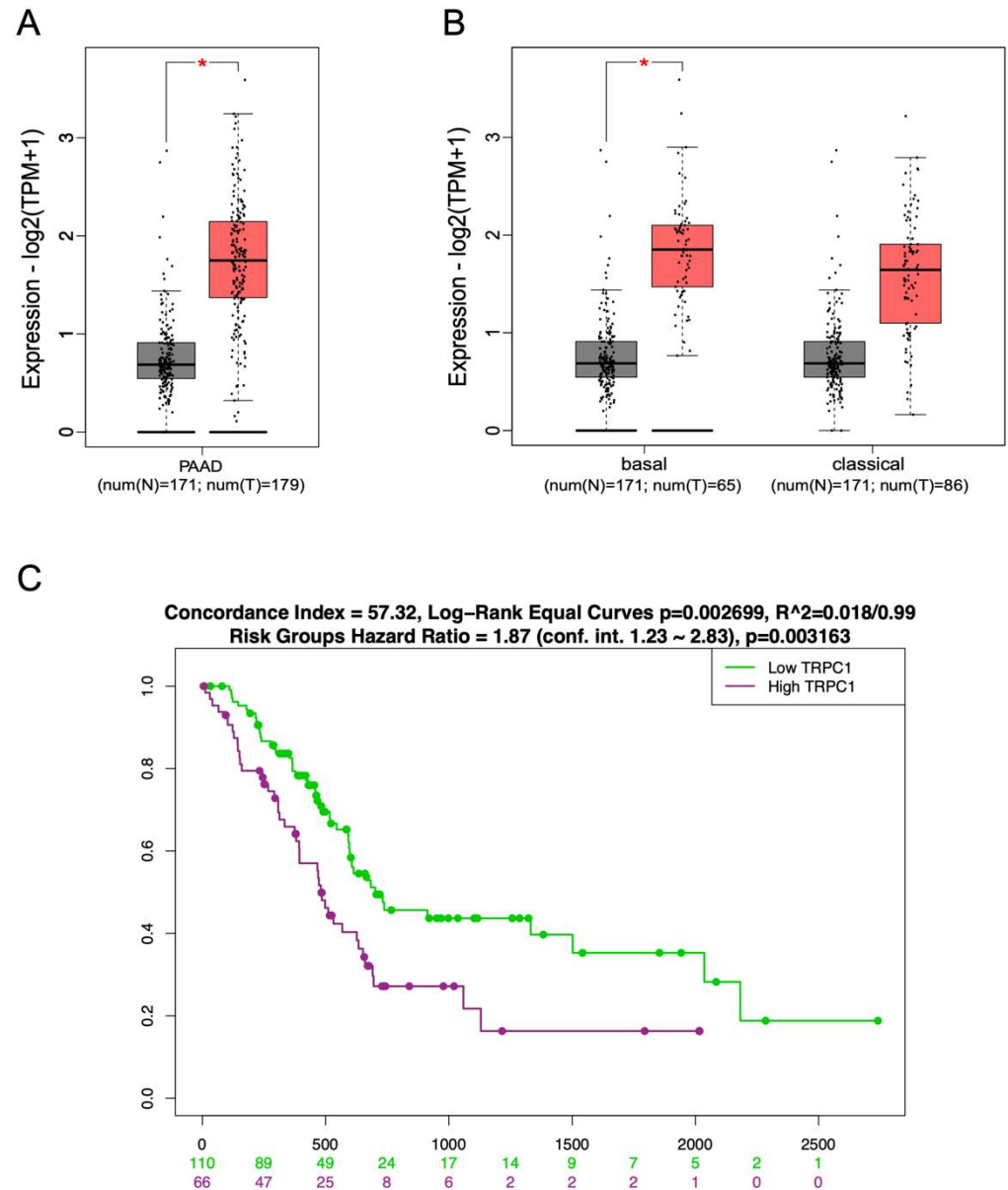


**Figure 1.** TRPC1 overexpression correlates with poor overall survival in PDAC patients. (A) Whisker boxplots of TRPC1 mRNA expression in normal samples (N) and PDAC tumor tissues (T) were generated by GEPIA2 using data from The Cancer Genome Atlas (TCGA) cohort PAAD and Genotype-Tissue Expression (GTEx) samples. \* Indicates  $p < 0.01$ . (B) Whisker boxplots of TRPC1 mRNA expression in normal samples (N) and PDAC tumor tissues (T) in both the basal and classical subtypes of PDAC were generated by GEPIA2 using data from the TCGA cohort PAAD and GTEx samples. \* Indicates  $p < 0.01$ . (C) Overall survival analysis of patients within the PAAD cohort with either a high or low expression of TRPC1 was generated using SurvExpress. The Kaplan-Meier curve was analyzed using the optimized SurvExpress Maximize algorithm. The number of analyzed patients across time (days) is indicated below the horizontal axis.

## 2.2. TRPC1 Is Overexpressed in Cell Lines with an Aggressive Phenotype and Is Localized to the Plasma Membrane

TRPC1 is located both in the plasma membrane and intracellular sites [39]. However, its localization in pancreatic ductal cells and PDAC cells is still unknown, although TRPC1 has been found in the apical and lateral regions of the basolateral membrane of pancreatic acinar cells [40]. Thus, we compared the TRPC1 expression and localization in human PDAC and adjacent non-tumor tissue samples from our local cohort (N = 21). Our immunohistochemistry (IHC) results confirmed the GEPIA2 analysis, showing a significant upregulation of TRPC1 by  $33 \pm 12.5\%$  ( $p < 0.05$ , Figure 2A,B). Moreover, TRPC1 was considerably more localized to the plasma membrane in tumor cells when compared to non-tumor cells, where TRPC1 was found mainly expressed in the cytoplasm ( $p < 0.0001$ , Figure 2A,C,D). Transcriptional expression of TRPC1 has been found in different types of commercially available PDAC cell lines (BxPC-3, CAPAN-1, CFPAC, and PANC-1) [41,42]. However, to our knowledge, its expression has not yet been compared to a normal pancreatic cell line. We investigated the protein expression of TRPC1 in different pancreatic cell lines. TRPC1 was overexpressed in five different PDAC cell lines, significantly in the MIA PaCa-2 cell line by  $83 \pm 22.6\%$  and in the PANC-1 cell line by  $88 \pm 8.9\%$  when compared to the normal-like pancreatic ductal cell line HPNE ( $n = 4-5$ ,  $p < 0.05$ , Figure 2E). Since the expression of TRPC1 was significantly upregulated in the particularly aggressive PDAC cell line PANC-1, this cell line was the focus of the subsequent study. Hence, we investigated the localization of TRPC1 in PANC-1 and HPNE cells. We found a robust membrane localization of TRPC1 in PANC-1 cells, which we did not find in HPNE cells, where it seems that TRPC1 tended to be localized in the cytoplasm (Figure 2F). Collectively, these findings suggest that TRPC1 is upregulated in human PDAC tissue and cell lines when compared to adjacent non-tumor tissue and a non-cancerous cell line. TRPC1 also localizes to the plasma membrane of tumor cells when compared to non-tumor cells.

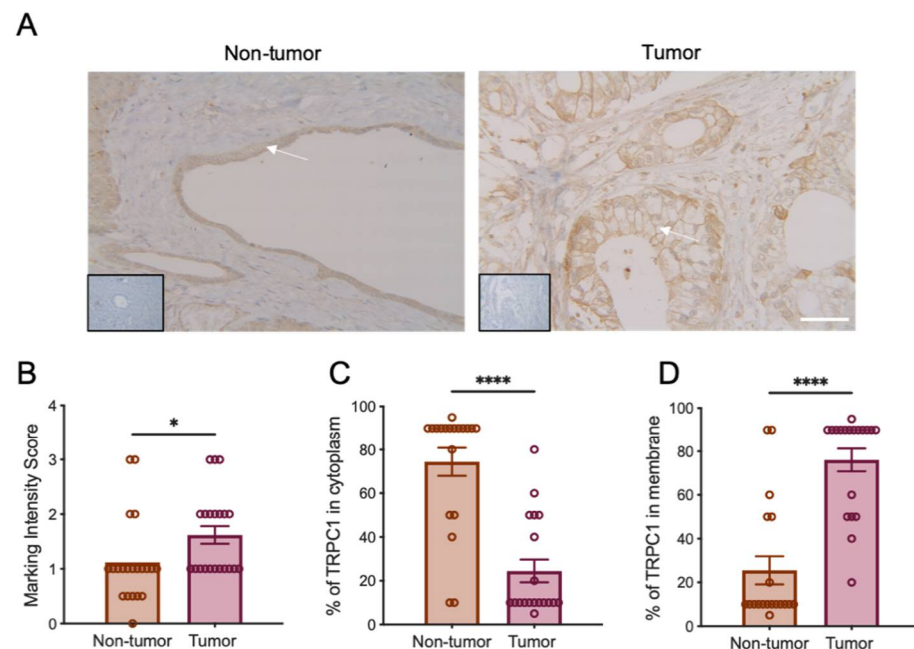
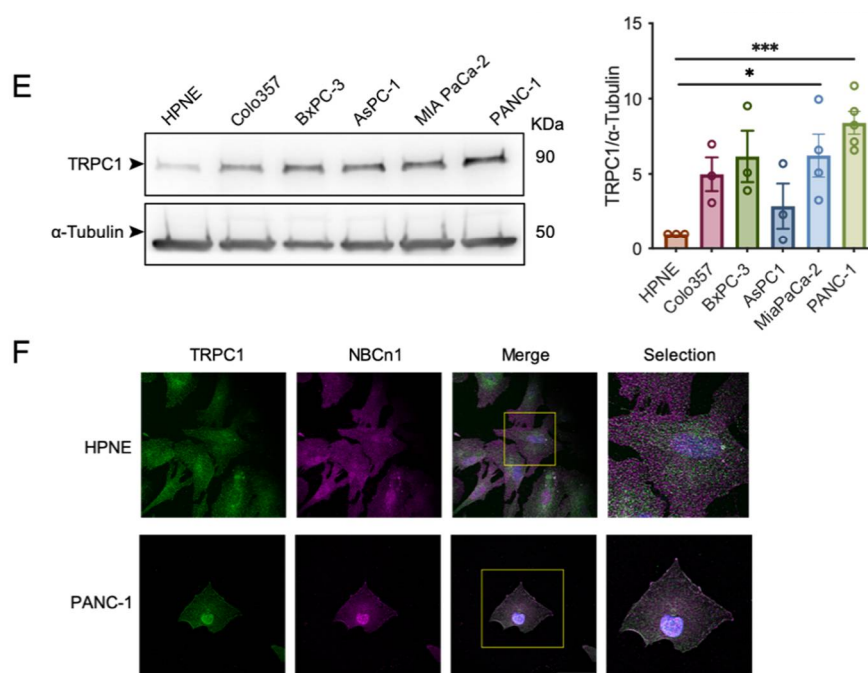


Figure 2. Cont.



**Figure 2.** TRPC1 is overexpressed in PDAC tissue and cell lines, where it localizes to the plasma membrane. (A) Representative images of TRPC1 expression in human PDAC tissue, performed by immunohistochemistry (IHC). White arrows indicate expression in the cytoplasm (left panel) and the plasma membrane (right panel). Inserts represent negative controls, scale bar = 40  $\mu$ m. (B) Quantification of TRPC1 marking intensity score between non-tumor and tumor tissue (N = 21). (C) Quantification of TRPC1 expressed in the cytoplasm and (D) membrane (N = 21). (E) Western blot analysis (left panel) and quantification (right panel) of TRPC1 expression in commercial-available PDAC cell lines ( $n = 3$ –5). (F) Representative immunofluorescent analysis of TRPC1 in HPNE and PANC-1 cells ( $n = 3$ ), scale bar = 20  $\mu$ m. Welch’s correction t-test was used to determine the significant difference between control and tumor conditions. \*, \*\* and \*\*\* indicate  $p < 0.05$ , 0.01, 0.001, and 0.0001, respectively.

### 2.3. The Knockdown of TRPC1 Inhibits PANC-1 Cell and Spheroid Growth

To study the role of TRPC1, we validated our knockdown (KD) model (Supplementary Figure S1). TRPC1 protein expression decreased by  $44 \pm 10\%$  after 72 h of siRNA transfection against TRPC1. Similar results were obtained by assessing the TRPC1 transcriptional levels 48, 72, and 96 h post-transfection (Supplementary Figure S1A). We investigated the role of TRPC1 in PANC-1 cell proliferation by the trypan blue assay. The KD of TRPC1 resulted in a significant decrease of PANC-1 cell viability by  $48 \pm 17.4\%$  and  $38 \pm 17.6\%$  after 72 and 96 h post-transfection, respectively ( $n = 4$ ,  $p < 0.05$ , Figure 3A). Even though our trypan blue assay indicated increased mortality 48 h post-transfection, our annexin-5 analysis did not show any significant difference in cell mortality between conditions (Supplementary Figure S2A–C). As 3D models imitate *in vivo* cell–cell and cell–extracellular matrix interactions better than traditional two-dimensional (2D) cell cultures [43], we established a 3D model of PANC-1 cell spheroids grown for nine days upon a KD of TRPC1. First, we confirmed the KD of TRPC1 after nine days, where TRPC1 protein levels decreased by  $22 \pm 1.0\%$  (Supplementary Figure S1C). This KD of TRPC1 significantly decreased the viability of spheroids after nine days by  $22 \pm 2.3\%$  ( $n = 3$ ,  $p < 0.05$ , Figure 3B). Collectively, these results suggest that silencing of TRPC1 inhibits PANC-1 cell and spheroid proliferation.

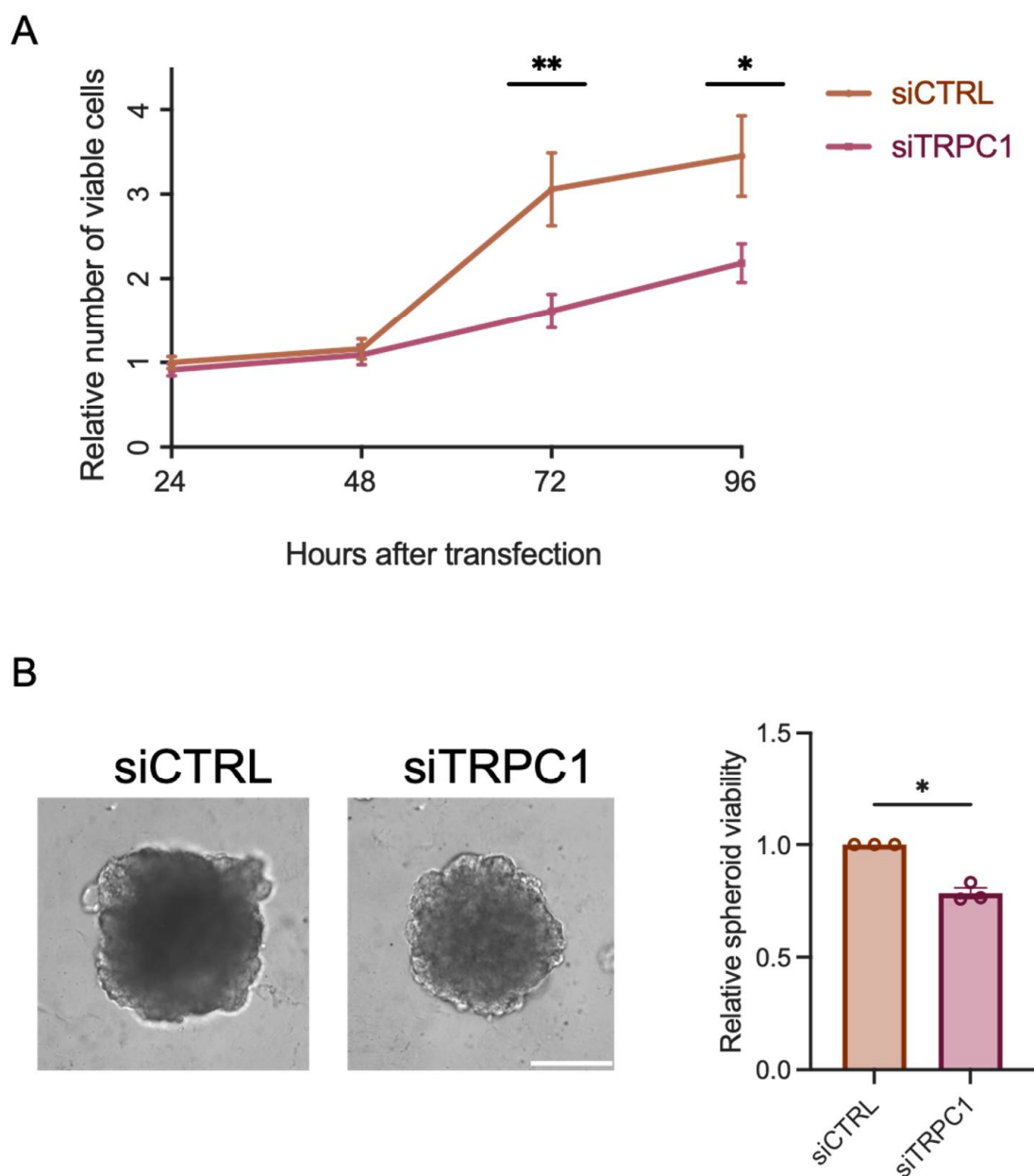


**Figure 3.** The knockdown of TRPC1 inhibits PANC-1 cell proliferation and spheroid growth. **(A)** trypan blue analysis of transfected PANC-1 cells shows the relative number of viable cells compared to siCTRL 24, 48, 72, and 96 h post-transfection ( $n = 4$ ). **(B)** Representative images of PANC-1 spheroids grown for nine days (left panel) and quantification of CellTiter-Glo<sup>®</sup> assay (right panel) ( $n = 3$ ), scale bar = 400  $\mu\text{m}$ . Welch's correction t-test was used to determine the significant difference between siCTRL and siTRPC1; \* and \*\* indicate  $p < 0.05$  and  $0.01$ , respectively.

#### 2.4. The Knockdown of TRPC1 Regulates Cell Cycle Progression by Reducing the Expression of CDK6, 2, and Cyclin A and Increasing the Expression of p21<sup>CIP1</sup>

To investigate the possible mechanism by which the KD of TRPC1 affects PANC-1 cell proliferation, the cell cycle distribution was examined by flow cytometry. We found that the KD of TRPC1 increased the number of PANC-1 cells in G0/G1 phase by  $13.8 \pm 3.7\%$  and decreased the number of cells by  $25.7\% \pm 10.3\%$  in S-phase ( $n = 4$ ,  $p < 0.05$ , Figure 4A). To further confirm the TRPC1-dependent regulation of cell cycle progression, we analyzed the expressions of several essential cell cycle-driven proteins involved in the G1- and S-phases. The immunoblot analysis showed that the expressions of CDK6 and CDK2 were

significantly decreased by  $44 \pm 5.3\%$ ,  $39 \pm 1.4\%$ , and Cyclin A by  $24 \pm 2.3\%$ , respectively, upon KD of TRPC1 ( $n = 3-4$ ,  $p < 0.05$ , Figure 4B). Moreover, the expression of p21<sup>CIP1</sup>, known to inhibit the CDK2 and CDK6 complexes, was significantly upregulated by  $23 \pm 4.6\%$  ( $n = 3$ ,  $p < 0.05$ , Figure 4B). However, TRPC1 KD failed to affect the expression of cyclin B1, D1, D3, and E, along with CDK1 and CDK4 (Supplementary Figure S3). Together, this suggests that TRPC1 depletion arrests cells in the G1 phase and decreases the cell fraction in the S-phase.

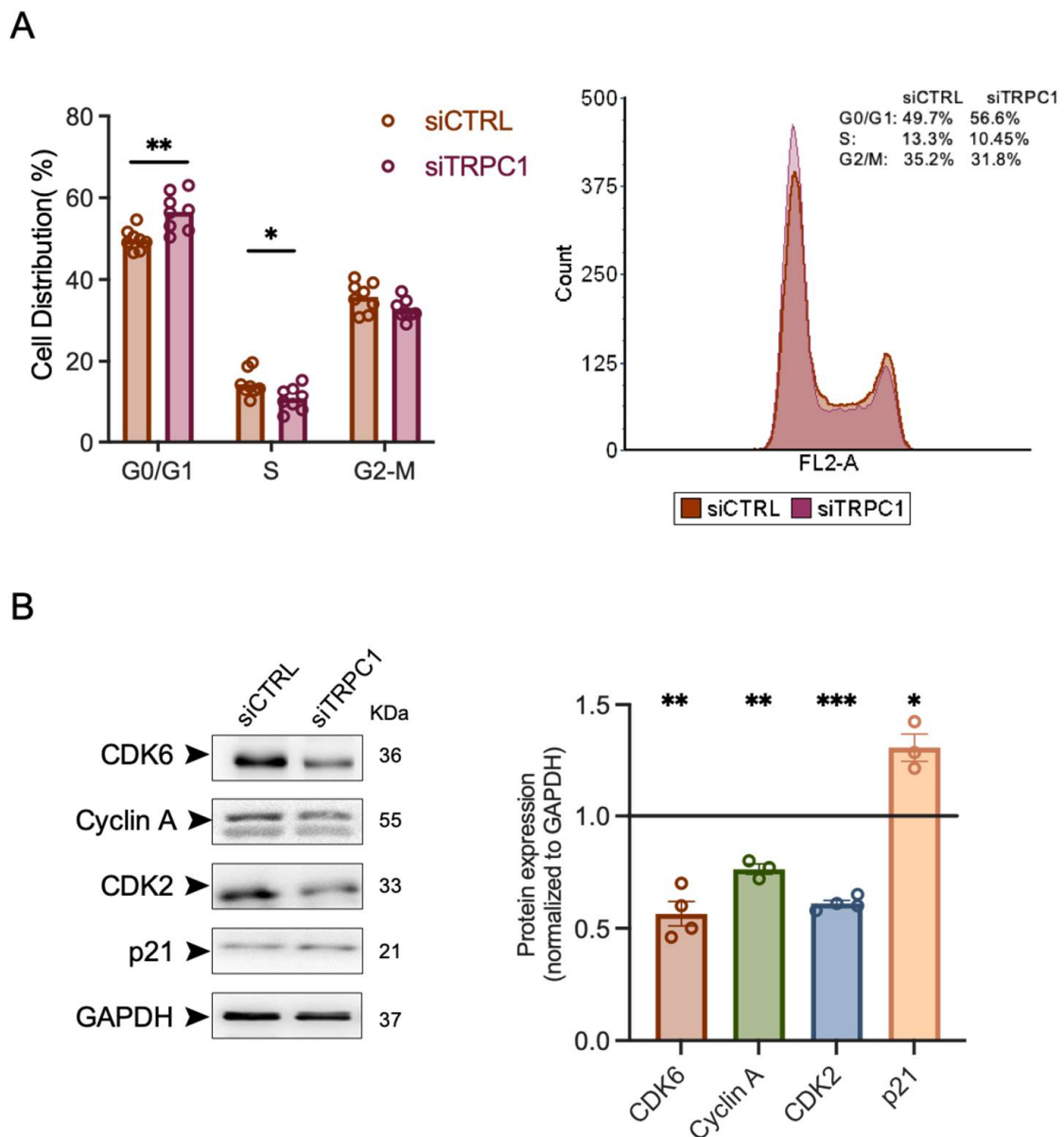


**Figure 4.** The knockdown of TRPC1 arrests PANC-1 cells in G1/S phases, decreases the expression of CDK6, 2, Cyclin A, and increases the expression of p21<sup>CIP1</sup>. (A) Quantification of cell cycle analysis representing the percentage of cells in each cell cycle phase of both transfected PANC-1 cells with either siCTRL or siTRPC1 (left panel) and representative data from FACS acquisition (generated with FCS Express 7) (right panel) ( $n = 4$ ). (B) Western blot analysis of relevant cyclin-dependent kinase complexes and cyclins and their inhibitor p21<sup>CIP1</sup> (left panel). Quantification of western blot analysis representing the expression of proteins in siTRPC1 lysates compared to siCTRL lysates (right panel) ( $n = 3-4$ ). Welch’s correction t-test was used to determine the significant difference between siCTRL and siTRPC1. \*, \*\* and \*\*\* indicate  $p < 0.05$ , 0.01 and 0.001, respectively.

### 2.5. The Knockdown of TRPC1 Does Not Affect $\text{Ca}^{2+}$ Entry nor Store-Operated $\text{Ca}^{2+}$ Entry and Decreases Cell Proliferation Independently of Extracellular $\text{Ca}^{2+}$

Although it has been shown that TRPC1 functions as a SOC channel in the PDAC cell line BxPC-3 [42], it is very controversial whether TRPC1 is a modulator of  $\text{Ca}^{2+}$  entry [44]. In different colorectal, thyroid, and hepatocellular cancer cells, TRPC1 did not contribute to cancer progression through SOCE [13,24,37,45]. Therefore, we investigated the role of TRPC1 in  $\text{Ca}^{2+}$  entry of PANC-1 cells using the manganese-quenching technique. TRPC1 silencing did not affect the  $\text{Mn}^{2+}$  quench ( $6 \pm 9.2\%$  increase,  $n = 342$  and  $382$ , for siCTRL and siTRPC1, respectively, Figure 5A). Furthermore, using the classical SOCE protocol, we showed that TRPC1 silencing did not participate in SOCE ( $2.6 \pm 3.2\%$  increase,  $n = 303$  and  $280$ , for siCTRL and siTRPC1, respectively, Figure 5B,C) or affected the intracellular  $\text{Ca}^{2+}$  concentration estimated by the basal ratio ( $1.8 \pm 1.7\%$  increase,  $n = 303$  and  $280$ , for siCTRL and siTRPC1, respectively, Figure 5B,D). As TRPC1 does not appear to be involved in  $\text{Ca}^{2+}$  entry in PANC-1 cells, we investigated whether PANC-1 cell proliferation was  $\text{Ca}^{2+}$ -dependent or independent. We evaluated the proliferation of PANC-1 cells cultured for 48 h in a medium depleted of  $\text{Ca}^{2+}$ . This extracellular  $\text{Ca}^{2+}$  chelation by EGTA did not decrease cell viability (Figure 5E). Moreover, TRPC1 silencing further decreased the cell proliferation regardless of the extracellular  $\text{Ca}^{2+}$  concentration by  $32 \pm 5.3\%$  and  $37.0 \pm 5.2\%$ , with or without  $\text{Ca}^{2+}$ , respectively ( $n = 3$ ,  $p < 0.01$ ). These results suggest that TRPC1 is not involved in the  $\text{Ca}^{2+}$  entry of PANC-1 cells and regulates cell proliferation by a  $\text{Ca}^{2+}$ -independent mechanism.

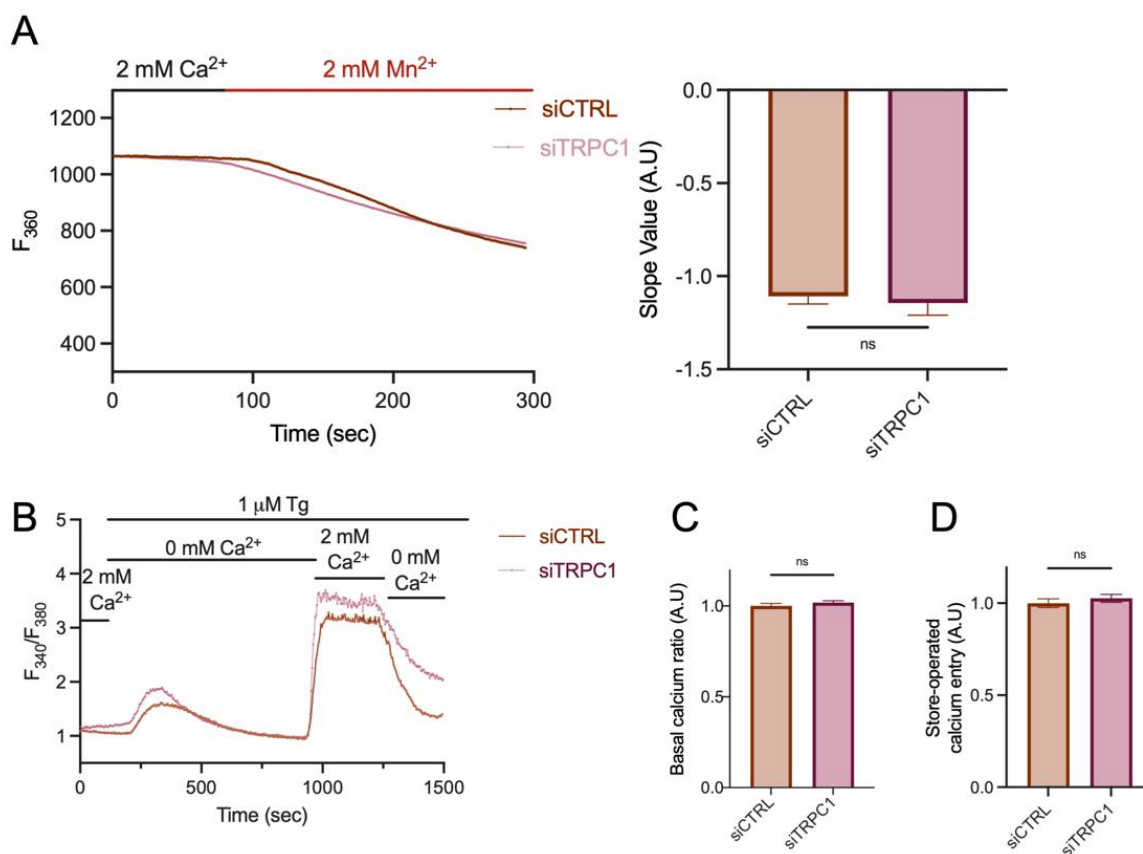
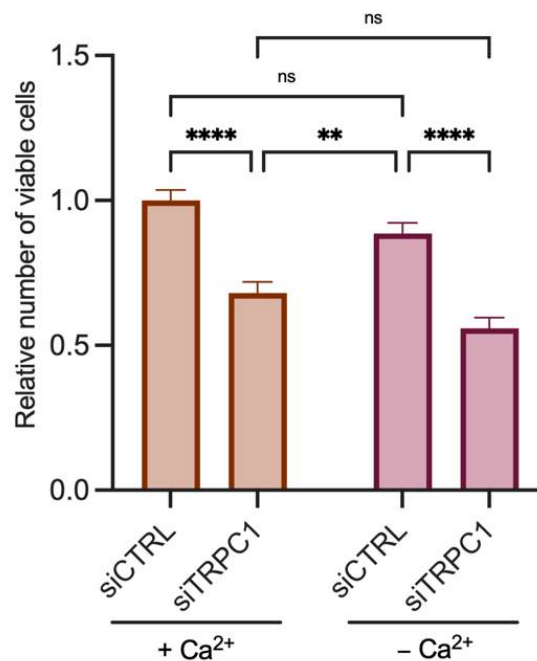


Figure 5. Cont.



E



**Figure 5.** The knockdown of TRPC1 does not affect Ca<sup>2+</sup> entry and the proliferative role of PANC-1 cells does not depend on extracellular Ca<sup>2+</sup> concentration. (A) Representative traces of Mn<sup>2+</sup> quenching in PANC-1 cells (left panel) and the quantification of siCTRL and siTRPC1 transfected PANC-1 cells (right panel) (number of analyzed cells siCTRL = 342 and siTRPC1 = 382). ns indicates non-significant. (B) Representative traces of the classical store-operated Ca<sup>2+</sup> entry protocol. Cells were perfused with 2 mM Ca<sup>2+</sup> for 1 min, then with 0 mM Ca<sup>2+</sup> and 1  $\mu$ M thapsigargin (Tg) for 12 min, followed by 2 mM Ca<sup>2+</sup> for 5 min, and finally perfused with 0 mM Ca<sup>2+</sup>. ns indicates non-significant. (C) Quantification of basal Ca<sup>2+</sup> ratio (0 mM Ca<sup>2+</sup>) in siCTRL and siTRPC1 transfected PANC-1 cells (number of analyzed cells siCTRL = 303 and siTRPC1 = 280). ns indicates non-significant. (D) Quantification of SOCE (2 mM Ca<sup>2+</sup> after internal Ca<sup>2+</sup>-store depletion) in siCTRL and siTRPC1 transfected PANC-1 cells (number of analyzed cells siCTRL = 303 and siTRPC1 = 280). (E) Trypan blue assay analysis of siCTRL and siTRPC1 transfected PANC-1 cells (for 72 h) either treated with medium containing extracellular Ca<sup>2+</sup> concentrations (+Ca<sup>2+</sup>), or with medium depleted for extracellular Ca<sup>2+</sup> (−Ca<sup>2+</sup>), for 48 h ( $n = 3$ ). Welch's correction t-test and Tukey's multiple comparison test (E) were used to determine significant difference between siCTRL and siTRPC1 conditions. \*\*, and \*\*\*\* indicate  $p < 0.01$ , and 0.0001, respectively.

### 2.6. TRPC1 Strongly Regulates AKT Phosphorylation in PANC-1 Cells

Two key downstream proteins responsible for cell proliferation are the serine/threonine kinases AKT and ERK1/2 [46]. The phosphorylation of these kinases has been shown to be dependent on TRPC1 expression [28,47]. We investigated the role of TRPC1 in the phosphorylation of AKT and ERK1/2 in transfected PANC-1 cells starved for 24 h, which were then mitogen-activated with FBS for 30 min. The immunoblot analysis revealed that the KD of TRPC1 significantly reduced AKT activation by  $39 \pm 7.8\%$ , while total AKT expression remained unchanged ( $n = 4$ ,  $p < 0.05$ , Figure 6A). A slight reduction of ERK1/2 phosphorylation ( $13 \pm 0.4\%$ , ( $n = 4$ ,  $p < 0.0001$ , Figure 6B) was observed in cells transfected with siTRPC1. These results indicate that TRPC1 regulates PANC-1 cell proliferation through activation of AKT.

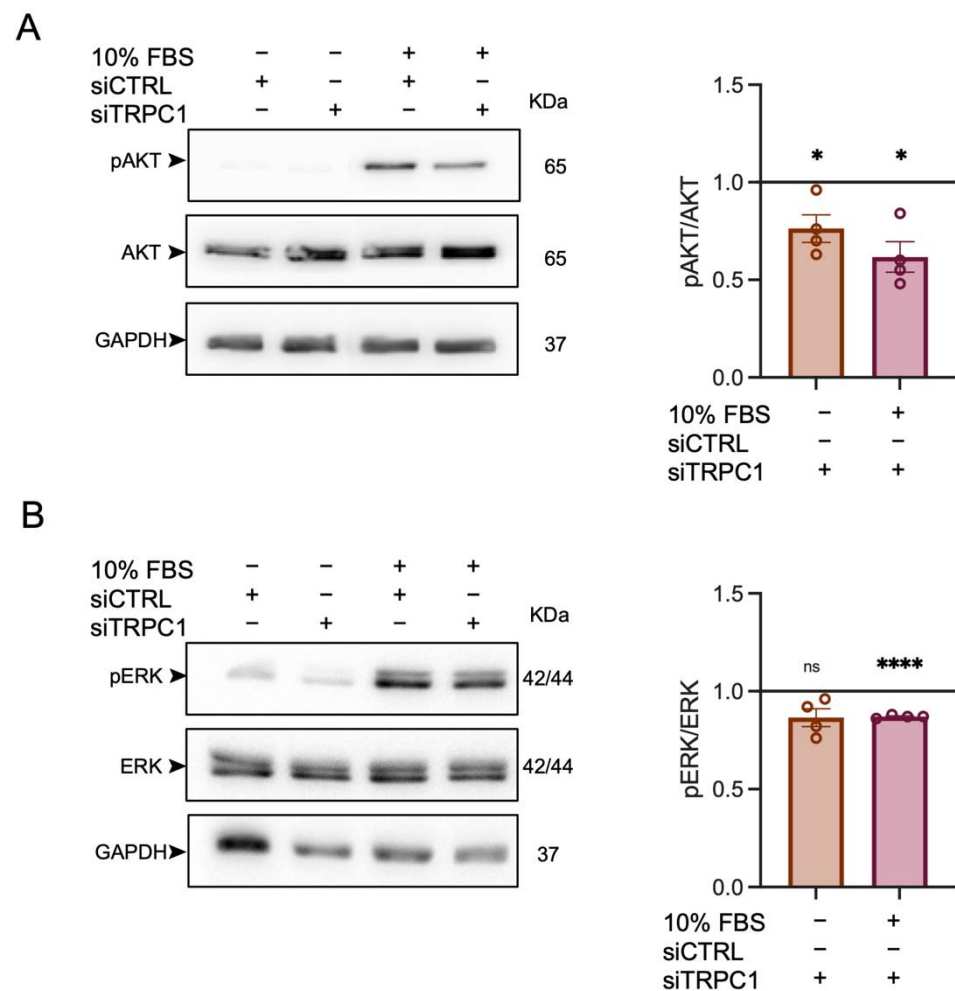


**Figure 6.** The knockdown of TRPC1 decreases PANC-1 cell proliferation through the phosphorylation of AKT pathways. **(A)** Western blot analysis of phosphorylated AKT (pAKT) and total AKT in transfected PANC-1 cells after mitogen-activation with FBS for either 0 or 30 min (left panel). Quantification of the western blot analysis compared to siCTRL either after 0 min or 30 min of mitogen activation (right panel). \* indicates  $p < 0.05$ . **(B)** Western blot analysis of phosphorylated ERK1/2 (pERK1/2) and total ERK in transfected PANC-1 cells after mitogen-action for either 0 or 30 min (left panel). Quantification of the western blot analysis compared to siCTRL either after 0 min or 30 min of mitogen activation (right panel). Welch's correction *t*-test was used to determine the significant difference between siCTRL and siTRPC1 conditions. ns indicate non-significant and \*\*\*\*  $p < 0.0001$ , respectively.

### 2.7. TRPC1 Interacts with PI3K, Which Is Attenuated upon the Knockdown of TRPC1

TRPC1 has been shown to be involved in activating the PI3K signaling pathway [13,38,47]. In addition, it has been demonstrated that CaM is a connexin between TRPC1 and the p85 $\alpha$  subunit of PI3K [13]. Thus, we investigated whether TRPC1 interacts with the PI3K-p85 $\alpha$  subunit in PANC-1 cells using Co-IP and PLA techniques. Our results by PLA analysis showed that TRPC1 and PI3K are located particularly close to each other (<40 nm) and can possibly interact. There was a relative decrease of  $57 \pm 7.8\%$  puncta per cell in siTRPC1 cells compared to siCTRL cells ( $n = 3$ ,  $p < 0.0001$ , Figure 7C). By co-IP, we found that TRPC1 interacts with PI3K and CaM in PANC-1 cells (Figure 7A). As an outcome of TRPC1 silencing, the interaction between TRPC1, PI3K, and CaM was reduced (Figure 7B) by  $32 \pm 4.5\%$ ,  $51 \pm 15.8\%$ , and  $31 \pm 0.1\%$ , respectively. These results suggest that the loss of TRPC1 can attenuate PI3K signaling.

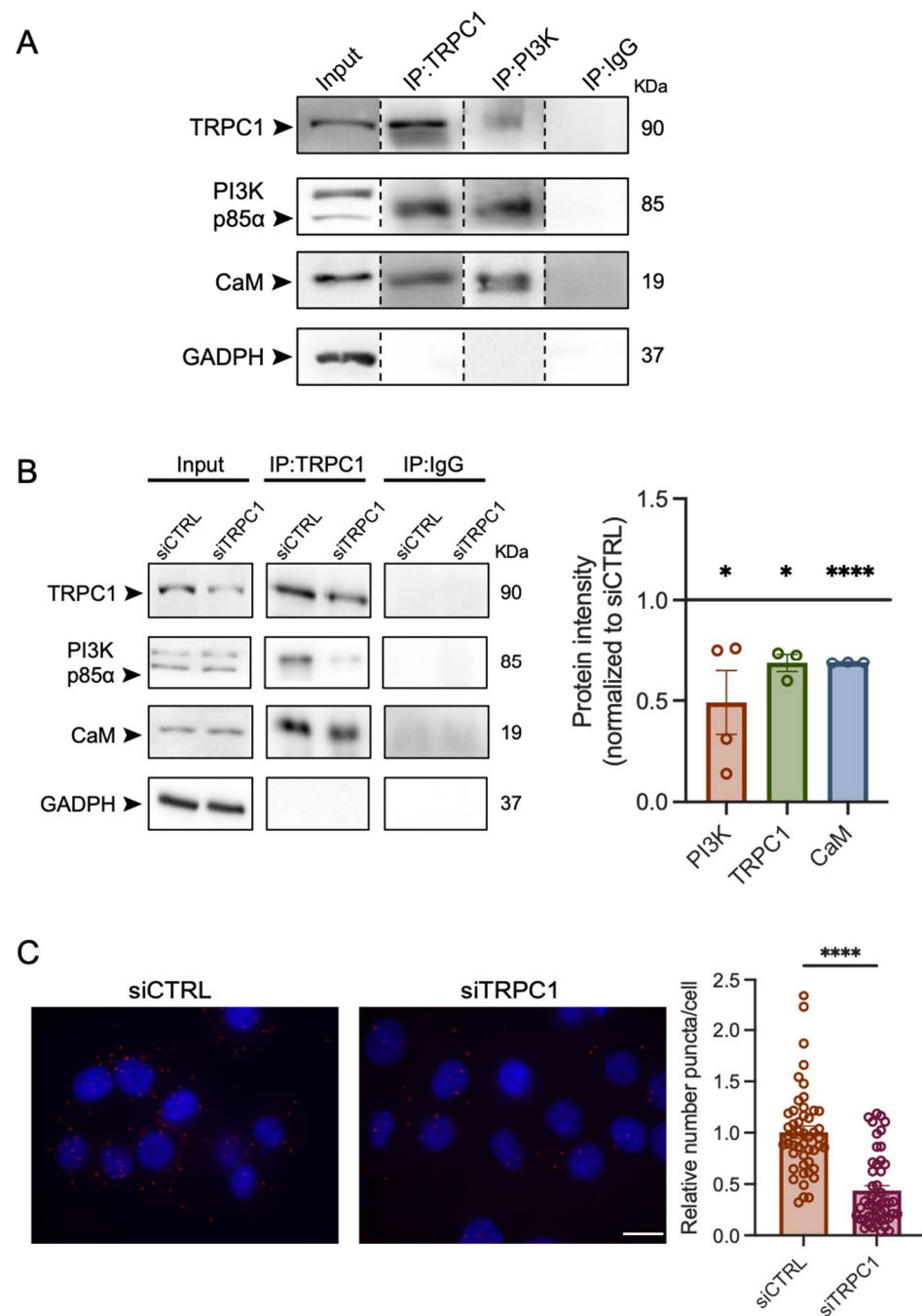


**Figure 7.** TRPC1 forms a complex with the PI3K p85α subunit and CaM, which is abolished upon TRPC1 knockdown. **(A)** Representative western blot analysis of co-immunoprecipitation of TRPC1 and PI3K p85α subunit with CaM in non-transfected PANC-1 cells. **(B)** Representative western blot analysis of co-immunoprecipitation of TRPC1 with PI3K p85α and CaM in transfected PANC-1 cells (left panel). Quantification of western blot analysis compared to siCTRL represents the effect of TRPC1 KD on the protein interaction (right panel) ( $n = 3-4$ ). \* and \*\*\*\* indicate  $p < 0.05$  and  $0.0001$ , respectively. **(C)** Representative images of proximity ligation assay (PLA) in transfected PANC-1 cells (left panel). Quantification of PLA where siTRPC1 is compared to the relative number of siCTRL ( $n = 3$ . At least 20 images were analyzed for each experiment, see material and methods for details) (right panel). \*\*\*\* indicates  $p < 0.0001$ , respectively.

### 3. Discussion

A wide range of physiological functions has been attributed to the expression and regulation of TRPC1, including cell proliferation, migration, invasion, and apoptosis [9,10,48,49]. In recent years, there has been increased interest in TRPC1 and its connection with tumor-related functions, and several studies have reported different downstream mechanisms of TRPC1 in several types of cancers [11]. However, there is sparse evidence of its involvement in PDAC progression. In this study, we revealed the role of TRPC1 and its downstream mechanisms that contribute to PDAC cell proliferation. TRPC1 is upregulated in various types of cancer, such as tongue, breast, gastric, ovarian, colorectal, and renal cell carcinoma, where its expression correlates with different clinical factors [12–21]. For instance, the high expression of TRPC1 correlated with low overall and event-free survival in colorectal cancer patients [13,17] and disease-free survival in lung cancer patients [21]. In endometrial cancer patients, the high expression of TRPC1 was correlated with low overall survival, even though the expression of TRPC1 was downregulated when comparing endometrial cancer with adjacent tissue samples [15]. In congruence with this, we show that TRPC1 is upregulated in PDAC tissue compared to non-tumor tissue samples. Interestingly, the expression of TRPC1 is higher in the basal-like subtype of PDAC, which is associated with a poorer clinical outcome and loss of differentiation [50]. In addition, our findings show that the high expression of TRPC1 correlated with low overall survival in PDAC patients. However, the dysregulated expression of TRPC1 will remain controversial and seems to be cell type-specific, as the upregulation of TRPC1 appears to have a protective role in prostate [51,52] and some breast cancer patients [33]. Consistent with the increased TRPC1 mRNA expression, TRPC1 protein expression also significantly increased in human PDAC samples, where TRPC1 localizes to the plasma membrane, compared to adjacent non-tumor tissue, where it localizes in the cytoplasmic compartments.

In addition to expression in human tissue, TRPC1 has been shown to be upregulated in cancer cell lines compared to a corresponding non-cancerous cell line. For instance, TRPC1 is upregulated in breast cancer cell lines [33] and colorectal cancer cell lines [13]. To our knowledge, the expression of TRPC1 has not yet been evaluated in commercially-available PDAC cell lines compared to a duct-like control cell line. Interestingly, TRPC1 expression markedly increased in the more aggressive PDAC cell line PANC-1, and the cell line was the focus of the subsequent study. Remarkably, in PANC-1 cells, the localization of TRPC1 is in the cell membrane when compared to the HPNE cells, where TRPC1 seems to be located in the cytoplasm.

To investigate the role of TRPC1 in PDAC proliferation and growth, we performed loss of function experiments in 2D and 3D cell models. We found that TRPC1 silencing inhibited 2D cell proliferation and spheroid growth. The same effect has been found in neuroblastoma [22], glioblastoma [23], thyroid [24], breast [12,25–27], lung, [28], liver [29,30], ovarian [31], and colon cancer [13]. This indicates that the upregulation of TRPC1 stimulates proliferation in several cancer types. Repressed cell proliferation is often associated with disruption of cell cycle progression by the dysregulation of cyclins and cyclin-dependent kinase (CDK) complexes [53]. In this study, the KD of TRPC1 accumulated cells in the G0/G1 phase reduced the number of cells in the S-phase and the expressions of CDK6, CDK2, Cyclin A, and increased p21<sup>CIP1</sup> expression. These proteins are essential in regulating progress through the G1/S phases of the cell cycle. Such a scenario has also been reported for other cancer cell models, for instance, in A549 lung cancer cells, where the KD of TRPC1 decreased the protein expression of Cyclin D1 and D3, leading to an increased number of cells in the G1 phase [28]. In addition, MCF-7 breast cancer cells accumulated in the G1 phase upon the KD of TRPC1 [12], which was also found in the thyroid cancer cell line ML-1, where the expression of the CDK6, Cyclin D2, and D3 decreased, and the expression of their regulating inhibitor p21 increased [24]. This indicates that TRPC1 is important for different cancer cell types to progress through the G1/S phases and that it is cell type-specific how CDK/Cyclin complexes regulate this progression.

The pathophysiological importance of TRPC1 in the plasma membrane is often associated with its role in  $\text{Ca}^{2+}$  entry, as the  $\text{Ca}^{2+}$  flux has been shown to be essential for tumor progression [11]. However, it is controversial whether TRPC1 regulates relevant cellular processes of tumorigenesis through  $\text{Ca}^{2+}$  as several studies have shown that these events can be regulated by TRPC1 independently of  $\text{Ca}^{2+}$  entry [13,24,30,34–36]. Even though SOCE and constitutive  $\text{Ca}^{2+}$ -entry have been shown to regulate cell proliferation through cell cycle progression, it is well accepted that transformed cells can proliferate independently from  $\text{Ca}^{2+}$ -entry [5,7,13,24]. This is consistent with our findings, where the KD of TRPC1 did not affect  $\text{Ca}^{2+}$ -entry, SOCE, which was slightly but not significantly increased, and the chelation of  $\text{Ca}^{2+}$  had no effect on PANC-1 cell proliferation, suggesting that the PANC-1 cell and spheroid proliferation is  $\text{Ca}^{2+}$  independent.

It is well known that the PI3K and MAPK signaling pathways play essential roles in cell proliferation and growth [54]. Inhibition of these proteins can lead to cell cycle arrest in PDAC cell lines [55]. Our findings show that KD of TRPC1 decreases the phosphorylation of AKT and, to a lesser extent, ERK1/2, which could explain the decrease of cell cycle regulating proteins and cell cycle arrest in the G1/S phases. This indicates that the PI3K signaling axis profoundly regulates PANC-1 cell proliferation through TRPC1. Hence, we investigated the physical interaction of TRPC1 and PI3K and its associated connecting protein CaM. It is known that TRPC channels can bind to CaM and thereby regulate physiological and pathophysiological processes [9]. In addition, CaM can bind to the PI3K p85 $\alpha$  subunit, which removes its inhibitory effect on the catalytic subunit p110, and sequentially activates PI3K signaling [56]. The physical interaction between TRPC1 and PI3K has been shown to regulate myoblast differentiation [57], and only one other study besides ours shows the interaction between TRPC1, PI3K, and CaM [13]. However, a similar interaction of CaM and PI3K with TRPC6 has been found to regulate bovine aortic endothelial cell migration [58]. Here, we found that abolishing TRPC1 decreased the interaction between these proteins. As the phosphorylation of AKT was significantly reduced upon KD of TRPC1, our findings suggest that TRPC1 regulates PANC-1 cell proliferation by forming a complex with PI3K and CaM, thereby activating downstream signaling. However, some studies have shown that KD of TRPC1 decreased SOCE and thereby AKT phosphorylation in different cancer cell models [28,29]. Our results show that the phosphorylation of AKT seems to be  $\text{Ca}^{2+}$ -independent. This finding is in congruence with other reports, where the KD of TRPC1 decreased the phosphorylation of AKT in a  $\text{Ca}^{2+}$ -independent manner. For instance, in the PTEN deficient breast cancer cell line MDA-MB-468, TRPC1 silencing reduced the phosphorylation of AKT even though it slightly increased SOCE levels [36,47]. The same was found in some colorectal cancer cell lines, where it was proposed that TRPC1 regulated the PI3K/CaM/AKT axis independently of  $\text{Ca}^{2+}$  [13].

In conclusion, we show for the first time that TRPC1 is upregulated in aggressive subtypes of PDAC patient tumor tissue and cell lines. TRPC1 regulates PDAC cell and spheroid proliferation through the direct interaction with the PI3K and CaM, thereby activating downstream signaling events implicated in G1 phase progression and G1/S transition, likely through a  $\text{Ca}^{2+}$ -independent mechanism.

## 4. Materials and Methods

### 4.1. Public Database Analysis

TRPC1 mRNA expression was investigated by using online available datasets. Whisker boxplots of TRPC1 mRNA expression were generated using GEPIA2 (<http://gepia2.cancer-pku.cn/>, accessed on 1 June 2021) that compiles Genotype-Tissue Expression (GTEx) (<http://www.GTEXportal.org/>, accessed on 1 June 2021), and The Cancer Genome Atlas (TCGA) (<http://www.cancergenome.nih.gov/>, accessed on 1 June 2021) datasets of normal and tumoral samples from different organs of interest, in our case pancreas and PDAC (PAAD). Survival analysis was performed using the SurvExpress online tool (available at [http:](http://)



[/bioinformatica.mty.itesm.mx/SurvExpress](https://bioinformatica.mty.itesm.mx/SurvExpress), accessed on 2 March 2022), as previously described [59].

#### 4.2. Immunohistochemistry in Human PDAC Samples

All experimental protocols were approved by the ethical committee of the University Hospital Center of Amiens (reference: PI2021\_843\_0027). Human tissue samples from PDAC patients were obtained and processed at the University Hospital Center of Amiens. Classical immunohistochemistry was performed from routinely processed formalin-fixed paraffin-embedded PDAC tumor material. First, 4  $\mu$ M thick sections were deparaffinized in xylene and then rehydrated in ethanol. Then, the endogenous peroxidase activity was blocked before the antigen retrieval. The cell conditioning solution CC1 (BenchMark XT, Ventana, Rotkreuz, Switzerland) was used for antigen retrieval. Automatic immunohistochemical staining was carried out on a BenchMark ULTRA system (Ventana, Rotkreuz, Switzerland) using antibodies against TRPC1 (1/50, Abcam, Waltham, MA, USA). Next, the biotin-labeled secondary antibody was applied, followed by the addition of avidin–biotin–peroxidase complex treatment. Reactions were developed using a chromogenic reaction with 3,3'-diaminobenzidine tetrahydrochloride (iVIEW DAB Detection Kit, Ventana). The tissue sections were counterstained with hematoxylin. The TRPC1 antibody was certified for immunohistochemical use by the manufacturer. Negative controls were performed with the same technique and conditions, without the addition of the primary antibody. Histological examination and quantitative evaluation were performed in cooperation with a pathologist (HS, PR), using a Leica inverted microscope. The marking intensity score ranged from 0 to 3 (0 = no immunostaining, 1 = weak immunostaining, 2 = moderate immunostaining, 3 = strong immunostaining). The TRPC1 localization was evaluated as a percentage in the cytoplasm or membrane.

#### 4.3. Cell Culture

The hTERT-immortalized Human Pancreatic Nestin-Expressing cells (HPNE) were purchased from the American Type Culture Collection (ATCC, Molsheim, France). HPNE were grown in 75% DMEM without glucose (Sigma, Cat no. D-503, St. Louis, MO, USA), 25% Medium M3 Base (Incell Corp., San Antonio, TX, USA, Cat no. M300F-500), which were completed with 10% fetal bovine serum (Cat no. P30-3031, PAN Biotech, Aidenbach, Germany), 5.5 mM glucose and 750 ng/mL puromycin. Colo357, BxPC-3, AsPC-1, MIA PaCa-2, and PANC-1 cells were kindly provided by Prof. Anna Trauzold (Institute of Experimental Cancer Research, Kiel University, Kiel, Germany). These cell lines were grown in RPMI-1640 (Sigma-Aldrich, Cat no. R8758), supplemented with 10% fetal bovine serum (Cat no. P30-3031, PAN Biotech), 1 mM sodium pyruvate (Gibco, Waltham, MA, USA), and 1% Glutamax (Gibco). Cells were grown at 37 °C, 95% humidity, 5% CO<sub>2</sub>, and passaged with trypsin-EDTA 0.25% (Sigma, Saint-Quentin-Fallavier, France) when cells reached a confluency of 70–80%. Cell cultures were not used for more than 20 passages.

#### 4.4. Transient Transfections

Cells were transfected with small interfering RNA (siRNA) by electroporation using nucleofection (Amaxa Biosystems, Lonza, Aubergenville, France). PANC-1 cells ( $1 \times 10^6$ ) were transiently nucleofected according to the manufacturer's protocol with 4  $\mu$ g of scrambled siRNA (siCTRL, duplex negative control, Eurogentec) or with siRNA directed against TRPC1, (siTRPC1, ON-TARGET plus SMART pool siRNA, Dharmacon Research, Chicago, IL, USA). All the experiments were performed 72 h after the siRNA transfection.

#### 4.5. 3D-Spheroid Growth and CellTiter Glo Assay

A total of 2000 transfected PANC-1 cells were seeded per well in round-bottomed, ultra-low attachment 96-well plates (Corning, NY, USA) in 200  $\mu$ L growth medium, supplemented with 2% GelTrex LDEV-Free reduced growth factor basement membrane matrix (ThermoFisher Scientific, Waltham, MA, USA). Cells were subsequently spun down



at 750 RCF for 20 min and were grown for 9 days at 37 °C with 95% humidity and 5% CO<sub>2</sub>. 100 µL medium was exchanged every second day. Light microscopic images of the spheroids at 10× magnification were acquired on days 2, 4, 7, and 9. On day 9, spheroids (in a replicate of 3) in 100 µL medium were transferred to a black 96-well plate where 100 µL CellTiter-Glo<sup>®</sup> 3D Reagent (Promega, Madison, WI, USA) was added. The black plate was wrapped in aluminum foil, shaken for 5 min, and then incubated for 25 min at room temperature. The luminescence signal was recorded using a FLUOStar Optima microplate reader (BMG Labtech, Ortenberg, Germany).

#### 4.6. Western Blot Analysis

Proteins were extracted and separated as previously described [60]. The primary antibodies used were: anti-TRPC1 (1:1000, Abcam, Waltham, MA, USA), anti- $\alpha$ Tubulin (Sigma-Aldrich, France), anti-CDK6 (1:500, Cell Signaling Tech., Danvers, MA, USA), anti-Cyclin A (1:500, Santacruz Biotechnology, Dallas, TX, USA), anti-CDK2 (1:500, Cell Signaling Tech., Danvers, MA, USA), anti-p21 (1:500, Cell Signaling Tech., Danvers, MA, USA), anti-GAPDH (1:2000, Cell Signaling Tech., Danvers, MA, USA), anti-PI3K p85 $\alpha$  (1:500, Bioworld Technology), and anti-Calmodulin (1:500, Santacruz Biotechnology, Dallas, TX, USA). Secondary antibodies were coupled to horseradish peroxidase, permitting protein detection with an enhanced chemiluminescence kit (Ozyme, Saint-Cyr-l'Ecole, France). Quantification was performed with the ImageJ analysis tool. All experiments were normalized to  $\alpha$ -Tubulin or GAPDH, which were used as reference proteins.

#### 4.7. Co-Immunoprecipitation

A total of 500 µg of proteins from non-transfected or transfected PANC-1 cells were used for co-immunoprecipitation with SureBeads<sup>™</sup> Protein A Magnetic Beads (Biorad, France). First, the beads were washed thoroughly, as described in the manufacturer's protocol. Then 1 µg of either TRPC1 antibody (Abcam, Waltham, MA, USA) or PI3K p85 $\alpha$  antibody was resuspended with the beads for 30 min. After another sequential washing step, protein lysates were added to the beads and slowly rotated for 2 h at room temperature. The beads were washed and eluted according to the manufacturer's protocol. After denaturation, proteins were used for a standard Western blot, as described above. For input, 50 µg of proteins from the corresponding co-immunoprecipitation samples were used.

#### 4.8. Trypan Blue Assay

The  $8 \times 10^4$  PANC-1 cells were seeded in 35 mm Petri-dishes for 72 h after siRNA transfection. Cells were washed in PBS, trypsinized, and diluted (1:5) in trypan blue solution (Sigma-Aldrich, France), then counted six times using the standard Malassez cell method. Proliferation was calculated as the total number of viable cells (cells alive/white cells), normalized to the control, and the mortality was calculated as the percentage of dead cells (blue cells), compared to the control. To test the effect of Ca<sup>2+</sup> on proliferation, the same procedure as described above was carried out, but after 24 h of seeding, the medium was changed to medium with standard conditions containing 1 mM Ca<sup>2+</sup> (referred to as conditions with Ca<sup>2+</sup>) or containing Ethylene Glycol Tetraacetic Acid (EGTA), to chelate Ca<sup>2+</sup> and to end with a final concentration of 30 µM (referred to conditions without Ca<sup>2+</sup>). Therefore, cells were transfected for 72 h, and Ca<sup>2+</sup> were chelated for 48 h.

#### 4.9. Flow Cytometry

Flow cytometry was carried out on ethanol-fixed cells by a propidium iodide assay. Duplicates of  $2 \times 10^5$  transfected PANC-1 cells were seeded in 60 mm Petri dishes and collected after 72 h. Cells were washed in PBS, trypsinized, collected in PBS + EDTA (5 mM), and fixed with cold absolute ethanol ( $\geq 99.8\%$ , Sigma-Aldrich) for at least 6 h, at 4 °C. Then, cells were pelleted, resuspended in PBS + EDTA (5 mM), treated with 20 µg/mL RNase A (Sigma-Aldrich) for 30 min at room temperature, and stained with 50 µg/mL

of propidium iodide (Sigma-Aldrich, St. Quentin Fallavier, France). Samples were then analyzed by a flow cytometer (Accuri<sup>®</sup>, Dominique Deutscher, Brumath, France), and the cell percentage in different phases was calculated using Cyflogic software and illustrated with FCS Express 7.

#### 4.10. Calcium Imaging

Ca<sup>2+</sup> imaging acquisition was performed as previously described [61]. Briefly,  $25 \times 10^3$  transfected PANC-1 cells were seeded on glass coverslips 72 h before each experiment. Then, cells were incubated with 3.33  $\mu$ M Fura-2/AM (Sigma, Saint-Quentin-Fallavier, France) at 37 °C in the dark for 45 min. Cells on the coverslip were washed twice with extracellular saline solution (145 mM NaCl, 5 mM KCl, 2 mM CaCl<sub>2</sub>, 1 mM MgCl<sub>2</sub>, 5 mM glucose, 10 mM HEPES, pH 7.4), and placed on the stage of a fluorescence microscope (Axiovert 200; Carl Zeiss, Oberkochen, Germany). Here, cells were excited at 340 and 380 nm using a monochromator (polychrome IV, TILL Photonics, Gräfelfing, Germany), and fluorescent emission was captured with a Cool SNAPHQ camera (Princeton Instruments, Lisses, France) after filtration through a long-pass filter (510 nm). Metafluor software (version 7.1.7.0, Molecular Devices, San Jose, CA, USA) was used for signal acquisition and data analysis. During acquisition, cells were continuously perfused with the saline solution. Store-operated Ca<sup>2+</sup> entry (SOCE) was triggered by applying the classical protocol, first by perfusing 2 mM Ca<sup>2+</sup> (for 1 min), then 0 mM Ca<sup>2+</sup> during 1 min followed by 1  $\mu$ M thapsigargin in 0 mM Ca<sup>2+</sup> for Ca<sup>2+</sup> store depletion for 12 min, followed by perfusion of 2 mM Ca<sup>2+</sup> (for 5 min). The intracellular Ca<sup>2+</sup> concentration is derived from the ratio of emitted fluorescence intensities for each of the excitation wavelengths (F340/F380). To estimate divalent cation influx under basal conditions, we used the manganese (Mn<sup>2+</sup>) quenching technique. After Fura2/AM loading, cells were washed and excited at 360 nm, where fluorescence was recorded at 510 nm. After 1.5 min, the Ca<sup>2+</sup> (2 mM) present in the saline solution was replaced by 2 mM Mn<sup>2+</sup> solution. The Mn<sup>2+</sup> quenching extracellular solution was composed of 145 mM NaCl, 5 mM KCl, 2 mM MnCl<sub>2</sub>, 1 mM MgCl<sub>2</sub>, 5 mM glucose, and 10 mM HEPES (pH 7.4). The Mn<sup>2+</sup> influx, a corroborate of the Ca<sup>2+</sup> influx, was estimated from the quenching rate of fluorescence at 360 nm by calculating the slope.

#### 4.11. Immunofluorescence

The  $8 \times 10^4$  non-transfected HPNE or PANC-1 cells were seeded on coverslips. After 48 h, cells were washed in cold PBS fixed for 20 min at room temperature in 4% paraformaldehyde (PFA, Sigma-Aldrich) and washed twice in PBS. Cells were permeabilized in 0.1% Triton<sup>™</sup>X-100 (Sigma, Saint-Quentin-Fallavier, France) for 10 min and blocked in 5% Bovine Serum Albumin (BSA, Sigma Aldrich no. A7906) for 30 min. Primary antibodies (anti-TRPC1, 1:100, Santacruz Biotechnology, Dallas, TX, USA, NBCn1 was used as a membrane marker, 1:400, Abcam, Waltham, MA, USA) were added overnight at 4 °C and secondary antibodies for 1 h at room temperature. Cells were treated with 4',6-diamidino-2-phenylindole (DAPI; 1%) for 5 min to stain nuclei, washed 3 times in 1% BSA, and mounted on slides using Prolong<sup>®</sup> Gold antifade reagent. Images were collected on an Olympus Cell Vivo IX83 with a Yokogawa CSU-W1 confocal scanning unit. Z-stacks were deconvoluted in Olympus Cell Sens software using a constrained iterative algorithm. No or negligible labeling was seen in the absence of primary antibodies (data not shown). Overlays and brightness/contrast/background adjustments were carried out using ImageJ software.

#### 4.12. Proximity Ligation Assay

The  $8 \times 10^4$  transfected PANC-1 cells were seeded on coverslips 72 h before the proximity ligation assay (PLA) experiment. As described before [61], cells were washed with PBS and fixed with PFA (4%) at room temperature for 20 min. Thereafter, cells were washed and permeabilized with 0.1% Triton<sup>™</sup> X-100 (Sigma, Saint-Quentin-Fallavier, France) for 10 min. The Duolink in situ PLA detection kit (Sigma-Aldrich, Saint-Quentin-

Fallavier, France) was used to detect interactions between TRPC1 and PI3K. Experiments were performed following the manufacturer's protocol. Red fluorescent oligonucleotides produced as the end product of the procedure were visualized using the Zeiss Observer Z1 microscope 60X oil objective (Carl Zeiss, Oberkochen, Germany). Images were analyzed using ImageJ software 1.53a (National Institute of Health, Bethesda, MD, USA), where puncta per cell were counted and normalized to the control. At least 20 pictures per condition were captured and analyzed.

#### 4.13. Statistical Analysis

All data are shown as representative images or as mean measurements with standard error of means (SEM) error bars and represent at least three independent experiments.  $N$  refers to the population size, where  $n$  refers to the number of independent experiments performed or to the number of cells analyzed. Welch's correction t-test or Tukey's multiple comparison test was applied to test for statistically significant differences between two groups. \*, \*\*, \*\*\*, and \*\*\*\* denotes  $p < 0.05$ ,  $p < 0.01$ ,  $p < 0.001$ , and  $p < 0.0001$ , respectively. All graphs and statistics were generated in GraphPad Prism 9.0 software.

**Supplementary Materials:** The following supporting information can be downloaded at: <https://www.mdpi.com/article/10.3390/ijms23147923/s1>. Refs. [60,62] are cited in the supplementary materials.

**Author Contributions:** Conceptualization, J.S., R.T., H.S., A.A., S.F.P. and H.O.-A.; methodology, J.S., S.K., F.H., A.G., P.R., S.G., R.T., H.S., A.A., S.F.P. and H.O.-A.; software, J.S. and H.O.-A.; validation, J.S., S.F.P., H.S. and H.O.-A.; formal analysis, J.S., S.F.P. and H.O.-A.; investigation, J.S., S.K., F.H., A.G., P.R., M.-S.T., S.G., R.T., H.S., A.A., S.F.P. and H.O.-A.; data curation, J.S., S.K., F.H., A.G., P.R., M.-S.T., S.G., R.T., H.S., A.A., S.F.P. and H.O.-A.; resources, S.G., R.T., H.S., S.F.P., A.A. and H.O.-A.; writing—original draft preparation, J.S. and H.O.-A.; writing—review and editing, J.S., S.K., F.H., A.G., P.R., S.G., R.T., H.S., A.A., S.F.P. and H.O.-A.; visualization, J.S. and H.O.-A.; supervision, R.T., H.S., S.F.P., A.A. and H.O.-A.; project administration, J.S., R.T., H.S., S.F.P., A.A. and H.O.-A.; funding acquisition, S.F.P. and H.O.-A. All authors have read and agreed to the published version of the manuscript.

**Funding:** This work is funded by the Marie Skłodowska-Curie Innovative Training Network (ITN) grant agreement number: 813834-pHioniC-H2020-MSCA-ITN-2018, and by the Ministère de l'Enseignement Supérieur et de la Recherche, the Région Hauts-de-France (Picardie), the FEDER (Fonds Européen de Développement Économique Régional), the Université Picardie Jules Verne, and the Ligue Contre le Cancer (Septentrion).

**Institutional Review Board Statement:** The study was conducted according to the tenets of the Declaration of Helsinki and was approved by an institutional review board "Direction de la Recherche, Clinique et de l'Innovation", CHU Amiens-Picardie (reference: Pan-Ionic: PI2021\_843\_0027).

**Informed Consent Statement:** Informed consent was obtained from all study participants.

**Data Availability Statement:** Not applicable.

**Acknowledgments:** We are grateful to Marie-Pierre Mabilbe (Anatomy and Pathology Department, Amiens Hospital) and Mette Flinck (Department of Biology, University of Copenhagen) for the excellent technical assistance, and to Anna Trauzold (Institute of Experimental Cancer Research, Kiel University, Kiel, Germany) for providing us with the PDAC cell lines.

**Conflicts of Interest:** The authors declare no conflict of interest.

## References

1. Kleeff, J.; Korc, M.; Apte, M.; La Vecchia, C.; Johnson, C.D.; Biankin, A.V.; Neale, R.E.; Tempero, M.; Tuveson, D.A.; Hruban, R.H.; et al. Pancreatic cancer. *Nat. Rev. Dis. Primers* **2016**, *2*, 16022. [CrossRef]
2. Siegel, R.L.; Miller, K.D.; Jemal, A. Cancer statistics, 2018. *CA A Cancer J. Clin.* **2018**, *68*, 7–30. [CrossRef]
3. Quinonero, F.; Mesas, C.; Doello, K.; Cabeza, L.; Perazzoli, G.; Jimenez-Luna, C.; Rama, A.R.; Melguizo, C.; Prados, J. The challenge of drug resistance in pancreatic ductal adenocarcinoma: A current overview. *Cancer Biol. Med.* **2019**, *16*, 688–699. [CrossRef]

4. Berridge, M.J.; Lipp, P.; Bootman, M.D. The versatility and universality of calcium signalling. *Nat. Rev. Mol. Cell Biol.* **2000**, *1*, 11–21. [[CrossRef](#)]
5. Borowiec, A.S.; Bidaux, G.; Pigat, N.; Goffin, V.; Bernichtein, S.; Capiod, T. Calcium channels, external calcium concentration and cell proliferation. *Eur. J. Pharmacol.* **2014**, *739*, 19–25. [[CrossRef](#)]
6. Hodeify, R.; Yu, F.; Courjaret, R.; Nader, N.; Dib, M.; Sun, L.; Adap, E.; Hubrack, S.; Machaca, K. Regulation and Role of Store-Operated Ca(2+) Entry in Cellular Proliferation. In *Calcium Entry Channels in Non-Excitable Cells*; Kozak, J.A., Putney, J.W., Jr., Eds.; CRC Press/Taylor & Francis: Boca Raton, FL, USA, 2018; pp. 215–240.
7. Capiod, T. The need for calcium channels in cell proliferation. *Recent Pat. Anticancer Drug Discov.* **2013**, *8*, 4–17. [[CrossRef](#)]
8. Tajada, S.; Villalobos, C. Calcium Permeable Channels in Cancer Hallmarks. *Front. Pharmacol.* **2020**, *11*, 968. [[CrossRef](#)]
9. Chen, X.; Sooch, G.; Demaree, I.S.; White, F.A.; Obukhov, A.G. Transient Receptor Potential Canonical (TRPC) Channels: Then and Now. *Cells* **2020**, *9*, 1983. [[CrossRef](#)]
10. Wang, H.; Cheng, X.; Tian, J.; Xiao, Y.; Tian, T.; Xu, F.; Hong, X.; Zhu, M.X. TRPC channels: Structure, function, regulation and recent advances in small molecular probes. *Pharmacol. Ther.* **2020**, *209*, 107497. [[CrossRef](#)]
11. Elzamzamy, O.M.; Penner, R.; Hazlehurst, L.A. The Role of TRPC1 in Modulating Cancer Progression. *Cells* **2020**, *9*, 388. [[CrossRef](#)]
12. Faouzi, M.; Hague, F.; Geerts, D.; Ay, A.S.; Potier-Cartreau, M.; Ahidouch, A.; Ouadid-Ahidouch, H. Functional cooperation between KCa3.1 and TRPC1 channels in human breast cancer: Role in cell proliferation and patient prognosis. *Oncotarget* **2016**, *7*, 36419–36435. [[CrossRef](#)]
13. Sun, Y.; Ye, C.; Tian, W.; Ye, W.; Gao, Y.Y.; Feng, Y.D.; Zhang, H.N.; Ma, G.Y.; Wang, S.J.; Cao, W.; et al. TRPC1 promotes the genesis and progression of colorectal cancer via activating CaM-mediated PI3K/AKT signaling axis. *Oncogenesis* **2021**, *10*, 67. [[CrossRef](#)]
14. Zhang, Y.; Lun, X.; Guo, W. Expression of TRPC1 and SBEM protein in breast cancer tissue and its relationship with clinicopathological features and prognosis of patients. *Oncol. Lett.* **2020**, *20*, 392. [[CrossRef](#)]
15. Wang, A.; Guo, H.; Long, Z. Integrative Analysis of Differently Expressed Genes Reveals a 17-Genes Prognosis Signature for Endometrial Carcinoma. *Biomed. Res. Int.* **2021**, *2021*, 4804694. [[CrossRef](#)]
16. Mandavilli, S.; Singh, B.B.; Sahnoun, A.E. Serum calcium levels, TRPM7, TRPC1, microcalcifications, and breast cancer using breast imaging reporting and data system scores. *Breast Cancer* **2012**, *2013*, 1–7. [[CrossRef](#)]
17. Ibrahim, S.; Dakik, H.; Vandier, C.; Chautard, R.; Paintaud, G.; Mazurier, F.; Lecomte, T.; Gueguinou, M.; Raoul, W. Expression Profiling of Calcium Channels and Calcium-Activated Potassium Channels in Colorectal Cancer. *Cancers* **2019**, *11*, 561. [[CrossRef](#)]
18. Liu, X.; Zou, J.; Su, J.; Lu, Y.; Zhang, J.; Li, L.; Yin, F. Downregulation of transient receptor potential cation channel, subfamily C, member 1 contributes to drug resistance and high histological grade in ovarian cancer. *Int. J. Oncol.* **2016**, *48*, 243–252. [[CrossRef](#)]
19. Chen, L.; Shan, G.; Ge, M.; Qian, H.; Xia, Y. Transient Receptor Potential Channel 1 Potentially Serves as a Biomarker Indicating T/TNM Stages and Predicting Long-Term Prognosis in Patients with Renal Cell Carcinoma. *Front. Surg.* **2022**, *9*, 853310. [[CrossRef](#)]
20. Xu, Z.; Shao, Z.; Wang, M.; Thorndike, E.; Song, Y.; Shang, Z. Expression of transient receptor potential canonical 1 (TRPC1) in tongue squamous cell carcinoma and correlations with clinicopathological features and outcomes. *Int. J. Clin. Exp. Pathol.* **2017**, *10*, 1477–1487.
21. Ke, C.; Long, S. Dysregulated transient receptor potential channel 1 expression and its correlation with clinical features and survival profile in surgical non-small-cell lung cancer patients. *J. Clin. Lab. Anal.* **2022**, *36*, e24229. [[CrossRef](#)]
22. Bollimuntha, S.; Singh, B.B.; Shavali, S.; Sharma, S.K.; Ebadi, M. TRPC1-mediated inhibition of 1-methyl-4-phenylpyridinium ion neurotoxicity in human SH-SY5Y neuroblastoma cells. *J. Biol. Chem.* **2005**, *280*, 2132–2140. [[CrossRef](#)]
23. Bomben, V.C.; Sontheimer, H. Disruption of transient receptor potential canonical channel 1 causes incomplete cytokinesis and slows the growth of human malignant gliomas. *Glia* **2010**, *58*, 1145–1156. [[CrossRef](#)]
24. Asghar, M.Y.; Magnusson, M.; Kempainen, K.; Sukumaran, P.; Lof, C.; Pulli, I.; Kalhori, V.; Tornquist, K. Transient Receptor Potential Canonical 1 (TRPC1) Channels as Regulators of Sphingolipid and VEGF Receptor Expression: Implications for Thyroid Cancer Cell Migration and Proliferation. *J. Biol. Chem.* **2015**, *290*, 16116–16131. [[CrossRef](#)]
25. Kaemmerer, E.; Turner, D.; Peters, A.A.; Roberts-Thomson, S.J.; Monteith, G.R. An automated epifluorescence microscopy imaging assay for the identification of phospho-AKT level modulators in breast cancer cells. *J. Pharmacol. Toxicol. Methods* **2018**, *92*, 13–19. [[CrossRef](#)]
26. El Hiani, Y.; Ahidouch, A.; Lehen'kyi, V.; Hague, F.; Gouilleux, F.; Mentaverri, R.; Kamel, S.; Lassoued, K.; Brule, G.; Ouadid-Ahidouch, H. Extracellular signal-regulated kinases 1 and 2 and TRPC1 channels are required for calcium-sensing receptor-stimulated MCF-7 breast cancer cell proliferation. *Cell Physiol. Biochem.* **2009**, *23*, 335–346. [[CrossRef](#)]
27. El Hiani, Y.; Lehen'kyi, V.; Ouadid-Ahidouch, H.; Ahidouch, A. Activation of the calcium-sensing receptor by high calcium induced breast cancer cell proliferation and TRPC1 cation channel over-expression potentially through EGFR pathways. *Arch. Biochem. Biophys.* **2009**, *486*, 58–63. [[CrossRef](#)]
28. Tajeddine, N.; Gailly, P. TRPC1 protein channel is major regulator of epidermal growth factor receptor signaling. *J. Biol. Chem.* **2012**, *287*, 16146–16157. [[CrossRef](#)]
29. Selli, C.; Erac, Y.; Kosova, B.; Erdal, E.S.; Tosun, M. Silencing of TRPC1 regulates store-operated calcium entry and proliferation in Huh7 hepatocellular carcinoma cells. *Biomed. Pharmacother.* **2015**, *71*, 194–200. [[CrossRef](#)]



30. Selli, C.; Pearce, D.A.; Sims, A.H.; Tosun, M. Differential expression of store-operated calcium- and proliferation-related genes in hepatocellular carcinoma cells following TRPC1 ion channel silencing. *Mol. Cell Biochem.* **2016**, *420*, 129–140. [[CrossRef](#)]
31. Zeng, B.; Yuan, C.; Yang, X.; Atkin, S.L.; Xu, S.Z. TRPC channels and their splice variants are essential for promoting human ovarian cancer cell proliferation and tumorigenesis. *Curr. Cancer Drug Targets* **2013**, *13*, 103–116. [[CrossRef](#)]
32. Zeng, Y.Z.; Zhang, Y.Q.; Chen, J.Y.; Zhang, L.Y.; Gao, W.L.; Lin, X.Q.; Huang, S.M.; Zhang, F.; Wei, X.L. TRPC1 Inhibits Cell Proliferation/Invasion and Is Predictive of a Better Prognosis of Esophageal Squamous Cell Carcinoma. *Front. Oncol.* **2021**, *11*, 627713. [[CrossRef](#)]
33. Zhang, L.Y.; Zhang, Y.Q.; Zeng, Y.Z.; Zhu, J.L.; Chen, H.; Wei, X.L.; Liu, L.J. TRPC1 inhibits the proliferation and migration of estrogen receptor-positive Breast cancer and gives a better prognosis by inhibiting the PI3K/AKT pathway. *Breast Cancer Res. Treat* **2020**, *182*, 21–33. [[CrossRef](#)]
34. Selli, C.; Erac, Y.; Tosun, M. Simultaneous measurement of cytosolic and mitochondrial calcium levels: Observations in TRPC1-silenced hepatocellular carcinoma cells. *J. Pharmacol. Toxicol. Methods* **2015**, *72*, 29–34. [[CrossRef](#)]
35. Madsen, C.P.; Klausen, T.K.; Fabian, A.; Hansen, B.J.; Pedersen, S.F.; Hoffmann, E.K. On the role of TRPC1 in control of Ca<sup>2+</sup> influx, cell volume, and cell cycle. *Am. J. Physiol. Cell Physiol.* **2012**, *303*, C625–C634. [[CrossRef](#)]
36. Davis, F.M.; Peters, A.A.; Grice, D.M.; Cabot, P.J.; Parat, M.O.; Roberts-Thomson, S.J.; Monteith, G.R. Non-stimulated, agonist-stimulated and store-operated Ca<sup>2+</sup> influx in MDA-MB-468 breast cancer cells and the effect of EGF-induced EMT on calcium entry. *PLoS ONE* **2012**, *7*, e36923. [[CrossRef](#)]
37. El Boustany, C.; Bidaux, G.; Enfissi, A.; Delcourt, P.; Prevarskaya, N.; Capiod, T. Capacitative calcium entry and transient receptor potential canonical 6 expression control human hepatoma cell proliferation. *Hepatology* **2008**, *47*, 2068–2077. [[CrossRef](#)]
38. Lepannetier, S.; Zanou, N.; Yerna, X.; Emeriau, N.; Dufour, I.; Masquelier, J.; Muccioli, G.; Tajeddine, N.; Gailly, P. Sphingosine-1-phosphate-activated TRPC1 channel controls chemotaxis of glioblastoma cells. *Cell Calcium* **2016**, *60*, 373–383. [[CrossRef](#)]
39. Rychkov, G.; Barritt, G.J. TRPC1 Ca(2+)-permeable channels in animal cells. *Handb. Exp. Pharmacol.* **2007**, *179*, 23–52. [[CrossRef](#)]
40. Hong, J.H.; Li, Q.; Kim, M.S.; Shin, D.M.; Feske, S.; Birnbaumer, L.; Cheng, K.T.; Ambudkar, I.S.; Muallem, S. Polarized but differential localization and recruitment of STIM1, Orai1 and TRPC channels in secretory cells. *Traffic* **2011**, *12*, 232–245. [[CrossRef](#)]
41. Kim, M.H.; Seo, J.B.; Burnett, L.A.; Hille, B.; Koh, D.S. Characterization of store-operated Ca<sup>2+</sup> channels in pancreatic duct epithelia. *Cell Calcium* **2013**, *54*, 266–275. [[CrossRef](#)]
42. Dong, H.; Shim, K.N.; Li, J.M.; Estrema, C.; Ornelas, T.A.; Nguyen, F.; Liu, S.; Ramamoorthy, S.L.; Ho, S.; Carethers, J.M.; et al. Molecular mechanisms underlying Ca<sup>2+</sup>-mediated motility of human pancreatic duct cells. *Am. J. Physiol. Cell Physiol.* **2010**, *299*, C1493–C1503. [[CrossRef](#)]
43. Ravi, M.; Paramesh, V.; Kaviya, S.R.; Anuradha, E.; Solomon, F.D. 3D cell culture systems: Advantages and applications. *J. Cell Physiol.* **2015**, *230*, 16–26. [[CrossRef](#)]
44. Ambudkar, I.S.; de Souza, L.B.; Ong, H.L. TRPC1, Orai1, and STIM1 in SOCE: Friends in tight spaces. *Cell Calcium* **2017**, *63*, 33–39. [[CrossRef](#)]
45. Sobradillo, D.; Hernandez-Morales, M.; Ubierna, D.; Moyer, M.P.; Nunez, L.; Villalobos, C. A reciprocal shift in transient receptor potential channel 1 (TRPC1) and stromal interaction molecule 2 (STIM2) contributes to Ca<sup>2+</sup> remodeling and cancer hallmarks in colorectal carcinoma cells. *J. Biol. Chem.* **2014**, *289*, 28765–28782. [[CrossRef](#)]
46. Saez-Rodriguez, J.; MacNamara, A.; Cook, S. Modeling Signaling Networks to Advance New Cancer Therapies. *Annu. Rev. Biomed. Eng.* **2015**, *17*, 143–163. [[CrossRef](#)]
47. Azimi, I.; Milevskiy, M.J.G.; Kaemmerer, E.; Turner, D.; Yapa, K.; Brown, M.A.; Thompson, E.W.; Roberts-Thomson, S.J.; Monteith, G.R. TRPC1 is a differential regulator of hypoxia-mediated events and Akt signalling in PTEN-deficient breast cancer cells. *J. Cell Sci.* **2017**, *130*, 2292–2305. [[CrossRef](#)]
48. Fabian, A.; Bertrand, J.; Lindemann, O.; Pap, T.; Schwab, A. Transient receptor potential canonical channel 1 impacts on mechanosignaling during cell migration. *Pflug. Arch.* **2012**, *464*, 623–630. [[CrossRef](#)]
49. Fels, B.; Bulk, E.; Petho, Z.; Schwab, A. The Role of TRP Channels in the Metastatic Cascade. *Pharmaceuticals* **2018**, *11*, 48. [[CrossRef](#)]
50. Park, W.; Chawla, A.; O'Reilly, E.M. Pancreatic Cancer: A Review. *JAMA* **2021**, *326*, 851–862. [[CrossRef](#)]
51. Perrouin-Verbe, M.A.; Schoentgen, N.; Talagas, M.; Garlantezec, R.; Uguen, A.; Doucet, L.; Rosec, S.; Marcorelles, P.; Potier-Cartreau, M.; Vandier, C.; et al. Overexpression of certain transient receptor potential and Orai channels in prostate cancer is associated with decreased risk of systemic recurrence after radical prostatectomy. *Prostate* **2019**, *79*, 1793–1804. [[CrossRef](#)]
52. Perrouin Verbe, M.A.; Bruyere, F.; Rozet, F.; Vandier, C.; Fromont, G. Expression of store-operated channel components in prostate cancer: The prognostic paradox. *Hum. Pathol.* **2016**, *49*, 77–82. [[CrossRef](#)]
53. Bonelli, P.; Tuccillo, F.M.; Borrelli, A.; Schiattarella, A.; Buonaguro, F.M. CDK/CCN and CDKI alterations for cancer prognosis and therapeutic predictivity. *Biomed. Res. Int.* **2014**, *2014*, 361020. [[CrossRef](#)]
54. De Luca, A.; Maiello, M.R.; D'Alessio, A.; Pergameno, M.; Normanno, N. The RAS/RAF/MEK/ERK and the PI3K/AKT signalling pathways: Role in cancer pathogenesis and implications for therapeutic approaches. *Expert Opin. Ther. Targets* **2012**, *16* (Suppl. S2), S17–S27. [[CrossRef](#)]
55. Roy, S.K.; Srivastava, R.K.; Shankar, S. Inhibition of PI3K/AKT and MAPK/ERK pathways causes activation of FOXO transcription factor, leading to cell cycle arrest and apoptosis in pancreatic cancer. *J. Mol. Signal* **2010**, *5*, 10. [[CrossRef](#)]

56. Nussinov, R.; Wang, G.; Tsai, C.J.; Jang, H.; Lu, S.; Banerjee, A.; Zhang, J.; Gaponenko, V. Calmodulin and PI3K Signaling in KRAS Cancers. *Trends Cancer* **2017**, *3*, 214–224. [[CrossRef](#)]
57. Zanou, N.; Schakman, O.; Louis, P.; Ruegg, U.T.; Dietrich, A.; Birnbaumer, L.; Gailly, P. Trpc1 ion channel modulates phosphatidylinositol 3-kinase/Akt pathway during myoblast differentiation and muscle regeneration. *J. Biol. Chem.* **2012**, *287*, 14524–14534. [[CrossRef](#)]
58. Chaudhuri, P.; Rosenbaum, M.A.; Sinharoy, P.; Damron, D.S.; Birnbaumer, L.; Graham, L.M. Membrane translocation of TRPC6 channels and endothelial migration are regulated by calmodulin and PI3 kinase activation. *Proc. Natl. Acad. Sci. USA* **2016**, *113*, 2110–2115. [[CrossRef](#)]
59. Jonckheere, N.; Van Seuning, I. Integrative analysis of the cancer genome atlas and cancer cell lines encyclopedia large-scale genomic databases: MUC4/MUC16/MUC20 signature is associated with poor survival in human carcinomas. *J. Transl. Med.* **2018**, *16*, 259. [[CrossRef](#)]
60. Radoslavova, S.; Folcher, A.; Lefebvre, T.; Kondratska, K.; Guenin, S.; Dhennin-Duthille, I.; Gautier, M.; Prevarskaya, N.; Ouadid-Ahidouch, H. Orai1 Channel Regulates Human-Activated Pancreatic Stellate Cell Proliferation and TGFbeta1 Secretion through the AKT Signaling Pathway. *Cancers* **2021**, *13*, 2395. [[CrossRef](#)]
61. Chamlali, M.; Kouba, S.; Rodat-Despoix, L.; Todesca, L.M.; Petho, Z.; Schwab, A.; Ouadid-Ahidouch, H. Orai3 Calcium Channel Regulates Breast Cancer Cell Migration through Calcium-Dependent and -Independent Mechanisms. *Cells* **2021**, *10*, 3487. [[CrossRef](#)]
62. Pfaffl, M.W.; Horgan, G.W.; Dempfle, L. Relative expression software tool (REST) for group-wise comparison and statistical analysis of relative expression results in real-time PCR. *Nucleic Acids Res.* **2002**, *30*, e36. [[CrossRef](#)]





Supplementary Figures

# The TRPC1 channel forms a PI3K/CaM complex and regulates pancreatic ductal adenocarcinoma cell proliferation in a $Ca^{2+}$ -independent manner

Julie Schnipper<sup>1</sup>, Sana Kouba<sup>1</sup>, Frédéric Hague<sup>1</sup>, Alban Girault<sup>1</sup>, Pierre Rybarczyk<sup>1,2</sup>, Marie-Sophie Telliez<sup>1</sup>, Stéphanie Guénin<sup>3</sup>, Riad Tebbakha<sup>1,2</sup>, Henri Sevestre<sup>1,2</sup>, Ahmed Ahidouch<sup>1,4</sup>, Stine Falsig Pedersen<sup>5</sup>, Halima Ouadid-Ahidouch<sup>1\*</sup>

- <sup>1</sup> Laboratory of Cellular and Molecular Physiology, UR UPJV 4667, University of Picardie Jules Verne, Amiens, France; julie\_schnipper@hotmail.com (JS), Sana Kouba sana.kouba@hotmail.com (SK), fh-lnc@u-picardie.fr (FH), alban.girault@u-picardie.fr (AG), marie-sophie.telliez@u-picardie.fr (MST),
  - <sup>2</sup> Anatomy and Pathology Department, Amiens Hospital, University of Picardie Jules Verne, Tumorothèque of Picardie, Amiens, France; Rybarczyk.Pierre@chu-amiens.fr (PR), Henrisevestre@gmail.com (HS), Tebbakha.Riad@chu-amiens.fr (RT)
  - <sup>3</sup> Centre de Ressources Régional en Biologie Moléculaire, Université de Picardie Jules Verne, Amiens, France; stephanie.vandecasteele@u-picardie.fr (SG)
  - <sup>4</sup> Biology department, University Ibn Zohr, Agadir, Morocco, ahidouch@gmail.com (AA)
  - <sup>5</sup> Section for Cell Biology and Physiology, Department of Biology, University of Copenhagen, Copenhagen Ø, Denmark; sfpedersen@bio.ku.dk (SFP)
- \* Correspondence: halima.ahidouch-ouadid@u-picardie.fr (HOA); Tel.: +33-322827646

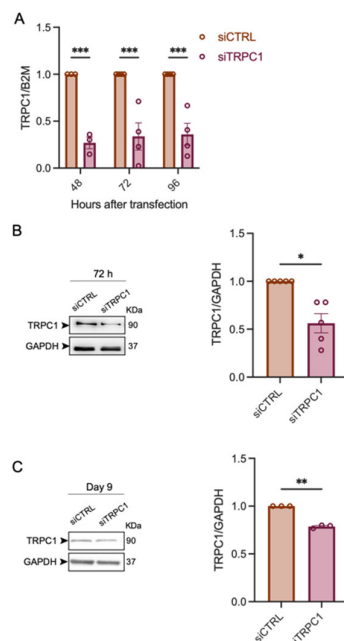


**Figure S1:** (A) TRPC1 mRNA expression evaluated by qPCR 48, 72 and 96 hours after transfection with siCTRL and siTRPC1 in PANC-1 lines (n = 3-4). Materials and methods for qPCR are described below. (B) TRPC1 protein expression evaluated 72 hours after transfection with siCTRL and siTRPC1 in PANC-1 lines (n = 5). (C) TRPC1 protein expression evaluated 9 days after transfection with siCTRL and siTRPC1 in PANC-1 spheroids (n = 3). \*, \*\* and \*\*\* indicate  $p < 0.05$ , 0.01 and 0.001, respectively.

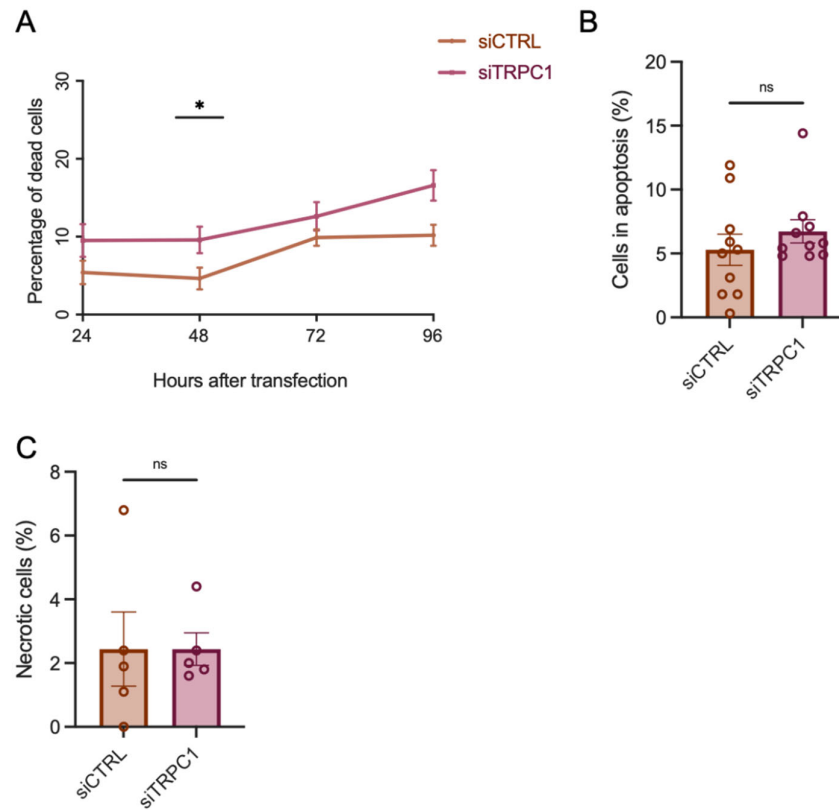


**Figure S2:** (A) Percentage of dead cells analysed by the Trypan Blue Assay after 24, 48, 72 and 96 h after transfection with siCTRL and siTRPC1 in PANC-1 cells, respectively (n = 4). (B) Quantification of Annexin-5 analysis of cells in apoptosis 72 h after transfection with siCTRL and siTRPC1 in PANC-1 cells (n = 3). Methods and materials for Annexin-5 analysis are described below. (C) Quantification of Annexin-5 analysis of cells necrotic cells 72 h after transfection with siCTRL and siTRPC1 in PANC-1 cells (n = 3). Methods and materials for Annexin-5 analysis are described below. ). \* indicate  $p < 0.05$  and ns indicate non-significant.

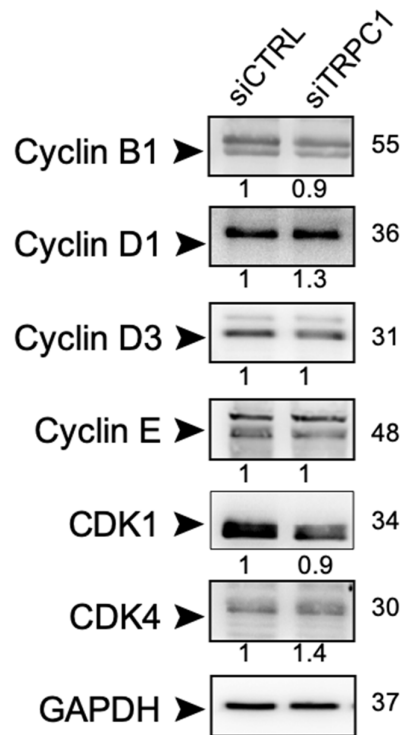


**Figure S3:** Westernblot analysis of different cell cycle regulating proteins 72 h after transfection with siCTRL and siTRPC1 in PANC-1 cells (n= 3-4, no significance was found).

### Supplemental Materials and Methods

#### Quantitative Real-Time PCR (qRT-PCR)

Total RNA was extracted with the Trizol reagent (Sigma, Saint-Quentin-Fallavier, France) method as previously described [60]. RNA concentration and purity were determined using a spectrophotometer (NanoDrop 2000, Wilmington, NC, USA). 2 µg of RNA was converted into cDNA with the MultiScribe™ Reverse Transcriptase kit (Applied Biosystems, Carlsbad, CA, USA). Real-time PCR was performed on a LightCycler 480 System (Roche, Basel, Switzerland) using SYBR Green I PCR master mix (Life Science, Roche, Basel, Switzerland), and sense and antisense PCR primers specific to TRPC1 (forward 5'GAGGTGATGGCGCTGAAGG-3' and reverse 5'-GCACGCCAGCAAGAAAAGC-3') and B2M (forward 5'GTCTTTCAGCAAGGACTGGTC3' and reverse CAAATGCGGCATCTTCAAACC3'). TRPC1 mRNA expression was normalized to B2M, used as housekeeping gene, and compared to the control sample, using the Pfaffl method [62].

#### FACS analysis of annexin V and propidium iodide staining

To evaluate the percentage of apoptotic and necrotic cells, we detected phosphatidylserine residues at the outer plasma membrane by the FITC Annexin V Apoptosis Detection Kit I (BD Biosciences Pharmingen, Le Pont-de-Claix, France).  $5 \times 10^5$  transfected PANC-1 cells were seeded, and collected after 72 h. Both detached and adherent cells were collected by trypsinization. Then the cells were pelleted, washed twice with ice-cold PBS and resuspended in 1× binding buffer (BD Biosciences

Pharmingen). Following the PE Annexin V Apoptosis Detection Kit staining protocol, we added FITC Annexin V and propidium iodide to the cell pellets and incubated them at 25°C in the dark for 15 min. Binding buffer was then added to each tube and samples were directly analysed by the flow cytometer (Accuri®) in order to determine the percentage of apoptotic cells.

## References

60. Radoslavova, S.; Folcher, A.; Lefebvre, T.; Kondratska, K.; Guenin, S.; Dhennin-Duthille, I.; Gautier, M.; Prevarskaya, N.; Ouadid-Ahidouch, H., Orai1 Channel Regulates Human-Activated Pancreatic Stellate Cell Proliferation and TGFbeta1 Secretion through the AKT Signaling Pathway. *Cancers (Basel)* **2021**, *13*, (10), DOI: 10.3390/cancers13102395.
62. Pfaffl, M. W.; Horgan, G. W.; Dempfle, L., Relative expression software tool (REST) for group-wise comparison and statistical analysis of relative expression results in real-time PCR. *Nucleic Acids Res* **2002**, *30*, (9), e36, DOI: 10.1093/nar/30.9.e36.

## Complementary results

We have shown that TRPC1 is highly expressed in PDAC tissue compared to adjacent tissue. Our complementary results revealed that patients with vascular and nerve tumor invasion and with overexpression of TRPC1 ( $n = 12/21$ ) displayed an increased plasma membrane localization of TRPC1. This was not found in patients without vascular or nerve invasion, indicating that the plasma membrane localization of TRPC1 correlates with aggressiveness.

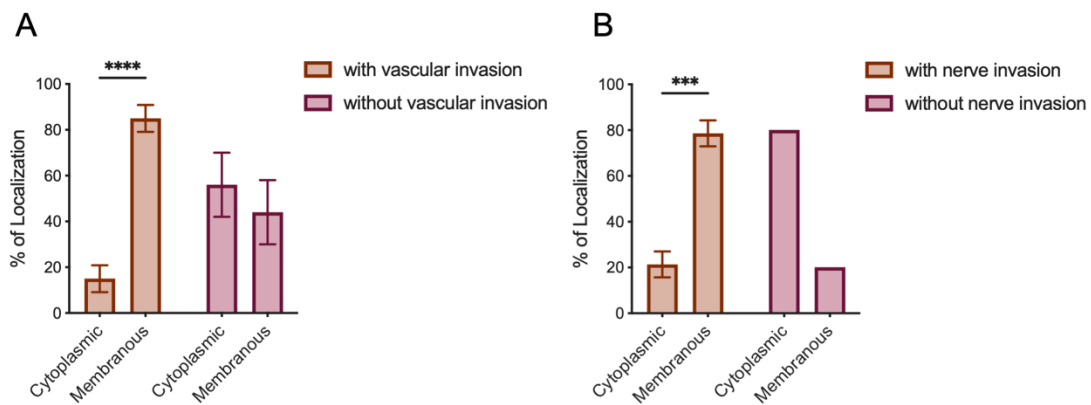


Figure 36. The localization of TRPC1 correlates with clinical factors. The plasma membrane localization of TRPC1 correlates with vascular invasion and nerve invasion in samples from patients with PDAC, where TRPC1 is upregulated ( $n=12$ ). \*\*\*\* indicates  $p < 0.0001$ .

## Part 2: Acid adaptation promotes TRPC1 plasma membrane localization leading to pancreatic ductal adenocarcinoma cell proliferation and migration through $\text{Ca}^{2+}$ entry and interaction with PI3K/CaM

### Summary

The unique tumor microenvironment of PDAC evolves throughout carcinogenesis. It comprises an excessive ECM, non-neoplastic cells such as PSCs, CAFs, and immune and endothelial cells. Solid PDAC tumors display high interstitial pressure, vascular collapse, poor perfusion, with high levels of inflammatory and oxidative stress and hypoxia. Together with the glycolytic shift in the cancer cells, this causes an extracellular acidification characteristic of the tumor microenvironment (Elingaard-Larsen et al. 2022). The tumor acidosis is not constant but rather temporal and spatial, with some regions exhibiting near-neutral to neutral pH values, and other areas are highly acidic with a pH as low as pH 5.6 (Vaupel et al. 1989, Helmlinger et al. 1997, Rohani et al. 2019, Boedtkjer and Pedersen 2020). The effect of extracellular acidity depends on the duration and extent of acidity. Several studies have shown that a long-term acidic treatment selects for a more aggressive phenotype, as only cells that have adapted to the hostile microenvironment can survive and proliferate. Interestingly, the acidic microenvironment renders the cancer cells more motile, invasive, and resistant to cytotoxic treatments. The acidic-induced selection is particularly of interest when the cancer cells encounter a less acidic or neutral microenvironment, as an increase in  $\text{pH}_i$  can enhance proliferation (Flinck et al. 2018, Boedtkjer and Pedersen 2020, Andersen et al. 2021, Elingaard-Larsen et al. 2022).

Ion channels, often known as sensors of the surrounding microenvironment, can be affected by  $\text{pH}_o$  changes and transduce the signal (Petho et al. 2020). Among ion channels is the TRPC1, known to be a mechanosensitive ion channel, for instance, by transducing signals from pressure and hypoxia (Fels et al. 2016, Azimi et al. 2017, Radoslavova et al. 2022). To date, it has not been shown how acidosis can affect TRPC1, but other TRPC channels are activated by acidification. As we have described that TRPC1 is overexpressed in human PDAC tissue and cell lines and how it regulates proliferation through the PI3K/CaM/AKT axis, we in the following study aimed to investigate how the fluctuating acidic tumor microenvironment could affect the function of TRPC1 and downstream mechanistic properties of PDAC.

To assess the influence of the fluctuating acidic tumor microenvironment, we developed a model where PANC-1 cells were grown in either normal conditions (pH 7.4), acid-adapted (30 days in pH 6.5), or in recovery conditions (cells adapted to pH 6.5 and reseeded for 14 days in pH 7.4).

Initially, our  $\text{pH}_i$  measurements demonstrated that acid-adapted PANC-1 cells exhibit a lower  $\text{pH}_i$  than cells grown in normal pH conditions. Further, acid-adapted cells measured in normal  $\text{pH}_o$  conditions exhibited an even more alkaline  $\text{pH}_i$ . Next, our western blot analysis, confocal imaging, and biotinylation assay



demonstrated that acid adaptation decreased the total expression of TRPC1 but favored its plasma membrane localization. The TRPC1 expression was further increased and maintained in the plasma membrane in the recovery conditions.

We further showed that acid adaptation promoted PANC-1 cell migration but inhibited proliferation. Interestingly, the proliferation was enhanced in recovery conditions in 2D and 3D models.

To demonstrate the role of TRPC1 in the acidic tumor microenvironment, we used the siRNA KD approach. We showed that TRPC1 KD inhibited PANC-1 cell migration in normal, acid-adapted, and -recovered conditions. Furthermore, we showed that silencing of TRPC1 strongly inhibited the proliferation of acid-recovered PANC-1 cells and spheroids, compared to the control, while this effect was less evident in acid-adapted conditions.

We aimed to investigate the underlying mechanism of the tumor microenvironment and TRPC1 in PANC-1 cells. Our flow cytometric analysis revealed that acid adaptation resulted in an increased number of cells in the G0/G1 phase and a decreased number in the G2/M phase. Notably, the acid-recovered cells showed an increased number of cells in the S phase. The TRPC1 KD resulted in a further accumulation of cells in the G0/G1 phase and a reduction in the G2/M phase. This phenotype was maintained in acid-recovered conditions. Along with the cell cycle analysis, our immunoblot analysis of cell cycle regulating proteins revealed that silencing of TRPC1 reduced the expression of CDK6, 2, and 1, and cyclin A while increasing the expression of p21. Notably, the TRPC1 KD had a more substantial effect in recovered conditions than in normal and acidic conditions.

As we previously have shown that TRPC1 forms a complex with PI3K and CaM, we aimed to demonstrate the role of the acidic tumor microenvironment and TRPC1 in association with PI3K signaling. Our confocal imaging and subsequent co-localization analysis showed that TRPC1 co-localized with the PI3K-p85 $\alpha$  subunit in acid-adapted conditions, which was maintained upon recovery. These results were confirmed by PLA and co-IP, which revealed a strong interaction between TRPC1 and the PI3K-p85 $\alpha$  subunit in acid-adapted PANC-1 cells. TRPC1 also interacted with the connecting protein CaM in all pH conditions. These interactions were attenuated upon TRPC1 silencing.

Thus, we aimed to investigate the downstream effect of the interaction between TRPC1 and PI3K. We found that the activation of ERK1/2 was profoundly inhibited upon TRPC1 KD in both acidic and recovered conditions, compared to what we previously observed in normal pH conditions. Furthermore, the TRPC1 silencing also decreased the activation of AKT, particularly in acid-recovered conditions. Additionally, inhibition of CaM reduced the activation of AKT solely in acid-recovered cells, while ERK1/2 levels were affected in all conditions, but notably in acid-adapted and acid-recovered conditions.

Our Ca<sup>2+</sup> imaging assay revealed that basal Ca<sup>2+</sup> entry was increased in acid-recovered cells compared to cells grown in normal and acidic conditions. Furthermore, the TRPC1 KD only affected the Ca<sup>2+</sup> entry in

acid-adapted and -recovered cells. TRPC1 silencing did not affect SOCE in either acid-adapted or recovered PANC-1 cells.

Given that TRPC1 could regulate the basal  $\text{Ca}^{2+}$ , we finally investigated if extracellular  $\text{Ca}^{2+}$  levels could influence cell migration and proliferation. Here, we found that low extracellular  $\text{Ca}^{2+}$  levels decreased cell proliferation and migration solely in acid-adapted and -recovered conditions but not in normal pH conditions. In these conditions, TRPC1 KD slightly reduced migration and proliferation.

Taken together, these data revealed a novel insight into the interplay between the tumor microenvironment and the mechanosensitive ion channel TRPC1. We showed that the fluctuations of the tumor microenvironment translocate TRPC1 to the plasma membrane, favoring the interaction with PI3K/CaM and  $\text{Ca}^{2+}$  entry that regulates PANC-1 migration and proliferation, both through the AKT and ERK1/2 axis (Figure 37).

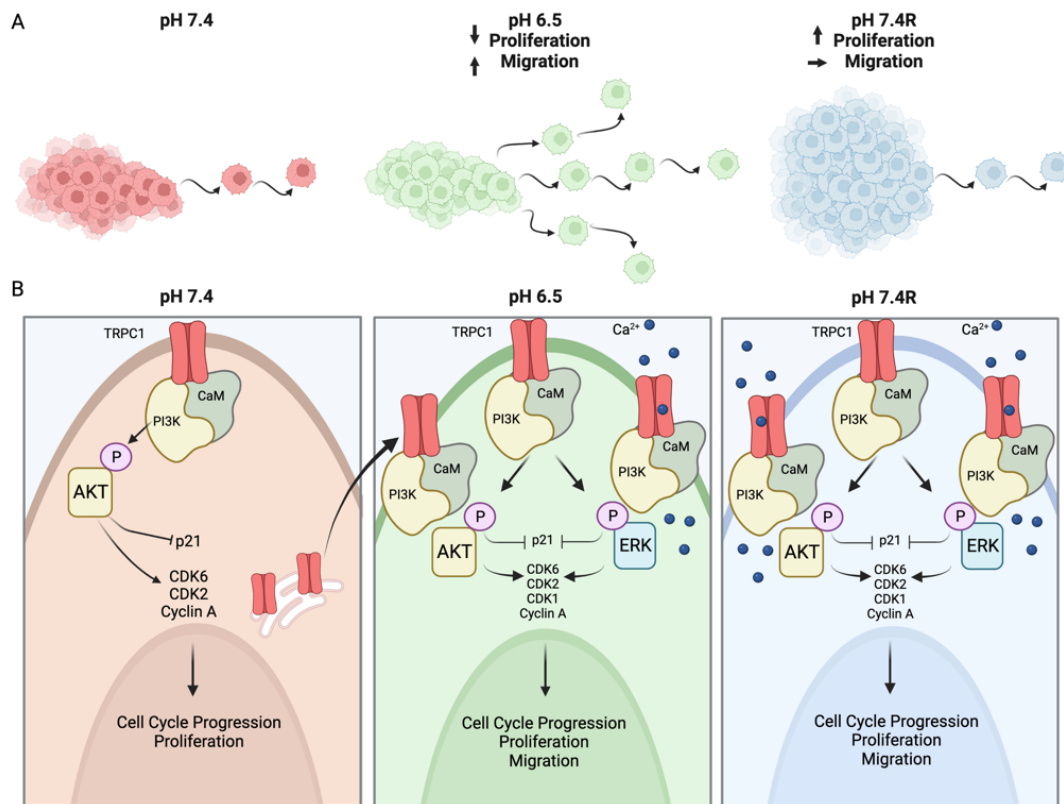







Figure 37. (A) Acid adaptation promotes migration but attenuates proliferation, whereas acid recovery impairs this migration but further accelerates proliferation. (B) The fluctuations of the acidic tumor microenvironment affect TRPC1 expression and localization. TRPC1 is downregulated in acid-adapted PANC-1 cells but favors plasma membrane localization, which is maintained in acid-recovered PANC-1 cells, where the expression of TRPC1 is upregulated. In the plasma membrane of acid-adapted and -recovered conditions, TRPC1 permits  $\text{Ca}^{2+}$  entry and, in interaction with the PI3K-p85 $\alpha$  subunit and CaM, regulates PANC-1 cell migration, proliferation and cell cycle progression. (The figure is generated with [www.Biorender.com](http://www.Biorender.com).)

## Article

# Acid Adaptation Promotes TRPC1 Plasma Membrane Localization Leading to Pancreatic Ductal Adenocarcinoma Cell Proliferation and Migration through Ca<sup>2+</sup> Entry and Interaction with PI3K/CaM

Julie Schnipper <sup>1</sup>, Sana Kouba <sup>1</sup>, Frédéric Hague <sup>1</sup>, Alban Girault <sup>1</sup>, Marie-Sophie Telliez <sup>1</sup>,  
Stéphanie Guénin <sup>2</sup>, Ahmed Ahidouch <sup>1,3</sup>, Stine Falsig Pedersen <sup>4</sup> and Halima Ouadid-Ahidouch <sup>1,\*</sup>

<sup>1</sup> Laboratory of Cellular and Molecular Physiology, UR UPJV 4667, University of Picardie Jules Verne, 80000 Amiens, France

<sup>2</sup> Regional Ressources Center for Molecular Biology (CRRBM), University of Picardie Jules Verne, 80000 Amiens, France

<sup>3</sup> Biology Department, Sciences Faculty, University Ibn Zohr, Agadir 80000, Morocco

<sup>4</sup> Section for Cell Biology and Physiology, Department of Biology, University of Copenhagen, 2100 Copenhagen Ø, Denmark

\* Correspondence: halima.ahidouch-ouadid@u-picardie.fr; Tel.: +33-322-827-646



**Citation:** Schnipper, J.; Kouba, S.; Hague, F.; Girault, A.; Telliez, M.-S.; Guénin, S.; Ahidouch, A.; Pedersen, S.F.; Ouadid-Ahidouch, H. Acid Adaptation Promotes TRPC1 Plasma Membrane Localization Leading to Pancreatic Ductal Adenocarcinoma Cell Proliferation and Migration through Ca<sup>2+</sup> Entry and Interaction with PI3K/CaM. *Cancers* **2022**, *14*, 4946. <https://doi.org/10.3390/cancers14194946>

Academic Editor: Iman Azimi

Received: 11 August 2022

Accepted: 7 October 2022

Published: 9 October 2022

**Publisher's Note:** MDPI stays neutral with regard to jurisdictional claims in published maps and institutional affiliations.



**Copyright:** © 2022 by the authors. Licensee MDPI, Basel, Switzerland. This article is an open access article distributed under the terms and conditions of the Creative Commons Attribution (CC BY) license (<https://creativecommons.org/licenses/by/4.0/>).

**Simple Summary:** Pancreatic ductal adenocarcinoma (PDAC) is one of the deadliest cancers globally, with a 5-year overall survival of less than 10%. The development and progression of PDAC are linked to its fluctuating acidic tumor microenvironment. Ion channels act as important sensors of this acidic tumor microenvironment. They transduce extracellular signals and regulate signaling pathways involved in all hallmarks of cancer. In this study, we evaluated the interplay between a pH-sensitive ion channel, the calcium (Ca<sup>2+</sup>) channel transient receptor potential C1 (TRPC1), and three different stages of the tumor microenvironment, normal pH, acid adaptation, and acid recovery, and its impact on PDAC cell migration, proliferation, and cell cycle progression. In acid adaptation and recovery conditions, TRPC1 localizes to the plasma membrane, where it interacts with PI3K and calmodulin, and permits Ca<sup>2+</sup> entry, which results in downstream signaling, leading to proliferation and migration. Thus, TRPC1 exerts a more aggressive role after adaptation to the acidic tumor microenvironment.

**Abstract:** Pancreatic ductal adenocarcinoma (PDAC) remains one of the most lethal malignancies, with a low overall survival rate of less than 10% and limited therapeutic options. Fluctuations in tumor microenvironment pH are a hallmark of PDAC development and progression. Many ion channels are bona fide cellular sensors of changes in pH. Yet, the interplay between the acidic tumor microenvironment and ion channel regulation in PDAC is poorly understood. In this study, we show that acid adaptation increases PANC-1 cell migration but attenuates proliferation and spheroid growth, which are restored upon recovery. Moreover, acid adaptation and recovery conditions favor the plasma membrane localization of the pH-sensitive calcium (Ca<sup>2+</sup>) channel transient receptor potential C1 (TRPC1), TRPC1-mediated Ca<sup>2+</sup> influx, channel interaction with the PI3K p85 $\alpha$  subunit and calmodulin (CaM), and AKT and ERK1/2 activation. Knockdown (KD) of TRPC1 suppresses cell migration, proliferation, and spheroid growth, notably in acid-recovered cells. KD of TRPC1 causes the accumulation of cells in G0/G1 and G2/M phases, along with reduced expression of CDK6, -2, and -1, and cyclin A, and increased expression of p21<sup>CIP1</sup>. TRPC1 silencing decreases the basal Ca<sup>2+</sup> influx in acid-adapted and -recovered cells, but not in normal pH conditions, and Ca<sup>2+</sup> chelation reduces cell migration and proliferation solely in acid adaptation and recovery conditions. In conclusion, acid adaptation and recovery reinforce the involvement of TRPC1 in migration, proliferation, and cell cycle progression by permitting Ca<sup>2+</sup> entry and forming a complex with the PI3K p85 $\alpha$  subunit and CaM.

**Keywords:** pancreatic ductal adenocarcinoma; tumor microenvironment; acid adaptation;  $\text{Ca}^{2+}$  signaling; TRPC1; cell migration; cell proliferation; spheroid growth; cell cycle progression; PI3K; calmodulin

## 1. Introduction

Pancreatic ductal adenocarcinoma (PDAC) accounts for up to 90% of pancreatic cancer incidences, and is the seventh leading cause of cancer-related deaths worldwide [1,2]. The poor prognosis of PDAC patients is mainly caused by late diagnosis, at a stage where the disease is often advanced, metastatic, and non-resectable [3,4]. The cytotoxic therapies available at present are modestly effective, and there is a compelling need to explore underlying PDAC development and progression mechanisms to develop better treatment options [3].

The development and progression of PDAC is linked to the physiology and microenvironment of the exocrine pancreas. Pancreatic epithelial and stromal cells are exposed to cyclic changes in the extracellular pH ( $\text{pH}_o$ ) due to the production of alkaline pancreatic juices rich in  $\text{HCO}_3^-$ . The apical exposure to this alkaline  $\text{pH}_o$  is coupled to the parallel acidification of the basolateral membrane, leading to an acidic pancreatic interstitium [5,6]. Interestingly, extracellular acidification is one of the key characteristics of the tumor microenvironment, where it is caused by low perfusion in combination with high extrusion of  $\text{H}^+$  from fermentative glycolysis and acid in the form of  $\text{CO}_2$  from oxidative phosphorylation [7–9]. While the interstitial space of solid tumors is generally acidic, and  $\text{pH}_o$  values as low as 5.6 have been measured, most values are in the range of 6.4–7. Where regions of the tumor with poor vascularization will typically be acidic, well-vascularized areas will exhibit a  $\text{pH}_o$  closer to neutral [8,10–12]. The intracellular pH ( $\text{pH}_i$ ) is more alkaline than the  $\text{pH}_o$  in tumors, yet cancer cells in an acidic microenvironment still exhibit an acidic  $\text{pH}_i$  [13,14] compared to healthy cells in the normal pancreas.

Long-term acidosis acts as an evolutionary selection pressure. It causes adaptive responses that can establish cancer cell populations with more malignant phenotypes in the form of invasive and metastatic potential [8,15–17]. In addition, acidosis limits proliferation by keeping the cancer cells in a dormant state [18]. This adaptation can be of particular impact once the cancer cells encounter a more neutral microenvironment, as an increase in  $\text{pH}_i$  can further accelerate proliferation [8,9,19,20]. Changes in the pH can produce a multitude of cellular physiological effects, as numerous proteins are sensitive to pH in the range encountered in tumors [19–21]. Transmembrane proteins, such as ion channels, can function as pH sensors and transduce extracellular signals as changes in  $\text{pH}_o$  [19,22]. They can potentially regulate signaling pathways related to all hallmarks of cancer by being affected by both  $\text{pH}_o$  and  $\text{pH}_i$  [19–21]. In recent years, the role of calcium ( $\text{Ca}^{2+}$ ) channels as drivers of cancer mechanisms has been extensively investigated [23–25]. The transient receptor potential canonical (TRPC) channel subfamily represents a group of  $\text{Ca}^{2+}$ -permeable non-selective cation channels [26]. Different physiochemical stimuli can activate their gating mechanisms and affect their expression, thus being categorized as cellular sensors [27]. The TRPC1 isoform is involved in various physiological and pathological processes [27,28] through different stimuli. For instance, the expression of TRPC1 increases and modulates proliferation and migration via hypoxia-induced signaling in breast and follicular thyroid cancer cells [29,30]. TRPC1 expression increases upon 24 h of pressure in pancreatic stellate cells (PSCs) [31,32]. The ambient pressure activates TRPC1 to form a complex with  $\alpha$  smooth muscle actin ( $\alpha\text{SMA}$ ) and phosphorylated SMAD2. This physical interaction between TRPC1/ $\alpha\text{SMA}$ /SMAD2 is essential for activating two major pathways underlying PSC activation, namely ERK1/2 and SMAD2 pathways, resulting in IL-6 secretion and PSC proliferation [32]. Interestingly, the TRPC1 plasma membrane expression decreases upon PI3K inhibition in glioblastoma cells, which is associated with reduced chemotaxis and cell migration [33]. Although the response of TRPC1 to acidification has, to our knowledge, not been reported, other TRPC channels have been shown to

be affected by acidification [34]. For instance, TRPC4 and TRPC5 are activated by acidic pH in HEK293 cell models. TRPC4 is activated by acidic  $\text{pH}_i$  (6.75–6.25), in combination with increased cytosolic  $\text{Ca}^{2+}$  levels and G-protein-coupled receptor activation [35], while TRPC5 is activated both through G-protein activation and directly through protonation (pH 6.5) [36].

We have recently shown that TRPC1 is overexpressed in PDAC tissue and cell lines but does not regulate either basal  $\text{Ca}^{2+}$  entry or store-operated  $\text{Ca}^{2+}$  entry (SOCE). However, TRPC1 regulates PANC-1 cell proliferation by interacting with phosphoinositol-3-kinase (PI3K) and calmodulin (CaM) and regulating AKT signaling in normal pH conditions [37]. In the present study, we demonstrate the role of the fluctuating acidic tumor microenvironment and TRPC1 in PDAC cell migration, proliferation, and cell cycle progression. We showed that in acid-adapted PDAC cells, total TRPC1 expression decreased, but plasma membrane localization increased. In acid-recovered cells, TRPC1 expression increased, high plasma membrane localization of the channel was maintained, and  $\text{Ca}^{2+}$  influx increased. As we have demonstrated before, TRPC1 formed a complex with PI3K/CaM, activating the downstream serine/threonine protein kinase AKT, but in this study, TRPC1 also activated the extracellular signal-regulated kinase 1 and 2 (ERK1/2) that synergistically control cell migration, proliferation, and cell cycle progression, in acid adaptation and recovery conditions.

## 2. Materials and Methods

### 2.1. Cell Culture and Experimental pH Setup

The normal duct-like cell line human pancreatic nestin-expressing cells (HPNE), immortalized with hTERT, was purchased from the American Type Culture Collection (ATCC, Molsheim, France). HPNE were grown in 75% DMEM without glucose (Sigma-Aldrich, Saint-Quentin-Fallavier, France), 25% Medium M3 Base (Incell Corp. Cat#M300F-500), and 10% fetal bovine serum (Cat#P30-3031, PAN Biotech), 5.5 mM glucose, and 750 ng/mL Puromycin. The human PDAC cell line PANC-1 cells were kindly provided by Prof. Anna Trauzold (Institute of Experimental Cancer Research, Kiel University, Kiel, Germany). PANC-1 cells were cultured in RPMI-1640 medium already containing glucose (Sigma-Aldrich, Saint-Quentin-Fallavier, France) supplemented with 10% fetal bovine serum (Cat#P30-3031, PAN Biotech), 1 mM sodium pyruvate (Gibco, Waltham, MA, USA), and 1% Glutamax (Gibco). Cells were grown at 37 °C, 95% humidity, 5%  $\text{CO}_2$ , and passaged with trypsin-EDTA 0.25% (Sigma-Aldrich, Saint-Quentin-Fallavier, France) when cells reached a confluency of 70–80%. Cell cultures were not used for more than 20 passages. The medium pH was adapted to pH 6.5 by adjusting the  $\text{HCO}_3^-$  concentration by adding the appropriate amount of  $\text{NaHCO}_3$  and ensuring equal osmolarity by changing  $[\text{NaCl}]$  as suggested by Michl et al., [38], and as performed previously by Flinck et al., Yao et al., and Hagelund and Trauzold [39–41]. All cell lines were regularly tested for mycoplasma.

PANC-1 cells were thawed and grown under normal pH conditions (pH 7.4), then transferred to medium with pH 6.5, and maintained in this medium for a period of 30 days. These cells are referred to as acid-adapted cells (pH 6.5). The acid-adapted PANC-1 cells were then reseeded in a pH 7.4 medium for 14 days and are referred to as acid-recovered cells (pH 7.4R).

### 2.2. Live Imaging of Intracellular pH

As previously described, the  $\text{pH}_i$  measurements of non-transfected PANC-1 cells were performed [41,42]. In detail,  $8 \times 10^4$  cells were seeded in WillCo glass-bottom dishes WillCo Wells, Amsterdam, The Netherlands. After 48 h of seeding, cells were incubated in a growth medium containing 4  $\mu\text{M}$  2,7-bis-(2-carboxyethyl)-5-(and-6)-carboxyfluorescein acetoxymethyl ester (BCECF-AM, Invitrogen) for 30 min in the dark at 37 °C, 95% humidity, 5%  $\text{CO}_2$ . Cells were washed twice in  $\text{HCO}_3^-$  containing Ringer solution; 115 mM (for pH 7.4) or 135 mM (for pH 6.5) NaCl, 24 mM (for pH 7.4) or 3 mM (for pH 6.5)  $\text{NaHCO}_3$ , 5 mM KCl, 1 mM  $\text{MgSO}_4$ , 1 mM  $\text{Na}_2\text{HPO}_4$ , 1 mM  $\text{CaCl}_2$ , 3.3 mM 3-(*N*-morpholino)



propanesulfonic acid (MOPS), 3.3 mM 2 [Tris(hydroxymethyl)-methylamino]-ethanesulfonic acid (TES), 5 mM 4-(2-hydroxyethyl)-1-piperazineethanesulfonic acid (HEPES), adjusted with NaOH or HCl to pH 7.4 or 6.5 at 37 °C. Then, the cells in the glass-bottom dish containing Ringer solution adjusted to the respective pH were placed in a temperature-controlled compartment (37 °C) equipped with gas. The steady-state pH<sub>i</sub> measurements were carried out using a Nikon Eclipse Ti microscope equipped with a Xenon lamp for fluorescence excitation, a 40× oil 1.4 NA objective, and EasyRatioPro imaging software (PTI), for 10 min. Emission was measured at 520 nm after excitation at 440 nm and 485 nm. Calibration was carried out using the high K<sup>+</sup>/nigericin technique [43], employing KCl solutions (156 mM KCl, 1 mM MgSO<sub>4</sub>, 1 mM CaCl<sub>2</sub>, 1 mM K<sub>2</sub>HPO<sub>4</sub>, 3.3 mM MOPS, 3.3 mM TES, 5 mM HEPES) of pH 6.6, 7.0, 7.4, and 7.8, and 10 μM Nigericin (Sigma-Aldrich), which generated a four-point linear calibration curve to calibrate pH<sub>i</sub> values. Fluorescence measured from the two excitation channels (440 nm and 485 nm) was corrected for their respective background fluorescence during each experiment. The background fluorescence was assessed by measuring in a cell-free area during the experiment. The ratio 485 nm/440 nm was then calculated, and the calibration data were fitted to a linear function in the applied pH range. The experimental data were inserted and converted to corrected steady-state pH values.

### 2.3. Transient Transfections

Cells were transfected with small interfering RNA (siRNA) by electroporation using nucleofection (Amaxa Biosystems, Lonza, Aubergenville, France) as previously described [37]. Briefly, PANC-1 cells (1 × 10<sup>6</sup>) grown under either normal pH, acid adaptation, or acid recovery conditions, were transiently nucleofected according to the manufacturer's protocol. To achieve this, 4 μg of scrambled siRNA (siCTRL, negative duplex control, Eurogentec) or siRNA directed against TRPC1 (siTRPC1, ON-TARGET plus SMART pool siRNA, Dharmacon Research, Chicago, IL, USA) were used. Experiments were performed 72 h after siRNA transfection unless otherwise indicated.

### 2.4. 3D Spheroid Growth and CellTiter-Glo Assay

Non-transfected or transfected PANC-1 cells grown under either normal or acid adaptation conditions were formed into spheroids in their respective medium or in normal pH conditions following acid adaptation to simulate the 2D model of acid recovery conditions. In total, 2000 PANC-1 cells were seeded in round-bottomed, ultralow attachment 96-well plates (Corning, NY, USA) in 200 μL growth medium, supplemented with 2% GelTrex LDEV-Free reduced growth factor basement membrane matrix (Thermo Fisher Scientific, Waltham, MA, USA). After seeding, cells were spun down at 750 RCF for 20 min and were grown for 9 days at 37 °C with 95% humidity and 5% CO<sub>2</sub>, and 100 μL of the respective pH medium was exchanged every second day. Light microscopic images of the spheroids at 10× magnification were acquired on days 2, 4, 7, and 9. On day 9, PANC-1 spheroids, either non-transfected or transfected cells (in replicates of three) were transferred to a black 96-well plate with 100 μL of the respective pH medium and 100 μL CellTiter-Glo<sup>®</sup> 3D Reagent (Promega, Madison, WI, USA). This plate was wrapped in aluminum foil, shaken for 5 min, and then incubated without shaking for 25 min at room temperature. The luminescence signal was recorded using a FLUOStar Optima microplate reader (BMG Labtech, Ortenberg, Germany).

### 2.5. Western Blot Analysis

Proteins were extracted, determined, and separated by the SDS-page technique as previously described [44]. The primary antibodies used were: anti-TRPC1 (1:1000, Abcam, Waltham, MA, USA), anti-GAPDH (1:2000, Cell Signaling Tech., Danvers, MA, USA), anti-CDK6 (1:500, Cell Signaling Tech., Danvers, MA, USA), anti-Cyclin A (1:500, Santacruz Biotechnology, Dallas, TX, USA), anti-CDK2 (1:500, Cell Signaling Tech., Danvers, MA, USA), anti-CDK1 (1:500, Cell Signaling Tech., Danvers, MA, USA), anti-p21<sup>CIP1</sup> (1:500, Cell Signaling Tech., Danvers, MA, USA), anti-PI3K p85α (1:500, Bioworld Technology, tebu-bio,



France), anti-calmodulin (1:500, Santacruz Biotechnology, Dallas, TX, USA), anti-pAKT (Ser473) (1:500, Cell Signaling Tech., Danvers, MA, USA), anti-AKT (1:500, Cell Signaling Tech., Danvers, MA, USA), anti-pERK1/2 (Thr202/Tyr204) (1:500, Cell Signaling Tech., Danvers, MA, USA), and anti-ERK1/2 (1:500, Cell Signaling Tech., Danvers, MA, USA). Secondary antibodies (1:4000, Cell Signaling Tech., Danvers, MA, USA) were coupled to horseradish peroxidase, and proteins were detected using enhanced chemiluminescence (Ozyme, Saint-Cyr-l'Ecole, France). Quantification was performed with the ImageJ software 1.53a (National Institute of Health, Bethesda, MD, USA) analysis tool. All experiments were normalized to the level of GAPDH.

### 2.6. Cell Surface Biotinylation Assay

To determine the membrane fraction of TRPC1,  $1 \times 10^6$  HPNE cells or  $8 \times 10^5$  PANC-1 cells grown in normal pH, acid adaptation, or acid recovery conditions were seeded in 60 mm Petri dishes for 48 h and collected as previously described [45]. Briefly, cells were washed three times with cold PBS, then incubated with 3 mg of sulfo-NHS-SS-biotin (Thermo Fisher Scientific) and slightly shaken for 1 h at 4 °C. The reaction was interrupted by the addition of cold PBS containing 10 mM glycine. Cells were scrapped with RIPA buffer, and ~ 10% of the total lysate was saved as the total lysate fraction. The remaining lysate portion (corresponding to the membrane fraction) was incubated with high-capacity streptavidin agarose beads (Thermo Fisher Scientific, Waltham, MA, USA) with gentle rotation overnight at 4 °C. After incubation, beads were washed four times with RIPA buffer. Proteins were eluted from the beads with 50 µL of Laemmli buffer 2X and heated at 60 °C for 30 min. Both total lysate samples and membrane fraction samples were used for Western blot analysis, as described above.

### 2.7. Co-Immunoprecipitation

The  $6 \times 10^5$  non-transfected or  $1 \times 10^6$  transfected PANC-1 cells grown in the three different pH conditions were seeded in 10 cm Petri dishes and collected after 72 h. As previously described [37], 500 µg of proteins were used for co-immunoprecipitation with SureBeads™ Protein A Magnetic Beads (Bio-Rad, France). Beads were washed thoroughly, according to the manufacturer's protocol. Then, 1 µg of either TRPC1 antibody (Abcam, Waltham, MA, USA), PI3K p85α antibody (Bioworld Technology, tebu-bio, France), or a control HRP-linked anti-rabbit IgG antibody (Cell Signaling Tech., Danvers, MA, USA) were resuspended with the beads for 30 min. Protein lysates were subsequently washed and added to the beads, which were slowly rotated for 2 h at room temperature. After another sequential washing step of the beads, proteins were eluted according to the manufacturer's protocol. After denaturation, proteins were subjected to Western blotting as described above. To detect the input, 50 µg of proteins from the corresponding co-immunoprecipitation samples were used.

### 2.8. Immunofluorescence Assay and Analysis

The  $8 \times 10^4$  non-transfected PANC-1 cells, grown under the three different pH conditions, were seeded on coverslips for 48 h. Immunofluorescent staining was performed as previously described [37]. Briefly, cells were washed in cold PBS and fixed for 20 min at room temperature in 4% paraformaldehyde (PFA, Sigma, Saint-Quentin-Fallavier, France). Cells were washed twice in PBS and permeabilized in 0.1% Triton™X-100 (Sigma, Saint-Quentin-Fallavier, France) for 10 min. Next, cells were blocked in 5% bovine serum albumin (BSA, Sigma, Saint-Quentin-Fallavier, France) for 30 min, followed by the addition of primary antibodies overnight at 4 °C. The antibodies used were anti-TRPC1, (1:100, Santacruz Biotechnology, Dallas, TX, USA), with Na<sup>+</sup>/HCO<sub>3</sub><sup>-</sup> co-transporter (NBCn1) used as a membrane marker (1:400, Abcam, Waltham, MA, USA), and anti-PI3K p85α (1:100, Bioworld Technology, tebu-bio, France). Secondary antibodies (AlexaFluor® 488/550 conjugated antibody 1:600) were applied for 1 h at room temperature, followed by treatment with 4',6-diamidino-2-phenylindole (DAPI; 1%) for 5 min to stain nuclei. Coverslips were

washed three times and mounted on slides using Prolong<sup>®</sup> Gold antifade reagent. Images were collected on an Olympus Cell Vivo IX83 with a Yokogawa CSU-W1 confocal scanning unit. Z-stacks were deconvoluted in Olympus Cell Sens software using a constrained iterative algorithm. No or negligible labeling was seen in the absence of primary antibodies. Overlays and brightness/contrast/background adjustments were carried out using ImageJ software. Mander's overlapping R coefficient was calculated using the ImageJ software plugin JACoP, which calculates the proportion of the green signal coincident with the magenta signal over the total intensity [46]. The threshold setting was the same for both images.

### 2.9. Boyden Chamber Assay

Cell migration was evaluated using a Boyden chamber assay with 8  $\mu\text{m}$  pore size cell culture inserts (Falcon<sup>®</sup>, Corning, Boulogne-Billancourt, France), as previously described [47]. Briefly,  $4 \times 10^4$  non-transfected or transfected PANC-1 cells, grown under the three different pH conditions, were seeded in the upper compartment of the chamber. Both the upper and lower compartments were filled with the respective culture medium containing 10% FBS. After 24 h of incubation at 37 °C, 95% humidity, and 5% CO<sub>2</sub>, inserts were washed in PBS and fixed in methanol for 15 min at room temperature, followed by staining with hematoxylin for 5 min. Inserts were washed in Milli-Q water and cleaned with a cotton swab; 20 adjacent fields were counted per insert at  $\times 400$  magnification. The number of migrating cells was normalized to their respective control (normal pH conditions (pH 7.4) for non-transfected PANC-1 cells and siCTRL in normal pH conditions (pH 7.4) for transfected PANC-1 cells). To ensure that there was no difference in viability between the conditions after 24 h, the trypan blue assay (as described below) was performed.

To investigate the effect of extracellular Ca<sup>2+</sup> concentrations on migration, we used the same Boyden chamber procedure as described above, but after 8 h of seeding, medium in the upper and lower chamber was changed to the respective medium, either with standard conditions containing 1 mM Ca<sup>2+</sup> (referred to as conditions with Ca<sup>2+</sup>) or containing ethylene glycol tetraacetic acid (EGTA), to chelate Ca<sup>2+</sup> and to end with a final concentration of 30  $\mu\text{M}$  (referred to conditions without Ca<sup>2+</sup>). Thus, cells were transfected for 72 h, where Ca<sup>2+</sup> were chelated for 24 h in total during the migration process.

### 2.10. Trypan Blue Assay

Non-transfected ( $4 \times 10^4$ ) or transfected ( $8 \times 10^4$ ) PANC-1 cells were seeded in 35 mm Petri dishes. Subsequently, 24, 48, 72, or 96 h after seeding, cells were washed in PBS, trypsinized, and diluted (1:5) in trypan blue solution (Sigma, Saint-Quentin-Fallavier, France). All conditions were counted six times using the standard Malassez cell method. Proliferation was calculated as the total number of viable cells (alive/white cells) normalized to the control. As previously described, we tested the effect of extracellular Ca<sup>2+</sup> concentrations on proliferation [37]. Here, the same counting procedure as described above was carried out, but after 24 h of seeding, the medium was changed to medium with standard conditions containing 1 mM Ca<sup>2+</sup> (referred to as conditions with Ca<sup>2+</sup>) or containing EGTA to chelate Ca<sup>2+</sup> and to end with a final concentration of 30  $\mu\text{M}$  (referred to conditions without Ca<sup>2+</sup>). Cells were transfected for 72 h, and Ca<sup>2+</sup> was chelated for 48 h.

### 2.11. Flow Cytometry

Flow cytometry was carried out as described previously [37]. Briefly, duplicates of  $2 \times 10^5$  non-transfected or transfected PANC-1 cells were seeded in 60 mm Petri dishes and collected after 72 h. Cells were washed in PBS, trypsinized, and collected in PBS + EDTA (5 mM), followed by fixation with cold absolute ethanol ( $\geq 99.8\%$ , Sigma, Saint-Quentin-Fallavier, France). Cells were kept at 4 °C for at least 6 h post-fixation. To prepare for analysis, cells were pelleted, resuspended in PBS + EDTA (5 mM), treated with 20  $\mu\text{g}/\text{mL}$  RNase A (Sigma-Aldrich, St. Quentin Fallavier, France) for 30 min at room temperature, and stained with 50  $\mu\text{g}/\text{mL}$  of propidium iodide (Sigma-Aldrich, St. Quentin Fallavier, France). The cell cycle distribution of each sample was determined by flow cytometry

analysis of nuclear DNA content using a flow cytometer (Accuri<sup>®</sup>, Dominique Deutscher, Brumath, France). The cell percentage in different phases was calculated using Cyflogic software and illustrated with FCS Express 7.

#### 2.12. Proximity Ligation Assay

The  $8 \times 10^4$  non-transfected or transfected PANC-1 cells grown in one of the three pH media were seeded on coverslips 72 h before the proximity ligation assay (PLA) experiment. As described before [47], cells were washed twice with PBS, then fixed with PFA (4%) at room temperature for 20 min. Cells were washed twice in PBS and permeabilized with 0.1% Triton<sup>™</sup> X-100 (Sigma, Saint-Quentin-Fallavier, France) for 10 min. The Duolink in situ PLA detection kit (Sigma-Aldrich, Saint-Quentin-Fallavier, France) was used to detect interactions between TRPC1 and the PI3K p85 $\alpha$  subunit. Experiments were performed according to the manufacturer's protocol. Red fluorescent oligonucleotides produced as the end product of the procedure were visualized using the Zeiss Observer Z1 microscope 60X oil objective (Carl Zeiss, Oberkochen, Germany). Images were analyzed using ImageJ, where puncta per cell were counted and normalized to the respective control; normal pH conditions (pH 7.4) for non-transfected cells, and siCTRL in their respective medium (pH 6.5 or 7.4R). A total of 20 pictures per condition were captured and analyzed, and are presented as relative number puncta/cell.

#### 2.13. Manganese Quench Assay

To estimate divalent cation influx under basal conditions, we used the manganese ( $Mn^{2+}$ ) quenching technique as previously described [47]. Briefly,  $25 \times 10^3$  transfected PANC-1 cells, grown under one of the three pH conditions, were seeded on glass coverslips for 72 h. At the beginning of each experiment, cells were incubated with 3.33  $\mu M$  Fura-2/AM (Sigma, Saint-Quentin-Fallavier, France) at 37 °C, 95% humidity, 5% CO<sub>2</sub> for 45 min in the dark. Cells on the coverslip were washed twice with extracellular saline solution (145 mM NaCl, 5 mM KCl, 2 mM CaCl<sub>2</sub>, 1 mM MgCl<sub>2</sub>, 5 mM glucose, 10 mM HEPES, pH 7.4 or pH 6.5), and placed on the stage of a fluorescence microscope (Axiovert 200; Carl Zeiss, Oberkochen, Germany). Cells were excited at 360 nm using a monochromator (polychrome IV, TILL Photonics, Gräfelfing, Germany), and fluorescent emission was captured with a Cool SNAPHQ camera (Princeton Instruments, Lisses, France) after filtration through a long-pass filter (510 nm). Metafluor software (version 7.1.7.0, Molecular Devices, San Jose, CA, USA) was used for signal acquisition and data analysis. After 1.5 min, the saline solution (including 2 mM Ca<sup>2+</sup>) was replaced by 2 mM Mn<sup>2+</sup> solution by perfusion. The Mn<sup>2+</sup> quenching extracellular solution contains 145 mM NaCl, 5 mM KCl, 2 mM MnCl<sub>2</sub>, 1 mM MgCl<sub>2</sub>, 5 mM glucose, and 10 mM HEPES, and was adjusted with NaOH or HCl to pH 7.4 or 6.5. The Mn<sup>2+</sup> influx, a corroborate of Ca<sup>2+</sup> influx, was estimated from the quenching rate of fluorescence at 360 nm by calculating the slope.

#### 2.14. Statistical Analysis

All data are shown as representative images or as mean measurements with standard error of means (SEM) error bars and represent at least three independent experiments. *N* refers to the number of independent experiments performed, or to the number of cells analyzed. Welch's correction *t*-test or Tukey's multiple comparison test was applied to test for statistically significant differences between two groups. \*, \*\*, and \*\*\* denotes  $p < 0.05$ ,  $p < 0.01$ , and  $p < 0.001$ , respectively. All graphs and statistics were generated in GraphPad Prism 9.0 software (San Diego, CA, USA).

### 3. Results

#### 3.1. Acid Adaptation Promotes Membrane Localization of TRPC1 in PANC-1 Cells

Before investigating the impact of the acidic tumor microenvironment on the growth and migration of PANC-1 cells, we studied the pH<sub>i</sub> values in different pH<sub>o</sub> conditions buffered with HCO<sub>3</sub><sup>-</sup>/CO<sub>2</sub>. We observed that PANC-1 cells grown in normal pH conditions

(pH 7.4) exhibited a  $pH_i$  of 7.3. This value decreased to 6.9 in acid-adapted cells (pH 6.5), and increased to 7.6 in acid-adapted cells measured at pH 7.4 ( $n = 6-11$ ,  $p < 0.05$ , Figure 1A).

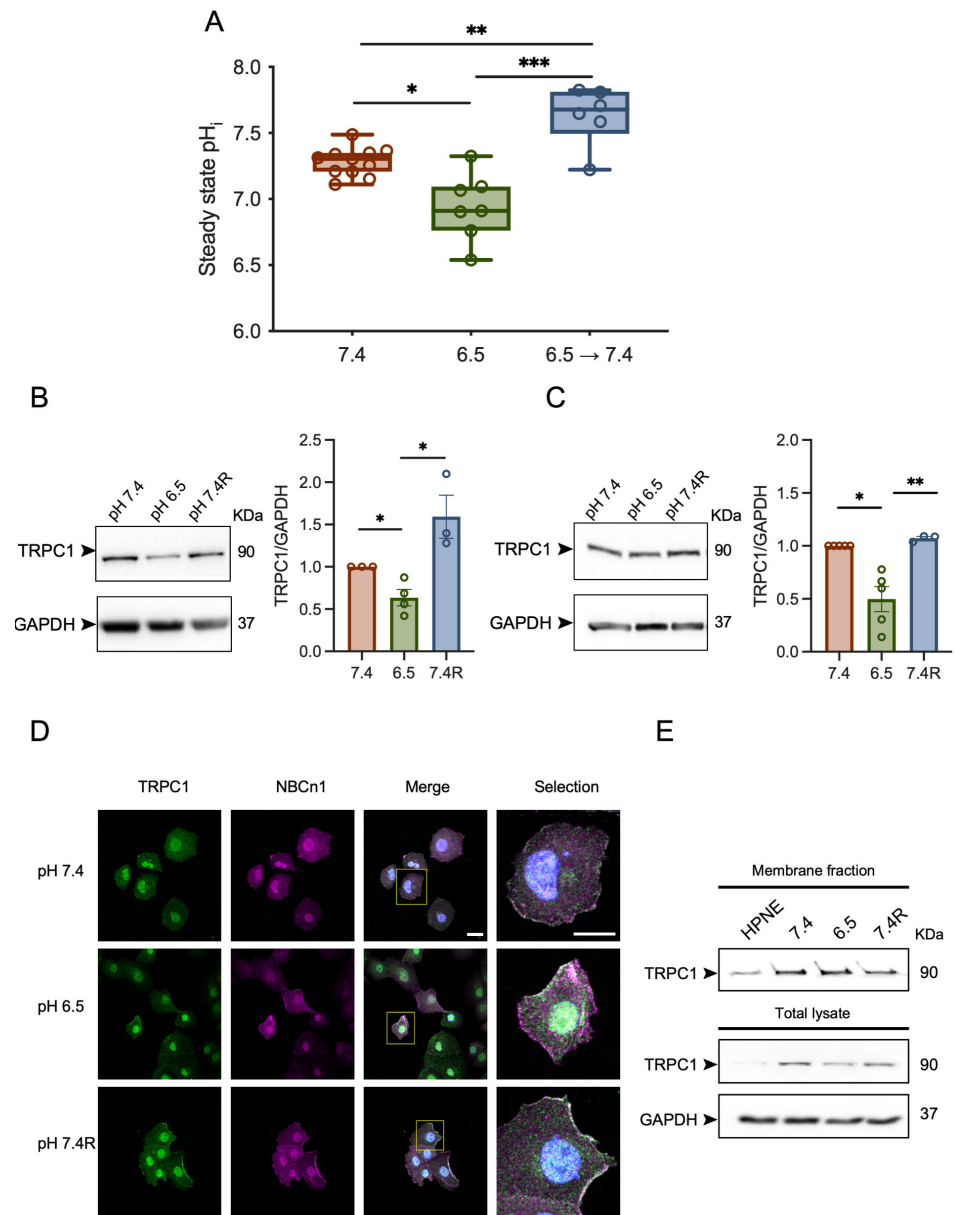


**Figure 1.** TRPC1 protein expression is affected by acid adaptation and recovery and favors the plasma membrane localization. (A) Steady state  $pH_i$  in PANC-1 cells grown in normal pH or acid adaptation conditions and measured in  $HCO_3^-$  Ringer adjusted to pH 7.4 or 6.5 (X-axis). 6.5 → 7.4 indicate acid-adapted cells measured in  $pH_e$  7.4. ( $n = 6-11$ ). (B) Western blot analysis (left panel) and quantification (right panel) of TRPC1 expression in PANC-1 cells grown under normal pH (7.4), acid adaptation (6.5) or acid recovery conditions (7.4R) ( $n = 3-4$ ). (C) Western blot analysis (left panel) and quantification (right panel) of TRPC1 expression in PANC-1 spheroids grown under normal pH (7.4), acid adaptation (6.5), or acid recovery conditions (7.4R) for 9 days ( $n = 3-5$ ). Welch’s correction  $t$ -test was used to determine the significant difference between different conditions. \*, \*\* and \*\*\* indicate  $p < 0.05$  and 0.01 and 0.001 respectively. (D) Representative immunofluorescent analysis of TRPC1 and the membrane protein  $Na^+ / HCO_3^-$  co-transporter (NBCn1, used as membrane marker) in PANC-1 cells grown under normal pH (7.4), acid adaptation (6.5) or acid recovery conditions (7.4R) ( $n = 3$ ), scale bars = 20  $\mu m$ . (E) Cell surface biotinylation followed by Western blotting indicating membrane fraction or total lysate of TRPC1. The uncropped blots are shown in File S1.

Recently, we have shown an overexpression of TRPC1 in human PDAC tissue and the aggressive PANC-1 cell line [37]. Hence, we investigated the effect of the acidic tumor microenvironment on the expression and the localization of TRPC1 in PANC-1 cells. The protein levels of TRPC1 were significantly reduced by  $37 \pm 9\%$  in acid-adapted PANC-1 cells compared to cells cultured in normal conditions ( $n = 3-4$ ,  $p < 0.05$ , Figure 1B). Moreover, TRPC1 protein expression in acid-recovered PANC-1 cells (pH 7.4R) was significantly increased by  $60 \pm 16.9\%$  compared to acid-adapted PANC-1 cells ( $n = 3-4$ ,  $p < 0.05$ , Figure 1B). The protein levels of TRPC1 in spheroid PANC-1 cells grown in different pH conditions were comparable with those found in the 2D model ( $n = 3-5$ ,  $p < 0.05$ , Figure 1C). Using surface biotinylation and confocal imaging, we found that TRPC1 was expressed in the plasma membrane of PANC-1 cells in all three pH conditions compared to a duct-like cell line HPNE. However, the membrane fraction was increased in the majority of acid-adapted cells ( $n = 3$ , Figure 1D,E). These results indicate that acid adaptation decreases the global expression of TRPC1, but favors its plasma membrane localization.

### *3.2. The Knockdown of TRPC1 Inhibits Cell Migration and the Growth of PANC-1 Cells and Spheroids under Acid Recovery Conditions*

It is well known that the acidic tumor microenvironment can promote migration and slow down the proliferation of cancer cells [8,41,48,49]. First, we investigated the effect of pH on cell migration and viability. As expected, we found that acid-adapted PANC-1 cells migrated more than cells grown in normal pH and acid recovery conditions ( $75 \pm 11.4\%$ ,  $n = 3$ ,  $p < 0.001$ , Figure 2A), and showed a significant decrease in viability ( $25 \pm 10.7\%$  and  $36 \pm 6.3\%$  for 72 h and 96 h of cell culture, respectively) when compared to cells cultured in pH 7.4 ( $n = 3$ ,  $p < 0.05$ , Figure 2B). Similar results were found in PANC-1 spheroids ( $n = 4$ ,  $p < 0.01$ , Figure 2C,D). Indeed, acid-adapted PANC-1 spheroids grown for 9 days displayed lower viability by  $25 \pm 4\%$  and by  $43 \pm 4.8\%$  compared to normal pH and recovery conditions, respectively ( $n = 4-5$ ,  $p < 0.01$ , Figure 2C,D).

To investigate the role of TRPC1, we validated our knockdown (KD) model. In normal pH, TRPC1 protein expression was reduced by  $44 \pm 10\%$  72 h post-transfection [37] and by  $46 \pm 3\%$  and  $59 \pm 6.6\%$  in acid adaptation and recovery conditions, respectively (Figure S1C). Similar results were found at the transcriptional level after 48, 72, and 96 h (Figure S1A,B). Silencing of TRPC1 reduced cell migration by  $25 \pm 6.8\%$  in normal pH,  $43 \pm 5.1\%$  in acid adaptation, and  $49 \pm 3.7\%$  in acid recovery conditions ( $n = 3-4$ ,  $p < 0.05$  and  $0.001$ , Figure 3A). We did not observe a significant effect of TRPC1 KD on viability after 24 h of seeding (Figure S2A). KD of TRPC1 in PANC-1 cells in normal pH conditions inhibited cell proliferation by  $48 \pm 17.4\%$  and  $38 \pm 17.6\%$  after 72 and 96 h, respectively [37], and spheroid growth by  $22 \pm 2.3\%$  [37]. KD of TRPC1 decreased the viability of acid-adapted and -recovered cells by  $31.5 \pm 12.2\%$  ( $n = 3-4$ ,  $p < 0.05$ , Figure 3B) and  $33 \pm 12\%$ , respectively 72 h post-transfection ( $n = 5$ ,  $p < 0.01$ , Figure 3C). In addition, the annexin-5 analysis did not show any significant effect on apoptosis or necrosis (Figure S2E,F). To investigate whether the acid adaptation and recovery emphasize the involvement of TRPC1 in spheroid growth, we developed a siRNA-based KD of TRPC1 in spheroids. First, we confirmed the KD of TRPC1 after 9 days, where TRPC1 protein levels were decreased by  $27 \pm 16\%$  and  $41 \pm 8\%$  in acid adaptation and recovery conditions, respectively (Figure S1D). This KD of TRPC1 significantly decreased the viability of spheroids by  $38 \pm 6.5\%$  in acid recovery conditions ( $n = 3$ ,  $p < 0.05$ , Figure 3D,E). However, the silencing of TRPC1 did not affect the viability of acid-adapted spheroids ( $n = 3$ , Figure 3D,E). These results indicate that TRPC1 contributes to cell migration and proliferation of PANC-1 cells considerably in acid recovery conditions.



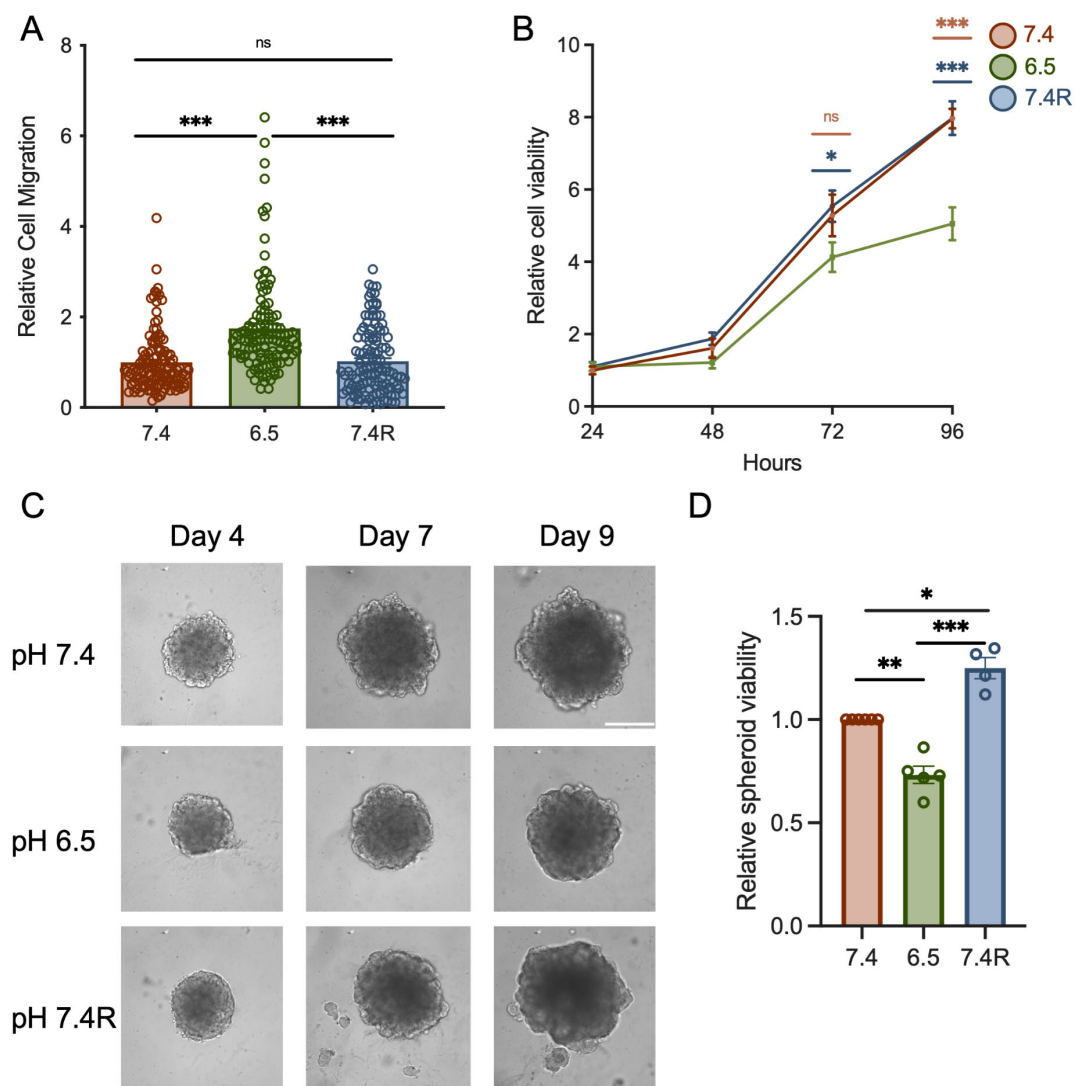


**Figure 2.** Acid adaptation promotes PANC-1 cell migration but attenuates proliferation, which is restored upon acid recovery. (A) Cell migration of PANC-1 cells grown under normal pH (7.4), acid-adapted (6.5), or acid recovery conditions (7.4R) analyzed by Boyden chamber assay ( $n = 3$ ). (B) Trypan blue analysis of PANC-1 cells grown under normal pH (7.4), acid-adapted (6.5), or acid recovery conditions (7.4R) shows the relative number of viable cells after 24, 48, 72, and 96 h after seeding ( $n = 3$ ). (C) Representative images of PANC-1 spheroids grown for 9 days and (D) viability quantification performed with CellTiter-Glo<sup>®</sup> assay ( $n = 4-5$ ), scale bar = 400  $\mu\text{m}$ . Welch's correction  $t$ -test was used to determine the significant difference between different conditions. ns indicates non-significance. \*, \*\*, and \*\*\* indicate  $p < 0.05$ , 0.01, and 0.001, respectively.

### 3.3. Knockdown of TRPC1 Accumulates Cells in the G0/G1 Phase and Decreases the Number of Cells in the G2/M Phase

To investigate the mechanism by which pH and TRPC1 KD affect PANC-1 cell proliferation, we examined the cell cycle distribution by flow cytometry. First, we discovered that non-transfected cells grown in both acid adaptation and recovery conditions accumulated in the G0/G1 phase compared to cells cultured under normal pH conditions by  $13.8 \pm 4\%$  and  $10.7 \pm 2.2\%$ , respectively ( $n = 3$ ,  $p < 0.01$ , Figure 4A). Furthermore, the number of cells in the S phase decreased significantly by  $21 \pm 6.4\%$  in acid adaptation conditions. It increased significantly by  $17 \pm 5\%$  in acid recovery conditions when compared to cells in normal pH conditions ( $n = 3$ ,  $p < 0.01$ , Figure 4A). In the G2-M phase, the number of cells were decreased by  $26 \pm 5.8\%$  and  $26 \pm 3.8\%$  in acid adaptation and recovery conditions,



respectively, compared to normal pH conditions ( $n = 3$ ,  $p < 0.01$  and  $0.001$ , Figure 4A). These results indicate that acid adaptation of PANC-1 cells arrests them in the G0/G1 phase. In contrast, when they recover from this acid adaptation, they accumulate in the S phase and proliferate to a greater extent than cells grown in control conditions.

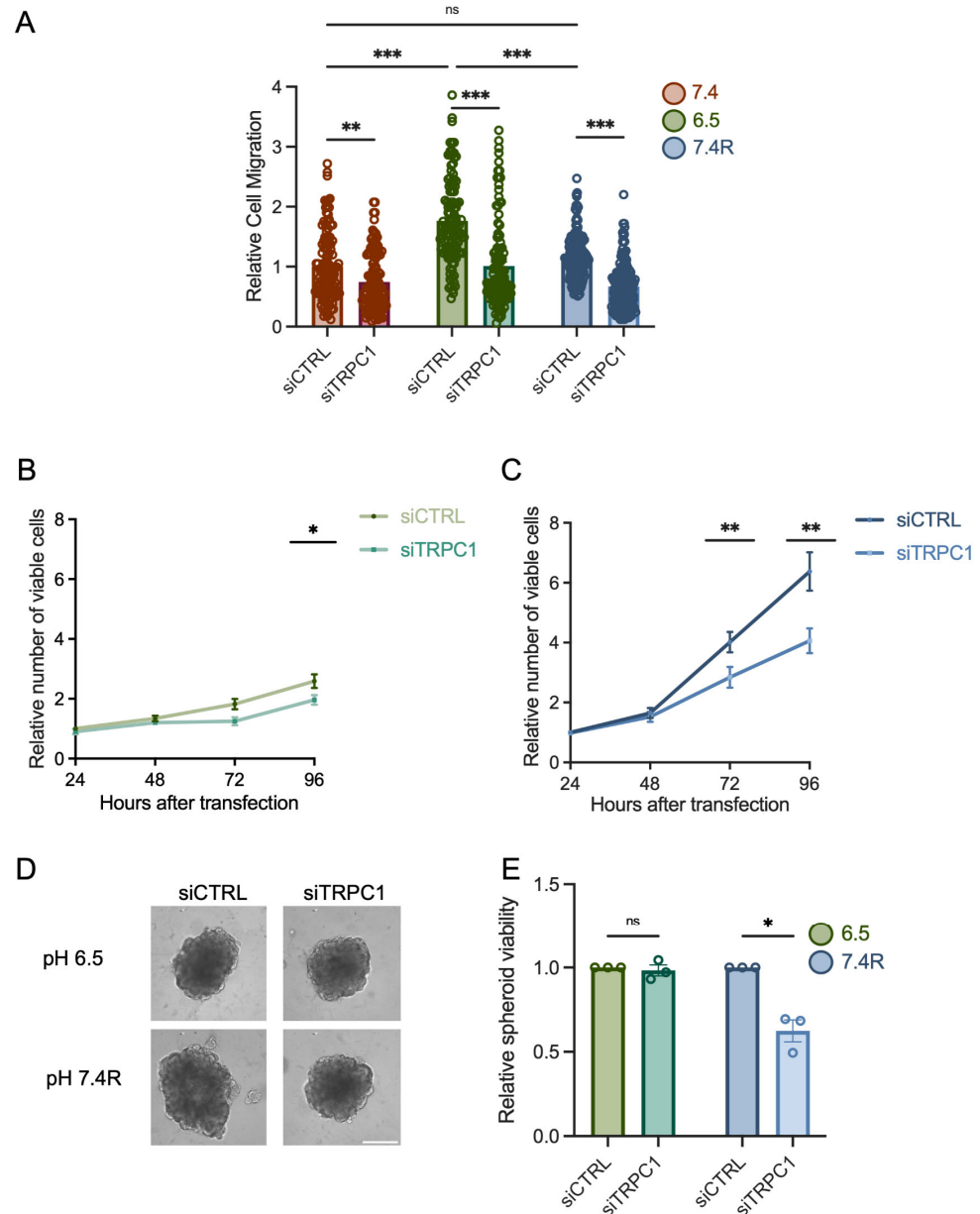


**Figure 3.** TRPC1 silencing inhibits cell migration, proliferation, and the growth of PANC-1 spheroids under acid recovery conditions. (A) Cell migration of siTRPC1 cells grown under normal pH (7.4), acid adaptation (6.5), or acid recovery conditions (7.4R) analyzed by Boyden chamber assay ( $n = 3-4$ ). Tukey's multiple comparison test was used to determine significant differences between conditions. (B) Trypan blue analysis of siTRPC1 PANC-1 cells grown under acid adaptation (6.5), or (C) acid recovery conditions (7.4R), showing the relative number of viable cells 24, 48, 72, and 96 h post-transfection ( $n = 3-5$ ). (D) Representative images of siTRPC1 transfected PANC-1 spheroids grown for 9 days, and (E) viability quantification performed with CellTiter-Glo<sup>®</sup> assay of siTRPC1 transfected spheroids grown under acid adaptation (6.5) or acid recovery (7.4R) ( $n = 3$ ), scale bar = 400  $\mu$ m. Welch's correction  $t$ -test was used to determine the significant difference between siCTRL and siTRPC1 conditions. ns indicates non-significance. \*, \*\*, and \*\*\* indicate  $p < 0.05$ ,  $0.01$ , and  $0.001$ , respectively.

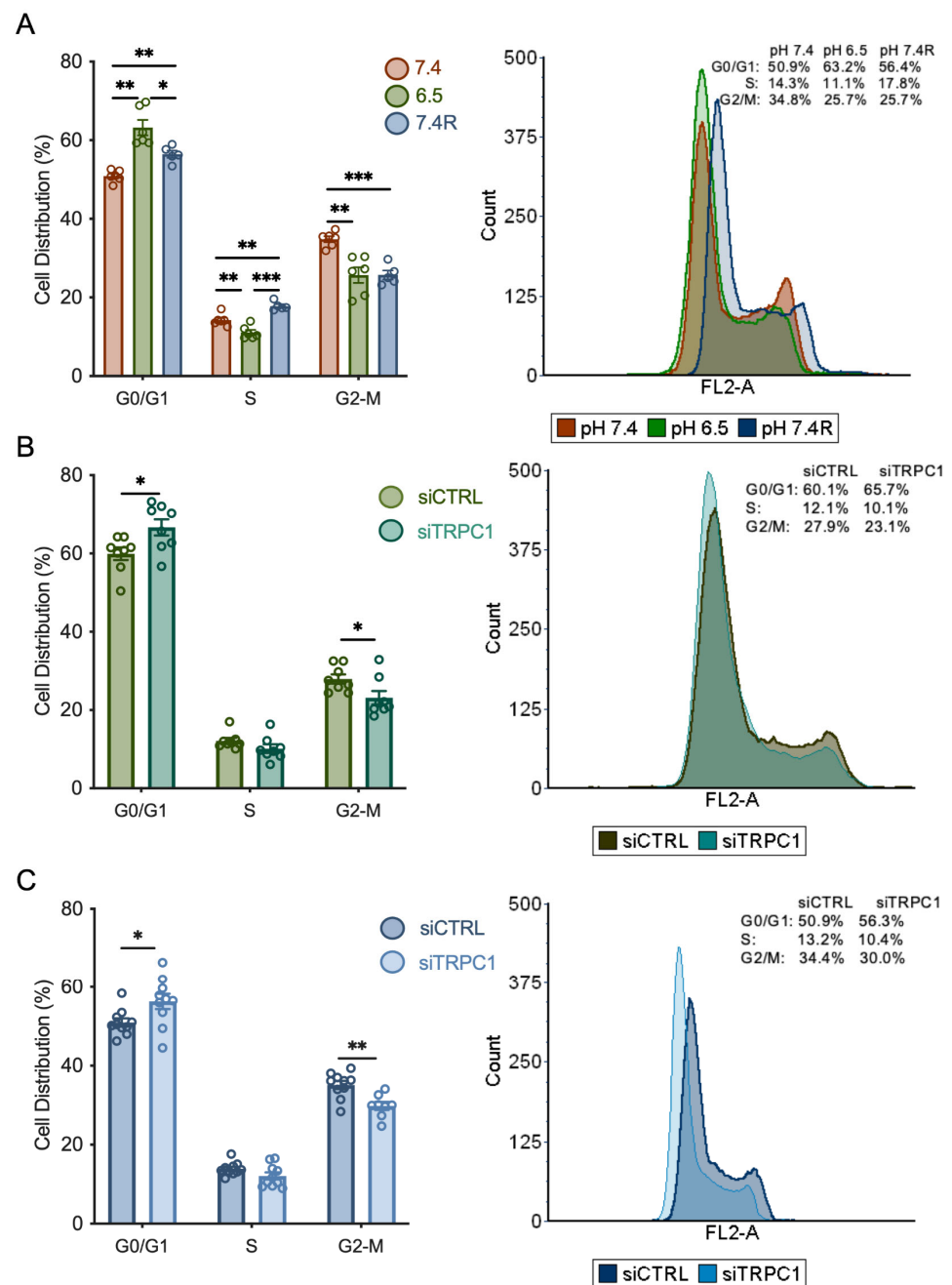


**Figure 4.** TRPC1 silencing accumulates cells in the G0/G1 phase and reduces the number of cells in the G2/M phase in both acid adaptation and recovery conditions. **(A)** Quantification of cell cycle analysis representing the percentage of cells in each cell cycle phase of non-transfected PANC-1 cells grown under normal pH (7.4), acid adaptation (6.5) or acid recovery conditions (7.4R) (left panel) and representative data from FACS acquisition (right panel). **(B)** Quantification of cell cycle analysis representing the percentage of cells in each cell cycle phase of siTRPC1 transfected PANC-1 cells grown under acid adaptation (6.5) or **(C)** acid recovery conditions (7.4R) (left panel), and representative data from FACS acquisition (right panel). Welch's correction *t*-test was used to determine the significant difference between different conditions. \*, \*\*, and \*\*\* indicate  $p < 0.05$ , 0.01, and 0.001, respectively.

In addition to the effect of pH, we investigated the role of TRPC1 in the cell cycle distribution in acid-adapted and -recovered cells. We have previously shown that silencing of TRPC1 accumulated cells grown in normal pH conditions in the G0/G1 phase and decreased the number of cells in the S phase [37]. Here, we show, in the acid adaptation

conditions, that TRPC1 silencing resulted in a slight accumulation ( $10 \pm 4.3\%$ ) of cells in the G0/G1 phase and a decrease in the number of cells in the G2/M phase by  $17 \pm 7.4\%$  ( $n = 4, p < 0.05$ , Figure 4B). This profile was maintained upon TRPC1 KD in acid recovery conditions; with an increase in the number of cells by  $9.4 \pm 4\%$  in the G0/G1 phase and a decrease of  $15.1 \pm 4\%$  in the G2/M phase ( $n = 4, p < 0.05$  and  $0.01$ , Figure 4C). These results suggest that TRPC1 is involved in G0/G1 progression, regardless of the pH condition. Furthermore, the role of TRPC1 in cell cycle progression shifts from the S phase in normal pH conditions to the G2/M phase in acidic and recovery conditions.

### 3.4. TRPC1 Strongly Modulates the Expression of CDKs and Cyclin A in Acid Adaptation and Recovery Conditions

In normal pH conditions, the KD of TRPC1 reduced the expression of CDK6, CDK2, and cyclin A and increased p21<sup>CIP1</sup> expression [37]. We investigated the effect of siTRPC1 on the expression of these proteins in both acid-adapted and -recovered cells. Our immunoblot analysis showed that the expression of CDK6 and CDK2 was more affected in acid-adapted and -recovered cells depleted of TRPC1. CDK6 protein expression was decreased by  $53 \pm 5.3\%$  and  $73 \pm 1.5\%$  and CDK2 expression was decreased by  $43 \pm 1.3\%$  and  $70 \pm 1.5\%$  in acid-adapted ( $n = 3-4, p < 0.01$  and  $0.001$ , Figure 5A,B) and -recovered cells ( $n = 3-6, p < 0.05$  and  $0.01$ , Figure 5A,C), respectively. A similar profile was observed for cyclin A and p21<sup>CIP1</sup> expression. The expression of cyclin A was reduced by  $45 \pm 7.8\%$  and  $44 \pm 4.2\%$ , and the expression of p21<sup>CIP1</sup> was upregulated by  $31\% \pm 6.2\%$  and  $34\% \pm 2.7\%$ , in acid-adapted and -recovered cells, respectively ( $n = 4, p < 0.05$  and  $0.01$ , Figure 5A,E,F). The expression of CDK1, the regulator driving cells through the G2/M phase, was not affected by TRPC1 KD in normal pH conditions [37]. In this study, the silencing of TRPC1 decreased CDK1 expression by  $20 \pm 4.9\%$  and  $45 \pm 1.4\%$  for cells grown in acid adaptation and recovery conditions, respectively ( $n = 3-5, p < 0.05$ , Figure 5A,D). Moreover, TRPC1 KD failed to affect the expression of cyclin B1, D1, D3, and E, along with CDK4 in both acid-adapted and -recovered cells (Figure S3A). Collectively, these results suggest that the depletion of TRPC1 has a stronger effect on the expression of the cell cycle regulating proteins, CDK1, -2, and -6, cyclin A, and p21<sup>CIP1</sup> in acid-recovered PANC-1 cells than in normal pH and acid-adapted cells.

### 3.5. TRPC1 Interacts Strongly with the PI3K p85 $\alpha$ Subunit and CaM under Acid Adaptation and Recovery Conditions

The PI3K signaling cascade is a regulator of cell cycle progression, as it activates transcription of cell cycle regulating proteins [50]. TRPC1 has been shown to be involved in activating the PI3K signaling pathway [30,33,51], and we have recently demonstrated that TRPC1 formed a complex with the PI3K p85 $\alpha$  subunit and its associated connecting protein CaM, thereby regulating PANC-1 cell proliferation under normal pH conditions [37]. Thus, we aimed to investigate the role of the acidic tumor microenvironment and TRPC1 in association with PI3K signaling. Through confocal imaging, we found that TRPC1 also co-localized with the PI3K p85 $\alpha$  subunit in acid-adapted PANC-1 cells, and that this was maintained under acid recovery conditions (Figure 6A). This co-localization was illustrated by the calculation of Mander's overlapping R coefficient, which was 0.13, 0.58, and 0.48 in normal pH, acid adaptation, and acid recovery conditions, respectively (Figure 6A). We further investigated the protein interaction between the PI3K p85 $\alpha$  subunit and TRPC1. With PLA analysis, we found an increase in the proximity between the PI3K p85 $\alpha$  subunit and TRPC1 in acid-adapted cells by  $43.8 \pm 5.6\%$  and by  $28 \pm 7.2\%$  in acid-recovered cells, compared to cells grown under normal pH conditions, respectively ( $n = 3, p < 0.01$  and  $0.001$ , Figure 6B,C). The proximity was decreased by  $21 \pm 6.7\%$  in acid-recovered cells compared to acid-adapted cells ( $n = 3, p < 0.01$ , Figure 6B,C). The protein-protein interaction was then confirmed by co-IP analysis, where we found similar results with the pull-down of both TRPC1 and PI3K p85 $\alpha$  (Figure 6D). In addition, we investigated the interaction between CaM and TRPC1. Indeed, CaM can function as a connecting protein between TRPC1 and the p85 $\alpha$  subunit of PI3K [51]. We found that CaM interacted with

TRPC1 and the PI3K p85 $\alpha$  subunit in all three pH conditions (Figure 6D). To strengthen the indication of a complex between TRPC1, PI3K, and CaM, we first performed PLA analysis on PANC-1 cells upon the silencing of TRPC1. We observed that the protein interaction between the PI3K p85 $\alpha$  subunit and TRPC1 was decreased by  $50.7 \pm 6.2\%$  and  $34.2 \pm 8.0\%$  under acid adaptation and recovery conditions, respectively ( $n = 3, p < 0.001$ , Figure 7A,B). Next, we determined the protein–protein interaction upon the KD of TRPC1 by co-IP. Compared to siCTRL conditions, the interaction between TRPC1 and the PI3K p85 $\alpha$  subunit was significantly decreased in siTRPC1 conditions by  $79.8 \pm 8.5\%$  and  $47.2 \pm 14.5\%$  in acid-adapted and -recovered cells, respectively ( $n = 4, p < 0.05$  and  $0.01$ , Figure 7C,D). Furthermore, a significant decrease in protein–protein interaction by  $40.3 \pm 10.8\%$  and  $23.0 \pm 6.0\%$  was observed between TRPC1 and CaM in acid-adapted and -recovered cells, respectively ( $n = 4, p < 0.05$  and  $0.01$ , Figure 7C,E). Collectively, these results indicate that TRPC1 interacts strongly with the PI3K p85 $\alpha$  subunit under acidic and recovery conditions, probably in assembly with CaM.

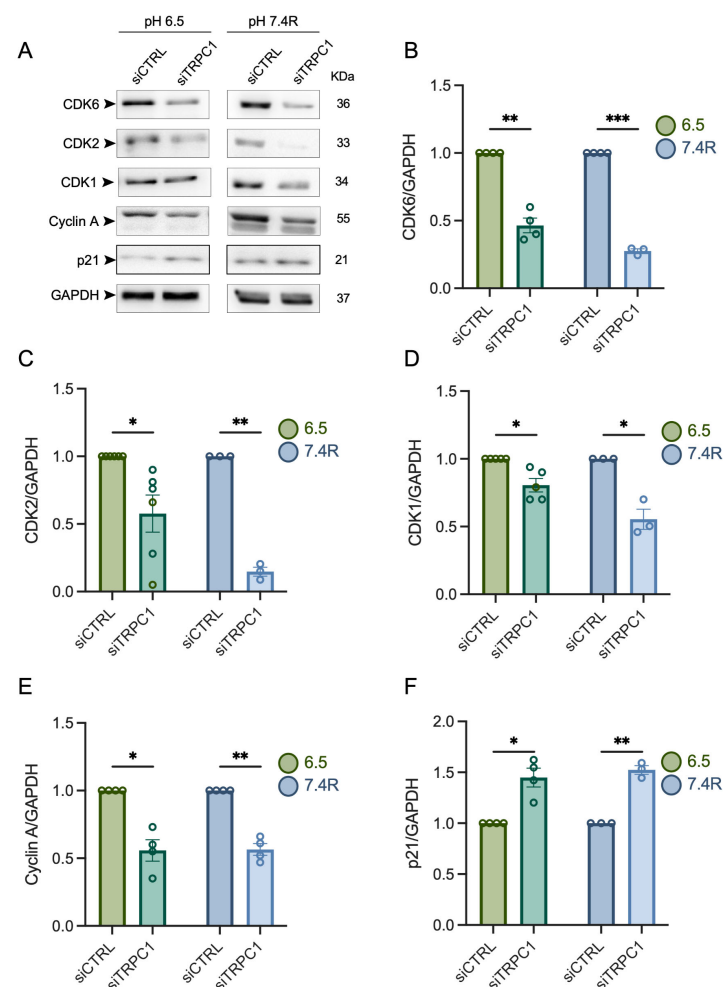


**Figure 5.** TRPC1 silencing decreases the expression of CDK6, -1, -2, and cyclin A and increases the expression of p21<sup>CIP1</sup> to a greater extent in acid recovery conditions. (A) Western blot analysis of relevant cyclin-dependent kinase complexes and cyclins and their inhibitor p21<sup>CIP1</sup> from cells grown under acid adaptation (6.5) or acid recovery conditions (7.4R). (B) Quantification of Western blot analysis representing the expression of CDK6, (C) CDK2, (D) CDK1, (E) cyclin A, and (F) p21<sup>CIP1</sup> in siTRPC1 lysates compared to siCTRL lysates from PANC-1 cells grown under acid adaptation (6.5) or acid recovery (7.4R) conditions ( $n = 3 - 6$ ). Welch's correction  $t$ -test was used to determine the significant difference between siCTRL and siTRPC1. \*, \*\*, and \*\*\* indicate  $p < 0.05$ ,  $0.01$ , and  $0.001$ , respectively. The uncropped blots are shown in File S1.

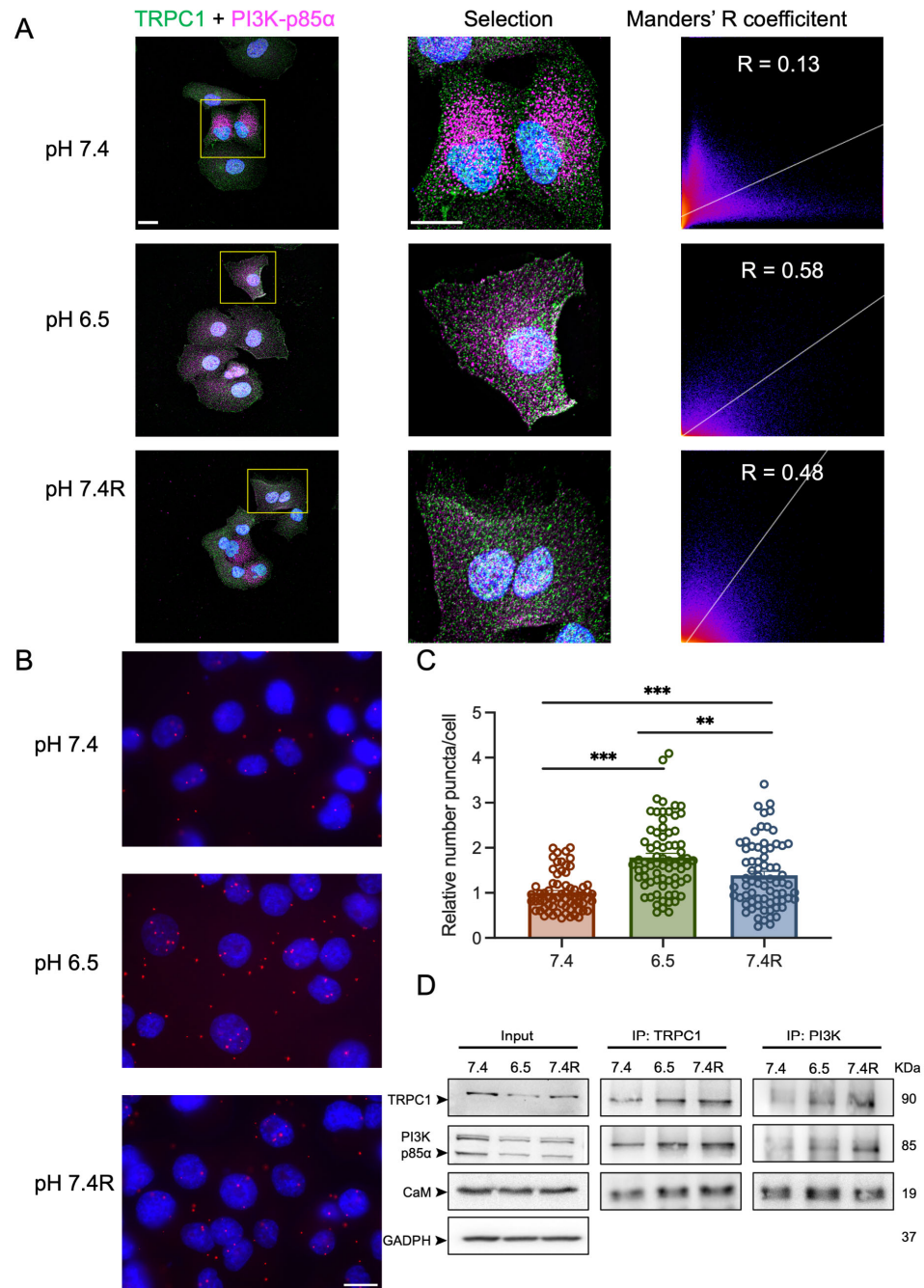


**Figure 6.** TRPC1 strongly interacts with the PI3K p85α subunit and CaM in acid adaptation and recovery conditions. **(A)** Representative immunofluorescent analysis of TRPC1 and the PI3K p85α subunit in PANC-1 cells grown under normal pH (7.4), acid adaptation (6.5) or acid recovery conditions (7.4R), scale bars = 20 μm. Mander's R coefficient was used to quantify the co-localization between the two fluorophores ( $n = 3$ ). **(B)** Representative images of proximity ligation assay (PLA) in PANC-1 cells grown under normal pH (7.4), acid adaptation (6.5), or acid recovery conditions (7.4R), scale bar = 10 μm. **(C)** Quantification of PLA where conditions are normalized to normal pH conditions (7.4) ( $n = 3$ ). Welch's correction  $t$ -test was used to determine the significant difference between different conditions. \*\* and \*\*\* indicate  $p < 0.01$  and  $0.001$ , respectively. **(D)** Representative Western blot analysis of co-immunoprecipitation of TRPC1 and PI3K p85α subunit with CaM in non-transfected PANC-1 cells grown under normal pH (7.4), acid adaptation (6.5) or acid recovery conditions (7.4R), ( $n = 3-5$ ). The control pull-down performed with rabbit IgG is presented in Figure S3B. The uncropped blots are shown in File S1.



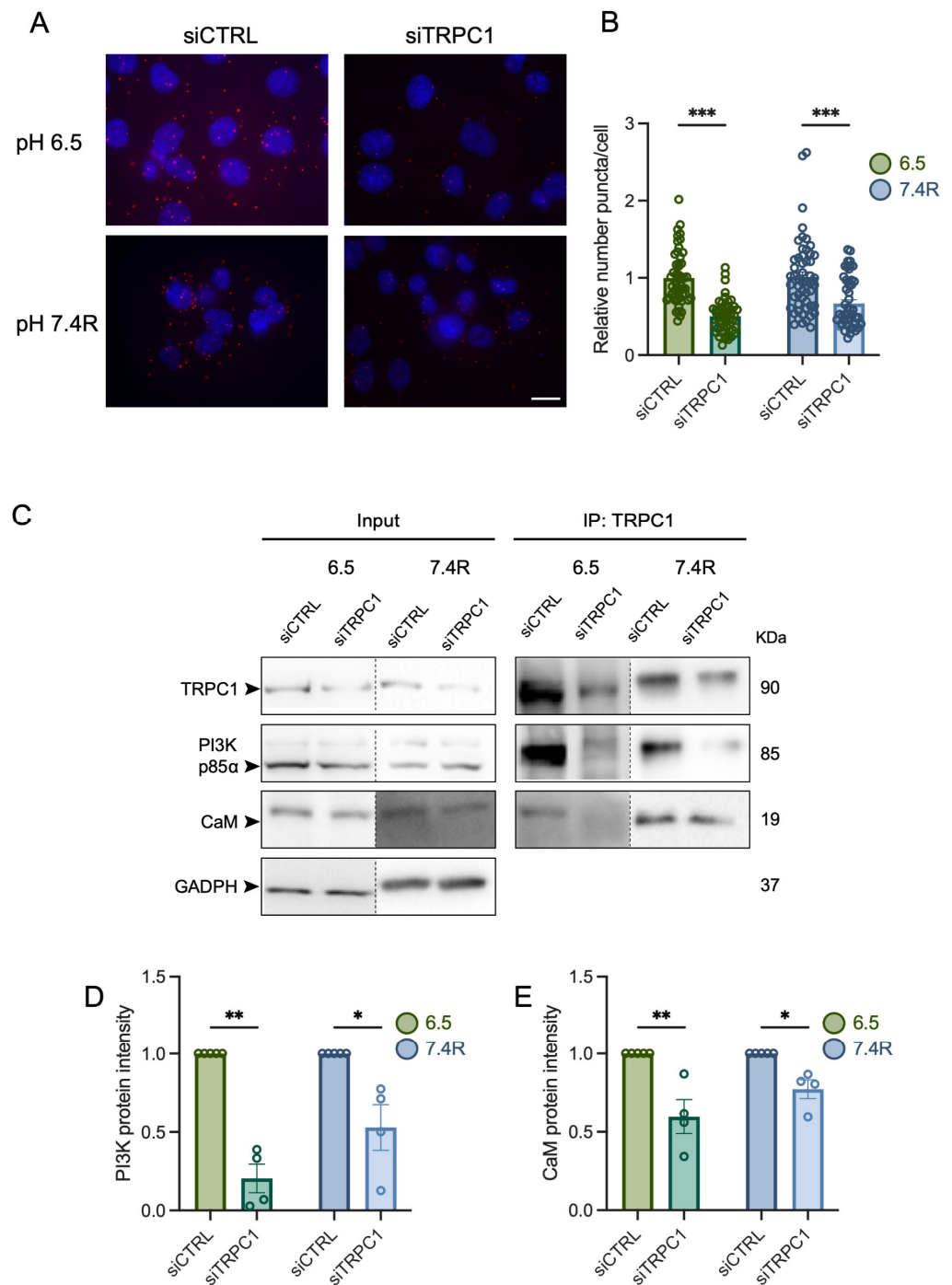


**Figure 7.** TRPC1 silencing inhibits the interaction between the PI3K p85α subunit and CaM. **(A)** Representative images of PLA in transfected PANC-1 cells grown under acid adaptation (6.5) or acid recovery conditions (7.4R). Scale bar = 10 μm. **(B)** Quantification of PLA in transfected PANC-1 cells grown under acid adaptation (6.5) or acid recovery conditions (7.4R), where siTRPC1 is compared to the relative number of siCTRL ( $n = 3$ ). Welch’s correction  $t$ -test was used to determine the significant difference between different conditions. **(C)** Representative Western blot analysis of co-immunoprecipitation of TRPC1 with PI3K p85α and CaM in transfected PANC-1 cells grown under acid adaptation (6.5) or acid recovery conditions (7.4R). The control pull-down performed with rabbit IgG is presented in Figure S3B. **(D)** Quantification of PI3K p85α subunit intensity and **(E)** CaM intensity from co-immunoprecipitation ( $n = 3-4$ ). Welch’s correction  $t$ -test was used to determine the significant difference between different conditions. \*, \*\*, and \*\*\* indicate  $p < 0.05$ , 0.01, and 0.001, respectively. The uncropped blots are shown in File S1.



### 3.6. The Knockdown of TRPC1 Decreases the Phosphorylation of AKT and ERK1/2 in Acid-Recovered PANC-1 Cells

In normal pH conditions, TRPC1 silencing regulates AKT to a greater extent than ERK1/2, with a decrease of  $39 \pm 7.8\%$  and  $13 \pm 0.4\%$ , respectively [37]. Hence, we investigated the effect of TRPC1 silencing on the phosphorylation of AKT and ERK1/2 in acid-adapted and -recovered cells. The KD of TRPC1 reduced the activation of AKT less in acid-adapted cells ( $27.4 \pm 4.2\%$ ), and more in acid-recovered cells ( $48.0 \pm 5.6\%$ ), when compared to normal pH ( $n = 4-5$ ,  $p < 0.01$ , Figure 8A,B). Moreover, AKT total expression remained unchanged. Silencing of TRPC1 reduced the activation of ERK1/2 strongly in acid-adapted and -recovered cells when compared to pH 7.4 ( $32.0 \pm 6.9\%$  and  $39.0 \pm 10.7\%$ ), respectively, without affecting the total ERK1/2 protein expression ( $n = 4$ ,  $p < 0.05$ , Figure 8C,D). Taken together, these results indicate that TRPC1 affects the activation of AKT to a greater extent in acid-recovered PANC-1 cells and ERK1/2 phosphorylation in both conditions.

Once we had established that TRPC1 and the PI3K p85 $\alpha$  subunit interact with CaM, and that TRPC1 regulates AKT and ERK1/2 phosphorylation, we investigated whether the inhibition of CaM affected the downstream signaling protein kinases AKT and/or ERK1/2. Treatment of cells with the CaM inhibitor W7 for 72 h decreased the phosphorylation of AKT by  $25 \pm 6.8\%$  in acid recovery conditions ( $n = 4$ ,  $p < 0.05$ , Figure S4E). No significant decrease was found in normal pH or acid adaptation conditions ( $n = 3-4$ , Figure S4A,C). Furthermore, we found that the treatment with W7 decreased the phosphorylation of ERK1/2 by  $23.8 \pm 1.9\%$ ,  $35.0 \pm 10.5\%$ , and  $40.0 \pm 6.0\%$  in normal pH, acid adaptation, and acid recovery conditions, respectively ( $n = 4$ ,  $p < 0.05$  and  $0.01$ , Figure S4B,D,F). These results indicate that CaM-dependent mechanisms regulate AKT solely in acid-recovered cells, while ERK1/2 levels are affected in all conditions and notably in acid-adapted and in acid-recovered PANC-1 cells.

### 3.7. PANC-1 Cell Migration and Proliferation Depend Mainly on Extracellular Ca<sup>2+</sup> Entry, Likely through TRPC1, in Acid-Adapted and -Recovered PANC-1 Cells

TRPC1 is not involved in SOCE, nor in basal Ca<sup>2+</sup> entry in normal pH conditions; instead, it regulates PANC-1 cell proliferation through a Ca<sup>2+</sup>-independent mechanism [37]. As TRPC1 was more localized at the plasma membrane in both acid-adapted and -recovered cells compared to control, we investigated whether TRPC1 participates in Ca<sup>2+</sup> entry in these conditions. First, we found an increase in Mn<sup>2+</sup> quenching in acid-recovered cells ( $34.7 \pm 5.8\%$  and  $57 \pm 6.2\%$ ), compared to cells grown in normal pH and acid adaptation conditions, respectively, ( $n = 150, 405$ , and  $325$ ,  $p < 0.01$  and  $0.001$ , Figure 9A–D). Furthermore, we found that KD of TRPC1 decreased Mn<sup>2+</sup> quenching by  $60.2 \pm 6.8\%$  in acid-adapted cells ( $n = 5$ ,  $p < 0.001$ , Figure 9B,D) and by  $21.5 \pm 6.8\%$  in acid-recovered cells ( $n = 5$ ,  $p < 0.01$ , Figure 9C,D), whereas no effect was observed in normal pH conditions ( $n = 3$ , Figure 9A,D). Moreover, TRPC1 KD elicited a decrease of  $12.8 \pm 2.4\%$  in the basal Ca<sup>2+</sup> ratio in acid-adapted cells only ( $n = 3$ ,  $p < 0.001$ , Figure S5A,B), and failed to affect SOCE in acid adaptation and recovery conditions ( $n = 4$ , respectively, Figure S5A,C–F).

Given the ability of TRPC1 to regulate basal Ca<sup>2+</sup> entry in acid-adapted and -recovered cells, and to understand whether Ca<sup>2+</sup> is involved in cell migration and proliferation, we cultured cells in normal and low Ca<sup>2+</sup> (30  $\mu$ M free Ca<sup>2+</sup>) medium. Cell migration decreased by  $40 \pm 3.7\%$  and  $34.2 \pm 5.6\%$  in acid-adapted and -recovered cells, respectively, in the low Ca<sup>2+</sup> medium ( $n = 3$  and  $4$ ,  $p < 0.001$ , Figure 10B,C). KD of TRPC1 in this condition reduced migration additionally by  $15.2 \pm 4.7\%$  and  $12.5 \pm 6.3\%$  in acid-adapted and -recovered cells, respectively ( $n = 3$  and  $4$ ,  $p < 0.001$  and  $< 0.05$ , Figure 10B,C). Furthermore, no significant difference was found between the cell migration of siTRPC1 cells in normal Ca<sup>2+</sup> medium and in siCTRL cells in low Ca<sup>2+</sup> medium, indicating that TRPC1 mainly regulates PANC-1 cell migration in a Ca<sup>2+</sup>-dependent manner in acid adaptation conditions ( $n = 3$ , Figure 10B). In normal pH conditions, low Ca<sup>2+</sup> medium failed to affect cell migration, and silencing of

TRPC1 reduced it to a similar extent with or without extracellular  $Ca^{2+}$  ( $27.1 \pm 4.7\%$  and  $30.4 \pm 5.9$ , respectively;  $n = 3$ ,  $p < 0.001$ , Figure 10A).

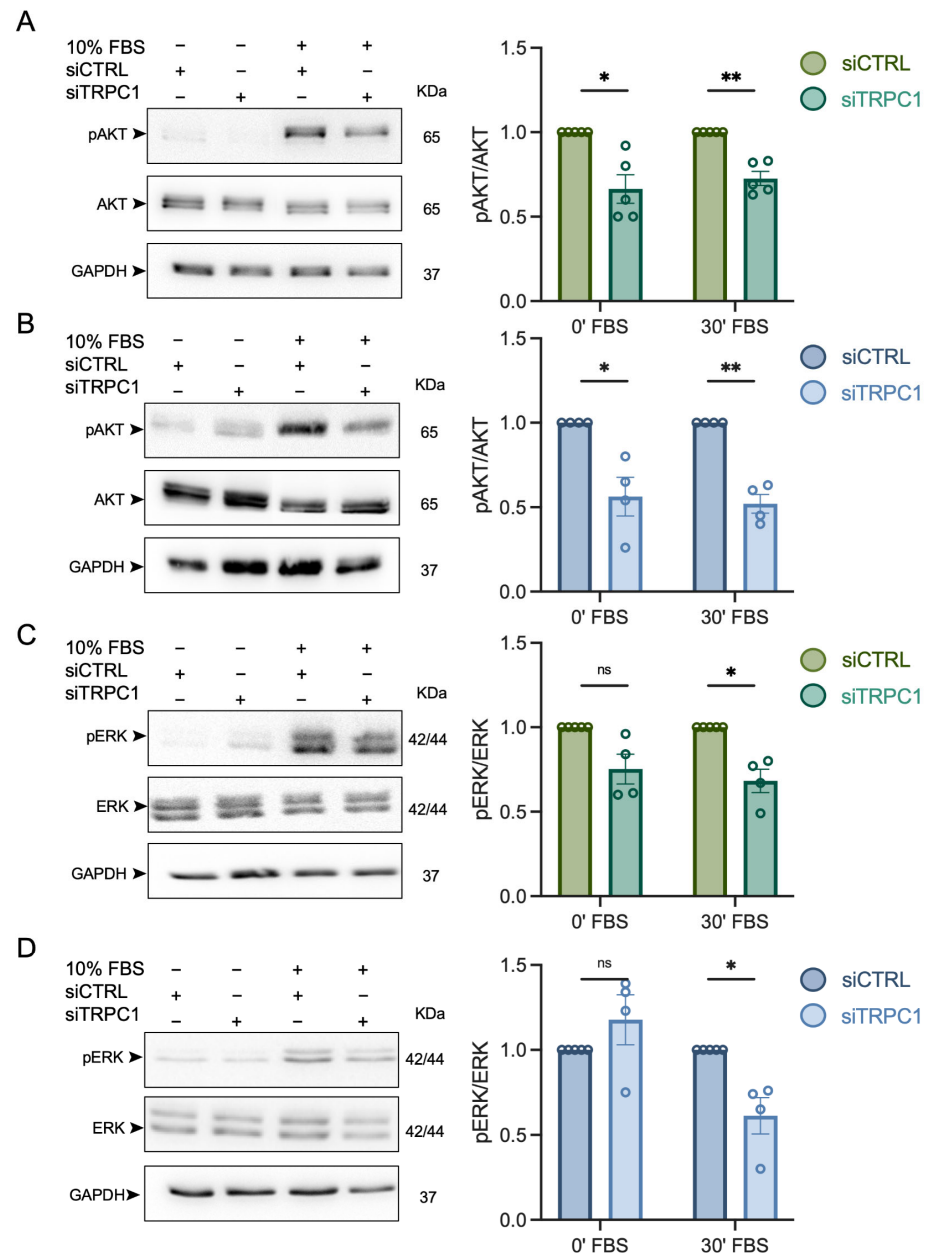


**Figure 8.** TRPC1 silencing inhibits the phosphorylation of AKT and ERK1/2, notably in acid recovery conditions. (A) Western blot analysis of phosphorylated AKT (pAKT) and total AKT in transfected PANC-1 cells grown in acid adaptation (6.5) conditions or (B) in acid recovery (7.4R) conditions after mitogen activation with FBS for either 0 or 30 min (left panel). Quantification of the Western blot analysis compared to siCTRL either after 0 min or 30 min of mitogen activation (right panel). (C) Western blot analysis of phosphorylated ERK1/2 (pERK1/2) and total ERK1/2 in transfected PANC-1 cells grown in acid adaptation (6.5) conditions or (D) in acid recovery conditions (7.4R) after mitogen activation with FBS for either 0 or 30 min (left panel). Quantification of the Western blot analysis compared to siCTRL either after 0 min or 30 min of mitogen activation (right panel). Welch’s correction *t*-test was used to determine the significant difference between siCTRL and siTRPC1. ns indicates non-significance. \* and \*\* indicate  $p < 0.05$  and  $0.01$ , respectively. The uncropped blots are shown in File S1.

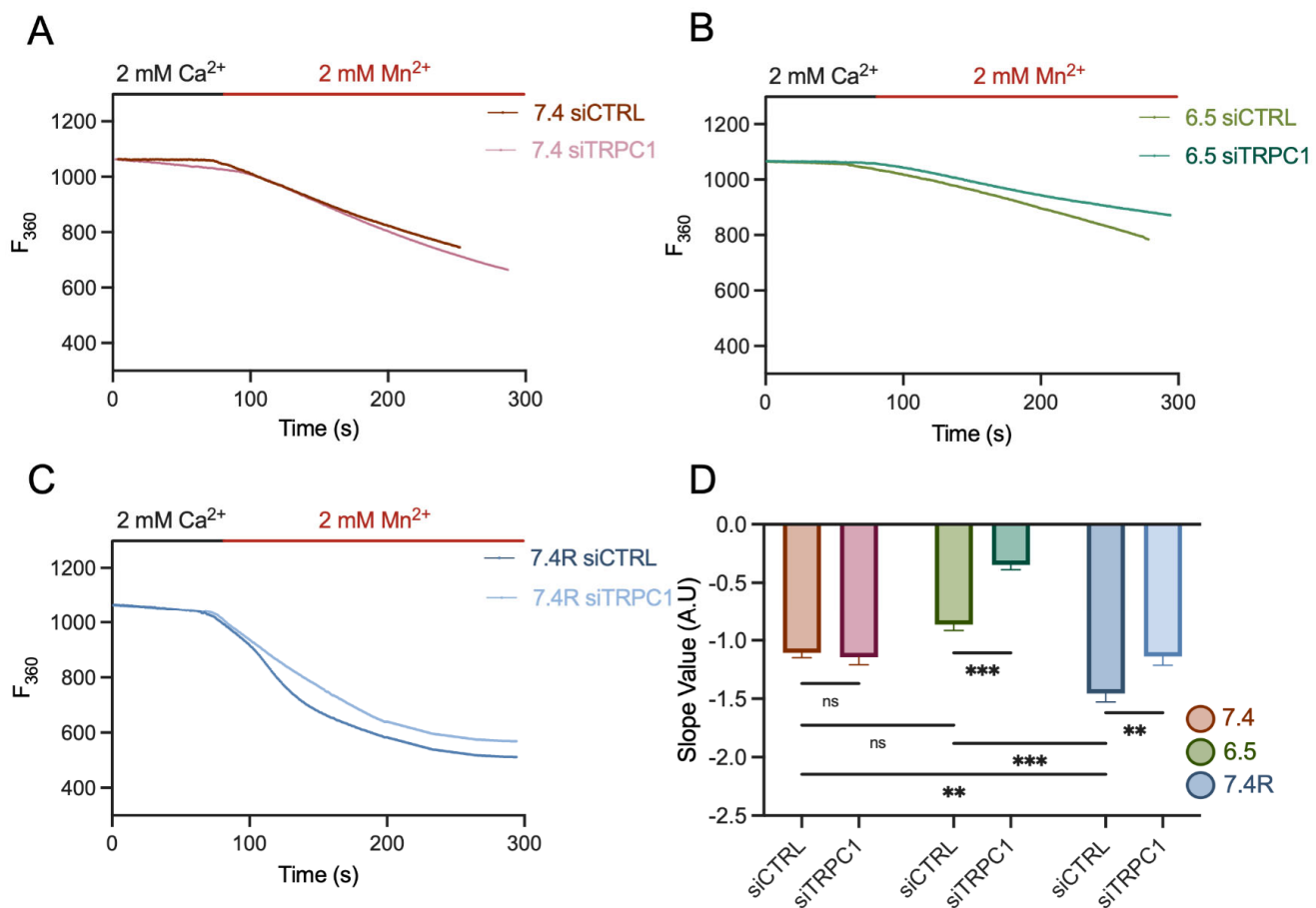


**Figure 9.** TRPC1 reduces basal  $\text{Ca}^{2+}$  entry in acid adaptation and recovery conditions. (A) Representative traces of  $\text{Mn}^{2+}$  quenching in transfected PANC-1 cells grown in normal pH conditions (7.4), (B) in acid adaptation (6.5) conditions, or (C) in acid recovery conditions (7.4R). (D) Quantification of siCTRL and siTRPC1 transfected PANC-1 cells in all three conditions (number of analyzed cells; pH 7.4 siCTRL  $n = 150$  and siTRPC  $n = 128$ , pH 6.5 siCTRL  $n = 405$  and siTRPC  $n = 326$ , pH 7.4R siCTRL  $n = 325$  and siTRPC  $n = 214$ ). Tukey's multiple comparison test was used to determine significant differences between conditions. ns indicates non-significance. \*\* and \*\*\* indicate  $p < 0.01$  and  $0.001$ , respectively.

Growth in low  $\text{Ca}^{2+}$  medium for 48 h decreased cell proliferation by  $24.1 \pm 5.3\%$  and  $30 \pm 3.5\%$  in acid adaptation and recovery conditions, respectively ( $n = 4$  and  $5$ ,  $p < 0.001$ , Figure 10D,E). Furthermore, in low  $\text{Ca}^{2+}$  conditions, KD of TRPC1 decreased cell proliferation additionally by  $16.2 \pm 5.8\%$  in acid-adapted and by  $15.3 \pm 4.9\%$  in acid-recovered cells ( $n = 4$  and  $5$ ,  $p < 0.01$  and  $0.001$ , Figure 10D,E). These results suggest that in acid-adapted and -recovered PANC-1 cells, proliferation and migration exhibit increased dependence on extracellular  $\text{Ca}^{2+}$  levels. TRPC1 permits  $\text{Ca}^{2+}$  entry, which regulates cell migration and proliferation by  $\text{Ca}^{2+}$ -dependent and, to some extent, -independent mechanisms.

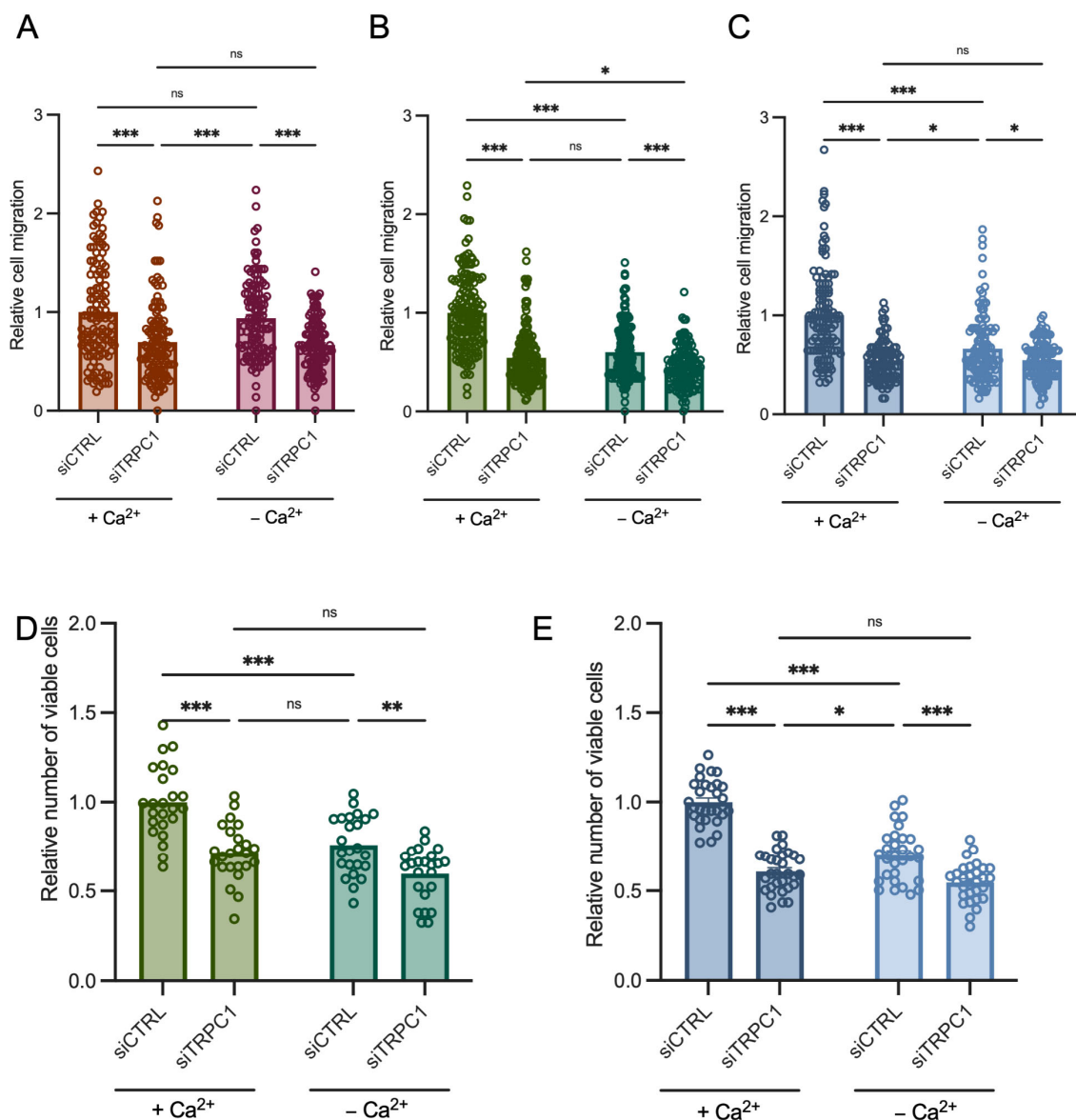


**Figure 10.** The role of TRPC1 in PANC-1 cell migration and proliferation shifts from being Ca<sup>2+</sup>-independent in normal pH conditions to being substantially Ca<sup>2+</sup>-dependent in acid adaptation and recovery conditions. (A) Boyden chamber assay analysis of transfected PANC-1 cells grown in normal pH conditions, (B) in acid-adapted (6.5) conditions, or (C) in acid-recovered (7.4R) conditions. Cells were transfected for 72 h in total. After 48 h, cells were seeded in Boyden inserts for 8 h, and were then treated with medium containing extracellular Ca<sup>2+</sup> concentrations (+ Ca<sup>2+</sup>), or with a medium depleted of extracellular Ca<sup>2+</sup> (− Ca<sup>2+</sup>), for 24 h (*n* = 3). (D) Trypan blue assay analysis of transfected PANC-1 cells grown in acid-adapted (6.5) conditions or (E) in acid-recovered (7.4R) conditions. Cells were transfected for 72 h in total and either treated with medium containing extracellular Ca<sup>2+</sup> concentrations (+ Ca<sup>2+</sup>), or with medium depleted of extracellular Ca<sup>2+</sup> (− Ca<sup>2+</sup>), for 48 h (*n* = 3). Tukey's multiple comparison test was used to determine significant differences between conditions. ns indicates non-significance. \*, \*\*, and \*\*\* indicate *p* < 0.05, 0.01, and 0.001, respectively.

#### 4. Discussion

Numerous studies have addressed the impact of TRPC1 dysregulation on hallmarks of cancer. However, the interplay between the acidic tumor microenvironment and TRPC1 expression and downstream mechanisms contributing to PDAC progression are unexplored.

The key findings of this study are: (i) The acidic tumor microenvironment promotes PDAC cell migration but attenuates proliferation, which is restored upon recovery. (ii) Acid adaptation reduces TRPC1 expression but favors its plasma membrane localization and its interaction with the PI3K p85 $\alpha$  subunit and CaM. (iii) TRPC1 regulates acid-adapted and -recovered PANC-1 cell migration and proliferation by both Ca<sup>2+</sup>-dependent and -independent mechanisms. This likely occurs through the PI3K/CaM axis and the downstream activation of AKT and ERK1/2.

Acid adaptation creates an evolutionary selection pressure that contributes to a malignant phenotype [52,53]. Our results show that acid adaptation reduces PANC-1 cell viability and spheroid growth. In congruence with this, other studies have found the same events in different types of cancer cells [54–56], including PDAC cell lines [40,57,58]. Although acid adaptation is becoming of interest, not much is known about the recovery of and fluctuations in the acidic microenvironment. However, one study has shown that oral squamous cell carcinomas can restore their proliferation capacity after 7 and 21 days of acid treatments (pH 6.8) followed by 7 days of recovery (pH 7.4). To our knowledge, we are the first to show that 14 days of acid recovery restores PANC-1 proliferation rates, and that PANC-1 spheroid viability is enhanced after 9 days of recovery in normal pH conditions.

It is well accepted that proliferation and cell cycle progression depend on a permissive and slightly alkaline pH<sub>i</sub> [41,48]. Our results show that acid-adapted PANC-1 cells exposed to pH 7.4 exhibited a more alkaline pH<sub>i</sub>. The acid adaptation and recovery conditions led to the accumulation of cells in G0/G1 phases and decreased the number of cells in G2/M phases. Regarding the S phase, the number of cells was increased in the acid recovery conditions, suggesting that acid adaptation promotes a more alkaline pH<sub>i</sub>, which results in the improved cell proliferation of acid-recovered PANC-1 cells.

Moreover, long-term acidosis enhances extracellular matrix degradation that promotes cell migration and invasion [8,15]. Our findings are in congruence with previous reports showing that acid adaptation increased the migratory abilities of cancer cells, including PANC-1 cells [39,52,54–56,59]. However, the cell migration was reduced upon recovery conditions to the same levels as for normal pH conditions. Similar results were found in prostate carcinoma cells, where acute acidosis (3 h) followed by 24 h of pH 7.4 treatment decreased cell motility [60]. In oral squamous carcinoma cells, no difference in cell migration was found between acid-adapted (21 days) and -recovered (7 days) conditions. However, after only 7 days of acid treatment and 7 days of recovery under normal conditions, cell migration increased [54]. In a mouse model of metastatic breast cancer, an increase in pH to 7.4 after acid adaptation led to reduced spontaneous metastases [61]. These results suggest that migratory properties of acid-recovered cells are cell type-specific and depend on the time of acidosis and recovery.

We recently demonstrated that TRPC1 does not contribute to Ca<sup>2+</sup> entry in PANC-1 cells grown under normal pH conditions [37]. Here, we show that there is a decrease in TRPC1 expression along with an increase in the plasma membrane fraction of TRPC1 in acid-adapted cells. In acid-recovered cells, the expression increased and increased plasma membrane localization of TRPC1 was maintained. In addition, TRPC1 was involved in Ca<sup>2+</sup> entry in acid adaptation and recovery conditions. Moreover, the Ca<sup>2+</sup> entry was increased upon acid recovery, indicating that PANC-1 cells grown in these conditions depend more on extracellular Ca<sup>2+</sup> concentrations. It is unknown whether TRPC1 expression and function are affected by changes in pH. However, acidic pH activates its homologs TRPC4 and TRPC5 [35,36], leading to Ca<sup>2+</sup> entry. In addition, other ion channels, transporters, and receptors can function as extracellular acid/base sensors, thereby increasing Ca<sup>2+</sup> concentrations [48,62]. Furthermore, it has been reported that TRPC1 plasma membrane levels are low when in an inactive form, and that the transfer and activation of the channel depends on Ca<sup>2+</sup> entry through ORAI1 and STIM1 [63,64]. Additional to other Ca<sup>2+</sup> channels, TRPC1 trafficking to the plasma membrane can depend on other membrane-bound proteins. For instance, the GTP-binding protein RhoA promotes the plasma membrane translocation [65] and activation of TRPC1, which leads to SOCE [66]. The interaction between RhoA and



TRPC1 leads to cell migration of intestinal epithelial cells [66]. In a glioblastoma cell line, TRPC1 translocation to the plasma membrane depends on PI3K mediated transport, which results in  $\text{Ca}^{2+}$  entry, chemotaxis, and cell migration [33]. We show that the interaction between TRPC1 and the PI3K p85 $\alpha$  subunit/CaM was enhanced after acid adaptation. Thus, our results suggest that the acidic tumor microenvironment induces the trafficking of TRPC1 to the plasma membrane, likely in association with the PI3K p85 $\alpha$  subunit and CaM, which are proteins near the plasma membrane. Here, TRPC1 promotes  $\text{Ca}^{2+}$  entry, in acid adaptation and recovery conditions. However, the precise mechanism of TRPC1 trafficking upon acid adaptation and recovery needs further investigation.

TRPC1 regulates the cell cycle G1 and S phases, leading to PANC-1 cell proliferation in a  $\text{Ca}^{2+}$ -independent manner [37]. In acidic and recovery conditions, we show that silencing of TRPC1 accumulated cells in the G0/G1 phases but decreased the number of cells in the G2/M phases. Remarkably, TRPC1 KD reduced the expression of CDK1, -2, -6, and cyclin A and increased the levels of p21<sup>CIP1</sup> excessively in acid recovery conditions compared to normal pH and acid adaptation conditions. In addition, TRPC1 KD inhibited PANC-1 cell proliferation and spheroid growth to a greater extent than in the two other conditions. This indicates that TRPC1 expression in acid recovery conditions is of more importance in cell proliferation and spheroid growth. Furthermore, the proliferation of PANC-1 cells in acidic and recovery conditions, contrary to normal pH conditions [37], depends on extracellular  $\text{Ca}^{2+}$  levels, as the proliferation rate was decreased upon  $\text{Ca}^{2+}$  chelation.

TRPC1 regulates the migratory properties of several cancer cell types, including PDAC cell lines [29,30,67–70]. In this study, KD of TRPC1 decreased the migratory properties of PANC-1 cells in normal, acid-adapted, and acid-recovered PANC-1 cells. However, the decrease was more prominent in acid recovery conditions. The migration of PANC-1 cells highly depends on extracellular  $\text{Ca}^{2+}$  solely in acid-adapted and -recovered cells, as cell migration decreased upon  $\text{Ca}^{2+}$  chelation. Meanwhile, no effect was found under normal pH conditions. These results indicate that, as for proliferation, TRPC1 regulates cell migration in the acidic tumor microenvironment through  $\text{Ca}^{2+}$ -dependent mechanisms.

TRPC1 forms a complex with the PI3K p85 $\alpha$  subunit and the associated connecting protein CaM, and activates AKT and, to a lesser extent, ERK1/2 in normal pH conditions [37,51]. We report that TRPC1 strongly formed a complex with the PI3K p85 $\alpha$  subunit, probably through CaM in acid-adapted and -recovered PANC-1 cells. This interaction was abolished upon the KD of TRPC1. Moreover, the silencing of TRPC1 resulted in a substantial decrease in AKT and ERK1/2 activation in acid-adapted and -recovered cells, which could result in the downregulation of cell-cycle-regulating proteins and, thereby, cell cycle arrest in the G0/G1 and G2/M phases. These results indicate that in these conditions, TRPC1 regulates proliferation and migration both through the PI3K and MAPK signaling axis, and that TRPC1 exerts a more aggressive role in acid-recovered PANC-1 cells.

AKT and ERK1/2 have previously been shown to be regulated through TRPC1 by  $\text{Ca}^{2+}$ -dependent and -independent mechanisms. The activation of AKT depends on  $\text{Ca}^{2+}$  through TRPC1 in lung cancer and hepatocellular carcinoma cell lines [71,72], and the activation of ERK1/2 depends on  $\text{Ca}^{2+}$  through TRPC1 in thyroid and different breast cancer cell lines [29,73,74]. Here, the activation of AKT and ERK1/2 seemed to be regulated, at least partially, by  $\text{Ca}^{2+}$  through TRPC1 in acid adaptation and recovery conditions. As TRPC1 forms a complex with PI3K p85 $\alpha$  subunit and the  $\text{Ca}^{2+}$  binding messenger CaM, we investigated whether the inhibition of CaM affected the activation of AKT and ERK1/2. This inhibition only decreased the activating phosphorylation of AKT in acid recovery conditions, where the activation of ERK1/2 was reduced in all conditions, but notably in acid-adapted and -recovered cells. Our results designate the importance of CaM and  $\text{Ca}^{2+}$  downstream signaling in acid recovery conditions.

Interestingly, in more than 90% of PDAC tumors, the oncogene *KRAS* is mutated, and *KRAS* G12D is the predominant driver mutation in this type of adenocarcinoma [75]. Furthermore, *KRAS* is involved in reprogramming cell metabolism, including glucose metabolism, and the mutations are known to promote aerobic glycolysis (also known as



the Warburg effect) [76]. The change in aerobic glycolysis in cancer cells is well known to produce waste products in the form of  $H^+$ , causing increased proton extrusion and an acidic extracellular space. As TRPC1 can potentially regulate MAPK signaling cascades through *KRAS* in liver and colorectal cancer cell lines [51,77], it would be interesting to further investigate the interplay between TRPC1, *KRAS*, and the metabolic changes implicated in the acidification of the tumor microenvironment of PDAC.

## 5. Conclusions

In conclusion, we show that pH fluctuations in the tumor microenvironment affect PDAC cell migration, proliferation, and spheroid growth. We demonstrate that acid adaptation permits TRPC1 localization to the plasma membrane. Here, TRPC1 reinforces a complex with PI3K p85 $\alpha$ /CaM and promotes  $Ca^{2+}$  entry. Synergically, this regulates AKT and ERK1/2 activation, which in turn controls cell cycle progression, proliferation, and migration. This indicates that the fluctuations in the acidic tumor microenvironment confer a more aggressive role to TRPC1 (Figure 11).

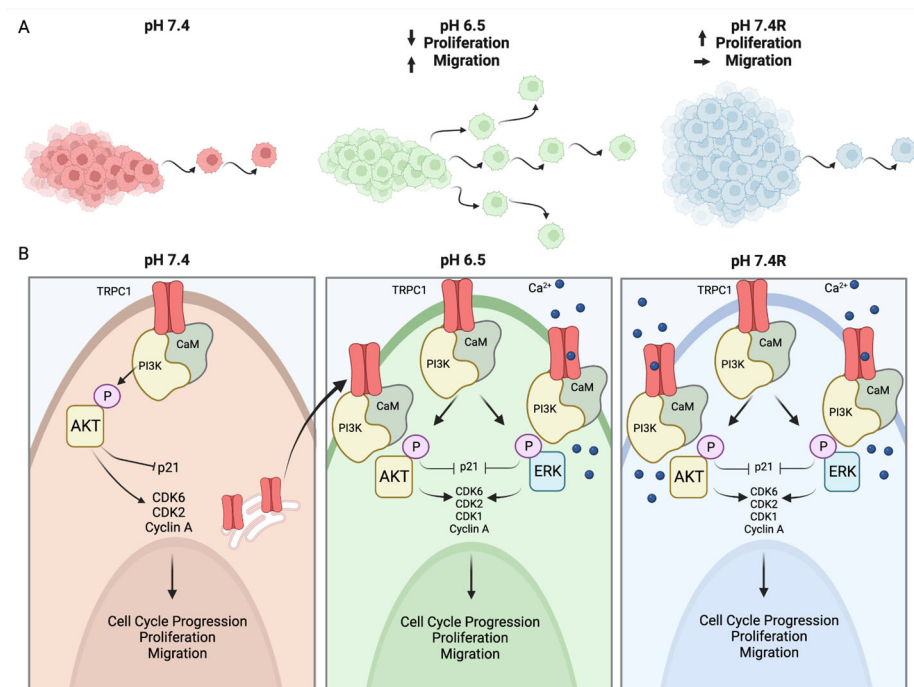


**Figure 11.** (A) Acid adaptation promotes migration but attenuates proliferation, whereas acid recovery impairs this migration but further accelerates proliferation. (B) The fluctuations in the acidic tumor microenvironment affect TRPC1 expression and localization. TRPC1 is downregulated in acid-adapted PANC-1 cells and favors plasma membrane localization, which is maintained in acid-recovered PANC-1 cells, where the expression of TRPC1 is upregulated. In the plasma membrane of acid-adapted and -recovered cells, TRPC1 permits  $Ca^{2+}$  entry and, in interactions with the PI3K p85 $\alpha$  subunit and CaM, regulates PANC-1 cell migration, proliferation, and cell cycle progression. The figure is generated with [www.Biorender.com](http://www.Biorender.com).

**Supplementary Materials:** The following supporting information can be downloaded at: <https://www.mdpi.com/article/10.3390/cancers14194946/s1>. Figure S1: Knockdown of TRPC1 in 2D and 3D models evaluated by qPCR and WB. Figure S2: Trypan blue assay performed in parallel with Boyden chamber assay to avoid any bias due to cell proliferation. Annexin-5 assay shows no effect upon siTRPC1. Figure S3: Representative WB of non-affected cell cycle regulating proteins upon the KD of TRPC1 and of the control pull-down with IgG-Rabbit for co-IP. Figure S4: Representative WB of PANC-1 cells treated with W7, blotted for pERK, ERK, pAKT and AKT. Figure S5: Representative traces of the classical store-operated  $Ca^{2+}$  entry protocol [78]. File S1. Full pictures of the Western blots.

**Author Contributions:** Conceptualization, J.S., A.A., S.F.P. and H.O.-A.; methodology, J.S., S.K., F.H., A.G., S.G., A.A., S.F.P. and H.O.-A.; software, J.S. and H.O.-A.; validation, J.S., S.F.P. and H.O.-A.; formal analysis, J.S., S.F.P. and H.O.-A.; investigation, J.S., S.K., F.H., A.G., M.-S.T., S.G., A.A., S.F.P. and H.O.-A.; data curation, J.S., S.K., F.H., A.G., M.-S.T., S.G., A.A., S.F.P. and H.O.-A.; resources, S.G., S.F.P., A.A. and H.O.-A.; writing—original draft preparation, J.S. and H.O.-A.; writing—review and editing, J.S., S.K., F.H., A.G., S.G., A.A., S.F.P. and H.O.-A.; visualization, J.S. and H.O.-A.; supervision, S.F.P., A.A. and H.O.-A.; project administration, J.S., S.F.P., A.A. and H.O.-A.; funding acquisition, S.F.P. and H.O.-A. All authors have read and agreed to the published version of the manuscript.

**Funding:** This work is funded by the Marie Skłodowska-Curie Innovative Training Network (ITN) Grant Agreement number: 813834—pHioniC—H2020-MSCA-ITN-2018, and by the Ministère de l’Enseignement Supérieur et de la Recherche, the Région Hauts-de-France (Picardie), the FEDER (Fonds Européen de Développement Économique Régional), the Université Picardie Jules Verne, and the Ligue Contre le Cancer (Septentrion).

**Institutional Review Board Statement:** Not applicable.

**Informed Consent Statement:** Not applicable.

**Data Availability Statement:** The data presented in this study are available in this article and Supplementary Material.

**Acknowledgments:** We are grateful to Mette Flinck (Department of Biology, University of Copenhagen) for excellent technical assistance, and to Anna Trauzold (Institute of Experimental Cancer Research, Kiel University, Kiel, Germany) for providing us with the PANC-1 cell line.

**Conflicts of Interest:** The authors declare no conflict of interest.

## References

- Sung, H.; Ferlay, J.; Siegel, R.L.; Laversanne, M.; Soerjomataram, I.; Jemal, A.; Bray, F. Global Cancer Statistics 2020: GLOBOCAN Estimates of Incidence and Mortality Worldwide for 36 Cancers in 185 Countries. *CA Cancer J. Clin.* **2021**, *71*, 209–249. [\[CrossRef\]](#)
- Wong, M.C.S.; Jiang, J.Y.; Liang, M.; Fang, Y.; Yeung, M.S.; Sung, J.J.Y. Global temporal patterns of pancreatic cancer and association with socioeconomic development. *Sci. Rep.* **2017**, *7*, 3165. [\[CrossRef\]](#) [\[PubMed\]](#)
- Park, W.; Chawla, A.; O’Reilly, E.M. Pancreatic Cancer: A Review. *JAMA* **2021**, *326*, 851–862. [\[CrossRef\]](#) [\[PubMed\]](#)
- Ferlay, J.; Soerjomataram, I.; Dikshit, R.; Eser, S.; Mathers, C.; Rebelo, M.; Parkin, D.M.; Forman, D.; Bray, F. Cancer incidence and mortality worldwide: Sources, methods and major patterns in GLOBOCAN 2012. *Int. J. Cancer* **2015**, *136*, E359–E386. [\[CrossRef\]](#) [\[PubMed\]](#)
- Novak, I.; Haanes, K.A.; Wang, J. Acid-base transport in pancreas-new challenges. *Front. Physiol.* **2013**, *4*, 380. [\[CrossRef\]](#) [\[PubMed\]](#)
- Pedersen, S.F.; Novak, I.; Alves, F.; Schwab, A.; Pardo, L.A. Alternating pH landscapes shape epithelial cancer initiation and progression: Focus on pancreatic cancer. *Bioessays* **2017**, *39*, 1600253. [\[CrossRef\]](#) [\[PubMed\]](#)
- Swietach, P.; Vaughan-Jones, R.D.; Harris, A.L.; Hulikova, A. The chemistry, physiology and pathology of pH in cancer. *Philos. Trans. R. Soc. Lond. B Biol. Sci.* **2014**, *369*, 20130099. [\[CrossRef\]](#) [\[PubMed\]](#)
- Boedtker, E.; Pedersen, S.F. The Acidic Tumor Microenvironment as a Driver of Cancer. *Annu. Rev. Physiol.* **2020**, *82*, 103–126. [\[CrossRef\]](#)
- Andersen, H.B.; Ialchina, R.; Pedersen, S.F.; Czaplinska, D. Metabolic reprogramming by driver mutation-tumor microenvironment interplay in pancreatic cancer: New therapeutic targets. *Cancer Metastasis Rev.* **2021**, *40*, 1093–1114. [\[CrossRef\]](#)
- Vaupel, P.; Kallinowski, F.; Okunieff, P. Blood flow, oxygen and nutrient supply, and metabolic microenvironment of human tumors: A review. *Cancer Res.* **1989**, *49*, 6449–6465.
- Rohani, N.; Hao, L.; Alexis, M.S.; Joughin, B.A.; Krismer, K.; Moufarrej, M.N.; Soltis, A.R.; Lauffenburger, D.A.; Yaffe, M.B.; Burge, C.B.; et al. Acidification of Tumor at Stromal Boundaries Drives Transcriptome Alterations Associated with Aggressive Phenotypes. *Cancer Res.* **2019**, *79*, 1952–1966. [\[CrossRef\]](#)
- Helmlinger, G.; Yuan, F.; Dellian, M.; Jain, R.K. Interstitial pH and pO<sub>2</sub> gradients in solid tumors in vivo: High-resolution measurements reveal a lack of correlation. *Nat. Med.* **1997**, *3*, 177–182. [\[CrossRef\]](#)
- Lee, S.; Axelsen, T.V.; Andersen, A.P.; Vahl, P.; Pedersen, S.F.; Boedtker, E. Disrupting Na<sup>(+)</sup>, HCO<sub>3</sub><sup>(-)</sup>-cotransporter NBCn1 (Slc4a7) delays murine breast cancer development. *Oncogene* **2016**, *35*, 2112–2122. [\[CrossRef\]](#)
- Lee, S.; Mele, M.; Vahl, P.; Christiansen, P.M.; Jensen, V.E.; Boedtker, E. Na<sup>(+)</sup>,HCO<sub>3</sub><sup>(-)</sup>-cotransport is functionally upregulated during human breast carcinogenesis and required for the inverted pH gradient across the plasma membrane. *Pflugers Arch.* **2015**, *467*, 367–377. [\[CrossRef\]](#)
- Pillai, S.R.; Damaghi, M.; Marunaka, Y.; Spugnini, E.P.; Fais, S.; Gillies, R.J. Causes, consequences, and therapy of tumors acidosis. *Cancer Metastasis Rev.* **2019**, *38*, 205–222. [\[CrossRef\]](#)

16. Martinez-Zaguilan, R.; Seftor, E.A.; Seftor, R.E.; Chu, Y.W.; Gillies, R.J.; Hendrix, M.J. Acidic pH enhances the invasive behavior of human melanoma cells. *Clin. Exp. Metastasis* **1996**, *14*, 176–186. [[CrossRef](#)]
17. Corbet, C.; Bastien, E.; Santiago de Jesus, J.P.; Dierge, E.; Martherus, R.; Vander Linden, C.; Doix, B.; Degavre, C.; Guilbaud, C.; Petit, L.; et al. TGFbeta2-induced formation of lipid droplets supports acidosis-driven EMT and the metastatic spreading of cancer cells. *Nat. Commun.* **2020**, *11*, 454. [[CrossRef](#)]
18. Peppicelli, S.; Andreucci, E.; Ruzzolini, J.; Laurenzana, A.; Margheri, F.; Fibbi, G.; Del Rosso, M.; Bianchini, F.; Calorini, L. The acidic microenvironment as a possible niche of dormant tumor cells. *Cell. Mol. Life Sci.* **2017**, *74*, 2761–2771. [[CrossRef](#)]
19. Petho, Z.; Najder, K.; Carvalho, T.; McMorrow, R.; Todesca, L.M.; Rugi, M.; Bulk, E.; Chan, A.; Lowik, C.; Reshkin, S.J.; et al. pH-Channeling in Cancer: How pH-Dependence of Cation Channels Shapes Cancer Pathophysiology. *Cancers* **2020**, *12*, 2484. [[CrossRef](#)]
20. Holzer, P. Acid-sensitive ion channels and receptors. In *Handbook of Experimental Pharmacology*; Springer: Berlin/Heidelberg, Germany, 2009. [[CrossRef](#)]
21. Damaghi, M.; Wojtkowiak, J.W.; Gillies, R.J. pH sensing and regulation in cancer. *Front. Physiol.* **2013**, *4*, 370. [[CrossRef](#)]
22. Audero, M.M.; Prevarskaya, N.; Fiorio Pla, A. Ca<sup>2+</sup> Signalling and Hypoxia/Acidic Tumour Microenvironment Interplay in Tumour Progression. *Int. J. Mol. Sci.* **2022**, *23*, 7377. [[CrossRef](#)]
23. Schnipper, J.; Ouadid-Ahidouch, H.; Dhennin-Duthille, I.; Ahidouch, A. Ion channel signature in healthy pancreas and pancreatic ductal adenocarcinoma. *Front. Pharmacol.* **2020**, *11*, 568993. [[CrossRef](#)]
24. Chamli, M.; Rodat-Despoix, L.; Ouadid-Ahidouch, H. Store-Independent Calcium Entry and Related Signaling Pathways in Breast Cancer. *Genes* **2021**, *12*, 994. [[CrossRef](#)]
25. Tajada, S.; Villalobos, C. Calcium Permeable Channels in Cancer Hallmarks. *Front. Pharmacol.* **2020**, *11*, 968. [[CrossRef](#)]
26. Wang, H.; Cheng, X.; Tian, J.; Xiao, Y.; Tian, T.; Xu, F.; Hong, X.; Zhu, M.X. TRPC channels: Structure, function, regulation and recent advances in small molecular probes. *Pharmacol. Ther.* **2020**, *209*, 107497. [[CrossRef](#)]
27. Fels, B.; Bulk, E.; Petho, Z.; Schwab, A. The Role of TRP Channels in the Metastatic Cascade. *Pharmaceuticals* **2018**, *11*, 48. [[CrossRef](#)]
28. Elzamzamy, O.M.; Penner, R.; Hazlehurst, L.A. The Role of TRPC1 in Modulating Cancer Progression. *Cells* **2020**, *9*, 388. [[CrossRef](#)]
29. Asghar, M.Y.; Magnusson, M.; Kempainen, K.; Sukumaran, P.; Lof, C.; Pulli, I.; Kalhori, V.; Tornquist, K. Transient Receptor Potential Canonical 1 (TRPC1) Channels as Regulators of Sphingolipid and VEGF Receptor Expression: Implications for thyroid cancer cell migration and proliferation. *J. Biol. Chem.* **2015**, *290*, 16116–16131. [[CrossRef](#)]
30. Azimi, I.; Milevskiy, M.J.G.; Kaemmerer, E.; Turner, D.; Yapa, K.; Brown, M.A.; Thompson, E.W.; Roberts-Thomson, S.J.; Monteith, G.R. TRPC1 is a differential regulator of hypoxia-mediated events and Akt signalling in PTEN-deficient breast cancer cells. *J. Cell Sci.* **2017**, *130*, 2292–2305. [[CrossRef](#)]
31. Fels, B.; Nielsen, N.; Schwab, A. Role of TRPC1 channels in pressure-mediated activation of murine pancreatic stellate cells. *Eur. Biophys. J.* **2016**, *45*, 657–670. [[CrossRef](#)]
32. Radoslavova, S.; Fels, B.; Petho, Z.; Gruner, M.; Ruck, T.; Meuth, S.G.; Folcher, A.; Prevarskaya, N.; Schwab, A.; Ouadid-Ahidouch, H. Trpc1 channels regulate the activation of pancreatic stellate cells through erk1/2 and smad2 pathways and perpetuate their pressure-mediated activation. *Cell Calcium*. **2022**, *106*, 102621. [[CrossRef](#)]
33. Lepannetier, S.; Zanou, N.; Yerna, X.; Emeriau, N.; Dufour, I.; Masquelier, J.; Muccioli, G.; Tajeddine, N.; Gailly, P. Sphingosine-1-phosphate-activated TRPC1 channel controls chemotaxis of glioblastoma cells. *Cell Calcium* **2016**, *60*, 373–383. [[CrossRef](#)]
34. Zheng, J. Molecular mechanism of TRP channels. *Compr. Physiol.* **2013**, *3*, 221–242. [[CrossRef](#)]
35. Thakur, D.P.; Wang, Q.; Jeon, J.; Tian, J.B.; Zhu, M.X. Intracellular acidification facilitates receptor-operated TRPC4 activation through PLCdelta1 in a Ca<sup>2+</sup>-dependent manner. *J. Physiol.* **2020**, *598*, 2651–2667. [[CrossRef](#)]
36. Semtner, M.; Schaefer, M.; Pinkenburg, O.; Plant, T.D. Potentiation of TRPC5 by protons. *J. Biol. Chem.* **2007**, *282*, 33868–33878. [[CrossRef](#)]
37. Schnipper, J.; Kouba, S.; Hague, F.; Girault, A.; Rybarczyk, P.; Telliez, M.S.; Guenin, S.; Tebbakha, R.; Sevestre, H.; Ahidouch, A.; et al. The TRPC1 Channel Forms a PI3K/CaM Complex and Regulates Pancreatic Ductal Adenocarcinoma Cell Proliferation in a Ca(2+)-Independent Manner. *Int. J. Mol. Sci.* **2022**, *23*, 7923. [[CrossRef](#)]
38. Michl, J.; Park, K.C.; Swietach, P. Evidence-based guidelines for controlling pH in mammalian live-cell culture systems. *Commun. Biol.* **2019**, *2*, 144. [[CrossRef](#)]
39. Yao, J.; Czaplinska, D.; Ialchina, R.; Schnipper, J.; Liu, B.; Sandelin, A.; Pedersen, S.F. Cancer Cell Acid Adaptation Gene Expression Response Is Correlated to Tumor-Specific Tissue Expression Profiles and Patient Survival. *Cancers* **2020**, *12*, 2183. [[CrossRef](#)]
40. Hagelund, S.; Trauzold, A. Impact of Extracellular pH on Apoptotic and Non-Apoptotic TRAIL-Induced Signaling in Pancreatic Ductal Adenocarcinoma Cells. *Front. Cell Dev. Biol.* **2022**, *10*, 768579. [[CrossRef](#)]
41. Flinck, M.; Kramer, S.H.; Schnipper, J.; Andersen, A.P.; Pedersen, S.F. The acid-base transport proteins NHE1 and NBCn1 regulate cell cycle progression in human breast cancer cells. *Cell Cycle* **2018**, *17*, 1056–1067. [[CrossRef](#)]
42. Olesen, C.W.; Vogensen, J.; Axholm, I.; Severin, M.; Schnipper, J.; Pedersen, I.S.; von Stemann, J.H.; Schroder, J.M.; Christensen, D.P.; Pedersen, S.F. Trafficking, localization and degradation of the Na(+),HCO3(-) co-transporter NBCn1 in kidney and breast epithelial cells. *Sci. Rep.* **2018**, *8*, 7435. [[CrossRef](#)]
43. Thomas, J.A.; Buchsbaum, R.N.; Zimniak, A.; Racker, E. Intracellular pH measurements in Ehrlich ascites tumor cells utilizing spectroscopic probes generated in situ. *Biochemistry* **1979**, *18*, 2210–2218. [[CrossRef](#)]

44. Radoslavova, S.; Folcher, A.; Lefebvre, T.; Kondratska, K.; Guenin, S.; Dhennin-Duthille, I.; Gautier, M.; Prevarskaya, N.; Ouadid-Ahidouch, H. Orai1 Channel Regulates Human-Activated Pancreatic Stellate Cell Proliferation and TGFbeta1 Secretion through the AKT Signaling Pathway. *Cancers* **2021**, *13*, 2395. [[CrossRef](#)] [[PubMed](#)]
45. Girault, A.; Peretti, M.; Badaoui, M.; Hemon, A.; Morjani, H.; Ouadid-Ahidouch, H. The N and C-termini of SPCA2 regulate differently Kv10.1 function: Role in the collagen 1-induced breast cancer cell survival. *Am. J. Cancer Res.* **2021**, *11*, 251–263.
46. Bolte, S.; Cordelieres, F.P. A guided tour into subcellular colocalization analysis in light microscopy. *J. Microsc.* **2006**, *224*, 213–232. [[CrossRef](#)]
47. Chamlali, M.; Kouba, S.; Rodat-Despoix, L.; Todesca, L.M.; Petho, Z.; Schwab, A.; Ouadid-Ahidouch, H. Orai3 Calcium Channel Regulates Breast Cancer Cell Migration through Calcium-Dependent and -Independent Mechanisms. *Cells* **2021**, *10*, 3487. [[CrossRef](#)] [[PubMed](#)]
48. Flinck, M.; Kramer, S.H.; Pedersen, S.F. Roles of pH in control of cell proliferation. *Acta Physiol.* **2018**, *223*, e13068. [[CrossRef](#)] [[PubMed](#)]
49. Smallbone, K.; Gavaghan, D.J.; Gatenby, R.A.; Maini, P.K. The role of acidity in solid tumour growth and invasion. *J. Theor. Biol.* **2005**, *235*, 476–484. [[CrossRef](#)]
50. Garcia, Z.; Kumar, A.; Marques, M.; Cortes, I.; Carrera, A.C. Phosphoinositide 3-kinase controls early and late events in mammalian cell division. *EMBO J.* **2006**, *25*, 655–661. [[CrossRef](#)]
51. Sun, Y.; Ye, C.; Tian, W.; Ye, W.; Gao, Y.Y.; Feng, Y.D.; Zhang, H.N.; Ma, G.Y.; Wang, S.J.; Cao, W.; et al. TRPC1 promotes the genesis and progression of colorectal cancer via activating CaM-mediated PI3K/AKT signaling axis. *Oncogenesis* **2021**, *10*, 67. [[CrossRef](#)] [[PubMed](#)]
52. Blaszczyk, W.; Swietach, P. What do cellular responses to acidity tell us about cancer? *Cancer Metastasis Rev.* **2021**, *40*, 1159–1176. [[CrossRef](#)]
53. White, K.A.; Grillo-Hill, B.K.; Barber, D.L. Cancer cell behaviors mediated by dysregulated pH dynamics at a glance. *J. Cell Sci.* **2017**, *130*, 663–669. [[CrossRef](#)] [[PubMed](#)]
54. De Bem Prunes, B.; Nunes, J.S.; da Silva, V.P.; Laureano, N.K.; Goncalves, D.R.; Machado, I.S.; Barbosa, S.; Lamers, M.L.; Rados, P.V.; Kurth, I.; et al. The role of tumor acidification in aggressiveness, cell dissemination and treatment resistance of oral squamous cell carcinoma. *Life Sci.* **2022**, *288*, 120163. [[CrossRef](#)]
55. Sutoo, S.; Maeda, T.; Suzuki, A.; Kato, Y. Adaptation to chronic acidic extracellular pH elicits a sustained increase in lung cancer cell invasion and metastasis. *Clin. Exp. Metastasis* **2020**, *37*, 133–144. [[CrossRef](#)]
56. Moellering, R.E.; Black, K.C.; Krishnamurty, C.; Baggett, B.K.; Stafford, P.; Rain, M.; Gatenby, R.A.; Gillies, R.J. Acid treatment of melanoma cells selects for invasive phenotypes. *Clin. Exp. Metastasis* **2008**, *25*, 411–425. [[CrossRef](#)]
57. Wu, T.C.; Liao, C.Y.; Lu, W.C.; Chang, C.R.; Tsai, F.Y.; Jiang, S.S.; Chen, T.H.; Lin, K.M.; Chen, L.T.; Chang, W.W. Identification of distinct slow mode of reversible adaptation of pancreatic ductal adenocarcinoma to the prolonged acidic pH microenvironment. *J. Exp. Clin. Cancer Res.* **2022**, *41*, 137. [[CrossRef](#)]
58. Shin, S.C.; Thomas, D.; Radhakrishnan, P.; Hollingsworth, M.A. Invasive phenotype induced by low extracellular pH requires mitochondria dependent metabolic flexibility. *Biochem. Biophys. Res. Commun.* **2020**, *525*, 162–168. [[CrossRef](#)] [[PubMed](#)]
59. Zhou, Z.H.; Wang, Q.L.; Mao, L.H.; Li, X.Q.; Liu, P.; Song, J.W.; Liu, X.; Xu, F.; Lei, J.; He, S. Chromatin accessibility changes are associated with enhanced growth and liver metastasis capacity of acid-adapted colorectal cancer cells. *Cell Cycle* **2019**, *18*, 511–522. [[CrossRef](#)] [[PubMed](#)]
60. Riemann, A.; Schneider, B.; Gundel, D.; Stock, C.; Thews, O.; Gekle, M. Acidic priming enhances metastatic potential of cancer cells. *Pflugers Arch.* **2014**, *466*, 2127–2138. [[CrossRef](#)]
61. Robey, I.F.; Baggett, B.K.; Kirkpatrick, N.D.; Roe, D.J.; Dosesco, J.; Sloane, B.F.; Hashim, A.I.; Morse, D.L.; Raghunand, N.; Gatenby, R.A.; et al. Bicarbonate increases tumor pH and inhibits spontaneous metastases. *Cancer Res.* **2009**, *69*, 2260–2268. [[CrossRef](#)] [[PubMed](#)]
62. Glitsch, M. Protons and Ca<sup>2+</sup>: Ionic allies in tumor progression? *Physiology* **2011**, *26*, 252–265. [[CrossRef](#)]
63. Cheng, K.T.; Liu, X.; Ong, H.L.; Swaim, W.; Ambudkar, I.S. Local Ca<sup>2+</sup> entry via Orai1 regulates plasma membrane recruitment of TRPC1 and controls cytosolic Ca<sup>2+</sup> signals required for specific cell functions. *PLoS Biol.* **2011**, *9*, e1001025. [[CrossRef](#)]
64. Ambudkar, I.S.; de Souza, L.B.; Ong, H.L. TRPC1, Orai1, and STIM1 in SOCE: Friends in tight spaces. *Cell Calcium* **2017**, *63*, 33–39. [[CrossRef](#)]
65. Mehta, D.; Ahmed, G.U.; Paria, B.C.; Holinstat, M.; Voyno-Yasenetskaya, T.; Tirupathi, C.; Minshall, R.D.; Malik, A.B. RhoA interaction with inositol 1,4,5-trisphosphate receptor and transient receptor potential channel-1 regulates Ca<sup>2+</sup> entry. Role in signaling increased endothelial permeability. *J. Biol. Chem.* **2003**, *278*, 33492–33500. [[CrossRef](#)]
66. Chung, H.K.; Rathor, N.; Wang, S.R.; Wang, J.Y.; Rao, J.N. RhoA enhances store-operated Ca<sup>2+</sup> entry and intestinal epithelial restitution by interacting with TRPC1 after wounding. *Am. J. Physiol. Gastrointest Liver Physiol.* **2015**, *309*, G759–G767. [[CrossRef](#)]
67. Zhang, L.Y.; Zhang, Y.Q.; Zeng, Y.Z.; Zhu, J.L.; Chen, H.; Wei, X.L.; Liu, L.J. TRPC1 inhibits the proliferation and migration of estrogen receptor-positive Breast cancer and gives a better prognosis by inhibiting the PI3K/AKT pathway. *Breast Cancer Res. Treat.* **2020**, *182*, 21–33. [[CrossRef](#)] [[PubMed](#)]
68. Schaar, A.; Sukumaran, P.; Sun, Y.; Dhasarathy, A.; Singh, B.B. TRPC1-STIM1 activation modulates transforming growth factor beta-induced epithelial-to-mesenchymal transition. *Oncotarget* **2016**, *7*, 80554–80567. [[CrossRef](#)]



69. Bomben, V.C.; Turner, K.L.; Barclay, T.T.; Sontheimer, H. Transient receptor potential canonical channels are essential for chemotactic migration of human malignant gliomas. *J. Cell Physiol.* **2011**, *226*, 1879–1888. [[CrossRef](#)] [[PubMed](#)]
70. Dong, H.; Shim, K.N.; Li, J.M.; Estrema, C.; Ornelas, T.A.; Nguyen, F.; Liu, S.; Ramamoorthy, S.L.; Ho, S.; Carethers, J.M.; et al. Molecular mechanisms underlying  $\text{Ca}^{2+}$ -mediated motility of human pancreatic duct cells. *Am. J. Physiol. Cell Physiol.* **2010**, *299*, C1493–C1503. [[CrossRef](#)]
71. Tajeddine, N.; Gailly, P. TRPC1 protein channel is major regulator of epidermal growth factor receptor signaling. *J. Biol. Chem.* **2012**, *287*, 16146–16157. [[CrossRef](#)]
72. Selli, C.; Erac, Y.; Kosova, B.; Erdal, E.S.; Tosun, M. Silencing of TRPC1 regulates store-operated calcium entry and proliferation in Huh7 hepatocellular carcinoma cells. *Biomed. Pharmacother.* **2015**, *71*, 194–200. [[CrossRef](#)] [[PubMed](#)]
73. El Hiani, Y.; Ahidouch, A.; Lehen'kyi, V.; Hague, F.; Gouilleux, F.; Mentaverri, R.; Kamel, S.; Lassoued, K.; Brule, G.; Ouadid-Ahidouch, H. Extracellular signal-regulated kinases 1 and 2 and TRPC1 channels are required for calcium-sensing receptor-stimulated MCF-7 breast cancer cell proliferation. *Cell Physiol. Biochem.* **2009**, *23*, 335–346. [[CrossRef](#)] [[PubMed](#)]
74. Davis, F.M.; Peters, A.A.; Grice, D.M.; Cabot, P.J.; Parat, M.O.; Roberts-Thomson, S.J.; Monteith, G.R. Non-stimulated, agonist-stimulated and store-operated  $\text{Ca}^{2+}$  influx in MDA-MB-468 breast cancer cells and the effect of EGF-induced EMT on calcium entry. *PLoS ONE* **2012**, *7*, e36923. [[CrossRef](#)] [[PubMed](#)]
75. Waters, A.M.; Der, C.J. KRAS: The Critical Driver and Therapeutic Target for Pancreatic Cancer. *Cold Spring Harb. Perspect. Med.* **2018**, *8*, a031435. [[CrossRef](#)] [[PubMed](#)]
76. Mukhopadhyay, S.; Vander Heiden, M.G.; McCormick, F. The Metabolic Landscape of RAS-Driven Cancers from biology to therapy. *Nat. Cancer* **2021**, *2*, 271–283. [[CrossRef](#)]
77. Selli, C.; Pearce, D.A.; Sims, A.H.; Tosun, M. Differential expression of store-operated calcium- and proliferation-related genes in hepatocellular carcinoma cells following TRPC1 ion channel silencing. *Mol. Cell Biochem.* **2016**, *420*, 129–140. [[CrossRef](#)] [[PubMed](#)]
78. Pfaffl, M.W.; Horgan, G.W.; Dempfle, L. Relative expression software tool (REST) for group-wise comparison and statistical analysis of relative expression results in real-time PCR. *Nucleic Acids Res.* **2002**, *30*, e36. [[CrossRef](#)]

*Supplementary Figures and Material and Methods*

# **Acid Adaptation Promotes TRPC1 Plasma Membrane Localization Leading to Pancreatic Ductal Adenocarcinoma Cell Proliferation and Migration through Ca<sup>2+</sup> Entry and Interaction with PI3K/CaM**

**Julie Schnipper <sup>1</sup>, Sana Kouba <sup>1</sup>, Frédéric Hague <sup>1</sup>, Alban Girault <sup>1</sup>, Marie-Sophie Telliez <sup>1</sup>, Stéphanie Guénin <sup>2</sup>, Ahmed Ahidouch <sup>1,3</sup>, Stine Falsig Pedersen <sup>4</sup> and Halima Ouadid-Ahidouch <sup>1,\*</sup>**

<sup>1</sup> Laboratory of Cellular and Molecular Physiology, UR UPJV 4667, University of Picardie Jules Verne, 80000 Amiens, France

<sup>2</sup> Regional Ressources Center for Molecular Biology (CRRBM), University of Picardie Jules Verne, 80000 Amiens, France

<sup>3</sup> Biology Department, Sciences Faculty, University Ibn Zohr, Agadir 80000, Morocco

<sup>4</sup> Section for Cell Biology and Physiology, Department of Biology, University of Copenhagen, 2100 Copenhagen Ø, Denmark

\* Correspondence: halima.ahidouch-ouadid@u-picardie.fr; Tel.: +33-322-827-646



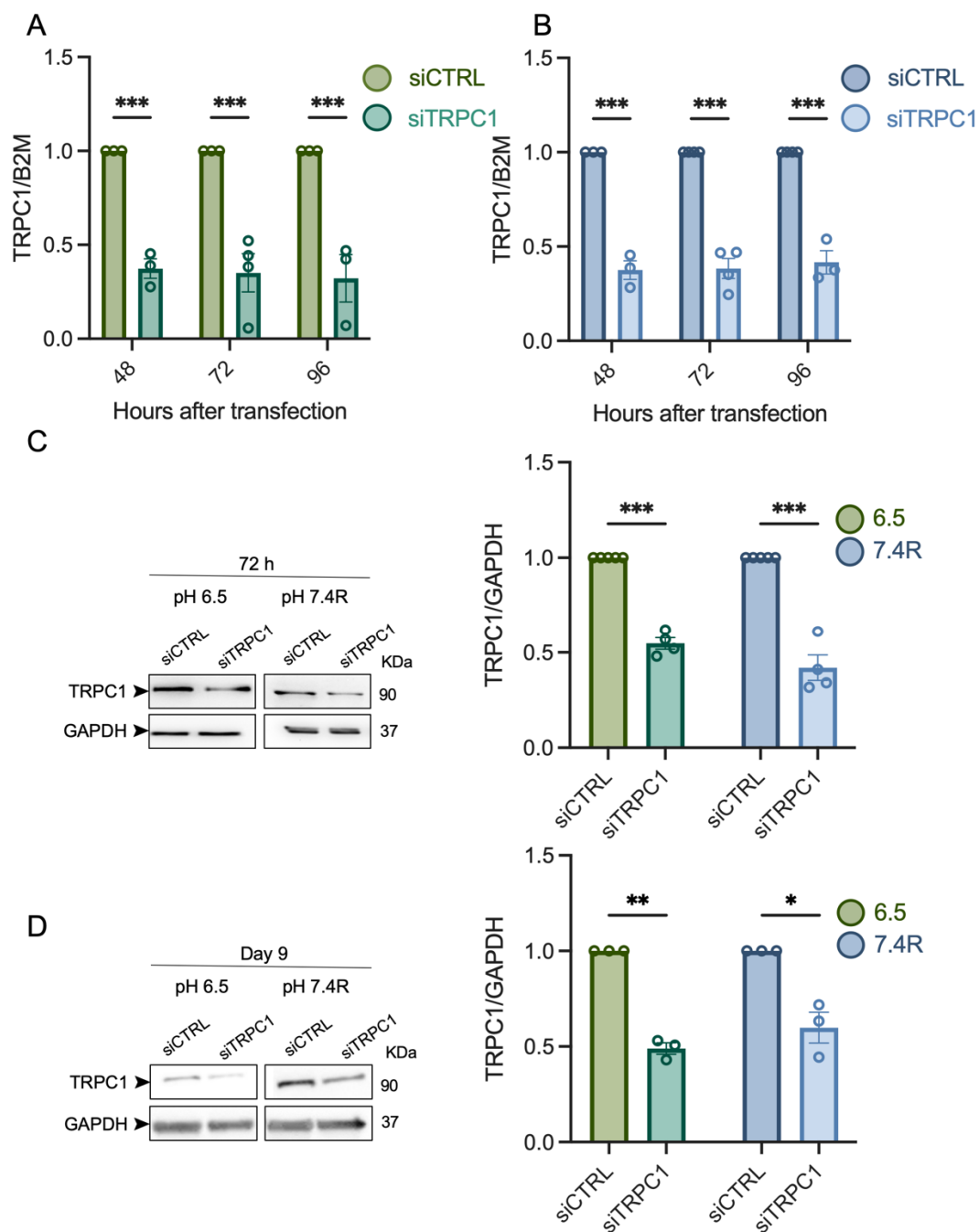


**Figure S1.** (A) TRPC1 mRNA expression evaluated by qPCR 48, 72 and 96 h after transfection with siCTRL and siTRPC1 in acid-adapted PANC-1 cells (6.5) ( $n = 3-4$ ). (B) TRPC1 mRNA expression evaluated by qPCR 48, 72 and 96 h after transfection with siCTRL and siTRPC1 in acid-recovered PANC-1 cells (7.4R) ( $n = 3-4$ ). Materials and methods for qPCR are described below. (C) TRPC1 protein expression evaluated 72 h after transfection with siCTRL and siTRPC1 in acid-adapted (6.5) or acid-recovered (7.4R) PANC-1 cells ( $n = 4$ , Western blot analysis left panel and quantification right panel). (D) TRPC1 protein expression evaluated 9 days after transfection with siCTRL and siTRPC1 in acid-adapted PANC-1 spheroids, grown in medium pH 6.5 or 7.4R ( $n = 3$ , Western blot analysis left panel and quantification right panel). Welch's correction t-test was used to determine the significant difference between siCTRL and siTRPC1 conditions. \*, \*\* and \*\*\* indicate  $p < 0.05$ , 0.01 and 0.001, respectively.

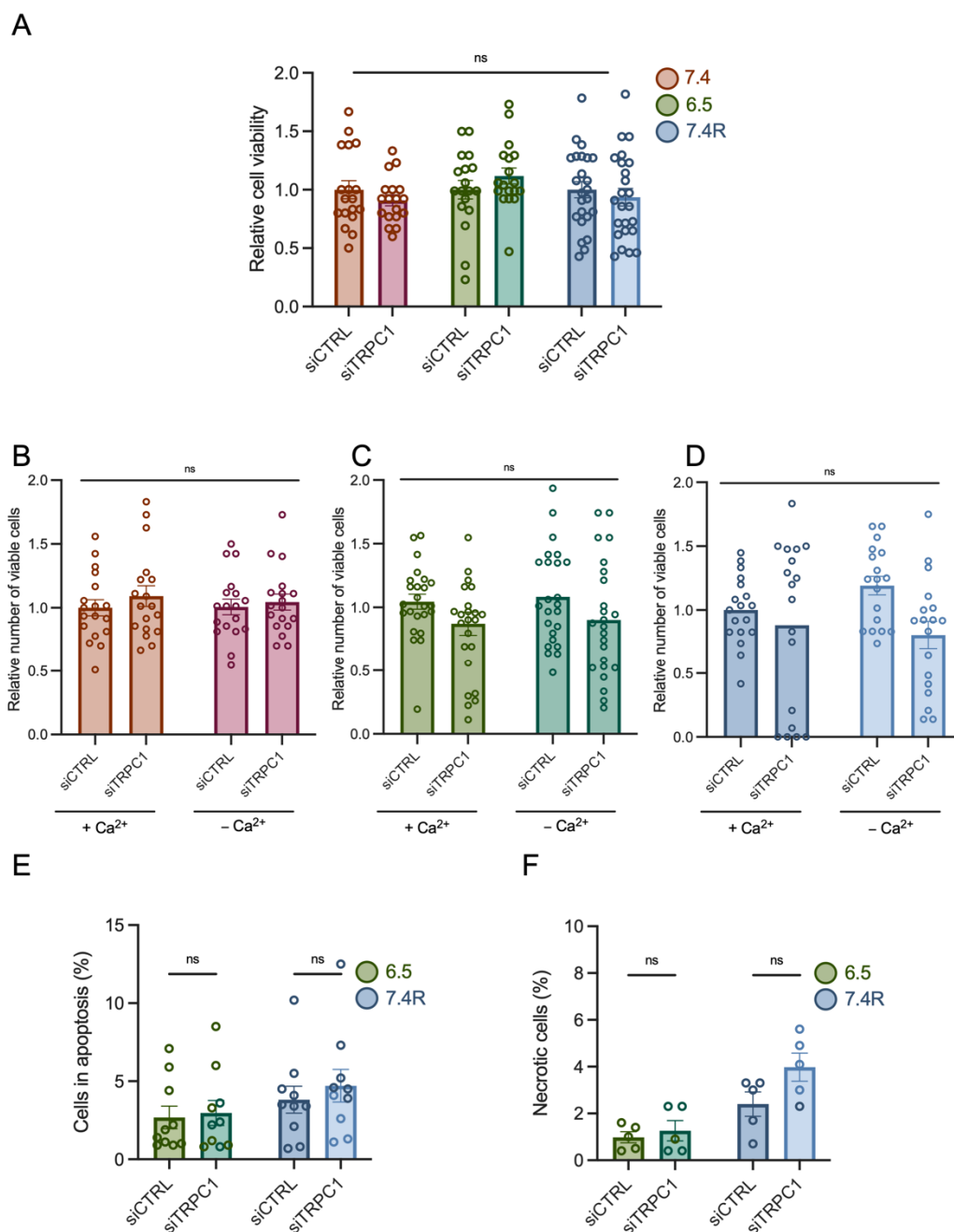


**Figure S2.** (A) Trypan blue assay performed in parallel with Boyden chamber assay (24 h after seeding). Welch's correction t-test was used to determine the significant difference between siCTRL and siTRPC1 conditions ( $n = 3-4$ ). Ns indicates non-significant. (B) Trypan blue assay performed in parallel with Boyden chamber assay, with (+ Ca<sup>2+</sup>) or without (- Ca<sup>2+</sup>) calcium for 24 h in PANC-1 cells grown under normal pH conditions (7.4), ( $n = 3$ ) (C) in acid-adapted ( $n = 4$ ) or, (D) acid-recovered conditions ( $n = 3$ ). Tukey's multiple comparison test was used to determine significant differences between conditions. Ns indicates non-significant. (E) Quantification of Annexin-5 analysis of cells in apoptosis or, (F) necrotic cells 72 h after transfection with siCTRL and siTRPC1 in acid-adapted (6.5) or acid-recovered (7.4R) PANC-1 cells ( $n = 3$ ). Welch's correction t-test was used to determine the significant differences between siCTRL and siTRPC1 conditions. Ns indicates non-significant. Materials and methods for Annexin-5 analysis are described below.

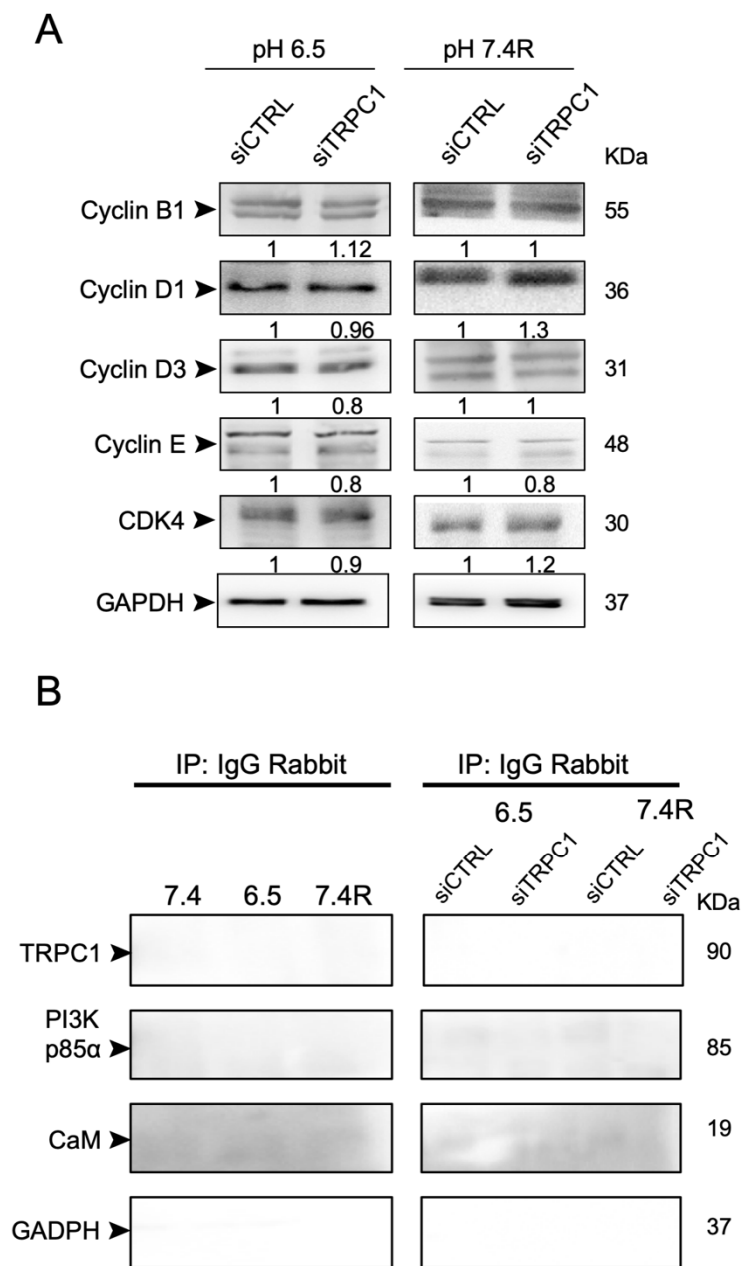


**Figure S3.** (A) Westernblot analysis of different cell cycle regulating proteins 72 h after transfection with siCTRL and siTRPC1 in acid-adapted (6.5) or acid-recovered (7.4R) PANC-1 cells ( $n= 3-4$ , no significance was found by using Welch's correction t-test). (B) Representative immunoblot of co-immunoprecipitation with a control IgG Rabbit.

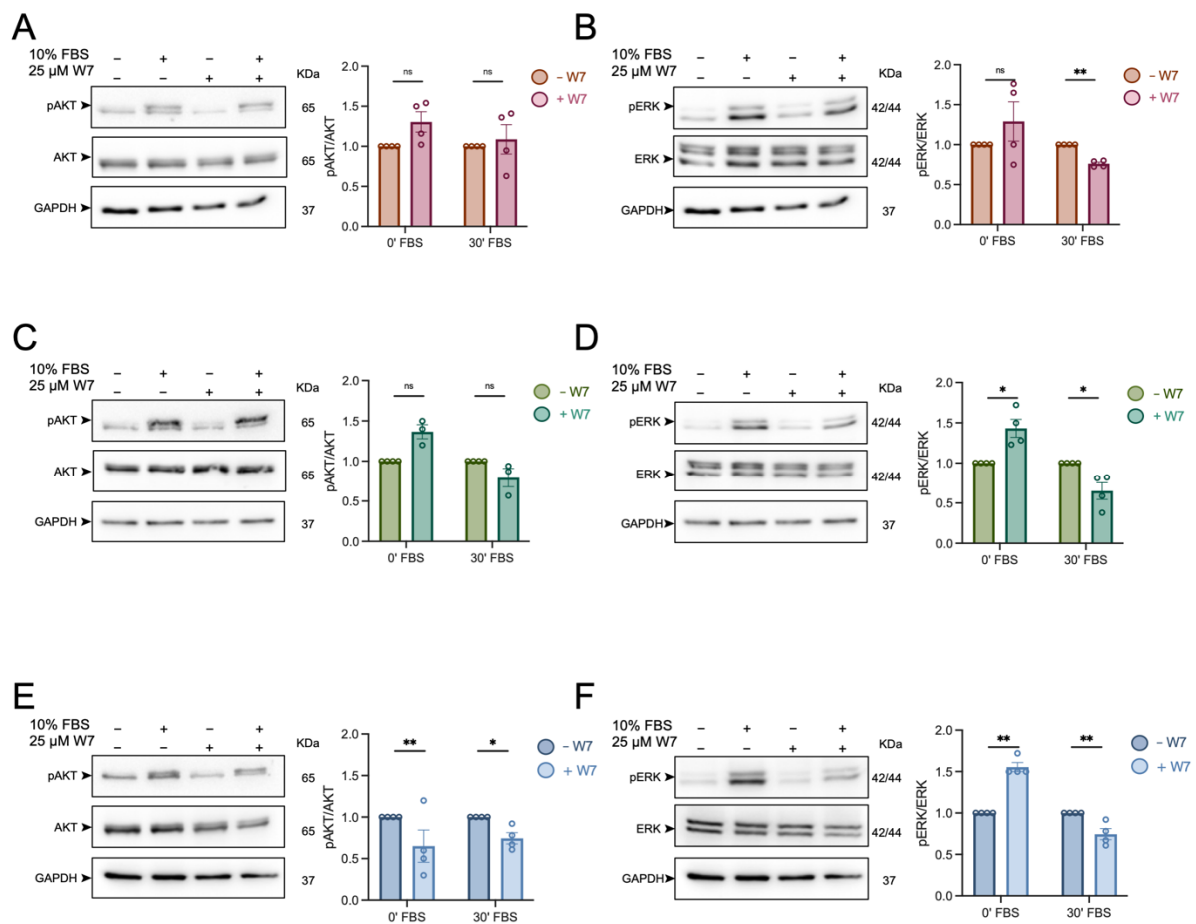


**Figure S4.** Representative immunoblot analysis of PANC-1 cells treated with 72 h of 25  $\mu$ M W7, including 24 h of starvation, followed by either 0 min or 30 min of mitogen activation with 10% FBS. (A) phosphorlyated AKT (pAKT) and total AKT in normal conditions (7.4). (B) phosphorlyated ERK1/2 (pERK) and total ERK1/2 in normal conditions (7.4). (C) phosphorlyated AKT (pAKT) and total AKT in acid-adapted conditions (6.5). (D) phosphorlyated ERK1/2 (pERK) and total ERK1/2 in acid-adapted conditions (6.5). (E) phosphorlyated AKT (pAKT) and total AKT in acid-recovered conditions (7.4R). (F) phosphorlyated ERK1/2 (pERK) and total ERK1/2 in acid-recovered conditions (7.4R). ( $n = 3-4$ ). Welch's correction t-test was used to determine the significant difference between conditions. Ns indicates non-significant. \* and \*\* indicate  $p < 0.05$  and  $0.01$ , respectively.

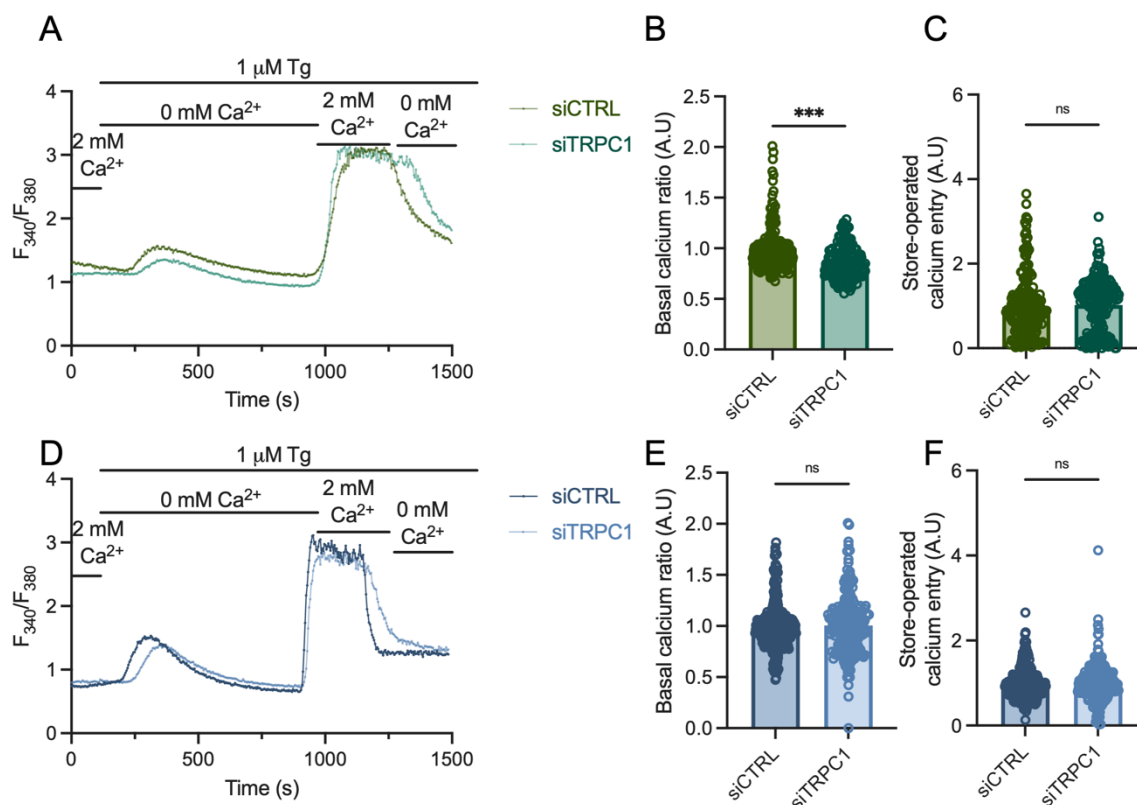


**Figure S5.** (A) Representative traces of the classical store-operated  $\text{Ca}^{2+}$  entry protocol. Acid-adapted (6.5) PANC-1 cells were perfused with 2 mM  $\text{Ca}^{2+}$  for 1 min, then with 0 mM  $\text{Ca}^{2+}$  and 1  $\mu\text{M}$  thapsigargin (Tg) for 12 min, followed by 2 mM  $\text{Ca}^{2+}$  for 5 min, and finally perfused with 0 mM  $\text{Ca}^{2+}$ . (B) Quantification of basal  $\text{Ca}^{2+}$  ratio (0 mM  $\text{Ca}^{2+}$ ) and (C) quantification of SOCE (2 mM  $\text{Ca}^{2+}$  after internal  $\text{Ca}^{2+}$ -store depletion) in in acid-adapted (6.5) and transfected PANC-1 cells (number of analyzed cells siCTRL = 183 and siTRPC1 = 158). (D) Representative traces of the classical store-operated  $\text{Ca}^{2+}$  entry protocol used on acid-recovered (7.4R) PANC-1 cells. (E) Quantification of basal  $\text{Ca}^{2+}$  ratio (0 mM  $\text{Ca}^{2+}$ ) and (F) quantification of SOCE (2 mM  $\text{Ca}^{2+}$  after internal  $\text{Ca}^{2+}$ -store depletion) in acid-recovered (7.4R) and transfected PANC-1 cells (number of analyzed cells siCTRL = 274 and siTRPC1 = 234). Welch's correction t-test was used to determine the significant difference between conditions. Ns indicates non-significant. \* indicates  $p < 0.05$ .

## Supplemental Materials and Methods

### *Store-operated Ca<sup>2+</sup> entry assay*

To investigate Store-operated Ca<sup>2+</sup> entry (SOCE) we used the same equipment and reagents as described in the Mn<sup>2+</sup> Quench Assay. SOCE was triggered by applying the classical protocol, first by perfusing a saline solution (145 mM NaCl, 5 mM KCl, 2 mM CaCl<sub>2</sub>, 1 mM MgCl<sub>2</sub>, 5 mM glucose, 10 mM HEPES, pH 7.4 or pH 6.5) containing 2 mM Ca<sup>2+</sup> (for 1 min), then 0 mM Ca<sup>2+</sup> during 1 min followed by 1 μM thapsigargin in 0 mM Ca<sup>2+</sup> for 12 min to induce Ca<sup>2+</sup> store depletion, followed by perfusion of 2 mM Ca<sup>2+</sup> (for 5 min). The intracellular Ca<sup>2+</sup> concentration is derived from the ratio of emitted fluorescence intensities for each of the excitation wavelengths (F340/F380), and emission at 510 nm.

### *Quantitative Real-Time PCR (qRT - PCR)*

The  $2.5 \times 10^4$  transfected (with either siCTRL or siTRPC1) PANC-1 cells, grown in either pH 6.5 or 7.4R conditions, were seeded for 48, 72, or 96 h respectively, to determine the KD of TRPC1 at the transcriptional level. At the specific time points, total RNA was extracted with the Trizol reagent (Sigma-Aldrich, Saint-Quentin-Fallavier, France) method as previously described [44,47]. After RNA extraction, RNA concentrations and purity were determined using a spectrophotometer (NanoDrop 2000, Wilmington, NC, USA). 2 μg of RNA was converted into cDNA with the MultiScribe™ Reverse Transcriptase kit (Applied Biosystems, Carlsbad, CA, USA). Real - time PCR was performed on a LightCycler 480 System (Roche, Basel, Switzerland) using SYBR Green I PCR master mix (Life Science, Roche, Basel, Switzerland). Sense and antisense PCR primers specific to TRPC1 (forward 5' GAGGTGATGGCGCTGAAGG-3' and reverse 5' - GCACGCCAGCAAGAAAAGC-3') and β 2 microglobulin (B2M) (forward 5GTCTTTCAGCAAGGACTGGTC - 3 ' and reverse CAAATGCGGCATCTTCAAACC3'). TRPC1 mRNA expression was normalized to B2M, used as housekeeping gene, and compared to the control sample, using the Pfaffl method [78].

### *FACS analysis of annexin V and propidium iodide staining*

To evaluate the percentage of apoptotic and necrotic cells, we detected phosphatidylserine residues at the outer plasma membrane by the FITC Annexin V Apoptosis Detection Kit I (BD Biosciences Pharmingen, Le Pont - de - Claix, France).  $5 \times 10^5$  transfected PANC - 1 cells, grown in either pH 6.5 or 7.4R conditions, were seeded and collected after 72 h. Both detached and adherent cells were collected by trypsinization. Cells were pelleted, washed twice with cold PBS and resuspended in 1X binding buffer (BD Biosciences Pharmingen). Following the Annexin V Apoptosis Detection Kit staining protocol, we added FITC Annexin V and propidium iodide to the cell pellets and incubated them at room temperature in the dark for 15 min. The binding buffer was then added to each sample, which were immediately analyzed by flow cytometry (Accuri®) in order to determine the percentage of apoptotic and necrotic cells.



## Complementary results

### TRPC1 silencing does not change the expression of other store-operated channels

As we did not find any difference in SOCE in either pH 7.4, 6.5 or 7.4R conditions we investigated if other major SOC could compensate for the loss of TRPC1. However, our immunoblot analysis did not show any significant upregulation of either ORAI1, ORAI3, STIM1 or STIM2 but to some extent the same expression as the control conditions, indicating that the expression of these channels are not affected by TRPC1 silencing (Figure 38).

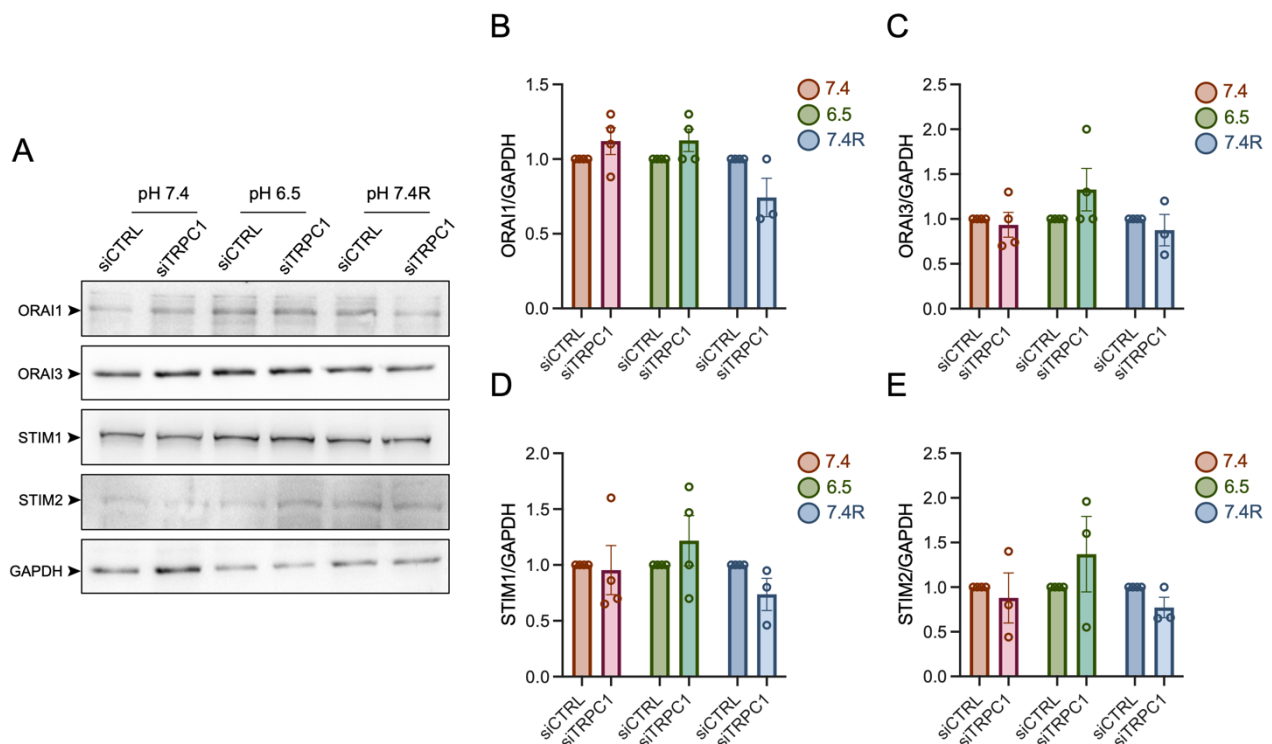


Figure 38. The protein expression of SOC do not change upon TRPC1 KD. A) Representative western blot of SOC in pH 7.4, 6.5 and 7.4R conditions. Quantification of B) ORAI1, C) ORAI3, D) STIM1, and E) STIM2. No significant difference was found between conditions (n=4).

### Acid adaptation does not affect the transcriptional expression of other Ca<sup>2+</sup> channels

Acidification has been shown to affect the function of several ion channels (Petho et al. 2020). For instance, acidification inhibits the function of ORAI channels and their activator, STIM1. Our study investigated the expression of different Ca<sup>2+</sup> channels in the aggressive PDAC cell lines PANC-1 and MiaPaCa-2. However, we did not find any significant difference in the mRNA expression of these ion channels (Figure 39), suggesting that even though the ion channels are functionally affected, their expression is not affected by acid adaptation.

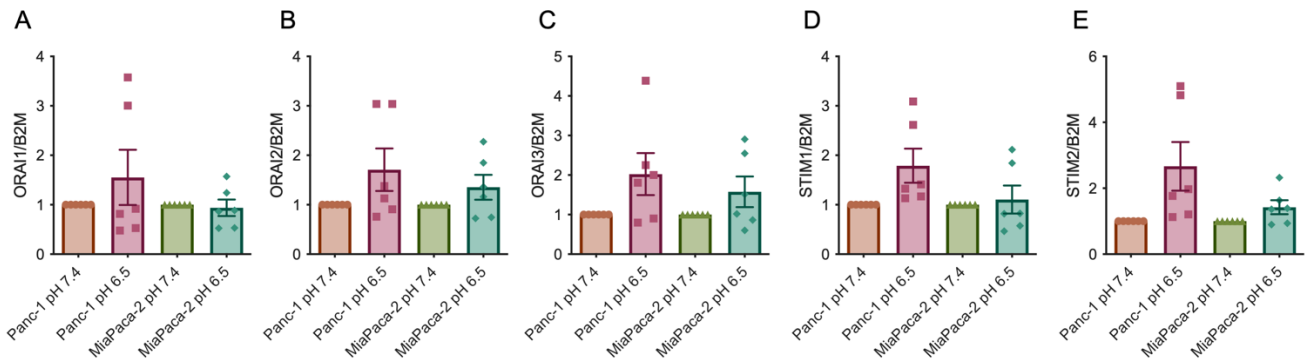


Figure 39. The expression of  $Ca^{2+}$  channels does not change upon acid adaptation. mRNA expression of A) *ORAI1*, B) *ORAI2*, C) *ORAI3*, D) *STIM1*, and E) *STIM2*. No significant difference was found between conditions.

### Acute acidification increases $Ca^{2+}$ entry through TRPC1

TRPC1 localizes to the plasma membrane in acid-adapted PANC-1 cells and regulates basal  $Ca^{2+}$  entry here. It has to our knowledge, not yet been shown if TRPC1 is functionally active upon acidification, as it has been shown for other TRPC channels. Thus, we aimed to investigate if acute acidification also could activate the  $Ca^{2+}$  entry through TRPC1. Here, our  $Mn^{2+}$  quench assay showed that PANC-1 cells grown in normal pH conditions (pH 7.4) display a higher  $Ca^{2+}$  entry when exposed acutely to pH 6.5 by  $16.8 \pm 7.6\%$  compared to cells exposed to pH 7.4 (Figure 40,  $n = 1$ ). The  $Ca^{2+}$  entry was abolished by  $18.7 \pm 6.3\%$  upon TRPC1 KD in normal pH conditions, and by  $59.2 \pm 8.9\%$  in pH 6.5 (Figure 40,  $n = 1$ ) (Figure 40). These results suggest that TRPC1 activates  $Ca^{2+}$  entry upon acute acidification.

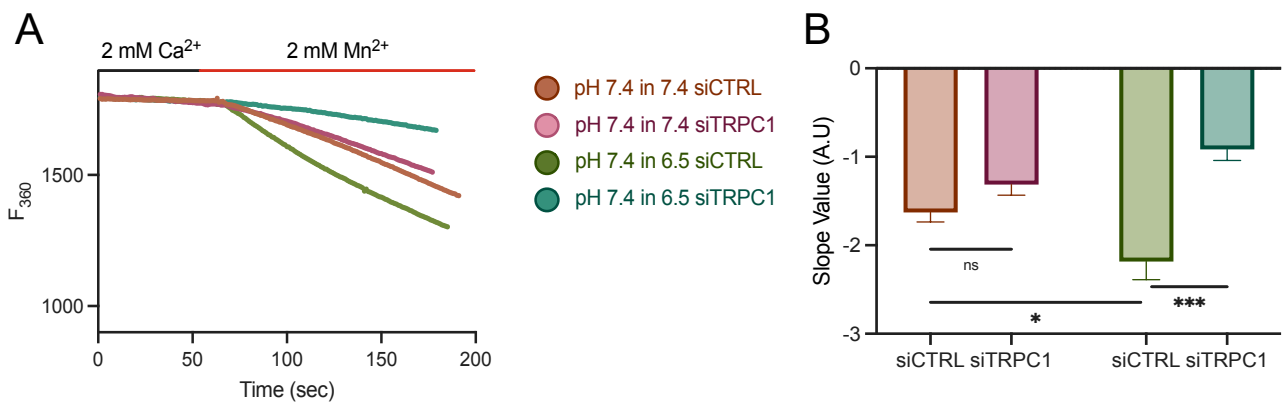


Figure 40. TRPC1 regulates  $Ca^{2+}$  entry upon acute acidification. PANC-1 cells grown in pH 7.4 were measured acutely in either pH 7.4 or 6.5 conditions. A) Representative traces from  $Mn^{2+}$  quench assay. B) Quantification of  $Mn^{2+}$  quench assay ( $n = 1$ ).

### The TRPC1 localization correlates with the acidic tumor microenvironment

We aimed to reveal the acidic tumor microenvironment in human PDAC tissue samples, with markers indicating acidity. We used two proteins that previously described the acidification of solid tumor microenvironments. The LAMP2 and the NBCn1 proteins. LAMP2 is highly expressed in more acidic regions

of breast cancer tumors (Damaghi et al. 2015). NBCn1 is involved in acidifying the tumor microenvironment and is consistently expressed in breast cancer tissue (Lee et al. 2015, Pedersen et al. 2017). We analyzed the marking intensity score and found that both LAMP2 and NBCn1 were highly expressed in both tumor and adjacent non-tumor cells (Figure 41A, B). LAMP2 was mainly located in the cytoplasm (91.7% and 83.6% in non-tumor and tumor tissue, respectively, n = 20), where NBCn1 was found both in the plasma membrane and the cytoplasm of non-tumor and tumor cells (~50% in cytoplasm and membrane, respectively, n = 20).

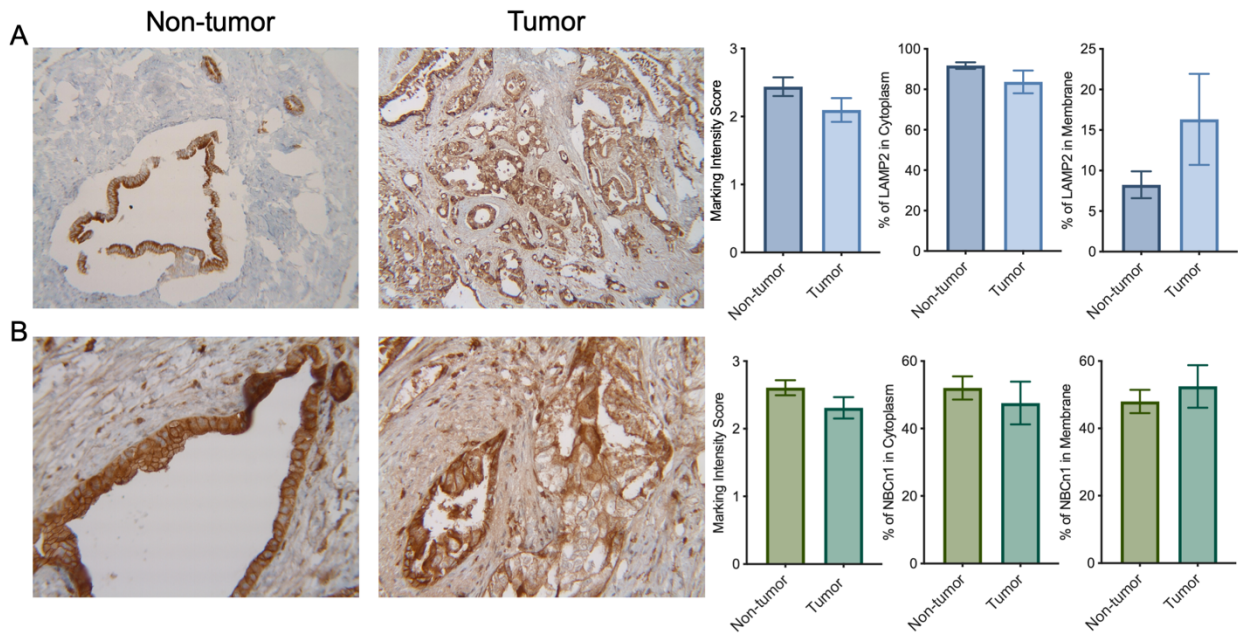


Figure 41. LAMP2 and NBCn1 expression in PDAC tissue. The protein expression (marking intensity score) and localization of A) LAMP2 and B) NBCn1 in non-tumor and tumor tissue. (n = 20). No significant difference was found between conditions.

We have previously demonstrated that TRPC1 localizes to the plasma membrane of tumor cells in human PDAC tissue and that acid adaptation enhances this localization. Therefore, we aimed to analyze if TRPC1 correlated with the LAMP2 or NBCn1 expression in PDAC tissue. Here, we found that the plasma membrane localization of TRPC1 is associated with the cytoplasmic localization of LAMP2 in tumor cells (Figure 42A).

Together, our results suggest that LAMP2 and NBCn1 are highly expressed in non-tumor and PDAC tissue, and TRPC1 plasma membrane localization correlates with the localization of LAMP2 in the cytoplasm.

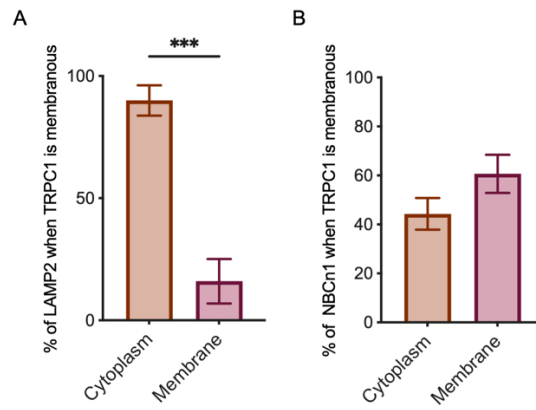


Figure 42. TRPC1 in the plasma membrane correlates with LAMP2 in the cytoplasm. A) The expression of LAMP2 in the cytoplasm or membrane when TRPC1 is expressed in the membrane. B) The expression of NBCn1 in the cytoplasm or membrane when TRPC1 is expressed in the membrane (n=20, \*\*\*,  $p < 0.001$ ).

# DISCUSSION

## Discussion, Part 1 & 2

The role of transmembrane proteins, including ion channels, in the healthy exocrine pancreas is well established. The ductal epithelial cells are, like other epithelia, well-organized. They are equipped with a highly polarized set of ion channels and transporters, which maintain the net bicarbonate excretion across the apical membrane, balanced by the net efflux of acid across the basolateral membrane to maintain their intracellular pH. Thus, the correct distribution of ion channels and transporters is vital to preserve the secreting function of the exocrine pancreas (Novak et al. 2013). However, it is well known that when epithelial cells transform into a malignant phenotype, they lose their apicobasal polarity, resulting in an altered localization of ion channels (Coradini *et al.* 2011, Pedersen and Stock 2013). Until present, the role of ion channels in the exocrine pancreas and PDAC have not been described. Thus, we made a comprehensive literature study, summarizing the localization and function of ion channels involved in fluid secretion and their role in the development and progression of PDAC. Additionally, we outlined how different ion channels can be potential biomarkers of PDAC. This work was published as a review named '*Ion channel signature in healthy pancreas and pancreatic ductal adenocarcinoma*' in *Frontiers in Pharmacology*.

In parallel with our literature study, we screened several ion channel expressions in PDAC cell lines, focusing on Ca<sup>2+</sup> channels, as presented here. Numerous studies have shown the implication of different Ca<sup>2+</sup> channels in cancer progression, including PDAC (Prevarskaya et al. 2007, Borowiec et al. 2014, Shapovalov et al. 2016, Humeau et al. 2018, Chen et al. 2019, Tajada and Villalobos 2020). We found that mRNA expression of Ca<sup>2+</sup> channels was upregulated in human PDAC tissue cell lines, compared to adjacent non-tumor tissue and a normal-like control cell line. However, their expression profile in our local cohort of human PDAC tissue was less evident. Only two Ca<sup>2+</sup> channels were significantly upregulated in our study, ORAI3, and TRPC1, and both channels seemed to localize to the plasma membrane of tumor cells. Furthermore, our transcriptomic analysis showed that TRPC1 was highly upregulated in the aggressive PDAC cell line PANC-1, whereas ORAI3 was primarily upregulated in the less aggressive PDAC cell lines BxPC-3 and AsPC-1. Interestingly, TP53 is mutated in these two cell lines, in contrast to the Colo357 cell line. Mutations in TP53 is known to result in the over expression of ORAI3 in other cancer cell types (Hasna *et al.* 2018). Furthermore, two recent reports have shown that ORAI3 was highly expressed in several PDAC cell lines (Arora et al. 2021, Dubois et al. 2021). We showed that ORAI3 was upregulated at the transcriptomic level with our TCGA approach. Arora et al. showed the same upregulation of ORAI3 and that patients with a high expression of ORAI3 displayed shorter overall survival time; however, this was not significant.

There is strong evidence that TRPC1 is involved in other types of cancer progression (Elzamzamy et al. 2020). Yet, only one study before ours has shown the role of TRPC1 in BxPC-3 cell migration (Dong et al. 2010). Taking the sparse knowledge into account with our preliminary results, which indicated an upregulation of TRPC1 in PDAC cell lines and tissue, we, therefore, aimed to investigate the downstream role of TRPC1 in PDAC cell proliferation and as a potential biomarker of PDAC. We worked with TCGA data, human PDAC



tissue from our local cohort, and the aggressive PANC-1 cell line to demonstrate this. The result obtained during this work was published in the article '*The TRPC1 channel forms a PI3K/CaM complex and regulates pancreatic ductal adenocarcinoma cell proliferation in a Ca<sup>2+</sup>-independent manner*' in the International Journal of Molecular Sciences.

We further aimed to investigate the interplay between TRPC1 and the fluctuations of the acidic tumor microenvironment, which is now in revision as the article '*Acid adaptation promotes TRPC1 plasma membrane localization leading to pancreatic ductal adenocarcinoma cell proliferation and migration through Ca<sup>2+</sup> entry and interaction with PI3K/CaM*' in Cancers.

#### TRPC1 is a potential biomarker of PDAC

Several studies have demonstrated that TRPC1 is a potential biomarker of different kinds of cancer, including tongue, breast, gastric, ovarian, colorectal, and renal cell carcinoma (Mandavilli et al. 2012, Faouzi et al. 2016, Liu et al. 2016, Xu et al. 2017, Ibrahim et al. 2019, Zhang et al. 2020, Sun et al. 2021, Wang et al. 2021, Chen et al. 2022, Ke and Long 2022). As we have summarized in our review, other ion channels have shown to be potential biomarkers of PDAC. In congruence with previous studies, we showed that TRPC1 was upregulated in human PDAC tissue, notably in the basal-like subtype of PDAC. The high expression of TRPC1 correlated with low overall survival. Additionally, the localization of TRPC1 in the plasma membrane was associated with nerve and vascular invasion. It has previously been reported that the GTP-binding protein RhoA promotes the plasma membrane localization and activation of TRPC1-mediated Ca<sup>2+</sup> entry in pulmonary artery endothelial cells and intestinal epithelial cells (Mehta et al. 2003, Chung et al. 2015). TRPC1 translocation to the plasma membrane depends on PI3K mediated transport, leading to Ca<sup>2+</sup> entry, which promotes glioma cell migration (Lepannetier *et al.* 2016). Furthermore, TRPC1 levels are low in the plasma membrane when in an inactive form. The transfer and activation of the channels depend on STIM1 Ca<sup>2+</sup> entry through ORAI1 (Cheng et al. 2011, Ambudkar et al. 2017). Collectively, our results and previous reports indicate that TRPC1 exerts an aggressive role when located in the plasma membrane of PDAC tumor cells. One could speculate if this role is designated the interplay between the acidic tumor microenvironment of PDAC and TRPC1, as the plasma membrane location of TRPC1 correlated with the acidification marker LAMP2, which has previously been described to correlate with acidosis of breast cancer tissue and cell lines (Damaghi et al. 2015).

#### TRPC1 localizes to the plasma membrane and is functionally active solely in acid-adapted and -recovered PANC-1 cells

As we demonstrated that TRPC1 is expressed in the cytoplasmic compartments of a normal-like duct cell line and non-tumor cells and translocate to the plasma membrane in PANC-1 and tumor cells of human PDAC tissue, we aimed to investigate how the localization was affected by the acidic tumor microenvironment. We found that the acid adaptation promoted the plasma membrane localization of TRPC1, which was maintained

in acid-recovered conditions. The interaction between TRPC1 with other complexes, promotes its translocation to the plasma membrane, as described above.

The enhanced TRPC1 plasma membrane localization resulted in  $\text{Ca}^{2+}$  entry solely in acid-adapted and -recovered conditions, as TRPC1 did not contribute to  $\text{Ca}^{2+}$  entry under normal pH conditions. This notion was supported by our  $\text{Ca}^{2+}$  entry experiments, where PANC-1 cells grown in normal pH conditions were acutely exposed to acidosis, which resulted in a decreased  $\text{Ca}^{2+}$  entry of 60% upon TRPC1 silencing. This effect was not found in normal pH conditions. These results indicate that TRPC1 is active upon acidification and leads to downstream mechanisms of  $\text{Ca}^{2+}$  entry, both in acid-adapted and acid-recovered conditions. Even though it has not previously been described whether TRPC1 is activated by acidification, other TRPC channels as TRPC4 and TRPC5, are activated upon low pH values (~6.5) (Semtner et al. 2007, Thakur et al. 2020). Thus, one could speculate that TRPC1 can translocate to the plasma membrane, where it becomes active and lead to  $\text{Ca}^{2+}$  entry. This could be due to its interaction with other ion channels, transporters, receptors or cytosolic proteins, which could also be affected by acidification and recovery.

TRPC1 regulates proliferation and migration through  $\text{Ca}^{2+}$ -dependent mechanisms in acid-adapted and -recovered conditions

To investigate the interplay between TRPC1 and the fluctuations of the acidic tumor microenvironment, we initially demonstrated the effect of acid adaptation and recovery on PANC-1 cells. As previously described for other cell lines, acid adaptation inhibited PANC-1 cell proliferation (Shin et al. 2020, Hagelund and Trauzold 2022, Wu et al. 2022) and induced their migratory properties (Sutoo et al. 2020, Yao *et al.* 2020). However, we found that the proliferation and viability of acid-recovered cells and spheroids were enhanced. Along was the number of acid-recovered cells increased in the S-phase. Interestingly, the acid-adapted cells exhibited a more alkaline  $\text{pH}_i$  when exposed to a neutral pH. Together, these results confirm that acid-adapted cells encountering a neutral microenvironment favors an increased  $\text{pH}_i$ , resulting in enhanced proliferation (Flinck M et al. 2018, Flinck et al. 2018). Additionally, we showed an improved migration property of PANC-1 cells, which was decreased in recovery conditions to the same level as for normal pH conditions. The same effect has been demonstrated in other cell lines, where the motility of acid-induced cells increased for a short period upon exposure to pH 7.4 but decreased to lower levels than in acid-induced conditions after longer exposures (Robey et al. 2009, Riemann et al. 2014, Riemann et al. 2016, de Bem Prunes et al. 2022). These results suggest that the migratory properties are cell type-specific and depend on the duration of acidosis and recovery.

The role of TRPC1 in  $\text{Ca}^{2+}$  entry is still under debate (Ambudkar et al. 2017, Elzamzamy et al. 2020). However, the activation of TRPC1 seems to depend on cell type and microenvironmental conditions. Our group and others have shown that  $\text{Ca}^{2+}$  entry through TRPC1 is activated upon ambient pressure leading to cell proliferation and migration of PSCs (Fels et al. 2016, Radoslavova et al. 2022). Furthermore, TRPC1 is overexpressed in hypoxic conditions where it regulates breast cancer cell migration through SOCE (Azimi et al. 2017). This study showed that silencing of TRPC1 did not affect constitutive  $\text{Ca}^{2+}$  entry or SOCE under

normal pH conditions. Additionally, the depletion of the extracellular  $\text{Ca}^{2+}$  did not affect either PANC-1 cell proliferation or migration. These results are in congruence with previous studies, showing that TRPC1 regulates cellular processes independently of  $\text{Ca}^{2+}$  entry (Davis et al. 2012, Madsen et al. 2012, Asghar et al. 2015, Selli et al. 2015, Selli et al. 2016, Sun et al. 2021). It is also in congruence with the literature, describing that transformed cells can proliferate in the absence of  $\text{Ca}^{2+}$  and that the downregulation of several ion channels has no effect on  $\text{Ca}^{2+}$  entry but attenuates proliferation (Capiod 2013, Borowiec et al. 2014). This designates the  $\text{Ca}^{2+}$ -independent role of TRPC1 in normal pH conditions.

Interestingly, TRPC1 regulates constitutive  $\text{Ca}^{2+}$  entry, but not SOCE, in acid-adapted and recovered PANC-1 cells. We aimed to investigate if other SOC was responsible for compensating for the loss of TRPC1. However, our results did not show any clear picture of an upregulation of other  $\text{Ca}^{2+}$  channels, indicating that other channels could compensate for the loss of TRPC1 during SOCE.

Indeed, our results suggest that TRPC1 is activated upon acidic conditions leading to  $\text{Ca}^{2+}$  entry. Additionally, PANC-1 cell proliferation and migration were reduced upon  $\text{Ca}^{2+}$  depletion in acid-adapted and -recovered conditions. Together with its translocation to the membrane, these results designate that TRPC1 becomes active in acid-adapted and -recovered cells where it regulates proliferation and migration also via a  $\text{Ca}^{2+}$ -dependent mechanism.

#### TRPC1 regulates proliferation and migration through the PI3K/AKT and MAPK/ERK1/2 axis in acid-recovered conditions

We showed that TRPC1 regulated proliferation and migration through PI3K/AKT and MAPK/ERK1/2, particularly in acid-recovered PANC-1 cells. TRPC1 strongly interacted with the PI3K-p85 $\alpha$  subunit, which removes its inhibitory effect on the catalytic subunit p110 and sequentially activates downstream PI3K signaling (Nussinov *et al.* 2017). The interaction between TRPC1 and the PI3K-p85 $\alpha$  subunit was enhanced in acid-adapted cells, and maintained in acid-recovered conditions. The silencing of TRPC1 resulted in potent inhibition of AKT and ERK1/2 phosphorylation in acid-adapted and recovered cells. This inhibition explains the downregulation of cell cycle regulating proteins and cell cycle arrest in the G0/G1 and G2/M phases. TRPC1 KD affected ERK1/2 phosphorylation to less extent in normal pH conditions, which was more evident in acidic and recovered conditions, indicating that TRPC1 regulates cell proliferation and migration through the PI3K and MAPK signaling axis and exerts a more aggressive role in acid-recovered PANC-1 cells.

As TRPC1 forms a complex with the  $\text{Ca}^{2+}$  binding protein CaM in all pH conditions, we investigated whether the inhibition of CaM, which is activated by  $\text{Ca}^{2+}$ , affected the downstream signaling pathways AKT and ERK1/2. Here, we revealed that this inhibition decreased the activation of AKT solely in acid-recovered PANC-1 cells. The activation of ERK1/2 was reduced in all conditions but to a greater extent in acid-adapted and -recovered cells. This designates the role of CaM and  $\text{Ca}^{2+}$  downstream signaling, notably in acid-adapted and -recovered conditions.

Taken together, this study shows that TRPC1 is upregulated in human PDAC tissue and cell lines. Its total expression is downregulated upon acid adaptation, but favors a localization in the plasma membrane. Acid-recovery restores the total expression of TRPC1 and maintains the expression in the plasma membrane. In acid-adapted and -recovered conditions, TRPC1 forms a complex with PI3K and CaM, and enhances Ca<sup>2+</sup> entry, which regulates AKT and ERK1/2 activation. This activation of the PI3K/AKT and MAPK/ERK1/2 signaling control cell cycle progression, proliferation and migration, notably in the acid-recovered conditions.

# EPIGENETIC PROJECT

# The acidic microenvironment affects the DNA methylation of ion channels

## Introduction

The term 'epigenetics' was described by C.H. Waddington in the 1940s and addressed as: 'the branch of biology which studies the causal interactions between genes and their products, which bring the phenotype into being' (Waddington 1975). Since then, implications of epigenetic changes have been extended in a wide range of biological processes, and accumulating evidence suggested that heritable changes in the genome can occur independently of alterations in somatic cells regardless of their differentiation status (Bird 2007). The heritable changes require fine-tuned epigenetic modifications, including DNA methylation, histone or chromatin post-translational modifications, and non-coding RNA regulations. If the fine-tuning of epigenetic modifications fails, it may cause inappropriate initiation or inhibition of gene expression, which leads to pathological changes, such as cancers (Jones and Baylin 2002, Egger *et al.* 2004).

Cancer is a consequence of genomic mutations, epigenetic alterations, and environmental factors (Easwaran *et al.* 2014). Numerous studies have characterized the genomic landscape of cancers from oncogene-driven signaling to the mutation spectrum of different cancer types. Epigenetic changes differ from genomic changes as they modify gene expression without permanent changes in the genomic sequence (Easwaran *et al.* 2014). These changes favor cancer cells as epigenetic alterations are reversible and faster regulated than genomic evolution. Except for the traditional changes that occur to somatic cells upon malignant transformation, multiple forces shape the landscape of cancer, including the tumor microenvironment. Current epigenetic modifications investigations are focused on the progress of cancer cell development and the interaction between the tumor microenvironment and cancer cells (Lu *et al.* 2020).

## DNA methylation patterns in PDAC

DNA methylation is the most extensively studied epigenetic modification and displays a fundamental function in development and diseases, including embryonic development, genomic imprinting, cell identity establishment, lineage specification, and X chromosome deactivation (Bird 1986, Gopalakrishnan *et al.* 2008, Lister *et al.* 2009, Zhang *et al.* 2020). DNA methylation appears by the covalent binding of a methyl group from S-adenosylmethionine to the 5' position of the cytosine pyrimidine ring. These methylations often occur in cytosine-phosphate-guanine (CpG) rich regions (also known as CpG islands), particularly concentrated in the promoter region of many genes. The binding of the methyl group can either prevent the access of transcription factors to the binding sites of DNA or recruit methyl-binding domain proteins, combined with histone modifications to rearrange the chromatin structure, leading to repressive gene expression (Issa 2004, Kanwal and Gupta 2012).

The enzymes, namely the DNA methyltransferases (DNMT) 1, 3a, and 3b, are orchestrated to catalyze adding the methyl group to the DNA (Bestor 2000). The DNMT1 is responsible for maintaining methylation patterns of the parental DNA strand to the newly synthesized daughter strand (Pradhan *et al.* 1999, Bestor



2000). DNMT3a and 3b are thought to be responsible for applying de novo methyl groups to the DNA. In contrast, demethylation is the reverse action that recovers silenced genes (Okano *et al.* 1999). The enzyme family Ten-eleven translocation methylcytosine dioxygenases (TET) can turn the 5-methylcytosine (m5C) into 5-hydroxymethylcytosine (5hmC). The homeostasis between methylation and demethylation of the genome occurs as a dynamic mechanism of gene expression regulation (Tahiliani *et al.* 2009, Scourzic *et al.* 2015). The extensive addition or removal of methyl groups from the DNA is referred to as hypermethylation or hypomethylation.

In PDAC, DNA methylation is a well-known mechanism to inactivate tumor suppressor genes. Specifically, the inactivation of the promoter region by methylation of the CDK2A/p16 tumor suppressor gene has been established. As described in cell cycle progression, the p16 protein (a CKI) inhibits the binding of cyclin D to their dependent kinases CDK4 and 6, and the loss of the p16 protein can result in increased phosphorylation of Rb and a subsequent progression through the G1 and S phase. It has been shown that this hypermethylation of *CDKN2A/p16* occurs in the early stages of PDAC (Fukushima *et al.* 2002). PanIN lesions of patients with chronic pancreatitis show a loss of p16 expression, suggesting that this alteration may contribute to PDAC development (Rosty *et al.* 2003). Methylation of the CpG islands of the *CDKN2A/p16* gene is one of the most common mechanisms to silence p16 in PDAC, emphasizing the significance of this epigenetic mechanism in modulating tumor progression in PDAC (Schutte *et al.* 1997, Wilentz *et al.* 1998, Fukushima *et al.* 2002). Other genes promoting PDAC progression have also been identified as hypermethylated (Zhang *et al.* 2021). On the contrary, several genes have shown to be hypomethylated in PDAC, including *CCND1* and 3 (coding for cyclin D1 and 3) and *S100A4* and *S100P* (calcium-binding protein), which are proteins involved in cell cycle progression, and cell motility and invasion (Bararia *et al.* 2020).

Interestingly, the expression of several types of ion channels is regulated by methylation in a wide range of cancers (Ouadid-Ahidouch *et al.* 2015). Regarding PDAC, different genes encoding ion channels are associated with DNA methylation. Two voltage-gated ion channels have shown to be hypermethylated. Namely, the *CACNA1* gene, coding for the Cav3.1 channel, was hypermethylated in 16% of PDAC tumors (Ueki *et al.* 2000). The *KCNA3* gene promoter (voltage-gated potassium channel, K<sub>v</sub>1.3) was hypermethylated, and its expression was decreased in 69.7% of PDAC tumors. Furthermore, this hypermethylation was associated with low overall survival (Brevet *et al.* 2009). A recent study exploring the genome-wide DNA methylation profile of PDAC tumors compared to non-tumor tissues showed that different actors of Ca<sup>2+</sup> signaling were associated with methylation patterns (Gregorio *et al.* 2020). They observed that Ca<sup>2+</sup> signaling pathways had a large number of genes significantly hypo- and hypermethylated. Interestingly, the *ORAI2* gene promoter was hypomethylated, associated with an increased expression. Furthermore, this expression correlated with better overall survival (Gregorio *et al.* 2020). In another study, investigating the DNA methylome of PDAC samples and from the TCGA cohort, authors found hypermethylation of *CACNB2*

(coding for the Voltage-dependent L-type calcium channel subunit beta-2), *KCNA6* (K<sub>v</sub>1.6) and *KCNA3*, as previously described (Chatterjee *et al.* 2021).

Changes in pH are a reciprocal concept concerning genomic stability. As described in the section ‘Cellular adaptation to extracellular acidosis in carcinogenesis’, changes in intracellular pH greatly affect genomic stability. These changes in pH<sub>i</sub> can be due to changes in pH<sub>o</sub>. Still, they can also be created by the cells’ biodynamics, as many genetic and epigenetic alterations exert their function by altering the metabolism in cancer cells, causing changes in pH (Ordway *et al.* 2020).

However, it is not well known how acidification directly affects epigenetic changes. The concept of histone acetylation is better described in terms of acidification. When pH<sub>i</sub> decreases, histones are globally deacetylated by histone deacetylases (HDACs), resulting in more condensed chromatin structure and repression of the gene. The released acetate anions from this process are co-exported with protons through MCTs to maintain the pH<sub>i</sub> (McBrian *et al.* 2013). In contrast, when pH<sub>i</sub> increases, histone acetyltransferases (HAT) are activated, and global histone acetylation increases, resulting in accessible chromatin and gene activation (McBrian *et al.* 2013). Although the relation between pH<sub>i</sub> and histone acetylation has been reported, little is known about the pH<sub>i</sub>-dependent mechanisms of gene expression due to gene promoter methylation. Acidification can affect gene expression by changing mRNA stability, and influence the stability of DNA binding proteins by changing their protein-protein and protein-DNA complex affinities, for instance, transcription factors such as AP-1, NFκB, and Sp1 (Xu and Fidler 2000, Torigoe *et al.* 2003). Sp1 binds CpG sites, protecting specific regions from methylation, and is activated by increasing acidity (Torigoe *et al.* 2003). Acidification can disrupt the oligomerization of DNMT3A, decreasing its catalytic activity. This could potentially result in specific gene promoter hypomethylation and, thus, an upregulation of oncogenes (Holz-Schietinger and Reich 2015).

How acid adaptation affects DNA methylation levels of ion channel promoter regions, and thus gene expression, has to our knowledge, never been studied before. In the following chapter, we aimed to reveal how acid adaptation could affect gene promoter methylation of, specifically, *ASIC1*, *SCN8A* (coding for the sodium voltage-gated channel alpha subunit 8, Nav1.6), and *TRPC1*.

- **VGSC/Na<sub>v</sub> channels**

Voltage-gated sodium channels (Na<sub>v</sub> channels) allow the permeability of Na<sup>+</sup> across the membrane. They are comprised of nine α subunit isoforms (Nav1.1-1.9) and four β subunits (β1-4) and are encoded by SCN\_A/B genes (de Lera Ruiz and Kraus 2015). Na<sub>v</sub> channels are known as critical proteins for the initiation of the action potential (Catterall 2000). It has been shown that a high membrane potential can facilitate the proliferation of cells, which is believed to be associated with the initiation of DNA synthesis and mitosis (Orr *et al.* 1972, Binggeli and Weinstein 1986). Cancer cells often have a higher membrane potential than their normal counterparts, which might be associated with their rapid proliferation (Yang and Brackenbury 2013). Interestingly, some tumor tissues have been shown to exhibit a higher level of Na<sup>+</sup> levels compared to non-

cancer tissues (Smith *et al.* 1978, Cameron *et al.* 1980, Sparks *et al.* 1983). This implies that intracellular Na<sup>+</sup> levels could determine the abnormal membrane potential in cancer cells. Thus, Na<sup>+</sup> permeable channels, such as Nav channels, might play a critical role in cancers (Mao *et al.* 2019). It has been demonstrated that Nav takes part in regulating the pH of the tumor microenvironment (Besson *et al.* 2015). This mechanism is caused by the high expression of Nav channels leading to a high influx of Na<sup>+</sup>. Interestingly, Nav channels are co-expressed with NHE1 (Carrithers *et al.* 2009, Brisson *et al.* 2011, Brisson *et al.* 2013). The high increase of Na<sup>+</sup> causes a high efflux of protons through NHE1. This decreases the extracellular pH, facilitating the activation of cathepsins that degrade the ECM, thereby enhancing pH-dependent tumor cell invasion and metastasis. (Carrithers *et al.* 2009, Gillet *et al.* 2009, Brisson *et al.* 2011, Brisson *et al.* 2013). Interestingly, the high influx of Na<sup>+</sup> can activate VGCCs, which increase intracellular Ca<sup>2+</sup> concentrations (Tong *et al.* 2009, Yao *et al.* 2011).

The Nav1.6 isoform is overexpressed in lymphoma, cervical, prostate, and colorectal cancers, where it promotes cell invasion and metastatic behaviors, probably in cooperation with NHE1 (Mao *et al.* 2019). Interestingly, another study showed, that a significantly lower level of Nav1.6 mRNA expression was found in colorectal adenocarcinomas tissues compared with paired neighboring non-cancerous tissues (Igci *et al.* 2015).

- ASICs

The acid-sensing ion channels (ASICs) are widely expressed throughout the nervous system, and recently they have been shown to be expressed in non-excitable tissues, such as vascular smooth muscle cells and epithelial-derived cancer cells (Cheng *et al.* 2018, Zhang *et al.* 2022). ASICs belong to the voltage-insensitive, amiloride-sensitive epithelial sodium channel (ENaC)/degenerin (dEG) channel family, which is a group of distantly related, non-voltage-gated Na<sup>+</sup> channels found in mammals (Garty and Palmer 1997, Benos and Stanton 1999). There are four isoforms encoded by ASIC functional genes in humans and rodents, namely ASIC1-4. Functional ASICs are aggregated by three homologous or heterologous subunits, which have different properties. The subunits allow for differences in pH sensitivity and ion selectivity between different ASICs (Rotin and Staub 2021). ASIC1-3 is directly affected by protons, whereas ASIC4 generally does not exhibit a functional role alone (Holzer 2009). When extracellular pH drops rapidly from 7.4 to <6.9, the ASICs are activated, allowing the passage of Na<sup>+</sup>, Ca<sup>2+</sup> and K<sup>+</sup> (permeability index Na<sup>+</sup> > Ca<sup>2+</sup> > K<sup>+</sup>). Although ASICs are rapidly deactivated after activation, they can still monitor long-term acidosis (Krishtal and Pidoplichko 1980, Waldmann *et al.* 1997, Waldmann *et al.* 1997). Several cancer types are associated with ASIC expression, including gliomas, breast, liver, colorectal and pancreatic cancer (Berdiev *et al.* 2003, Sheng *et al.* 2021, Zhang *et al.* 2022). In PDAC cancer cells, ASIC1 and 3 are upregulated and promote EMT, as described in the section 'Calcium and pH'.

## Results

ASIC1 and Nav1.6 expression is dysregulated in human PDAC tissue and affected by acid adaptation in PDAC cell lines

We have shown that TRPC1 is upregulated in human PDAC tissue and downregulated upon acid adaptation. We found that ASIC1 tended to be upregulated by 50% (Figure 43A,  $n = 2$ ), and Nav1.6 was downregulated by  $33 \pm 13.2\%$  (Figure 43B,  $n = 20$ ,  $p < 0.05$ ) in PDAC tissue compared to adjacent non-tumor tissue. By investigating the mRNA levels of ASIC1 and Nav1.6, we showed that ASIC1 was highly upregulated by  $79.5 \pm 10.0\%$  (Figure 43C,  $n = 3$ ,  $p < 0.001$ ) in acid-adapted PANC-1 and by  $81.5 \pm 15.7\%$  ( $n = 3$ ,  $p < 0.01$ ) in acid-adapted MiaPaCa-2 cells. Nav1.6 was significantly downregulated in MiaPaCa-2 cells upon acid adaptation by  $44 \pm 9.8\%$  (Figure 43D,  $n = 3$ ,  $p < 0.01$ ), indicating that the expression of certain Na<sup>+</sup> channels is affected by acid adaptation.

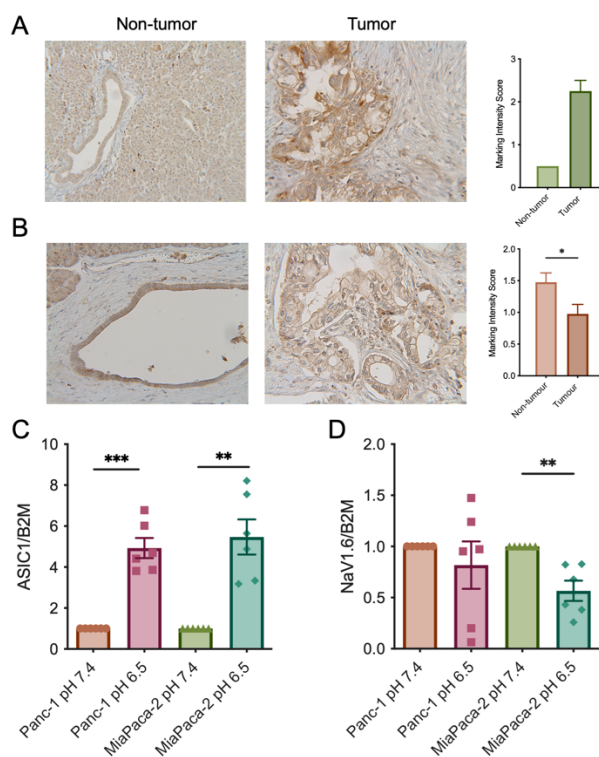


Figure 43. The Na<sup>+</sup> channels ASIC1 and Nav1.6 are dysregulated in human PDAC tissue and upon acid adaptation. A) The protein expression of Nav1.6 in human PDAC and adjacent non-tumor tissue ( $n = 2$ ). B) The protein expression of ASIC1 in human PDAC and adjacent non-tumor tissue ( $n = 20$ ). C) ASIC1 mRNA expression in acid-adapted PANC-1 and MiaPaCa-2 cells, compared to cells grown in normal pH conditions ( $n = 3$ ). D) Nav1.6 mRNA expression in acid-adapted PANC-1 and MiaPaCa-2 cells, compared to cells grown in normal pH conditions ( $n = 3$ ).

ASIC1 seems to be hypomethylated in acid-adapted MiaPaCa-2 cells, but hypermethylated in acid-adapted PANC-1 cells

Initially, we investigated the methylation levels by semiquantitative analysis of the *ASIC1* promoter region in MiaPaCa-2 and PANC-1 cells. The semiquantitative method was used to calculate the ratio between the C and the G on the specific CpG sites from at least 10 pooled clones. We found that *ASIC1* seems to be hypomethylated in acid-adapted MiaPaCa-2 cells, as the sum of methylation levels from all the CpG sites was less than 2%, compared to cells grown in normal pH conditions, where the sum of methylation where 61.5% in average (Figure 44, n = 2). On the contrary, PANC-1 cells seemed to be hypermethylated in the *ASIC1* promoter region, as the sum of methylation on average was 303% (Figure 45, n = 2).

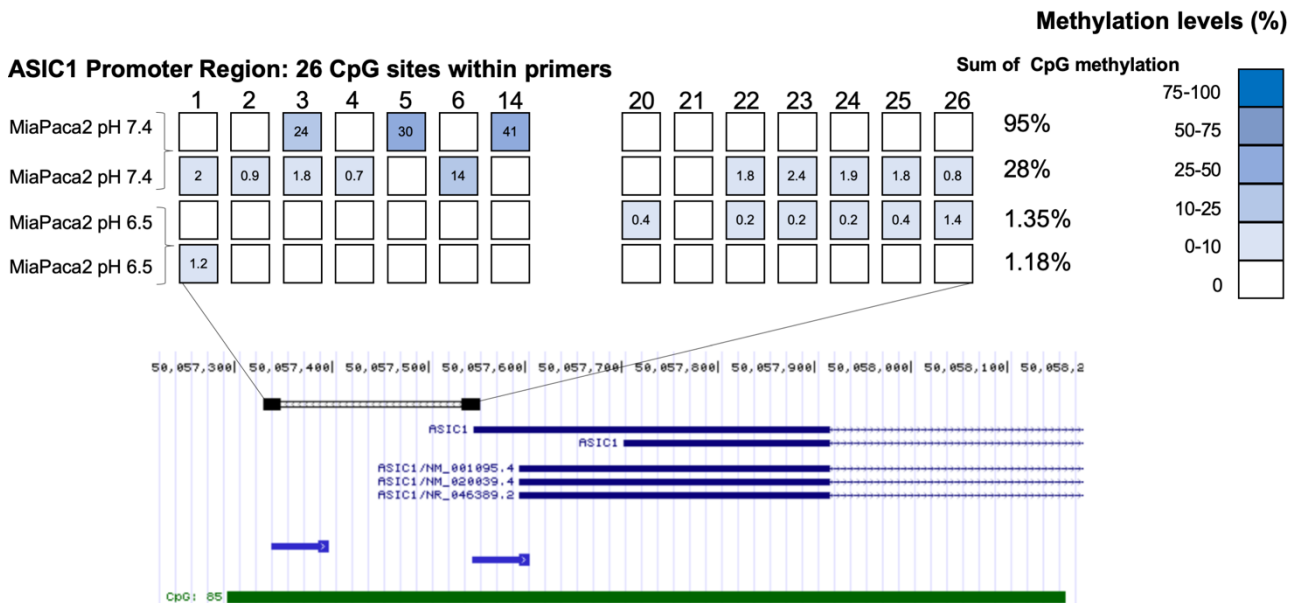


Figure 44. Semiquantitative analysis of DNA methylation levels of the *ASIC1* promoter region in MiaPaCa-2 cells. Promoter sites in *ASIC1* gene within the specifically designed primers (black dotted box). MiaPaCa-2 cells grown at pH 7.4 are more methylated than MiaPaCa-2 cells grown at pH 6.5. The sum of the methylation represents the sum of the methylation levels of the 26 CpG sites calculated by the semiquantitative analysis method. (CpG sites that are not shown are not methylated). (n=2).

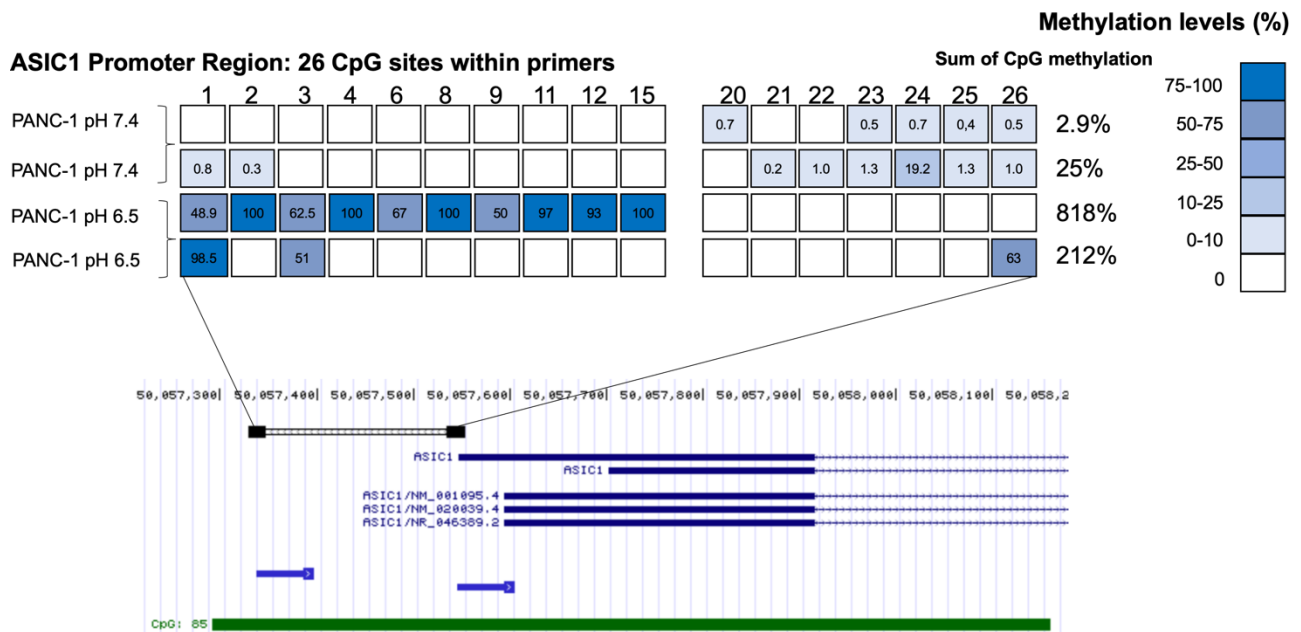


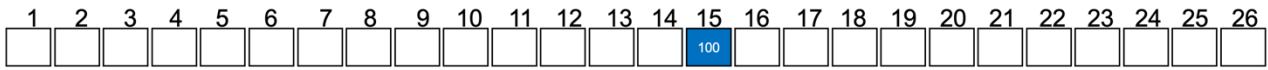
Figure 45. Semiquantitative analysis of DNA methylation levels of the *ASIC1* promoter region in PANC-1 cells. Promoter sites in *ASIC1* gene within the specifically designed primers (black dotted box). PANC-1 cells grown at pH 6.5 are more methylated than PANC-1 cells grown at pH 7.4. The sum of the methylation represents the sum of the methylation levels of the 26 CpG sites calculated by the semiquantitative analysis method. (CpG sites that are not shown are not methylated). (n=2).

The quantitative analysis method reveals that the *ASIC1* region is not hypomethylated upon acid-adaptation. As our results indicated that the *ASIC1* promoter region could be hypomethylated in MiaPaCa-2 cells, we chose to investigate further the methylation levels of the *ASIC1* promoter region in this cell line by the quantitative analysis method, where bisulfite-converted DNA from single clones is sequenced separately. The outcome will be either a C or a G. With this method, we found that none of the CpG sites within the *ASIC1* gene promoter were methylated in acid-adapted MiaPaCa-2 cells. However, we only found one CpG site methylated in one out of 14 clones of MiaPaCa-2 cells (Figure 46, n = 2). This indicates that methylation of the *ASIC1* promoter region is not strongly affected by acid adaptation compared to that of normal pH conditions.



### ASIC1 promoter region

MiaPaca-2 pH 7.4



MiaPaca-2 pH 6.5

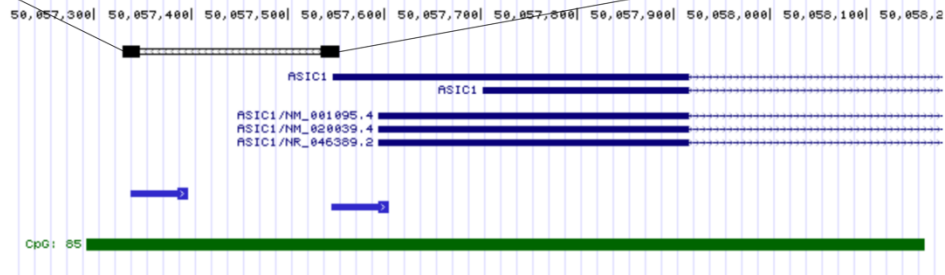
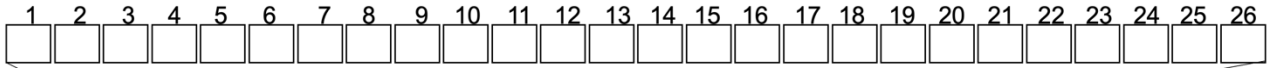


Figure 46. Quantitative analysis of DNA methylation levels of the ASIC1 promoter region in MiaPaCa-2 cells. Promoter sites in ASIC1 gene within the specifically designed primers (black dotted box). One clone from MiaPaCa-2 cells grown at pH 7.4 are more methylated than MiaPaCa-2 cells grown at pH 6.5 at the 15<sup>th</sup> CpG site (n=2, clones in total; 7.4: 14, 6.5: 14).

The *SCN8A* gene promoter is hypermethylated in acid-adapted PANC-1 cells

As the Nav1.6 channel was downregulated in human PDAC tissue and the MiaPaCa-2 cell line upon acid adaptation, by the semiquantitative analysis method, we investigated if the *SCN8A* promoter displayed methylation levels in these conditions. We showed an increased tendency by 7.9% of DNA methylation in the *SCN8A* gene promoter in a pool of clones (Figure 47, n = 2). Thus, we used the quantitative analysis method to investigate if any CpG sites in this promoter region were methylated. Here, we used another primer pair with 52 CpG sites included instead of 11, which we used for the semi-quantitative analysis. Our results showed that four CpG sites in the *SCN8A* gene promoter were methylated in PANC-1 cells, in contrast to two CpG sites in cells grown in normal pH conditions. The four CpG sites were methylated in three different clones out of 11, from acid-adapted PANC-1 cells, and the two methylated CpG sites were from two clones out of 9, from PANC-1 cells grown in normal pH conditions (Figure 48, n = 2). This could suggest that the promoter region of the *SCN8A* gene is hypermethylated upon acid adaptation.

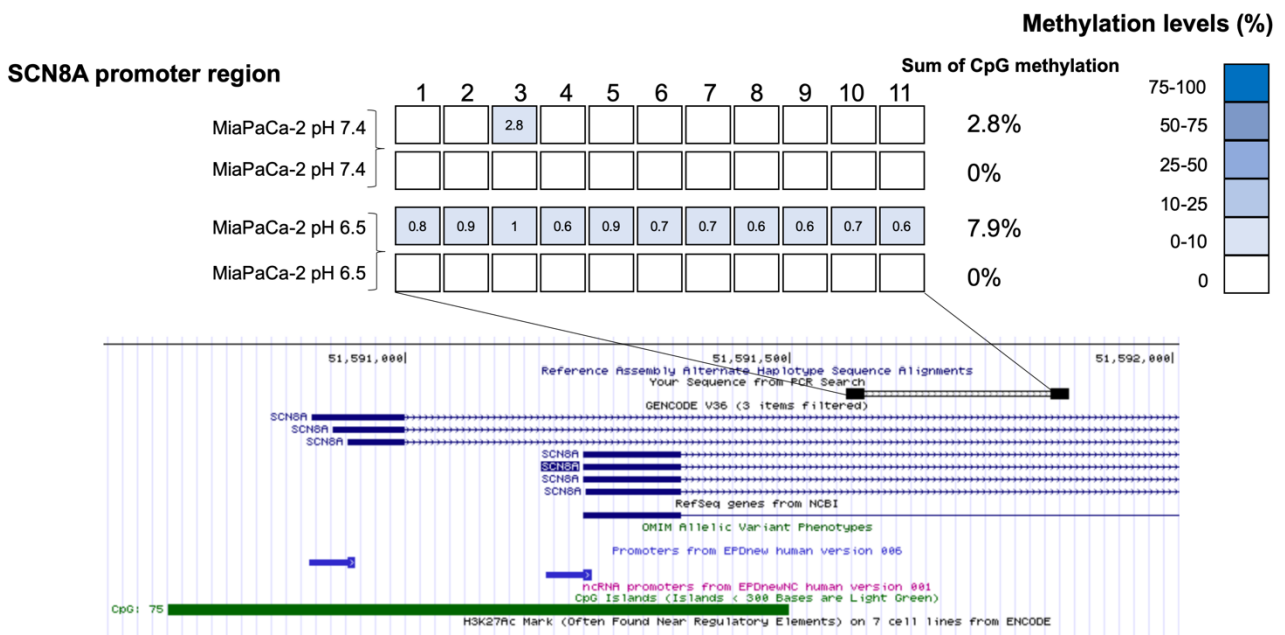


Figure 47. Semiquantitative analysis of DNA methylation levels of the *SCN8A* promoter region in MiaPaCa-2 cells. Promoter sites in *SCN8A* gene within the specifically designed primers (black dotted box). MiaPaCa-2 cells grown at pH 6.5 are more methylated than MiaPaCa-2 cells grown at pH 7.4. The sum of the methylation represents the sum of the methylation levels of the 11 CpG sites calculated by the semiquantitative analysis method ( $n=2$ ).

**SCN8A Promoter Region: 52 CpG sites within primers**

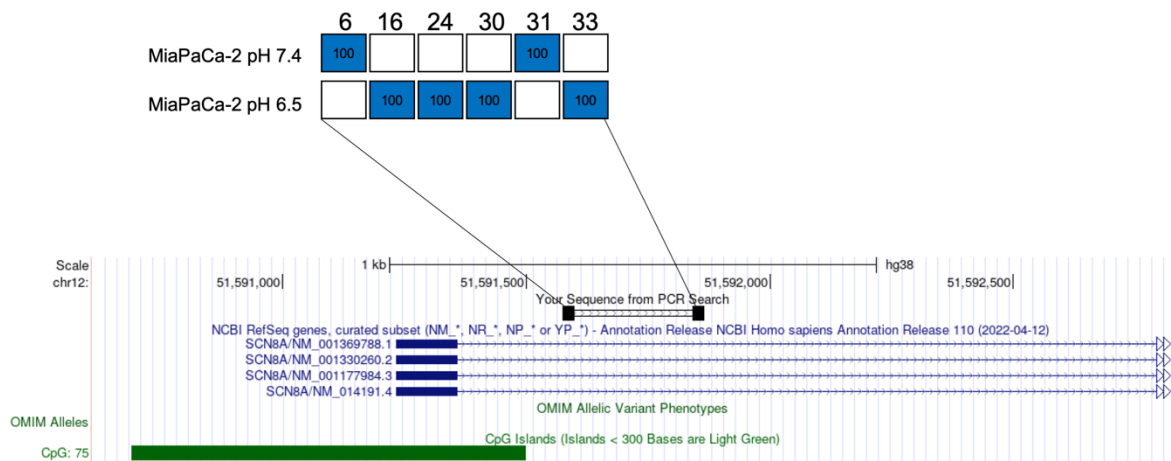


Figure 48. Quantitative analysis of DNA methylation levels of the *SCN8A* promoter region in MiaPaCa-2 cells. Promoter sites in *SCN8A* gene within the specifically designed primers (black dotted box). Three clones from MiaPaCa-2 cells grown at pH 6.5 are more methylated at the 16<sup>th</sup>, 24<sup>th</sup>, 30<sup>th</sup>, and 33<sup>rd</sup> CpG site ( $n=2$ , clones in total 11) than MiaPaCa-2 cells grown at pH 7.4 which were methylated at the 6<sup>th</sup> and 31<sup>st</sup> CpG site in two different clones ( $n=2$ , clones in total 9) (CpG sites which are not showed, are not methylated).

The *TRPC1* gene promoter is hypomethylated upon acid-adaptation

As *TRPC1* was downregulated at the protein level upon acid adaptation, we initially used the quantitative analysis method to investigate DNA methylation of the *TRPC1* gene promoter. We observed that there were five out of 12 clones (Figure 49, n = 2) displaying methylation in different CpG sites in the *TRPC1* promoter region in PANC-1 cells grown in normal pH conditions, where there were no clones out of 8 displaying methylation in any CpG sites in acid-adapted PANC-1 cells (Figure 49, n = 2). This suggests that the gene promoter of *TRPC1* is hypomethylated upon acid adaptation.

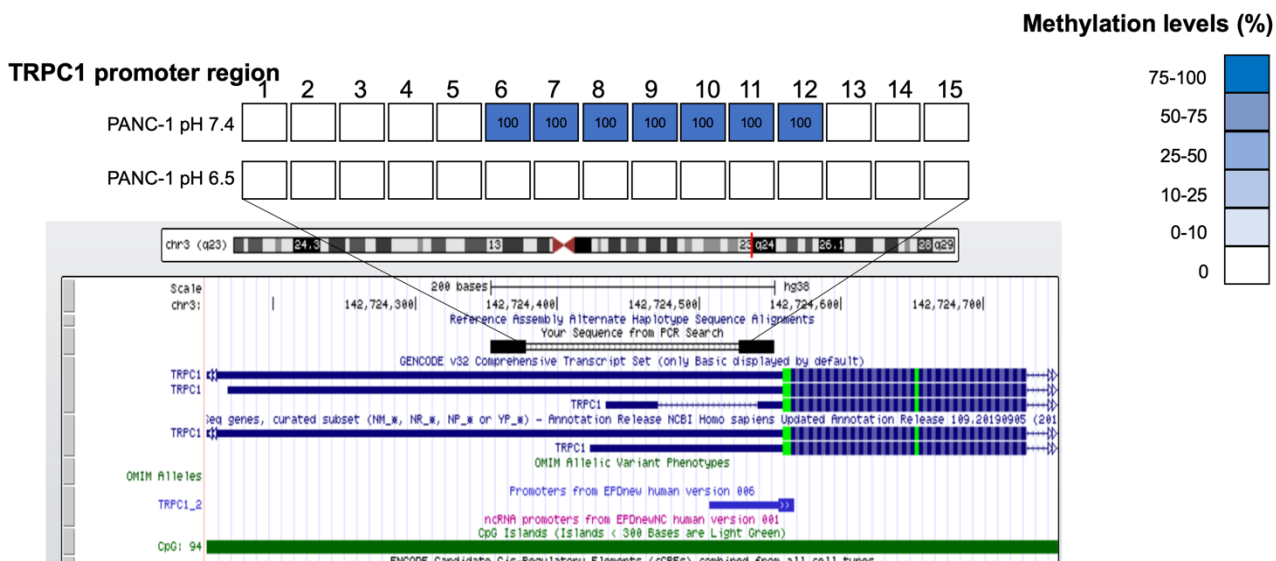


Figure 49. Quantitative analysis of DNA methylation levels of the *TRPC1* promoter region in PANC-1 cells. Promoter sites in the *TRPC1* gene within the specifically designed primers (black dotted box). Five clones from PANC-1 cells grown in pH 7.4 are more methylated at the 6<sup>th</sup>-12<sup>th</sup> CpG site (n=2, clones in total 12) than PANC-1 cells grown in pH 6.5 were not methylated in any CpG sites (n=2, clones in total 8).

## Discussion

It is well-known that epigenetic changes affect gene expression and are essential drivers of carcinogenesis (Lu et al. 2020). Of interest is DNA methylation as this epigenetic mechanism is persistent and can be passed down through generations to provide further generations a ‘memory’ to survive the tumor microenvironment. In contrast, the more transient modalities as histone acetylation that, are imposed to help cancer cells survive acute disruption in their microenvironmental homeostasis (Ordway et al. 2020). Studies have shown that genetic and epigenetic alterations contribute to PDAC development and progression (Roalso *et al.* 2022).

Interestingly, the expression of several ion channels is known to be regulated by either hypo- or hypermethylation of their gene promoter in different cancer types, including PDAC (Ouadid-Ahidouch et al. 2015). Furthermore, acidosis can affect genetic stability and cause double-stranded DNA breaks (Morita et al. 1992). Epigenetic changes themselves exert their function by altering the metabolism of cancer cells and are acquired by signaling cascades initiated by sensing the extracellular microenvironment (Ordway et al. 2020). However, it is not known how the acidic tumor microenvironment affects DNA methylation alterations of ion channel gene promoters and if this can be the cause of up-or down-regulation of specific ion channels. In this study, we used a bisulfite sequencing approach and a quantitative and semi-quantitative analysis method to explore the DNA methylation levels of genes coding for ion channels whose expression is affected by acid adaptation (Figure 50). We showed that  $Na_v1.6$  was downregulated in acid-adapted MiaPaCa-2 cells and human PDAC tissue, compared to adjacent non-tumor tissue. Furthermore, we showed that the *SCN8A* gene promoter is hypermethylated in acid-adapted MiaPaCa-2 cells compared to cells grown in normal pH conditions. However, it cannot be anticipated that this hypermethylation, shown in very few clones, regulates the expression of *SCN8A* alone. To further investigate if the hypermethylation causes the downregulation of *SCN8A*, a demethylation agent as 5-azadeoxycytidine could be used to remove the m5C and then investigate if both the hypermethylation will disappear and the expression of  $Na_v1.6$  will increase.

We furthermore showed that the gene promoter regions of *ASIC1* and *TRPC1* were not hypo- or hypermethylated upon acid adaptation, respectively, when compared to normal pH conditions. This indicates that pH does not modulate DNA methylation at these specific promoter sites, and might not regulate the expression of *ASIC1* and *TRPC1*.

One could speculate if the acid adaptation affects other epigenetic alterations causing the aberrant expression of *ASIC1* and *TRPC1*. Acidosis is known to deacetylate histones globally by activating HDACs, resulting in gene silencing (McBrian et al. 2013). This could be the case for the *TRPC1* gene promoter, as the protein expression of TRPC1 is decreased upon acid adaptation. In addition, there was no remarkable change in the DNA methylation of the *ASIC1* gene promoter and these specific CpG sites. One could argue that acidosis increases the activation of specific transcription factors binding to CpG sites and protects the promoter from methylation, such as Sp1 (Torigoe et al. 2003). Epigenetic approaches cannot investigate these activities.

However, this case is more complex to explain, it could be worth investigating if the DNA methylation or histone modification are found on other sites of the gene promoter.

Taken together, further studies and replicates are needed to conclude how acid-adaptation affects DNA methylation and other epigenetic changes of ion channel gene promoters.

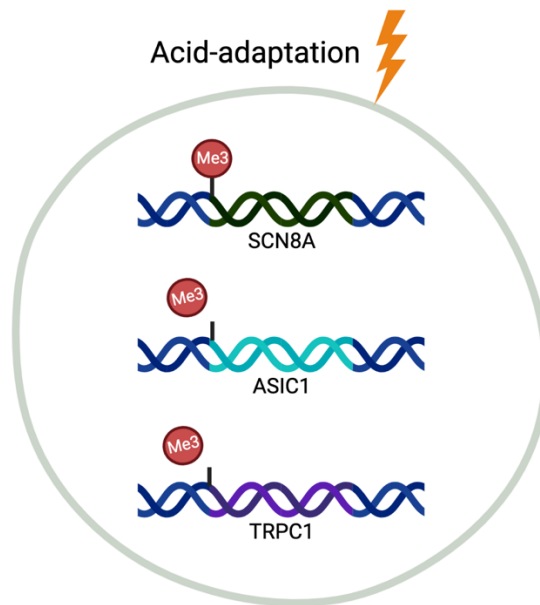


Figure 50. Graphical summary of hypo- or hypermethylation in the gene promoters investigated in this study.

# CONCLUSION AND FUTURE PERSPECTIVES



This thesis has given novel insight into the role of ion channels, specifically the impact of TRPC1 and the acidic microenvironment in PDAC progression. First, we elucidated the role of TRPC1 in PDAC cell proliferation and if it could be used as a potential biomarker. Next, we evaluated the interplay between fluctuations of the acidic microenvironment and TRPC1, resulting in downstream signaling events that regulate PDAC cell proliferation and migration. Finally, we investigated whether DNA methylation of specific pH-sensitive ion channels regulated their expression.

Thus, in this thesis work, we specifically highlighted that:

1. Ion channels are involved in PDAC development and progression
2. TRPC1 is overexpressed in human PDAC tissue and cell lines, which correlates with aggressive clinical factors and a poor outcome.
3. Acid adaptation increases TRPC1 plasma membrane localization, even if its total expression is decreased.
4. In acid-recovered conditions, the total TRPC1 expression is increased, and the plasma membrane localization maintained.
5. TRPC1 regulates PDAC cell proliferation and migration through PI3K/CaM in a  $\text{Ca}^{2+}$ -independent manner in normal pH conditions, where it regulates these processes through  $\text{Ca}^{2+}$ -dependent mechanisms upon acid adaptation and recovery.
6. The TRPC1/PI3K/CaM complex controls cell cycle progression, proliferation, and migration through AKT and ERK1/2 activation.
7. The *SCN8A* gene promoter tends to be hypermethylated, causing its downregulation in acid-adapted MiaPaCa-2 cells.
8. ORAI1, 2 and 3 and STIM1 are upregulated at the transcriptional level in human PDAC samples, where only ORAI3 is overexpressed in human PDAC tissue at the protein level.

To complete our story about the interplay between the acidic tumor microenvironment and TRPC1, it could be of purpose to further investigate different factors (Figure 51):

In this study, TRPC1 regulates PANC-1 cell proliferation in a  $\text{Ca}^{2+}$ -independent manner in normal pH conditions. Although, through  $\text{Ca}^{2+}$ -dependent mechanisms in acid-adapted and -recovered conditions. We hypothesize this is due to the TRPC1 translocalization in the plasma membrane in these conditions. Thus, it could be interesting to investigate if TRPC1 activation is caused directly by acidification and recovery. This could be explored by using the patch-clamp technique.

It would also be interesting to investigate the trafficking of TRPC1 to the plasma membrane in these conditions. It is proposed that TRPC1 is active in the membrane when activated by forming a complex with ORAI1/STIM1. Thus, it could be interesting to see how the fluctuations of the acidic tumor microenvironment affect these processes.

Furthermore, we showed that the inhibition of CaM (Ca<sup>2+</sup>-activated protein) decreases the activation of ERK1/2 to a smaller extent in normal pH conditions than in acid-adapted and -recovered conditions. Notably, the activation of AKT was only affected by CaM inhibition in acid-recovered cells, suggesting that the activation of ERK1/2 and AKT in acid-recovered conditions are strongly Ca<sup>2+</sup>-dependent. The inhibition of CaM is an indirect way to investigate if these processes, to some extent, are Ca<sup>2+</sup>-dependent. Thus, exploring the direct effect of Ca<sup>2+</sup> depletion on ERK1/2 and AKT activation could be of interest. Furthermore, these findings could reveal if the proliferation and migration of acid-recovered PANC-1 cells are more dependent on Ca<sup>2+</sup> entry through TRPC1 than on the TRPC1/PI3K/CaM complex.

This study also showed that the acidic tumor microenvironment enhanced PANC-1 cell migration. Additionally, the inhibition of TRPC1 decreased cell migration in all pH conditions. While it is well known that acidosis enhances the EMT process of cancer cells, including PDAC cells (Wu et al. 2022) and that hypoxia induces TRPC1-dependent breast-cancer cell migration (Azimi et al. 2017), it is not known how the interplay between the acidic microenvironment and TRPC1 regulates the EMT process and hence invasion and migration of PDAC cells. Therefore, it could be interesting to elucidate if TRPC1 is involved in this process by investigating epithelial markers and parameters of cell motility.

To further investigate the role of TRPC1 and the acidic tumor microenvironment in PDAC cell cycle progression, it could be of interest to synchronize PDAC cells, expose them to the fluctuations of the acidic environment and investigate the expression of TRPC1 in the different phases of the cell cycle. Here, it would also be interesting to examine if the silencing of TRPC1 affected the cell cycle phases differently. This study showed that in non-synchronized cells, TRPC1 KD accumulated cells in the G0/G1 phase in all conditions. However, the TRPC1 KD decreased the number of cells in the S-phase in normal pH conditions and increased the number of cells in the G2/M phases in acidic and recovered conditions, indicating that the role of TRPC1 shifts in different conditions.

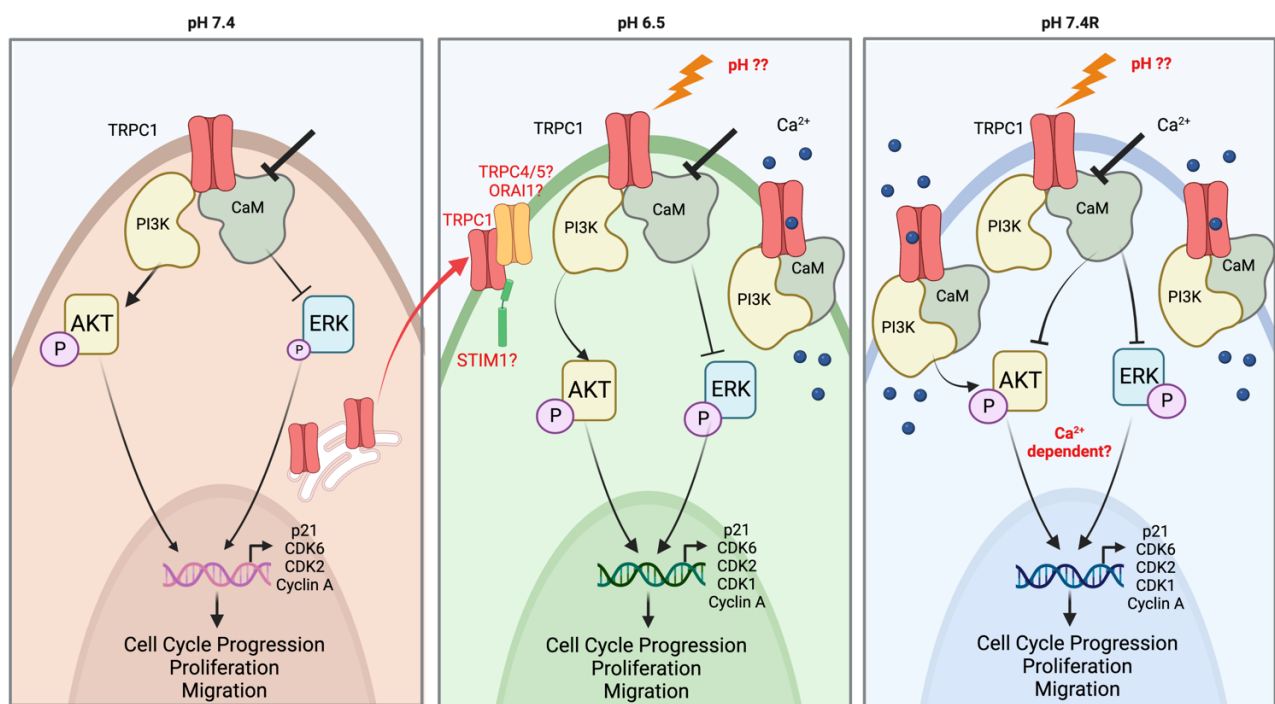


Figure 51. Concluding and perspective figure of how acid adaptation and TRPC1 affect PDAC progression. Questions still to be elucidated are marked in red color: Is TRPC1 activated by acidic pH? Does TRPC1 translocate to the plasma membrane by forming a complex with other channels? Are downstream signaling of TRPC1 in acid-recovered conditions  $Ca^{2+}$  dependent?

We revealed that both the acidic tumor microenvironment and TRPC1 affected the growth of PANC-1 spheroids. Moreover, we have recently shown that in activated PSCs, TRPC1 is involved in cell proliferation and secretion of the cytokine IL-6 (Radoslavova et al. 2022). Thus, it could be interesting to develop a 3D model with a co-culture of PDAC cells and PSCs and investigate the role of TRPC1 by comparing the aggressiveness, in the form of proliferation and invasion, between the different pH conditions and the co-cultured and not co-cultured conditions (Figure 52A).

We elucidated that TRPC1 localization and the downstream mechanism were affected by the fluctuations of the acidic microenvironment. These processes could, to some extent, be studied *in vivo* by using a TRPC1 deficient mouse model and a pH indicator such as pHlourin, SNARF, or pHLIPS. TRPC1-deficient mice have been shown to decrease the number of colorectal cancer metastases and tumor growth. *In vivo* results from a TRPC1 deficient mouse model, which will take the acidic microenvironment into account, could provide data about the proportion of acidic tissue in the tumor, tumor size, and metastases profile (Figure 52B).

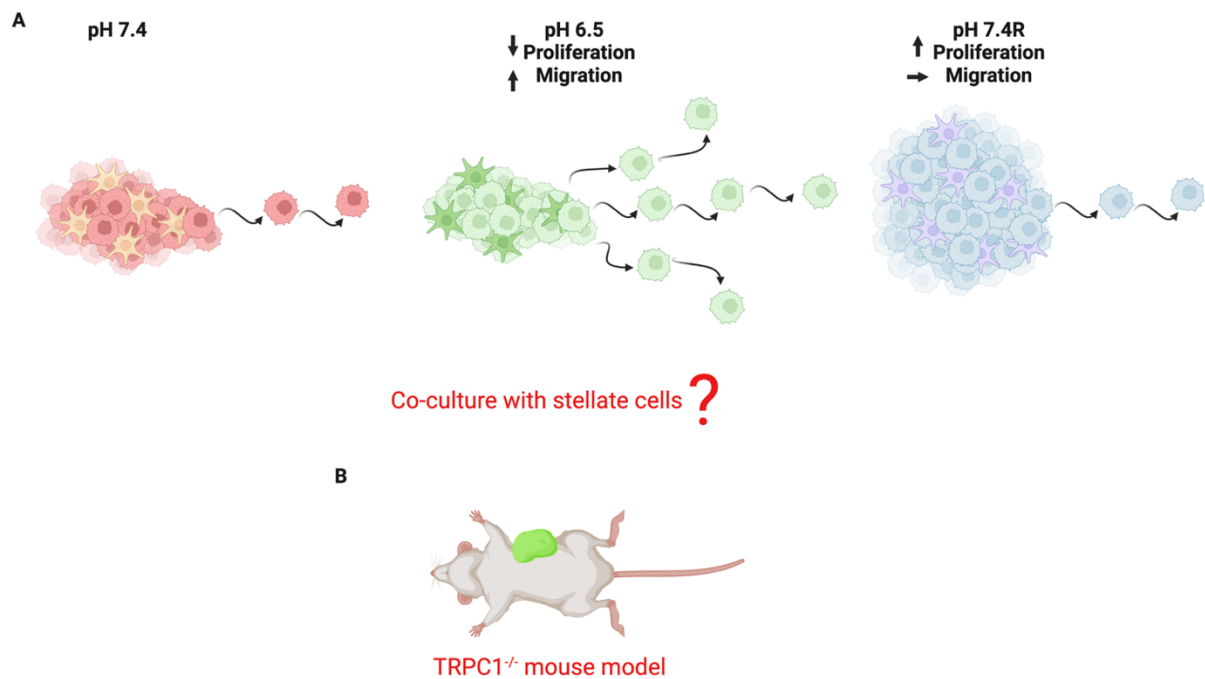


Figure 52. Concluding and perspective figure of how A) co-culture with stellate cells in a 3D model could affect PDAC proliferation and invasion, and B) a TRPC1 deficient mouse model with fluorescent indicators could provide in vivo inside of the role of TRPC1 and the tumor microenvironment

Other future perspectives of this thesis work could include the following:

Several ion channels, including TRPC1, have been shown to correlate with clinical factors (Lastraioli *et al.* 2015). In our local cohort, only the plasma membrane localization of TRPC1 correlated with clinical factors. However, to implement ion channel expression as a screening method, the marking intensity profile would be preferable. To encounter this, a larger cohort is needed to investigate if the channel expression correlates with clinical factors and can function as a diagnostic and prognostic element in clinical practice. There are several methods to examine, for instance, nerve and vascular invasion. However, it is less used in clinical practice to demonstrate the direct invasion mechanisms, such as ECM degradation, EMT, and cell-cell adhesion. Since dysregulation of ion channels is involved in these cellular processes, they could be potential partners to investigate along with classical invasion markers.

The acidic tumor microenvironment in human PDAC tissue is a difficult task to overcome. First, the pH changes are rapidly affected, for instance, during the surgical procedure when the tumor is removed and upon tissue fixation. However, it is still interesting to investigate how the acidic tumor microenvironment in its present form behaves. In our study, we implemented both NBCn1 and LAMP2 as potential biomarkers of acidification. However, tumor cells and normal cells in the adjacent tumor tissue showed a high expression of these proteins, meaning they are essential both in normal ducts and PDAC cells. As there is not yet a standardized method to investigate the acidification of human tissue, it could be of interest if other acid-extruding transporters acidifying the extracellular space could be highly expressed in PDAC tissue.

# RÉSUMÉ

## INTRODUCTION

L'adénocarcinome canalaire pancréatique (ACP), présentant une survie globale à 5 ans inférieure à 10 %, est l'un des cancers les plus meurtriers au monde. Étant donné que l'ACP devrait devenir la principale cause de mortalité par cancer à l'échelle mondiale d'ici 2030 (Rahib et al. 2014), une meilleure compréhension des mécanismes moléculaires sous-jacents à la maladie est nécessaire dans le but de développer des thérapies et biomarqueurs efficaces.

Plusieurs études ont montré qu'une dérégulation de sécrétion de suc pancréatique exocrine peut contribuer au développement de pathologies du pancréas exocrine, y compris l'ACP. Les principaux rôles du tissu pancréatique exocrine sain sont la sécrétion d'enzymes et de fluides riches en ions bicarbonates, au cours de laquelle les canaux ioniques participent à affiner ces processus biologiques. Par conséquent, la dérégulation des canaux ioniques tant au niveau de leur expression mais également de leur activité est liée à un grand nombre de pathologies (Kim, 2014). De plus, cette dérégulation peut également entraîner la transformation d'un comportement cellulaire normal en un comportement malin (Litan et Langhans, 2015). Au cours des dernières décennies, une expression aberrante de nombreux canaux ioniques a été rapportée dans divers types de cancers (Pedersen et Stock, 2013 ; Djamgoz et al., 2014). Ainsi, une expression et une activité anormales des canaux ioniques pourraient être classées comme des caractéristiques du cancer (« Hallmarks of cancer ») (Hanahan et Weinberg, 2011).

Le développement et la progression de l'ACP sont également liés à la physiologie et au microenvironnement du pancréas exocrine. Les cellules épithéliales et stromales pancréatiques sont exposées à des changements cycliques du pH extracellulaire (pHE) dus à la production de sucs pancréatiques alcalins riches en ion bicarbonate ( $\text{HCO}_3^-$ ). L'exposition apicale à ce pHE alcalin est couplée à l'acidification parallèle au niveau de la membrane basolatérale, conduisant à un interstitium pancréatique acide (Novak et al. 2013, Pedersen et al. 2017). Fait intéressant, l'acidification extracellulaire est l'une des principales caractéristiques du microenvironnement tumoral. Celle-ci est causée conjointement par une faible perfusion sanguine et une forte extrusion de protons ( $\text{H}^+$ ) de la glycolyse fermentative et de l'acide sous forme de  $\text{CO}_2$  provenant de la phosphorylation oxydative (Swietach et al. 2014, Boedtkjer et Pedersen 2020, Andersen et al. 2021). L'espace interstitiel des tumeurs solides est généralement acide et bien que des valeurs de pHE aussi basses que 5,6 ont été mesurées, la plupart des valeurs se situent entre 6,4 et 7. En revanche, les zones bien vascularisées présentent un pHE plus proche de la neutralité (Vaupel et al. 1989, Helmlinger et al. 1997, Rohani et al. 2019, Boedtkjer et Pedersen 2020). Le pH intracellulaire (pHi) est plus alcalin que le pHE des tumeurs, mais les cellules cancéreuses dans un microenvironnement acide présentent toujours un pHi acide (Lee et al. 2015, Lee et al. 2016) par rapport aux cellules saines du pancréas normal. Des preuves solides ont été rapportées quant à l'impact du microenvironnement tumoral acide sur l'agressivité de l'ACP en termes de prolifération, de migration et d'invasion ainsi que de résistance à l'apoptose (Orth et al. 2019). Cependant, les mécanismes sous-jacents sont encore mal compris.



Bien que les canaux ioniques soient exposés au microenvironnement acide de la tumeur, le dialogue entre eux n'est pas intégralement étudié. Plus précisément, le rôle des canaux  $\text{Ca}^{2+}$  et de leurs voies de signalisation sous-jacentes sont connus pour être impliqués dans la cancérogenèse (Prevarskaya et al. 2007, Shapovalov et al. 2016, Chen et al. 2019). Parmi les canaux calciques impliqués dans l'entrée du  $\text{Ca}^{2+}$  figure la famille des canaux TRP (*Transient Receptor Potential*). La sous-famille TRPC (C pour *Canonical*) sont sensibles au pH (Wang et al. 2020). Le premier membre de la famille TRPC est TRPC1. TRPC1 est particulièrement connu pour être impliqué dans la cancérogenèse d'une façon dépendante et indépendante du  $\text{Ca}^{2+}$  (Elzamzamy et al. 2020). TRPC1 régule principalement la prolifération, par les voies de signalisation de la *phosphoinositol-3-kinase* (PI3K) et de la *mitogen-activated protein kinase* (MAPK) plusieurs cancers, ce qui s'est avéré vrai par exemple dans le cancer du sein et du côlon (Azimi et al. 2017, El Hiani et al. 2006, El Hiani et al. 2009, Sun et al. 2021). De plus, TRPC1 favorise l'entrée de  $\text{Ca}^{2+}$  dans la cancérogenèse du cancer du sein dans des conditions tumorales hypoxique (Azimi et al. 2017). Concernant l'ACP, une seule étude a rapporté que l'entrée de  $\text{Ca}^{2+}$  via TRPC1 favorise la migration cellules cancéreuses BxPC-3 (Dong et al. 2010). En revanche, la façon dont TRPC1 est affecté par le microenvironnement tumoral n'est pas élucidé. Notre groupe ainsi que d'autres ont récemment montré que TRPC1 est activé par la pression ambiante, une caractéristique du microenvironnement tumoral dans les cellules stellaires pancréatiques (CSP). Cette activation de TRPC1 favorise la prolifération et la migration des CSP de manière dépendante du  $\text{Ca}^{2+}$  (Fels et al. 2016, Radoslavova et al. 2022). Ainsi, les objectifs de cette thèse étaient de comprendre le rôle du canal TRPC1 dans l'agressivité de l'ACP dans un microenvironnement tumoral acide.

Les objectifs spécifiques du présent projet étaient les suivants :

1. Comparer le profil d'expression des canaux  $\text{Ca}^{2+}$  dans les tissus non tumoral et tumoral de patients atteints de l'ACP, ainsi que dans des lignées cellulaires normales et cancéreuses pancréatiques.
2. Caractériser l'effet du microenvironnement tumoral acide sur l'expression des canaux  $\text{Ca}^{2+}$
3. Étudier l'implication du microenvironnement tumoral acide et de TRPC1 dans la prolifération et la migration des cellules d'ACP et déterminer les voies de signalisation sous-jacentes.

Enfin, nous avons également cherché à déterminer si le microenvironnement acide pouvait affecter la méthylation de l'ADN de certains canaux ioniques.

## RESULTATS

1. Les canaux  $\text{Ca}^{2+}$  sont surexprimés dans les tissus humains d'ACP et dans des lignées cellulaires cancéreuses

Plusieurs canaux ioniques, dont les canaux  $\text{Ca}^{2+}$ , sont dérégulés dans différents types de cancer (Tajada et Villalobos 2020). Même si plusieurs études ont démontré l'implication de ces canaux  $\text{Ca}^{2+}$  dans la progression de l'ACP, un aperçu complet de leur expression dans le tissu cancéreux pancréatique humain n'a pas encore été réalisé. Ainsi, nous avons comparé l'expression de l'ARNm des canaux  $\text{Ca}^{2+}$  entre le tissu pancréatique non

tumoral et les échantillons d'ACP humains à l'aide de la base de données TCGA-PAAD d'échantillons normaux et tumoraux. Nous avons constaté que les canaux ORAI1, ORAI2, ORAI3, TRPC1 ainsi que la protéine STIM1 étaient surexprimés dans les tissus d'ACP. De plus, les résultats de notre cohorte locale ont confirmé que ORAI3 et TRPC1 étaient significativement surexprimés dans le tissu d'ACP humain par rapport au tissu non tumoral adjacent. Fait intéressant, nous avons observé que les canaux ORAI3 et TRPC1 étaient localisés au niveau membranaire dans les cellules tumorales, tandis que leur expression était cytoplasmique dans les cellules non tumorales. En outre, nous avons étudié l'expression transcriptionnelle de ces canaux  $Ca^{2+}$  dans différentes lignées cellulaires d'ACP. Durant ce travail, nous avons démontré que les profils d'expression des canaux  $Ca^{2+}$  différaient entre les lignées cellulaires. En effet, TRPC1 était surexprimé dans la lignée cellulaire d'ACP très agressive PANC-1 par rapport à la lignée cellulaire HPNE de type normal. ORAI3 et STIM2 semblaient être surexprimés dans les lignées cellulaires cancéreuses moins agressives BxPC-3 et AsPC-1. STIM1 était significativement surexprimé dans les cellules AsPC-1 et PANC-1. L'ensemble de ces résultats indiquent que STIM, ORAI et TRPC1 sont surexprimés dans le tissu d'ACP humain, au moins au niveau transcriptomique. De plus, ils sont exprimés de manière différentielle entre les lignées cellulaires. Le rôle cancéreux d'ORAI3 a récemment été démontré dans des lignées cellulaires et des tissus humains d'ACP (Arora et al. 2021, Dubois et al. 2021).

## 2. Le canal TRPC1 forme un complexe avec PI3K/CaM et régule la prolifération cellulaire de l'ACP de manière indépendante du $Ca^{2+}$ .

*Article 1 : "The TRPC1 Channel Forms a PI3K/CaM Complex and Regulates Pancreatic Ductal Adenocarcinoma Cell Proliferation in a  $Ca^{2+}$ -Independent Manner". International Journal Of Molecular Sciences, 2022.*

Lors de notre étude, nous avons montré que TRPC1 était systématiquement surexprimé dans le tissu d'ACP humain aux niveaux transcriptomique et protéique. En outre, il est fortement exprimé dans la lignée cellulaire cancéreuse pancréatique agressive, PANC-1.

Dans cette étude, nous avons démontré que la surexpression de TRPC1, au niveau transcriptionnel, analysée à l'aide de la base de données TCGA-PAAD, était significativement plus élevée dans le sous-type d'ACP agressif de type basal par rapport au sous-type classique. De plus, les patients présentant des niveaux élevés de TRPC1 présentaient une survie globale significativement plus faible par rapport aux patients présentant de faibles niveaux d'expression de TRPC1. Au niveau des lignées cellulaires, l'expression de TRPC1 était significativement plus élevée dans les cellules cancéreuses MiaPaCa-2 et PANC-1 par rapport à la lignée cellulaire saine HPNE. Comme TRPC1 était surexprimé dans la lignée agressive PANC-1, nous avons choisi d'étudier les mécanismes par lesquels TRPC1 régulent les processus cellulaires cancéreux dans cette lignée cellulaire. Dans cette lignée, TRPC1 présentait majoritairement une localisation au niveau de la membrane

plasmique, que nous n'avons pas retrouvé dans les cellules HPNE dans lesquelles TRPC1 était localisé au niveau cytosolique. Ces données étaient en accord avec ce que nous avons trouvé dans le tissu d'ACP humain. Pour étudier les mécanismes en aval par lesquels TRPC1 régule les processus cancéreux pancréatique, nous avons développé un modèle de perte de fonction de TRPC1 grâce à une approche siARN. L'efficacité de cette invalidation moléculaire de TRPC1 a été validée par qPCR et Western Blot.

Par la suite, nous avons étudié le rôle de TRPC1 dans la prolifération des cellules PANC-1 et de sphéroïdes pancréatiques. Nous avons démontré que l'inhibition moléculaire de TRPC1 diminuait la prolifération cellulaire et la viabilité des sphéroïdes. De plus, une analyse par cytométrie en flux, a révélé que siTRPC1 entraînait une accumulation de cellules dans la phase G1 ainsi qu'un nombre réduit de cellules dans la phase S. Ces observations étaient en corrélation avec la diminution de l'expression des protéines de régulation du cycle cellulaire CDK6, CDK2 et la cycline A, ainsi qu'une augmentation de l'expression de p21.

Nous avons cherché à déterminer la signature  $Ca^{2+}$  spécifique à TRPC1 dans les cellules PANC-1. En effet, nous avons constaté que le siTRPC1 n'affecte ni l'entrée calcique basale, ni l'entrée de calcium dépendante des stocks calciques (SOCE). De plus, le rôle prolifératif des cellules PANC-1 ne dépendait pas de l'entrée calcique, car nous n'avons pas trouvé de différences significatives entre la prolifération des cellules PANC-1 cultivées dans un milieu de culture normal et un milieu présentant une faible concentration de  $Ca^{2+}$  extracellulaire.

La lignée cellulaire PANC-1 présente des mutations au sein de trois oncogènes connus (KRAS, TP53, CDKN2A). De plus, il a été rapporté que TRPC1 régule la prolifération des cellules cancéreuses par les voies de signalisation en aval de ces oncogènes (Elzamzamy et al. 2020). Ainsi, nous avons cherché à déterminer siTRPC1 régulait la prolifération des cellules PANC-1 par les voies PI3K/AKT et MAPK/ERK. Nous avons constaté que siTRPC1 diminuait principalement l'activation de AKT et, dans une moindre mesure, ERK, indiquant que TRPC1 régule la prolifération des cellules PANC-1 via l'axe de signalisation PI3K/AKT plutôt que la voie de signalisation MAPK.

Nous avons, par la suite, étudié l'interaction physique entre la sous-unité PI3K-p85 et TRPC1. Notre expérience de PLA a montré une proximité entre TRPC1 et la sous-unité PI3K-p85. Cette interaction a été confirmée par co-IP. En effet, TRPC1 interagit fortement avec PI3K et leur protéine de liaison, la calmoduline (CaM). Cette interaction a été abolie lors de l'extinction moléculaire de TRPC1.

L'ensemble de ces données ont révélé que TRPC1 pourrait être un biomarqueur potentiel de l'ACP en étant régulé à la hausse dans les tissus humains d'ACP et les lignées cellulaires cancéreuses pancréatiques. Nous avons démontré que TRPC1 régule la prolifération des cellules PANC-1 et la croissance de sphéroïdes pancréatiques par l'interaction directe avec les protéines PI3K et CaM, activant ainsi cette voie de signalisation régulant la progression des cellules dans les phases G1 et S, probablement par des mécanismes indépendants du  $Ca^{2+}$ .

3. L'adaptation des cellules à un pH acide favorise (i) la localisation TRPC1 au niveau de la membrane plasmique, et (ii) à la prolifération et à la migration des cellules d'ACP de manière dépendante de l'entrée de  $Ca^{2+}$  et de l'interaction avec PI3K/CaM

*Article 2 : "Acid adaptation promotes TRPC1 plasma membrane localization leading to pancreatic ductal adenocarcinoma cell proliferation and migration through  $Ca^{2+}$  entry and interaction with PI3K/CaM". Cancers, 2022.*

Les canaux ioniques, souvent appelés capteurs du microenvironnement, peuvent être affectés par les changements de pH extracellulaire ( $pH_e$ ) et impacter les voies de signalisation (Petho et al. 2020). TRPC1 est connu pour être activé suite à la variation de pression et à l'hypoxie (Fels et al. 2016, Azimi et al. 2017, Radoslavova et al. 2022). À ce jour, il n'a pas été démontré comment l'acidose peut affecter TRPC1, bien que d'autres canaux de la famille TRPC sont activés par l'acidification. L'objectif de ce 2<sup>ème</sup> article était d'étudier si le microenvironnement tumoral acide pourrait affecter la fonction de TRPC1 et les voies de signalisation sous-jacentes.

Pour évaluer l'influence du microenvironnement tumoral acide, nous avons développé un protocole expérimental où les cellules PANC-1 ont été cultivées dans des conditions normales (pH 7,4), adaptées à un environnement acide (30 jours à pH 6,5) ou dans des conditions de récupération (cellules adaptées à pH 6,5 et réensemencé pendant 14 jours à pH 7,4).

Nos mesures de pH intracellulaire ( $pH_i$ ) ont démontré que les cellules PANC-1 adaptées à l'acide (pH 6,5) présentent un  $pH_i$  inférieur à celui des cellules cultivées dans des conditions de pH normales (pH 7,4). De plus, les cellules adaptées à l'acide puis récupérées dans des conditions de  $pH_e$  normales (pH 7,4R) présentaient un  $pH_i$  plus alcalin.

Ensuite, notre analyse par Western Blot, imagerie confocale et test de biotinylation ont démontré que l'adaptation acide diminuait l'expression totale de TRPC1 mais favorisait sa localisation au niveau de la membrane plasmique. L'expression de TRPC1 était encore plus augmentée et maintenue au niveau membranaire dans les conditions de récupération. Nous avons en outre montré que l'adaptation acide favorisait la migration des cellules PANC-1 mais réduisait la prolifération. Similaires résultats ont été trouvés dans les modèles 2D et 3D.

Pour démontrer le rôle de TRPC1 dans le microenvironnement tumoral acide, nous avons également choisi l'approche par siRNA afin d'inhiber l'expression de TRPC1. Nous avons montré que siTRPC1 inhibait la migration des cellules PANC-1 dans les conditions normales, adaptées à l'acide et de récupération. De plus, nous avons montré que l'invalidation moléculaire de TRPC1 inhibait fortement la prolifération, en 2D et en 3D, des cellules PANC-1 récupérées de l'environnement acide, par rapport au contrôle, alors que cet effet était moins évident dans des conditions adaptées à l'acide.

Notre objectif était d'étudier les mécanismes sous-jacents du microenvironnement tumoral acide et de TRPC1 dans les cellules PANC-1. Notre analyse par cytométrie en flux a révélé que l'adaptation acide entraînait une

augmentation du nombre de cellules dans la phase G0/G1 et une diminution dans la phase G2/M. Par ailleurs, les cellules récupérées à l'acide ont montré un nombre accru de cellules en phase S. L'invalidation moléculaire de TRPC1 a entraîné une nouvelle accumulation de cellules dans la phase G0/G1 et une réduction dans la phase G2/M. Ce phénotype a été maintenu dans des conditions de récupération.

Parallèlement à l'analyse du cycle cellulaire, notre analyse par Western Blot des protéines régulatrices du cycle cellulaire a révélé que le siTRPC1 réduisait l'expression de CDK6, 2 et 1 et de la cycline A tout en augmentant l'expression de p21. Notamment, l'inhibition de l'expression de TRPC1 a eu un effet plus substantiel dans des conditions récupérées que dans des conditions normales et acides.

Nous avons précédemment montré que TRPC1 forme un complexe avec PI3K et CaM. Ainsi, nous avons cherché à démontrer le rôle du microenvironnement tumoral acide et de TRPC1 en association avec la signalisation PI3K. Par imagerie confocale et analyse de colocalisation, nous avons montré que TRPC1 était colocalisé avec la sous-unité PI3K-p85 $\alpha$  dans des conditions adaptées au pH acide puis se maintenait après la récupération des cellules dans un milieu normal. Ces résultats ont été confirmés par PLA et co-IP, qui ont révélé une forte interaction entre TRPC1 et la sous-unité PI3K-p85 $\alpha$  dans les cellules PANC-1 cultivées dans un pH 6,5. TRPC1 interagit également avec la protéine CaM dans toutes les conditions de pH. Ces interactions ont été atténuées lors de l'extinction moléculaire de TRPC1.

Nous avons constaté que l'activation de ERK1/2 était profondément inhibée lorsque les cellules étaient transfectées avec siTRPC1 dans des conditions acides et récupérées, par rapport à ce que nous avons précédemment observé dans des conditions de pH normales. De plus, siTRPC1 a également diminué l'activation de AKT, en particulier dans des conditions de récupération d'acide. De plus, l'inhibition de la CaM a réduit l'activation de AKT uniquement dans les cellules récupérées de l'environnement acide, tandis que les niveaux de ERK1/2 ont été affectés dans toutes les conditions.

Les expériences d'imagerie calciques ont révélé que l'entrée basale de Ca<sup>2+</sup> était augmentée dans les cellules récupérées à l'acide par rapport aux cellules cultivées dans des conditions normales et acides. De plus, siTRPC1 n'affectait l'entrée du Ca<sup>2+</sup> que dans les cellules adaptées au pH acide et récupérées. En revanche, siTRPC1 n'a aucun effet sur l'entrée calcique capacitive (SOCE) dans les cellules PANC-1 adaptées à l'acide ou récupérées. Nous avons, par la suite, cherché à savoir si les niveaux de Ca<sup>2+</sup> extracellulaire pourrait influencer la migration et la prolifération cellulaires. Nous avons constaté que la faible concentration de Ca<sup>2+</sup> extracellulaire diminuaient la prolifération et la migration cellulaires uniquement dans des conditions adaptées et récupérées du milieu acide, mais pas lorsque les cellules sont cultivées dans un milieu de culture à pH normal. Dans ces conditions (bas calcium extracellulaire), siTRPC1 a induit une légère réduction de la migration et la prolifération cellulaires.

L'ensemble de ces données a révélé un nouvel aperçu de l'interaction entre le microenvironnement tumoral et le canal ionique TRPC1. Nous avons montré que l'acidification du pH du microenvironnement tumoral favoriserait la translocation du TRPC1 à la membrane plasmique, favorisant ainsi l'interaction avec PI3K/CaM

et l'entrée de  $\text{Ca}^{2+}$ , qui en retour, augmente la migration et la prolifération des cellules PANC-1, via les voies de signalisation AKT et ERK1/2.

#### 4. La localisation cellulaire de TRPC1 est liée au microenvironnement acide de la tumeur : étude sur les échantillons de tissus non cancéreux et cancéreux du pancréas.

L'objectif de cette étude était de déterminer si l'expression de TRPC1 est localisée dans les parties acides de la tumeur. Nous avons utilisé deux protéines dont l'expression est dépendante de l'acidification du microenvironnement des tumeurs solides : les protéines LAMP2 et NBCn1. En effet, LAMP2 est fortement exprimé dans les régions les plus acides des tumeurs cancéreuses du sein (Damaghi et al. 2015), tandis que NBCn1 est impliqué dans l'acidification du microenvironnement tumoral et est constamment exprimé dans les tissus du cancer du sein (Lee et al. 2015, Pedersen et al. 2017). Nous avons analysé le score d'intensité de marquage de ces deux marqueurs et nous avons constaté que LAMP2 et NBCn1 étaient exprimés dans les cellules tumorales ainsi que dans les cellules non tumorales adjacentes. LAMP2 était principalement localisé dans le cytoplasme, tandis que NBCn1 a été retrouvée exprimée à la fois au niveau de la membrane plasmique et au niveau du cytoplasme des cellules non tumorales et tumorales. Nous avons précédemment démontré que TRPC1 était localisé à la membrane plasmique des cellules tumorales dans le tissu d'ACP humain et que l'adaptation acide améliore cette localisation. Par conséquent, nous avons cherché à montrer si l'expression de TRPC1 à la membrane était corrélée avec l'expression de LAMP2 ou NBCn1 dans le tissu d'ACP. Durant cette partie du travail, nous avons constaté que la localisation de la membrane plasmique de TRPC1 est associée à la localisation cytoplasmique de LAMP2 dans les cellules tumorales. Nos résultats suggèrent que LAMP2 et NBCn1 sont exprimés dans les tissus non tumoraux et d'ACP, et que la localisation membranaire de TRPC1 est corrélée avec la localisation cytosolique de LAMP2.

#### 5. Le microenvironnement acide affecte la méthylation de l'ADN des canaux ioniques

Il est connu que la dérégulation de l'expression de plusieurs types de canaux ioniques dans le cancer est liée une dérégulation de la méthylation de leur ADN (Oquadid-Ahidouch et al. 2015). En ce qui concerne l'ACP, différents gènes codant pour les canaux ioniques sont associés à la méthylation de l'ADN (Brevet et al., 2009, Gregorio et al. 2020, Chatterjee et al. 2021). Les changements de pH peuvent affecter la stabilité génomique et réciproquement. Ces changements de  $\text{pH}_i$  peuvent être dus à des changements de  $\text{pH}_e$ . Pourtant, ils peuvent également être créés par la biodynamique des cellules, car de nombreuses altérations génétiques et épigénétiques exercent leur fonction en modifiant le métabolisme des cellules cancéreuses, provoquant des changements de pH (Ordway et al. 2020). Cependant, nous ne comprenons pas très bien comment l'acidification affecte directement les changements épigénétiques. La façon dont l'adaptation acide affecte les niveaux de méthylation de l'ADN des régions promotrices des canaux ioniques, et donc l'expression des gènes, n'a, à notre connaissance, jamais été étudiée auparavant. Dans cette dernière partie de mon travail de thèse,



nous avons cherché à déterminer si l'adaptation acide pourrait affecter la méthylation du promoteur des gènes codant les canaux ioniques, en particulier, ASIC1, SCN8A (codant pour la sous-unité alpha 8 du canal voltage-dépendant du sodium, NaV1.6) et TRPC1. Nous avons utilisé une approche de séquençage au bisulfite de sodium et une méthode d'analyse quantitative et semi-quantitative pour explorer les niveaux de méthylation de l'ADN des gènes codant pour les canaux ioniques dont l'expression pourrait être affectée par l'adaptation acide. Nous avons montré que l'expression de NaV1.6 était régulée négativement dans les cellules MiaPaCa-2 adaptées à l'acide et le tissu d'ACP humain, par rapport au tissu non tumoral adjacent. De plus, nous avons montré que le promoteur du gène SCN8A est hyperméthylé dans les cellules MiaPaCa-2 adaptées à l'acide par rapport aux cellules cultivées dans des conditions de pH normale. En outre, nous avons montré que les régions promotrices des gènes ASIC1 et TRPC1 ne présentait pas de modifications quant à leur méthylation lors de l'adaptation acide par rapport aux conditions de pH normales.

D'autres expériences complémentaires sont nécessaires pour valider nos résultats préliminaires et comprendre comment l'adaptation à l'acide affecte la méthylation de l'ADN et d'autres modifications épigénétiques des promoteurs de gènes de canaux ioniques.

### CONCLUSION ET PERSPECTIVES

Pour conclure, ce travail de thèse a donné un nouvel aperçu du rôle des canaux ioniques, en particulier de l'impact de TRPC1 et du microenvironnement acide dans la progression de l'ACP. Tout d'abord, nous avons élucidé le rôle de TRPC1 dans la prolifération des cellules cancéreuses pancréatiques et s'il pouvait être utilisé comme biomarqueur potentiel. Ensuite, nous avons montré que le dialogue entre les fluctuations du microenvironnement acide et TRPC1, active une cascade de signalisation qui régule la prolifération et la migration des cellules d'ACP.

Ainsi, durant ce travail de thèse, nous avons spécifiquement mis en évidence que (Figure 53):

1. L'expression de certains canaux ioniques est dérégulée dans le développement et la progression de l'ACP.
2. TRPC1 est surexprimé dans les tissus et les lignées cellulaires d'ACP humaines, et est corrélé à des facteurs cliniques agressifs et à un mauvais pronostic.
3. L'adaptation acide augmente la localisation membranaire de TRPC1, même si son expression totale est réduite.
4. Les cellules récupérées du milieu acide présentent une expression totale de TRPC1 augmentée et une localisation de TRPC1 à la membrane plasmique est maintenue.
5. TRPC1 régule la prolifération et la migration des cellules d'ACP via la voie de signalisation PI3K/CaM indépendamment du  $Ca^{2+}$  dans des conditions de pH normales, tandis qu'il régule ces

processus cellulaires via des mécanismes dépendants du  $\text{Ca}^{2+}$  lors de l'adaptation à l'acide et de la récupération du milieu acide.

6. Le complexe TRPC1/PI3K/CaM contrôle la progression des cellules dans le cycle cellulaire, la prolifération et la migration via l'activation d'AKT et ERK1/2.
7. Le promoteur du gène SCN8A a tendance à être hyperméthylé, provoquant sa régulation à la baisse dans les cellules MiaPaCa-2 adaptées à un microenvironnement acide.

Pour compléter ce travail portant sur l'interaction entre le microenvironnement tumoral acide et le canal TRPC1, nous proposons d'étudier plus en détails les différents mécanismes impliqués (Figure 53). Par exemple, il pourrait être intéressant d'étudier :

1. Si l'activation de TRPC1 est causée directement par l'acidification et/ou la récupération des cellules d'un milieu acide.
2. Le mécanisme permettant la translocation de TRPC1 vers la membrane plasmique dans différentes conditions de pH et si celle-ci dépend de la formation d'un complexe avec ORAI1 et/ou STIM1 par exemple.
3. L'effet direct de l'appauvrissement en  $\text{Ca}^{2+}$  sur l'activation de ERK1/2 et AKT.
4. Si TRPC1 est impliqué dans le processus de transition épithélio-mésenchymateuse en étudiant les marqueurs épithéliaux et les paramètres de motilité cellulaire.
5. Le rôle de TRPC1 en comparant l'agressivité, sous forme de prolifération et d'invasion cellules, entre les différentes conditions de pH et les cellules cancéreuses co-cultivées ou non avec des cellules stellaires pancréatiques.

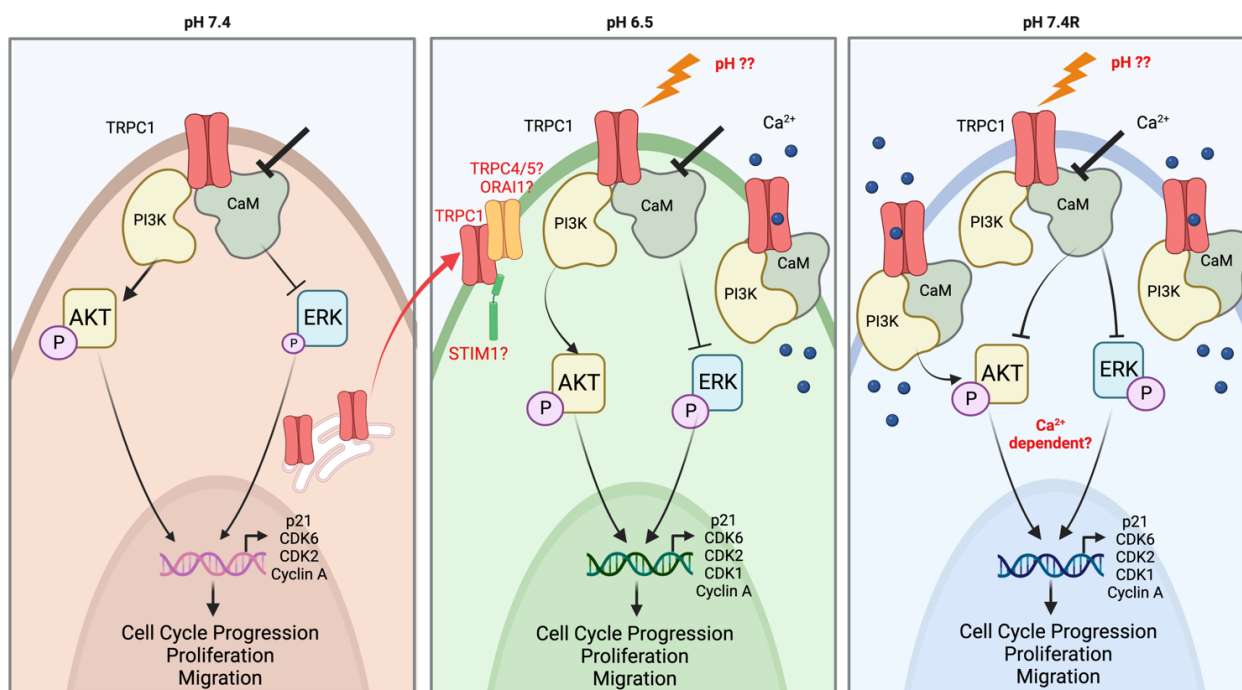


Figure 53. Représentation schématique présentant les divers mécanismes par lesquels TRPC1 module la progression de l'ACP. Les mécanismes restant à élucider sont marqués en rouge : TRPC1 est-il activé par un pH acide ? TRPC1 se transloque-t-il vers la membrane plasmique en formant un complexe avec d'autres canaux ioniques ? Les voies de signalisation activées par TRPC1 dans des conditions de récupération des cellules du milieu acide dépendent-elles du  $Ca^{2+}$  ?

## References

- Al-Hawary, M. M., I. R. Francis, S. T. Chari, *et al.* (2014). "Pancreatic ductal adenocarcinoma radiology reporting template: consensus statement of the society of abdominal radiology and the american pancreatic association." *Gastroenterology* 146(1): 291-304 e291.
- Alfonso, A., A. G. Cabado, M. R. Vieytes, *et al.* (2000). "Calcium-pH crosstalks in rat mast cells: cytosolic alkalization, but not intracellular calcium release, is a sufficient signal for degranulation." *Br J Pharmacol* 130(8): 1809-1816.
- Alfonso, S., O. Benito, S. Alicia, *et al.* (2008). "Regulation of the cellular localization and function of human transient receptor potential channel 1 by other members of the TRPC family." *Cell Calcium* 43(4): 375-387.
- Almirza, W. H., P. H. Peters, E. J. van Zoelen, *et al.* (2012). "Role of Trpc channels, Stim1 and Orai1 in PGF(2alpha)-induced calcium signaling in NRK fibroblasts." *Cell Calcium* 51(1): 12-21.
- Alvarez, J. and M. Montero (2002). "Measuring [Ca<sup>2+</sup>] in the endoplasmic reticulum with aequorin." *Cell Calcium* 32(5-6): 251-260.
- Ambudkar, I. S., L. B. de Souza and H. L. Ong (2017). "TRPC1, Orai1, and STIM1 in SOCE: Friends in tight spaces." *Cell Calcium* 63: 33-39.
- Amith, S. R., J. M. Wilkinson, S. Baksh, *et al.* (2015). "The Na<sup>(+)</sup>/H<sup>(+)</sup> exchanger (NHE1) as a novel co-adjuvant target in paclitaxel therapy of triple-negative breast cancer cells." *Oncotarget* 6(2): 1262-1275.
- Andersen, A. P., M. Flinck, E. K. Oernbo, *et al.* (2016). "Roles of acid-extruding ion transporters in regulation of breast cancer cell growth in a 3-dimensional microenvironment." *Mol Cancer* 15(1): 45.
- Andersen, A. P., J. M. Moreira and S. F. Pedersen (2014). "Interactions of ion transporters and channels with cancer cell metabolism and the tumour microenvironment." *Philos Trans R Soc Lond B Biol Sci* 369(1638): 20130098.
- Andersen, A. P., J. Samsoe-Petersen, E. K. Oernbo, *et al.* (2018). "The net acid extruders NHE1, NBCn1 and MCT4 promote mammary tumor growth through distinct but overlapping mechanisms." *Int J Cancer* 142(12): 2529-2542.
- Andersen, H. B., R. Ialchina, S. F. Pedersen, *et al.* (2021). "Metabolic reprogramming by driver mutation-tumor microenvironment interplay in pancreatic cancer: new therapeutic targets." *Cancer Metastasis Rev* 40(4): 1093-1114.
- Aneiros, E., L. Cao, M. Papakosta, *et al.* (2011). "The biophysical and molecular basis of TRPV1 proton gating." *EMBO J* 30(6): 994-1002.
- Apte, M. V., R. C. Pirola and J. S. Wilson (2012). "Pancreatic stellate cells: a starring role in normal and diseased pancreas." *Front Physiol* 3: 344.
- Aronson, P. S. (1985). "Kinetic properties of the plasma membrane Na<sup>+</sup>-H<sup>+</sup> exchanger." *Annu Rev Physiol* 47: 545-560.
- Arora, S., J. Tanwar, N. Sharma, *et al.* (2021). "Orai3 Regulates Pancreatic Cancer Metastasis by Encoding a Functional Store Operated Calcium Entry Channel." *Cancers (Basel)* 13(23).
- Asghar, M. Y., M. Magnusson, K. Kemppainen, *et al.* (2015). "Transient Receptor Potential Canonical 1 (TRPC1) Channels as Regulators of Sphingolipid and VEGF Receptor Expression: IMPLICATIONS FOR THYROID CANCER CELL MIGRATION AND PROLIFERATION." *J Biol Chem* 290(26): 16116-16131.
- Ashley, S. W., M. Schwarz, C. Alvarez, *et al.* (1994). "Pancreatic interstitial pH regulation: effects of secretory stimulation." *Surgery* 115(4): 503-509.
- Audero, M. M., N. Prevarskaya and A. Fiorio Pla (2022). "Ca<sup>(2+)</sup> Signalling and Hypoxia/Acidic Tumour Microenvironment Interplay in Tumour Progression." *Int J Mol Sci* 23(13).
- Azimi, I., M. J. G. Milevskiy, E. Kaemmerer, *et al.* (2017). "TRPC1 is a differential regulator of hypoxia-mediated events and Akt signalling in PTEN-deficient breast cancer cells." *J Cell Sci* 130(14): 2292-2305.
- Bachem, M. G., E. Schneider, H. Gross, *et al.* (1998). "Identification, culture, and characterization of pancreatic stellate cells in rats and humans." *Gastroenterology* 115(2): 421-432.

- Bai, C. X., A. Giamarchi, L. Rodat-Despoix, *et al.* (2008). "Formation of a new receptor-operated channel by heteromeric assembly of TRPP2 and TRPC1 subunits." *EMBO Rep* 9(5): 472-479.
- Bailey, P., D. K. Chang, K. Nones, *et al.* (2016). "Genomic analyses identify molecular subtypes of pancreatic cancer." *Nature* 531(7592): 47-52.
- Bararia, A., S. Dey, S. Gulati, *et al.* (2020). "Differential methylation landscape of pancreatic ductal adenocarcinoma and its precancerous lesions." *Hepatobiliary Pancreat Dis Int* 19(3): 205-217.
- Bardeesy, N. and R. A. DePinho (2002). "Pancreatic cancer biology and genetics." *Nat Rev Cancer* 2(12): 897-909.
- Barrera, N. P., Y. Shaifita, I. McFadzean, *et al.* (2007). "AFM imaging reveals the tetrameric structure of the TRPC1 channel." *Biochem Biophys Res Commun* 358(4): 1086-1090.
- Beck, A., A. Fleig, R. Penner, *et al.* (2014). "Regulation of endogenous and heterologous Ca(2+)(+) release-activated Ca(2+)(+) currents by pH." *Cell Calcium* 56(3): 235-243.
- Bendell, J. C., G. A. Manji, S. Pant, *et al.* (2020). "A phase I study to evaluate the safety and tolerability of AB680 combination therapy in participants with gastrointestinal malignancies." *Journal of Clinical Oncology* 38(4\_suppl): TPS788-TPS788.
- Benos, D. J. and B. A. Stanton (1999). "Functional domains within the degenerin/epithelial sodium channel (Deg/ENaC) superfamily of ion channels." *J Physiol* 520 Pt 3: 631-644.
- Berdiev, B. K., J. Xia, L. A. McLean, *et al.* (2003). "Acid-sensing ion channels in malignant gliomas." *J Biol Chem* 278(17): 15023-15034.
- Berra-Romani, R., P. Faris, S. Negri, *et al.* (2019). "Arachidonic Acid Evokes an Increase in Intracellular Ca(2+) Concentration and Nitric Oxide Production in Endothelial Cells from Human Brain Microcirculation." *Cells* 8(7).
- Berridge, M. J., M. D. Bootman and H. L. Roderick (2003). "Calcium signalling: dynamics, homeostasis and remodelling." *Nat Rev Mol Cell Biol* 4(7): 517-529.
- Berridge, M. J., P. Lipp and M. D. Bootman (2000). "The versatility and universality of calcium signalling." *Nat Rev Mol Cell Biol* 1(1): 11-21.
- Bertoli, C., J. M. Skotheim and R. A. de Bruin (2013). "Control of cell cycle transcription during G1 and S phases." *Nat Rev Mol Cell Biol* 14(8): 518-528.
- Besson, P., V. Driffort, E. Bon, *et al.* (2015). "How do voltage-gated sodium channels enhance migration and invasiveness in cancer cells?" *Biochim Biophys Acta* 1848(10 Pt B): 2493-2501.
- Bestor, T. H. (2000). "The DNA methyltransferases of mammals." *Hum Mol Genet* 9(16): 2395-2402.
- Bettaieb, L., M. Brule, A. Chomy, *et al.* (2021). "Ca(2+) Signaling and Its Potential Targeting in Pancreatic Ductal Carcinoma." *Cancers (Basel)* 13(12).
- Binggeli, R. and R. C. Weinstein (1986). "Membrane potentials and sodium channels: hypotheses for growth regulation and cancer formation based on changes in sodium channels and gap junctions." *J Theor Biol* 123(4): 377-401.
- Bird, A. (2007). "Perceptions of epigenetics." *Nature* 447(7143): 396-398.
- Bird, A. P. (1986). "CpG-rich islands and the function of DNA methylation." *Nature* 321(6067): 209-213.
- Blaszczak, W. and P. Swietach (2021). "What do cellular responses to acidity tell us about cancer?" *Cancer Metastasis Rev* 40(4): 1159-1176.
- Boedtkjer, E., J. F. Bentzon, V. S. Dam, *et al.* (2016). "Na<sup>+</sup>, HCO<sub>3</sub><sup>-</sup>-cotransporter NBCn1 increases pH<sub>i</sub> gradients, filopodia, and migration of smooth muscle cells and promotes arterial remodelling." *Cardiovasc Res* 111(3): 227-239.
- Boedtkjer, E., L. Bunch and S. F. Pedersen (2012). "Physiology, pharmacology and pathophysiology of the pH regulatory transport proteins NHE1 and NBCn1: similarities, differences, and implications for cancer therapy." *Curr Pharm Des* 18(10): 1345-1371.
- Boedtkjer, E., J. M. Moreira, M. Mele, *et al.* (2013). "Contribution of Na<sup>+</sup>,HCO<sub>3</sub><sup>-</sup>-cotransport to cellular pH control in human breast cancer: a role for the breast cancer susceptibility locus NBCn1 (SLC4A7)." *Int J Cancer* 132(6): 1288-1299.
- Boedtkjer, E. and S. F. Pedersen (2020). "The Acidic Tumor Microenvironment as a Driver of Cancer." *Annu Rev Physiol* 82:21.1-21.24.

- Bollimuntha, S., E. Cornatzer and B. B. Singh (2005). "Plasma membrane localization and function of TRPC1 is dependent on its interaction with beta-tubulin in retinal epithelium cells." *Vis Neurosci* 22(2): 163-170.
- Bollimuntha, S., B. B. Singh, S. Shavali, *et al.* (2005). "TRPC1-mediated inhibition of 1-methyl-4-phenylpyridinium ion neurotoxicity in human SH-SY5Y neuroblastoma cells." *J Biol Chem* 280(3): 2132-2140.
- Bomben, V. C. and H. Sontheimer (2010). "Disruption of transient receptor potential canonical channel 1 causes incomplete cytokinesis and slows the growth of human malignant gliomas." *Glia* 58(10): 1145-1156.
- Bomben, V. C., K. L. Turner, T. T. Barclay, *et al.* (2011). "Transient receptor potential canonical channels are essential for chemotactic migration of human malignant gliomas." *J Cell Physiol* 226(7): 1879-1888.
- Bondar, V. M., B. Sweeney-Gotsch, M. Andreeff, *et al.* (2002). "Inhibition of the phosphatidylinositol 3'-kinase-AKT pathway induces apoptosis in pancreatic carcinoma cells in vitro and in vivo." *Mol Cancer Ther* 1(12): 989-997.
- Borowiec, A. S., G. Bidaux, N. Pigat, *et al.* (2014). "Calcium channels, external calcium concentration and cell proliferation." *Eur J Pharmacol* 739: 19-25.
- Bouron, A., K. Kiselyov and J. Oberwinkler (2015). "Permeation, regulation and control of expression of TRP channels by trace metal ions." *Pflugers Arch* 467(6): 1143-1164.
- Boynton, A. L., J. F. Whitfield and R. J. Isaacs (1976). "The different roles of serum and calcium in the control of proliferation of BALB/c 3T3 mouse cells." *In Vitro* 12(2): 120-123.
- Boynton, A. L., J. F. Whitfield, R. J. Isaacs, *et al.* (1977). "The control of human WI-38 cell proliferation by extracellular calcium and its elimination by SV-40 virus-induced proliferative transformation." *J Cell Physiol* 92(2): 241-247.
- Bravo-Cordero, J. J., L. Hodgson and J. Condeelis (2012). "Directed cell invasion and migration during metastasis." *Curr Opin Cell Biol* 24(2): 277-283.
- Brevet, M., D. Fucks, D. Chatelain, *et al.* (2009). "Deregulation of 2 potassium channels in pancreas adenocarcinomas: implication of KV1.3 gene promoter methylation." *Pancreas* 38(6): 649-654.
- Brini, M. and E. Carafoli (2011). "The plasma membrane Ca(2)+ ATPase and the plasma membrane sodium calcium exchanger cooperate in the regulation of cell calcium." *Cold Spring Harb Perspect Biol* 3(2).
- Brisson, L., V. Driffort, L. Benoist, *et al.* (2013). "NaV1.5 Na(+) channels allosterically regulate the NHE-1 exchanger and promote the activity of breast cancer cell invadopodia." *J Cell Sci* 126(Pt 21): 4835-4842.
- Brisson, L., L. Gillet, S. Calaghan, *et al.* (2011). "Na(V)1.5 enhances breast cancer cell invasiveness by increasing NHE1-dependent H(+) efflux in caveolae." *Oncogene* 30(17): 2070-2076.
- Brundage, R. A., K. E. Fogarty, R. A. Tuft, *et al.* (1991). "Calcium gradients underlying polarization and chemotaxis of eosinophils." *Science* 254(5032): 703-706.
- Brundage, R. A., K. E. Fogarty, R. A. Tuft, *et al.* (1993). "Chemotaxis of newt eosinophils: calcium regulation of chemotactic response." *Am J Physiol* 265(6 Pt 1): C1527-1543.
- Busco, G., R. A. Cardone, M. R. Greco, *et al.* (2010). "NHE1 promotes invadopodial ECM proteolysis through acidification of the peri-invadopodial space." *FASEB J* 24(10): 3903-3915.
- Cahalan, M. D. (2009). "STIMulating store-operated Ca(2+) entry." *Nat Cell Biol* 11(6): 669-677.
- Cairns, S. P., H. Westerblad and D. G. Allen (1993). "Changes in myoplasmic pH and calcium concentration during exposure to lactate in isolated rat ventricular myocytes." *J Physiol* 464: 561-574.
- Cameron, I. L., N. K. Smith, T. B. Pool, *et al.* (1980). "Intracellular concentration of sodium and other elements as related to mitogenesis and oncogenesis in vivo." *Cancer Res* 40(5): 1493-1500.
- Canales Coutino, B. and R. Mayor (2021). "Mechanosensitive ion channels in cell migration." *Cells Dev* 166: 203683.
- Capiod, T. (2013). "The need for calcium channels in cell proliferation." *Recent Pat Anticancer Drug Discov* 8(1): 4-17.
- Cardone, R. A., V. Casavola and S. J. Reshkin (2005). "The role of disturbed pH dynamics and the Na+/H+ exchanger in metastasis." *Nat Rev Cancer* 5(10): 786-795.



- Cardone, R. A., M. R. Greco, K. Zeeberg, *et al.* (2015). "A novel NHE1-centered signaling cassette drives epidermal growth factor receptor-dependent pancreatic tumor metastasis and is a target for combination therapy." *Neoplasia* 17(2): 155-166.
- Carrithers, M. D., G. Chatterjee, L. M. Carrithers, *et al.* (2009). "Regulation of podosome formation in macrophages by a splice variant of the sodium channel SCN8A." *J Biol Chem* 284(12): 8114-8126.
- Case, R. M., D. Eisner, A. Gurney, *et al.* (2007). "Evolution of calcium homeostasis: from birth of the first cell to an omnipresent signalling system." *Cell Calcium* 42(4-5): 345-350.
- Casey, J. R., S. Grinstein and J. Orlowski (2010). "Sensors and regulators of intracellular pH." *Nat Rev Mol Cell Biol* 11(1): 50-61.
- Catterall, W. A. (2000). "From ionic currents to molecular mechanisms: the structure and function of voltage-gated sodium channels." *Neuron* 26(1): 13-25.
- Catterall, W. A. (2011). "Voltage-gated calcium channels." *Cold Spring Harb Perspect Biol* 3(8): a003947.
- Cazacu, I. M., N. Farkas, A. Garami, *et al.* (2018). "Pancreatitis-Associated Genes and Pancreatic Cancer Risk: A Systematic Review and Meta-analysis." *Pancreas* 47(9): 1078-1086.
- Chang, M. C., J. M. Wong and Y. T. Chang (2014). "Screening and early detection of pancreatic cancer in high risk population." *World J Gastroenterol* 20(9): 2358-2364.
- Chang, Q., I. Jurisica, T. Do, *et al.* (2011). "Hypoxia predicts aggressive growth and spontaneous metastasis formation from orthotopically grown primary xenografts of human pancreatic cancer." *Cancer Res* 71(8): 3110-3120.
- Chao, M., H. Wu, K. Jin, *et al.* (2016). "A nonrandomized cohort and a randomized study of local control of large hepatocarcinoma by targeting intratumoral lactic acidosis." *Elife* 5.
- Chatterjee, A., A. Bararia, D. Ganguly, *et al.* (2021). "Altered DNA methylation in ion transport and immune signalling genes is associated with severity in Pancreatic Ductal Adenocarcinoma." *bioRxiv*: 2021.2006.2014.448193.
- Chen, C., J. D. Vincent and I. J. Clarke (1994). "Ion channels and the signal transduction pathways in the regulation of growth hormone secretion." *Trends Endocrinol Metab* 5(6): 227-233.
- Chen, K. H., P. Y. Tung, J. C. Wu, *et al.* (2008). "An acidic extracellular pH induces Src kinase-dependent loss of beta-catenin from the adherens junction." *Cancer Lett* 267(1): 37-48.
- Chen, L., G. Shan, M. Ge, *et al.* (2022). "Transient Receptor Potential Channel 1 Potentially Serves as a Biomarker Indicating T/TNM Stages and Predicting Long-Term Prognosis in Patients With Renal Cell Carcinoma." *Front Surg* 9: 853310.
- Chen, W. H., C. R. Chen, K. T. Yang, *et al.* (2001). "Arachidonic acid-induced H<sup>+</sup> and Ca<sup>2+</sup> increases in both the cytoplasm and nucleoplasm of rat cerebellar granule cells." *J Physiol* 537(Pt 2): 497-510.
- Chen, W. T., C. C. Lee, L. Goldstein, *et al.* (1994). "Membrane proteases as potential diagnostic and therapeutic targets for breast malignancy." *Breast Cancer Res Treat* 31(2-3): 217-226.
- Chen, X. S., L. Y. Li, Y. D. Guan, *et al.* (2016). "Anticancer strategies based on the metabolic profile of tumor cells: therapeutic targeting of the Warburg effect." *Acta Pharmacol Sin* 37(8): 1013-1019.
- Chen, Y. F., P. C. Lin, Y. M. Yeh, *et al.* (2019). "Store-Operated Ca(2+) Entry in Tumor Progression: From Molecular Mechanisms to Clinical Implications." *Cancers (Basel)* 11(7): :899.
- Cheng, K. T., X. Liu, H. L. Ong, *et al.* (2008). "Functional requirement for Orai1 in store-operated TRPC1-STIM1 channels." *J Biol Chem* 283(19): 12935-12940.
- Cheng, K. T., X. Liu, H. L. Ong, *et al.* (2011). "Local Ca(2)<sup>+</sup> entry via Orai1 regulates plasma membrane recruitment of TRPC1 and controls cytosolic Ca(2)<sup>+</sup> signals required for specific cell functions." *PLoS Biol* 9(3): e1001025.
- Cheng, Y. R., B. Y. Jiang and C. C. Chen (2018). "Acid-sensing ion channels: dual function proteins for chemo-sensing and mechano-sensing." *J Biomed Sci* 25(1): 46.
- Chin, D. and A. R. Means (2000). "Calmodulin: a prototypical calcium sensor." *Trends Cell Biol* 10(8): 322-328.
- Chow, J. Y., H. Dong, K. T. Quach, *et al.* (2008). "TGF-beta mediates PTEN suppression and cell motility through calcium-dependent PKC-alpha activation in pancreatic cancer cells." *Am J Physiol Gastrointest Liver Physiol* 294(4): G899-905.

- Chowdhury, M. A., A. A. Peters, S. J. Roberts-Thomson, *et al.* (2013). "Effects of differentiation on purinergic and neurotensin-mediated calcium signaling in human HT-29 colon cancer cells." *Biochem Biophys Res Commun* 439(1): 35-39.
- Chung, H. K., N. Rathor, S. R. Wang, *et al.* (2015). "RhoA enhances store-operated Ca<sup>2+</sup> entry and intestinal epithelial restitution by interacting with TRPC1 after wounding." *Am J Physiol Gastrointest Liver Physiol* 309(9): G759-767.
- Collisson, E. A., A. Sadanandam, P. Olson, *et al.* (2011). "Subtypes of pancreatic ductal adenocarcinoma and their differing responses to therapy." *Nat Med* 17(4): 500-503.
- Conroy, T., P. Hammel, M. Hebbar, *et al.* (2018). "FOLFIRINOX or Gemcitabine as Adjuvant Therapy for Pancreatic Cancer." *N Engl J Med* 379(25): 2395-2406.
- Cooper, D. S., H. S. Yang, P. He, *et al.* (2009). "Sodium/bicarbonate cotransporter NBCn1/slc4a7 increases cytotoxicity in magnesium depletion in primary cultures of hippocampal neurons." *Eur J Neurosci* 29(3): 437-446.
- Coradini, D., C. Casarsa and S. Oriana (2011). "Epithelial cell polarity and tumorigenesis: new perspectives for cancer detection and treatment." *Acta Pharmacol Sin* 32(5): 552-564.
- Corbet, C. and O. Feron (2017). "Tumour acidosis: from the passenger to the driver's seat." *Nat Rev Cancer* 17(10): 577-593.
- Corbet, C., A. Pinto, R. Martherus, *et al.* (2016). "Acidosis Drives the Reprogramming of Fatty Acid Metabolism in Cancer Cells through Changes in Mitochondrial and Histone Acetylation." *Cell Metab* 24(2): 311-323.
- Cosens, D. J. and A. Manning (1969). "Abnormal electroretinogram from a *Drosophila* mutant." *Nature* 224(5216): 285-287.
- Counillon, L., Y. Bouret, I. Marchiq, *et al.* (2016). "Na<sup>(+)</sup>/H<sup>(+)</sup> antiporter (NHE1) and lactate/H<sup>(+)</sup> symporters (MCTs) in pH homeostasis and cancer metabolism." *Biochim Biophys Acta* 1863(10): 2465-2480.
- Coupaye-Gerard, B., C. Bookstein, P. Duncan, *et al.* (1996). "Biosynthesis and cell surface delivery of the NHE1 isoform of Na<sup>+</sup>/H<sup>+</sup> exchanger in A6 cells." *Am J Physiol* 271(5 Pt 1): C1639-1645.
- Cucu, D., G. Chiritoiu, S. Petrescu, *et al.* (2014). "Characterization of functional transient receptor potential melastatin 8 channels in human pancreatic ductal adenocarcinoma cells." *Pancreas* 43(5): 795-800.
- Daemen, A., D. Peterson, N. Sahu, *et al.* (2015). "Metabolite profiling stratifies pancreatic ductal adenocarcinomas into subtypes with distinct sensitivities to metabolic inhibitors." *Proc Natl Acad Sci U S A* 112(32): E4410-4417.
- Damaghi, M., N. K. Tafreshi, M. C. Lloyd, *et al.* (2015). "Chronic acidosis in the tumour microenvironment selects for overexpression of LAMP2 in the plasma membrane." *Nat Commun* 6: 8752.
- Damaghi, M., J. W. Wojtkowiak and R. J. Gillies (2013). "pH sensing and regulation in cancer." *Front Physiol* 4: 370.
- Daugirdas, J. T., J. Arrieta, M. Ye, *et al.* (1995). "Intracellular acidification associated with changes in free cytosolic calcium. Evidence for Ca<sup>2+</sup>/H<sup>+</sup> exchange via a plasma membrane Ca<sup>(2+)</sup>-ATPase in vascular smooth muscle cells." *J Clin Invest* 95(4): 1480-1489.
- Davis, F. M., A. A. Peters, D. M. Grice, *et al.* (2012). "Non-stimulated, agonist-stimulated and store-operated Ca<sup>2+</sup> influx in MDA-MB-468 breast cancer cells and the effect of EGF-induced EMT on calcium entry." *PLoS One* 7(5): e36923.
- de Bem Prunes, B., J. S. Nunes, V. P. da Silva, *et al.* (2022). "The role of tumor acidification in aggressiveness, cell dissemination and treatment resistance of oral squamous cell carcinoma." *Life Sci* 288: 120163.
- de la Roche, J., M. J. Eberhardt, A. B. Klinger, *et al.* (2013). "The molecular basis for species-specific activation of human TRPA1 protein by protons involves poorly conserved residues within transmembrane domains 5 and 6." *J Biol Chem* 288(28): 20280-20292.
- de Lera Ruiz, M. and R. L. Kraus (2015). "Voltage-Gated Sodium Channels: Structure, Function, Pharmacology, and Clinical Indications." *J Med Chem* 58(18): 7093-7118.
- Deer, E. L., J. Gonzalez-Hernandez, J. D. Coursen, *et al.* (2010). "Phenotype and genotype of pancreatic cancer cell lines." *Pancreas* 39(4): 425-435.
- DeHaven, W. I., B. F. Jones, J. G. Petranka, *et al.* (2009). "TRPC channels function independently of STIM1 and Orail." *J Physiol* 587(Pt 10): 2275-2298.

- Deng, H., J. Shi, M. Wilkerson, *et al.* (2008). "Usefulness of S100P in diagnosis of adenocarcinoma of pancreas on fine-needle aspiration biopsy specimens." *Am J Clin Pathol* 129(1): 81-88.
- Derynck, R. and Y. E. Zhang (2003). "Smad-dependent and Smad-independent pathways in TGF-beta family signalling." *Nature* 425(6958): 577-584.
- DeWitt, J., B. Devereaux, M. Chriswell, *et al.* (2004). "Comparison of endoscopic ultrasonography and multidetector computed tomography for detecting and staging pancreatic cancer." *Ann Intern Med* 141(10): 753-763.
- Dhennin-Duthille, I., M. Gautier, M. Faouzi, *et al.* (2011). "High expression of transient receptor potential channels in human breast cancer epithelial cells and tissues: correlation with pathological parameters." *Cell Physiol Biochem* 28(5): 813-822.
- Dierge, E., E. Debock, C. Guilbaud, *et al.* (2021). "Peroxidation of n-3 and n-6 polyunsaturated fatty acids in the acidic tumor environment leads to ferroptosis-mediated anticancer effects." *Cell Metab* 33(8): 1701-1715 e1705.
- Dietrich, A., M. Fahlbusch and T. Gudermann (2014). "Classical Transient Receptor Potential 1 (TRPC1): Channel or Channel Regulator?" *Cells* 3(4): 939-962.
- Dietrich, A., H. Kalwa, U. Storch, *et al.* (2007). "Pressure-induced and store-operated cation influx in vascular smooth muscle cells is independent of TRPC1." *Pflugers Arch* 455(3): 465-477.
- Dong, H., K. N. Shim, J. M. Li, *et al.* (2010). "Molecular mechanisms underlying Ca<sup>2+</sup>-mediated motility of human pancreatic duct cells." *Am J Physiol Cell Physiol* 299(6): C1493-1503.
- Donoso, P., M. Beltran and C. Hidalgo (1996). "Luminal pH regulated calcium release kinetics in sarcoplasmic reticulum vesicles." *Biochemistry* 35(41): 13419-13425.
- Du, J., J. Xie and L. Yue (2009). "Modulation of TRPM2 by acidic pH and the underlying mechanisms for pH sensitivity." *J Gen Physiol* 134(6): 471-488.
- Dubois, C., K. Kondratska, A. Kondratskyi, *et al.* (2021). "ORAI3 silencing alters cell proliferation and promotes mitotic catastrophe and apoptosis in pancreatic adenocarcinoma." *Biochim Biophys Acta Mol Cell Res* 1868(7): 119023.
- Easwaran, H., H. C. Tsai and S. B. Baylin (2014). "Cancer epigenetics: tumor heterogeneity, plasticity of stem-like states, and drug resistance." *Mol Cell* 54(5): 716-727.
- Edling, C. E., F. Selvaggi, R. Buus, *et al.* (2010). "Key role of phosphoinositide 3-kinase class IB in pancreatic cancer." *Clin Cancer Res* 16(20): 4928-4937.
- Egger, G., G. Liang, A. Aparicio, *et al.* (2004). "Epigenetics in human disease and prospects for epigenetic therapy." *Nature* 429(6990): 457-463.
- Eijkelkamp, N., K. Quick and J. N. Wood (2013). "Transient receptor potential channels and mechanosensation." *Annu Rev Neurosci* 36: 519-546.
- El Boustany, C., G. Bidaux, A. Enfissi, *et al.* (2008). "Capacitative calcium entry and transient receptor potential canonical 6 expression control human hepatoma cell proliferation." *Hepatology* 47(6): 2068-2077.
- El Boustany, C., M. Katsogiannou, P. Delcourt, *et al.* (2010). "Differential roles of STIM1, STIM2 and Orai1 in the control of cell proliferation and SOCE amplitude in HEK293 cells." *Cell Calcium* 47(4): 350-359.
- El Hiani, Y., A. Ahidouch, V. Lehen'kyi, *et al.* (2009). "Extracellular signal-regulated kinases 1 and 2 and TRPC1 channels are required for calcium-sensing receptor-stimulated MCF-7 breast cancer cell proliferation." *Cell Physiol Biochem* 23(4-6): 335-346.
- El Hiani, Y., A. Ahidouch, M. Roudbaraki, *et al.* (2006). "Calcium-sensing receptor stimulation induces nonselective cation channel activation in breast cancer cells." *J Membr Biol* 211(2): 127-137.
- El Hiani, Y., V. Lehen'kyi, H. Ouadid-Ahidouch, *et al.* (2009). "Activation of the calcium-sensing receptor by high calcium induced breast cancer cell proliferation and TRPC1 cation channel over-expression potentially through EGFR pathways." *Arch Biochem Biophys* 486(1): 58-63.
- Elingaard-Larsen, L. O., M. G. Rolver, E. E. Sorensen, *et al.* (2022). "How Reciprocal Interactions Between the Tumor Microenvironment and Ion Transport Proteins Drive Cancer Progression." *Rev Physiol Biochem Pharmacol* 182: 1-38.

- Ellingsen, C., S. Walenta, T. Hompland, *et al.* (2013). "The Microenvironment of Cervical Carcinoma Xenografts: Associations with Lymph Node Metastasis and Its Assessment by DCE-MRI." *Transl Oncol* 6(5): 607-617.
- Elzamzamy, O. M., R. Penner and L. A. Hazlehurst (2020). "The Role of TRPC1 in Modulating Cancer Progression." *Cells* 9(2).
- Estrella, V., T. Chen, M. Lloyd, *et al.* (2013). "Acidity generated by the tumor microenvironment drives local invasion." *Cancer Res* 73(5): 1524-1535.
- Evans, J. H. and J. J. Falke (2007). "Ca<sup>2+</sup> influx is an essential component of the positive-feedback loop that maintains leading-edge structure and activity in macrophages." *Proc Natl Acad Sci U S A* 104(41): 16176-16181.
- Ezzat, N. E., N. S. Tahoun and Y. M. Ismail (2016). "The role of S100P and IMP3 in the cytologic diagnosis of pancreatic adenocarcinoma." *J Egypt Natl Canc Inst* 28(4): 229-234.
- Faouzi, M., F. Hague, D. Geerts, *et al.* (2016). "Functional cooperation between KCa3.1 and TRPC1 channels in human breast cancer: Role in cell proliferation and patient prognosis." *Oncotarget* 7(24): 36419-36435.
- Fares, J., M. Y. Fares, H. H. Khachfe, *et al.* (2020). "Molecular principles of metastasis: a hallmark of cancer revisited." *Signal Transduct Target Ther* 5(1): 28.
- Feig, C., A. Gopinathan, A. Neesse, *et al.* (2012). "The pancreas cancer microenvironment." *Clin Cancer Res* 18(16): 4266-4276.
- Felmlee, M. A., R. S. Jones, V. Rodriguez-Cruz, *et al.* (2020). "Monocarboxylate Transporters (SLC16): Function, Regulation, and Role in Health and Disease." *Pharmacol Rev* 72(2): 466-485.
- Fels, B., N. Nielsen and A. Schwab (2016). "Role of TRPC1 channels in pressure-mediated activation of murine pancreatic stellate cells." *Eur Biophys J* 45(7): 657-670.
- Ferlay, J., C. Partensky and F. Bray (2016). "More deaths from pancreatic cancer than breast cancer in the EU by 2017." *Acta Oncol* 55(9-10): 1158-1160.
- Feske, S., Y. Gwack, M. Prakriya, *et al.* (2006). "A mutation in Orai1 causes immune deficiency by abrogating CRAC channel function." *Nature* 441(7090): 179-185.
- Fiorio Pla, A., D. Maric, S. C. Brazer, *et al.* (2005). "Canonical transient receptor potential 1 plays a role in basic fibroblast growth factor (bFGF)/FGF receptor-1-induced Ca<sup>2+</sup> entry and embryonic rat neural stem cell proliferation." *J Neurosci* 25(10): 2687-2701.
- Flinck M, Kramer SH, Schnipper J, *et al.* (2018). "The acid-base transport proteins NHE1 and NBCn1 regulate cell cycle progression in human breast cancer cells." *Cell Cycle* In press.
- Flinck, M., S. H. Kramer and S. F. Pedersen (2018). "Roles of pH in control of cell proliferation." *Acta Physiol (Oxf)*: e13068.
- Flinck, M., S. H. Kramer, J. Schnipper, *et al.* (2018). "The acid-base transport proteins NHE1 and NBCn1 regulate cell cycle progression in human breast cancer cells." *Cell Cycle*: 1-12.
- Formigli, L., C. Sassoli, R. Squecco, *et al.* (2009). "Regulation of transient receptor potential canonical channel 1 (TRPC1) by sphingosine 1-phosphate in C2C12 myoblasts and its relevance for a role of mechanotransduction in skeletal muscle differentiation." *J Cell Sci* 122(Pt 9): 1322-1333.
- Fukumura, D., L. Xu, Y. Chen, *et al.* (2001). "Hypoxia and acidosis independently up-regulate vascular endothelial growth factor transcription in brain tumors in vivo." *Cancer Res* 61(16): 6020-6024.
- Fukushima, N., N. Sato, T. Ueki, *et al.* (2002). "Aberrant methylation of preproenkephalin and p16 genes in pancreatic intraepithelial neoplasia and pancreatic ductal adenocarcinoma." *Am J Pathol* 160(5): 1573-1581.
- Gao, H. L., W. Q. Wang, X. J. Yu, *et al.* (2020). "Molecular drivers and cells of origin in pancreatic ductal adenocarcinoma and pancreatic neuroendocrine carcinoma." *Exp Hematol Oncol* 9: 28.
- Garrison, S. R., A. Dietrich and C. L. Stucky (2012). "TRPC1 contributes to light-touch sensation and mechanical responses in low-threshold cutaneous sensory neurons." *J Neurophysiol* 107(3): 913-922.
- Garty, H. and L. G. Palmer (1997). "Epithelial sodium channels: function, structure, and regulation." *Physiol Rev* 77(2): 359-396.
- Gatenby, R. A. and R. J. Gillies (2004). "Why do cancers have high aerobic glycolysis?" *Nat Rev Cancer* 4(11): 891-899.

- Gautier, M., I. Dhennin-Duthille, A. S. Ay, *et al.* (2014). "New insights into pharmacological tools to TR(i)P cancer up." *Br J Pharmacol* 171(10): 2582-2592.
- Ge, P., L. Wei, M. Zhang, *et al.* (2018). "TRPC1/3/6 inhibition attenuates the TGF-beta1-induced epithelial-mesenchymal transition in gastric cancer via the Ras/Raf1/ERK signaling pathway." *Cell Biol Int* 42(8): 975-984.
- Gerweck, L. E., S. Vijayappa and S. Kozin (2006). "Tumor pH controls the in vivo efficacy of weak acid and base chemotherapeutics." *Mol Cancer Ther* 5(5): 1275-1279.
- Ghiorzo, P. (2014). "Genetic predisposition to pancreatic cancer." *World J Gastroenterol* 20(31): 10778-10789.
- Gillet, L., S. Roger, P. Besson, *et al.* (2009). "Voltage-gated Sodium Channel Activity Promotes Cysteine Cathepsin-dependent Invasiveness and Colony Growth of Human Cancer Cells." *J Biol Chem* 284(13): 8680-8691.
- Gonzalez, A., F. Pfeiffer, A. Schmid, *et al.* (1998). "Effect of intracellular pH on acetylcholine-induced Ca<sup>2+</sup> waves in mouse pancreatic acinar cells." *Am J Physiol* 275(3): C810-817.
- Gopalakrishnan, S., B. O. Van Emburgh and K. D. Robertson (2008). "DNA methylation in development and human disease." *Mutat Res* 647(1-2): 30-38.
- Gorbatenko, A., C. W. Olesen, E. Boedtkjer, *et al.* (2014). "Regulation and roles of bicarbonate transporters in cancer." *Front Physiol* 5: 130.
- Gouaux, E. and R. Mackinnon (2005). "Principles of selective ion transport in channels and pumps." *Science* 310(5753): 1461-1465.
- Grabmayr, H., C. Romanin and M. Fahrner (2020). "STIM Proteins: An Ever-Expanding Family." *Int J Mol Sci* 22(1).
- Grant, T. J., K. Hua and A. Singh (2016). "Molecular Pathogenesis of Pancreatic Cancer." *Prog Mol Biol Transl Sci* 144: 241-275.
- Grau, A. M., L. Zhang, W. Wang, *et al.* (1997). "Induction of p21waf1 expression and growth inhibition by transforming growth factor beta involve the tumor suppressor gene DPC4 in human pancreatic adenocarcinoma cells." *Cancer Res* 57(18): 3929-3934.
- Greaves, M. and C. C. Maley (2012). "Clonal evolution in cancer." *Nature* 481(7381): 306-313.
- Gregorio, C., S. C. Soares-Lima, B. Alemar, *et al.* (2020). "Calcium Signaling Alterations Caused by Epigenetic Mechanisms in Pancreatic Cancer: From Early Markers to Prognostic Impact." *Cancers (Basel)* 12(7).
- Gress, D., S. Edge, F. Greene, *et al.* (2017). Principles of Cancer Staging: 3-30.
- Grutzmann, R., M. Foerder, I. Alldinger, *et al.* (2003). "Gene expression profiles of microdissected pancreatic ductal adenocarcinoma." *Virchows Arch* 443(4): 508-517.
- Gueguinou, M., T. Harnois, D. Crottes, *et al.* (2016). "SK3/TRPC1/Orai1 complex regulates SOCE-dependent colon cancer cell migration: a novel opportunity to modulate anti-EGFR mAb action by the alkyl-lipid Ohmlin." *Oncotarget* 7(24): 36168-36184.
- Guse, A. H., E. Roth and F. Emmrich (1994). "Ca<sup>2+</sup> release and Ca<sup>2+</sup> entry induced by rapid cytosolic alkalization in Jurkat T-lymphocytes." *Biochem J* 301 ( Pt 1): 83-88.
- Habtezion, A., A. S. Gukovskaya and S. J. Pandol (2019). "Acute Pancreatitis: A Multifaceted Set of Organelle and Cellular Interactions." *Gastroenterology* 156(7): 1941-1950.
- Haeberle, L. and I. Esposito (2019). "Pathology of pancreatic cancer." *Transl Gastroenterol Hepatol* 4: 50.
- Hagelund, S. and A. Trauzold (2022). "Impact of Extracellular pH on Apoptotic and Non-Apoptotic TRAIL-Induced Signaling in Pancreatic Ductal Adenocarcinoma Cells." *Front Cell Dev Biol* 10: 768579.
- Halestrap, A. P. and M. C. Wilson (2012). "The monocarboxylate transporter family--role and regulation." *IUBMB Life* 64(2): 109-119.
- Halling, D. B., B. J. Liebeskind, A. W. Hall, *et al.* (2016). "Conserved properties of individual Ca<sup>2+</sup>-binding sites in calmodulin." *Proc Natl Acad Sci U S A* 113(9): E1216-1225.
- Hanahan, D. (2022). "Hallmarks of Cancer: New Dimensions." *Cancer Discov* 12(1): 31-46.
- Hanahan, D. and R. A. Weinberg (2011). "Hallmarks of cancer: the next generation." *Cell* 144(5): 646-674.
- Hartel, M., F. F. di Mola, F. Selvaggi, *et al.* (2006). "Vanilloids in pancreatic cancer: potential for chemotherapy and pain management." *Gut* 55(4): 519-528.

- Hasna, J., F. Hague, L. Rodat-Despoix, *et al.* (2018). "Orai3 calcium channel and resistance to chemotherapy in breast cancer cells: the p53 connection." *Cell Death Differ* 25(4): 693-707.
- Hazelton, B., B. Mitchell and J. Tupper (1979). "Calcium, magnesium, and growth control in the WI-38 human fibroblast cell." *J Cell Biol* 83(2 Pt 1): 487-498.
- He, B., F. Liu, J. Ruan, *et al.* (2012). "Silencing TRPC1 expression inhibits invasion of CNE2 nasopharyngeal tumor cells." *Oncol Rep* 27(5): 1548-1554.
- Hegyí, P., J. Maleth, V. Venglovecz, *et al.* (2011). "Pancreatic ductal bicarbonate secretion: challenge of the acinar Acid load." *Front Physiol* 2: 36.
- Hegyí, P. and O. H. Petersen (2013). "The exocrine pancreas: the acinar-ductal tango in physiology and pathophysiology." *Rev Physiol Biochem Pharmacol* 165: 1-30.
- Helmlinger, G., F. Yuan, M. Dellian, *et al.* (1997). "Interstitial pH and pO<sub>2</sub> gradients in solid tumors in vivo: high-resolution measurements reveal a lack of correlation." *Nat Med* 3(2): 177-182.
- Hingorani, S. R., L. Wang, A. S. Multani, *et al.* (2005). "Trp53R172H and KrasG12D cooperate to promote chromosomal instability and widely metastatic pancreatic ductal adenocarcinoma in mice." *Cancer Cell* 7(5): 469-483.
- Hodeify, R., F. Yu, R. Courjaret, *et al.* (2018). Regulation and Role of Store-Operated Ca<sup>2+</sup> Entry in Cellular Proliferation. *Calcium Entry Channels in Non-Excitable Cells*. J. A. Kozak and J. W. Putney, Jr. Boca Raton (FL): 215-240.
- Hoffman, L., M. M. Farley and M. N. Waxham (2013). "Calcium-calmodulin-dependent protein kinase II isoforms differentially impact the dynamics and structure of the actin cytoskeleton." *Biochemistry* 52(7): 1198-1207.
- Hofschroer, V., K. Najder, M. Rugi, *et al.* (2020). "Ion Channels Orchestrate Pancreatic Ductal Adenocarcinoma Progression and Therapy." *Front Pharmacol* 11: 586599.
- Holinstat, M., D. Mehta, T. Kozasa, *et al.* (2003). "Protein kinase Calpha-induced p115RhoGEF phosphorylation signals endothelial cytoskeletal rearrangement." *J Biol Chem* 278(31): 28793-28798.
- Holz-Schietinger, C. and N. O. Reich (2015). "De novo DNA methyltransferase DNMT3A: Regulation of oligomeric state and mechanism of action in response to pH changes." *Biochim Biophys Acta* 1850(6): 1131-1139.
- Holzer, P. (2009). "Acid-sensitive ion channels and receptors." *Handb Exp Pharmacol*(194): 283-332.
- Hong, J. H., Q. Li, M. S. Kim, *et al.* (2011). "Polarized but differential localization and recruitment of STIM1, Orai1 and TRPC channels in secretory cells." *Traffic* 12(2): 232-245.
- Hu, Y. L., X. Mi, C. Huang, *et al.* (2017). "Multiple H<sup>+</sup> sensors mediate the extracellular acidification-induced [Ca<sup>2+</sup>]<sub>i</sub> elevation in cultured rat ventricular cardiomyocytes." *Sci Rep* 7: 44951.
- Huang, B. Z., S. J. Pandol, C. Y. Jeon, *et al.* (2020). "New-Onset Diabetes, Longitudinal Trends in Metabolic Markers, and Risk of Pancreatic Cancer in a Heterogeneous Population." *Clin Gastroenterol Hepatol* 18(8): 1812-1821 e1817.
- Huang, F. T., J. F. Peng, W. J. Cheng, *et al.* (2017). "MiR-143 Targeting TAK1 Attenuates Pancreatic Ductal Adenocarcinoma Progression via MAPK and NF-kappaB Pathway In Vitro." *Dig Dis Sci* 62(4): 944-957.
- Huang, X. Y., H. C. Wang, Z. Yuan, *et al.* (2012). "Norepinephrine stimulates pancreatic cancer cell proliferation, migration and invasion via beta-adrenergic receptor-dependent activation of P38/MAPK pathway." *Hepatogastroenterology* 59(115): 889-893.
- Humeau, J., J. M. Bravo-San Pedro, I. Vitale, *et al.* (2018). "Calcium signaling and cell cycle: Progression or death." *Cell Calcium* 70: 3-15.
- Humez, S., M. Monet, F. van Coppenolle, *et al.* (2004). "The role of intracellular pH in cell growth arrest induced by ATP." *Am J Physiol Cell Physiol* 287(6): C1733-1746.
- Iacobuzio-Donahue, C. A., B. Fu, S. Yachida, *et al.* (2009). "DPC4 gene status of the primary carcinoma correlates with patterns of failure in patients with pancreatic cancer." *J Clin Oncol* 27(11): 1806-1813.
- Ibrahim, S., H. Dakik, C. Vandier, *et al.* (2019). "Expression Profiling of Calcium Channels and Calcium-Activated Potassium Channels in Colorectal Cancer." *Cancers (Basel)* 11(4).
- Icard, P. and H. Lincet (2012). "A global view of the biochemical pathways involved in the regulation of the metabolism of cancer cells." *Biochim Biophys Acta* 1826(2): 423-433.



- Igci, Y. Z., E. Bozgeyik, E. Borazan, *et al.* (2015). "Expression profiling of SCN8A and NDUFC2 genes in colorectal carcinoma." *Exp Oncol* 37(1): 77-80.
- Ikura, M. (1996). "Calcium binding and conformational response in EF-hand proteins." *Trends Biochem Sci* 21(1): 14-17.
- Ishiguro, H., A. Yamamoto, M. Nakakuki, *et al.* (2012). "Physiology and pathophysiology of bicarbonate secretion by pancreatic duct epithelium." *Nagoya J Med Sci* 74(1-2): 1-18.
- Ishikawa, H., H. Sakurai, M. Hasegawa, *et al.* (2004). "Expression of hypoxic-inducible factor 1alpha predicts metastasis-free survival after radiation therapy alone in stage IIIB cervical squamous cell carcinoma." *Int J Radiat Oncol Biol Phys* 60(2): 513-521.
- Issa, J. P. (2004). "CpG island methylator phenotype in cancer." *Nat Rev Cancer* 4(12): 988-993.
- Javadrashid, D., A. Baghbanzadeh, A. Derakhshani, *et al.* (2021). "Pancreatic Cancer Signaling Pathways, Genetic Alterations, and Tumor Microenvironment: The Barriers Affecting the Method of Treatment." *Biomedicines* 9(4).
- Jayanth, V. R., M. T. Bayne and M. E. Varnes (1994). "Effects of extracellular and intracellular pH on repair of potentially lethal damage, chromosome aberrations and DNA double-strand breaks in irradiated plateau-phase A549 cells." *Radiat Res* 139(2): 152-162.
- Jeffs, G. J., B. P. Meloni, A. J. Bakker, *et al.* (2007). "The role of the Na(+)/Ca(2+) exchanger (NCX) in neurons following ischaemia." *J Clin Neurosci* 14(6): 507-514.
- Jiang, H. N., B. Zeng, Y. Zhang, *et al.* (2013). "Involvement of TRPC channels in lung cancer cell differentiation and the correlation analysis in human non-small cell lung cancer." *PLoS One* 8(6): e67637.
- Jiang, J., M. Li and L. Yue (2005). "Potentiation of TRPM7 inward currents by protons." *J Gen Physiol* 126(2): 137-150.
- Jin, M. Z. and W. L. Jin (2020). "The updated landscape of tumor microenvironment and drug repurposing." *Signal Transduct Target Ther* 5(1): 166.
- Jones, P. A. and S. B. Baylin (2002). "The fundamental role of epigenetic events in cancer." *Nat Rev Genet* 3(6): 415-428.
- Jordt, S. E., M. Tominaga and D. Julius (2000). "Acid potentiation of the capsaicin receptor determined by a key extracellular site." *Proc Natl Acad Sci U S A* 97(14): 8134-8139.
- Kaemmerer, E., D. Turner, A. A. Peters, *et al.* (2018). "An automated epifluorescence microscopy imaging assay for the identification of phospho-AKT level modulators in breast cancer cells." *J Pharmacol Toxicol Methods* 92: 13-19.
- Kahl, C. R. and A. R. Means (2003). "Regulation of cell cycle progression by calcium/calmodulin-dependent pathways." *Endocr Rev* 24(6): 719-736.
- Kaneda, M. M., P. Cappello, A. V. Nguyen, *et al.* (2016). "Macrophage PI3Kgamma Drives Pancreatic Ductal Adenocarcinoma Progression." *Cancer Discov* 6(8): 870-885.
- Kanwal, R. and S. Gupta (2012). "Epigenetic modifications in cancer." *Clin Genet* 81(4): 303-311.
- Kao, J. P., J. M. Alderton, R. Y. Tsien, *et al.* (1990). "Active involvement of Ca<sup>2+</sup> in mitotic progression of Swiss 3T3 fibroblasts." *J Cell Biol* 111(1): 183-196.
- Karasinska, J. M., J. T. Topham, S. E. Kalloger, *et al.* (2020). "Altered Gene Expression along the Glycolysis-Cholesterol Synthesis Axis Is Associated with Outcome in Pancreatic Cancer." *Clin Cancer Res* 26(1): 135-146.
- Kato, Y., S. Ozawa, C. Miyamoto, *et al.* (2013). "Acidic extracellular microenvironment and cancer." *Cancer Cell Int* 13(1): 89.
- Ke, C. and S. Long (2022). "Dysregulated transient receptor potential channel 1 expression and its correlation with clinical features and survival profile in surgical non-small-cell lung cancer patients." *J Clin Lab Anal* 36(3): e24229.
- Keener, J. and J. Sneyd (2009). Mathematical Physiology I: Cellular Physiology. New York, NY, Springer New York : Imprint: Springer.
- Khan, H. Y., G. B. Mpilla, R. Sexton, *et al.* (2020). "Calcium Release-Activated Calcium (CRAC) Channel Inhibition Suppresses Pancreatic Ductal Adenocarcinoma Cell Proliferation and Patient-Derived Tumor Growth." *Cancers (Basel)* 12(3): :750.

- Khananshvili, D. (2014). "Sodium-calcium exchangers (NCX): molecular hallmarks underlying the tissue-specific and systemic functions." *Pflugers Arch* 466(1): 43-60.
- Kiang, J. G. (1991). "Effect of intracellular pH on cytosolic free [Ca<sup>2+</sup>] in human epidermoid A-431 cells." *Eur J Pharmacol* 207(4): 287-296.
- Kim, D. and T. W. Smith (1988). "Cellular mechanisms underlying calcium-proton interactions in cultured chick ventricular cells." *J Physiol* 398: 391-410.
- Kim, J. B. (2014). "Channelopathies." *Korean J Pediatr* 57(1): 1-18.
- Kim, M. S., W. Zeng, J. P. Yuan, *et al.* (2009). "Native Store-operated Ca<sup>2+</sup> Influx Requires the Channel Function of Orai1 and TRPC1." *J Biol Chem* 284(15): 9733-9741.
- Kirkegard, J., F. V. Mortensen and D. Cronin-Fenton (2017). "Chronic Pancreatitis and Pancreatic Cancer Risk: A Systematic Review and Meta-analysis." *Am J Gastroenterol* 112(9): 1366-1372.
- Kondratska, K., A. Kondratskyi, M. Yassine, *et al.* (2014). "Orai1 and STIM1 mediate SOCE and contribute to apoptotic resistance of pancreatic adenocarcinoma." *Biochim Biophys Acta* 1843(10): 2263-2269.
- Krebs, J. (2017). "The Plasma Membrane Calcium Pump (PMCA): Regulation of Cytosolic Ca<sup>2+</sup>, Genetic Diversities and Its Role in Sub-plasma Membrane Microdomains." *Adv Exp Med Biol* 981: 3-21.
- Kretsinger, R. H. and C. E. Nockolds (1973). "Carp muscle calcium-binding protein. II. Structure determination and general description." *J Biol Chem* 248(9): 3313-3326.
- Krishtal, O. A. and V. I. Pidoplichko (1980). "A receptor for protons in the nerve cell membrane." *Neuroscience* 5(12): 2325-2327.
- Krizaj, D., A. J. Mercer, W. B. Thoreson, *et al.* (2011). "Intracellular pH modulates inner segment calcium homeostasis in vertebrate photoreceptors." *Am J Physiol Cell Physiol* 300(1): C187-197.
- Kroemer, G. and J. Pouyssegur (2008). "Tumor cell metabolism: cancer's Achilles' heel." *Cancer Cell* 13(6): 472-482.
- Kurdyukov, S. and M. Bullock (2016). "DNA Methylation Analysis: Choosing the Right Method." *Biology (Basel)* 5(1).
- L'Allemain, G., S. Paris and J. Pouyssegur (1984). "Growth factor action and intracellular pH regulation in fibroblasts. Evidence for a major role of the Na<sup>+</sup>/H<sup>+</sup> antiport." *J Biol Chem* 259(9): 5809-5815.
- Lamonte, G., X. Tang, J. L. Chen, *et al.* (2013). "Acidosis induces reprogramming of cellular metabolism to mitigate oxidative stress." *Cancer Metab* 1(1): 23.
- Larsson, C. (2006). "Protein kinase C and the regulation of the actin cytoskeleton." *Cell Signal* 18(3): 276-284.
- Lastraioli, E., J. Iorio and A. Arcangeli (2015). "Ion channel expression as promising cancer biomarker." *Biochim Biophys Acta* 1848(10 Pt B): 2685-2702.
- Lauritzen, G., M. B. Jensen, E. Boedtkjer, *et al.* (2010). "NBCn1 and NHE1 expression and activity in DeltaNERbB2 receptor-expressing MCF-7 breast cancer cells: contributions to pH<sub>i</sub> regulation and chemotherapy resistance." *Exp Cell Res* 316(15): 2538-2553.
- Le Floch, R., J. Chiche, I. Marchiq, *et al.* (2011). "CD147 subunit of lactate/H<sup>+</sup> symporters MCT1 and hypoxia-inducible MCT4 is critical for energetics and growth of glycolytic tumors." *Proc Natl Acad Sci U S A* 108(40): 16663-16668.
- Lee, E. Y. and W. J. Muller (2010). "Oncogenes and tumor suppressor genes." *Cold Spring Harb Perspect Biol* 2(10): a003236.
- Lee, K. P., S. Choi, J. H. Hong, *et al.* (2014). "Molecular determinants mediating gating of Transient Receptor Potential Canonical (TRPC) channels by stromal interaction molecule 1 (STIM1)." *J Biol Chem* 289(10): 6372-6382.
- Lee, M. G., E. Ohana, H. W. Park, *et al.* (2012). "Molecular mechanism of pancreatic and salivary gland fluid and HCO<sub>3</sub> secretion." *Physiol Rev* 92(1): 39-74.
- Lee, S., M. Mele, P. Vahl, *et al.* (2015). "Na<sup>+</sup>,HCO<sub>3</sub><sup>-</sup> cotransport is functionally upregulated during human breast carcinogenesis and required for the inverted pH gradient across the plasma membrane." *Pflugers Arch* 467(2): 367-377.
- Leggett, S. E., A. M. Hruska, M. Guo, *et al.* (2021). "The epithelial-mesenchymal transition and the cytoskeleton in bioengineered systems." *Cell Commun Signal* 19(1): 32.
- Lepannetier, S., N. Zanou, X. Yerna, *et al.* (2016). "Sphingosine-1-phosphate-activated TRPC1 channel controls chemotaxis of glioblastoma cells." *Cell Calcium* 60(6): 373-383.

- Lewis, B. (2010). Cell Cycle Control in Pancreatic Cancer Pathogenesis. Pancreatic Cancer. New York, NY, Springer New York: 333-367.
- Lewit-Bentley, A. and S. Rety (2000). "EF-hand calcium-binding proteins." *Curr Opin Struct Biol* 10(6): 637-643.
- Li, M., J. Du, J. Jiang, *et al.* (2007). "Molecular determinants of Mg<sup>2+</sup> and Ca<sup>2+</sup> permeability and pH sensitivity in TRPM6 and TRPM7." *J Biol Chem* 282(35): 25817-25830.
- Li, S., B. Hao, Y. Lu, *et al.* (2012). "Intracellular alkalinization induces cytosolic Ca<sup>2+</sup> increases by inhibiting sarco/endoplasmic reticulum Ca<sup>2+</sup>-ATPase (SERCA)." *PLoS One* 7(2): e31905.
- Li, Y., J. Zhang, J. Xu, *et al.* (2021). "The Metabolism Symbiosis Between Pancreatic Cancer and Tumor Microenvironment." *Front Oncol* 11: 759376.
- Liot, S., J. Balas, A. Aubert, *et al.* (2021). "Stroma Involvement in Pancreatic Ductal Adenocarcinoma: An Overview Focusing on Extracellular Matrix Proteins." *Front Immunol* 12: 612271.
- Lister, R., M. Pelizzola, R. H. Downen, *et al.* (2009). "Human DNA methylomes at base resolution show widespread epigenomic differences." *Nature* 462(7271): 315-322.
- Liu, X., K. T. Cheng, B. C. Bandyopadhyay, *et al.* (2007). "Attenuation of store-operated Ca<sup>2+</sup> current impairs salivary gland fluid secretion in TRPC1(-/-) mice." *Proc Natl Acad Sci U S A* 104(44): 17542-17547.
- Liu, X., J. Zou, J. Su, *et al.* (2016). "Downregulation of transient receptor potential cation channel, subfamily C, member 1 contributes to drug resistance and high histological grade in ovarian cancer." *Int J Oncol* 48(1): 243-252.
- Lockwich, T. P., X. Liu, B. B. Singh, *et al.* (2000). "Assembly of Trp1 in a signaling complex associated with caveolin-scaffolding lipid raft domains." *J Biol Chem* 275(16): 11934-11942.
- Longnecker, D. S. (2021). Anatomy and Histology of the Pancreas. The Pancreapedia: Exocrine Pancreas Knowledge Base. [DOI: 10.3998/panc.2021.01].
- Loveday, B. P. T., L. Lipton and B. N. Thomson (2019). "Pancreatic cancer: An update on diagnosis and management." *Aust J Gen Pract* 48(12): 826-831.
- Lu, M., R. Branstrom, E. Berglund, *et al.* (2010). "Expression and association of TRPC subtypes with Orail and STIM1 in human parathyroid." *J Mol Endocrinol* 44(5): 285-294.
- Lu, Y., Y. T. Chan, H. Y. Tan, *et al.* (2020). "Epigenetic regulation in human cancer: the potential role of epigenetic drug in cancer therapy." *Mol Cancer* 19(1): 79.
- Maalouf, N. M. (2011). Calcium Homeostasis. Textbook of Endocrine Physiology. W. J. Kovacs and S. R. Ojeda, Oxford University Press: 0.
- Madsen, C. P., T. K. Klausen, A. Fabian, *et al.* (2012). "On the role of TRPC1 in control of Ca<sup>2+</sup> influx, cell volume, and cell cycle." *Am J Physiol Cell Physiol* 303(6): C625-634.
- Makohon-Moore, A. and C. A. Iacobuzio-Donahue (2016). "Pancreatic cancer biology and genetics from an evolutionary perspective." *Nat Rev Cancer* 16(9): 553-565.
- Malumbres, M. and M. Barbacid (2005). "Mammalian cyclin-dependent kinases." *Trends Biochem Sci* 30(11): 630-641.
- Mandavilli, S., B. B. Singh and A. E. Sahnoun (2012). "Serum calcium levels, TRPM7, TRPC1, microcalcifications, and breast cancer using breast imaging reporting and data system scores." *Breast Cancer (Dove Med Press)* 2013(5): 1-7.
- Mao, W., J. Zhang, H. Korner, *et al.* (2019). "The Emerging Role of Voltage-Gated Sodium Channels in Tumor Biology." *Front Oncol* 9: 124.
- Marchi, S. and P. Pinton (2014). "The mitochondrial calcium uniporter complex: molecular components, structure and physiopathological implications." *J Physiol* 592(5): 829-839.
- Margetis, A. T. (2022). "Metabolic targeting of malignant tumors: a need for systemic approach." *J Cancer Res Clin Oncol*.
- Marin, M., C. Sellier, A. F. Paul-Antoine, *et al.* (2010). "Calcium dynamics during physiological acidification in *Xenopus* oocyte." *J Membr Biol* 236(3): 233-245.
- Maroto, R., A. Raso, T. G. Wood, *et al.* (2005). "TRPC1 forms the stretch-activated cation channel in vertebrate cells." *Nat Cell Biol* 7(2): 179-185.
- Martin, C., S. F. Pedersen, A. Schwab, *et al.* (2011). "Intracellular pH gradients in migrating cells." *Am J Physiol Cell Physiol* 300(3): C490-495.

- Martinez-Zaguilan, R., R. M. Lynch, G. M. Martinez, *et al.* (1993). "Vacuolar-type H(+)-ATPases are functionally expressed in plasma membranes of human tumor cells." *Am J Physiol* 265(4 Pt 1): C1015-1029.
- Martinez-Zaguilan, R., E. A. Seftor, R. E. Seftor, *et al.* (1996). "Acidic pH enhances the invasive behavior of human melanoma cells." *Clin Exp Metastasis* 14(2): 176-186.
- McBrian, M. A., I. S. Behbahan, R. Ferrari, *et al.* (2013). "Histone acetylation regulates intracellular pH." *Mol Cell* 49(2): 310-321.
- Mccudden, C. R. (2013). "pH-adjusted ionized calcium." *Acute Care* 28, 166–177, <https://acutecaretesting.org/en/articles/ph-adjusted-ionized-calcium>.
- McGuire, C., K. Cotter, L. Stransky, *et al.* (2016). "Regulation of V-ATPase assembly and function of V-ATPases in tumor cell invasiveness." *Biochim Biophys Acta* 1857(8): 1213-1218.
- McWilliams, R. R., G. M. Petersen, K. G. Rabe, *et al.* (2010). "Cystic fibrosis transmembrane conductance regulator (CFTR) gene mutations and risk for pancreatic adenocarcinoma." *Cancer* 116(1): 203-209.
- Mehra, S., N. Deshpande and N. Nagathihalli (2021). "Targeting PI3K Pathway in Pancreatic Ductal Adenocarcinoma: Rationale and Progress." *Cancers (Basel)* 13(17).
- Mehta, D., G. U. Ahmmmed, B. C. Paria, *et al.* (2003). "RhoA interaction with inositol 1,4,5-trisphosphate receptor and transient receptor potential channel-1 regulates Ca<sup>2+</sup> entry. Role in signaling increased endothelial permeability." *J Biol Chem* 278(35): 33492-33500.
- Michl, J., Y. Wang, S. Monterisi, *et al.* (2022). "CRISPR-Cas9 screen identifies oxidative phosphorylation as essential for cancer cell survival at low extracellular pH." *Cell Rep* 38(10): 110493.
- Mikoshiba, K. (2007). "The IP3 receptor/Ca<sup>2+</sup> channel and its cellular function." *Biochem Soc Symp*(74): 9-22.
- Minelli, A., S. Lyons, C. Nolte, *et al.* (2000). "Ammonium triggers calcium elevation in cultured mouse microglial cells by initiating Ca(2+) release from thapsigargin-sensitive intracellular stores." *Pflugers Arch* 439(3): 370-377.
- Mizrahi, J. D., R. Surana, J. W. Valle, *et al.* (2020). "Pancreatic cancer." *Lancet* 395(10242): 2008-2020.
- Moellering, R. E., K. C. Black, C. Krishnamurty, *et al.* (2008). "Acid treatment of melanoma cells selects for invasive phenotypes." *Clin Exp Metastasis* 25(4): 411-425.
- Moffitt, R. A., R. Marayati, E. L. Flate, *et al.* (2015). "Virtual microdissection identifies distinct tumor- and stroma-specific subtypes of pancreatic ductal adenocarcinoma." *Nat Genet* 47(10): 1168-1178.
- Molina-Montes, E., P. Gomez-Rubio, M. Marquez, *et al.* (2018). "Risk of pancreatic cancer associated with family history of cancer and other medical conditions by accounting for smoking among relatives." *Int J Epidemiol* 47(2): 473-483.
- Molina-Montes, E., L. Van Hoogstraten, P. Gomez-Rubio, *et al.* (2020). "Pancreatic Cancer Risk in Relation to Lifetime Smoking Patterns, Tobacco Type, and Dose-Response Relationships." *Cancer Epidemiol Biomarkers Prev* 29(5): 1009-1018.
- Molinari, G. and E. Nervo (2021). "Role of protons in calcium signaling." *Biochem J* 478(4): 895-910.
- Monteith, G. R., N. Prevarskaya and S. J. Roberts-Thomson (2017). "The calcium-cancer signalling nexus." *Nat Rev Cancer* 17(6): 367-380.
- Montell, C. and G. M. Rubin (1989). "Molecular characterization of the Drosophila trp locus: a putative integral membrane protein required for phototransduction." *Neuron* 2(4): 1313-1323.
- Montrose, M. H. and H. Murer (1988). *Kinetics of Na<sup>+</sup>/H<sup>+</sup> Exchange*, CRC Press.
- Moore, P. S., B. Sipos, S. Orlandini, *et al.* (2001). "Genetic profile of 22 pancreatic carcinoma cell lines. Analysis of K-ras, p53, p16 and DPC4/Smad4." *Virchows Arch* 439(6): 798-802.
- Morita, T., T. Nagaki, I. Fukuda, *et al.* (1992). "Clastogenicity of low pH to various cultured mammalian cells." *Mutat Res* 268(2): 297-305.
- Morris, J. P. t., S. C. Wang and M. Hebrok (2010). "KRAS, Hedgehog, Wnt and the twisted developmental biology of pancreatic ductal adenocarcinoma." *Nat Rev Cancer* 10(10): 683-695.
- Muallem, S., S. J. Pandol and T. G. Beeker (1989). "Modulation of agonist-activated calcium influx by extracellular pH in rat pancreatic acini." *Am J Physiol* 257(6 Pt 1): G917-924.
- Muller, P. A. and K. H. Vousden (2013). "p53 mutations in cancer." *Nat Cell Biol* 15(1): 2-8.
- Neri, D. and C. T. Supuran (2011). "Interfering with pH regulation in tumours as a therapeutic strategy." *Nat Rev Drug Discov* 10(10): 767-777.

- Nesin, V. and L. Tsiokas (2014). "Trpc1." *Handb Exp Pharmacol* 222: 15-51.
- Ng, L. C., K. G. O'Neill, D. French, *et al.* (2012). "TRPC1 and Orai1 interact with STIM1 and mediate capacitative Ca<sup>2+</sup> entry caused by acute hypoxia in mouse pulmonary arterial smooth muscle cells." *Am J Physiol Cell Physiol* 303(11): C1156-1172.
- Nielsen, N., K. Kondratska, T. Ruck, *et al.* (2017). "TRPC6 channels modulate the response of pancreatic stellate cells to hypoxia." *Pflugers Arch* 469(12): 1567-1577.
- Niemeyer, B. A., L. Mery, C. Zawar, *et al.* (2001). "Ion channels in health and disease. 83rd Boehringer Ingelheim Fonds International Titisee Conference." *EMBO Rep* 2(7): 568-573.
- Nilius, B. and G. Owsianik (2011). "The transient receptor potential family of ion channels." *Genome Biol* 12(3): 218.
- Nishi, T. and M. Forgac (2002). "The vacuolar (H<sup>+</sup>)-ATPases--nature's most versatile proton pumps." *Nat Rev Mol Cell Biol* 3(2): 94-103.
- Nishiguchi, H., T. Hayashi, T. Shigetomi, *et al.* (1997). "Changes in intracellular Ca<sup>2+</sup> concentration produced by the alteration of intracellular pH in rat parotid acinar cells." *Jpn J Physiol* 47(1): 41-49.
- Nitschke, R., A. Riedel, S. Ricken, *et al.* (1996). "The effect of intracellular pH on cytosolic Ca<sup>2+</sup> in HT29 cells." *Pflugers Arch* 433(1-2): 98-108.
- North, R. A. (2002). "Molecular physiology of P2X receptors." *Physiol Rev* 82(4): 1013-1067.
- Novak, I., K. A. Haanes and J. Wang (2013). "Acid-base transport in pancreas-new challenges." *Front Physiol* 4: 380.
- Novak, I. and J. Praetorius (2020). Fundamentals of Bicarbonate Secretion in Epithelia. Basic Epithelial Ion Transport Principles and Function: Ion Channels and Transporters of Epithelia in Health and Disease - Vol. 1. K. L. Hamilton and D. C. Devor. Cham, Springer International Publishing: 461-541.
- Nussinov, R., G. Wang, C. J. Tsai, *et al.* (2017). "Calmodulin and PI3K Signaling in KRAS Cancers." *Trends Cancer* 3(3): 214-224.
- Ohta, Y., E. Nishida and H. Sakai (1986). "Type II Ca<sup>2+</sup>/calmodulin-dependent protein kinase binds to actin filaments in a calmodulin-sensitive manner." *FEBS Lett* 208(2): 423-426.
- Okano, M., D. W. Bell, D. A. Haber, *et al.* (1999). "DNA methyltransferases Dnmt3a and Dnmt3b are essential for de novo methylation and mammalian development." *Cell* 99(3): 247-257.
- Okeke, E., T. Parker, H. Dingsdale, *et al.* (2016). "Epithelial-mesenchymal transition, IP3 receptors and ER-PM junctions: translocation of Ca<sup>2+</sup> signalling complexes and regulation of migration." *Biochem J* 473(6): 757-767.
- Ong, E. C., V. Nesin, C. L. Long, *et al.* (2013). "A TRPC1 protein-dependent pathway regulates osteoclast formation and function." *J Biol Chem* 288(31): 22219-22232.
- Ong, H. L. and I. S. Ambudkar (2011). "The dynamic complexity of the TRPC1 channelosome." *Channels (Austin)* 5(5): 424-431.
- Ong, H. L., K. T. Cheng, X. Liu, *et al.* (2007). "Dynamic assembly of TRPC1-STIM1-Orai1 ternary complex is involved in store-operated calcium influx. Evidence for similarities in store-operated and calcium release-activated calcium channel components." *J Biol Chem* 282(12): 9105-9116.
- Ong, H. L., L. B. de Souza and I. S. Ambudkar (2016). "Role of TRPC Channels in Store-Operated Calcium Entry." *Adv Exp Med Biol* 898: 87-109.
- Orchard, C. H., S. R. Houser, A. A. Kort, *et al.* (1987). "Acidosis facilitates spontaneous sarcoplasmic reticulum Ca<sup>2+</sup> release in rat myocardium." *J Gen Physiol* 90(1): 145-165.
- Ordway, B., P. Swietach, R. J. Gillies, *et al.* (2020). "Causes and Consequences of Variable Tumor Cell Metabolism on Heritable Modifications and Tumor Evolution." *Front Oncol* 10: 373.
- Orlowski, J. and S. Grinstein (2011). "Na<sup>+</sup>/H<sup>+</sup> exchangers." *Compr Physiol* 1(4): 2083-2100.
- Orr, C. W., M. Yoshikawa-Fukada and J. D. Ebert (1972). "Potassium: effect on DNA synthesis and multiplication of baby-hamster kidney cells: (cell cycle-membrane potential-synchronization-transformation)." *Proc Natl Acad Sci U S A* 69(1): 243-247.
- Orth, M., P. Metzger, S. Gerum, *et al.* (2019). "Pancreatic ductal adenocarcinoma: biological hallmarks, current status, and future perspectives of combined modality treatment approaches." *Radiat Oncol* 14(1): 141.
- Ouadid-Ahidouch, H., L. Rodat-Despoix, F. Matifat, *et al.* (2015). "DNA methylation of channel-related genes in cancers." *Biochim Biophys Acta* 1848(10 Pt B): 2621-2628.

- Paillamanque, J., C. Madrid, E. M. Carmona, *et al.* (2016). "Effects of Fatty Acids on Intracellular [Ca<sup>2+</sup>], Mitochondrial Uncoupling and Apoptosis in Rat Pachytene Spermatocytes and Round Spermatids." *PLoS One* 11(7): e0158518.
- Pallagi, P., P. Hegyi and Z. Rakonczay, Jr. (2015). "The Physiology and Pathophysiology of Pancreatic Ductal Secretion: The Background for Clinicians." *Pancreas* 44(8): 1211-1233.
- Pani, B., X. Liu, S. Bollimuntha, *et al.* (2013). "Impairment of TRPC1-STIM1 channel assembly and AQP5 translocation compromise agonist-stimulated fluid secretion in mice lacking caveolin1." *J Cell Sci* 126(Pt 2): 667-675.
- Pani, B., H. L. Ong, S. C. Brazer, *et al.* (2009). "Activation of TRPC1 by STIM1 in ER-PM microdomains involves release of the channel from its scaffold caveolin-1." *Proc Natl Acad Sci U S A* 106(47): 20087-20092.
- Pantel, K. and R. H. Brakenhoff (2004). "Dissecting the metastatic cascade." *Nat Rev Cancer* 4(6): 448-456.
- Park, K., R. L. Evans, G. E. Watson, *et al.* (2001). "Defective fluid secretion and NaCl absorption in the parotid glands of Na<sup>+</sup>/H<sup>+</sup> exchanger-deficient mice." *J Biol Chem* 276(29): 27042-27050.
- Park, W., A. Chawla and E. M. O'Reilly (2021). "Pancreatic Cancer: A Review." *JAMA* 326(9): 851-862.
- Parks, S. K., J. Chiche and J. Pouyssegur (2013). "Disrupting proton dynamics and energy metabolism for cancer therapy." *Nat Rev Cancer* 13(9): 611-623.
- Parks, S. K. and J. Pouyssegur (2015). "The Na<sup>(+)</sup>/HCO<sub>3</sub><sup>(-)</sup> Co-Transporter SLC4A4 Plays a Role in Growth and Migration of Colon and Breast Cancer Cells." *J Cell Physiol* 230(8): 1954-1963.
- Pedersen, S. F. and L. Counillon (2019). "The SLC9A-C Mammalian Na<sup>(+)</sup>/H<sup>(+)</sup> Exchanger Family: Molecules, Mechanisms, and Physiology." *Physiol Rev* 99(4): 2015-2113.
- Pedersen, S. F. and B. Nilius (2007). "Transient receptor potential channels in mechanosensing and cell volume regulation." *Methods Enzymol* 428: 183-207.
- Pedersen, S. F., I. Novak, F. Alves, *et al.* (2017). "Alternating pH landscapes shape epithelial cancer initiation and progression: Focus on pancreatic cancer." *Bioessays* 39(6).
- Pedersen, S. F. and C. Stock (2013). "Ion channels and transporters in cancer: pathophysiology, regulation, and clinical potential." *Cancer Res* 73(6): 1658-1661.
- Penner, R., C. Fasolato and M. Hoth (1993). "Calcium influx and its control by calcium release." *Curr Opin Neurobiol* 3(3): 368-374.
- Peppicelli, S., E. Andreucci, J. Ruzzolini, *et al.* (2017). "The acidic microenvironment as a possible niche of dormant tumor cells." *Cell Mol Life Sci* 74(15): 2761-2771.
- Peppicelli, S., F. Bianchini, A. Toti, *et al.* (2015). "Extracellular acidity strengthens mesenchymal stem cells to promote melanoma progression." *Cell Cycle* 14(19): 3088-3100.
- Perez-Escuredo, J., V. F. Van Hee, M. Sboarina, *et al.* (2016). "Monocarboxylate transporters in the brain and in cancer." *Biochim Biophys Acta* 1863(10): 2481-2497.
- Periasamy, M. and A. Kalyanasundaram (2007). "SERCA pump isoforms: their role in calcium transport and disease." *Muscle Nerve* 35(4): 430-442.
- Perrouin Verbe, M. A., F. Bruyere, F. Rozet, *et al.* (2016). "Expression of store-operated channel components in prostate cancer: the prognostic paradox." *Hum Pathol* 49: 77-82.
- Perrouin-Verbe, M. A., N. Schoentgen, M. Talagas, *et al.* (2019). "Overexpression of certain transient receptor potential and Orai channels in prostate cancer is associated with decreased risk of systemic recurrence after radical prostatectomy." *Prostate* 79(16): 1793-1804.
- Petersen, O. H. (2014). "Calcium signalling and secretory epithelia." *Cell Calcium* 55(6): 282-289.
- Petho, Z., K. Najder, T. Carvalho, *et al.* (2020). "pH-Channeling in Cancer: How pH-Dependence of Cation Channels Shapes Cancer Pathophysiology." *Cancers (Basel)* 12(9).
- Peti-Peterdi, J., R. Chambrey, Z. Bebok, *et al.* (2000). "Macula densa Na<sup>(+)</sup>/H<sup>(+)</sup> exchange activities mediated by apical NHE2 and basolateral NHE4 isoforms." *Am J Physiol Renal Physiol* 278(3): F452-463.
- Pigozzi, D., T. Ducret, N. Tajeddine, *et al.* (2006). "Calcium store contents control the expression of TRPC1, TRPC3 and TRPV6 proteins in LNCaP prostate cancer cell line." *Cell Calcium* 39(5): 401-415.
- Pillai, S. R., M. Damaghi, Y. Marunaka, *et al.* (2019). "Causes, consequences, and therapy of tumors acidosis." *Cancer Metastasis Rev* 38(1-2): 205-222.
- Poenie, M., J. Alderton, R. Y. Tsien, *et al.* (1985). "Changes of free calcium levels with stages of the cell division cycle." *Nature* 315(6015): 147-149.

- Porporato, P. E., S. Dhup, R. K. Dadhich, *et al.* (2011). "Anticancer targets in the glycolytic metabolism of tumors: a comprehensive review." *Front Pharmacol* 2: 49.
- Pradhan, S., A. Bacolla, R. D. Wells, *et al.* (1999). "Recombinant human DNA (cytosine-5) methyltransferase. I. Expression, purification, and comparison of de novo and maintenance methylation." *J Biol Chem* 274(46): 33002-33010.
- Prakriya, M. and R. S. Lewis (2015). "Store-Operated Calcium Channels." *Physiol Rev* 95(4): 1383-1436.
- Preston, S. F., R. I. Sha'afi and R. D. Berlin (1991). "Regulation of Ca<sup>2+</sup> influx during mitosis: Ca<sup>2+</sup> influx and depletion of intracellular Ca<sup>2+</sup> stores are coupled in interphase but not mitosis." *Cell Regul* 2(11): 915-925.
- Prevarskaya, N., R. Skryma and Y. Shuba (2018). "Ion Channels in Cancer: Are Cancer Hallmarks Oncochannelopathies?" *Physiol Rev* 98(2): 559-621.
- Prevarskaya, N., L. Zhang and G. Barritt (2007). "TRP channels in cancer." *Biochim Biophys Acta* 1772(8): 937-946.
- Puleo, F., R. Nicolle, Y. Blum, *et al.* (2018). "Stratification of Pancreatic Ductal Adenocarcinomas Based on Tumor and Microenvironment Features." *Gastroenterology* 155(6): 1999-2013 e1993.
- Putney, L. K. and D. L. Barber (2003). "Na-H exchange-dependent increase in intracellular pH times G2/M entry and transition." *J Biol Chem* 278(45): 44645-44649.
- Quail, D. F. and J. A. Joyce (2013). "Microenvironmental regulation of tumor progression and metastasis." *Nat Med* 19(11): 1423-1437.
- Radoslavova, S., B. Fels, Z. Petho, *et al.* (2022). "TRPC1 channels regulate the activation of pancreatic stellate cells through ERK1/2 and SMAD2 pathways and perpetuate their pressure-mediated activation." *Cell Calcium* 106: 102621.
- Radoslavova, S., A. Folcher, T. Lefebvre, *et al.* (2021). "Orai1 Channel Regulates Human-Activated Pancreatic Stellate Cell Proliferation and TGFbeta1 Secretion through the AKT Signaling Pathway." *Cancers (Basel)* 13(10).
- Raghunand, N., X. He, R. van Sluis, *et al.* (1999). "Enhancement of chemotherapy by manipulation of tumour pH." *Br J Cancer* 80(7): 1005-1011.
- Rahib, L., B. D. Smith, R. Aizenberg, *et al.* (2014). "Projecting cancer incidence and deaths to 2030: the unexpected burden of thyroid, liver, and pancreas cancers in the United States." *Cancer Res* 74(11): 2913-2921.
- Rawla, P., T. Sunkara and V. Gaduputi (2019). "Epidemiology of Pancreatic Cancer: Global Trends, Etiology and Risk Factors." *World J Oncol* 10(1): 10-27.
- Reddy, G. P. (1994). "Cell cycle: regulatory events in G1-->S transition of mammalian cells." *J Cell Biochem* 54(4): 379-386.
- Reshkin, S. J., A. Bellizzi, R. A. Cardone, *et al.* (2003). "Paclitaxel induces apoptosis via protein kinase A- and p38 mitogen-activated protein-dependent inhibition of the Na<sup>+</sup>/H<sup>+</sup> exchanger (NHE) NHE isoform 1 in human breast cancer cells." *Clin Cancer Res* 9(6): 2366-2373.
- Rich, I. N., D. Worthington-White, O. A. Garden, *et al.* (2000). "Apoptosis of leukemic cells accompanies reduction in intracellular pH after targeted inhibition of the Na<sup>(+)</sup>/H<sup>(+)</sup> exchanger." *Blood* 95(4): 1427-1434.
- Riemann, A., M. Rauschner, M. Giesselmann, *et al.* (2019). "Extracellular Acidosis Modulates the Expression of Epithelial-Mesenchymal Transition (EMT) Markers and Adhesion of Epithelial and Tumor Cells." *Neoplasia* 21(5): 450-458.
- Riemann, A., B. Schneider, D. Gundel, *et al.* (2016). "Acidosis Promotes Metastasis Formation by Enhancing Tumor Cell Motility." *Adv Exp Med Biol* 876: 215-220.
- Riemann, A., B. Schneider, D. Gundel, *et al.* (2014). "Acidic priming enhances metastatic potential of cancer cells." *Pflugers Arch* 466(11): 2127-2138.
- Rijkers, A. P., O. J. Bakker, U. Ahmed Ali, *et al.* (2017). "Risk of Pancreatic Cancer After a Primary Episode of Acute Pancreatitis." *Pancreas* 46(8): 1018-1022.
- Roalso, M. T. T., O. H. Hald, M. Alexeeva, *et al.* (2022). "Emerging Role of Epigenetic Alterations as Biomarkers and Novel Targets for Treatments in Pancreatic Ductal Adenocarcinoma." *Cancers (Basel)* 14(3).



- Robey, I. F., B. K. Baggett, N. D. Kirkpatrick, *et al.* (2009). "Bicarbonate increases tumor pH and inhibits spontaneous metastases." *Cancer Res* 69(6): 2260-2268.
- Rofstad, E. K., B. Mathiesen, K. Kindem, *et al.* (2006). "Acidic extracellular pH promotes experimental metastasis of human melanoma cells in athymic nude mice." *Cancer Res* 66(13): 6699-6707.
- Rohani, N., L. Hao, M. S. Alexis, *et al.* (2019). "Acidification of Tumor at Stromal Boundaries Drives Transcriptome Alterations Associated with Aggressive Phenotypes." *Cancer Res* 79(8): 1952-1966.
- Rojas, J. D., S. R. Sennoune, D. Maiti, *et al.* (2006). "Vacuolar-type H<sup>+</sup>-ATPases at the plasma membrane regulate pH and cell migration in microvascular endothelial cells." *Am J Physiol Heart Circ Physiol* 291(3): H1147-1157.
- Rosty, C., J. Geradts, N. Sato, *et al.* (2003). "p16 Inactivation in pancreatic intraepithelial neoplasias (PanINs) arising in patients with chronic pancreatitis." *Am J Surg Pathol* 27(12): 1495-1501.
- Rotin, D. and O. Staub (2021). "Function and Regulation of the Epithelial Na(+) Channel ENaC." *Compr Physiol* 11(3): 2017-2045.
- Rune, S. J. and N. A. Lassen (1968). "Diurnal variations in the acid-base balance of blood." *Scand J Clin Lab Invest* 22(2): 151-156.
- Russa, A. D., N. Ishikita, K. Masu, *et al.* (2008). "Microtubule remodeling mediates the inhibition of store-operated calcium entry (SOCE) during mitosis in COS-7 cells." *Arch Histol Cytol* 71(4): 249-263.
- Rybarczyk, P., M. Gautier, F. Hague, *et al.* (2012). "Transient receptor potential melastatin-related 7 channel is overexpressed in human pancreatic ductal adenocarcinomas and regulates human pancreatic cancer cell migration." *Int J Cancer* 131(6): E851-861.
- Rybarczyk, P., A. Vanlaeys, B. Brassart, *et al.* (2017). "The Transient Receptor Potential Melastatin 7 Channel Regulates Pancreatic Cancer Cell Invasion through the Hsp90alpha/uPA/MMP2 pathway." *Neoplasia* 19(4): 288-300.
- Rychkov, G. and G. J. Barritt (2007). "TRPC1 Ca(2+)-permeable channels in animal cells." *Handb Exp Pharmacol*(179): 23-52.
- Rychkov, G. Y., F. H. Zhou, M. K. Adams, *et al.* (2022). "Orai1- and Orai2-, but not Orai3-mediated ICRAC is regulated by intracellular pH." *J Physiol* 600(3): 623-643.
- Sadeghi, M., B. Ordway, I. Rafiei, *et al.* (2020). "Integrative Analysis of Breast Cancer Cells Reveals an Epithelial-Mesenchymal Transition Role in Adaptation to Acidic Microenvironment." *Front Oncol* 10: 304.
- Sakura, H. and F. M. Ashcroft (1997). "Identification of four trp1 gene variants murine pancreatic beta-cells." *Diabetologia* 40(5): 528-532.
- Samanta, A., T. E. T. Hughes and V. Y. Moiseenkova-Bell (2018). "Transient Receptor Potential (TRP) Channels." *Subcell Biochem* 87: 141-165.
- Schaar, A., P. Sukumaran, Y. Sun, *et al.* (2016). "TRPC1-STIM1 activation modulates transforming growth factor beta-induced epithelial-to-mesenchymal transition." *Oncotarget* 7(49): 80554-80567.
- Schito, L. and S. Rey (2017). "Hypoxic pathobiology of breast cancer metastasis." *Biochim Biophys Acta Rev Cancer* 1868(1): 239-245.
- Schlappack, O. K., A. Zimmermann and R. P. Hill (1991). "Glucose starvation and acidosis: effect on experimental metastatic potential, DNA content and MTX resistance of murine tumour cells." *Br J Cancer* 64(4): 663-670.
- Schmidt-Hansen, M., S. Berendse and W. Hamilton (2016). "Symptoms of Pancreatic Cancer in Primary Care: A Systematic Review." *Pancreas* 45(6): 814-818.
- Schnipper, J., H. Ouadid-Ahidouch, I. Dhennin-Duthille, *et al.* (2020). "Ion channel signature in healthy pancreas and pancreatic ductal adenocarcinoma." *Front. Pharmacol.*
- Schonichen, A., B. A. Webb, M. P. Jacobson, *et al.* (2013). "Considering protonation as a posttranslational modification regulating protein structure and function." *Annu Rev Biophys* 42: 289-314.
- Schutte, M., R. H. Hruban, J. Geradts, *et al.* (1997). "Abrogation of the Rb/p16 tumor-suppressive pathway in virtually all pancreatic carcinomas." *Cancer Res* 57(15): 3126-3130.
- Schwaller, B. (2010). "Cytosolic Ca<sup>2+</sup> buffers." *Cold Spring Harb Perspect Biol* 2(11): a004051.
- Scourzic, L., E. Mouly and O. A. Bernard (2015). "TET proteins and the control of cytosine demethylation in cancer." *Genome Med* 7(1): 9.

- Scrimgeour, N. R., D. P. Wilson and G. Y. Rychkov (2012). "Glu(1)(0)(6) in the Orai1 pore contributes to fast Ca(2+)-dependent inactivation and pH dependence of Ca(2+) release-activated Ca(2+) (CRAC) current." *Biochem J* 441(2): 743-753.
- Selli, C., Y. Erac, B. Kosova, *et al.* (2015). "Silencing of TRPC1 regulates store-operated calcium entry and proliferation in Huh7 hepatocellular carcinoma cells." *Biomed Pharmacother* 71: 194-200.
- Selli, C., Y. Erac and M. Tosun (2015). "Simultaneous measurement of cytosolic and mitochondrial calcium levels: observations in TRPC1-silenced hepatocellular carcinoma cells." *J Pharmacol Toxicol Methods* 72: 29-34.
- Selli, C., D. A. Pearce, A. H. Sims, *et al.* (2016). "Differential expression of store-operated calcium- and proliferation-related genes in hepatocellular carcinoma cells following TRPC1 ion channel silencing." *Mol Cell Biochem* 420(1-2): 129-140.
- Semenza, G. L. (2010). "Defining the role of hypoxia-inducible factor 1 in cancer biology and therapeutics." *Oncogene* 29(5): 625-634.
- Semenza, G. L. (2010). "HIF-1: upstream and downstream of cancer metabolism." *Curr Opin Genet Dev* 20(1): 51-56.
- Semtner, M., M. Schaefer, O. Pinkenburg, *et al.* (2007). "Potentiation of TRPC5 by protons." *J Biol Chem* 282(46): 33868-33878.
- Sennoune, S. R., K. Bakunts, G. M. Martinez, *et al.* (2004). "Vacuolar H<sup>+</sup>-ATPase in human breast cancer cells with distinct metastatic potential: distribution and functional activity." *Am J Physiol Cell Physiol* 286(6): C1443-1452.
- Sennoune, S. R., D. Luo and R. Martinez-Zaguilan (2004). "Plasmalemmal vacuolar-type H<sup>+</sup>-ATPase in cancer biology." *Cell Biochem Biophys* 40(2): 185-206.
- Shapovalov, G., A. Ritaine, R. Skryma, *et al.* (2016). "Role of TRP ion channels in cancer and tumorigenesis." *Semin Immunopathol* 38(3): 357-369.
- Sharma, S., R. Goswami, D. X. Zhang, *et al.* (2019). "TRPV4 regulates matrix stiffness and TGFbeta1-induced epithelial-mesenchymal transition." *J Cell Mol Med* 23(2): 761-774.
- Sheng, Y., B. Wu, T. Leng, *et al.* (2021). "Acid-sensing ion channel 1 (ASIC1) mediates weak acid-induced migration of human malignant glioma cells." *Am J Cancer Res* 11(3): 997-1008.
- Shi, G., W. Cui, Y. Liu, *et al.* (2022). "TRPC1 correlates with poor tumor features, radiotherapy efficacy and survival in tongue squamous cell carcinoma." *Biomark Med* 16(11): 867-877.
- Shin, S. C., D. Thomas, P. Radhakrishnan, *et al.* (2020). "Invasive phenotype induced by low extracellular pH requires mitochondria dependent metabolic flexibility." *Biochem Biophys Res Commun*.
- Singh, B. B., X. Liu, J. Tang, *et al.* (2002). "Calmodulin regulates Ca(2+)-dependent feedback inhibition of store-operated Ca(2+) influx by interaction with a site in the C terminus of TrpC1." *Mol Cell* 9(4): 739-750.
- Skou, J. C. and M. Esmann (1992). "The Na,K-ATPase." *J Bioenerg Biomembr* 24(3): 249-261.
- Smith, N. R., R. L. Sparks, T. B. Pool, *et al.* (1978). "Differences in the intracellular concentration of elements in normal and cancerous liver cells as determined by X-ray microanalysis." *Cancer Res* 38(7): 1952-1959.
- Smyth, J. T., J. G. Petranka, R. R. Boyles, *et al.* (2009). "Phosphorylation of STIM1 underlies suppression of store-operated calcium entry during mitosis." *Nat Cell Biol* 11(12): 1465-1472.
- Sobradillo, D., M. Hernandez-Morales, D. Ubierna, *et al.* (2014). "A reciprocal shift in transient receptor potential channel 1 (TRPC1) and stromal interaction molecule 2 (STIM2) contributes to Ca<sup>2+</sup> remodeling and cancer hallmarks in colorectal carcinoma cells." *J Biol Chem* 289(42): 28765-28782.
- Song, H., M. Dong, J. Zhou, *et al.* (2018). "Expression and prognostic significance of TRPV6 in the development and progression of pancreatic cancer." *Oncol Rep* 39(3): 1432-1440.
- Sparks, R. L., T. B. Pool, N. K. Smith, *et al.* (1983). "Effects of amiloride on tumor growth and intracellular element content of tumor cells in vivo." *Cancer Res* 43(1): 73-77.
- Speake, T. and A. C. Elliott (1998). "Modulation of calcium signals by intracellular pH in isolated rat pancreatic acinar cells." *J Physiol* 506 ( Pt 2): 415-430.
- Srivastava, J., D. L. Barber and M. P. Jacobson (2007). "Intracellular pH sensors: design principles and functional significance." *Physiology (Bethesda)* 22: 30-39.

- Staaf, S., I. Maxvall, U. Lind, *et al.* (2009). "Down regulation of TRPC1 by shRNA reduces mechanosensitivity in mouse dorsal root ganglion neurons in vitro." *Neurosci Lett* 457(1): 3-7.
- Starkus, J., A. Beck, A. Fleig, *et al.* (2007). "Regulation of TRPM2 by extra- and intracellular calcium." *J Gen Physiol* 130(4): 427-440.
- Stock, C. and S. F. Pedersen (2017). "Roles of pH and the Na(+)/H(+) exchanger NHE1 in cancer: From cell biology and animal models to an emerging translational perspective?" *Semin Cancer Biol* 43: 5-16.
- Stock, C. and A. Schwab (2015). "Ion channels and transporters in metastasis." *Biochim Biophys Acta* 1848(10 Pt B): 2638-2646.
- Storck, H., B. Hild, S. Schimmelpfennig, *et al.* (2017). "Ion channels in control of pancreatic stellate cell migration." *Oncotarget* 8(1): 769-784.
- Stuwe, L., M. Muller, A. Fabian, *et al.* (2007). "pH dependence of melanoma cell migration: protons extruded by NHE1 dominate protons of the bulk solution." *J Physiol* 585(Pt 2): 351-360.
- Sukumaran, P., Y. Sun, M. Vyas, *et al.* (2015). "TRPC1-mediated Ca(2+)(+) entry is essential for the regulation of hypoxia and nutrient depletion-dependent autophagy." *Cell Death Dis* 6: e1674.
- Sun, Y., L. Birnbaumer and B. B. Singh (2015). "TRPC1 regulates calcium-activated chloride channels in salivary gland cells." *J Cell Physiol* 230(11): 2848-2856.
- Sun, Y., C. Ye, W. Tian, *et al.* (2021). "TRPC1 promotes the genesis and progression of colorectal cancer via activating CaM-mediated PI3K/AKT signaling axis." *Oncogenesis* 10(10): 67.
- Sun, Z., L. Wang, L. Han, *et al.* (2021). "Functional Calsequestrin-1 Is Expressed in the Heart and Its Deficiency Is Causally Related to Malignant Hyperthermia-Like Arrhythmia." *Circulation* 144(10): 788-804.
- Sutoo, S., T. Maeda, A. Suzuki, *et al.* (2020). "Adaptation to chronic acidic extracellular pH elicits a sustained increase in lung cancer cell invasion and metastasis." *Clin Exp Metastasis* 37(1): 133-144.
- Suzuki, A., T. Maeda, Y. Baba, *et al.* (2014). "Acidic extracellular pH promotes epithelial mesenchymal transition in Lewis lung carcinoma model." *Cancer Cell Int* 14(1): 129.
- Suzuki, M., A. Mizuno, K. Kodaira, *et al.* (2003). "Impaired pressure sensation in mice lacking TRPV4." *J Biol Chem* 278(25): 22664-22668.
- Swietach, P. (2019). "What is pH regulation, and why do cancer cells need it?" *Cancer Metastasis Rev* 38(1-2): 5-15.
- Swietach, P., R. D. Vaughan-Jones, A. L. Harris, *et al.* (2014). "The chemistry, physiology and pathology of pH in cancer." *Philos Trans R Soc Lond B Biol Sci* 369(1638): 20130099.
- Swietach, P., J. B. Youm, N. Saegusa, *et al.* (2013). "Coupled Ca<sup>2+</sup>/H<sup>+</sup> transport by cytoplasmic buffers regulates local Ca<sup>2+</sup> and H<sup>+</sup> ion signaling." *Proc Natl Acad Sci U S A* 110(22): E2064-2073.
- Tahiliani, M., K. P. Koh, Y. Shen, *et al.* (2009). "Conversion of 5-methylcytosine to 5-hydroxymethylcytosine in mammalian DNA by MLL partner TET1." *Science* 324(5929): 930-935.
- Tajada, S. and C. Villalobos (2020). "Calcium Permeable Channels in Cancer Hallmarks." *Front Pharmacol* 11: 968.
- Tajeddine, N. and P. Gailly (2012). "TRPC1 protein channel is major regulator of epidermal growth factor receptor signaling." *J Biol Chem* 287(20): 16146-16157.
- Takuwa, N., W. Zhou, M. Kumada, *et al.* (1992). "Ca<sup>2+</sup>/calmodulin is involved in growth factor-induced retinoblastoma gene product phosphorylation in human vascular endothelial cells." *FEBS Lett* 306(2-3): 173-175.
- Talathi, S. S., R. Zimmerman and M. Young (2022). *Anatomy, Abdomen and Pelvis, Pancreas*. StatPearls. Treasure Island (FL).
- Tani, D., M. K. Monteilh-Zoller, A. Fleig, *et al.* (2007). "Cell cycle-dependent regulation of store-operated I(CRAC) and Mg<sup>2+</sup>-nucleotide-regulated MagNum (TRPM7) currents." *Cell Calcium* 41(3): 249-260.
- Tanimura, S. and K. Takeda (2017). "ERK signalling as a regulator of cell motility." *J Biochem* 162(3): 145-154.
- Tawfik, D., A. Zaccagnino, A. Bernt, *et al.* (2020). "The A818-6 system as an in-vitro model for studying the role of the transportome in pancreatic cancer." *BMC Cancer* 20(1): 264.
- Thakur, D. P., Q. Wang, J. Jeon, *et al.* (2020). "Intracellular acidification facilitates receptor-operated TRPC4 activation through PLCdelta1 in a Ca(2+) -dependent manner." *J Physiol* 598(13): 2651-2667.

- Thebault, S., M. Flourakis, K. Vanoverberghe, *et al.* (2006). "Differential role of transient receptor potential channels in Ca<sup>2+</sup> entry and proliferation of prostate cancer epithelial cells." *Cancer Res* 66(4): 2038-2047.
- Thews, O. and A. Riemann (2019). "Tumor pH and metastasis: a malignant process beyond hypoxia." *Cancer Metastasis Rev* 38(1-2): 113-129.
- Thibault, B., F. Ramos-Delgado, E. Pons-Tostivint, *et al.* (2021). "Pancreatic cancer intrinsic PI3K activity accelerates metastasis and rewires macrophage component." *EMBO Mol Med* 13(7): e13502.
- Thomas, R. C. (2002). "The effects of HCl and CaCl<sub>2</sub> injections on intracellular calcium and pH in voltage-clamped snail (*Helix aspersa*) neurons." *J Gen Physiol* 120(4): 567-579.
- Thomlinson, R. H. and L. H. Gray (1955). "The histological structure of some human lung cancers and the possible implications for radiotherapy." *Br J Cancer* 9(4): 539-549.
- Tong, X. P., X. Y. Li, B. Zhou, *et al.* (2009). "Ca<sup>2+</sup> signaling evoked by activation of Na<sup>+</sup> channels and Na<sup>+</sup>/Ca<sup>2+</sup> exchangers is required for GABA-induced NG2 cell migration." *J Cell Biol* 186(1): 113-128.
- Torigoe, T., H. Izumi, Y. Yoshida, *et al.* (2003). "Low pH enhances Sp1 DNA binding activity and interaction with TBP." *Nucleic Acids Res* 31(15): 4523-4530.
- Totiger, T. M., S. Srinivasan, V. R. Jala, *et al.* (2019). "Urolithin A, a Novel Natural Compound to Target PI3K/AKT/mTOR Pathway in Pancreatic Cancer." *Mol Cancer Ther* 18(2): 301-311.
- Trebak, M., G. Vazquez, G. S. Bird, *et al.* (2003). "The TRPC3/6/7 subfamily of cation channels." *Cell Calcium* 33(5-6): 451-461.
- Trivedi, B. and W. H. Danforth (1966). "Effect of pH on the kinetics of frog muscle phosphofructokinase." *J Biol Chem* 241(17): 4110-4112.
- Truong, L. H. and S. Pauklin (2021). "Pancreatic Cancer Microenvironment and Cellular Composition: Current Understandings and Therapeutic Approaches." *Cancers (Basel)* 13(19).
- Tsai, F. C., G. H. Kuo, S. W. Chang, *et al.* (2015). "Ca<sup>2+</sup> signaling in cytoskeletal reorganization, cell migration, and cancer metastasis." *Biomed Res Int* 2015: 409245.
- Tsai, H. J. and J. S. Chang (2019). "Environmental Risk Factors of Pancreatic Cancer." *J Clin Med* 8(9).
- Tsujikawa, H., A. S. Yu, J. Xie, *et al.* (2015). "Identification of key amino acid residues responsible for internal and external pH sensitivity of Orai1/STIM1 channels." *Sci Rep* 5: 16747.
- Tsunoda, Y. (1990). "Cytosolic free calcium spiking affected by intracellular pH change." *Exp Cell Res* 188(2): 294-301.
- Tsunoda, Y., E. L. Stuenkel and J. A. Williams (1990). "Characterization of sustained [Ca<sup>2+</sup>]<sub>i</sub> increase in pancreatic acinar cells and its relation to amylase secretion." *Am J Physiol* 259(5 Pt 1): G792-801.
- Ueki, T., M. Toyota, T. Sohn, *et al.* (2000). "Hypermethylation of multiple genes in pancreatic adenocarcinoma." *Cancer Res* 60(7): 1835-1839.
- Ulareanu, R., G. Chiritoiu, F. Cojocar, *et al.* (2017). "N-glycosylation of the transient receptor potential melastatin 8 channel is altered in pancreatic cancer cells." *Tumour Biol* 39(8): 1010428317720940.
- Vachiranubhap, B., Y. H. Kim, N. C. Balci, *et al.* (2009). "Magnetic resonance imaging of adenocarcinoma of the pancreas." *Top Magn Reson Imaging* 20(1): 3-9.
- Valls, C., E. Andia, A. Sanchez, *et al.* (2002). "Dual-phase helical CT of pancreatic adenocarcinoma: assessment of resectability before surgery." *AJR Am J Roentgenol* 178(4): 821-826.
- Van Petegem, F. (2012). "Ryanodine receptors: structure and function." *J Biol Chem* 287(38): 31624-31632.
- Vandecaetsbeek, I., P. Vangheluwe, L. Raeymaekers, *et al.* (2011). "The Ca<sup>2+</sup> pumps of the endoplasmic reticulum and Golgi apparatus." *Cold Spring Harb Perspect Biol* 3(5).
- Vanden Abeele, F., Y. Shuba, M. Roudbaraki, *et al.* (2003). "Store-operated Ca<sup>2+</sup> channels in prostate cancer epithelial cells: function, regulation, and role in carcinogenesis." *Cell Calcium* 33(5-6): 357-373.
- Vander Heiden, M. G., L. C. Cantley and C. B. Thompson (2009). "Understanding the Warburg effect: the metabolic requirements of cell proliferation." *Science* 324(5930): 1029-1033.
- Vangeel, L. and T. Voets (2019). "Transient Receptor Potential Channels and Calcium Signaling." *Cold Spring Harb Perspect Biol* 11(6).
- Vaupel, P., F. Kallinowski and P. Okunieff (1989). "Blood flow, oxygen and nutrient supply, and metabolic microenvironment of human tumors: a review." *Cancer Res* 49(23): 6449-6465.

- Vig, M., C. Peinelt, A. Beck, *et al.* (2006). "CRACM1 is a plasma membrane protein essential for store-operated Ca<sup>2+</sup> entry." *Science* 312(5777): 1220-1223.
- Volpi, M. and R. D. Berlin (1988). "Intracellular elevations of free calcium induced by activation of histamine H1 receptors in interphase and mitotic HeLa cells: hormone signal transduction is altered during mitosis." *J Cell Biol* 107(6 Pt 2): 2533-2539.
- Waddington, C. H. (1975). The evolution of an evolutionist. Edinburgh, Edinburgh University Press.
- Waldmann, R., F. Bassilana, J. de Weille, *et al.* (1997). "Molecular cloning of a non-inactivating proton-gated Na<sup>+</sup> channel specific for sensory neurons." *J Biol Chem* 272(34): 20975-20978.
- Waldmann, R., G. Champigny, F. Bassilana, *et al.* (1997). "A proton-gated cation channel involved in acid-sensing." *Nature* 386(6621): 173-177.
- Walenta, S. and W. F. Mueller-Klieser (2004). "Lactate: mirror and motor of tumor malignancy." *Semin Radiat Oncol* 14(3): 267-274.
- Walenta, S., N. F. Voelxen and W. Mueller-Klieser (2016). "Lactate-An Integrative Mirror of Cancer Metabolism." *Recent Results Cancer Res* 207: 23-37.
- Walenta, S., M. Wetterling, M. Lehrke, *et al.* (2000). "High lactate levels predict likelihood of metastases, tumor recurrence, and restricted patient survival in human cervical cancers." *Cancer Res* 60(4): 916-921.
- Walter, F. M., K. Mills, S. C. Mendonca, *et al.* (2016). "Symptoms and patient factors associated with diagnostic intervals for pancreatic cancer (SYMPTOM pancreatic study): a prospective cohort study." *Lancet Gastroenterol Hepatol* 1(4): 298-306.
- Wang, A., H. Guo and Z. Long (2021). "Integrative Analysis of Differently Expressed Genes Reveals a 17- Gene Prognosis Signature for Endometrial Carcinoma." *Biomed Res Int* 2021: 4804694.
- Wang, H., X. Cheng, J. Tian, *et al.* (2020). "TRPC channels: Structure, function, regulation and recent advances in small molecular probes." *Pharmacol Ther* 209: 107497.
- Wang, L., Z. Fan, J. Zhang, *et al.* (2015). "Evaluating tumor metastatic potential by imaging intratumoral acidosis via pH-activatable near-infrared fluorescent probe." *Int J Cancer* 136(4): E107-116.
- Wang, Y., J. He, H. Jiang, *et al.* (2018). "Nicotine enhances storeoperated calcium entry by upregulating HIF1alpha and SOCC components in nonsmall cell lung cancer cells." *Oncol Rep* 40(4): 2097-2104.
- Warburg, O. (1956). "On the origin of cancer cells." *Science* 123(3191): 309-314.
- Waters, A. M. and C. J. Der (2018). "KRAS: The Critical Driver and Therapeutic Target for Pancreatic Cancer." *Cold Spring Harb Perspect Med* 8(9).
- Webb, B. A., M. Chimenti, M. P. Jacobson, *et al.* (2011). "Dysregulated pH: a perfect storm for cancer progression." *Nat Rev Cancer* 11(9): 671-677.
- Wei, C., X. Wang, M. Chen, *et al.* (2009). "Calcium flickers steer cell migration." *Nature* 457(7231): 901-905.
- Wei, C., X. Wang, M. Zheng, *et al.* (2012). "Calcium gradients underlying cell migration." *Curr Opin Cell Biol* 24(2): 254-261.
- Wes, P. D., J. Chevesich, A. Jeromin, *et al.* (1995). "TRPC1, a human homolog of a Drosophila store-operated channel." *Proc Natl Acad Sci U S A* 92(21): 9652-9656.
- Whitcott, C. J., C. H. Diep, P. Jiang, *et al.* (2015). "Desmoplasia in Primary Tumors and Metastatic Lesions of Pancreatic Cancer." *Clin Cancer Res* 21(15): 3561-3568.
- White, K. A., D. G. Ruiz, Z. A. Szpiech, *et al.* (2017). "Cancer-associated arginine-to-histidine mutations confer a gain in pH sensing to mutant proteins." *Sci Signal* 10(495).
- Whitfield, J. F., A. L. Boynton, J. P. MacManus, *et al.* (1979). "The regulation of cell proliferation by calcium and cyclic AMP." *Mol Cell Biochem* 27(3): 155-179.
- Wicks, E. E. and G. L. Semenza (2022). "Hypoxia-inducible factors: cancer progression and clinical translation." *J Clin Invest* 132(11).
- Wilentz, R. E., J. Geradts, R. Maynard, *et al.* (1998). "Inactivation of the p16 (INK4A) tumor-suppressor gene in pancreatic duct lesions: loss of intranuclear expression." *Cancer Res* 58(20): 4740-4744.
- Wu, H., M. Ying and X. Hu (2016). "Lactic acidosis switches cancer cells from aerobic glycolysis back to dominant oxidative phosphorylation." *Oncotarget* 7(26): 40621-40629.
- Wu, T. C., C. Y. Liao, W. C. Lu, *et al.* (2022). "Identification of distinct slow mode of reversible adaptation of pancreatic ductal adenocarcinoma to the prolonged acidic pH microenvironment." *J Exp Clin Cancer Res* 41(1): 137.

- Wu, Y., B. Gao, Q. J. Xiong, *et al.* (2017). "Acid-sensing ion channels contribute to the effect of extracellular acidosis on proliferation and migration of A549 cells." *Tumour Biol* 39(6): 1010428317705750.
- Xu, L. and I. J. Fidler (2000). "Acidic pH-induced elevation in interleukin 8 expression by human ovarian carcinoma cells." *Cancer Res* 60(16): 4610-4616.
- Xu, Z., Z. Shao, M. Wang, *et al.* (2017). "Expression of transient receptor potential canonical 1 (TRPC1) in tongue squamous cell carcinoma and correlations with clinicopathological features and outcomes." *Int J Clin Exp Pathol* 10:1477-1487.
- Yachida, S., S. Jones, I. Bozic, *et al.* (2010). "Distant metastasis occurs late during the genetic evolution of pancreatic cancer." *Nature* 467(7319): 1114-1117.
- Yachida, S., C. M. White, Y. Naito, *et al.* (2012). "Clinical significance of the genetic landscape of pancreatic cancer and implications for identification of potential long-term survivors." *Clin Cancer Res* 18(22): 6339-6347.
- Yamagata, M., K. Hasuda, T. Stamato, *et al.* (1998). "The contribution of lactic acid to acidification of tumours: studies of variant cells lacking lactate dehydrogenase." *Br J Cancer* 77(11): 1726-1731.
- Yamaguchi, H., J. Wyckoff and J. Condeelis (2005). "Cell migration in tumors." *Curr Opin Cell Biol* 17(5): 559-564.
- Yang, K., Y. Li, G. Lian, *et al.* (2018). "KRAS promotes tumor metastasis and chemoresistance by repressing RKIP via the MAPK-ERK pathway in pancreatic cancer." *Int J Cancer* 142(11): 2323-2334.
- Yang, M. and W. J. Brackenbury (2013). "Membrane potential and cancer progression." *Front Physiol* 4: 185.
- Yang, M., X. Zhong and Y. Yuan (2020). "Does Baking Soda Function as a Magic Bullet for Patients With Cancer? A Mini Review." *Integr Cancer Ther* 19: 1534735420922579.
- Yang, W., J. Zou, R. Xia, *et al.* (2010). "State-dependent inhibition of TRPM2 channel by acidic pH." *J Biol Chem* 285(40): 30411-30418.
- Yao, J., D. Czaplinska, R. Ialchina, *et al.* (2020). "Cancer Cell Acid Adaptation Gene Expression Response Is Correlated to Tumor-Specific Tissue Expression Profiles and Patient Survival." *Cancers (Basel)* 12(8).
- Yao, L., P. Fan, Z. Jiang, *et al.* (2011). "Nav1.5-dependent persistent Na<sup>+</sup> influx activates CaMKII in rat ventricular myocytes and N1325S mice." *Am J Physiol Cell Physiol* 301(3): C577-586.
- Yee, N. S., Q. Li, A. A. Kazi, *et al.* (2014). "Aberrantly Over-Expressed TRPM8 Channels in Pancreatic Adenocarcinoma: Correlation with Tumor Size/Stage and Requirement for Cancer Cells Invasion." *Cells* 3(2): 500-516.
- Yee, N. S., W. Zhou and M. Lee (2010). "Transient receptor potential channel TRPM8 is over-expressed and required for cellular proliferation in pancreatic adenocarcinoma." *Cancer Lett* 297(1): 49-55.
- Yilmaz, M. and G. Christofori (2010). "Mechanisms of motility in metastasizing cells." *Mol Cancer Res* 8(5): 629-642.
- Ying, H., P. Dey, W. Yao, *et al.* (2016). "Genetics and biology of pancreatic ductal adenocarcinoma." *Genes Dev* 30(4): 355-385.
- Yu, A. S., Z. Yue, J. Feng, *et al.* (2018). Regulation of Orai/STIM Channels by pH. Calcium Entry Channels in Non-Excitable Cells. J. A. Kozak and J. W. Putney, Jr. Boca Raton (FL): 161-176.
- Yu, F., L. Sun and K. Machaca (2009). "Orai1 internalization and STIM1 clustering inhibition modulate SOCE inactivation during meiosis." *Proc Natl Acad Sci U S A* 106(41): 17401-17406.
- Zaccagnino, A., C. Pilarsky, D. Tawfik, *et al.* (2016). "In silico analysis of the transportome in human pancreatic ductal adenocarcinoma." *Eur Biophys J* 45(7): 749-763.
- Zamponi, G. W., J. Striessnig, A. Koschak, *et al.* (2015). "The Physiology, Pathology, and Pharmacology of Voltage-Gated Calcium Channels and Their Future Therapeutic Potential." *Pharmacol Rev* 67(4): 821-870.
- Zeng, B., C. Yuan, X. Yang, *et al.* (2013). "TRPC channels and their splice variants are essential for promoting human ovarian cancer cell proliferation and tumorigenesis." *Curr Cancer Drug Targets* 13(1): 103-116.
- Zeng, Y. Z., Y. Q. Zhang, J. Y. Chen, *et al.* (2021). "TRPC1 Inhibits Cell Proliferation/Invasion and Is Predictive of a Better Prognosis of Esophageal Squamous Cell Carcinoma." *Front Oncol* 11: 627713.
- Zhang, L., Q. Lu and C. Chang (2020). "Epigenetics in Health and Disease." *Adv Exp Med Biol* 1253: 3-55.
- Zhang, L., L. Zheng, X. Yang, *et al.* (2022). "Pathology and physiology of acidsensitive ion channels in the digestive system (Review)." *Int J Mol Med* 50(1).

- Zhang, L. Y., Y. Q. Zhang, Y. Z. Zeng, *et al.* (2020). "TRPC1 inhibits the proliferation and migration of estrogen receptor-positive Breast cancer and gives a better prognosis by inhibiting the PI3K/AKT pathway." *Breast Cancer Res Treat* 182(1): 21-33.
- Zhang, Y., X. Lun and W. Guo (2020). "Expression of TRPC1 and SBEM protein in breast cancer tissue and its relationship with clinicopathological features and prognosis of patients." *Oncol Lett* 20(6): 392.
- Zhang, Z., L. Ren, Q. Zhao, *et al.* (2020). "TRPC1 exacerbate metastasis in gastric cancer via ciRS-7/miR-135a-5p/TRPC1 axis." *Biochem Biophys Res Commun* 529(1): 85-90.
- Zhang, Z., R. Zhu, W. Sun, *et al.* (2021). "Analysis of Methylation-driven Genes in Pancreatic Ductal Adenocarcinoma for Predicting Prognosis." *J Cancer* 12(21): 6507-6518.
- Zhang, Z. Y., L. J. Pan and Z. M. Zhang (2010). "Functional interactions among STIM1, Orai1 and TRPC1 on the activation of SOCs in HL-7702 cells." *Amino Acids* 39(1): 195-204.
- Zhong, T., W. Zhang, H. Guo, *et al.* (2022). "The regulatory and modulatory roles of TRP family channels in malignant tumors and relevant therapeutic strategies." *Acta Pharm Sin B* 12(4): 1761-1780.
- Zhou, Y., B. Sun, W. Li, *et al.* (2019). "Pancreatic Stellate Cells: A Rising Translational Physiology Star as a Potential Stem Cell Type for Beta Cell Neogenesis." *Front Physiol* 10: 218.
- Zhou, Z. H., J. W. Song, W. Li, *et al.* (2017). "The acid-sensing ion channel, ASIC2, promotes invasion and metastasis of colorectal cancer under acidosis by activating the calcineurin/NFAT1 axis." *J Exp Clin Cancer Res* 36(1): 130.
- Zhu, S., H. Y. Zhou, S. C. Deng, *et al.* (2017). "ASIC1 and ASIC3 contribute to acidity-induced EMT of pancreatic cancer through activating Ca(2+)/RhoA pathway." *Cell Death Dis* 8(5): e2806.
- Zhu, X., P. B. Chu, M. Peyton, *et al.* (1995). "Molecular cloning of a widely expressed human homologue for the *Drosophila trp* gene." *FEBS Lett* 373(3): 193-198.
- Zitt, C., A. Zobel, A. G. Obukhov, *et al.* (1996). "Cloning and functional expression of a human Ca<sup>2+</sup>-permeable cation channel activated by calcium store depletion." *Neuron* 16(6): 1189-1196.



# Appendices

## Appendix 1

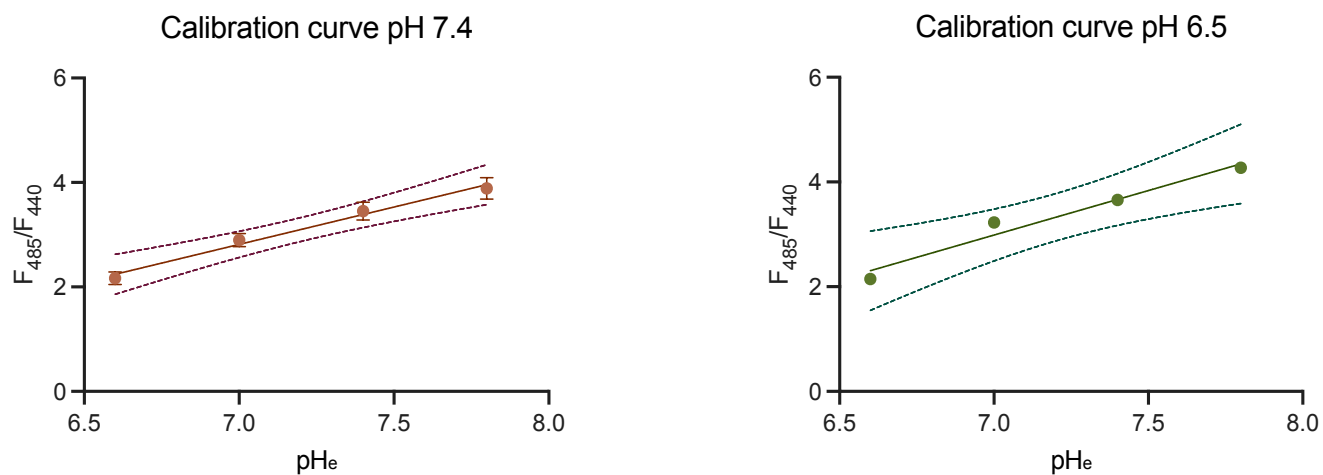


Figure 54. Calibration curve made as described in 'Intracellular pH calibration'. PANC-1 cells grown in either pH 7.4 or pH 6.5 were calibrated with KCl ringers, and  $pH_i$  was calculated by using the slope.

# Effects of the Tumor Environment on Ion Channels: Implication for Breast Cancer Progression



Halima Ouadid-Ahidouch, Hamid Morjani, Julie Schnipper, Alban Girault, and Ahmed Ahidouch

## Contents

1	Introduction .....	2
2	Impact of Tumor Microenvironment on Breast Cancer Hallmarks .....	3
2.1	Extracellular Matrix .....	4
2.2	Impact of Hypoxia on Breast Carcinoma Behavior .....	6
2.3	pH in Mammary Tissue .....	7
3	Dialogue Between Microenvironmental Elements and Ion Channels: Effect on Breast Cancer Hallmarks .....	8
3.1	Collagen Induces Breast Cancer Survival and Migration Through Potassium Channels .....	8
3.2	EGF and TGF- $\beta$ Modulate EMT, Invasion, Migration, and Proliferation Through Potassium, Calcium, and Sodium Channels .....	10
3.3	Involvement of Ion Channels in the Adaptation of Cells to Live in: .....	15
4	Conclusion and Perspectives .....	26
	References .....	27

**Abstract** In recent years, it has been shown that breast cancer consists not only of neoplastic cells, but also of significant alterations in the surrounding stroma or tumor microenvironment. These alterations are now recognized as a critical element for breast cancer development and progression, as well as potential therapeutic targets. Furthermore, there is no doubt that ion channels are deregulated in breast cancer and

---

H. Ouadid-Ahidouch (✉), J. Schnipper, and A. Girault  
Laboratory of Cellular and Molecular Physiology, UR UPJV 4667, University of Picardie Jules Verne, Amiens, France  
e-mail: [halima.ahidouch-ouadid@u-picardie.fr](mailto:halima.ahidouch-ouadid@u-picardie.fr)

H. Morjani  
BioSpecT EA7506, Faculty of Pharmacy, Reims University, Reims, France

A. Ahidouch  
Laboratory of Cellular and Molecular Physiology, UR UPJV 4667, University of Picardie Jules Verne, Amiens, France

Department of Biology, Faculty of Sciences, Ibn-Zohr University, Agadir, Morocco

some of which are prognostic markers of clinical outcome. Their dysregulation is also associated with aberrant signaling pathways. The number of published data on ion channels modifications by the microenvironment has significantly increased last years. Here, we summarize the state of the art on the cross talk between the tumor microenvironment and ion channels, in particular collagen 1, EGF, TGF- $\beta$ , ATP, hypoxia, and pH, on the development and progression of breast cancer.

**Keywords** ATP · Breast cancer · Collagen 1 · EGF · Hypoxia · Ion channels · pH · TGF- $\beta$  · Tumor microenvironment

## Abbreviations

BC	Breast cancer
DDR	Discoidin domain receptor
ECM	Extracellular matrix
EGF	Epidermal growth factor
EGFR	Epidermal growth factor receptor
EMT	Epithelial-to-mesenchymal transition
ER	Endoplasmic reticulum
GSTO1	Glutathione S-transferase omega 1
HIF	Hypoxia inducible factor
MCU	Mitochondrial calcium uniporter
MMP	Metalloproteinase
ROS	Reactive oxygen species
SICE	Store-independent calcium entry
TGF- $\beta$	Transforming growth factor $\beta$
TME	Tumor microenvironment
TNBC	Triple-negative breast cancer
VEGF	Vascular endothelial growth factor

## 1 Introduction

While enormous progress has been made in understanding the genetics of tumors and the fundamental molecular mechanisms involved in tumor progression, it is only in recent years that we have been interested in the role of the tumor microenvironment in cancer development including breast cancer (BC) (Soysal et al. 2015). Breast tissue represents an organ whose stroma plays a very important role in the development of the mammary gland. Indeed, during mammogenesis, the growth of the milk ducts and lobules requires infiltration of the epithelial cells into the surrounding stromal tissue. This mechanism requires remodeling of the microenvironment to allow the growth and migration of epithelial cells in a “similar” manner to an infiltrating tumor. Thus, many processes related to the microenvironment are

deregulated and used by cancer cells during its tumor progression. The tumor microenvironment (TME) communicates and dynamically interacts with cancer cells permanently. It is not surprising that its components are key players in the cancer development and progression. The TME is a dynamic entity composed of stromal cells, including fibroblasts, adipocytes, endothelial cells, and immune cells. Furthermore, it is also composed of extracellular matrix (ECM) which contains soluble factors and adhesive components, which greatly influence cancer progression (Hui and Chen 2015).

The composition and the dynamic of TME in BC have been extensively reviewed (Soysal et al. 2015). However, very little data are reported in the literature concerning the relationship between ion channels and the TME in BC. Ion channels have recently been identified as “new markers” in oncological research. Studies over the last 20 years have clearly shown the contribution of these channels to the aggressiveness of cancer and more and more studies suggest them as key players in interactions between tumor cells and TME through signals’ transduction of cell signaling from the TME (Andersen et al. 2014; Arcangeli et al. 2014; Brucher and Jamall 2014). This review is divided into two parts. The first deals with the effect of the different components of extra cellular matrix (collagen 1, EGF, TGF- $\beta$ , and ATP), hypoxia, and pH on BC progression. The second part will summarize the works that explored the possible involvement of ion channels in the TME-dependent effect on BC.

## **2 Impact of Tumor Microenvironment on Breast Cancer Hallmarks**

In recent decades, several works have underlined the importance of the microenvironment in BC progression (Balkwill et al. 2012; Dias et al. 2019). Indeed, several studies have highlighted the importance of bidirectional communication between tumor cells and their microenvironment in the modulation of their phenotype. The TME consists of stromal cells and ECM components. Stromal cells components include cancer associated fibroblasts (Houthuijzen and Jonkers 2018), cancer associated adipocytes (Attane et al. 2018), immune cells (Tower et al. 2019), and endothelial cells (Hida et al. 2018). ECM consists of adhesion factors, including type 1 and 6 collagens, which are overexpressed in aggressive breast tumors (Phillips et al. 2019). Soluble factors, which correspond to the “secretome” of stromal cells, include among others transforming growth factor- $\beta$  (TGF- $\beta$ ) (Drabsch and ten Dijke 2012; Imamura et al. 2012) and epidermal growth factor (EGF) (De Luca et al. 2008; Masuda et al. 2012). All these factors are involved in cell proliferation, survival, epithelial-to-mesenchymal transition (EMT), migration, invasion, and metastasis.

## 2.1 Extracellular Matrix

One of the components of the breast TME is the ECM, which plays an important role in the regulation of BC progression (Kaushik et al. 2016; Pickup et al. 2014). ECM contains adhesive and soluble factors and among adhesives components, type 1 collagen (collagen 1) is one of important factors that regulates the tumorigenesis, EMT, migration, invasion, metastasis, and response to anticancer therapies (Xu et al. 2019).

### 2.1.1 Collagen 1 and Breast Cancer Cell Phenotype

The collagen superfamily is the major component of this ECM, particularly type 1 collagen, which is the most abundant in several organs such as breast, skin, and lung. Biophysical investigations have given an evidence for different molecular fingerprints for collagen (fiber alignment, stiffness, and density) in breast carcinoma tissues when compared to normal tissues. In fact, analysis of mammographic and particularly collagen density, analyzed by second harmonic generation microscopy (SHG), has shown a relationship between collagen density and BC risk and progression (Boyd et al. 2009; Provenzano et al. 2008). Kakkad et al. have investigated the relationship between lymph node metastasis and the properties of collagen in the primary breast tumors. They demonstrated an increase in collagen density only in primary tumors associated with positive lymph node metastasis (Kakkad et al. 2012). Concerning the collagen stiffness, Stowers et al. have recently shown using the non-malignant MCF-10A epithelial breast cells, that matrix stiffening induces a malignant phenotypic transition and thus could be involved in the acquisition of invasive and metastatic properties in normal epithelial cells (Stowers et al. 2017). Finally, Morris et al. have shown that, in metastatic BC cells, higher collagen density induced an alteration in cell metabolism. Such observed shift was associated with changes in gene expression profile (Morris et al. 2016).

Collagen 1 consists of three subunits, two  $\alpha 1$  chains and one  $\alpha 2$  chain. The combination of these three chains leads to a right triple helix measuring 300 nm long and 1.5 nm in diameter (Mouw et al. 2014). Amino acid sequence of the subunits consists of a Gly-X-Y triplet repeats. X and Y correspond frequently to proline and hydroxyproline, respectively. In addition to its architectural function, collagen 1 also modulates the behavior of surrounding cells by interacting with them *via* specific receptors. The most studied receptors of collagen 1 are  $\beta 1$ -integrin heterodimers ( $\alpha 1\beta 1$ ,  $\alpha 2\beta 1$ ,  $\alpha 10\beta 1$ , and  $\alpha 11\beta 1$ ) (Humphries et al. 2006). Several studies have underlined the importance of integrins in the regulation of cancer stemness, metastasis, and drug resistance (Seguin et al. 2015).  $\alpha 1\beta 1$  and  $\alpha 2\beta 1$  integrins have been reported to mediate invasion in mouse breast tumor cells (Lochter et al. 1999). Kim et al. have demonstrated that collagen is able to induce MMP-2 activation in BC cells and that  $\alpha 2\beta 1$  integrin signaling was involved in this process (Kim et al. 2007). Collagen also activates pro-MMP-2 and estrogen-induced proliferation in human



breast epithelial cells *via*  $\alpha 2\beta 1$  integrin and  $\beta 1$  integrin, respectively (Kim et al. 2007; Xie and Haslam 2008).  $\alpha 2\beta 1$  integrin signaling has been identified as survival pathway in doxorubicin-induced apoptosis in BC cells (Aoudjit and Vuori 2001). The same group demonstrated later, but in other cell models, that such mechanism involves an overexpression of ABCC1/MRP-1 protein which is a member of the large ATP-binding cassette transporters (ABC) family (El Azreq et al. 2012). More recently, Bendas group described a functional role of collagen 1- $\beta 1$  integrin axis in mediated chemoresistance *via* upregulation of ABC transporters in BC cells (Baltes et al. 2020).

Discoidin domain receptors DDR1 and DDR2 have also been reported to interact with collagen 1 (Carafoli and Hohenester 2013; Fu et al. 2013; Leitinger 2014) and to play a role in tumor progression (Rammal et al. 2016; Valiathan et al. 2012). These receptors, which harbor a tyrosine kinase activity, recognize GVMGFO sequence of collagen 1 (Konitsiotis et al. 2008) and exhibit a relatively late and prolonged activation (Vogel et al. 1997). DDR1 seems to be preferentially expressed in luminal-like breast carcinoma, whereas the basal-like one expressed predominantly DDR2 (Saby et al. 2019; Takai et al. 2018). Moreover, the high level of DDR2 expression is associated with high BC grade (Toy et al. 2015). More recently, DDR1 mutations were strongly associated with poor prognosis in estrogen receptor-positive BC (Griffith et al. 2018). However, among the basal-like cell lines, MDA-MB-231 cells are the exception since they express weakly DDR1 and do not express DDR2 (Saby et al. 2019; Juin et al. 2014). It is important to note that as reported by Saby et al., mRNA analysis *in silico* using the Broad-Novartis Cancer Cell Line Encyclopedia (CCLE) showed that 58 BC cell lines were separated into two distinct groups. The first one includes cells with a relatively high level of DDR1 and a low level of DDR2, and is essentially composed of cells with epithelial-like phenotype (E-cadherin) like the MCF-7 cells. The second group includes cells with a low level of DDR1. This group is composed by cells with basal-like phenotype (Vimentin) like the MDA-MB-231 cells which do not express DDR2. The other cell lines harboring basal-like phenotype like MDA-MB-157, MDA-MB-436, and others present an overexpression of DDR2 (Saby et al. 2019). Moreover, Toy et al. have shown for some of those basal-like BC cells, that the low level of DDR1 expression could be compensated by an increase in DDR2 expression (Toy et al. 2015).

Maquoi group was the first to show the role of the collagen/DDR1 axis as a tumor suppressor in breast carcinoma. Indeed, this group showed that the 3D collagen matrix, by activating DDR1, inhibited the proliferation and induced apoptosis in luminal-like MCF-7 and ZR75-1 BC cells (Maquoi et al. 2012). In more recent works, DDR1 has been shown to activate an apoptotic signaling pathway by inducing BIK expression (Assent et al. 2015; Saby et al. 2018). While such phenotype was not observed in MDA-MB-231 cells (Maquoi et al. 2012), enforced expression of DDR1 in these cells restored cell proliferation suppression and apoptosis (Saby et al. 2019). Concerning involvement of DDR2 in BC progression, the first data have been reported by Longmore group, who demonstrated that this receptor was able to enhance invasion and metastasis by stabilizing SNAIL1 (Zhang et al. 2013). Another work has demonstrated that DDR2 not only in tumor cells, but

also in cancer associated fibroblasts, is important for BC metastasis (Corsa et al. 2016). More recent data have shown that DDR2 controls breast tumor metastasis *via* the regulation of the matrix stiffness and integrin signal transduction in cancer associated fibroblasts. Thus, DDR2 has been proposed at a promising target for the treatment of metastatic BC (Grither and Longmore 2018).

### 2.1.2 Cytokines and Growth Factors

Among cytokines and growth factors, TGF- $\beta$  and EGF are respectively important players in BC progression. TGF- $\beta$  is secreted in the extracellular environment by several cell types, including macrophages, T cells, and monocytes. This factor is produced in a latent form until it is activated to interact with its receptors and this activation is highly controlled (Yu and Feng 2019). TGF- $\beta$  has been associated with poor prognosis in patients with BC (de Kruijf et al. 2013). At the functional level, it has been shown recently that this factor plays a crucial role in induction of EMT and invasion in BC cells (Pang et al. 2016). Moreover, inhibition of TGF- $\beta$  has been described to sensitize triple-negative breast carcinoma to chemotherapy (TNBC) (Bhola et al. 2013).

EGF is expressed by several human tissues and promotes a variety of cell phenotypes *in vivo* and *in vitro* (Kajikawa et al. 1991). The paracrine signaling of epidermal growth factor (EGF) and its associated receptor EGFR has been shown to have an important role in driving BC progression and metastasis (Lo et al. 2007; Olsen et al. 2012). While it is known to promote cell proliferation (Wee and Wang 2017), EGF has also been described to have an important role in bone metastasis process (De Luca et al. 2008; Lu and Kang 2010). EGF has also been reported to promote EMT in BC (Kim et al. 2016). Therefore, overexpression of EGFR and its activation by EGF have been depicted to be predictive markers for poor clinical outcome in BC patients (Tischkowitz et al. 2007; Carey et al. 2010).

## 2.2 *Impact of Hypoxia on Breast Carcinoma Behavior*

Because of the weak vascular network associated with the exacerbated proliferation, solid tumors present often a very low oxygen level. Consequently, this generates hypoxia environment in the tumor (Semenza 2012) and particularly in breast carcinoma cells (Gilkes and Semenza 2013). In the context of breast cancer, it has been evaluated that partial pressure of oxygen is almost of 10 mm of mercury (Hg, range from 2.5 to 30 mmHg) compared to 65 mmHg in normal breast tissue. Transcriptomic studies on a large cohort of BC have shown the role of a family of transcription factors, HIF-1 $\alpha$  and HIF-2 $\alpha$  (HIF for hypoxia inducible factors), which are activated under hypoxia conditions, in the regulation of the expression of key genes encoding proteins involved in the various processes of tumor progression (The Cancer Genome Atlas Network 2012). Some of the first works have demonstrated



that upregulation of HIF-1 $\alpha$  was related to tumors and associated metastasis in human breast carcinoma and that this factor was a poor prognosis factor (Schindl et al. 2002; Zhong et al. 1999; Bos et al. 2003). Concerning the stroma matrix receptors which could be involved in metastasis process, a recent work has shown that the fibronectin receptor  $\alpha 5\beta 1$  receptor was overexpressed by activation of HIF-1 $\alpha$  in hypoxic conditions and that this integrin heterodimer was responsible for BC metastasis to lymph nodes and lung (Ju et al. 2017). In other works, the level of HIF-1 $\alpha$  expression has been associated with carcinogenesis process and an increase in proliferation rate of BC (Bos et al. 2001; Schwab et al. 2012). After demonstrating that hypoxia was able to induce vascular endothelial growth factor (VEGF) expression and to initiate angiogenesis (Shweiki et al. 1992), other works reported that HIF-1 $\alpha$  expression in hypoxic conditions was responsible for this effect (Semenza 2000). Drug resistance has also been associated with HIF-1 $\alpha$  expression in hypoxic conditions (Sullivan et al. 2008). Another work has demonstrated that HIF-1 $\alpha$  expression was necessary for drug resistance in BC stem cells (Samanta et al. 2014). Xiang et al. have shown recently that HIF-1 $\alpha$  was involved in the expression of TAZ, one of the matrix stroma sensors, and its recruitment into the nucleus to induced BC stem cell phenotype in hypoxic conditions (Xiang et al. 2014).

### 2.3 *pH in Mammary Tissue*

It has recently been well described how the acidic tumor microenvironment drives cancer progression (Boedtkjer and Pedersen 2020). The tightly regulated pH of cells is important to maintain a cellular homeostasis as chemical processes in the cytoplasm and in cell compartments which require an optimal pH (Andersen et al. 2014; White et al. 2017). The balance between the intracellular (pH<sub>i</sub>) and extracellular pH (pH<sub>e</sub>) is involved in regulating metabolic pathways *via* a fine-tuned balance between proton production and extrusion. The disruption of such balance in tumors is a consequence of the combination of high metabolic demands of cancer cells, in conjunction with poor perfusion and regional hypoxia. The low oxygen environment makes cells undergo a metabolic switch towards a more glycolytic phenotype, thus a higher production of protons (Warburg effect) (Gatenby and Gillies 2008). Excessive proton production induces intracellular acidification and apoptosis (Gottlieb et al. 1996; Damaghi et al. 2013). To compensate the high proton production, cells adapt by increasing the expression and activity of net acid extruders, keeping the intracellular pH normal or slightly alkaline. As a consequence, the microenvironment becomes acidic. A reversed pH gradient is associated with cancer progression, with acidic pH<sub>e</sub> stimulating invasion and migration (Damaghi et al. 2013; Webb et al. 2011; Hanahan and Weinberg 2011) and the slightly alkaline pH<sub>i</sub> promotes cell survival and increased proliferation (Damaghi et al. 2013; Flinck et al. 2018). This ability to sense pH changes in tumors is important for both normal stromal cells and cancer cells to survive. A study carried out by Hashim et al. has shown that BC cell

lines MCF-7 and MDA-MB-231 showed a  $\text{pH}_e$  as low as  $\sim 6.8$  vs  $7.4$  in normal tissue, and a normal or slightly alkaline  $\text{pH}_i$ ,  $\sim 7.4$ – $7.6$  vs  $7.2$  in normal tissue (Hashim et al. 2011). The essential pH regulation in both normal tissue and tumors are maintained by plasma membrane transporters and enzymes, including  $\text{Na}^+/\text{H}^+$  exchanger 1 (NHE1),  $\text{Na}^+/\text{HCO}_3^-$  co-transporters,  $\text{Na}^+$  driven  $\text{Cl}^-/\text{HCO}_3^-$  exchanger, the anion exchangers AE1 and AE2, monocarboxylate transporters (MCT1, MCT2, MCT3, and MCT4), and the V-ATPase (Andersen et al. 2014; Damaghi et al. 2013). Several of these transporters are involved in driving cancer proliferation, migration, and invasion (Boedtkjer and Pedersen 2020; Flinck et al. 2018; Andersen et al. 2016; Ma et al. 2019).

### **3 Dialogue Between Microenvironmental Elements and Ion Channels: Effect on Breast Cancer Hallmarks**

#### ***3.1 Collagen Induces Breast Cancer Survival and Migration Through Potassium Channels***

Although some studies have reported the effect of collagen type 1 or fibronectin on potassium and calcium channels in several cancers (Badaoui et al. 2018; Cherubini et al. 2005; Manoli et al. 2019; Toral et al. 2007), the relationship between matrix proteins and ion channels has been poorly studied in BC. Ouadid-Ahidouch's team has demonstrated a role of a complex composed by Kv10.1 potassium channel, Orai1 channel, and SPCA2 (Golgi ATPase), in signal transduction induced by collagen 1 in BC cells' survival. In non-invasive  $\text{ER}^+$  BC cell lines (MCF-7, T47-D), collagen 1, under free serum culture medium, promotes cell survival through the tyrosine kinase DDR1 receptor but not  $\beta 1$ -integrin (Badaoui et al. 2018). Indeed, collagen 1, by activating DDR1, activates ERK1/2 that increases Kv10.1 and Orai1 expression and activity leading to an increase in the basal calcium entry independently of the reticular stores (store-independent calcium entry, SICE) that activates the ERK pathway that, in turn, promotes the expression of the oncogene c-Myc leading therefore to cell survival. Peretti et al. (2019) deeply demonstrated how collagen 1 favors the interaction of the complex Kv10.1/Orai1 and SPCA2. Collagen 1 increases the plasma membrane fraction of Kv10.1 and Orai1 channels and promotes their co-localization and interaction with SPCA2 in the lipid rafts. SPCA2 is indispensable to both Orai1 and Kv10.1 trafficking to plasma membrane in the presence of collagen 1. Silencing of SPCA2 induces Orai1 retention in the cytoplasmic compartment and in the Golgi for Kv10.1. Moreover, Kv10.1, Orai1, SPCA2, and DDR1 are highly expressed and co-localized in aggressive BC tissues, while in non-tumor samples, these proteins are less expressed at the plasma membrane and the expression of Kv10.1 is restricted to the Golgi (Peretti et al. 2019).

Collagen 1 is also involved in BC aggressiveness. Collagen fiber alignment facilitates persistence by limiting cell protrusions, thus promoting cell migration and invasion (Riching et al. 2014), and redirect cell migration to move only in one direction (Ray et al. 2017). Basal-like BC MDA-MB-231 cells possess a high metastatic capacity and they also expressed Kv10.1 channel that regulates cell migration through two mechanisms: (1) by regulating calcium entry through Orai1 channels (Hammadi et al. 2012) and (2) by interacting with  $\beta$ 1-integrin and focal adhesion kinase (Ouadid-Ahidouch et al. 2016). The extracellular matrix through fibronectin and collagen 1 also positively modulates Kv10.1-dependent cell migration. The MDA-MB-231 cell line adopts a more elongated morphology and increased migration rate when growing on double coating with fibronectin and collagen 1. Several studies have also shown that fibronectin is able to increase potassium Kv11.1 channel activity, which is part of the same subfamily as Kv10.1 in the neuroblastoma and colorectal cancers (Cherubini et al. 2005; Crociani et al. 2013). In BC, fibronectin could increase both the interaction and the co-localization of Kv10.1 with  $\beta$ 1 integrin (unpublished data).

### 3.1.1 Stiffness, Mechanosensitive Ion Channels, and Breast Cancer

Malignant tumor extracellular matrix is often stiffer than the matrix surrounding adjacent non-malignant cells (Ingber 2008) and such pressures could stimulate mechanosensitive ion channels (Petho et al. 2019). Functional expression of Piezo channels has been described in BC cell lines (Li et al. 2015), and their relevance to BC has just been investigated recently. Piezo 1 is functional in MCF-7 BC cell line but not in MCF-10A normal mammary epithelial cell line. Pharmacological blockade of this channel reduced cellular motility of MCF-7 but not that of MCF-10A cells (Li et al. 2015). Moreover, BC patients with high Piezo1 mRNA levels showed a shorter overall survival when compared to those showing low Piezo1 expression levels (Li et al. 2015). Recently, in brain metastatic BC cell line MDA-MB-231-BrM2, Valverde's team has clearly reported that calcium influx *via* Piezo2 regulates cell migration by regulating the cytoskeleton organization through the RhoA-mDia pathway (Pardo-Pastor et al. 2018). Lou et al., by using the "Atlas database analysis," identified a decreased Piezo2 expression in BC compared with normal control tissues (Lou et al. 2019). They also investigated the relation between Piezo2 expression level and the overall survival of patients, and they found that high expression of this channel is correlated to a favorable prognosis in BC. Moreover, the expression of Piezo2 is potentially targeted by five miRNAs and correlated with the downregulation of 109 genes enriched in Hedgehog signaling pathway, including regulated cell adhesion molecules downregulated by oncogenes (Lou et al. 2019).

The mechanoreceptor TRPM7 has been shown to reduce the cytoskeletal tension through Myosin II activity in MDA-MB-231 cell line (Kuipers et al. 2018; Guilbert et al. 2013). Silencing of TRPM7 or its pharmacological inhibition, by waixenicin A, increased cytoskeletal tension likely through reducing SOX4 expression. Moreover,



the increase of matrix stiffness (in a collagen coating model) decreased both the expression of TRPM7 and SOX4. They also found that both the mRNA expression of SOX4 and TRPM7 are positively correlated with primary breast tumor samples. The authors suggested SOX4 as a downstream transcriptional target of TRPM7 signaling in mesenchymal-type BC cell lines (Kuipers et al. 2018).

To our knowledge, only one study has reported on the involvement of voltage-activated T-type calcium channels in MCF-7 BC cell proliferation (Basson et al. 2015) in relation with matrix density. The increase of extracellular pressure up to 40 mmHg activates T-type calcium channel (Cav3.3) leading to calcium influx and activation of PKC- $\beta$ , which in turn activates NF- $\kappa$ B (Basson et al. 2015).

### ***3.2 EGF and TGF- $\beta$ Modulate EMT, Invasion, Migration, and Proliferation Through Potassium, Calcium, and Sodium Channels***

#### **3.2.1 EGF**

Abnormal expression and activity of EGF and EGFR promote EMT in cancer cells through ERK1/2 and PI3K/Akt pathways, which are involved in proliferation, metastasis, and invasion (Thiery 2002; Ellerbroek et al. 2001; Grunert et al. 2003). It has previously been shown that EGF, EGFR, and the phosphorylation of its tyrosine residues modulate the activity of ion channels (Levitan 1994), including potassium (Bowlby et al. 1997; Zhang et al. 2011; Peppelenbosch et al. 1991), calcium (Peppelenbosch et al. 1991, 1992), chloride (Jeulin et al. 2008), and voltage-gated sodium channels (Fraser et al. 1638). Tyrosine kinases and phosphatases regulate the function ion channels activities that are involved in cancer proliferation, migration, invasion, and apoptosis (Davis et al. 2001; Azimi and Monteith 2016). These pathways are associated with EMT, induced by EGF and EGFR. Furthermore, several studies have identified that EMT induces changes in the expression and activity of different plasma membrane ion channels including potassium, calcium, and sodium, which will in turn regulate tumor invasion (Azimi and Monteith 2016).

The calcium-activated potassium channel  $K_{Ca}3.1$  (SK4) has been studied in several types of cancer including BC (Zhang et al. 2016). A blockage of SK4 has shown to inhibit proliferation and promote apoptosis in MDA-MB-231 cells. Furthermore, it has been shown that MDA-MB-231 and MDA-MB-468 cell lines can undergo EMT mediated by EGF/basic fibroblast growth factor (bFGF), whereas MCF-7 and T47D cells are not able to undergo EMT at all (Zhang et al. 2016). In addition, in MDA-MB-231 cells (harboring the most significant mesenchymal phenotype compared to other cell lines) the mRNA expression of SK4 is upregulated, and the decrease of SK4 channel expression downregulates the expression of the mesenchymal markers Vimentin and SNAIL1. The authors concluded that the expression of SK4 is associated with EGF/bFGF-induced EMT and that it might drive both the EMT and migration process in TNBC cells (Zhang et al. 2016).

It is well studied that remodeling of calcium permeable channels, their expression, and  $\text{Ca}^{2+}$  signaling are linked to EMT, and that they promote the expression of several proteins associated with cells transforming to a more mesenchymal phenotype (Azimi and Monteith 2016). The Monteith's team has deeply investigated the role of  $\text{Ca}^{2+}$  during the EMT process in BC cells (Davis et al. 2012, 2013, 2014). They have observed that treatment with EGF increases EMT markers as Twist, SNAIL1, and Vimentin in MDA-MB-468 cells and have identified specific channels involved in  $\text{Ca}^{2+}$  remodeling as regulators of EMT induced by EGF (Davis et al. 2012, 2014). TRPM7 is involved in EGF-mediated EMT by enhancing Vimentin protein expression. Furthermore, TRPM7 silencing results in a reduction of the EGF induced STAT-3 phosphorylation, but does not alter the cytosolic  $\text{Ca}^{2+}$  response induced by EGF (Davis et al. 2014). In another study, the same authors found not only a higher expression of EMT related markers, but also an increased expression of Orai1 and  $\text{Ca}^{2+}$  entry. In this study, they found that EGF-induced EMT in MDA-MB-468 cells is associated with reduced agonist-stimulated and store-operated  $\text{Ca}^{2+}$  influx. It is known that both Orai1 and TRPC1 maintain the constitutive  $\text{Ca}^{2+}$  influx, but here it has been shown that only Orai1, and not TRPC1, is associated with EGF-mediated EMT (Davis et al. 2012). Orai1 silencing inhibited non-stimulated  $\text{Ca}^{2+}$  influx, agonist-stimulated, and store-operated  $\text{Ca}^{2+}$  influx, whereas the silencing of TRPC1 only inhibited non-stimulated  $\text{Ca}^{2+}$  influx, but in a manner dependent on Orai1 (Davis et al. 2012). This suggests that the altered activity of Orai1 and TRPC1 plays a role in EGF-mediated EMT. In addition, TRPC1 silencing has been shown to be associated with a significant reduction in ERK1/2 signaling function, showing that TRPC1 is involved in proliferation. Ouadid-Ahidouch's team has also reported the involvement of TRPC1 in MCF-7 cell proliferation induced both by EGF and the activation of the calcium sensing receptor (CaSR). Indeed, CaSR stimulation by extracellular  $\text{Ca}^{2+}$  ( $[\text{Ca}^{2+}]_o$ ) (1.4–5.0 mM) increases TRPC1 expression, *via* ERK1/2 activation, and calcium influx leading to cell proliferation (El Hiani et al. 2009a). Additionally, cell proliferation is also obtained through a subsequent EGFR transactivation consecutive to CaSR activation in these cells (El Hiani et al. 2009b). In fact, both inhibitors of EGFR kinase (AG1478) and MMP (GM6001) reduce ERK1/2 activation, TRPC1 overexpression, and cell proliferation induced by  $[\text{Ca}^{2+}]_o$ . These data indicate the role of the CaSR-EGFR and ERK axis in response to extracellular calcium concentration in tumor environment of BC (Kadio et al. 2016).

Davis et al. have found that EMT in BC is also associated with the altered gene expression of specific endoplasmic reticular (ER) calcium channels and pumps (Davis et al. 2013). The expression of the ER channels inositol 1,4,5-triphosphate receptor  $\text{IP}_3\text{R1}$ ,  $\text{IP}_3\text{R3}$ , and ryanodine receptor RYR2 has been shown to be upregulated in EGF-treated MDA-MB-468 cells when compared to the non-treated cells. Under the same conditions, the ER pump SERCA2 is significantly upregulated, whereas the SERCA3 is downregulated. This suggests that EGF-induced EMT in BC induces changes in the expression of ER channels and pumps and thereby storage and  $\text{Ca}^{2+}$  signaling (Davis et al. 2013).

Voltage-gated sodium ( $\text{Na}_v$ ) channels are widely expressed in metastatic cells of different types of cancer, including BC (Roger et al. 2015; Onkal and Djamgoz 2009; Fraser et al. 2005).  $\text{Na}_v1.5$  is upregulated in BC, which promotes invasion and metastasis phenotype (Roger et al. 2015; Gonzalez-Gonzalez et al. 2019a; Brackenbury 2012). Recently, it has been shown that  $\text{Na}_v1.5$  channels are involved in EGF-induced EMT. EGF induces both the expression and activity of  $\text{Na}_v1.5$  in MDA-MB-231 cells (Gonzalez-Gonzalez et al. 2019a). Furthermore, the mobility of MDA-MB-231 cells is increased when induced with EGF through the functional expression of  $\text{Na}_v1.5$ . It can be suggested that  $\text{Na}_v1.5$  channels are not acting alone during cell migration induced with EGF. As the activation of  $\text{Na}_v1.5$  depolarizes the plasma membrane, other ion transporters could be activated by this environmental modification such as NHE or chloride channels (Gonzalez-Gonzalez et al. 2019a). In addition, the influx of  $\text{Na}^+$  through  $\text{Na}_v1.5$  channels stimulates the activity of NHE1, resulting in a higher proton extrusion, acidifying the extracellular environment, and thus activating metalloproteinases, which can promote the invasive and migratory capacity of cells (Gonzalez-Gonzalez et al. 2019a; Brisson et al. 2011; Gillet et al. 2009). Disrupting the homeostasis of ions as  $\text{Na}^+$ ,  $\text{Ca}^{2+}$ , and  $\text{H}^+$  could potentially activate protein kinases and downstream pathways that affect migration, invasion, or proliferation (Gonzalez-Gonzalez et al. 2019a). Rho family GTPase, Rac1 has been shown to be involved in migration by regulating cytoskeletal rearrangement and lamellipodia formation (Yang et al. 2019).  $\text{Na}_v1.5$ -dependent plasma membrane depolarization leads to Rac1 co-localization with phosphatidylserine and thereby activation. The activation of Rac1 in MDA-MB-231 cells results in lamellipodial protrusion formation, migration, and thereby a more invasive phenotype (Yang et al. 2019).

The sodium content has shown to be higher in mammary adenocarcinomas than in normal lactating mammary epithelium (Amara et al. 2016; Sparks et al. 1983), even though it is not clear if tumor functions are correlated with the extra- or intracellular sodium concentration (Amara et al. 2016). Recently, it has been shown that treatment with NaCl and pro-inflammatory interleukin 17 (IL-17) has a synergistic inflammatory effect on the growth in BC cell lines. This treatment also enhanced the production of reactive nitrogen and oxygen (RNS/ROS) species, which correlated with an upregulation of the epithelial sodium channel (ENaC) expression level in various BC (Amara et al. 2016; Blaug et al. 2001; Boyd and Naray-Fejes-Toth 2007). Treatment with NaCl, IL-17, and knockdown of ENaC reduce RNS/ROS species production. Furthermore, the same treatment enhances expression and phosphorylation of ERK1/2 in MDA-MB-231 cells. These data suggest that ENaC plays a role in proliferation through downstream ERK1/2 signaling and in the inflammatory process in BC (Amara et al. 2016).

### 3.2.2 TGF- $\beta$

Transforming growth factor beta (TGF- $\beta$ ) is another EMT inducer *via* the canonical or the non-canonical pathways in epithelial cells (Dumont and Arteaga 2000;



Muraoka et al. 2002). Cell calcium entry, especially upon store depletion, is also involved in TGF- $\beta$ -induced EMT by promoting cellular migration and potentially leading to metastasis. TGF- $\beta$  treatment is known to increase migration, calpain activity, expression of EMT markers (Vimentin, N-cadherin) and decrease expression of epithelial markers (E-cadherin) in NMuMG and MDA-MB-231 cells (Schaar et al. 2016). TGF- $\beta$ -treatment increases store-mediated  $\text{Ca}^{2+}$  entry, *via* TRPC1 / STIM1 that activates calpain leading to migration, a loss of E-cadherin and MMP activation. Silencing of TRPC1 or STIM1, or using pharmacological inhibition of SOCE (SKF-96365) decreased TGF- $\beta$  induced  $\text{Ca}^{2+}$  current, and inhibited calpain activation and cell migration (Schaar et al. 2016). Moreover, the overexpression of TRPC1 increases  $\text{Ca}^{2+}$  entry and promotes TGF- $\beta$ -mediated cell migration. TGF- $\beta$  affects more the activity of TRPC1/STIM1 but neither the expression of STIM1 nor that of Orai1. TGF- $\beta$  also suppresses cell proliferation of both MDA-MB-231 and MCF-7 cells by inducing cell cycle arrest at the G0/G1 phase by accumulating p21 and reducing cyclin E expression (Cheng et al. 2016). These effects are calcium dependent since they are altered by EGTA or by pharmacological inhibition of SOCE. Treatment of MDA-MB-231 cells with TGF- $\beta$  decreases both STIM1 expression and thapsigargin-induced calcium entry. Moreover, stably STIM1 overexpressing in MDA-MB-231 cells suppresses the TGF- $\beta$ -induced effects. TGF- $\beta$  increases the expression of the transcriptional inhibitory factor of STIM1 (Wilms' tumor suppressor 1, WT1). Silencing of WT1 restores the expression of STIM1 in the presence of TGF- $\beta$ . Moreover, both TGF- $\beta$  and thapsigargin increased ERK1/2 phosphorylation and pharmacological inhibition of SOCE reduces the TGF- $\beta$ -induced ERK phosphorylation (Cheng et al. 2016). Hu et al. have found that TGF- $\beta$ -induced EMT through downregulating of Oct4 that upregulates STIM1 and Orai1 expression leading to an increase in SOC entry (Hu et al. 2011).

Recently, Figiel and co-workers have proposed a new mechanism involving three partners Zeb1 (EMT transcription factor), SK3 channel, and calcium influx, probably through SOC channels, in the regulation of prostate cancer cell migration stimulated by TGF- $\beta$  (Figiel et al. 2019). They showed that TGF- $\beta$  increases the expression of Zeb1 and SK3 channel, which lead to calcium influx and migration. The expression of Zeb1 by TGF- $\beta$  is dependent on calcium influx and Zeb1 controls the transcriptional activity of the SK3 channel gene. Moreover, both linoleic acid and eicosapentaenoic acid inhibit the migration induced by TGF- $\beta$  likely by disrupting lipid raft SK3- $\text{Ca}^{2+}$  channels complexes.

### **3.2.3 ATP, *via* Purinergic Receptors, Regulates Proliferation, Invasion, Migration, and EMT**

ATP is a nucleotide firstly known to provide energy to different biological processes in living cells. In physiological conditions, intracellular ATP rate (5–10 mM) is relatively high when compared to extracellular medium (10–100 nM) (Gilbert et al. 2019). However, this balance is totally changed in case of cancer. Indeed, real-time extracellular ATP concentration monitoring showed that it could reach hundreds of

millimolar in the tumor microenvironment (Falzoni et al. 2013; Pellegatti et al. 2008). Cell damage as well as non-lytic pathways has been reported to explain the high extracellular ATP rate. Among these pathways, vesicular exocytosis and ATP efflux through ATP release channels and nucleotide transporters have been reported (Yegutkin 2008). Otherwise, the involved cells are both infiltrating inflammatory cells and tumor cells in response to inflammation, hypoxia, or to some therapies.

Extracellular ATP is sensed at P2 purinergic receptors. Burnstock and Kennedy (Kennedy and Burnstock 1985) have proposed the distinction between P2X and P2Y receptors based on pharmacological criteria. Cloning and transduction mechanisms led to the nomenclature of P2X ionotropic ligand-gated ion channel receptors and P2Y metabotropic G protein-coupled receptors (Burnstock 1996). Seven subunits (named P2X1-7) assemble as homo- or hetero-trimers to form the channel of P2X receptors. ATP is the physiologic agonist of these receptors whose activation results in the alteration of cytosolic calcium concentration. On the other hand, there are eight isoforms of P2Y receptors named P2Y1 & 2; P2Y4 & 6; and P2Y11-14. They differ from each other by the nature of their agonists and by the signal transduction pathways that their activation triggers. Indeed, P2Y1 & 2; P2Y4 & 6 are coupled to a  $G_q$  protein that, in turn, activate a phospholipase  $C\beta$ , while P2Y12-14 is coupled to a  $G_i$  protein that inhibits the adenylyl cyclase. Among the  $G_q$  coupled subfamily, P2Y2 is the only ATP-active isoform. It is also considered UTP equally active. ADP, UTP, and UDP are respectively the preferred ligands of the P2Y1, P2Y4, and P2Y6 isoforms. Among the  $G_i$  coupled subfamily, ADP is the preferred ligand of P2Y12&13 while P2Y14 is activated by sugar nucleotides such as UDP-glucose and UDP-galactose. P2Y11 is a special case in that it is coupled to both a  $G_q$  and a  $G_s$  protein, thus when activated by ATP it results in an increase of intracellular calcium and cAMP concentrations (Di Virgilio 2012).

The effect of ATP depends on its concentration in the extracellular medium and the panel of P2 receptors expressed in tumor and/or stromal cells. In MCF-7 BC cells, all P2Y receptors are expressed but not all the P2X isoforms. Indeed, P2X1 and P2X3 transcripts are not expressed. Moreover, the transcript profile shows a relative strong expression of P2X4 when compared to P2X2 & 5. P2X6 & 7 are not significantly expressed. When exposed to 30  $\mu\text{M}$   $[\text{ATP}]_o$ , MCF-7 shows a 50 pA inward current, which seems to be a P2X-like current. Extracellular ATP treatment does not significantly affect cell death or proliferation. However, cell migration is increased. As assessed by specific siRNA and the use of different inhibitors, ATP-induced migration results in the activation of the nucleotide on P2Y2 receptor leading to an increase in  $[\text{Ca}^{2+}]_{\text{cyt}}$  and subsequent activation of MEK pathway (Chadet et al. 2014).

Highly invasive MDA-MB-435s BC cell line expresses P2X4, P2X5, P2X6, and P2X7. However, P2X7 isoform is by far the most expressed and seems to be the only active form. Furthermore, in MDA-MB-435 cells, millimolar concentrations of ATP activate an inward current, leading to an increase in  $[\text{Ca}^{2+}]_{\text{cyt}}$ . P2X7R activation regulates MDA-MB-435s apoptosis, migration, and invasiveness. Indeed, ATP concentrations over 3 mM result in significant cell death that is inhibited both by KN62 and A740003 P2X7R inhibitors. Additionally, millimolar ATP exposition

induces elongation of “Neurite-like” MDA-MB-435s prolongations, which are hallmarks of a migratory cell profile. The ATP induces regulation cell migration through activation of SK3 potassium channels by the calcium-induced influx. P2X7R activation is also involved in MDA-MB-435s cell invasiveness in a dose-dependent manner both in vitro and in vivo through regulating cathepsin B active forms (Jelassi et al. 2011).

Recently, Maffey et al. (2017) reported that mesenchymal stem cells from tumor microenvironment promote BC stem cell proliferation, and metastasis through purinergic signaling. Such processes take place through exosomes and microvesicles that increase cytosolic calcium concentration. A significant increase in cell responsiveness is observed when exogenous ATP is added to the cells. In these cells, ATP acts through P2X ionotropic receptors as assessed by P2X inhibition experiments. Indeed, P2X7 inhibition by A438079 leads to a significant decrease in cell metabolism activity and cell growth. Moreover, ATP depletion in the extracellular medium leads to a significant decrease in BC cell invasiveness.

ATP action is modulated by other factors present in tumor microenvironment such as EGF (Davis et al. 2011). Davis et al. have shown that EGF induces changes in response to ATP in MDA-MB-468 BC cells. Indeed, in the presence of ATP, EGF induces a significant change in the calcium profile and expression of EMT markers such as Vimentin. Analysis of purinergic receptors has shown that P2X5 isoform is upregulated (4.6-folds) in the presence of EGF. Upregulation of this isoform is confirmed (13-folds) in mesenchymal-like BC cells when compared to epithelial-like cells. Moreover, P2X5 knockdown leads to a decrease in Vimentin which remains significant despite its weak expression (Davis et al. 2011).

A synthetic presentation of the different actors previously described is reported in Table 1 and in Figs. 1 and 2.

### ***3.3 Involvement of Ion Channels in the Adaptation of Cells to Live in:***

#### **3.3.1 Hypoxic Conditions**

As depicted previously, hypoxia is an important feature of the tumor microenvironment, which promotes, e.g., BC adaptation, resistance, and aggressiveness. In addition, hypoxia regulates different parameters of the tumor microenvironment like angiogenesis, extracellular matrix composition, or stromal cells' functions. However, underlying mechanisms are not yet clearly defined. Among the numerous tracks currently explored, ion channels could be good candidates due to their involvement in multiple tumor processes and their membrane localization. Indeed, a large information panel is already available regarding their role in the response to oxygen variations in the cardiovascular and neuronal system but few elements are evaluated in tumor context.



**Table 1** Ion channels involved in the dialogue with microenvironment: links to matrix, EGF, TGF- $\beta$ , and ATP

Channel family	Type/name	Involved in cancer progression by	Signaling pathway	References
Potassium channels	Kv10.1	Survival induced by collagen 1	DDR1, ERK phosphorylation, increased expression and membrane fraction of Kv10.1 and Orai1, increased co-localization of Kv10.1 and Orai1 through SPCA2, increased SICE, increased $[Ca^{2+}]_i$ , increased c-Myc expression and cell survival	Badaoui et al. (2018), Peretti et al. (2019)
	Kv10.1	Migration induced by fibronectin and collagen 1	Increasing co-localization and interaction between Kv10.1 and $\beta$ 1-integrin	Unpublished Personal data
	SK4, KCa3.1	EMT induced by EGF/bFGF	Increased Vimentin and snail mRNA expression	Zhang et al. (2016)
Orai and TRP	Orai1 & TRPC1	EMT induced by EGF	Reduced non-stimulated and agonist-stimulated, $Ca^{2+}$ entry through Orai1 and TRPC1	Davis et al. (2012)
	TRPC1	MDA-MB-468 cell proliferation	ERK1/2 phosphorylation, cell proliferation	Davis et al. (2012)
	TRPM7	Maintains BC mesenchymal phenotype/response to matrix rigidity	Increased cytoskeletal tension through reducing SOX4 expression	Kuipers et al. (2018)
	TRPC1	TGF- $\beta$ -induced EMT	Increased store-mediated $Ca^{2+}$ entry, activation of calpain, loss of E-cadherin, and MMP activation	Schaar et al. (2016)
	Orai1 and STIM1	TGF- $\beta$ -induced EMT	Inhibition of Oct4 expression that upregulates STIM1 and Orai1 expression leading to increase SOC	Hu et al. (2011)
	TRPM7	EGF-induced EMT	Increased Vimentin expression along with STAT3 activation	Davis et al. (2014)
PIEZO	PIEZO1	Cellular motility	Silencing of PIEZO 1 reduces cell motility	Li et al. (2015)
	PIEZO2	Migration	Regulating the cytoskeleton organization through the RhoA-mDia pathway	Pardo-Pastor et al. (2018)
Sodium channels	Nav1.5	Increased migration induced by EGF	EGF increased Nav1.5 expression	Gonzalez-Gonzalez et al. (2019b)
	Nav1.5	Increased migration	Depolarization of the resting $V_m$ ( $Na^+$ -dependent) that increases Rac activation	Yang et al. (2019)

(continued)

**Table 1** (continued)

Channel family	Type/name	Involved in cancer progression by	Signaling pathway	References
Others				
STIM	STIM1	TGF- $\beta$ inhibiting cell proliferation	Increased expression of Wilms' tumor suppressor 1 (WT1), reduction of STIM1 expression, reduction of SOCE, reduction or ERK phosphorylation, increased P21 expression and reduction of cyclin E expression, cell cycle arrest in G0-G1 phase	Cheng et al. (2016)
ER intracellular calcium transporters	IP3R RYR SERCA	EMT induced by EGF	A high increase of RYR2 expression A slight increase in IP <sub>3</sub> R1 and IP <sub>3</sub> R3 and SERCA2 expression A decrease of expression of SERCA3	Davis et al. (2013)
P2X ionotropic ligand-gated ion channel	P2X7	Growth Proliferation Mammosphere formation Spheroid size Invasion	Stimulate invasiveness through P2X7, enhancing Ca <sup>2+</sup> and Na <sup>+</sup> influx and K <sup>+</sup> efflux	Maffey et al. (2017)
	P2X5	EMT	Potentiate the EGF-induced Vimentin protein expression and reduced E-cadherin expression	Davis et al. (2011)

Some reports described the involvement of Ca<sup>2+</sup> signaling in response of BC cells to hypoxia. It has been previously described that hypoxia could induce EMT (Gonzalez and Medici 2014). In fact, Davis et al. demonstrated that Ca<sup>2+</sup> chelation reduces the hypoxia-induced EMT in MDA-MB-468 cells (Davis et al. 2014). By deciphering the putative molecular support, they analyzed the role of TRPM7 channel but they could not demonstrate that this channel is involved in the modulation of the [Ca<sup>2+</sup>]<sub>cyt</sub> even though it participates to the regulation of EMT markers.

Works from the Monteith's lab brought information about other calcium channels involved in the response of BC cells to hypoxia. In fact, TRPC1 seems to be involved in hypoxia-mediated events (Azimi et al. 2017). More precisely, hypoxia increases TRPC1 mRNA expression that regulates SNAIL and Claudin 4 expression and participates to the regulation of EGFR and STAT3 phosphorylation. In addition, TRPC1 is also involved in autophagy process through the EGFR pathway. In a recent study, the same group demonstrated that BC molecular subtypes present different calcium channel expression profile. Accurately, they showed that Orai3 channel is more specific to luminal cell type compared to Orai1, which is mostly

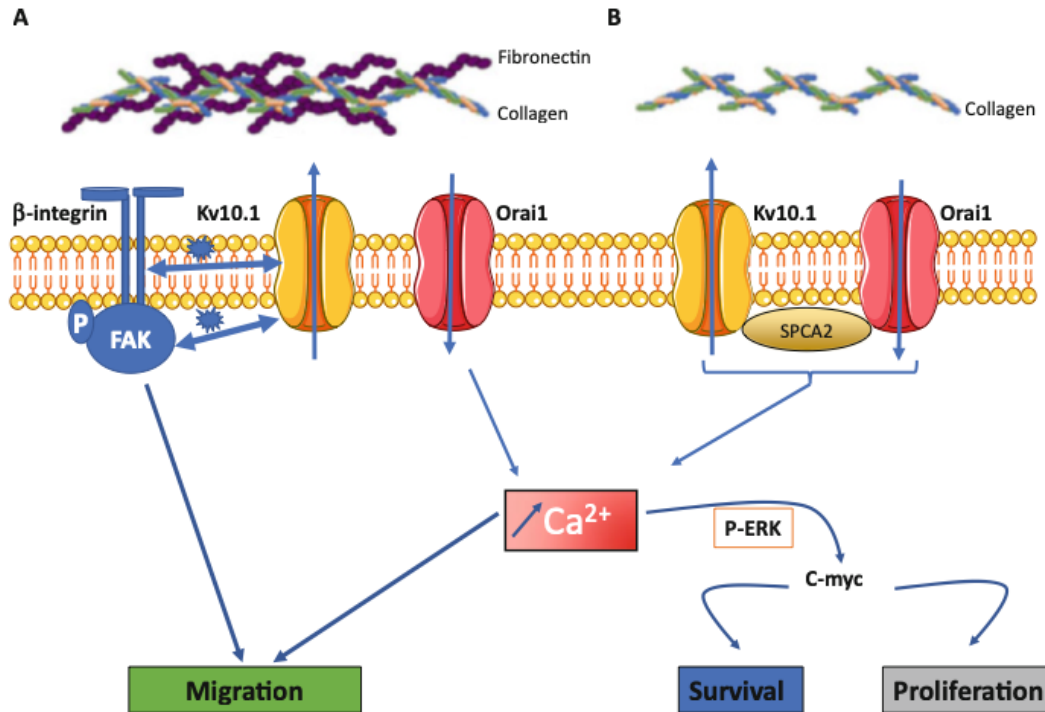


**Fig. 1** Schematic illustration of ion channels, involved in collagen 1-induced effects in breast cancer. (a) Effect of collagen and fibronectin on cell migration in the highly metastatic MDA-MB-231 breast cancer cell line. (b) Effect of collagen on the survival and proliferation in the non-invasive MCF-7 breast cancer cells

expressed and active in the basal cell type (Azimi et al. 2019). They further analyzed Orai3's involvements in hypoxia and they demonstrated that: (1) Orai3's expression is increased in hypoxia through HIF-1 $\alpha$  pathway; (2) this channel is not involved in the regulation of EMT markers' expression; (3) Orai3 regulates EGFR autophosphorylation without any effect on migration; (4) it participates to the hypoxia regulation of migration and to the inflammatory/immune response gene profile.

In a similar manner, Liu and collaborators demonstrated that Orai1 is also involved in the response to hypoxia (Liu et al. 2018). More precisely, they showed that Orai1 is involved in a Notch1 signaling pathway associated with a store-operated  $\text{Ca}^{2+}$  entry and NFAT4 to participate to the aggressiveness of TNBC cells. Intracellular  $\text{Ca}^{2+}$  transporters could also be involved in the TNBC phenotype. Indeed, it has been shown that mitochondrial calcium uniporter (MCU) could regulate the HIF-1 $\alpha$  pathway, and subsequent expressed genes, as well as the ROS production, participating to the metastatic processes (Tosatto et al. 2016). The results of this study suggest that MCU could be an actor in the response to hypoxia.

It is now clearly established that hypoxia also promotes resistance to therapy (Yeldag et al. 2018). In this context, Lu et al. demonstrated that  $[\text{Ca}^{2+}]_{\text{cyt}}$  concentration is increased by carboplatin treatment in a TNBC model (Lu et al. 2017). More precisely, glutathione S-transferase omega 1 (GSTO1), which is regulated by



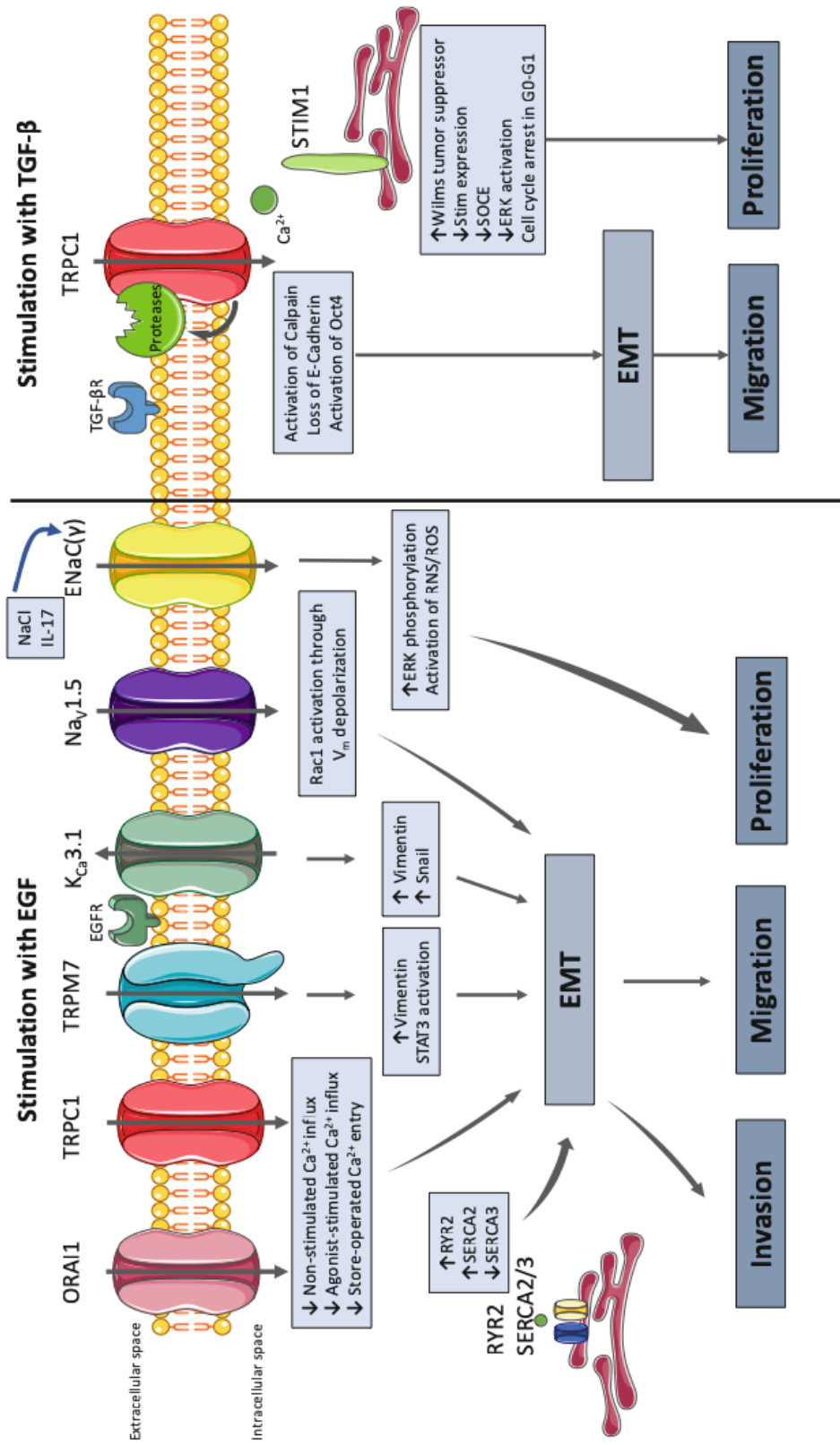


**Fig. 2** Ion transporters regulation by EGF and TGF-β and conferring breast cancer invasion, migration, and proliferation. Black arrows indicate the sequence of events for each channel type. See text for details. Green color indicates SERCA2 and 3 and STIM1 that are located in the ER

HIF-1 $\alpha$  and HIF-2 $\alpha$  and whose expression is increased by carboplatin, interacts with RyR1 and promotes Ca<sup>2+</sup> release from the internal store. The Ca<sup>2+</sup> raise activates the PYK2-SRC-STAT3 pathway promoting the BC stem cell phenotype and induces consequently chemoresistance. In a similar way, it has been shown that TRPC5, which is overexpressed in Adriamycin-treated MCF-7 cells, participates to the VEGF secretion regulation through a HIF-1 $\alpha$  pathway suggesting an involvement of this channel in the cell response to hypoxia (Zhu et al. 2015).

Regarding the potassium channels, some studies also described their involvement in BC properties in response to hypoxia. Firstly, Mu and collaborators highlighted the amplification of *KCNN9* potassium channel gene (Mu et al. 2003). They then described an improvement of the hypoxia resistance of the cells by using *in vitro* and *in vivo* models, which is not affected by the p53 status. A second subclass of the potassium channel family has been described in the hypoxia context: the voltage-gated potassium channels. Eag1 channel, also named Kv10.1, which was among the first Kv channels highlighted in oncogenic process, has been initially involved in the hypoxia homeostasis (Downie et al. 2008). By using Eag1-expressing CHO cells, authors demonstrated that Eag1 channel participates to the HIF-1 $\alpha$  expression's regulation and thereby VEGF secretion and vascularization. According to the involvement of Eag1 in the proliferation and in the motility of different BC cell models (Ouadid-Ahidouch et al. 2016), Lai et al. analyzed the putative expression relationship of this channel and HIF-1 $\alpha$  in human samples (Lai et al. 2014). Through their observational study, they demonstrated that the co-expression of the 2 actors is positively correlated with node status, tumor stage, and tumor size suggesting an interest to use this association like a potential biomarker. In addition, recent data obtained in our laboratory demonstrated that Eag1 channel could participate to the regulation of MDA-MB-231 cells' migration in hypoxia condition (unpublished data). To the best of our knowledge, only another study described the role of Kv3.1 and Kv3.4 in the control of BC cell migration and invasion (Song et al. 2018).

Little information about other players of the BC cell's transportome is available. However, it has been described an increase in aquaporin 1 in HIF-1 $\alpha$  expression in BC tissues (Yin et al. 2008). In addition, P2X7 has been involved in the regulation of tumor cell invasion, in hypoxia context, through a signaling pathway involving RAGE, Akt, ERK1/2, NF- $\kappa$ B translocation, and MMP-2, -9 expression (Tafari et al. 2011).

Despite the fact that NaV channels are already well described in the promotion of the BC cell aggressiveness and in the response to oxygen variations in myocytes and carotid bodies, there is no study about their involvement in hypoxic breast tumors.

Ion channels and transportome actors, involved in the answer to hypoxia, are classified in Table 2 and Fig. 3.

Finally, there is a very closed link between pH modification in tumor microenvironment and hypoxia. In this way, it is clear that acid-sensing ion channels and H<sup>+</sup> transporters could be modulated in this context but the concept has still not been demonstrated.

**Table 2** Ion channels involved in the relation between hypoxia and pH and breast cancer cells

Channel family	Type/name	Involved in cancer progression by	Signaling pathway	References
Relation with pH homeostasis in breast cancer tumor				
Voltage gated ion channels by:				
Sodium	Na <sub>v</sub> 1.5	Invasion Migration	Invasiveness through NHE1, enhancing H <sup>+</sup> efflux → activating ECM degradation by cathepsin invasion and migration through Src/Y421 activation	Brisson et al. (2011, 2013), Gillet et al. (2009)
Proton	Hv1	Invasion Migration	Invasion and migration → regulating pH <sub>e</sub> → secretion of cathepsin matrix metalloproteinase → ECM degradation	Wang et al. (2011, 2012)
Other				
Calcium-activated chloride channel	CLCA2	Proliferation Apoptosis	Proliferation and apoptosis induced by p53 in response to DNA damage	Walia et al. (2009)
Acid-sensing ion channels	ASIC1	Proliferation Invasion Migration	Through ROS-AKT-NF-κB, ERK1/2, and Ca <sup>2+</sup>	Gupta et al. (2014, 2016)
Relation with hypoxia in breast cancer tumor				
Calcium channels				
	TRPC1	EMT	Regulation of gene expression and of EGFR and STAT3 phosphorylation	Azimi et al. (2017)
	TRPC5	VEGF secretion	Through HIF-1α pathway	Zhu et al. (2015)
	Orai3	Hypoxia response	Regulation of EGFR autophosphorylation and participation to the control of migration and inflammatory/immune gene profile	Azimi et al. (2019)
	Orai1	Migration Invasion Angiogenesis	Through Notch1/Orai1/SOCE/NFAT4	Liu et al. (2018)
	MCU	Aggressiveness	Through HIF-1α pathway and subsequent genes' regulation	Tosatto et al. (2016)
	RyR1	BCSC promotion Chemoresistance	Through GSTO1/RyR1/PYK2/Src/STAT3	Lu et al. (2017)

(continued)

**Table 2** (continued)

Channel family	Type/name	Involved in cancer progression by	Signaling pathway	References
Potassium channels				
	TASK-3 ( <i>KCNK9</i> )	Hypoxia resistance	Genetic amplification promotes the resistance to drastic environment like hypoxia	Mu et al. (2003)
	Eag1		Co-expression with HIF-1 $\alpha$ correlates with tumor size, node status, and tumor stage	Lai et al. (2014)
	Kv3.1/ Kv3.4	Migration Invasion	Increased expression in hypoxia	Song et al. (2018)
Other				
	Aquaporin 1		Co-expression with HIF-1 $\alpha$ in breast cancer tissues	Yin et al. (2008)
	P2X7	Invasion	In association with RAGE and through a Akt/Erk1/2/NF- $\kappa$ B translocation	Tafani et al. (2011)

### 3.3.2 Acidic Conditions

The major regulators of pH in tumor cells are the transporters and carbonic anhydrases involved in the extrusion of H<sup>+</sup> excess to maintain the alkaline pH<sub>i</sub>. Whereas these transporters have often been reported to be important in tumor progression, the roles of pH sensing ion channels are less described. Here, we describe the pH sensing ion channels, mediated primarily through their expression at the cell surface in BC. A synthetic presentation is available in Table 2 and in Fig. 4.

A type of ion channels, being voltage independent but affected by pH, is the acid-sensing ion channels (ASICs), where eight subunits encoded by five genes have been identified. ASICs are H<sup>+</sup> cation-gated channels and are activated by extracellular acid. Some types (ASIC1) are both Na<sup>+</sup> and Ca<sup>2+</sup> permeable where other types are only Na<sup>+</sup> permeable (Damaghi et al. 2013). ASICs are mainly expressed in the central and peripheral nervous system and belong to the degenerin/epithelial sodium channel (DEG/ENaC) superfamily. Despite being expressed in the nervous system, ASICs have shown to be expressed in glioma cells and BC (Berdiev et al. 2003; Gupta et al. 2016). As ASICs have been reported to play an important role in acidosis-associated physiological and pathophysiological conditions (Wu et al. 2017), they may be involved in cancer progression, due to the acidic extracellular environment. ASIC1 is highly expressed in malignant BC tissue, compared to normal breast tissue, and genetic alterations of ASIC1 expression correlate with the overall survival of patients (Gupta et al. 2016). Furthermore, downregulation and pharmacological inhibition of ASIC1, with amiloride or psalmotoxin, suppressed tumor growth *in vitro* and *in vivo*. *In vivo* studies have shown that ASIC1 also leads



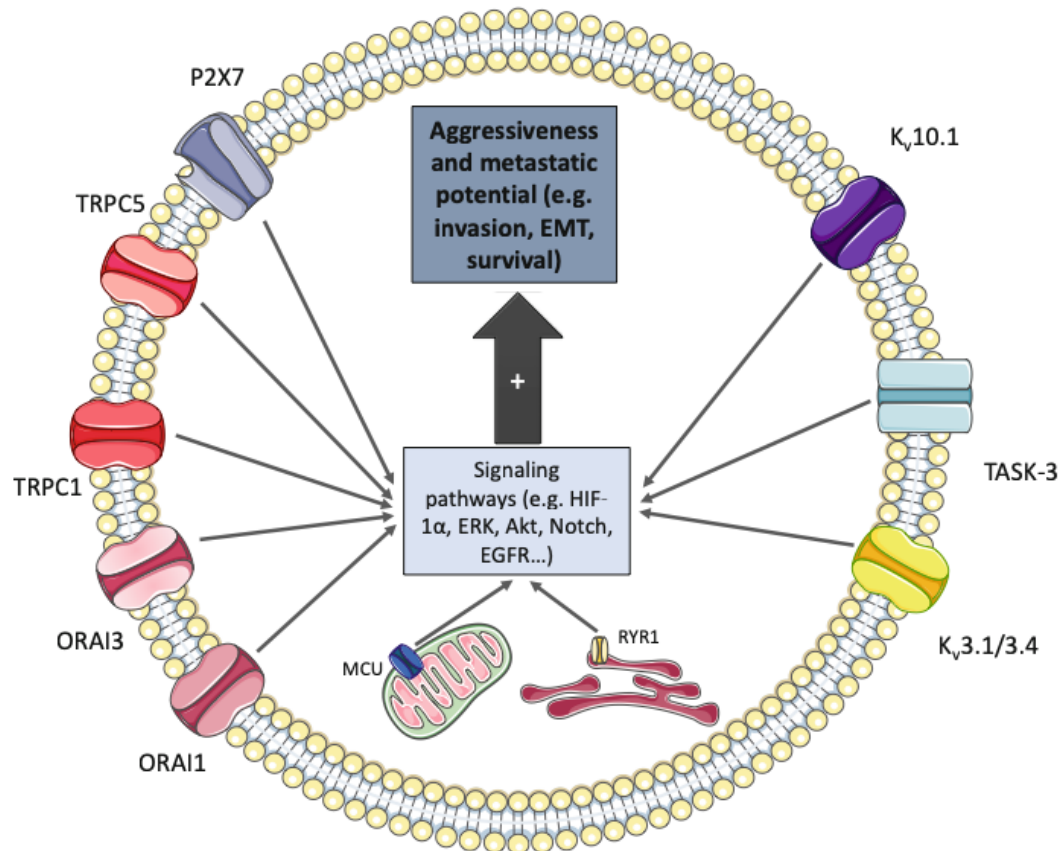


**Fig. 3** Schematic representation of the different ion channels described in hypoxia context of breast cancer. Membrane or intracellular  $\text{Ca}^{2+}$  and  $\text{K}^{+}$  transporters are modulated by hypoxia or modulate hypoxia signaling to promote aggressiveness/metastatic potential of breast cancer cells. Function and expression modulation of the channels are involved in signaling pathways promoting angiogenesis, survival, chemoresistance, invasion, migration, and EMT. Integral descriptions are included in the main text

to metastatic activity for lung tumor nodules, compared to the control. Together, these studies show that ASIC1 is important for BC growth, invasion, and metastasis. ASIC1 is expressed in some BC cell lines (MCF-7 and LM-4142), and acidification of breast cancer cells ( $\text{pH}_e$  6.6) leads to a high production of reactive oxygen species (ROS) levels (Gupta et al. 2014, 2016). Indeed, ASIC1 activation regulates proliferation, invasiveness, migration, apoptosis, and angiogenesis through ROS-AKT-NF- $\kappa$ B pathway (Gupta et al. 2014, 2016). Furthermore, the inhibition or silencing of ASIC1 suppressed acidosis-induced activation of ERK1/2, AKT, and NF- $\kappa$ B (Gupta et al. 2016). These findings show that ASIC1 is required for ROS production in BC cells, and ROS is a central molecule in regulating downstream pathways in an acidic environment. ASICs are also responsible for  $\text{Ca}^{2+}$  entry, and activation of ASIC1 leads to a rise in  $[\text{Ca}^{2+}]_{\text{cyt}}$  in neurons (Gupta et al. 2016).  $\text{Ca}^{2+}$  is involved in cancer as it regulates invasion and migration signaling (Davis et al. 2012; Gupta et al. 2016; Monteith et al. 2017). ROS production has been shown to be decreased by calcium chelators, indicating that ASIC1 regulation of  $\text{Ca}^{2+}$  is important for ROS

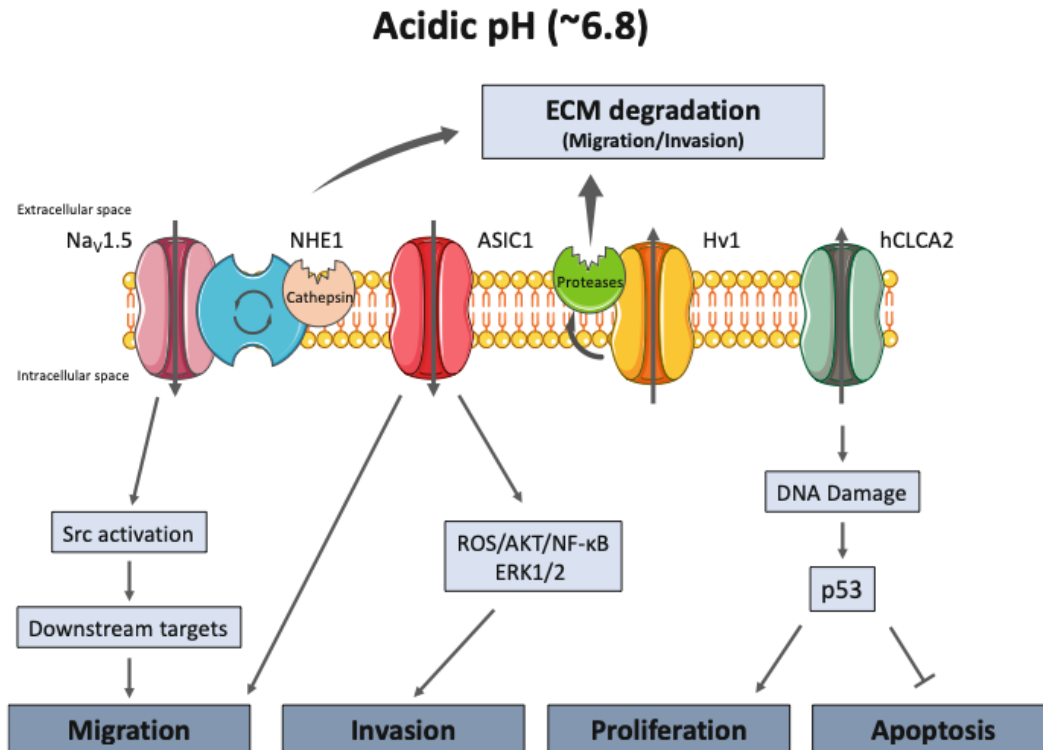


**Fig. 4** Schematic illustration of ion channels, involved in pH regulation and sensing in breast cancer

generation under acidic conditions (Gupta et al. 2016). Taken together, these suggest that there is a crosslink between ASICs and Ca<sup>2+</sup> influx and that ASICs can be involved in the regulation of Ca<sup>2+</sup> signaling pathway.

Another type of ion channel involved in pH regulation is the voltage gated proton channel Hv1, which is highly selective for H<sup>+</sup>, and no other cations. Hv1 is specifically expressed in highly metastatic human BC and the downregulation of Hv1 inhibits the metastatic by reducing invasion, migration, and H<sup>+</sup> secretion (Wang et al. 2011). As previously described, acidic pH<sub>e</sub> promotes degradation of ECM, which increases the secretion and activation of proteases. The proteases need the low pH<sub>e</sub> to have optimal activity. Among many proteases, the cathepsins and the MMPs are essentially involved in degradation and remodeling of ECM (Wang et al. 2011). The secretion and activation of some proteases are pH-regulated and MMP-9 showed reduced activity in MDA-MB-231 cells with suppressed Hv1. This indicates that secretion of protons by Hv1, ensuring the acidic pH<sub>e</sub>, promotes invasion and metastasis by activating and secreting proteases, such as MMP-9 (Wang et al. 2011). In addition, a knockdown of Hv1 in MDA-MB-231 cells decreases proliferation, invasiveness but also inhibited pH recovery and proton secretion, affecting cell capacity of acidifying pH<sub>e</sub> (Wang et al. 2012). Furthermore, the high expression of Hv1 in tumors from patients is correlated with tumor progression and patients were more likely to have a shorter overall survival. High expression of Hv1 is associated with a poor prognosis, thus making Hv1 a prognostic factor (Wang et al. 2012). The



metastatic potential of MDA-MB-231 cells correlates with the high Hv1 expression in the plasma membrane. Taken together, the regulation of pH by Hv1 and the acidic  $\text{pH}_e$  in cancer cells affect the secretion, activity, and cellular distribution of proteases, thus making the BC cells showing a more aggressive phenotype, with high proliferation, invasiveness, and migration. The knockdown of Hv1 showed inhibition of tumor progression, development, and metastasis, making Hv1 a molecular biomarker and target of BC therapy (Wang et al. 2012).

$\text{Na}_V1.5$  has been shown to interact with the predominant regulator of  $\text{pH}_i$  NHE1, in the caveolae to enhance the  $\text{H}^+$  efflux, resulting in an acidification of the pericellular microenvironment (Brisson et al. 2011; Gillet et al. 2009).  $\text{Na}_V1.5$  and NHE1 co-localize in the plasma membrane of cancer cells and extracellular matrix assays suggest that they are both involved in the same pH-dependent invasiveness regulatory pathway (Brisson et al. 2011). The invasive properties of both channels in cancer cells have been shown to be activated through acidic extracellular cathepsins, mainly cathepsin B and S (Gillet et al. 2009). From high-grade BC biopsies and highly invasive BC cells lines, the overexpression of  $\text{Na}_V1.5$  has been associated with ECM remodeling and an increased risk of developing metastasis (Gillet et al. 2009; Brisson et al. 2013). In addition, it has been shown that  $\text{Na}_V1.5$  interacts with NHE1, allosterically increasing NHE1 activity in a pH range of 6.4–7.0, suggesting more proton extrusion at more acidic  $\text{pH}_i$ . This interaction is supposed to occur in caveolae of the invadopodia compartment, hence responsible for increased ECM degradation and invasiveness (Brisson et al. 2013). A more aggressive phenotype of the BC cells could be explained by the enhanced Src kinase activity and the phosphorylation of Y421 cortactin, involved in migration and invasion (Brisson et al. 2013; Liu et al. 1999). These data suggest that  $\text{Na}_V1.5$  is regulated by pH and enhances NHE1 activity, promoting degradation of ECM and leads to invasion and migration in BC cells (Brisson et al. 2011, 2013).

Some other ion channels sensitive to the pH are expressed in BC. Among the  $\text{Ca}^{2+}$  channels, one example is the transient receptor potential vanilloid 1 (TRPV1), which is proton sensitive. The modulation of these channels has been reported to play a functional role in TNBC, where they have been shown to be overexpressed (Weber et al. 2016) and associated with growth and progression (Weber et al. 2016; Wu et al. 2014). Furthermore, the chloride channel protein 2 (CLC-2) has shown to be opened by mild acidification but is completely inhibited by strong acidification (Arreola et al. 2002). CLC-2 is highly expressed in epithelial cells and in the colon where it has been suggested to have role in electroneutral salt absorption (Sandoval et al. 2011). CLC channels are expressed in BC cells and tissue and especially CLC-3 is over expressed (Zhou et al. 2018) and is related to invasion, migration, and cell cycle regulation (Peretti et al. 2015). Moreover, metastatic BC cells transfected with hCLCA2 presented a reduced  $\text{pH}_i$  from 7.49 to 6.67, an acidic  $\text{pH}_i$  known to activate apoptosis. The acidification of the cytosol by hCLCA2 could explain its inhibitory effect on proliferation and cell survival, as pH has profound effects on these events (Walia et al. 2009). In addition, mammary epithelial cells and lung fibroblast expressing cystic fibrosis conductance regulator (CFTR) have been found

to induce a drop in pH to  $\sim 6.7$  to initiate apoptosis, whereas the CFTR mutant did not (Barriere et al. 2001; Gottlieb and Dosanjh 1996).

Concerning potassium channels, the two-pore domain potassium channel (K2P) family includes some members that are pH sensitive (Dookeran and Auer 2017). Members of the subfamily, the TWIK-related alkaline pH activated potassium channels including TASK-2, TALK-1, and TALK-2, are stimulated by an extracellular alkalization (Dookeran and Auer 2017; Pei et al. 2003; Patel and Lazdunski 2004). These channels are of interest as their genes have been found to be either altered or upregulated in BC tissue, and in some cell types are found to be required for apoptosis (Dookeran and Auer 2017; Pei et al. 2003; Patel and Lazdunski 2004; Williams et al. 2013). These channels are inhibited by an extracellular acidification, which may contribute to cancer cells avoiding apoptosis through these channels (Andersen et al. 2014). Another subfamily of the K<sub>2</sub>P is the TWIK-related acid sensitive (TASK) family, which is inhibited by extracellular acidification. All the genes have been found upregulated in BC tissue and the gene coding for TASK-3 (KCNK9) is recognized as a proto-oncogene and its overexpression promotes tumorigenesis (Pei et al. 2003; Patel and Lazdunski 2004; Dookeran et al. 2017). Taken together, these channels (CLC and K2P) would be potential actors to regulate downstream signaling pathways of these cancer hallmarks through an acidification of the tumor environment.

## 4 Conclusion and Perspectives

We have summarized here the modulation of ion channels expression and/or activity by the tumor microenvironment and how this involves changes in BC development and progression.

To better understand the complex nature of BC, several cell lines were used to study the tumor microenvironment impact on BC progression: luminal-like, basal-like, proliferative, invasive, and expressing “or not” different receptors for estrogen, progesterone, or HER-2. However, the results obtained remain fragmentary and represent only an approximation of how the processes take place in patient’s tumor. Moreover, tumor heterogeneity constitutes one of the major obstacles in cancer treatment leading to the recurrence of cancer. It is progressively becoming clear that there is significant response heterogeneity in drug responses within cancer cell populations. So far, most of the studies investigating the role of ion channels in cancer progression were dealing with cancer cells *in vitro*. Up to now their modulation by the microenvironment, which is crucial for tumor progression, has not been largely studied in BC and there is little knowledge about their expression profile and their role in clonal cell populations. Consequently, experimental approaches must be improved in order to get closer to the reality of the disease. For this purpose, it would be appropriate to investigate the role of ion channels by using different models including 3D cell culture, organoids, co-culture models, or microfluidic systems. Indeed, such approach could better enable to inform us about the interactions

between different cell types present in tumor environment and tumor cells and the role of ion channels in these interactions.

**Acknowledgments** This work was supported by the UPJV “Université de Picardie Jules Verne,” the “Région Hauts-de-France,” the CNO (“Cancéropôle Nord-Ouest”), and the Marie Skłodowska-Curie Innovative Training Network (ITN), Grant Agreement number: 813834 – pHioniC – H2020-MSCA-ITN-2018.

**Declaration of Competing Interest** The authors declare that they have no conflict of interest.

## References

- Amara S, Ivy MT, Myles EL, Tiriveedhi V (2016) Sodium channel gammaENaC mediates IL-17 synergized high salt induced inflammatory stress in breast cancer cells. *Cell Immunol* 302:1–10. <https://doi.org/10.1016/j.cellimm.2015.12.007>
- Andersen AP, Moreira JM, Pedersen SF (2014) Interactions of ion transporters and channels with cancer cell metabolism and the tumour microenvironment. *Philos Trans R Soc Lond B Biol Sci* 369(1638):20130098. <https://doi.org/10.1098/rstb.2013.0098>
- Andersen AP, Flinck M, Oernbo EK, Pedersen NB, Viuff BM, Pedersen SF (2016) Roles of acid-extruding ion transporters in regulation of breast cancer cell growth in a 3-dimensional microenvironment. *Mol Cancer* 15(1):45. <https://doi.org/10.1186/s12943-016-0528-0>
- Aoudjit F, Vuori K (2001) Integrin signaling inhibits paclitaxel-induced apoptosis in breast cancer cells. *Oncogene* 20(36):4995–5004. <https://doi.org/10.1038/sj.onc.1204554>
- Arcangeli A, Crociani O, Bencini L (2014) Interaction of tumour cells with their microenvironment: ion channels and cell adhesion molecules. A focus on pancreatic cancer. *Philos Trans R Soc Lond B Biol Sci* 369(1638):20130101. <https://doi.org/10.1098/rstb.2013.0101>
- Arreola J, Begenisich T, Melvin JE (2002) Conformation-dependent regulation of inward rectifier chloride channel gating by extracellular protons. *J Physiol* 541(Pt 1):103–112. <https://doi.org/10.1113/jphysiol.2002.016485>
- Assent D, Bourgot I, Hennuy B, Geurts P, Noel A, Foidart JM, Maquoi E (2015) A membrane-type-1 matrix metalloproteinase (MT1-MMP)-discoidin domain receptor 1 axis regulates collagen-induced apoptosis in breast cancer cells. *PLoS One* 10(3):e0116006. <https://doi.org/10.1371/journal.pone.0116006>
- Attane C, Milhas D, Hoy AJ, Muller C (2018) Metabolic remodeling induced by adipocytes: a new Achilles' heel in invasive breast cancer? *Curr Med Chem*. <https://doi.org/10.2174/0929867325666180426165001>
- Azimi I, Monteith GR (2016) Plasma membrane ion channels and epithelial to mesenchymal transition in cancer cells. *Endocr Relat Cancer* 23(11):R517–R525. <https://doi.org/10.1530/ERC-16-0334>
- Azimi I, Milevskiy MJG, Kaemmerer E, Turner D, Yapa K, Brown MA, Thompson EW, Roberts-Thomson SJ, Monteith GR (2017) TRPC1 is a differential regulator of hypoxia-mediated events and Akt signalling in PTEN-deficient breast cancer cells. *J Cell Sci* 130(14):2292–2305. <https://doi.org/10.1242/jcs.196659>
- Azimi I, Milevskiy MJG, Chalmers SB, Yapa K, Robitaille M, Henry C, Baillie GJ, Thompson EW, Roberts-Thomson SJ, Monteith GR (2019) ORAI1 and ORAI3 in breast cancer molecular subtypes and the identification of ORAI3 as a hypoxia sensitive gene and a regulator of hypoxia responses. *Cancer* 11(2). <https://doi.org/10.3390/cancers11020208>
- Badaoui M, Mimsy-Julienne C, Saby C, Van Gulick L, Peretti M, Jeannesson P, Morjani H, Ouadid-Ahidouch H (2018) Collagen type 1 promotes survival of human breast cancer cells



- by overexpressing Kv10.1 potassium and Orail calcium channels through DDR1-dependent pathway. *Oncotarget* 9(37):24653–24671. <https://doi.org/10.18632/oncotarget.19065>
- Balkwill FR, Capasso M, Hagemann T (2012) The tumor microenvironment at a glance. *J Cell Sci* 125(Pt 23):5591–5596. <https://doi.org/10.1242/jcs.116392>
- Baltes F, Pfeifer V, Silbermann K, Caspers J, von Rekowski KW, Schlesinger M, Bendas G (2020) beta1-Integrin binding to collagen type 1 transmits breast cancer cells into chemoresistance by activating ABC efflux transporters. *Biochim Biophys Acta Mol Cell Res* 1867:118663. <https://doi.org/10.1016/j.bbamcr.2020.118663>
- Barriere H, Poujeol C, Tauc M, Blasi JM, Counillon L, Poujeol P (2001) CFTR modulates programmed cell death by decreasing intracellular pH in Chinese hamster lung fibroblasts. *Am J Physiol Cell Physiol* 281(3):C810–C824. <https://doi.org/10.1152/ajpcell.2001.281.3.C810>
- Basson MD, Zeng B, Downey C, Sirivelu MP, Tepe JJ (2015) Increased extracellular pressure stimulates tumor proliferation by a mechanosensitive calcium channel and PKC-beta. *Mol Oncol* 9(2):513–526. <https://doi.org/10.1016/j.molonc.2014.10.008>
- Berdiev BK, Xia J, McLean LA, Markert JM, Gillespie GY, Mapstone TB, Naren AP, Jovov B, Bubien JK, Ji HL, Fuller CM, Kirk KL, Benos DJ (2003) Acid-sensing ion channels in malignant gliomas. *J Biol Chem* 278(17):15023–15034. <https://doi.org/10.1074/jbc.M300991200>
- Bhola NE, Balko JM, Dugger TC, Kuba MG, Sanchez V, Sanders M, Stanford J, Cook RS, Arteaga CL (2013) TGF-beta inhibition enhances chemotherapy action against triple-negative breast cancer. *J Clin Invest* 123(3):1348–1358. <https://doi.org/10.1172/JCI65416>
- Blaug S, Hybiske K, Cohn J, Firestone GL, Machen TE, Miller SS (2001) ENaC- and CFTR-dependent ion and fluid transport in mammary epithelia. *Am J Physiol Cell Physiol* 281(2):C633–C648. <https://doi.org/10.1152/ajpcell.2001.281.2.C633>
- Boedtker E, Pedersen SF (2020) The acidic tumor microenvironment as a driver of cancer. *Annu Rev Physiol* 82:21.1–21.24
- Bos R, Zhong H, Hanrahan CF, Mommers EC, Semenza GL, Pinedo HM, Abeloff MD, Simons JW, van Diest PJ, van der Wall E (2001) Levels of hypoxia-inducible factor-1 alpha during breast carcinogenesis. *J Natl Cancer Inst* 93(4):309–314. <https://doi.org/10.1093/jnci/93.4.309>
- Bos R, van der Groep P, Greijer AE, Shvarts A, Meijer S, Pinedo HM, Semenza GL, van Diest PJ, van der Wall E (2003) Levels of hypoxia-inducible factor-1alpha independently predict prognosis in patients with lymph node negative breast carcinoma. *Cancer* 97(6):1573–1581. <https://doi.org/10.1002/cncr.11246>
- Bowlby MR, Fadool DA, Holmes TC, Levitan IB (1997) Modulation of the Kv1.3 potassium channel by receptor tyrosine kinases. *J Gen Physiol* 110(5):601–610. <https://doi.org/10.1085/jgp.110.5.601>
- Boyd C, Naray-Fejes-Toth A (2007) Steroid-mediated regulation of the epithelial sodium channel subunits in mammary epithelial cells. *Endocrinology* 148(8):3958–3967. <https://doi.org/10.1210/en.2006-1741>
- Boyd NF, Martin LJ, Yaffe M, Minkin S (2009) Mammographic density. *Breast Cancer Res* 11 (Suppl 3):S4. <https://doi.org/10.1186/bcr2423>
- Brackenbury WJ (2012) Voltage-gated sodium channels and metastatic disease. *Channels (Austin)* 6(5):352–361. <https://doi.org/10.4161/chan.21910>
- Brisson L, Gillet L, Calaghan S, Besson P, Le Guennec JY, Roger S, Gore J (2011) Na(V)1.5 enhances breast cancer cell invasiveness by increasing NHE1-dependent H(+) efflux in caveolae. *Oncogene* 30(17):2070–2076. <https://doi.org/10.1038/ncr.2010.574>
- Brisson L, Driffort V, Benoist L, Poet M, Counillon L, Antelmi E, Rubino R, Besson P, Labbal F, Chevalier S, Reshkin SJ, Gore J, Roger S (2013) NaV1.5 Na(+) channels allosterically regulate the NHE-1 exchanger and promote the activity of breast cancer cell invadopodia. *J Cell Sci* 126 (Pt 21):4835–4842. <https://doi.org/10.1242/jcs.123901>

- Brucher BL, Jamall IS (2014) Cell-cell communication in the tumor microenvironment, carcinogenesis, and anticancer treatment. *Cell Physiol Biochem* 34(2):213–243. <https://doi.org/10.1159/000362978>
- Burnstock G (1996) P2 purinoceptors: historical perspective and classification. *Ciba Found Symp* 198:1–28.; discussion 29–34. <https://doi.org/10.1002/9780470514900.ch1>
- Carafoli F, Hohenester E (2013) Collagen recognition and transmembrane signalling by discoidin domain receptors. *Biochim Biophys Acta* 1834(10):2187–2194. <https://doi.org/10.1016/j.bbapap.2012.10.014>
- Carey L, Winer E, Viale G, Cameron D, Gianni L (2010) Triple-negative breast cancer: disease entity or title of convenience? *Nat Rev Clin Oncol* 7(12):683–692. <https://doi.org/10.1038/nrclinonc.2010.154>
- Chadet S, Jelassi B, Wannous R, Angoulvant D, Chevalier S, Besson P, Roger S (2014) The activation of P2Y2 receptors increases MCF-7 breast cancer cells migration through the MEK-ERK1/2 signalling pathway. *Carcinogenesis* 35(6):1238–1247. <https://doi.org/10.1093/carcin/bgt493>
- Cheng H, Wang S, Feng R (2016) STIM1 plays an important role in TGF-beta-induced suppression of breast cancer cell proliferation. *Oncotarget* 7(13):16866–16878. <https://doi.org/10.18632/oncotarget.7619>
- Cherubini A, Hofmann G, Pillozzi S, Guasti L, Crociani O, Cilia E, Di Stefano P, Degani S, Balzi M, Olivotto M, Wanke E, Becchetti A, Defilippi P, Wymore R, Arcangeli A (2005) Human ether-a-go-go-related gene 1 channels are physically linked to beta1 integrins and modulate adhesion-dependent signaling. *Mol Biol Cell* 16(6):2972–2983. <https://doi.org/10.1091/mbc.e04-10-0940>
- Corsa CA, Brenot A, Grither WR, Van Hove S, Loza AJ, Zhang K, Ponik SM, Liu Y, DeNardo DG, Eliceiri KW, Keely PJ, Longmore GD (2016) The action of discoidin domain receptor 2 in basal tumor cells and stromal cancer-associated fibroblasts is critical for breast cancer metastasis. *Cell Rep* 15(11):2510–2523. <https://doi.org/10.1016/j.celrep.2016.05.033>
- Crociani O, Zanieri F, Pillozzi S, Lastraioli E, Stefanini M, Fiore A, Fortunato A, D'Amico M, Masselli M, De Lorenzo E, Gasparoli L, Chiu M, Bussolati O, Becchetti A, Arcangeli A (2013) hERG1 channels modulate integrin signaling to trigger angiogenesis and tumor progression in colorectal cancer. *Sci Rep* 3:3308. <https://doi.org/10.1038/srep03308>
- Damaghi M, Wojtkowiak JW, Gillies RJ (2013) pH sensing and regulation in cancer. *Front Physiol* 4:370. <https://doi.org/10.3389/fphys.2013.00370>
- Davis MJ, Wu X, Nurkiewicz TR, Kawasaki J, Gui P, Hill MA, Wilson E (2001) Regulation of ion channels by protein tyrosine phosphorylation. *Am J Physiol Heart Circ Physiol* 281(5):H1835–H1862. <https://doi.org/10.1152/ajpheart.2001.281.5.H1835>
- Davis FM, Kenny PA, Soo ET, van Denderen BJ, Thompson EW, Cabot PJ, Parat MO, Roberts-Thomson SJ, Monteith GR (2011) Remodeling of purinergic receptor-mediated Ca<sup>2+</sup> signaling as a consequence of EGF-induced epithelial-mesenchymal transition in breast cancer cells. *PLoS One* 6(8):e23464. <https://doi.org/10.1371/journal.pone.0023464>
- Davis FM, Peters AA, Grice DM, Cabot PJ, Parat MO, Roberts-Thomson SJ, Monteith GR (2012) Non-stimulated, agonist-stimulated and store-operated Ca<sup>2+</sup> influx in MDA-MB-468 breast cancer cells and the effect of EGF-induced EMT on calcium entry. *PLoS One* 7(5):e36923. <https://doi.org/10.1371/journal.pone.0036923>
- Davis FM, Parsonage MT, Cabot PJ, Parat MO, Thompson EW, Roberts-Thomson SJ, Monteith GR (2013) Assessment of gene expression of intracellular calcium channels, pumps and exchangers with epidermal growth factor-induced epithelial-mesenchymal transition in a breast cancer cell line. *Cancer Cell Int* 13(1):76. <https://doi.org/10.1186/1475-2867-13-76>
- Davis FM, Azimi I, Faville RA, Peters AA, Jalink K, Putney JW Jr, Goodhill GJ, Thompson EW, Roberts-Thomson SJ, Monteith GR (2014) Induction of epithelial-mesenchymal transition (EMT) in breast cancer cells is calcium signal dependent. *Oncogene* 33(18):2307–2316. <https://doi.org/10.1038/onc.2013.187>

- de Kruijf EM, Dekker TJ, Hawinkels LJ, Putter H, Smit VT, Kroep JR, Kuppen PJ, van de Velde CJ, ten Dijke P, Tollenaar RA, Mesker WE (2013) The prognostic role of TGF-beta signaling pathway in breast cancer patients. *Ann Oncol* 24(2):384–390. <https://doi.org/10.1093/annonc/mds333>
- De Luca A, Carotenuto A, Rachiglio A, Gallo M, Maiello MR, Aldinucci D, Pinto A, Normanno N (2008) The role of the EGFR signaling in tumor microenvironment. *J Cell Physiol* 214(3):559–567. <https://doi.org/10.1002/jcp.21260>
- Di Virgilio F (2012) Purines, purinergic receptors, and cancer. *Cancer Res* 72(21):5441–5447. <https://doi.org/10.1158/0008-5472.CAN-12-1600>
- Dias AS, Almeida CR, Helguero LA, Duarte IF (2019) Metabolic crosstalk in the breast cancer microenvironment. *Eur J Cancer* 121:154–171. <https://doi.org/10.1016/j.ejca.2019.09.002>
- Hooker K, Auer P (2017) The emerging role of two-pore domain potassium channels in breast cancer. *J Glob Epidemiol Environ Health* 2017:27–36
- Hooker KA, Zhang W, Stayner L, Argos M (2017) Associations of two-pore domain potassium channels and triple negative breast cancer subtype in The Cancer Genome Atlas: systematic evaluation of gene expression and methylation. *BMC Res Notes* 10(1):475. <https://doi.org/10.1186/s13104-017-2777-4>
- Downie BR, Sanchez A, Knotgen H, Contreras-Jurado C, Gymnopoulos M, Weber C, Stuhmer W, Pardo LA (2008) Egr1 expression interferes with hypoxia homeostasis and induces angiogenesis in tumors. *J Biol Chem* 283(52):36234–36240. <https://doi.org/10.1074/jbc.M801830200>
- Drabsch Y, ten Dijke P (2012) TGF-beta signalling and its role in cancer progression and metastasis. *Cancer Metastasis Rev* 31(3-4):553–568. <https://doi.org/10.1007/s10555-012-9375-7>
- Dumont N, Arteaga CL (2000) Transforming growth factor-beta and breast cancer: tumor promoting effects of transforming growth factor-beta. *Breast Cancer Res* 2(2):125–132. <https://doi.org/10.1186/bcr44>
- El Azreq MA, Naci D, Aoudjit F (2012) Collagen/beta1 integrin signaling up-regulates the ABCC1/ MRP-1 transporter in an ERK/MAPK-dependent manner. *Mol Biol Cell* 23(17):3473–3484. <https://doi.org/10.1091/mbc.E12-02-0132>
- El Hiani Y, Ahidouch A, Lehen'kyi V, Hague F, Gouilleux F, Mentaverri R, Kamel S, Lassoued K, Brule G, Ouadid-Ahidouch H (2009a) Extracellular signal-regulated kinases 1 and 2 and TRPC1 channels are required for calcium-sensing receptor-stimulated MCF-7 breast cancer cell proliferation. *Cell Physiol Biochem* 23(4-6):335–346. <https://doi.org/10.1159/000218179>
- El Hiani Y, Lehen'kyi V, Ouadid-Ahidouch H, Ahidouch A (2009b) Activation of the calcium-sensing receptor by high calcium induced breast cancer cell proliferation and TRPC1 cation channel over-expression potentially through EGFR pathways. *Arch Biochem Biophys* 486(1):58–63. <https://doi.org/10.1016/j.abb.2009.03.010>
- Ellerbroek SM, Halbleib JM, Benavidez M, Warmka JK, Wattenberg EV, Stack MS, Hudson LG (2001) Phosphatidylinositol 3-kinase activity in epidermal growth factor-stimulated matrix metalloproteinase-9 production and cell surface association. *Cancer Res* 61(5):1855–1861
- Falzone S, Donvito G, Di Virgilio F (2013) Detecting adenosine triphosphate in the pericellular space. *Interface Focus* 3(3):20120101. <https://doi.org/10.1098/rsfs.2012.0101>
- Figiel S, Bery F, Chantome A, Fontaine D, Pasqualin C, Maupoil V, Domingo I, Guibon R, Bruyere F, Potier-Cartreau M, Vandier C, Fromont G, Maheo K (2019) A novel calcium-mediated EMT pathway controlled by lipids: an opportunity for prostate cancer adjuvant therapy. *Cancer* 11(11). <https://doi.org/10.3390/cancers11111814>
- Flinck M, Kramer SH, Pedersen SF (2018) Roles of pH in control of cell proliferation. *Acta Physiol (Oxf)*:e13068. <https://doi.org/10.1111/apha.13068>
- Fraser SP, Ozerlat-Gunduz I, Brackenbury WJ, Fitzgerald EM, Campbell TM, Coombes RC (1638) Djamgoz MB (2014) Regulation of voltage-gated sodium channel expression in cancer: hormones, growth factors and auto-regulation. *Philos Trans R Soc Lond B Biol Sci* 369:20130105. <https://doi.org/10.1098/rstb.2013.0105>



- Fraser SP, Diss JK, Chioni AM, Mycielska ME, Pan H, Yamaci RF, Pani F, Siwy Z, Krasowska M, Grzywna Z, Brackenbury WJ, Theodorou D, Koyuturk M, Kaya H, Battaloglu E, De Bella MT, Slade MJ, Tolhurst R, Palmieri C, Jiang J, Latchman DS, Coombes RC, Djamgoz MB (2005) Voltage-gated sodium channel expression and potentiation of human breast cancer metastasis. *Clin Cancer Res* 11(15):5381–5389. <https://doi.org/10.1158/1078-0432.CCR-05-0327>
- Fu HL, Valiathan RR, Arkwright R, Sohail A, Mihai C, Kumarasiri M, Mahasenan KV, Mobashery S, Huang P, Agarwal G, Fridman R (2013) Discoidin domain receptors: unique receptor tyrosine kinases in collagen-mediated signaling. *J Biol Chem* 288(11):7430–7437. <https://doi.org/10.1074/jbc.R112.444158>
- Gatenby RA, Gillies RJ (2008) A microenvironmental model of carcinogenesis. *Nat Rev Cancer* 8(1):56–61. <https://doi.org/10.1038/nrc2255>
- Gilbert SM, Oliphant CJ, Hassan S, Peille AL, Bronsert P, Falzoni S, Di Virgilio F, McNulty S, Lara R (2019) ATP in the tumour microenvironment drives expression of nP2X7, a key mediator of cancer cell survival. *Oncogene* 38(2):194–208. <https://doi.org/10.1038/s41388-018-0426-6>
- Gilkes DM, Semenza GL (2013) Role of hypoxia-inducible factors in breast cancer metastasis. *Future Oncol* 9(11):1623–1636. <https://doi.org/10.2217/fon.13.92>
- Gillet L, Roger S, Besson P, Lecaille F, Gore J, Bougnoux P, Lalmanach G, Le Guennec JY (2009) Voltage-gated sodium channel activity promotes cysteine cathepsin-dependent invasiveness and colony growth of human cancer cells. *J Biol Chem* 284(13):8680–8691. <https://doi.org/10.1074/jbc.M806891200>
- Gonzalez DM, Medici D (2014) Signaling mechanisms of the epithelial-mesenchymal transition. *Sci Signal* 7(344):re8. <https://doi.org/10.1126/scisignal.2005189>
- Gonzalez-Gonzalez L, Gonzalez-Ramirez R, Flores A, Avelino-Cruz JE, Felix R, Monjaraz E (2019a) Epidermal growth factor potentiates migration of MDA-MB 231 breast cancer cells by increasing NaV1.5 channel expression. *Oncology*:1–10. <https://doi.org/10.1159/000501802>
- Gonzalez-Gonzalez L, Gonzalez-Ramirez R, Flores A, Avelino-Cruz JE, Felix R, Monjaraz E (2019b) Epidermal growth factor potentiates migration of MDA-MB 231 breast cancer cells by increasing NaV1.5 channel expression. *Oncology* 97(6):373–382. <https://doi.org/10.1159/000501802>
- Gottlieb RA, Dosanjh A (1996) Mutant cystic fibrosis transmembrane conductance regulator inhibits acidification and apoptosis in C127 cells: possible relevance to cystic fibrosis. *Proc Natl Acad Sci U S A* 93(8):3587–3591. <https://doi.org/10.1073/pnas.93.8.3587>
- Gottlieb RA, Nordberg J, Skowronski E, Babior BM (1996) Apoptosis induced in Jurkat cells by several agents is preceded by intracellular acidification. *Proc Natl Acad Sci U S A* 93(2):654–658
- Griffith OL, Spies NC, Anurag M, Griffith M, Luo J, Tu D, Yeo B, Kunisaki J, Miller CA, Krysiak K, Hundal J, Ainscough BJ, Skidmore ZL, Campbell K, Kumar R, Fronick C, Cook L, Snider JE, Davies S, Kavuri SM, Chang EC, Magrini V, Larson DE, Fulton RS, Liu S, Leung S, Voduc D, Bose R, Dowsett M, Wilson RK, Nielsen TO, Mardis ER, Ellis MJ (2018) The prognostic effects of somatic mutations in ER-positive breast cancer. *Nat Commun* 9(1):3476. <https://doi.org/10.1038/s41467-018-05914-x>
- Grither WR, Longmore GD (2018) Inhibition of tumor-microenvironment interaction and tumor invasion by small-molecule allosteric inhibitor of DDR2 extracellular domain. *Proc Natl Acad Sci U S A* 115(33):E7786–E7794. <https://doi.org/10.1073/pnas.1805020115>
- Grunert S, Jechlinger M, Beug H (2003) Diverse cellular and molecular mechanisms contribute to epithelial plasticity and metastasis. *Nat Rev Mol Cell Biol* 4(8):657–665. <https://doi.org/10.1038/nrml175>
- Guilbert A, Gautier M, Dhennin-Duthille I, Rybarczyk P, Sahni J, Sevestre H, Scharenberg AM, Ouadid-Ahidouch H (2013) Transient receptor potential melastatin 7 is involved in oestrogen receptor-negative metastatic breast cancer cells migration through its kinase domain. *Eur J Cancer* 49(17):3694–3707. <https://doi.org/10.1016/j.ejca.2013.07.008>

- Gupta SC, Singh R, Pochampally R, Watabe K, Mo YY (2014) Acidosis promotes invasiveness of breast cancer cells through ROS-AKT-NF-kappaB pathway. *Oncotarget* 5(23):12070–12082. <https://doi.org/10.18632/oncotarget.2514>
- Gupta SC, Singh R, Asters M, Liu J, Zhang X, Pabbidi MR, Watabe K, Mo YY (2016) Regulation of breast tumorigenesis through acid sensors. *Oncogene* 35(31):4102–4111. <https://doi.org/10.1038/onc.2015.477>
- Hammadi M, Chopin V, Matifat F, Dhennin-Duthille I, Chasseraud M, Sevestre H, Ouadid-Ahidouch H (2012) Human ether a-gogo K(+) channel 1 (hEag1) regulates MDA-MB-231 breast cancer cell migration through Orai1-dependent calcium entry. *J Cell Physiol* 227(12):3837–3846. <https://doi.org/10.1002/jcp.24095>
- Hanahan D, Weinberg RA (2011) Hallmarks of cancer: the next generation. *Cell* 144(5):646–674. <https://doi.org/10.1016/j.cell.2011.02.013>
- Hashim AI, Zhang X, Wojtkowiak JW, Martinez GV, Gillies RJ (2011) Imaging pH and metastasis. *NMR Biomed* 24(6):582–591. <https://doi.org/10.1002/nbm.1644>
- Hida K, Maishi N, Annan DA, Hida Y (2018) Contribution of tumor endothelial cells in cancer progression. *Int J Mol Sci* 19(5). <https://doi.org/10.3390/ijms19051272>
- Houthuijzen JM, Jonkers J (2018) Cancer-associated fibroblasts as key regulators of the breast cancer tumor microenvironment. *Cancer Metastasis Rev* 37(4):577–597. <https://doi.org/10.1007/s10555-018-9768-3>
- Hu J, Qin K, Zhang Y, Gong J, Li N, Lv D, Xiang R, Tan X (2011) Downregulation of transcription factor Oct4 induces an epithelial-to-mesenchymal transition via enhancement of Ca<sup>2+</sup> influx in breast cancer cells. *Biochem Biophys Res Commun* 411(4):786–791. <https://doi.org/10.1016/j.bbrc.2011.07.025>
- Hui L, Chen Y (2015) Tumor microenvironment: sanctuary of the devil. *Cancer Lett* 368(1):7–13. <https://doi.org/10.1016/j.canlet.2015.07.039>
- Humphries JD, Byron A, Humphries MJ (2006) Integrin ligands at a glance. *J Cell Sci* 119(Pt 19):3901–3903. <https://doi.org/10.1242/jcs.03098>
- Imamura T, Hikita A, Inoue Y (2012) The roles of TGF-beta signaling in carcinogenesis and breast cancer metastasis. *Breast Cancer* 19(2):118–124. <https://doi.org/10.1007/s12282-011-0321-2>
- Ingber DE (2008) Can cancer be reversed by engineering the tumor microenvironment? *Semin Cancer Biol* 18(5):356–364. <https://doi.org/10.1016/j.semcancer.2008.03.016>
- Jelassi B, Chantome A, Alcaraz-Perez F, Baroja-Mazo A, Cayuela ML, Pelegrin P, Surprenant A, Roger S (2011) P2X(7) receptor activation enhances SK3 channels- and cystein cathepsin-dependent cancer cells invasiveness. *Oncogene* 30(18):2108–2122. <https://doi.org/10.1038/onc.2010.593>
- Jeulin C, Seltzer V, Bailbe D, Andreau K, Marano F (2008) EGF mediates calcium-activated chloride channel activation in the human bronchial epithelial cell line 16HBE14o-: involvement of tyrosine kinase p60c-src. *Am J Physiol Lung Cell Mol Physiol* 295(3):L489–L496. <https://doi.org/10.1152/ajplung.90282.2008>
- Ju JA, Godet I, Ye IC, Byun J, Jayatilaka H, Lee SJ, Xiang L, Samanta D, Lee MH, Wu PH, Wirtz D, Semenza GL, Gilkes DM (2017) Hypoxia selectively enhances integrin alpha5beta1 receptor expression in breast cancer to promote metastasis. *Mol Cancer Res* 15(6):723–734. <https://doi.org/10.1158/1541-7786.MCR-16-0338>
- Juin A, Di Martino J, Leitinger B, Henriët E, Gary AS, Paysan L, Bomo J, Baffet G, Gauthier-Rouvière C, Rosenbaum J, Moreau V, Saltel F (2014) Discoidin domain receptor 1 controls linear invadosome formation via a Cdc42-Tuba pathway. *J Cell Biol* 207(4):517–533. <https://doi.org/10.1083/jcb.201404079>
- Kadio B, Yaya S, Basak A, Dje K, Gomes J, Mesenge C (2016) Calcium role in human carcinogenesis: a comprehensive analysis and critical review of literature. *Cancer Metastasis Rev* 35(3):391–411. <https://doi.org/10.1007/s10555-016-9634-0>
- Kajikawa K, Yasui W, Sumiyoshi H, Yoshida K, Nakayama H, Ayhan A, Yokozaki H, Ito H, Tahara E (1991) Expression of epidermal growth factor in human tissues. *Immunohistochemical*



- and biochemical analysis. *Virchows Arch A Pathol Anat Histopathol* 418(1):27–32. <https://doi.org/10.1007/bf01600241>
- Kakkad SM, Solaiyappan M, Argani P, Sukumar S, Jacobs LK, Leibfritz D, Bhujwala ZM, Glunde K (2012) Collagen I fiber density increases in lymph node positive breast cancers: pilot study. *J Biomed Opt* 17(11):116017. <https://doi.org/10.1117/1.JBO.17.11.116017>
- Kaushik S, Pickup MW, Weaver VM (2016) From transformation to metastasis: deconstructing the extracellular matrix in breast cancer. *Cancer Metastasis Rev* 35(4):655–667. <https://doi.org/10.1007/s10555-016-9650-0>
- Kennedy C, Burnstock G (1985) Evidence for two types of P2-purinoceptor in longitudinal muscle of the rabbit portal vein. *Eur J Pharmacol* 111(1):49–56. [https://doi.org/10.1016/0014-2999\(85\)90112-8](https://doi.org/10.1016/0014-2999(85)90112-8)
- Kim IY, Jeong SJ, Kim ES, Kim SH, Moon A (2007) Type I collagen-induced pro-MMP-2 activation is differentially regulated by H-Ras and N-Ras in human breast epithelial cells. *J Biochem Mol Biol* 40(5):825–831. <https://doi.org/10.5483/bmbrep.2007.40.5.825>
- Kim J, Kong J, Chang H, Kim H, Kim A (2016) EGF induces epithelial-mesenchymal transition through phospho-Smad2/3-Snail signaling pathway in breast cancer cells. *Oncotarget* 7(51):85021–85032. <https://doi.org/10.18632/oncotarget.13116>
- Konitsiotis AD, Raynal N, Bihan D, Hohenester E, Farndale RW, Leitinger B (2008) Characterization of high affinity binding motifs for the discoidin domain receptor DDR2 in collagen. *J Biol Chem* 283(11):6861–6868. <https://doi.org/10.1074/jbc.M709290200>
- Kuipers AJ, Middelbeek J, Vrenken K, Perez-Gonzalez C, Poelmans G, Klarenbeek J, Jalink K, Treppe X, van Leeuwen FN (2018) TRPM7 controls mesenchymal features of breast cancer cells by tensional regulation of SOX4. *Biochimica et biophysica acta Molecular basis of disease* 1864(7):2409–2419. <https://doi.org/10.1016/j.bbadis.2018.04.017>
- Lai Q, Wang T, Guo Q, Zhang Y, Wang Y, Yuan L, Ling R, He Y, Wang W (2014) Positive correlation between the expression of hEag1 and HIF-1alpha in breast cancers: an observational study. *BMJ Open* 4(5):e005049. <https://doi.org/10.1136/bmjopen-2014-005049>
- Leitinger B (2014) Discoidin domain receptor functions in physiological and pathological conditions. *Int Rev Cell Mol Biol* 310:39–87. <https://doi.org/10.1016/B978-0-12-800180-6.00002-5>
- Levitan IB (1994) Modulation of ion channels by protein phosphorylation and dephosphorylation. *Annu Rev Physiol* 56:193–212. <https://doi.org/10.1146/annurev.ph.56.030194.001205>
- Li C, Rezaia S, Kammerer S, Sokolowski A, Devaney T, Gorischek A, Jahn S, Hackl H, Groschner K, Windpassinger C, Malle E, Bauernhofer T, Schreibmayer W (2015) Piezo1 forms mechanosensitive ion channels in the human MCF-7 breast cancer cell line. *Sci Rep* 5:8364. <https://doi.org/10.1038/srep08364>
- Liu J, Huang C, Zhan X (1999) Src is required for cell migration and shape changes induced by fibroblast growth factor 1. *Oncogene* 18(48):6700–6706. <https://doi.org/10.1038/sj.onc.1203050>
- Liu X, Wang T, Wang Y, Chen Z, Hua D, Yao X, Ma X, Zhang P (2018) Orail is critical for Notch-driven aggressiveness under hypoxic conditions in triple-negative breast cancers. *Biochim Biophys Acta Mol Basis Disease* 1864(4 Pt A):975–986. <https://doi.org/10.1016/j.bbadis.2018.01.003>
- Lo HW, Hsu SC, Xia W, Cao X, Shih JY, Wei Y, Abbruzzese JL, Hortobagyi GN, Hung MC (2007) Epidermal growth factor receptor cooperates with signal transducer and activator of transcription 3 to induce epithelial-mesenchymal transition in cancer cells via up-regulation of TWIST gene expression. *Cancer Res* 67(19):9066–9076. <https://doi.org/10.1158/0008-5472.CAN-07-0575>
- Lochter A, Navre M, Werb Z, Bissell MJ (1999) alpha1 and alpha2 integrins mediate invasive activity of mouse mammary carcinoma cells through regulation of stromelysin-1 expression. *Mol Biol Cell* 10(2):271–282. <https://doi.org/10.1091/mbc.10.2.271>
- Lou W, Liu J, Ding B, Jin L, Xu L, Li X, Chen J, Fan W (2019) Five miRNAs-mediated PIEZO2 downregulation, accompanied with activation of Hedgehog signaling pathway, predicts poor prognosis of breast cancer. *Aging* 11(9):2628–2652. <https://doi.org/10.18632/aging.101934>

- Lu X, Kang Y (2010) Epidermal growth factor signalling and bone metastasis. *Br J Cancer* 102(3):457–461. <https://doi.org/10.1038/sj.bjc.6605490>
- Lu H, Chen I, Shimoda LA, Park Y, Zhang C, Tran L, Zhang H, Semenza GL (2017) Chemotherapy-induced Ca(2+) release stimulates breast cancer stem cell enrichment. *Cell Rep* 18(8):1946–1957. <https://doi.org/10.1016/j.celrep.2017.02.001>
- Ma Z, Yuan D, Cheng X, Tuo B, Liu X, Li T (2019) Function of ion transporters in maintaining acid-base homeostasis of the mammary gland and the pathophysiological role in breast cancer. *Am J Physiol Regul Integr Comp Physiol*. <https://doi.org/10.1152/ajpregu.00202.2019>
- Maffey A, Storini C, Diceglie C, Martelli C, Sironi L, Calzarossa C, Tonna N, Lovchik R, Delamarque E, Ottobrini L, Bianco F (2017) Mesenchymal stem cells from tumor microenvironment favour breast cancer stem cell proliferation, cancerogenic and metastatic potential, via ionotropic purinergic signalling. *Sci Rep* 7(1):13162. <https://doi.org/10.1038/s41598-017-13460-7>
- Manoli S, Coppola S, Duranti C, Lulli M, Magni L, Kuppala N, Nielsen N, Schmidt T, Schwab A, Becchetti A, Arcangeli A (2019) The activity of Kv 11.1 potassium channel modulates F-actin organization during cell migration of pancreatic ductal adenocarcinoma cells. *Cancer* 11(2). <https://doi.org/10.3390/cancers11020135>
- Maquoi E, Assent D, Detilleux J, Pequeux C, Foidart JM, Noel A (2012) MT1-MMP protects breast carcinoma cells against type I collagen-induced apoptosis. *Oncogene* 31(4):480–493. <https://doi.org/10.1038/onc.2011.249>
- Masuda H, Zhang D, Bartholomeusz C, Doihara H, Hortobagyi GN, Ueno NT (2012) Role of epidermal growth factor receptor in breast cancer. *Breast Cancer Res Treat* 136(2):331–345. <https://doi.org/10.1007/s10549-012-2289-9>
- Monteith GR, Prevarskaya N, Roberts-Thomson SJ (2017) The calcium-cancer signalling nexus. *Nat Rev Cancer* 17(6):367–380. <https://doi.org/10.1038/nrc.2017.18>
- Morris BA, Burkel B, Ponik SM, Fan J, Condeelis JS, Aguirre-Ghiso JA, Castracane J, Denu JM, Keely PJ (2016) Collagen matrix density drives the metabolic shift in breast cancer cells. *EBioMedicine* 13:146–156. <https://doi.org/10.1016/j.ebiom.2016.10.012>
- Mouw JK, Ou G, Weaver VM (2014) Extracellular matrix assembly: a multiscale deconstruction. *Nat Rev Mol Cell Biol* 15(12):771–785. <https://doi.org/10.1038/nrm3902>
- Mu D, Chen L, Zhang X, See LH, Koch CM, Yen C, Tong JJ, Spiegel L, Nguyen KC, Servoss A, Peng Y, Pei L, Marks JR, Lowe S, Hoey T, Jan LY, McCombie WR, Wigler MH, Powers S (2003) Genomic amplification and oncogenic properties of the KCNK9 potassium channel gene. *Cancer Cell* 3(3):297–302. [https://doi.org/10.1016/s1535-6108\(03\)00054-0](https://doi.org/10.1016/s1535-6108(03)00054-0)
- Muraoka RS, Dumont N, Ritter CA, Dugger TC, Brantley DM, Chen J, Easterly E, Roebuck LR, Ryan S, Gotwals PJ, Koteliansky V, Arteaga CL (2002) Blockade of TGF-beta inhibits mammary tumor cell viability, migration, and metastases. *J Clin Invest* 109(12):1551–1559. <https://doi.org/10.1172/JCI15234>
- Olsen DA, Bechmann T, Ostergaard B, Wamberg PA, Jakobsen EH, Brandslund I (2012) Increased concentrations of growth factors and activation of the EGFR system in breast cancer. *Clin Chem Lab Med* 50(10):1809–1818. <https://doi.org/10.1515/cclm-2011-0823>
- Onkal R, Djamgoz MB (2009) Molecular pharmacology of voltage-gated sodium channel expression in metastatic disease: clinical potential of neonatal Nav1.5 in breast cancer. *Eur J Pharmacol* 625(1-3):206–219. <https://doi.org/10.1016/j.ejphar.2009.08.040>
- Ouadid-Ahidouch H, Ahidouch A, Pardo LA (2016) Kv10.1 K(+) channel: from physiology to cancer. *Pflugers Arch* 468(5):751–762. <https://doi.org/10.1007/s00424-015-1784-3>
- Pang MF, Georgoudaki AM, Lambut L, Johansson J, Tabor V, Hagikura K, Jin Y, Jansson M, Alexander JS, Nelson CM, Jakobsson L, Betsholtz C, Sund M, Karlsson MC, Fuxe J (2016) TGF-beta1-induced EMT promotes targeted migration of breast cancer cells through the lymphatic system by the activation of CCR7/CCL21-mediated chemotaxis. *Oncogene* 35(6):748–760. <https://doi.org/10.1038/onc.2015.133>
- Pardo-Pastor C, Rubio-Moscardo F, Vogel-Gonzalez M, Serra SA, Afthinos A, Mrkonjic S, Destaing O, Abenza JF, Fernandez-Fernandez JM, Trepate X, Albiges-Rizo C,



- Konstantopoulos K, Valverde MA (2018) Piezo2 channel regulates RhoA and actin cytoskeleton to promote cell mechanobiological responses. *Proc Natl Acad Sci U S A* 115(8):1925–1930. <https://doi.org/10.1073/pnas.1718177115>
- Patel AJ, Lazdunski M (2004) The 2P-domain K<sup>+</sup> channels: role in apoptosis and tumorigenesis. *Pflugers Arch* 448(3):261–273. <https://doi.org/10.1007/s00424-004-1255-8>
- Pei L, Wisner O, Slavin A, Mu D, Powers S, Jan LY, Hoey T (2003) Oncogenic potential of TASK3 (Kcnk9) depends on K<sup>+</sup> channel function. *Proc Natl Acad Sci U S A* 100(13):7803–7807. <https://doi.org/10.1073/pnas.1232448100>
- Pellegatti P, Raffaghello L, Bianchi G, Piccardi F, Pistoia V, Di Virgilio F (2008) Increased level of extracellular ATP at tumor sites: in vivo imaging with plasma membrane luciferase. *PLoS One* 3(7):e2599. <https://doi.org/10.1371/journal.pone.0002599>
- Peppelenbosch MP, Tertoolen LG, de Laat SW (1991) Epidermal growth factor-activated calcium and potassium channels. *J Biol Chem* 266(30):19938–19944
- Peppelenbosch MP, Tertoolen LG, den Hertog J, de Laat SW (1992) Epidermal growth factor activates calcium channels by phospholipase A2/5-lipoxygenase-mediated leukotriene C4 production. *Cell* 69(2):295–303. [https://doi.org/10.1016/0092-8674\(92\)90410-e](https://doi.org/10.1016/0092-8674(92)90410-e)
- Peretti M, Angelini M, Savalli N, Florio T, Yuspa SH, Mazzanti M (2015) Chloride channels in cancer: Focus on chloride intracellular channel 1 and 4 (CLIC1 AND CLIC4) proteins in tumor development and as novel therapeutic targets. *Biochim Biophys Acta* 1848(10 Pt B):2523–2531. <https://doi.org/10.1016/j.bbame.2014.12.012>
- Peretti M, Badaoui M, Girault A, Van Gulick L, Mabilille MP, Tebbakha R, Sevestre H, Morjani H, Ouadid-Ahidouch H (2019) Original association of ion transporters mediates the ECM-induced breast cancer cell survival: Kv10.1-Orai1-SPCA2 partnership. *Sci Rep* 9(1):1175. <https://doi.org/10.1038/s41598-018-37602-7>
- Petho Z, Najder K, Bulk E, Schwab A (2019) Mechanosensitive ion channels push cancer progression. *Cell Calcium* 80:79–90. <https://doi.org/10.1016/j.ceca.2019.03.007>
- Phillips L, Gill AJ, Baxter RC (2019) Novel prognostic markers in triple-negative breast cancer discovered by MALDI-mass spectrometry imaging. *Front Oncol* 9:379. <https://doi.org/10.3389/fonc.2019.00379>
- Pickup MW, Mouw JK, Weaver VM (2014) The extracellular matrix modulates the hallmarks of cancer. *EMBO Rep* 15(12):1243–1253. <https://doi.org/10.15252/embr.201439246>
- Provenzano PP, Inman DR, Eliceiri KW, Knittel JG, Yan L, Rueden CT, White JG, Keely PJ (2008) Collagen density promotes mammary tumor initiation and progression. *BMC Med* 6:11. <https://doi.org/10.1186/1741-7015-6-11>
- Rammal H, Saby C, Magnien K, Van-Gulick L, Garnotel R, Buache E, El Btaouri H, Jeannesson P, Morjani H (2016) Discoidin domain receptors: potential actors and targets in cancer. *Front Pharmacol* 7:55. <https://doi.org/10.3389/fphar.2016.00055>
- Ray A, Slama ZM, Morford RK, Madden SA, Provenzano PP (2017) Enhanced directional migration of cancer stem cells in 3D aligned collagen matrices. *Biophys J* 112(5):1023–1036. <https://doi.org/10.1016/j.bpj.2017.01.007>
- Riching KM, Cox BL, Salick MR, Pehlke C, Riching AS, Ponik SM, Bass BR, Crone WC, Jiang Y, Weaver AM, Eliceiri KW, Keely PJ (2014) 3D collagen alignment limits protrusions to enhance breast cancer cell persistence. *Biophys J* 107(11):2546–2558. <https://doi.org/10.1016/j.bpj.2014.10.035>
- Roger S, Gillet L, Le Guennec JY, Besson P (2015) Voltage-gated sodium channels and cancer: is excitability their primary role? *Front Pharmacol* 6:152. <https://doi.org/10.3389/fphar.2015.00152>
- Saby C, Rammal H, Magnien K, Buache E, Brassart-Pasco S, Van-Gulick L, Jeannesson P, Maquoi E, Morjani H (2018) Age-related modifications of type I collagen impair DDR1-induced apoptosis in non-invasive breast carcinoma cells. *Cell Adh Migr* 12(4):335–347. <https://doi.org/10.1080/19336918.2018.1472182>
- Saby C, Collin G, Sinane M, Buache E, Van Gulick L, Saltel F, Maquoi E, Morjani H (2019) DDR1 and MT1-MMP expression levels are determinant for triggering BIK-mediated apoptosis by 3D

- type I collagen matrix in invasive basal-like breast carcinoma cells. *Front Pharmacol* 10:462. <https://doi.org/10.3389/fphar.2019.00462>
- Samanta D, Gilkes DM, Chaturvedi P, Xiang L, Semenza GL (2014) Hypoxia-inducible factors are required for chemotherapy resistance of breast cancer stem cells. *Proc Natl Acad Sci U S A* 111(50):E5429–E5438. <https://doi.org/10.1073/pnas.1421438111>
- Sandoval M, Burgos J, Sepulveda FV, Cid LP (2011) Extracellular pH in restricted domains as a gating signal for ion channels involved in transepithelial transport. *Biol Pharm Bull* 34(6):803–809. <https://doi.org/10.1248/bpb.34.803>
- Schaar A, Sukumaran P, Sun Y, Dhasarathy A, Singh BB (2016) TRPC1-STIM1 activation modulates transforming growth factor beta-induced epithelial-to-mesenchymal transition. *Oncotarget* 7(49):80554–80567. <https://doi.org/10.18632/oncotarget.12895>
- Schindl M, Schoppmann SF, Samonigg H, Hausmaninger H, Kwasny W, Gnant M, Jakesz R, Kubista E, Birner P, Oberhuber G, Austrian Breast and Colorectal Cancer Study Group (2002) Overexpression of hypoxia-inducible factor 1alpha is associated with an unfavorable prognosis in lymph node-positive breast cancer. *Clin Cancer Res* 8(6):1831–1837
- Schwab LP, Peacock DL, Majumdar D, Ingels JF, Jensen LC, Smith KD, Cushing RC, Seagroves TN (2012) Hypoxia-inducible factor 1alpha promotes primary tumor growth and tumor-initiating cell activity in breast cancer. *Breast Cancer Res* 14(1):R6. <https://doi.org/10.1186/bcr3087>
- Seguin L, Desgrosellier JS, Weis SM, Cheresh DA (2015) Integrins and cancer: regulators of cancer stemness, metastasis, and drug resistance. *Trends Cell Biol* 25(4):234–240. <https://doi.org/10.1016/j.tcb.2014.12.006>
- Semenza GL (2000) Hypoxia, clonal selection, and the role of HIF-1 in tumor progression. *Crit Rev Biochem Mol Biol* 35(2):71–103. <https://doi.org/10.1080/10409230091169186>
- Semenza GL (2012) Hypoxia-inducible factors: mediators of cancer progression and targets for cancer therapy. *Trends Pharmacol Sci* 33(4):207–214. <https://doi.org/10.1016/j.tips.2012.01.005>
- Shweiki D, Itin A, Soffer D, Keshet E (1992) Vascular endothelial growth factor induced by hypoxia may mediate hypoxia-initiated angiogenesis. *Nature* 359(6398):843–845. <https://doi.org/10.1038/359843a0>
- Song MS, Park SM, Park JS, Byun JH, Jin HJ, Seo SH, Ryu PD, Lee SY (2018) Kv3.1 and Kv3.4, are involved in cancer cell migration and invasion. *Int J Mol Sci* 19(4). <https://doi.org/10.3390/ijms19041061>
- Soysal SD, Tzankov A, Muenst SE (2015) Role of the tumor microenvironment in breast cancer. *Pathobiology* 82(3–4):142–152. <https://doi.org/10.1159/000430499>
- Sparks RL, Pool TB, Smith NK, Cameron IL (1983) Effects of amiloride on tumor growth and intracellular element content of tumor cells in vivo. *Cancer Res* 43(1):73–77
- Stowers RS, Allen SC, Sanchez K, Davis CL, Ebel ND, Van Den Berg C, Suggs LJ (2017) Extracellular matrix stiffening induces a malignant phenotypic transition in breast epithelial cells. *Cell Mol Bioeng* 10(1):114–123. <https://doi.org/10.1007/s12195-016-0468-1>
- Sullivan R, Pare GC, Frederiksen LJ, Semenza GL, Graham CH (2008) Hypoxia-induced resistance to anticancer drugs is associated with decreased senescence and requires hypoxia-inducible factor-1 activity. *Mol Cancer Ther* 7(7):1961–1973. <https://doi.org/10.1158/1535-7163.MCT-08-0198>
- Tafani M, Schito L, Pellegrini L, Villanova L, Marfe G, Anwar T, Rosa R, Indelicato M, Fini M, Pucci B, Russo MA (2011) Hypoxia-increased RAGE and P2X7R expression regulates tumor cell invasion through phosphorylation of Erk1/2 and Akt and nuclear translocation of NF- $\kappa$ B. *Carcinogenesis* 32(8):1167–1175. <https://doi.org/10.1093/carcin/bgr101>
- Takai K, Drain AP, Lawson DA, Littlepage LE, Karpuj M, Kessenbrock K, Le A, Inoue K, Weaver VM, Werb Z (2018) Discoidin domain receptor 1 (DDR1) ablation promotes tissue fibrosis and hypoxia to induce aggressive basal-like breast cancers. *Genes Dev* 32(3–4):244–257. <https://doi.org/10.1101/gad.301366.117>



- Thiery JP (2002) Epithelial-mesenchymal transitions in tumour progression. *Nat Rev Cancer* 2 (6):442–454. <https://doi.org/10.1038/nrc822>
- Tischkowitz M, Brunet JS, Begin LR, Huntsman DG, Cheang MC, Akslen LA, Nielsen TO, Foulkes WD (2007) Use of immunohistochemical markers can refine prognosis in triple negative breast cancer. *BMC Cancer* 7:134. <https://doi.org/10.1186/1471-2407-7-134>
- Toral C, Mendoza-Garrido ME, Azorin E, Hernandez-Gallegos E, Gomora JC, Delgadillo DM, Solano-Agama C, Camacho J (2007) Effect of extracellular matrix on adhesion, viability, actin cytoskeleton and K<sup>+</sup> currents of cells expressing human ether a go-go channels. *Life Sci* 81 (3):255–265. <https://doi.org/10.1016/j.lfs.2007.05.014>
- Tosatto A, Sommaggio R, Kummerow C, Bentham RB, Blacker TS, Berecz T, Duchon MR, Rosato A, Bogeski I, Szabadkai G, Rizzuto R, Mammucari C (2016) The mitochondrial calcium uniporter regulates breast cancer progression via HIF-1alpha. *EMBO Mol Med* 8(5):569–585. <https://doi.org/10.15252/emmm.201606255>
- Tower H, Ruppert M, Britt K (2019) The immune microenvironment of breast cancer progression. *Cancer* 11(9). <https://doi.org/10.3390/cancers11091375>
- Toy KA, Valiathan RR, Nunez F, Kidwell KM, Gonzalez ME, Fridman R, Kleer CG (2015) Tyrosine kinase discoidin domain receptors DDR1 and DDR2 are coordinately deregulated in triple-negative breast cancer. *Breast Cancer Res Treat* 150(1):9–18. <https://doi.org/10.1007/s10549-015-3285-7>
- Valiathan RR, Marco M, Leitinger B, Kleer CG, Fridman R (2012) Discoidin domain receptor tyrosine kinases: new players in cancer progression. *Cancer Metastasis Rev* 31(1-2):295–321. <https://doi.org/10.1007/s10555-012-9346-z>
- Vogel W, Gish GD, Alves F, Pawson T (1997) The discoidin domain receptor tyrosine kinases are activated by collagen. *Mol Cell* 1(1):13–23. [https://doi.org/10.1016/s1097-2765\(00\)80003-9](https://doi.org/10.1016/s1097-2765(00)80003-9)
- Walia V, Ding M, Kumar S, Nie D, Premkumar LS, Elble RC (2009) hCLCA2 is a p53-inducible inhibitor of breast cancer cell proliferation. *Cancer Res* 69(16):6624–6632. <https://doi.org/10.1158/0008-5472.CAN-08-4101>
- Wang Y, Li SJ, Pan J, Che Y, Yin J, Zhao Q (2011) Specific expression of the human voltage-gated proton channel Hv1 in highly metastatic breast cancer cells, promotes tumor progression and metastasis. *Biochem Biophys Res Commun* 412(2):353–359. <https://doi.org/10.1016/j.bbrc.2011.07.102>
- Wang Y, Li SJ, Wu X, Che Y, Li Q (2012) Clinicopathological and biological significance of human voltage-gated proton channel Hv1 protein overexpression in breast cancer. *J Biol Chem* 287(17):13877–13888. <https://doi.org/10.1074/jbc.M112.345280>
- Webb BA, Chimenti M, Jacobson MP, Barber DL (2011) Dysregulated pH: a perfect storm for cancer progression. *Nat Rev Cancer* 11(9):671–677. <https://doi.org/10.1038/nrc3110>
- Weber LV, Al-Refae K, Wolk G, Bonatz G, Altmuller J, Becker C, Gisselmann G, Hatt H (2016) Expression and functionality of TRPV1 in breast cancer cells. *Breast Cancer (Dove Med Press)* 8:243–252. <https://doi.org/10.2147/BCTT.S121610>
- Wee P, Wang Z (2017) Epidermal Growth Factor Receptor Cell Proliferation Signaling Pathways. *Cancer* 9(5). <https://doi.org/10.3390/cancers9050052>
- White KA, Grillo-Hill BK, Barber DL (2017) Cancer cell behaviors mediated by dysregulated pH dynamics at a glance. *J Cell Sci* 130(4):663–669. <https://doi.org/10.1242/jcs.195297>
- Williams S, Bateman A, O'Kelly I (2013) Altered expression of two-pore domain potassium (K2P) channels in cancer. *PLoS One* 8(10):e74589. <https://doi.org/10.1371/journal.pone.0074589>
- Wu TT, Peters AA, Tan PT, Roberts-Thomson SJ, Monteith GR (2014) Consequences of activating the calcium-permeable ion channel TRPV1 in breast cancer cells with regulated TRPV1 expression. *Cell Calcium* 56(2):59–67. <https://doi.org/10.1016/j.ceca.2014.04.006>
- Wu Y, Gao B, Xiong QJ, Wang YC, Huang DK, Wu WN (2017) Acid-sensing ion channels contribute to the effect of extracellular acidosis on proliferation and migration of A549 cells. *Tumour Biol* 39(6):1010428317705750. <https://doi.org/10.1177/1010428317705750>
- Xiang L, Gilkes DM, Hu H, Takano N, Luo W, Lu H, Bullen JW, Samanta D, Liang H, Semenza GL (2014) Hypoxia-inducible factor 1 mediates TAZ expression and nuclear localization to

- induce the breast cancer stem cell phenotype. *Oncotarget* 5(24):12509–12527. <https://doi.org/10.18632/oncotarget.2997>
- Xie JW, Haslam SZ (2008) Extracellular matrix, Rac1 signaling, and estrogen-induced proliferation in MCF-7 breast cancer cells. *Breast Cancer Res Treat* 110(2):257–268. <https://doi.org/10.1007/s10549-007-9719-0>
- Xu S, Xu H, Wang W, Li S, Li H, Li T, Zhang W, Yu X, Liu L (2019) The role of collagen in cancer: from bench to bedside. *J Transl Med* 17(1):309. <https://doi.org/10.1186/s12967-019-2058-1>
- Yang M, James AD, Suman R, Kasprowicz R, Nelson M, O'Toole PJ, Brackenbury WJ (2019) Voltage-dependent activation of Rac1 by Nav 1.5 channels promotes cell migration. *J Cell Physiol*. <https://doi.org/10.1002/jcp.29290>
- Yegutkin GG (2008) Nucleotide- and nucleoside-converting ectoenzymes: Important modulators of purinergic signalling cascade. *Biochim Biophys Acta* 1783(5):673–694. <https://doi.org/10.1016/j.bbamcr.2008.01.024>
- Yeldag G, Rice A, Del Rio HA (2018) Chemoresistance and the self-maintaining tumor microenvironment. *Cancer* 10(12). <https://doi.org/10.3390/cancers10120471>
- Yin T, Yu S, Xiao L, Zhang J, Liu C, Lu Y, Liu C (2008) Correlation between the expression of aquaporin 1 and hypoxia-inducible factor 1 in breast cancer tissues. *J Huazhong Univ Sci Technol Med Sci* 28(3):346–348. <https://doi.org/10.1007/s11596-008-0327-y>
- Yu Y, Feng XH (2019) TGF-beta signaling in cell fate control and cancer. *Curr Opin Cell Biol* 61:56–63. <https://doi.org/10.1016/j.ceb.2019.07.007>
- Zhang DY, Zhang YH, Sun HY, Lau CP, Li GR (2011) Epidermal growth factor receptor tyrosine kinase regulates the human inward rectifier potassium K(IR)2.3 channel, stably expressed in HEK 293 cells. *Br J Pharmacol* 164(5):1469–1478. <https://doi.org/10.1111/j.1476-5381.2011.01424.x>
- Zhang K, Corsa CA, Ponik SM, Prior JL, Piwnicka-Worms D, Eliceiri KW, Keely PJ, Longmore GD (2013) The collagen receptor discoidin domain receptor 2 stabilizes SNAIL1 to facilitate breast cancer metastasis. *Nat Cell Biol* 15(6):677–687. <https://doi.org/10.1038/ncb2743>
- Zhang P, Yang X, Yin Q, Yi J, Shen W, Zhao L, Zhu Z, Liu J (2016) Inhibition of SK4 potassium channels suppresses cell proliferation, migration and the epithelial-mesenchymal transition in triple-negative breast cancer cells. *PLoS One* 11(4):e0154471. <https://doi.org/10.1371/journal.pone.0154471>
- Zhong H, De Marzo AM, Laughner E, Lim M, Hilton DA, Zagzag D, Buechler P, Isaacs WB, Semenza GL, Simons JW (1999) Overexpression of hypoxia-inducible factor 1 alpha in common human cancers and their metastases. *Cancer Res* 59(22):5830–5835
- Zhou FM, Huang YY, Tian T, Li XY, Tang YB (2018) Knockdown of chloride channel-3 inhibits breast cancer growth in vitro and in vivo. *J Breast Cancer* 21(2):103–111. <https://doi.org/10.4048/jbc.2018.21.2.103>
- Zhu Y, Pan Q, Meng H, Jiang Y, Mao A, Wang T, Hua D, Yao X, Jin J, Ma X (2015) Enhancement of vascular endothelial growth factor release in long-term drug-treated breast cancer via transient receptor potential channel 5-Ca(2+)-hypoxia-inducible factor 1alpha pathway. *Pharmacol Res* 93:36–42. <https://doi.org/10.1016/j.phrs.2014.12.006>

Article

# Cancer Cell Acid Adaptation Gene Expression Response Is Correlated to Tumor-Specific Tissue Expression Profiles and Patient Survival

Jiayi Yao <sup>1,2,†</sup>, Dominika Czaplinska <sup>3,†</sup>, Renata Ialchina <sup>3,†</sup>, Julie Schnipper <sup>3</sup>, Bin Liu <sup>4</sup> ,  
Albin Sandelin <sup>1,2,\*</sup>  and Stine Falsig Pedersen <sup>3,\*</sup> 

<sup>1</sup> The Bioinformatics Centre, Department of Biology, University of Copenhagen, DK2200 Copenhagen, Denmark; jiayi.yao@bio.ku.dk

<sup>2</sup> Biotech Research and Innovation Centre, University of Copenhagen, DK2200 Copenhagen, Denmark

<sup>3</sup> Section for Cell Biology and Physiology, Department of Biology, University of Copenhagen, DK2100 Copenhagen, Denmark; dominika.czaplinska@bio.ku.dk (D.C.); renata.ialchina@bio.ku.dk (R.I.); julie\_schnipper@hotmail.com (J.S.)

<sup>4</sup> Cell Death and Metabolism, Center for Autophagy, Recycling and Disease, Danish Cancer Society Research Center, DK2100 Copenhagen, Denmark; liu@cancer.dk

\* Correspondence: albin@binf.ku.dk (A.S.); sfpedersen@bio.ku.dk (S.F.P.)

† These authors contributed equally to this work.

Received: 17 June 2020; Accepted: 31 July 2020; Published: 5 August 2020



**Abstract:** The acidic pH of the tumor microenvironment plays a critical role in driving cancer development toward a more aggressive phenotype, but the underlying mechanisms are unclear. To this end, phenotypic and genotypic changes induced by adaptation of cancer cells to chronic acidosis have been studied. However, the generality of acid adaptation patterns across cell models and their correlation to the molecular phenotypes and aggressiveness of human cancers are essentially unknown. Here, we define an acid adaptation expression response shared across three cancer cell models, dominated by metabolic rewiring, extracellular matrix remodeling, and altered cell cycle regulation and DNA damage response. We find that many genes which are upregulated by acid adaptation are significantly correlated to patient survival, and more generally, that there are clear correlations between acid adaptation expression response and gene expression change between normal and tumor tissues, for a large subset of cancer patients. Our data support the notion that tumor microenvironment acidity is one of the key factors driving the selection of aggressive cancer cells in human patient tumors, yet it also induces a growth-limiting genotype that likely limits cancer cell growth until the cells are released from acidosis, for instance during invasion.

**Keywords:** RNA sequencing; tumor microenvironment; chronic acidosis; survival analysis; acid adaptation; medical transcriptomics

## 1. Introduction

Invasive cancers, regardless of their origin, acquire characteristic phenotypic traits during their development, including self-sufficiency with respect to growth signals, apoptosis evasion, profound metabolic changes, chemotherapy resistance, and the ability to invade and spread to secondary niches [1]. These changes are the result of a clonal evolution process, in which the combination of somatic mutations and evolutionary selection pressure leads to the preferential expansion of clones of cells that are particularly fit for survival and expansion in the harsh tumor microenvironment [2–4].

The microenvironmental conditions in solid tumors are a result of rapid cancer cell proliferation and growth which, in combination with insufficient vascularization, leads to hypoxia, glucose depletion,

accumulation of lactate and other metabolites, and profound acidosis. While serum pH is around 7.4, corresponding to a  $H^+$  concentration ( $[H^+]$ ) of ~40 nM, the extracellular pH ( $pH_e$ ) in tumors can reach 6.2–6.8, i.e.,  $[H^+]$  ~630–160 nM [5–9]. A plethora of studies have investigated the impact of hypoxia on cancer development and the therapeutic potential of targeting hypoxia-inducible factors (reviewed in, e.g., [10]). In contrast, the role of extracellular acidosis in this process remains incompletely understood. Recent studies, mostly employing the acid adaptation of cultured cancer cells, have supported the hypothesis that extracellular acidosis is a driver of cancer aggressiveness. Thus, adaptation to acidosis was shown to favor epithelial-to-mesenchymal transition (EMT) [11,12], invasiveness and metastasis in cell culture and xenograft models of melanoma, cervical cancer, and breast and colon cancer [13–16]. Accordingly, studies of mouse breast tumors in vivo showed that acidosis (detected by pH (low) insertion peptide (pHLIP) labeling), carbonic anhydrase (CA9) expression and plasma membrane-localized LAMP2 correlated with invasive features such as the absence of laminin and the expression of matrix metalloproteinase (MMP)-9 and -14 [17]. Other phenotypic changes induced by the adaptation of cancer cells to acidosis include a shift from glycolytic metabolism toward increased glutaminolysis, fatty acids uptake and  $\beta$ -oxidation [9,15,18–20]. Cancer cell proliferation and growth are, however, generally reduced, or unaltered, as long as acidic  $pH_e$  is maintained [12,13].

The molecular mechanisms through which growth under chronic extracellular acidosis leads to this profound rewiring of cancer cells are poorly understood. While several studies have examined global changes in gene expression upon acidosis or lactic acidosis [15,21,22], the overlap between the changes induced by acidosis and those found in patient tumors, and the correlation of acidosis-responsive gene expression to overall patient survival, have to our knowledge never been comprehensively examined. Because acidic growth seems to drive at least some phenotypes akin to those found in highly aggressive cancers, an important question is whether there is a generic response to acid adaptation that is shared between cancer cells, and whether this response reflects the expression changes observed between tumors and normal tissues in patient samples. Such correlations may indicate that an acidic microenvironment can increase cancer aggressiveness, which in turn should be correlated to patient survival.

In the present study, by applying RNA-seq to three acid-adapted cancer cell lines we identify a shared acid adaptation response gene signature, which we compare with rich expression data from human tumors and normal tissue across many cancers, and overall survival data from the same patients. Our results reveal significant overlaps between gene signatures of acid-adapted cells and tumor tissues for subsets of patients, and we identify sets of shared genes from these signatures that correlate significantly—positively as well as negatively—with patient survival.

## 2. Results

### 2.1. Gene Expression Changes Induced by Chronic Adaptation of Cancer Cells to Acidosis

To understand the changes in gene expression profile induced by changes in environmental pH ( $pH_e$ ) across multiple cancer cell types, rather than in a single cancer cell type, we adapted three different cancer cell lines to growth at either pH 7.6 or 6.5 by adjusting the  $HCO_3^-$  concentration of the medium [23], followed by culturing at the respective pH for at least 1 month at 5%  $CO_2$ . Cells were lysed, and RNA was isolated and subjected to global RNA-seq in triplicates (Figure 1A, top). Principal component (PC) analysis of gene expression estimates from RNA-seq libraries showed that PC1 and PC2 separated the three cell lines, while PC3 and PC4 separated acid-adapted cells from control cells, indicating a shared acid adaptation response across the three cell lines (Figure 1B). Given this, we set out to analyze the shared acid adaptation response, and compared it to tumor-specific expression profiles and patient survival using a strategy outlined in Figure 1A.



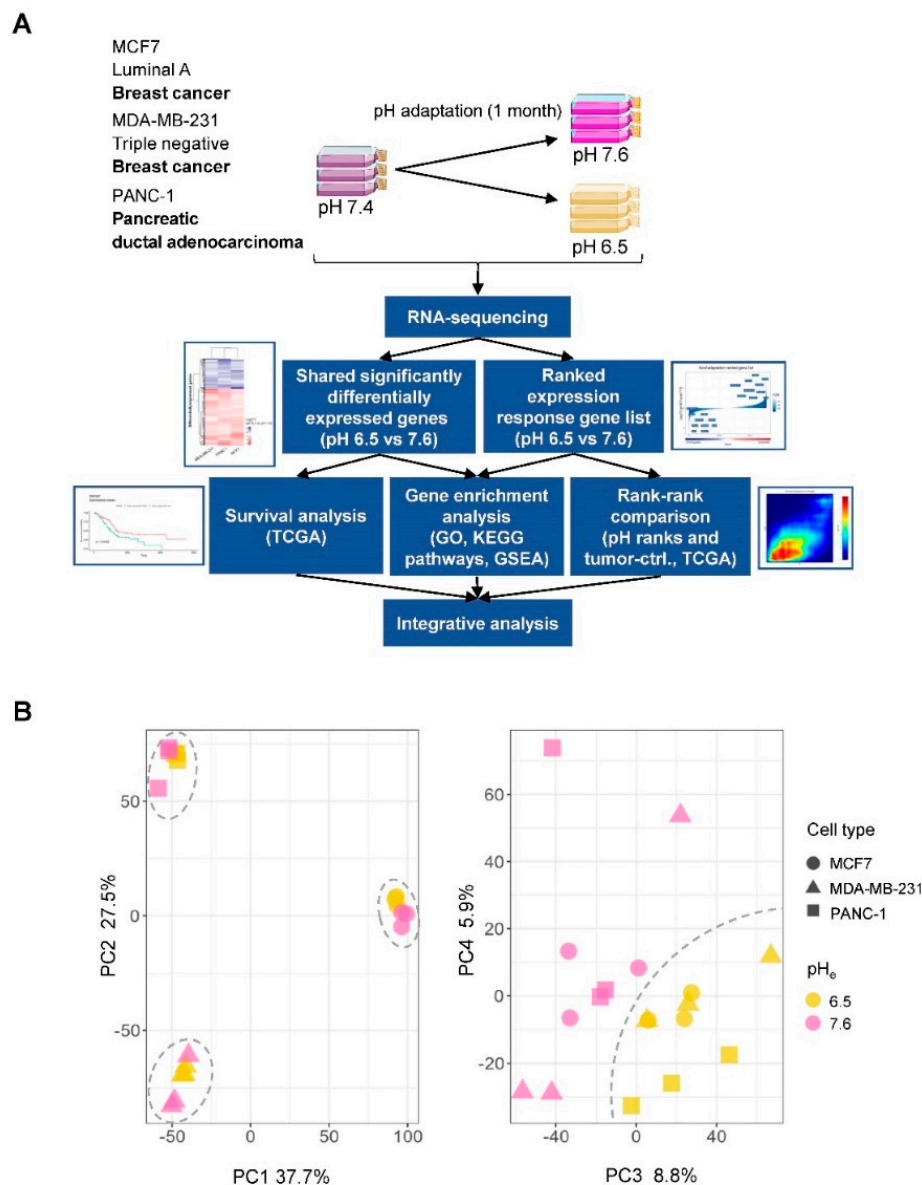


**Figure 1.** Overview of study procedures and analyses. **(A)** Overview of the experimental design, and individual and integrative analyses performed. Three cancer cell lines in triplicates (MDA-MB-231, MCF7 and PANC-1) were acid-adapted to pH 6.5 and 7.6 over a period of 1 month and subjected to RNA-sequencing analysis (RNA-seq). Below this, an overview of computational analyses performed is shown. Briefly, we used two strategies to define a shared acid adaptation gene expression profile: by defining sets of statistically significant genes, or by ranking genes by their expression fold change (pH 6.5 vs. 7.6; Figure 2). These lists were then subject to over-representation analyses (Figure 2), survival analysis in multiple cancers (Figure 3), and comparison to tumor-control tissue (ctrl.) RNA-seq experiments from patient samples (Figures 4 and 5), to identify a final list of genes that are up-/downregulated in acid adaptation as well as in tumor vs. ctrl. experiments, and whose in vivo expression is associated with overall patient survival (Figure 6). **(B)** Principle component analysis (PCA) based on gene expression. The x- and y-axes show principle components (PCs) 1 and 2 in left panel, 3 and 4 in right panel. Percentage explained variance is shown at each axis. Each dot corresponds to one RNA-seq library. Symbol shapes correspond to cell lines and color corresponds to pH treatment. In the left panel, dashed circles show three groups corresponding to cell lines. In the right panel, the dashed line divides samples by pH treatment.

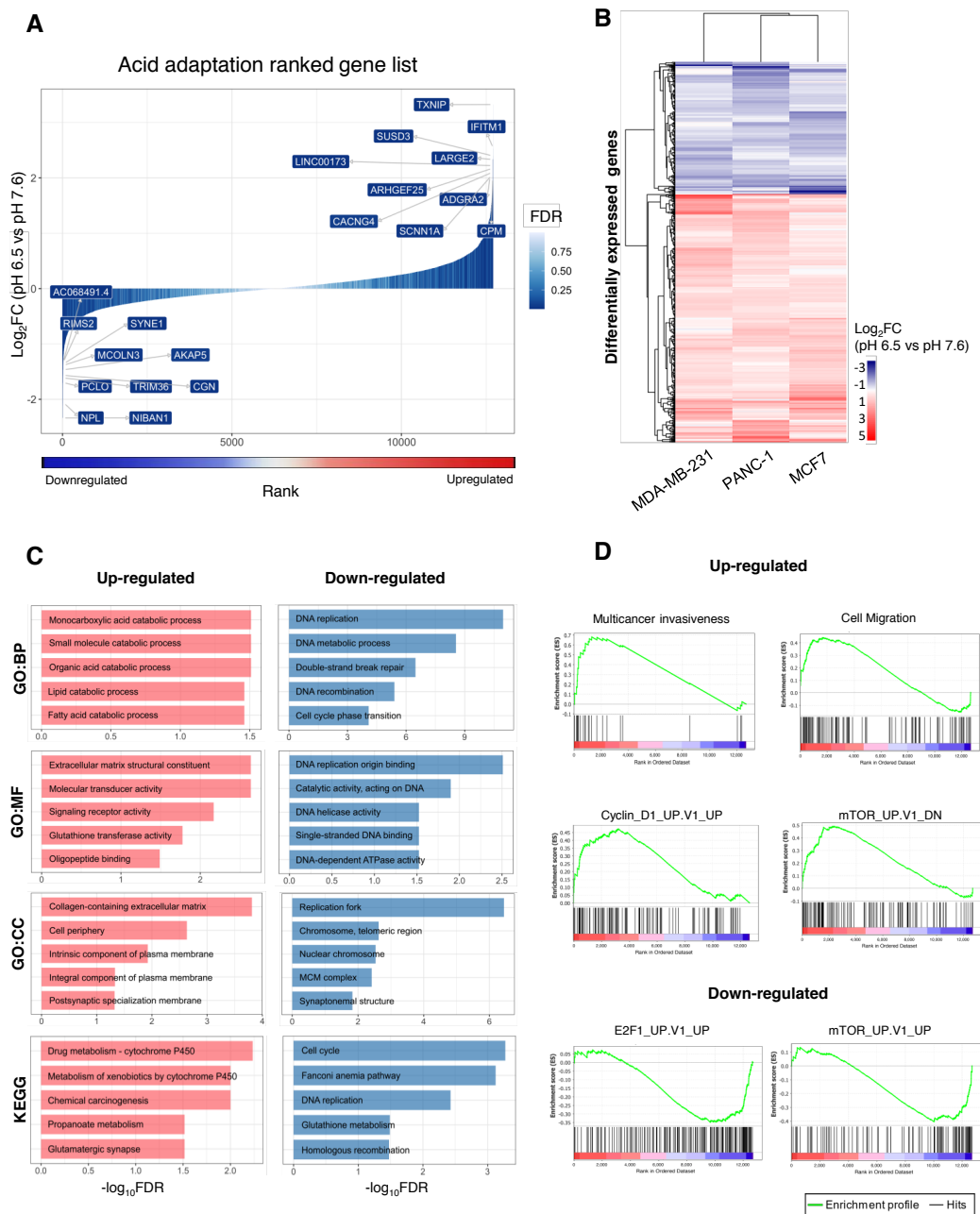


**Figure 2.** Identification of a shared acid adaptation expression response. (A) Fold change-based ranking of all genes differentially expressed in chronically acid-adapted cancer cells. The x-axis corresponds to the rank assigned to each gene from 1 to N based on gene expression fold change (pH 6.5 vs. pH 7.6) in log<sub>2</sub> scale (y-axis), also illustrated by blue–red gradient below. Bar color intensity indicates differential expression significance, expressed as false discovery rate (FDR). Genes with the largest absolute fold change are labelled on the plot. (B) Heatmap visualization of differential expression change in chronically acid-adapted cells. Rows correspond to significantly differentially expressed genes (480 upregulated and 256 downregulated), and columns correspond to three cancer cell lines (MDA-MB-231, PANC-1 and MCF7). Color indicates average log<sub>2</sub> fold change of gene expression (pH 6.5 vs. pH 7.6) across three replicates per condition. (C) Gene Ontology (GO) term analysis of differentially expressed genes in chronically acid-adapted cells. The x-axis shows GO term enrichment FDR values in  $-\log_{10}$  scale for differentially expressed genes defined above. The y-axis shows the top 5 GO terms from three categories (BP—Biological process, MF—Molecular function, CC—Cellular Component) and pathways from the KEGG (Kyoto Encyclopedia of Genes and Genomes) database, ordered by FDR. Bar colors correspond to up- or downregulated gene sets as in (B,D) Gene set enrichment analyses (GSEA) based on acid adaptation-ranked gene list from A to gene lists in the SigDB database. A subset of comparisons is shown as GSEA plots: the SigDB gene list identifier



is shown on top of each plot. The *y*-axis in subplot shows the enrichment score, reflecting how much the chosen gene set is over-represented at the top or bottom of the ranked acid adaptation gene list. In the *x*-axis, red indicates upregulation at pH 6.5, and blue downregulation, as in Figure 2A. Vertical lines in the lower part of the plot show where in the ranked acid adaptation gene list the genes in the selected SigDB gene list occurred.

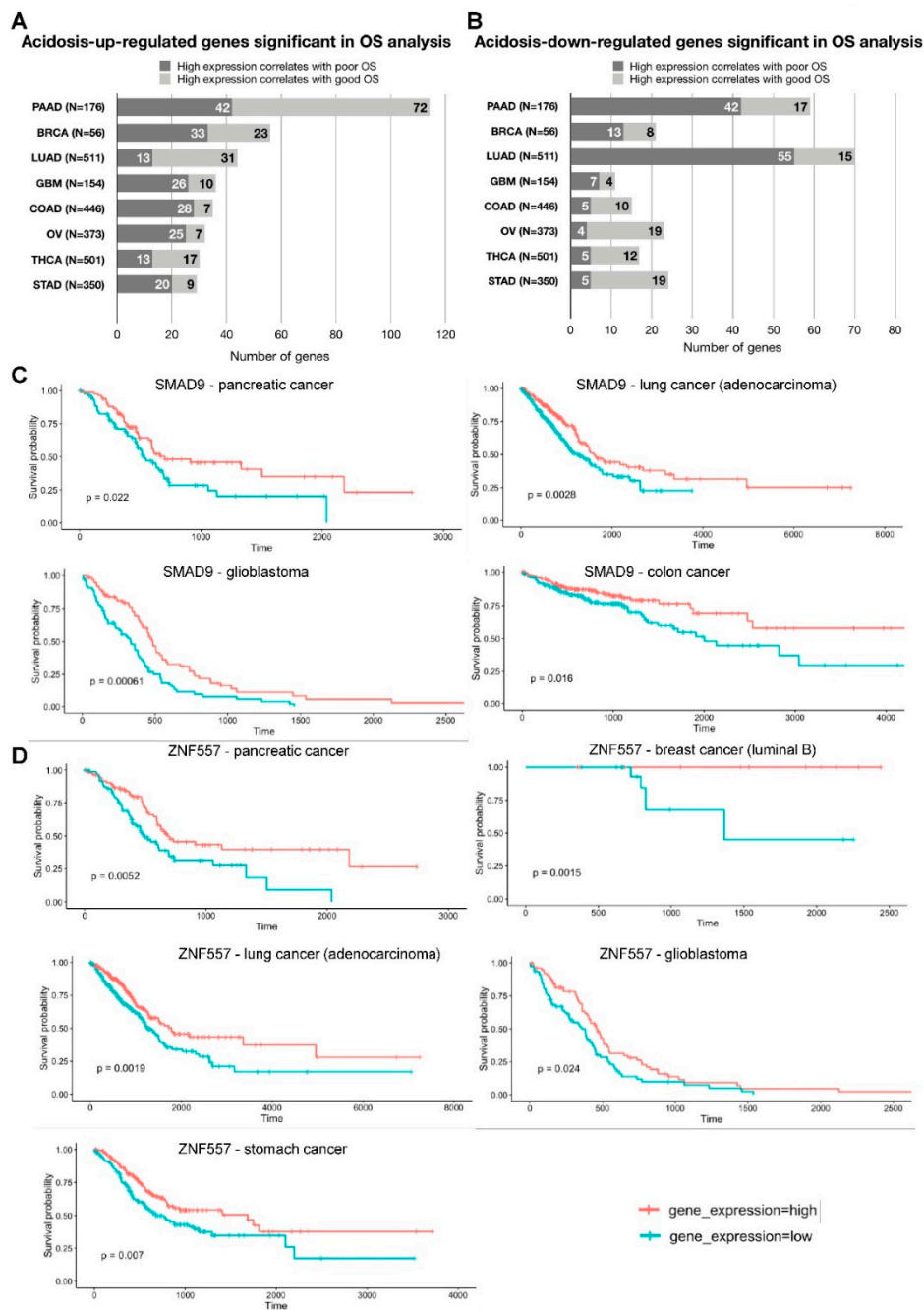


**Figure 3.** Correlation of genes differentially regulated in chronically acid adaptation cancer cells with patients' overall survival. (A) Summary of patient overall survival (OS) analysis based on acid adaptation-upregulated genes. Bars show the number of genes significantly associated with overall survival (*x*-axis), stratified by whether high patient gene expression correlates with poorer or better OS (indicated by bar color). The *y*-axis shows cancer type, where N is the number of patients analyzed. PAAD—pancreatic cancer, BRCA—breast cancer (luminal B), LUAD—lung cancer (adenocarcinoma),

GBM—glioblastoma, COAD—colon cancer, OV—ovarian cancer, THCA—thyroid cancer, STAD—stomach cancer. (B) Summary of patient OS analysis based on acid adaptation-downregulated genes. Arranged as in (A,C) Survival analysis based on SMAD9 expression levels. Kaplan–Meier overall survival analysis in pancreatic cancer, lung adenocarcinoma, glioblastoma and colon cancer patients, respectively, based on SMAD9 expression levels (GDC TCGA datasets). The *y*-axis shows survival probability, the *x*-axis shows time in days. Red line: patient group with high expression of the analyzed gene. Blue line: patient group with low expression of the analyzed gene. Survival analysis *p*-value is shown. (D) Survival analysis based on ZNF557 expression levels. Kaplan–Meier overall survival analysis in pancreatic cancer, breast cancer (luminal B), lung adenocarcinoma, glioblastoma and stomach cancer patients respectively, based on ZNF557 expression levels, arranged as in (C).

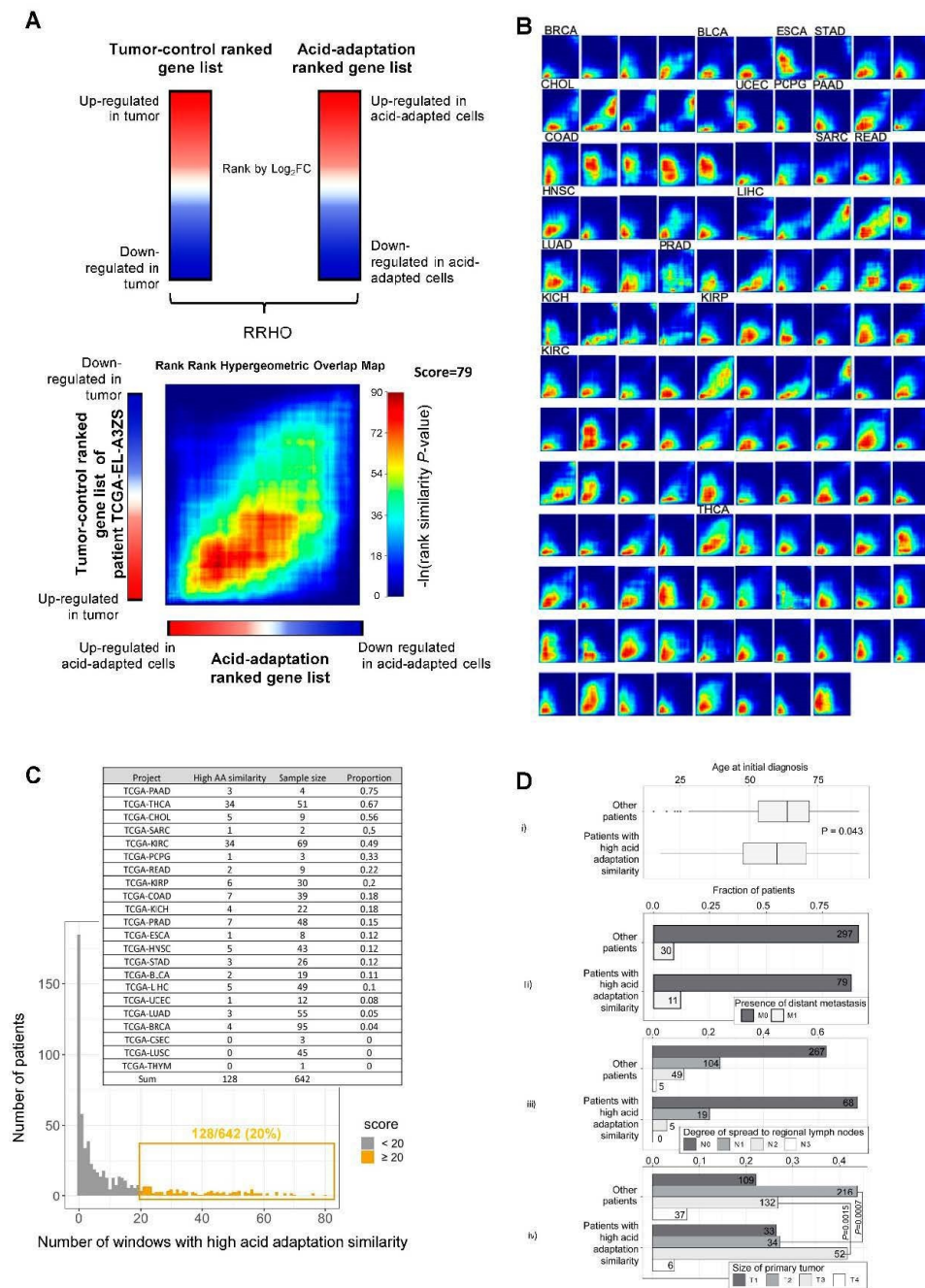


**Figure 4.** Rank–rank analysis of acid adaptation and patient tumor–ctrl. ranked gene lists. (A) Conceptual overview of rank–rank hypergeometric overlap (RRHO) analysis. Genes are ranked by their log2 fold expression change based on either tumor–ctrl. comparison for a given patient (left) or by acid adaptation

response (pH 6.5 vs. 7.6). These ranked gene lists are compared in the rank–rank heat map below (exemplified by the comparison of data from the TCGA patient TCGA-EL-A3ZS and the acid adaptation gene list), identifying windows of genes with correlated ranks in respective gene lists and the significance of such correlated ranks, as indicated by color (based on  $\ln(\text{hypergeometric } p\text{-values})$  as shown). (B) Heat maps resulting from patient tumor–ctrl. vs. acid adaptation gene list RRHO analyses showing high gene rank similarity. Each heat map corresponds to patient tumor–ctrl. vs. acid adaptation gene list analysis as in (A), where the acid adaptation gene list is always at the  $x$ -axis and the color scale is as in (A). Cancer types are indicated on top of heat maps: consecutive heat maps to the right have the same cancer type unless otherwise indicated (BRCA—breast cancer (luminal B), BLCA—bladder urothelial carcinoma, ESCA—esophageal carcinoma, STAD—stomach cancer, CHOL—cholangiocarcinoma, UCEC—uterine corpus endometrial carcinoma, PCPG—pheochromocytoma and paraganglioma, PAAD—pancreatic cancer, COAD—colon cancer, SARC—sarcoma, READ—renal adenocarcinoma, HNSC—head and neck squamous cell carcinoma, LIHC—liver hepatocellular carcinoma, LUAD—lung cancer (adenocarcinoma), PRAD—prostate adenocarcinoma, KICH—kidney chromophobe, KIRP—kidney renal papillary cell carcinoma, KIRC—kidney renal clear cell carcinoma, THCA—thyroid cancer). (C) Distribution of RRHO similarity scores across TCGA patients. The  $y$ -axis shows the number of patients with a given RRHO similarity score ( $x$ -axis) calculated as the fraction of windows with a  $p < 0.05$  in rank–rank heat maps (out of a total of 100 windows). Analyses resulting in  $>20$  windows with  $p < 0.05$  (highlighted in yellow) were considered “high acid adaptation similarity”. The number of analyzed patients and the number of analyses resulting in high acid adaptation similarity scores are shown as an insert table. (D) Relation between high acid adaptation similarity score and patient metadata. Subpanel i shows the distribution of age of diagnosis split by whether patients are in the “high acid adaptation similarity” group, visualized as box plots.  $p$ -value is from two-sided  $t$  test. Subpanel ii–iv shows fraction of patients classified by TNM staging system. T: size of the primary tumor. T1, T2, T3, T4—size and/or extension of the primary tumor. N: degree of spread to regional lymph nodes. N0—no regional lymph nodes metastasis; N1—regional lymph node metastasis present (at some sites, tumor spread to closest or small number of regional lymph nodes); N2—tumor spreads to an extent between N1 and N3; N3—tumor spread to more distant or numerous regional lymph nodes. M: presence of distant metastasis. M0—no distant metastasis; M1—metastasis to distant organs (beyond regional lymph nodes). Bars are split by whether patients are in the “high acid adaptation similarity” group.  $p$ -values from Fisher exact tests are shown, testing the decrease in T1 and increase in T2 in the “high acid adaptation similarity” group vs. remaining patients. Numbers on bars show patient counts.

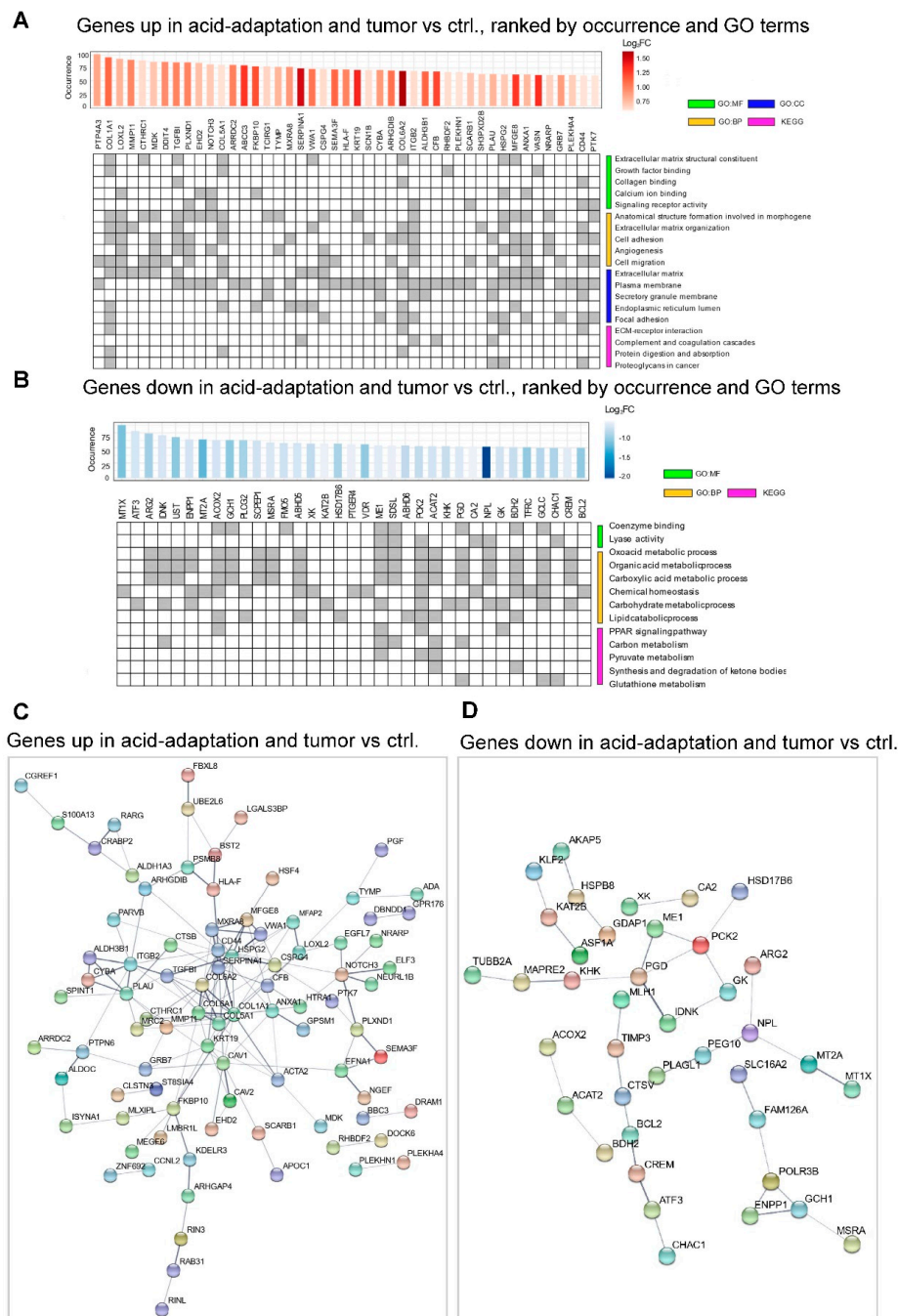


**Figure 5.** Analysis of overlapping genes between pH ranks and tumor–ctrl. ranks with high similarity. (A) Gene ontology (GO) and KEGG pathway analysis of genes upregulated in acid adaptation and correlated in gene expression rank in tumor–ctrl. comparisons in  $\geq 50$  patients. The upper bar plot shows the number of tumor–ctrl. vs. acid adaptation RRHO analyses in which the gene was identified as significant. Bar color indicates  $\log_2$  expression FC in the acid adaptation experiment (pH 6.5 vs. 7.6). Gene identifiers are shown below. Rows in the bottom panel correspond to selected GO terms with high significance from three sources (BP—Biological process, MF—Molecular function, CC—Cellular Component) and pathways from the KEGG database. Columns are genes as indicated above. Grey cells indicate that a given gene is labelled with a given GO term or pathway. (B) Gene ontology (GO) analysis of genes downregulated in acid adaptation correlated in gene expression rank in tumor–ctrl. comparisons in  $\geq 50$  patients, arranged as in (A). (C) STRING database analysis of genes from panel (A). Nodes are genes. Connections indicate STRING database evidence of protein interaction. Fully unconnected genes are not shown. (D) STRING database analysis of genes from panel (B), arranged as in (C).

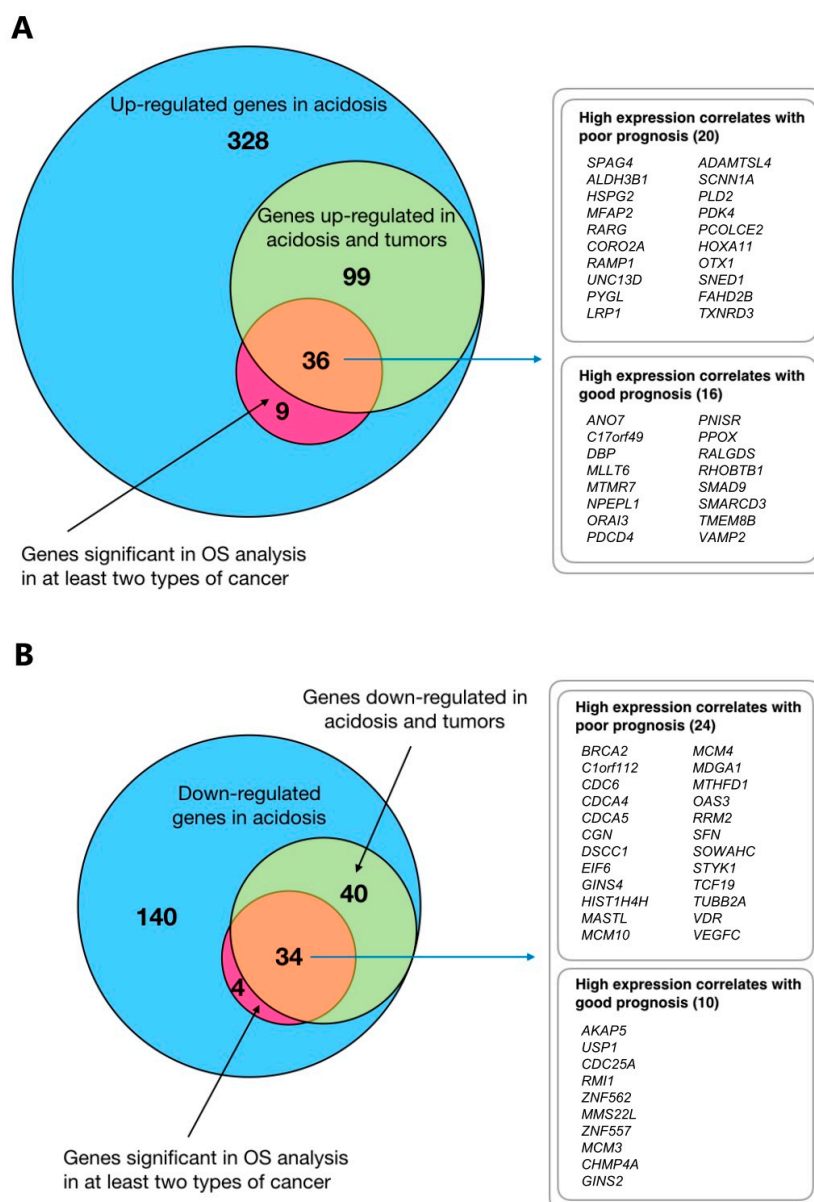


**Figure 6.** Integrative analysis. (A) Overlaps between upregulated genes, OS and RRHO analyses. Venn diagrams show overlaps between acid adaptation-upregulated genes (from Figure 2B), of genes significant in overall survival (OS) analysis in at least two types of cancer (based on TCGA data, Figure 4), and genes identified as having significant rank correlations between acid adaptation and tumor-control gene rank lists (RRHO analysis, Figures 4 and 5). (B) Overlaps between downregulated genes, OS and RRHO analyses Venn diagrams arranged as in (A) but focused on acid adaptation-downregulated genes.

## 2.2. Identification of a Shared Acid Adaptation Gene Response Profile

The Limma method was used to identify genes with a significant and shared expression response to acid adaptation using a linear model (See Materials and Methods). Out of the 12,750 expressed genes, 478 were significantly upregulated, and 255 were downregulated across all three cell lines (abs ( $\log_2$  fold change,  $\log_2FC$ ) > 0.5, False Discovery Rate (FDR) < 0.05). Figure 2A shows a shared  $\log_2FC$ -ranked list of all expressed genes, colored by significance, while Figure 2B shows the mean  $\log_2FC$  in each cell line across triplicates for differentially expressed genes. Tables S1 and S2 list all significantly up- and downregulated genes, respectively. The response to pH was overall highly similar between the three cancer cell lines, although the magnitude of change in the expressions of specific genes differed between cell lines (Figure 2B). Among the top 10 upregulated genes was thioredoxin-interacting



protein (*TXNIP*, also known as Vitamin D3-upregulated protein 1, *VDUP1*), previously reported to be upregulated in response to extracellular acidosis [22,24] (Figure 2A). The *TXNIP* protein has several important physiological roles: it is a potent negative regulator of glycolysis, and involved in redox homeostasis, differentiation and growth. *TXNIP* is generally downregulated in cancers, at least in part because it is negatively regulated by oncogenes such as *Myc* and *ErbB2*, and low *TXNIP* expression is associated with poor prognosis [25–27]. Confirming the relevance of this pathway, the *TXNIP* paralogs *ARRDC2* and *ARRDC4* were also among the significantly upregulated genes (Table S1).

Interestingly, several cation channels previously implicated in cancer development were significantly upregulated. For example, the  $\alpha$  subunit of the epithelial sodium channel *ENaC* (*SCNN1A*) and the  $\gamma 4$  subunit of the voltage-dependent calcium channel (*CACNG4*) (Figure 2A) were among the 10 most upregulated genes. The genes encoding the acid-stimulated ion channel-1 (*ASIC1*), and the  $\beta 1$  subunit of the voltage-gated sodium channel (*SCN1B*), were also significantly upregulated in acid-adapted cells (Table S1). In accordance with our findings, *ASIC1* and *ASIC2* are upregulated in colorectal cancer cells subjected to acidosis [28]. ASICs and *ENaC* belong to the same channel family, and both *ASIC1* [29] and *ENaC* [30] are acutely activated by acidic pH, and both channels are implicated in cancer development [11,31]. Similarly, both *CACNG4* [32] and *SCN1B* [33] are upregulated in cancer tissue and their gene products have been assigned a role in cancer progression.

Other highly upregulated genes included interferon-induced transmembrane protein 1 (*IFITM1*), which, together with other interferon-regulated genes, are highly upregulated in several cancers and assigned key roles in driving aggressiveness and chemotherapy resistance [34,35]. In addition, the genes encoding Sushi-containing Domain-3 (*SUSD3*), an estrogen-regulated membrane-localized protein previously found to be upregulated by chronic acidosis [15] and to play a key role in breast cancer cell migration [36], and *LARGE2*, a bifunctional glycosyltransferase involved in proteoglycan modification and hence in cell–extracellular matrix (ECM) interaction [37], were among the 10 most upregulated genes (Figure 2A).

The 10 most downregulated genes across all three acid-adapted cell lines included, firstly, the gene encoding the multidomain scaffold protein A-kinase anchoring protein-5 (*AKAP5*, a.k.a. *AKAP79/150*). *AKAP5* is a key regulator of cellular cAMP and  $\text{Ca}^{2+}$  signaling and, downstream from this, a plethora of physiological processes, including glucose metabolism [38]. *AKAP5* is not widely linked to cancer in the literature, yet low *AKAP5* expression was correlated with poor prognosis in some stomach adenocarcinomas [39]. *NIBAN1*, a.k.a. *FAM129A*, which was also downregulated by acidic growth, is frequently upregulated in cancers, favoring cell motility yet decreasing autophagy [40,41]. Furthermore, mucolipin-3 (*MCOLN3*) was strongly downregulated upon acidosis-induced selection. Interestingly, *MCOLN3* codes for a predominantly endosomal  $\text{Ca}^{2+}$  channel of the TRP channel family, which is inhibited by acidic pH and plays important roles in endosomal  $\text{Ca}^{2+}$  and pH homeostasis [42]. Other genes strongly downregulated across all three cell lines included those coding for the tight junction protein cingulin (*CGN*), the E3 ubiquitin ligase *TRIM36*, and *SYNE1* (a.k.a. Nesprin-1), a nuclear envelope protein.

Gene Ontology (GO) terms associated to ECM composition and remodeling, and lipid and carboxylic acid metabolism, were over-represented in the upregulated genes, while GO terms associated with cell proliferation, replication fork function and DNA repair were over-represented in the downregulated genes (Figure 2C). Furthermore, the upregulation of cation channels (Figure 2A and above) was reflected in GO term analysis (Table S3, while Table S4 shows the GO terms for downregulated genes). KEGG pathway analysis showed an over-representation of cytochrome P450-drug and xenobiotic metabolism, chemical carcinogenesis, propanoate metabolism and glutaminergic synapse pathways in the upregulated genes, while downregulated genes were over-represented in the cell cycle, DNA replication, homologous recombination, glutathione metabolism and Fanconi anemia pathways. Notably, a downregulated glutathione metabolism was previously reported in acid-adapted cells, and shown to reflect a shift from glutathione production towards utilization of glutamine as a metabolic fuel [18]. The ranked acid adaptation gene set from Figure 2A was



used to complement the above GO analysis with gene set enrichment analysis (GSEA) using the SigDb database of gene sets (Figure 2D). This revealed a clear gene rank enrichment of several oncological gene sets: acid adaptation-upregulated genes were enriched for gene sets associated with increased migration and invasiveness, gene sets upregulated after expression of CyclinD1 (CCND1) (a key regulator of G1-S phase transition), and genes downregulated after mTOR inhibition (Figure 2D). The link to mTOR signaling is notable, given the key role of mTOR in metabolic control. The pH sensitivity of mTOR signaling has previously been assigned a role in the impact of acidosis on metabolism, albeit in a short-term study (i.e., not long enough for acid-induced selection) where cytoplasmic acidosis was found to inhibit mTOR signaling [43,44]. Acid adaptation-downregulated genes were, correspondingly, enriched in gene sets upregulated by mTOR inhibition, or by overexpression of the transcription factor E2F1, a key player in the control of cell cycle progression.

Taken together, these analyses show that across multiple cancer cell types, chronic acidosis is associated with gene expression changes expected to reflect a profound metabolic shift, including the downregulation of fermentative glycolysis and upregulation of glutamine- and lipid-based metabolism, and the downregulation of cell division and DNA repair, as well as changes in ECM remodeling and ion channel activity.

### 2.3. *In Vivo* Expression of Genes Reacting to Chronic Acidosis Is Predictive of Cancer Patient Survival

The above analysis indicated that there was an overlap between cancer-regulated and acid adaptation-regulated gene sets, motivating a global investigation into whether the expression of acid adaptation-induced genes in patient tumors is correlated to patient overall survival (OS). To do this, RNA-seq data for multiple cancer types from the TCGA database were used. For each gene differentially expressed in all cell lines in the acid adaptation experiment above, patients were classified based on their mRNA expression of the specific genes into a high and low expression group, respectively, using the median expression of genes as the cut-off value.

Kaplan–Meier analysis showed that 267 genes upregulated by chronic acidosis and 138 genes downregulated by chronic acidosis were significantly associated with OS. Specifically, expression of 114 genes upregulated by chronic acidosis in all cell lines was significantly correlated with OS of pancreatic cancer patients. In luminal B breast cancer, 56 acid adaptation-upregulated genes correlated significantly with OS, followed by lung cancer (adenocarcinoma), glioblastoma, colon cancer, ovarian cancer, thyroid cancer and stomach cancer (44, 36, 35, 32, 30 and 29 genes, respectively; Figure 3A). In pancreatic, lung and thyroid cancer, a high expression of the majority of acid adaptation-upregulated genes correlated with better OS. Breast, glioblastoma, colon, ovarian and stomach cancer cohorts shared the reverse pattern: for the majority of acid adaptation-upregulated genes, high expression correlated with poor OS outcome (Figure 3A). Additionally, we found 70 acid adaptation-downregulated genes whose expression correlated with OS of lung adenocarcinoma patients. The counts in descending order for other types of cancer were: Pancreatic cancer—59, stomach cancer—24, ovarian cancer—23, luminal B breast cancer—21, thyroid cancer—17, colon cancer—15 and glioblastoma—11 (Figure 3B). High expressions of the majority of acid adaptation-downregulated genes in lung adenocarcinoma, pancreatic cancer, breast cancer and glioblastoma correlated with poor OS. On the contrary, high expressions of the majority of acid adaptation-downregulated genes in stomach, ovarian, thyroid and colon cancers were associated with better OS (Figure 3B).

The data in Figure 3A,B are collectively consistent with the hypothesis that in stomach, ovarian and colon cancers, acidosis-related changes in gene expression may be more likely to be linked to worse OS, whereas in pancreatic and lung cancer, they are more likely to be linked to better OS. A necessary caveat is that these analyses are only correlative (see also Discussion), and the statistical power of the OS analysis is limited by the number of patient datasets available.

Two genes stood out in terms of their high correlation with OS in multiple cancers. Among the acid adaptation-upregulated genes, high expression of the gene encoding the transcription regulator SMAD9 (a.k.a. SMAD8) showed correlation with good OS in four types of cancer (pancreatic, lung, colon and

glioblastoma; Figure 3C, Table 1). SMAD9, a receptor-SMAD activated by Bone Morphogenetic Protein (BMP) receptors, was also upregulated by acidosis in colon cancer cells [45]. Although the link of high expression to better OS makes SMAD9 upregulation an unlikely driver of acidosis-induced pro-tumorigenic effects, activating SMAD9 mutations were linked to some gastric cancers [46]. We also identified 5 genes (*LGR4*, *RARG*, *PNISR*, *PCOLCE2*, *RALGDS*) that shared the same patterns across three types of cancer, and 39 genes with two overlaps across eight cancer types (Table 1). As high expression of *LGR4*, *RARG* and *PCOLCE2* correlated with poor OS, these are interesting candidates for genes selected for in acidosis and linked to poor OS. The most common gene classes (based on the UniProt database) among genes with significant OS analysis results in at least two types of cancer were transcription regulators (9 genes), followed by genes involved in transport processes (8 genes), differentiation/morphogenesis (5 genes) and metabolism (4 genes) (Table 1).

Another gene with multiple cancer OS associations was the transcription factor *ZNF557*, which was downregulated by acid adaptation. Its low expression was associated with a worse OS outcome in five types of cancer (pancreatic, breast luminal B, lung adenocarcinoma, stomach and glioblastoma) (Figure 3D, Table 2). This supports that upregulation of *ZNF557*, an essentially unstudied member of the KRAB-ZNF family of zinc finger transcription factors and a transcriptional target of STAT3 [47], may be particularly relevant to the pro-tumorigenic effects of the acidic microenvironment, a possibility to be addressed in future studies. We furthermore discovered 5 genes (*MDGA1*, *VEGFC*, *MCM10*, *CTBP1-DT*, *CHMP4A*) with three OS correlations, and 22 genes with two OS correlations, across eight cancer types (Table 2). Of these, low expressions of *CTBP1-DT* and *CHMP4A* correlated with poor OS, making them possible candidates for acidosis-stimulated cancer aggressiveness. Among the acid adaptation-downregulated genes significant in OS analysis in at least two types of cancer, we found 17 genes associated with DNA replication/repair/cell cycle, 5 involved in transcription regulation and 4 playing key roles in differentiation and morphogenesis (Table 2).

All 182 acid adaptation-upregulated, and 84 acid adaptation-downregulated, genes that were significant in OS analysis in only one type of cancer are listed in Tables S5 and S6, respectively. Genes that showed contradictory OS results across cancer types (i.e., high and low expression was significantly associated with poor OS in different cancers) are listed in Table S7 (acid adaptation-upregulated) and Table S8 (acid adaptation-downregulated). Figures S1–S16 show plots for all genes with statistically significant OS results.

Taken together, these results show that a large fraction of acid adaptation-responsive genes correlate with patient survival across multiple cancers. Importantly, these genes fall into four major groups: acid adaptation-upregulated genes correlating with either good or poor OS, and acid adaptation-downregulated genes correlating with either better or worse OS across several types of cancers.

**Table 1.** Acid adaptation-upregulated genes significant in OS analysis in at least two types of cancers.

Gene Name	Log <sub>2</sub> FC	FDR	Correlation with Poor OS	Types of Cancer										Molecular Function/Biological Process (UniProt)	
				PAAD	BRCA	LUAD	GBM	COAD	OV	THCA	STAD				
4 OVERLAPS															
SMAD9	1.1723	0.0091	Low expression												DNA-binding, transcription regulation
3 OVERLAPS															
LGR4	0.7849	0.0127	High expression												Differentiation, immunity
RARG	0.6840	0.0117	High expression												DNA-binding, transcription regulation
PNISR	0.5890	0.0258	Low expression												RNA-binding
PCOLCE2	0.5538	0.0408	High expression												Collagen biosynthesis
RALGDS	0.5128	0.0249	Low expression												GTPase regulator, signal transduction
2 OVERLAPS															
SCNN1A	2.0490	0.0100	High expression												Ion transport
PLA2R1	1.6361	0.0249	High expression												Endocytosis
PDK4	1.6088	0.0351	High expression												Ser/Thr protein kinase, metabolism
SNED1	1.5574	0.0302	High expression												Cell-matrix adhesion
ADAMTSL4	1.5083	0.0176	High expression												Peptidase, apoptosis
RAMPI	1.4724	0.0169	High expression												Transport, angiogenesis
MFAP2	1.3770	0.0154	High expression												Embryonic morphogenesis
HSPG2	1.2833	0.0073	High expression												Angiogenesis, morphogenesis, GTPase activity
GNG7	1.2239	0.0142	Low expression												
HOXA11	1.1569	0.0346	High expression												DNA-binding, transcription regulation
ALDH3B1	1.1061	0.0081	High expression												Oxidoreductase, metabolism
CORO2A	1.0708	0.0321	High expression												Actin-binding, signal transduction
LRPI	1.0403	0.0380	High expression												Endocytosis
TMEM8B	0.9897	0.0045	Low expression												Cell adhesion, growth regulation

Table 1. Cont.

Gene Name	Log <sub>2</sub> FC	FDR	Correlation with Poor OS	Types of Cancer										Molecular Function/Biological Process (UniProt)	
				PAAD	BRCA	LUAD	GBM	COAD	OV	THCA	STAD				
ZNF710-AS1	0.9413	0.0330	Low expression												lncRNA
PYGL	0.8856	0.0251	High expression												Transferase, metabolism
TMED7-TICAM2	0.8634	0.0325	High expression												Golgi organization, protein transport
NPEPL1	0.8764	0.0117	Low expression												Aminopeptidase
SMARCD3	0.8743	0.0058	Low expression												Chromatin regulator, neurogenesis
RHOBTB1	0.8684	0.0234	Low expression												GTPase activity, actin organization
UNC13D	0.8587	0.0368	High expression												Exocytosis
DBP	0.8034	0.0249	Low expression												DNA-binding, transcription regulation
PDCD4	0.7330	0.0077	Low expression												RNA-binding, apoptosis
MTMR7	0.7273	0.0329	Low expression												Phosphatase
OTX1	0.6797	0.0091	High expression												DNA-binding, morphogenesis
TXNRD3	0.6584	0.0125	High expression												Differentiation, electron transport
PPOX	0.6399	0.0279	Low expression												Oxidoreductase, heme biosynthesis
SPAG4	0.6392	0.0404	High expression												Differentiation, spermatogenesis
ANO7	0.6260	0.0329	Low expression												Lipid transport
FAHD2B	0.6164	0.0069	High expression												Hydrolase
ORAI3	0.6063	0.0224	Low expression												Calcium channel
NOP53	0.5938	0.0156	High expression												Host-virus interaction, ribosome biogenesis
C17orf49	0.5910	0.0081	Low expression												Chromatin regulator, DNA-binding
VAMP2	0.5901	0.0073	Low expression												Exocytosis, protein transport
ZNF487	0.5872	0.0377	Low expression												DNA-binding, transcription regulation

Table 1. Cont.

Gene Name	Log <sub>2</sub> FC	FDR	Correlation with Poor OS	Types of Cancer							Molecular Function/Biological Process (UniProt)
				PAAD	BRCA	LUAD	GBM	COAD	OV	THCA	
<i>TDRD3</i>	0.5832	0.0058	Low expression								Chromatin regulator, RNA-binding
<i>FRG1HP</i>	0.5302	0.0376	Low expression								Pseudogene
<i>PLD2</i>	0.5226	0.0306	High expression								Hydrolase, lipid metabolism, motility
<i>MLLT6</i>	0.5118	0.0038	Low expression								Histone-binding, metal ion-binding

PAAD—pancreatic cancer (dark blue), BRCA—breast cancer—luminal B (pink), LUAD—lung cancer—adenocarcinoma (turquoise), GBM—glioblastoma (orange), COAD—colon cancer (red), OV—ovarian cancer (purple), THCA—thyroid cancer (grey), STAD—stomach cancer (green). Molecular function and/or biological processes according to UniProt database [48].

Table 2. Acid adaptation-upregulated genes significant in OS analysis in at least two types of cancers.

Gene Name	Log <sub>2</sub> FC	FDR	Correlation with Poor OS	Types of Cancer							Molecular Function/Biological Process (UniProt)	
				PAAD	BRCA	LUAD	GBM	COAD	OV	THCA		STAD
5 OVERLAPS												
<i>ZNF557</i>	-0.5999	0.0069	Low expression									DNA-binding, transcription factor, metal on binding
3 OVERLAPS												
<i>MDGAI</i>	-1.2003	0.0153	High expression									Differentiation, neurogenesis
<i>VEGFC</i>	-0.8963	0.0345	High expression									Growth factor, angiogenesis, differentiation
<i>MCM10</i>	-0.8486	0.0249	High expression									DNA-binding, DNA replication, DNA damage
<i>CTBP1-DT</i>	-0.5490	0.0098	Low expression									Oxidoreductase, differentiation, transcription
<i>CHMP4A</i>	-0.5182	0.0247	Low expression									Protein transport
2 OVERLAPS												
<i>CGN</i>	-1.5661	0.0112	High expression									Tight junction regulation

Table 2. Cont.

Gene Name	Log <sub>2</sub> FC	FDR	Correlation with Poor OS	Types of Cancer										Molecular Function/Biological Process (UniProt)		
				PAAD	BRCA	LUAD	GBM	COAD	OV	THCA	STAD					
AKAP5	-1.4671	0.0408	Low expression													Calmodulin-binding
HIST1H4H	-1.3143	0.0276	High expression													DNA-binding
STYK1	-1.0844	0.0290	High expression													Protein tyrosine kinase
CDC25A	-1.0023	0.0182	Low expression													Protein phosphatase, cell cycle, cell division
RRM2	-0.9925	0.0325	High expression													Oxidoreductase, DNA replication
VDR	-0.9901	0.0131	High expression													Vitamin D3 receptor, DNA-binding, transcription
CDC6	-0.8805	0.0110	High expression													Cell cycle, cell division, DNA replication
GINS4	-0.8574	0.0376	High expression													DNA replication
AC019069.1	-0.8118	0.0467	High expression													lncRNA
TCF19	-0.7835	0.0296	High expression													DNA-binding, transcription factor
GINS2	-0.7784	0.0182	Low expression													DNA replication
SOWAHC	-0.7653	0.0201	High expression													Ankyrin repeat domain-containing protein
BRCA2	-0.7332	0.0375	High expression													DNA-binding, DNA recombination, DNA damage
AC092279.1	-0.6853	0.0203	Low expression													lncRNA
CDC45	-0.6652	0.0425	High expression													Cell cycle, cell division
TUBB2A	-0.6559	0.0360	High expression													GTP-binding, microtubule cytoskeleton organization
OAS3	-0.6518	0.0117	High expression													RNA-binding, antiviral defense, immunity
SEN	-0.6382	0.0158	High expression													DNA damage response
MTHFD1	-0.6333	0.0107	High expression													Embryonic morphogenesis
ZNF562	-0.6041	0.0069	Low expression													DNA-binding, transcription factor, metal ion binding



Table 2. Cont.

Gene Name	Log <sub>2</sub> FC	FDR	Correlation with Poor OS	Types of Cancer										Molecular Function/Biological Process (UniProt)	
				PAAD	BRCA	LUAD	GBM	COAD	OV	THCA	STAD				
<i>MASTL</i>	-0.6008	0.0482	High expression												Ser/Thr protein kinase, cell division
<i>CDC44</i>	-0.5907	0.0236	High expression												Cell division
<i>MMS22L</i>	-0.5725	0.0418	Low expression												DNA repair
<i>RMI1</i>	-0.5661	0.0443	Low expression												DNA replication
<i>C1orf112</i>	-0.5581	0.0415	High expression												Uncharacterized protein C1orf112
<i>MIR4435-2HG</i>	-0.5537	0.0105	High expression												lncRNA
<i>MCM4</i>	-0.5328	0.0482	High expression												DNA-binding, cell cycle, DNA replication
<i>DSCC1</i>	-0.5268	0.0492	High expression												DNA-binding, cell cycle, DNA replication
<i>USP1</i>	-0.5192	0.0330	Low expression												Protease, DNA repair
<i>MCM3</i>	-0.5129	0.0471	Low expression												Transferase, mRNA transport, immunity
<i>EIF6</i>	-0.5008	0.0100	High expression												Ribosome biogenesis, protein synthesis

PAAD—pancreatic cancer (dark blue), BRCA—breast cancer—luminal B (pink), LUAD—lung cancer—adenocarcinoma (turquoise), GBM—glioblastoma (orange), COAD—colon cancer (red), OV—ovarian cancer (purple), THCA—thyroid cancer (grey), STAD—stomach cancer (green). Molecular function and/or biological processes according to UniProt database [48].

#### 2.4. RRHO Analysis Identifies Substantial Overlap between Genes Upregulated in Acid Adapted Cells and Patient Tumor Tissue

Given that the expression level *in vivo* of a substantial number of acidosis-induced genes was correlated with overall patient survival, we reasoned that it would be informative to directly compare the acid adaptation gene expression response and the gene expression change between tumor and ctrl. tissue. This requires paired normal and tumor tissue data from the same patient, and we therefore downloaded TCGA RNA-seq data for 642 patients for which such paired data was available. For each patient, we ranked genes according to the tumor vs. ctrl. tissue RNA-seq  $\log_2FC$ . We will refer to such lists as “tumor–ctrl. ranked gene lists”. Each such ranked list was compared to a ranked gene list based on the pH 6.5 vs. 7.6,  $\log_2FC$ , as shown in Figure 2A, referred to as the “acid adaptation ranked gene list”. Using the rank–rank hypergeometric test method (RRHO) (Figure 4A), we sought to identify patients whose tumor–ctrl. ranked gene lists had a significantly similar gene order to that of the acid adaptation ranked gene list, and the set of genes that had similar orders in many such pairwise comparisons. In brief, RRHO analysis identifies windows of the two rank gene lists which have higher rank similarities than expected, and assigns *p*-values for each such window based on hypergeometric tests, which can be visualized as a heat map. For example, the heat map in Figure 4A shows an RRHO comparison between the patient TCGA-EL-A3ZS tumor–ctrl. ranked gene list (*y*-axis) vs. the acid adaptation ranked gene list (*x*-axis), where color intensity in the heat map indicates the gene rank similarity significance in a given window across respective ranked lists. In this example, we observed a high overlap in the upregulated genes between the tumor–ctrl. ranked gene list of the TCGA-EL-A3ZS patient and the acid adaptation ranked gene list (red areas), and a less strong but still substantial rank similarity between modestly downregulated genes in both sets (yellow–green areas). To identify clear cases of substantial rank similarity between patient tumor–ctrl. ranked lists and the acid adaptation ranked lists, we counted the fraction of windows in the heat map matrix which had a *p*-value < 0.05, and defined this number as the “acid adaptation similarity”. If >20% of windows had *p* < 0.05, we considered the patient tumor–ctrl. rank gene list to be highly similar to the acid adaptation ranked gene list. The group of 128/642 (~20%) tumor–ctrl. ranked gene lists satisfying this criterion were defined as the ‘high acid adaptation similarity group’ (Figure 4C).

Within this group, in most cases, the genes with highest rank similarity were upregulated in pH 6.5 vs. 7.4 and upregulated in tumor vs. ctrl. Figure 4B shows all heat maps from patients in the high acid adaptation similarity group, while Figure 4C shows the distribution of patient ranked gene lists having a given fraction of windows with *p* < 0.05. Interestingly, some cancer types had particularly high proportions of patients within the high acid adaptation similarity group; for example, 34/51 (~63%) of thyroid cancer patients (TCGA-THCA), 34/69 (~49%) of kidney renal clear cell carcinoma (TCGA-KIRC) patients, and 3/4 (75%) of pancreatic adenocarcinoma (TCGA-PAAD) patients exhibited this pattern. The insert in Figure 4C shows the numbers of patients in each cancer type in the high acid adaptation similarity group. Notably, for some cancer types only small paired tumor–ctrl. sample sets were available; hence, for these cancers, the calculated fractions are less certain.

Next, we investigated if patients in the high acid similarity group had specific clinical characteristics. We observed that patients in the high acid adaptation similarity group had a weakly significant average lower age than remaining patients (two-sided *t*-test, *p* = 0.043, means 58.99 and 62.15) (Figure 4D(i)). To investigate metastasis status, we obtained tumor–normal–metastasis (TNM) staging system data from the TCGA database and filtered for M0–M1 stages (presence or not of distant metastasis, 417 patients), N0–N3 stages (degree of spread to regional lymph nodes, 517 patients), and T1–T4 stages (size of the primary tumor, 619 patients) (Figure 4D(ii–iv)). We found no significant relation between acid adaptation similarity groups and metastasis or node status, but patients in the high acid adaptation similarity group were less likely to be classified as T2 (two-sided Fisher’s exact test, *p* = 0.0007, odds ratio = 0.48), and more likely to be classified as T3 (two-sided Fisher’s exact test, *p* = 0.0015, odds ratio = 1.95). This is in congruence with the notion that an acidic gene signature is more likely to correlate with a more advanced primary tumor stage than with earlier stages.

Overall, the RRHO analysis strongly indicates high similarity in acid adaptation response and tumor–ctrl. expression profiles for a subset of patients spread across many cancers, in particular for the upregulated genes. To investigate the overlap on a gene, rather than patient, basis for each tumor–ctrl. and acid adaptation RRHO analysis, we extracted the set of genes that had significant rank similarities. We then sorted these genes via how many times they were identified in the overlap sets among all 128 comparisons. Figure 5A,B show significant GO term and KEGG pathway annotation of such genes occurring in  $\geq 50$  comparisons. STRING [49] protein–protein interaction plots for the up- and downregulated genes with occurrence  $\geq 50$  are shown in Figure 5D,E. The GO/KEGG analyses show that the upregulated overlapping genes were significantly associated with ECM remodeling and cell migration and invasion, whereas the downregulated overlapping genes were generally associated with metabolic processes. STRING analysis confirmed this pattern, with upregulated overlapping genes showing a predominant clustering of genes related to ECM components and remodeling (Figure 5C). Downregulated overlapping genes were less clearly clustered, but a cluster of metabolism-related genes including *ME1*, *PCK2*, *PGD*, *GK*, *IDNK* and *KHK* was evident (Figure 5D).

Collectively, these analyses show that there is a substantial overlap between gene sets up/downregulated by acid adaptation and genes up/downregulated in tumor vs. matched normal tissue, respectively. Furthermore, they indicate that the upregulated overlapping gene sets are strongly dominated by genes involved in cell motility, invasiveness and ECM remodeling, consistent with the notion that these are key processes through which microenvironmental acidosis favors cancer development.

### 2.5. Integration of Survival Data and Rank–Rank Analysis

Above, we have shown that (i) the in vivo expression of many genes selected for during acid adaptation is correlated to overall survival, and (ii) for around 20% of cancer patients investigated, there is a clear correlation in ranked gene expression (tumor–ctrl. vs. acid adaptation response). Seeking to identify a set of genes that both correlated in ranked gene expression between adapted cells and tumors, and was linked to survival, we plotted the overlap of acid adaptation-up- and downregulated genes identified in the respective analyses as Venn diagrams (Figure 6). For survival-related genes, we chose a conservative approach where only genes that were significantly related to survival in at least two cancer types were included. Remarkably, the large majority of such genes overlapped with genes identified by the RRHO analysis, resulting in two consensus gene lists of 36 and 34 genes, respectively (Figure 6A,B), which could be further split based on whether their in vivo expression correlated with higher or lower patient survival.

As expected, the acid adaptation and tumor-upregulated genes that were associated with poor prognosis (Figure 6A, top list) included multiple genes related to ECM and cell motility in various cancers, such as those encoding sperm-associated antigen-4 (SPAG4) [50], microfibril-associated protein-2 (MFAP2) [51], the ADAM protease ADAMTSL4 [52], and ECM components heparan-sulfate proteoglycan-2 (HSPG2) and Procollagen C-Endopeptidase Enhancer 2 (PCOLCE2). Thioredoxin reductase-3 (TXNRD3), likely important for alleviating oxidative stress, the transcription factors HOXA11 and OTX1, as well as the ENaC subunit SCNN1A, discussed above, were also found in this gene set. The upregulated genes for which high expression correlated with good prognosis in the cancers studied (Figure 6A, lower list) included *SMAD9*, discussed above, as well as genes coding for two transport proteins, the  $\text{Ca}^{2+}$  channel ORAI3 and the TMEM16 family member ANO7, which is a lipid transporter and/or ion channel. It should, however, be noted that although *ANO7* upregulation is associated with good prognosis in breast and colon cancer (Table 1), it is in fact associated with poor prognosis in prostate cancer [53].

The acid adaptation-downregulated genes overlapping with genes downregulated in patient cancers, and for which high expression was associated with good prognosis (i.e., potential candidates for pro-tumorigenic effects of acid adaptation, Figure 6B, lower list) included *AKAP5* and *ZNF557*, described above, as well as several DNA replication- and repair-related genes, including the genes

encoding the DNA repair protein MMS22L, the DNA replication licensing factor MCM3, and the replication fork complex protein GINS2. Conversely, the downregulated genes for which high expression correlates with poor prognosis (Figure 6B, top list) were dominated by other genes involved in DNA replication, repair and cell cycle control, such as *BRCA2*, *CDC6*, *CDCA4*, *CDCA5* and *EIF6*.

Collectively, these results reveal that genes regulated similarly in acid-adapted cells and in tumor tissue can be linked to both poor and good prognosis, consistent with the notion that tumor acidosis may be both a driver and a repressor of cancer progression. This indicates that while acidosis is likely to favor cancer progression through the upregulation of ECM/motility related genes, it limits it through the downregulation of DNA replication pathways.

### 3. Discussion

Acidosis is one of the key characteristics of the microenvironment of solid tumors [3,9,20,54]. Agreeing with the idea that cancer is largely an evolutionary disease driven by selection pressure, it has been proposed that chronic acidosis selects for changes in cancer cell genotype and phenotype that increase their “fitness”, and hence aggressiveness [3,55,56]. Such adaptations would potentially render the cells resistant not only to sustained acidosis, but also to other stress stimuli, such as nutrient limitations, hypoxia and chemotherapy, as well as to anti-tumor immunity [9,57,58]. Although individual genes and pathways have previously been compared between acid-adapted cells and patient tumors (e.g., [15,24,59]), a comprehensive integrative analysis comparing genes upregulated by acidosis, genes upregulated in patient tumors and their relation to patient survival is lacking. This was the aim of the work presented here.

Our analyses show that hundreds of genes are similarly regulated by chronic acidosis, in three cancer cell lines from human breast and pancreatic cancers, allowing for the identification of a characteristic gene set shared between cancer cells selected for growth in an acidic microenvironment. Both the up- and downregulated genes show significant overlaps with genes up- and downregulated in patient tumor tissue, compared to normal tissue, for subsets of patients across multiple cancers. Finally, numerous acid-regulated genes correlate with overall patient survival in at least one cancer type, and many in two or more cancers, pointing to a possible functional role. Importantly, survival correlations were both positive and negative, i.e., some genes selected for by acidosis and in patient tissue correlate with increased, and some with decreased, overall survival; furthermore, the effect on survival is often cancer-specific.

It is important to note that although the overlap between acid adaptation and tumor-specific expression was strong, the overall causality is unclear. Extracellular acidosis within tumors may causally lead to cancer aggression in vivo or potentiate an existing aggressive tumor behavior, or the correlations we observe may be caused by an unobserved factor. To detangle these questions and understand their true relevance to tumor growth and metastasis, it will be necessary to measure and manipulate extracellular acidity in tumors in vivo or in advanced in vitro models, that can mimic not only acidosis but other physicochemical, as well as cellular, components of the tumor microenvironment.

A limitation of this work is that a given gene may favor the development of one cancer type and counteract another (Tables S7 and S8), and hence correlations demonstrated here will not apply to all cancers. This notwithstanding, clear patterns were observed.

A number of specific observations deserve special attention with respect to their relation to cancer biology. Firstly, our findings are fully in line with the existing studies proposing that tumor acidosis can promote cancer invasiveness. This includes the prominent pattern of upregulation by acidosis of genes involved in ECM remodeling and invasiveness, as well as the striking extent of upregulation of *ASIC1*, the ENAC  $\alpha$  subunit, and other cation channel genes, many of which have been assigned important roles in cell–cell adhesion and invasion [60,61]. Second, our analyses also support several existing studies that clearly show that adaptation to acidosis is not associated with increased growth of the cancer cells [13,15]. The strong upregulation of *TXNIP* and its paralogs *ARRD2* and *ARRD4* by chronic acidosis is consistent with previous reports of the effect of acidosis [18,24] and lactic

acidosis [22] on this family of proteins, which are key negative regulators of glycolytic metabolism. In previous work, TXNIP upregulation in acidosis has been shown to involve MondoA [22,24]. The metabolic signature induced by chronic acidosis in this and previous reports is characterized by the downregulation of fermentative glycolysis and the upregulation of glutamine- and lipid-based metabolism [18,62]. In contrast to this, cancer cells are often highly glycolytic, and accordingly, frequently exhibit TXNIP downregulation [25–27]. Interestingly, combined inhibition of mTOR and histone deacetylases strongly upregulated TXNIP, triggering oxidative stress-induced cell death in KRAS-driven tumors [63]. This makes it tempting to speculate that TXNIP could be responsible not only for the metabolic shift away from fermentative glycolysis, but also for oxidative stress and growth restriction in acid-adapted cells.

Other mechanisms from those discussed in this work are likely to contribute to the effect of microenvironmental acidosis on cancer aggressiveness. For instance, extracellular acidosis may impact genomic instability and cause epigenetic changes in cancer cells, in line with the substantial downregulation of DNA damage response mechanisms observed in this work [9,17]. Numerous studies have established the strong inhibitory effect of acidosis on cell cycle progression [64]. After several weeks to a few months of culture in acidic medium, cancer cells attain a growth rate similar to that of normal cells grown at pH 7.4, yet not higher [13,15]. This is in itself remarkable, given the acidosis-induced downregulation of pathways associated with cell cycle progression and DNA replication observed in this study. It is, however, consistent with the notion that the acidic TME is likely to act as a brake on proliferation, and may be seen as a niche favoring cells with limited growth but high growth potential [56,65], such as cancer stem cells. Such cells would be growth-limited in an acidic environment, but could have the capacity for extremely rapid growth when encountering regions of normal  $pH_e$  [9]. In this regard, therapeutic strategies targeting pathways selected for by chronic acidosis, yet functionally limited by these conditions, may be particularly interesting. Similarly, otherwise highly successful strategies of limiting tumor growth by counteracting acidosis [66,67] could carry the risk of exacerbating aggressiveness if applied at a stage when pH normalization might unleash aggressive growth.

## 4. Materials and Methods

### 4.1. Cell Culture and Acid Adaptation

Human breast cancer cell lines MDA-MB-231, MCF7 and human pancreatic adenocarcinoma cell line PANC-1 were cultured in RPMI-1640 Medium (Sigma Aldrich, Catalog No. R1383, Saint Louis, MO, USA) supplemented with 10% Fetal Bovine Serum (Sigma Aldrich, Cat. No. F9665, Saint Louis, MO, USA) and 1% Penicillin/Streptomycin (Sigma Aldrich, Cat. No. P0781, Saint Louis, MO, USA). Medium pH was adapted by adjusting the  $HCO_3^-$  concentration by adding the appropriate amount of  $NaHCO_3$ , ensuring equal osmolarity by adjusting  $[NaCl]$ . Cells were adapted to pH 7.6 and 6.5 by adding the appropriately pH-adjusted medium to freshly split cells, and maintaining cells in this medium, splitting or adding fresh medium twice per week for 1 month, until approximately equal growth rates were observed.

### 4.2. RNA Isolation and RNA Sequencing

Cells were grown to 70–90% confluence in 10 cm<sup>2</sup> Petri dishes. RNA isolation was performed using a Nucleospin RNA purification kit (Macherey-Nagel, Cat. # NC0707522, Düren, Germany) and following the manufacturer's instructions. RNA library preparation and sequencing were done as a paid service by BGI (Hongkong), producing 100 bp paired-end non-stranded libraries with ~20 M reads per library, using the BGI-seq platform. Three replicate libraries were made for each cell type and condition (in total 18 libraries).



#### 4.3. Analyses of RNA-Seq Data

RNA-seq reads were pseudoaligned to Gencode transcriptome release 34 and quantified using Salmon v1.1.0 with `flags-validateMappings` for selective alignment and `-l A` for automatic library type inference [68]; Trimmed Mean of M values (TMM) normalization [69] and pre-filtering for low counts were performed using `calcNormFactors` and `filterByExpr` function in edgeR package [70,71]. Voom transformation [29] was then applied with a design matrix that used pH treatment as coefficient. To perform differential expression analyses in shared response to pH, inter-subject correlation within three cell lines was performed by `duplicateCorrelation` function, and was put into the linear model fit using Limma R package [72]. Differential expression, given the above settings, was defined as Benjamini–Hochberg FDR < 0.05 and an absolute  $\log_2$  FC > 0.5. Validation of key up/downregulated genes by qPCR and immunoblotting is provided in a manuscript in preparation and confirms the RNA-seq results.

#### 4.4. GO Enrichment Analysis and Gene Set Enrichment Analysis (GSEA)

Enrichment tests for GO-terms were performed on differentially expressed genes sets as defined above using gProfiler [73]. The background gene set was set to all expressed genes in the experiment. Significance threshold was set to Benjamini–Hochberg FDR < 0.05. The Gene Set Enrichment Analysis (GSEA) pre-ranked function was performed on the fold change ranked acid adaptation gene list using the Broad Institute GSEA java tool version 4.0.3. C6: Oncogenic signatures database v7.1, gene sets WU\_CELL\_MIGRATION (M2001) and ANASTASSIOU\_MULTICANCER\_INVASIVENESS\_SIGNATURE (M2572) were used and the number of permutations was set to 1000 [74].

#### 4.5. RRHO Analysis

First, using Limma and Voom as above, we ranked all expressed genes from the RNA-seq experiments by their shared acid adaptation response across cells ( $\log_2$  fold change pH 6.5 vs. pH 7.4). We will refer to this ranked gene list as the ‘acid adaptation ranked gene list’. To be able to compare this to human data, we extracted processed patient RNA-seq data from Cancer Genome Atlas (TCGA) [75] using the University of California Santa Cruz Xena portal [76]. For every patient and cancer where expression data from paired tumor and control tissue were available, and for each such case, we ranked genes according to their  $\log_2$  fold change (tumor vs. control (ctrl.) tissue). Next, we compared the acid adaptation ranked list to each ranked patient gene lists in a pairwise fashion, using the Rank–Rank Hypergeometric Overlap (RRHO) method [77], as implemented in R [78]. For each comparison, we obtained heat maps showing rank–rank correlations, colored by log-transformed hypergeometric *P*-value of local rank overlaps between sets, and the identifiers of genes in each overlap.

#### 4.6. Patient Survival Analysis

TCGA cancer patient data was downloaded from the University of California Santa Cruz Xena portal [76]. The following datasets containing gene expression RNAseq counts, survival data and phenotype information were analyzed: GDC TCGA Pancreatic Cancer (PAAD), GDC TCGA Breast Cancer (BRCA), GDC TCGA Lung Adenocarcinoma (LUAD), GDC TCGA Glioblastoma (GBM), GDC TCGA Colon Cancer (COAD), GDC TCGA Ovarian Cancer (OV), GDC TCGA Thyroid Cancer (THCA) and GDC TCGA Stomach Cancer (STAD).

Kaplan–Meier analysis was performed to estimate the overall survival of patients. Patients were categorized into high and low gene expression groups according to the cut-off value determined by median gene expression. *p*-values for significance of difference between the two groups were calculated using the log-rank test. Statistical analyses were performed using R’s “survival” and “survminer” packages. *p*-values < 0.05 were considered statistically significant.



#### 4.7. Data Availability

RNA-sequencing data from this study has been deposited in GEO database under accession number GSE152345.

### 5. Conclusions

We have defined a shared acid adaptation expression response across three cancer cell models, dominated by ECM remodeling, metabolic rewiring and altered cell cycle regulation. Many genes which are upregulated by acid adaptation are significantly correlated to patient survival, and there are clear correlations between acid adaptation expression response and expression change between normal and tumor tissues for a large subset of cancer patients. Importantly, our analyses reveal that genes whose expressions are changed by acid adaptation are linked both to increased and decreased overall patient survival. Thus, in conclusion, our data support the notion that adaptation to microenvironmental acidosis can drive the selection of highly invasive cancer cells and ECM remodeling in human patient tumors. However, consistent with existing experimental data, they also show that acid adaptation exerts inherently growth-limiting effects, which could be important for cancer stem cell maintenance but may per se limit full-blown cancer development, until selected against or otherwise eliminated. Future studies should address what dictates the balance between these effects, and hence the net effects of acid adaptation on cancer development in vivo.

**Supplementary Materials:** The following are available online at <http://www.mdpi.com/2072-6694/12/8/2183/s1>, Figures S1–S16: Kaplan–Meier overall survival analysis of cancer patients stratified by acidosis up- and downregulated gene expression levels, Table S1: Upregulated genes in pH 6.5 vs. pH 7.6, Table S2: Downregulated genes in pH 6.5 vs. pH 7.6, Table S3: GO and KEGG analysis of upregulated genes in pH 6.5 vs. pH 7.6, Table S4: GO and KEGG analysis of downregulated genes in pH 6.5 vs. pH 7.6, Table S5: Acidosis-upregulated genes significant in overall survival analysis in one type of cancer, Table S6: Acidosis-downregulated genes significant in overall survival analysis in one type of cancer; Table S7: Acidosis-upregulated genes, which showed contradictory survival analysis results across cancer types, Table S8: Acid adaptation-downregulated genes, which showed contradictory survival analysis results across cancer types.

**Author Contributions:** Conceived and designed the study: J.Y., D.C., R.I., A.S., and S.F.P., Designed and executed experimental work for RNA sequencing: J.S., B.L., Analyzed the data: J.Y., D.C., and R.I., with inputs and supervision from A.S. and S.F.P., Prepared the figures: J.Y., D.C., and R.I., Wrote the paper: J.Y., D.C., R.I., A.S., and S.F.P., with inputs from all co-authors. All authors have read and agreed to the published version of the manuscript.

**Funding:** This study was supported by funds from the Danish Cancer society (A.S. and S.F.P.), the Novo Nordisk Foundation (A.S. and S.F.P.), the European Union (H2020-MSCA-ITN-2018, grant 813834, A.S. and S.F.P.) and the Carlsberg Foundation (A.S.).

**Acknowledgments:** The authors thank Kristoffer Vitting Seerup, Jens Waaben and Kasper Haldrup Björnsson for help with exploratory RNA-seq analyses.

**Conflicts of Interest:** The authors declare no conflicts of interest.

### References

1. Hanahan, D.; Weinberg, R.A. Hallmarks of cancer: The next generation 1. *Cell* **2011**, *144*, 646–674. [[CrossRef](#)] [[PubMed](#)]
2. Nowell, P.C. The clonal evolution of tumor cell populations. *Science* **1976**, *194*, 23–28. [[CrossRef](#)] [[PubMed](#)]
3. Gatenby, R.A.; Gillies, R.J. A microenvironmental model of carcinogenesis. *Nat. Rev. Cancer* **2008**, *8*, 56–61. [[CrossRef](#)] [[PubMed](#)]
4. Merlo, L.M.; Pepper, J.W.; Reid, B.J.; Maley, C.C. Cancer as an evolutionary and ecological process. *Nat. Rev. Cancer* **2006**, *6*, 924–935. [[CrossRef](#)] [[PubMed](#)]
5. Hashim, A.I.; Zhang, X.; Wojtkowiak, J.W.; Martinez, G.V.; Gillies, R.J. Imaging pH and metastasis. *NMR Biomed.* **2011**, *24*, 582–591. [[CrossRef](#)]
6. Vaupel, P.; Kallinowski, F.; Okunieff, P. Blood flow, oxygen and nutrient supply, and metabolic microenvironment of human tumors: A review. *Cancer Res.* **1989**, *49*, 6449–6465.

7. Webb, B.A.; Chimenti, M.; Jacobson, M.P.; Barber, D.L. Dysregulated pH: A perfect storm for cancer progression. *Nat. Rev. Cancer* **2011**, *11*, 671–677. [[CrossRef](#)]
8. Elingaard-Larsen, L.O.; Rolver, M.G.; Sorensen, E.E.; Pedersen, S.F. How reciprocal interactions between the tumor microenvironment and ion transport proteins drive cancer progression. In *Reviews of Physiology, Biochemistry and Pharmacology*; Springer: Berlin/Heidelberg, Germany, 2020.
9. Boedtker, E.; Pedersen, S.F. The Acidic Tumor Microenvironment as a Driver of Cancer. *Annu. Rev. Physiol.* **2020**, *82*, 103–126. [[CrossRef](#)]
10. Semenza, G.L. Hypoxia-inducible factors: Mediators of cancer progression and targets for cancer therapy 12. *Trends Pharmacol. Sci.* **2012**, *33*, 207–214. [[CrossRef](#)]
11. Zhu, S.; Zhou, H.Y.; Deng, S.C.; Deng, S.J.; He, C.; Li, X.; Chen, J.Y.; Jin, Y.; Hu, Z.L.; Wang, F.; et al. ASIC1 and ASIC3 contribute to acidity-induced EMT of pancreatic cancer through activating Ca<sup>2+</sup>/RhoA pathway. *Cell Death Dis.* **2017**, *8*, e2806. [[CrossRef](#)]
12. Peppicelli, S.; Bianchini, F.; Torre, E.; Calorini, L. Contribution of acidic melanoma cells undergoing epithelial-to-mesenchymal transition to aggressiveness of non-acidic melanoma cells. *Clin. Exp. Metastasis* **2014**, *31*, 423–433. [[CrossRef](#)] [[PubMed](#)]
13. Moellering, R.E.; Black, K.C.; Krishnamurty, C.; Baggett, B.K.; Stafford, P.; Rain, M.; Gatenby, R.A.; Gillies, R.J. Acid treatment of melanoma cells selects for invasive phenotypes. *Clin. Exp. Metastasis* **2008**, *25*, 411–425. [[CrossRef](#)] [[PubMed](#)]
14. Estrella, V.; Chen, T.; Lloyd, M.; Wojtkowiak, J.; Cornell, H.H.; Ibrahim-Hashim, A.; Bailey, K.; Balagurunathan, Y.; Rothberg, J.M.; Sloane, B.F.; et al. Acidity generated by the tumor microenvironment drives local invasion. *Cancer Res.* **2013**, *73*, 1524–1535. [[CrossRef](#)] [[PubMed](#)]
15. Corbet, C.; Bastien, E.; de Jesus, J.P.S.; Dierge, E.; Martherus, R.; Vander Linden, C.; Doix, B.; Degavre, C.; Guilbaud, C.; Petit, L.; et al. TGFβ<sub>2</sub>-induced formation of lipid droplets supports acidosis-driven EMT and the metastatic spreading of cancer cells. *Nat. Commun.* **2020**, *11*, 454. [[CrossRef](#)] [[PubMed](#)]
16. Martínez-Zaguilán, R.; Seftor, E.A.; Seftor, R.E.; Chu, Y.W.; Gillies, R.J.; Hendrix, M.J. Acidic pH enhances the invasive behavior of human melanoma cells. *Clin. Exp. Metastasis* **1996**, *14*, 176–186. [[CrossRef](#)] [[PubMed](#)]
17. Rohani, N.; Hao, L.; Alexis, M.S.; Joughin, B.A.; Krismer, K.; Moufarrej, M.N.; Soltis, A.R.; Lauffenburger, D.A.; Yaffe, M.B.; Burge, C.B.; et al. Acidification of Tumor at Stromal Boundaries Drives Transcriptome Alterations Associated with Aggressive Phenotypes. *Cancer Res.* **2019**, *79*, 1952–1966. [[CrossRef](#)]
18. LaMonte, G.; Tang, X.; Chen, J.L.; Wu, J.; Ding, C.K.; Keenan, M.M.; Sangokoya, C.; Kung, H.N.; Ilkayeva, O.; Boros, L.G.; et al. Acidosis induces reprogramming of cellular metabolism to mitigate oxidative stress. *Cancer Metab.* **2013**, *1*, 23. [[CrossRef](#)]
19. Corbet, C.; Draoui, N.; Polet, F.; Pinto, A.; Drozak, X.; Riant, O.; Feron, O. The SIRT1/HIF2α axis drives reductive glutamine metabolism under chronic acidosis and alters tumor response to therapy. *Cancer Res.* **2014**, *74*, 5507–5519. [[CrossRef](#)]
20. Corbet, C.; Feron, O. Tumour acidosis: From the passenger to the driver's seat. *Nat. Rev. Cancer* **2017**, *17*, 577–593. [[CrossRef](#)]
21. Pellegrini, P.; Serviss, J.T.; Lundbäck, T.; Bancaro, N.; Mazurkiewicz, M.; Kolosenko, I.; Yu, D.; Haraldsson, M.; D'Arcy, P.; Linder, S.; et al. A drug screening assay on cancer cells chronically adapted to acidosis. *Cancer Cell Int.* **2018**, *18*, 147. [[CrossRef](#)]
22. Chen, J.L.; Merl, D.; Peterson, C.W.; Wu, J.; Liu, P.Y.; Yin, H.; Muoio, D.M.; Ayer, D.E.; West, M.; Chi, J.T. Lactic acidosis triggers starvation response with paradoxical induction of TXNIP through MondoA. *PLoS Genet* **2010**, *6*, e1001093. [[CrossRef](#)] [[PubMed](#)]
23. Michl, J.; Park, K.C.; Swietach, P. Evidence-based guidelines for controlling pH in mammalian live-cell culture systems. *Commun. Biol.* **2019**, *2*, 144. [[CrossRef](#)] [[PubMed](#)]
24. Wilde, B.R.; Ye, Z.; Lim, T.Y.; Ayer, D.E. Cellular acidosis triggers human MondoA transcriptional activity by driving mitochondrial ATP production. *Elife* **2019**, *8*, e40199. [[CrossRef](#)] [[PubMed](#)]
25. Jia, J.J.; Geng, W.S.; Wang, Z.Q.; Chen, L.; Zeng, X.S. The role of thioredoxin system in cancer: Strategy for cancer therapy. *Cancer Chemother. Pharmacol.* **2019**, *84*, 453–470. [[CrossRef](#)]
26. Cadenas, C.; Franckenstein, D.; Schmidt, M.; Gehrman, M.; Hermes, M.; Geppert, B.; Schormann, W.; Maccoux, L.J.; Schug, M.; Schumann, A.; et al. Role of thioredoxin reductase 1 and thioredoxin interacting protein in prognosis of breast cancer. *Breast Cancer Res.* **2010**, *12*, R44. [[CrossRef](#)]

27. Shen, L.; O'Shea, J.M.; Kaadige, M.R.; Cunha, S.; Wilde, B.R.; Cohen, A.L.; Welm, A.L.; Ayer, D.E. Metabolic reprogramming in triple-negative breast cancer through Myc suppression of TXNIP. *Proc. Natl. Acad. Sci. USA* **2015**, *112*, 5425–5430. [[CrossRef](#)]
28. Zhou, Z.H.; Song, J.W.; Li, W.; Liu, X.; Cao, L.; Wan, L.M.; Tan, Y.X.; Ji, S.P.; Liang, Y.M.; Gong, F. The acid-sensing ion channel, ASIC2, promotes invasion and metastasis of colorectal cancer under acidosis by activating the calcineurin/NFAT1 axis. *J. Exp. Clin. Cancer Res.* **2017**, *36*, 130. [[CrossRef](#)]
29. Waldmann, R.; Champigny, G.; Bassilana, F.; Heurteaux, C.; Lazdunski, M. A proton-gated cation channel involved in acid-sensing. *Nature* **1997**, *386*, 173–177. [[CrossRef](#)]
30. Collier, D.M.; Snyder, P.M. Extracellular protons regulate human ENaC by modulating Na<sup>+</sup> self-inhibition. *J. Biol. Chem.* **2009**, *284*, 792–798. [[CrossRef](#)]
31. Wu, L.; Ling, Z.H.; Wang, H.; Wang, X.Y.; Gui, J. Upregulation of SCNN1A Promotes Cell Proliferation, Migration, and Predicts Poor Prognosis in Ovarian Cancer Through Regulating Epithelial-Mesenchymal Transformation. *Cancer Biother. Radiopharm.* **2019**, *34*, 642–649. [[CrossRef](#)]
32. Kanwar, N.; Carmine-Simmen, K.; Nair, R.; Wang, C.; Moghadas-Jafari, S.; Blaser, H.; Tran-Thanh, D.; Wang, D.; Wang, P.; Wang, J.; et al. Amplification of a calcium channel subunit CACNG4 increases breast cancer metastasis. *EBioMedicine* **2020**, *52*, 102646. [[CrossRef](#)] [[PubMed](#)]
33. Nelson, M.; Millican-Slater, R.; Forrest, L.C.; Brackenbury, W.J. The sodium channel  $\beta$ 1 subunit mediates outgrowth of neurite-like processes on breast cancer cells and promotes tumour growth and metastasis. *Int. J. Cancer* **2014**, *135*, 2338–2351. [[CrossRef](#)] [[PubMed](#)]
34. Lui, A.J.; Geanes, E.S.; Ogony, J.; Behbod, F.; Marquess, J.; Valdez, K.; Jewell, W.; Tawfik, O.; Lewis-Wambi, J. IFITM1 suppression blocks proliferation and invasion of aromatase inhibitor-resistant breast cancer in vivo by JAK/STAT-mediated induction of p21. *Cancer Lett.* **2017**, *399*, 29–43. [[CrossRef](#)] [[PubMed](#)]
35. Sari, I.N.; Yang, Y.G.; Phi, L.T.; Kim, H.; Baek, M.J.; Jeong, D.; Kwon, H.Y. Interferon-induced transmembrane protein 1 (IFITM1) is required for the progression of colorectal cancer. *Oncotarget* **2016**, *7*, 86039–86050. [[CrossRef](#)] [[PubMed](#)]
36. Moy, I.; Todorovic, V.; Dubash, A.D.; Coon, J.S.; Parker, J.B.; Buranapramest, M.; Huang, C.C.; Zhao, H.; Green, K.J.; Bulun, S.E. Estrogen-dependent sushi domain containing 3 regulates cytoskeleton organization and migration in breast cancer cells. *Oncogene* **2015**, *34*, 323–333. [[CrossRef](#)] [[PubMed](#)]
37. Inamori, K.I.; Beedle, A.M.; de Bernabe, D.B.; Wright, M.E.; Campbell, K.P. LARGE2-dependent glycosylation confers laminin-binding ability on proteoglycans. *Glycobiology* **2016**, *26*, 1284–1296. [[CrossRef](#)]
38. Hinke, S.A.; Navedo, M.F.; Ulman, A.; Whiting, J.L.; Nygren, P.J.; Tian, G.; Jimenez-Caliani, A.J.; Langeberg, L.K.; Cirulli, V.; Tengholm, A.; et al. Anchored phosphatases modulate glucose homeostasis. *EMBO J.* **2012**, *31*, 3991–4004. [[CrossRef](#)]
39. Zhong, Z.; Ye, Z.; He, G.; Zhang, W.; Wang, J.; Huang, S. Low expression of A-kinase anchor protein 5 predicts poor prognosis in non-mucin producing stomach adenocarcinoma based on TCGA data. *Ann. Transl. Med.* **2020**, *8*, 115. [[CrossRef](#)]
40. Feng, X.; Yan, N.; Sun, W.; Zheng, S.; Jiang, S.; Wang, J.; Guo, C.; Hao, L.; Tian, Y.; Liu, S.; et al. miR-4521-FAM129A axial regulation on ccRCC progression through TIMP-1/MMP2/MMP9 and MDM2/p53/Bcl2/Bax pathways. *Cell Death Discov.* **2019**, *5*, 89. [[CrossRef](#)]
41. Nozima, B.H.; Mendes, T.B.; Pereira, G.; Araldi, R.P.; Iwamura, E.S.M.; Smaili, S.S.; Carvalheira, G.M.G.; Cerutti, J.M. FAM129A regulates autophagy in thyroid carcinomas in an oncogene-dependent manner. *Endocr. Relat. Cancer* **2019**, *26*, 227–238. [[CrossRef](#)]
42. Lelouvier, B.; Puertollano, R. Mucolipin-3 regulates luminal calcium, acidification, and membrane fusion in the endosomal pathway. *J. Biol. Chem.* **2011**, *286*, 9826–9832. [[CrossRef](#)] [[PubMed](#)]
43. Walton, Z.E.; Patel, C.H.; Brooks, R.C.; Yu, Y.; Ibrahim-Hashim, A.; Riddle, M.; Porcu, A.; Jiang, T.; Ecker, B.L.; Tameire, F.; et al. Acid Suspends the Circadian Clock in Hypoxia through Inhibition of mTOR. *Cell* **2018**, *174*, 72–87.e32. [[CrossRef](#)] [[PubMed](#)]
44. Walton, Z.E.; Brooks, R.C.; Dang, C.V. mTOR Senses Intracellular pH through Lysosome Dispersion from RHEB. *Bioessays* **2019**, *41*, e1800265. [[CrossRef](#)]
45. Zhou, Z.H.; Wang, Q.L.; Mao, L.H.; Li, X.Q.; Liu, P.; Song, J.W.; Liu, X.; Xu, F.; Lei, J.; He, S. Chromatin accessibility changes are associated with enhanced growth and liver metastasis capacity of acid-adapted colorectal cancer cells. *Cell Cycle* **2019**, *18*, 511–522. [[CrossRef](#)] [[PubMed](#)]

46. Ngeow, J.; Yu, W.; Yehia, L.; Niazi, F.; Chen, J.; Tang, X.; Heald, B.; Lei, J.; Romigh, T.; Tucker-Kellogg, L.; et al. Exome Sequencing Reveals Germline SMAD9 Mutation That Reduces Phosphatase and Tensin Homolog Expression and Is Associated With Hamartomatous Polyposis and Gastrointestinal Ganglioneuromas. *Gastroenterology* **2015**, *149*, 886–889.e5. [[CrossRef](#)] [[PubMed](#)]
47. Li, X.; Burton, E.M.; Koganti, S.; Zhi, J.; Doyle, F.; Tenenbaum, S.A.; Horn, B.; Bhaduri-McIntosh, S. KRAB-ZFP Repressors Enforce Quiescence of Oncogenic Human Herpesviruses. *J. Virol.* **2018**, *92*, e00298-18. [[CrossRef](#)]
48. The Universal Protein Resource (UniProt). Available online: <https://www.uniprot.org/> (accessed on 3 June 2020).
49. Szklarczyk, D.; Gable, A.L.; Lyon, D.; Junge, A.; Wyder, S.; Huerta-Cepas, J.; Simonovic, M.; Doncheva, N.T.; Morris, J.H.; Bork, P.; et al. STRING v11: Protein-protein association networks with increased coverage, supporting functional discovery in genome-wide experimental datasets. *Nucleic Acids Res.* **2019**, *47*, D607–D613. [[CrossRef](#)]
50. Ji, Y.; Jiang, J.; Huang, L.; Feng, W.; Zhang, Z.; Jin, L.; Xing, X. Sperm associated antigen 4 (SPAG4) as a new cancer marker interacts with Nesprin3 to regulate cell migration in lung carcinoma. *Oncol. Rep.* **2018**, *40*, 783–792. [[CrossRef](#)]
51. Wang, J.K.; Wang, W.J.; Cai, H.Y.; Du, B.B.; Mai, P.; Zhang, L.J.; Ma, W.; Hu, Y.G.; Feng, S.F.; Miao, G.Y. MFAP2 promotes epithelial-mesenchymal transition in gastric cancer cells by activating TGF-beta/SMAD2/3 signaling pathway. *Onco. Targets Ther.* **2018**, *11*, 4001–4017. [[CrossRef](#)]
52. Zhao, Z.; Zhang, K.N.; Chai, R.C.; Wang, K.Y.; Huang, R.Y.; Li, G.Z.; Wang, Y.Z.; Chen, J.; Jiang, T. ADAMTSL4, a Secreted Glycoprotein, Is a Novel Immune-Related Biomarker for Primary Glioblastoma Multiforme. *Dis. Markers* **2019**, *2019*, 1802620. [[CrossRef](#)]
53. Kaikkonen, E.; Rantapero, T.; Zhang, Q.; Taimen, P.; Laitinen, V.; Kallajoki, M.; Jambulingam, D.; Ettala, O.; Knaapila, J.; Bostrom, P.J.; et al. ANO7 is associated with aggressive prostate cancer. *Int. J. Cancer* **2018**, *143*, 2479–2487. [[CrossRef](#)] [[PubMed](#)]
54. Swietach, P.; Vaughan-Jones, R.D.; Harris, A.L.; Hulikova, A. The chemistry, physiology and pathology of pH in cancer. *Philos. Trans. R. Soc. Lond. B Biol. Sci.* **2014**, *369*, 20130099. [[CrossRef](#)] [[PubMed](#)]
55. Damaghi, M.; Gillies, R. Phenotypic changes of acid adapted cancer cells push them toward aggressiveness in their evolution in the tumor microenvironment. *Cell Cycle* **2016**, *16*, 1739–1743. [[CrossRef](#)] [[PubMed](#)]
56. Pedersen, S.F.; Novak, I.; Alves, F.; Schwab, A.; Pardo, L.A. Alternating pH landscapes shape epithelial cancer initiation and progression: Focus on pancreatic cancer. *Bioessays* **2017**, *39*, 1600253. [[CrossRef](#)] [[PubMed](#)]
57. Wojtkowiak, J.W.; Verduzco, D.; Schramm, K.J.; Gillies, R.J. Drug resistance and cellular adaptation to tumor acidic pH microenvironment. *Mol. Pharm.* **2011**, *8*, 2032–2038. [[CrossRef](#)] [[PubMed](#)]
58. Pilon-Thomas, S.; Kodumudi, K.N.; El-Kenawi, A.E.; Russell, S.; Weber, A.M.; Luddy, K.; Damaghi, M.; Wojtkowiak, J.W.; Mule, J.J.; Ibrahim-Hashim, A.; et al. Neutralization of Tumor Acidity Improves Antitumor Responses to Immunotherapy. *Cancer Res.* **2016**, *76*, 1381–1390. [[CrossRef](#)] [[PubMed](#)]
59. Damaghi, M.; Tafreshi, N.K.; Lloyd, M.C.; Sprung, R.; Estrella, V.; Wojtkowiak, J.W.; Morse, D.L.; Koomen, J.M.; Bui, M.M.; Gatenby, R.A.; et al. Chronic acidosis in the tumour microenvironment selects for overexpression of LAMP2 in the plasma membrane. *Nat. Commun.* **2015**, *6*, 8752. [[CrossRef](#)]
60. Bon, E.; Driffort, V.; Gradek, F.; Martinez-Caceres, C.; Anchin, M.; Pelegrin, P.; Cayuela, M.L.; Marionneau-Lambot, S.; Oullier, T.; Guibon, R.; et al. SCN4B acts as a metastasis-suppressor gene preventing hyperactivation of cell migration in breast cancer. *Nat. Commun.* **2016**, *7*, 13648. [[CrossRef](#)]
61. Haworth, A.S.; Brackenbury, W.J. Emerging roles for multifunctional ion channel auxiliary subunits in cancer. *Cell Calcium* **2019**, *80*, 125–140. [[CrossRef](#)]
62. Corbet, C.; Pinto, A.; Martherus, R.; de Jesus, J.P.S.; Polet, F.; Feron, O. Acidosis Drives the Reprogramming of Fatty Acid Metabolism in Cancer Cells through Changes in Mitochondrial and Histone Acetylation. *Cell Metab.* **2018**, *24*, 311–323. [[CrossRef](#)]
63. Malone, C.F.; Emerson, C.; Ingraham, R.; Barbosa, W.; Guerra, S.; Yoon, H.; Liu, L.L.; Michor, F.; Haigis, M.; Macleod, K.F.; et al. mTOR and HDAC Inhibitors Converge on the TXNIP/Thioredoxin Pathway to Cause Catastrophic Oxidative Stress and Regression of RAS-Driven Tumors. *Cancer Discov.* **2017**, *7*, 1450–1463. [[CrossRef](#)] [[PubMed](#)]
64. Flinck, M.; Kramer, S.H.; Pedersen, S.F. Roles of pH in control of cell proliferation. *Acta Physiol. (Oxf.)* **2018**, *223*, e13068. [[CrossRef](#)] [[PubMed](#)]

65. Peppicelli, S.; Andreucci, E.; Ruzzolini, J.; Laurenzana, A.; Margheri, F.; Fibbi, G.; Del Rosso, M.; Bianchini, F.; Calorini, L. The acidic microenvironment as a possible niche of dormant tumor cells. *Cell Mol. Life Sci.* **2017**, *74*, 2761–2771. [[CrossRef](#)] [[PubMed](#)]
66. Robey, I.F.; Baggett, B.K.; Kirkpatrick, N.D.; Roe, D.J.; Donescu, J.; Sloane, B.F.; Hashim, A.I.; Morse, D.L.; Raghunand, N.; Gatenby, R.A.; et al. Bicarbonate increases tumor pH and inhibits spontaneous metastases. *Cancer Res.* **2009**, *69*, 2260–2268. [[CrossRef](#)] [[PubMed](#)]
67. Ibrahim-Hashim, A.; Cornnell, H.H.; Abrahams, D.; Lloyd, M.; Bui, M.; Gillies, R.J.; Gatenby, R.A. Systemic buffers inhibit carcinogenesis in TRAMP mice. *J. Urol.* **2012**, *188*, 624–631. [[CrossRef](#)] [[PubMed](#)]
68. Patro, R.; Duggal, G.; Love, M.I.; Irizarry, R.A.; Kingsford, C. Salmon provides fast and bias-aware quantification of transcript expression. *Nat. Methods* **2017**, *14*, 417–419. [[CrossRef](#)]
69. Robinson, M.D.; Oshlack, A. A scaling normalization method for differential expression analysis of RNA-seq data. *Genome Biol.* **2010**, *11*, R25. [[CrossRef](#)]
70. McCarthy, D.J.; Chen, Y.; Smyth, G.K. Differential expression analysis of multifactor RNA-Seq experiments with respect to biological variation. *Nucleic Acids Res.* **2012**, *40*, 4288–4297. [[CrossRef](#)]
71. Robinson, M.D.; McCarthy, D.J.; Smyth, G.K. edgeR: A Bioconductor package for differential expression analysis of digital gene expression data. *Bioinformatics* **2009**, *26*, 139–140. [[CrossRef](#)]
72. Ritchie, M.E.; Phipson, B.; Wu, D.; Hu, Y.; Law, C.W.; Shi, W.; Smyth, G.K. limma powers differential expression analyses for RNA-sequencing and microarray studies. *Nucleic Acids Res.* **2015**, *43*, e47. [[CrossRef](#)]
73. Raudvere, U.; Kolberg, L.; Kuzmin, I.; Arak, T.; Adler, P.; Peterson, H.; Vilo, J. g:Profiler: A web server for functional enrichment analysis and conversions of gene lists (2019 update). *Nucleic Acids Res.* **2019**, *47*, W191–W198. [[CrossRef](#)] [[PubMed](#)]
74. Subramanian, A.; Tamayo, P.; Mootha, V.K.; Mukherjee, S.; Ebert, B.L.; Gillette, M.A.; Paulovich, A.; Pomeroy, S.L.; Golub, T.R.; Lander, E.S.; et al. Gene set enrichment analysis: A knowledge-based approach for interpreting genome-wide expression profiles. *Proc. Natl. Acad. Sci. USA* **2005**, *102*, 15545–15550. [[CrossRef](#)] [[PubMed](#)]
75. The Cancer Genome Atlas (TCGA). Available online: <http://cancergenome.nih.gov/> (accessed on 3 June 2020).
76. University of California Santa Cruz (UCSC) Xena Functional Genomic Browser. Available online: <https://xenabrowser.net/> (accessed on 3 June 2020).
77. R Package (Version 1.28.0) for Rank-Rank Hypergeometric Overlap (RRHO) Test. Available online: <https://bioconductor.org/packages/release/bioc/html/RRHO.html> (accessed on 3 June 2020).
78. Plaisier, S.B.; Taschereau, R.; Wong, J.A.; Graeber, T.G. Rank-rank hypergeometric overlap: Identification of statistically significant overlap between gene-expression signatures. *Nucleic Acids Res.* **2010**, *38*, e169. [[CrossRef](#)] [[PubMed](#)]





## Abstract

The transient receptor potential canonical 1 channel (TRPC1) is one of the most prominent nonselective cation channels involved in several diseases, including cancer progression. TRPCs can be activated by different physio-chemical stimuli of their surroundings, for instance, pH. Another hallmark of cancer is the variable extracellular pH landscape, notably in epithelial cancers such as pancreatic ductal adenocarcinoma (PDAC). PDAC progression and development are linked to the physiology and microenvironment of the exocrine pancreas. There are strong indications that PDAC aggressiveness is caused by the interplay between the tumor acidic microenvironment and ion channel dysregulation. However, this interaction has never been studied before. Here, we investigate if TRPC1 is involved in PDAC progression in the form of proliferation and migration and if the pH fluctuations of the acidic tumor microenvironment affect these processes.

We found that TRPC1 was significantly upregulated in PDAC tumor tissue compared to adjacent normal tissue, and in the aggressive PDAC cell line PANC-1, compared to a duct-like cell line, hTERT-HPNE. To investigate if fluctuations of the acidic tumor microenvironment affect TRPC1 dysregulation, PANC-1 cells were incubated in a medium with a pH of 7.4 or 6.5 over 30 days, where after cells were recovered in pH 7.4 for 14 days (7.4R). Acid adaptation (6.5) reduced TRPC1 protein expression but favored its membrane localization compared to the control (7.4). pH recovery treatment (7.4R) resulted in an upregulation of TRPC1 expression with a high membrane localization, both in 2D and 3D models. We found that pH fluctuations and the siRNA-based knock-down (KD) of TRPC1 affected 2D and spheroid PANC-1 proliferation, respectively. In our 2D model, flow cytometry and cell cycle regulating protein immunoblotting showed that TRPC1 KD affected the progression through G0/G1 phase under all conditions and S-phase under control pH 7.4, which shifts to the G2/M phase in pH 6.5 and 7.4R. In addition, pH 6.5 enhanced, and the KD of TRPC1 decreased cell migration, respectively. Furthermore, we found that TRPC1 interacted strongly with PI3K under acidic conditions and CaM under all conditions, and a KD of TRPC1 decreased both this interaction and the activation of AKT and ERK1/2. Finally, basal Ca<sup>2+</sup> entry was significantly reduced upon the KD of TRPC1 in pH 6.5 and 7.4R, where the entry was enhanced. The reduction of extracellular Ca<sup>2+</sup> concentration resulted in an additional decrease in proliferation and migration of cells transfected with siTRPC1 growing in pH 6.5 and 7.4R, but not in normal pH 7.4 conditions.

Collectively, our results show that TRPC1 is upregulated in PDAC tissue and cell lines. The acidic tumor microenvironment favors its plasma membrane localization, and its interaction with PI3K/CaM and Ca<sup>2+</sup> entry leads to PDAC cells proliferation and migration.

In addition, we performed an expression profile screening of ORAI channels, their partner STIM1, and a voltage-activated sodium channel (Nav1.6), and an acid-sensing ion channel (ASIC1) in PDAC tissues and cell lines, and investigated whether the acidic tumor microenvironment affects epigenetic regulation of ion channel expression. We found that ORAI3 was upregulated in PDAC tissue compared to normal tissue, where STIM1 and Nav1.6 were significantly downregulated. Moreover, ORAI3 was more localized in the plasma membrane in tumor tissue. Acid-adaptation had a differential effect on Ca<sup>2+</sup> channel expression. Furthermore, our preliminary results show that the acidic tumor microenvironment does not affect the methylation levels of the ASIC1 or TRPC1 promoter region, but so some extend the SCN8A gene promoter.

**Keywords:** Pancreatic cancer - Tumor microenvironment - Ion channels - Epigenetics

## Résumé

Le canal TRPC1 (pour *transient receptor potential canonical 1*) est l'un des canaux cationiques non sélectifs les plus impliqués dans plusieurs maladies, y compris la progression du cancer. Les TRPC peuvent être activés par différents stimuli physico-chimiques dont le pH. Par ailleurs, l'une des caractéristiques du cancer représente les variations pH extracellulaire, notamment dans l'adénocarcinome canalaire pancréatique (ACP). Il existe de fortes indications quant à l'agressivité de l'ACP qui est causée par l'interaction entre le microenvironnement acide de la tumeur et la dérégulation des canaux ioniques. Cependant, cette interaction n'a jamais été étudiée. Lors de ce travail, nous avons étudié si TRPC1 ainsi que les fluctuations du pH acide du microenvironnement tumoral régulent la progression de l'ACP et plus particulièrement la prolifération et de migration cellulaires.

Nous avons constaté que TRPC1 était surexprimé dans le tissu tumoral pancréatique par rapport au tissu normal, et dans la lignée cellulaire agressive PANC-1, par rapport à une lignée cellulaire de type canalaire, hTERT-HPNE. Pour déterminer si les fluctuations du microenvironnement acide de la tumeur affectent la dérégulation de TRPC1, les cellules PANC-1 ont été incubées dans un milieu présentant un pH de 7,4 ou 6,5 pendant 30 jours, après quoi les cellules ont été récupérées à pH 7,4 pendant 14 jours (7,4 R). L'adaptation acide (6,5) a réduit l'expression de la protéine TRPC1 mais a favorisé sa localisation membranaire par rapport au contrôle (7,4). Dans des conditions de pH 7,4R, les cellules cancéreuses présentaient une expression de TRPC1 exacerbée avec une localisation membranaire élevée, à la fois dans les modèles 2D et 3D. Nous avons constaté que les fluctuations de pH et l'invalidation moléculaire par siARN (KD) de TRPC1 affectaient respectivement la prolifération de PANC-1 dans un modèle 2D et sphéroïde. Dans notre modèle 2D, nous avons montré que TRPC1 KD affectait la progression à travers la phase G0/G1 dans toutes les conditions et la phase S lorsque les cellules sont cultivées dans un milieu pH 7,4, et la phase G2/M dans les conditions pH 6,5 et 7,4 R. En outre, pH 6,5 a amélioré tandis que le KD de TRPC1 a diminué la migration cellulaire. De plus, nous avons constaté que TRPC1 interagissait fortement avec PI3K dans des conditions acides, et CaM dans toutes les conditions. Le KD de TRPC1 diminuait à la fois cette interaction et l'activation de AKT et ERK1/2. Enfin, l'entrée basale de Ca<sup>2+</sup> a été significativement réduite par le KD de TRPC1 dans les conditions de pH 6,5 et 7,4R. La réduction de la concentration de Ca<sup>2+</sup> extracellulaire a entraîné une diminution additionnelle de la prolifération et de la migration des cellules transfectées avec siTRPC1 cultivées à pH 6,5 et 7,4R, mais pas dans des conditions normales de pH 7,4.

Collectivement, nos résultats montrent que TRPC1 est régulé positivement dans les tissus et lignées d'ACP. Le microenvironnement acide de la tumeur favorise sa localisation membranaire et son interaction avec PI3K/CaM. Enfin, le Ca<sup>2+</sup> transitant par TRPC1 participe à la prolifération et à la migration cellulaires.

De plus, nous avons effectué un criblage du profil d'expression des canaux ORAI, de leur partenaire STIM1, d'un canal sodique activé par le voltage (Nav1.6) et d'un canal ionique détectant l'acidité (ASIC1) dans les tissus et lignées d'ACP. Nous avons examiné si le microenvironnement acide affecte la régulation épigénétique des canaux ioniques. Nous avons constaté qu'ORAI3 était régulé positivement dans le tissu ACP par rapport au tissu normal, tandis que STIM1 et Nav1.6 étaient régulés négativement. De plus, ORAI3 était préférentiellement localisé au niveau membranaire dans le tissu tumoral. De plus, nos résultats préliminaires montrent que le microenvironnement acide de la tumeur n'affecte pas les niveaux de méthylation de la région promotrice des gènes codant pour ASIC1 ou TRPC1, mais également du gène SCN8A.

**Mots clés:** Cancer du pancréas - Microenvironnement tumoral - Canaux ioniques - Epigénétique